



U.S. DEPARTMENT OF  
**ENERGY**

Frontiers in Catalysis:  
Heterogeneous, Surface,  
Photo- and Electrochemical

Meeting of the Catalysis Science Program  
Chemical Sciences, Geosciences and Biosciences  
Division

Office of Basic Energy Sciences  
U.S. Department of Energy  
Annapolis, Maryland  
October 2-5, 2011

This document was produced under contract number DE-AC05-06OR23100 between the U.S. Department of Energy and Oak Ridge Associated Universities.

## FOREWORD

The 2011 Catalysis Science Program Meeting is sponsored by the Division of Chemical Sciences, Geosciences and Biosciences, Office of Basic Energy Sciences (OBES), U.S. Department of Energy. It is being held on October 2 through October 5, 2011, at the Westin Annapolis Hotel, Annapolis, Maryland. The purposes of this meeting are to discuss the recent advances in the physico-chemical, materials and biological bases of catalysis science, to foster exchange of ideas and cooperation among participants, and to discuss the new challenges and opportunities recently emerging in catalytic technologies.

Catalysis activities within OBES emphasize fundamental research aimed at initially understanding and finally controlling the chemical reactivity of matter in the presence of catalytic substances and thermal or nonthermal energy sources. The long-term goal of this research is to discover fundamental principles and produce ever more insightful approaches to predict structure-reactivity behavior. Such knowledge, integrated with advances in chemical and materials synthesis, *operando* analytical instrumentation, theoretical and chemical kinetics and dynamics methods, will allow the control of chemical reactions along desired pathways. Ultimately, this new knowledge should impact the efficiency of conversion of natural resources (mass and energy) into fuels, chemicals, materials, or other forms of energy, while minimizing the impact to the environment.

Special thanks go to our invited speakers and guest junior scientists, who will expose us to recent advances in their fields; to the program investigators and their students, postdocs, and collaborators, for their dedication to the continuous success and visibility of the Catalysis Science Program; and to the session chairs, for their invaluable help. We also thank the Oak Ridge Institute for Science and Education staff for the logistical and web support and the compilation of this volume.

Robert J. Davis<sup>1</sup> and Raul Miranda<sup>2</sup>

<sup>1</sup>University of Virginia

<sup>2</sup>Office of Basic Energy Sciences - U.S. Department of Energy

This page is intentionally blank.

# AGENDA

## Sunday Afternoon and Evening, October 2

3:00 - 5:00 pm                      Registration  
(*Outside Senate A&B*)

5:00 - 6:00 pm                      Dinner  
(*Capitol C&D*)

### Session I, Chair: Steven Suib

6:15 - 6:30 pm                      Welcoming Remarks

6:30 - 7:15 pm                      **Invited Speaker: Peidong Yang (UC Berkeley, LBNL)**  
"Metal Nanocrystals: Shape Control, Assembly, Surface  
Chemistry and Catalysis"

7:15 - 7:50 pm                      Jeffrey Brinker (U New Mexico) "Catalytic and Transport  
Behaviors of Model Porous and Composite Nanostructures"

7:50 - 8:25 pm                      Alexander Katz (UC Berkeley) "Control of Heterogeneous  
Catalysis via Design of Organic-Inorganic Interfaces"

8:25 - 10:00 pm                      **Social Hour/Poster Session I (Odd Numbers)**  
(*Senate A&B*)

## Monday Morning, October 3

7:00 - 8:15 am                      Breakfast  
(*Outside Senate A&B*)

### Session II, Chair: Cynthia Friend

8:30 - 9:15 am                      **Invited Speaker: Hans-Peter Steinrück (Erlangen-  
Nürnberg U)** "Surface Science Goes Liquid!"

9:15 - 9:50 am                      Christopher Jones (GA Tech U) "Developing the Science of  
Immobilized Molecular Catalysts"

9:50 - 10:15 am                      Coffee Break  
(*Outside Senate A&B*)

10:15 - 10:50 am                      Peter Stair (Northwestern U) "Structure/Composition/Function  
Relationship in Supported Nanoscale Catalysts for  
Hydrogen"

10:50 - 11:25 am                      Jose Rodriguez (Brookhaven NL) "Catalysis: Reactivity and  
Structure"

11:25 - 12:00 pm                      Francisco Zaera (UC Riverside) "Design and Characterization  
of Novel Photocatalysts with Core-Shell Nanostructures"

12:20 pm                              Lunch

### Monday Afternoon, October 3

1:00 - 3:00 pm                      Networking

#### Session III, Chair: Michael Henderson

- 3:00 - 3:45 pm                      **Invited Speaker: Morris Bullock (PNNL)**  
"Design and Development of Molecular Electrocatalysts for Energy Conversions"
- 3:45 - 4:05 pm                      Guofeng Wang (Pittsburgh U) "Theoretically Relating the Surface Composition of Pt Alloys to Their Performance as the Electrocatalysts of Low-Temperature Fuel Cells"
- 4:05 - 4:25 pm                      William Mustain (U Connecticut) "Understanding the Effects of Surface Chemistry and Microstructure on the Activity and Stability of Pt Electrocatalysts on Non-Carbon Supports"
- 4:25 - 5:00 pm                      Raymond Gorte (U Pennsylvania) "Thermodynamic Properties of Supported Catalysts"
- 5:00 - 6:00 pm                      Dinner

### Monday Evening, October 3

#### Session IV, Chair: Charles Campbell

- 6:15 - 7:00 pm                      **Invited Speaker: Xinhe Bao (Dalian Inst)**  
"Enhanced Catalysis by Nano Confinements"
- 7:00 - 7:35 pm                      Ludwig Bartels (UC Riverside) "Dynamics at a Surface: Understanding Fundamental Surface Processes as an Approach to Tailored Surface Activity"
- 7:35 - 8:10 pm                      Beatriz Roldán Cuenya (U Central Florida) "Influence of the Oxidation State of Supported Size-Selected Pt Nanoparticles on Catalytic Decomposition and Oxidation of High-Order Alcohols: Activity, Selectivity and Lifetime"
- 8:20 - 10:00 pm                      **Social Hour/Poster Session II (Even Numbers)**

### Tuesday Morning, October 4

7:00 - 8:15 am                      Breakfast  
(*Outside Senate A&B*)

#### Session V, Chair: Nicholas Delgass

- 8:30 - 9:15 am                      **Invited Speaker: Thorsten Bernhardt (U Ulm)**  
"Molecular Mechanism, Kinetics, and Dynamics of Metal Cluster Catalyzed Reactions in an Ion Trap"
- 9:15 - 9:50 am                      Peng Chen (Cornell U) "Single-Molecule Sub-Diffraction Imaging of Nanoscale Catalysis"

9:50 - 10:15 am	Coffee Break ( <i>Outside Senate A&amp;B</i> )
10:15 - 10:50 am	Maria Flytzani-Stephanopoulos (Tufts U) "Nanostructured, Metal-Ion Modified Oxide Catalysts for the Water-Gas Shift and Methanol Steam Reforming Reactions"
10:50 - 11:25 am	Ping Liu (BNL) "Theoretical Studies in Heterogeneous Catalysis and Electrocatalysis"
11:25 - 12:00 pm	Perla Balbuena (Texas A&M U) "Modeling Catalyzed Growth of Single-Wall Carbon Nanotubes"
12:20 pm	Lunch

### Tuesday Afternoon, October 4

1:00 - 3:00 pm                      Networking

#### **Session VI, Chair: Robert Davis**

3:00 - 3:45 pm	<b>Invited Speaker: Bert Weckhuysen (Utrecht U)</b> "In Situ Spectroscopy of Catalytic Solids at the Single Particle Level"
3:45 - 4:20 pm	Jingguang Chen (U Delaware) "Structure-Property Relationship in Metal Carbides and Bimetallic Alloys"
4:20 - 5:00 pm	Selected speakers
5:00 - 6:00 pm	Dinner

### Tuesday Evening, October 4

#### **Session VII, Chair: Manos Mavrikakis**

6:15 - 7:00 pm	<b>Invited Speaker: Jens Nørskov (SLAC/Stanford U)</b> "Understanding Activity and Selectivity in Syngas Reactions"
7:00 - 7:35 pm	William Schneider (Notre Dame U) "Towards Realistic Reaction Environments in Catalysis Simulation"
7:35 - 8:10 pm	Eric McFarland (UC Santa Barbara) "Investigations of C-X Bond Activation on Doped Metal Oxide Catalysts"
8:20 - 10:00 pm	<b>Social Hour/Poster Session III (All)</b>

## Wednesday Morning, October 5

7:00 - 8:15 am Breakfast  
(*Outside Senate A&B*)

### Session VIII, Chair: Harold Kung

8:30 - 9:15 am **Invited Speaker: Johannes Lercher (PNNL/TU Munich)**  
"Catalytic Depolymerization and Hydrodeoxygenation of Lignin"

9:15 - 9:50 am YuYe Tong (Georgetown U) "In Situ NMR/IR/Raman and Ab Initio DFT Investigations of Pt-Based Mono- and Bi-metallic Nanoscale Electrocatalysts: From Sulfur-Poisoning to Polymer Promoters to Surface Activity Indexes"

9:50 - 10:15 am Coffee Break  
(*Outside Senate A&B*)

10:15 - 10:50 am Dionisios Vlachos (U Delaware) "Modern Catalytic Technologies for Converting Biomass to Renewable Fuels and Chemicals"

10:50 - 11:25 am Robert Bartynski (Rutgers U) "Nanoscale Surface Chemistry and Electrochemistry of Clean and Metal-Covered Faceted Substrates: Structure, Reactivity, and Electronic Properties"

11:25 - 12:00 pm Selected speakers

12:20 pm **Working Lunch: Future directions for the program. Discussion and conclusions**



## Table of Contents

<b>Foreword</b> .....	i
<b>Agenda</b> .....	iii
 <b>Sunday Evening, Session I</b>	
<b>Invited Speaker: Peidong Yang</b> – <i>Metal Nanocrystals: Shape Control, Assembly, Surface Chemistry and Catalysis</i> .....	3
Jeffrey Brinker – <i>Catalytic and Transport Behaviors of Model Porous and Composite Nanostructures</i> .....	4
Alexander Katz – <i>Control of Heterogeneous Catalysis via Design of Organic-Inorganic Interfaces</i> .....	7
 <b>Monday Morning, Session II</b>	
<b>Invited Speaker: Hans-Peter Steinrueck</b> – <i>Surface Science Goes Liquid!</i> .....	13
Christopher Jones – <i>Developing the Science of Immobilized Molecular Catalysts</i> ..	14
Peter Stair – <i>Structure/Composition/Function Relationship in Supported Nanoscale Catalysts for Hydrogen</i> .....	20
Jose Rodriguez – <i>Catalysis: Reactivity and Structure</i> .....	26
Francisco Zaera – <i>Design and Characterization of Novel Photocatalysts with Core-Shell Nanostructures</i> .....	32
 <b>Monday Afternoon, Session III</b>	
<b>Invited Speaker: Morris Bullock</b> – <i>Design and Development of Molecular Electrocatalysts for Energy Conversions</i> .....	41
Guofeng Wang – <i>Theoretically Relating the Surface Composition of Pt Alloys to Their Performance as the Electrocatalysts of Low-Temperature Fuel Cells</i> .....	42
William Mustain – <i>Understanding the Effects of Surface Chemistry and Microstructure on the Activity and Stability of Pt Electrocatalysts on Non-carbon Supports</i> .....	45
Raymond Gorte – <i>Thermodynamic Properties of Supported Catalysts</i> .....	48
 <b>Monday Evening, Session IV</b>	
<b>Invited Speaker: Xinhe Bao</b> – <i>Enhanced Catalysis by Nano Confinements</i> .....	53

Ludwig Bartels – *Dynamics at a Surface: Understanding Fundamental Surface Processes as an Approach to Tailored Surface Activity*.....56

Beatriz Roldán Cuenya – *Influence of the Oxidation State of Supported Size-Selected Pt Nanoparticles on Catalytic Decomposition and Oxidation of High-Order Alcohols: Activity, Selectivity, and Lifetime*.....57

### **Tuesday Morning, Session V**

**Invited Speaker: Thorsten Bernhardt** – *Molecular Mechanism, Kinetics, and Dynamics of Metal Cluster Catalyzed Reactions in an Ion Trap* .....63

Peng Chen – *Single-Molecule Sub-diffraction Imaging of Nanoscale Catalysis*.....64

Maria Flytzani-Stephanopoulos – *Nanostructured, Metal-Ion Modified Oxide Catalysts for the Water-Gas Shift and Methanol Steam Reforming Reactions* .....65

Ping Liu – *Theoretical Studies in Heterogeneous Catalysis and Electrocatalysis*.....71

Perla Balbuena – *Modeling Catalyzed Growth of Single-Wall Carbon Nanotubes*....72

### **Tuesday Afternoon, Session VI**

**Invited Speaker: Bert Weckhuysen** – *In Situ Spectroscopy of Catalytic Solids at the Single Particle Level* .....77

Jingguang Chen – *Structure-Property Relationship in Metal Carbides and Bimetallic Alloys* .....78

### **Tuesday Evening, Session VII**

**Invited Speaker: Jens Nørskov** – *Understanding Activity and Selectivity in Syngas Reactions* .....83

William Schneider – *Towards Realistic Reaction Environments in Catalysis Simulation*.....87

Eric McFarland – *Investigations of C-X Bond Activation on Doped Metal Oxide Catalysts* .....90

### **Wednesday Morning, Session VIII**

**Invited Speaker: Johannes Lercher** – *Catalytic Depolymerization and Hydrodeoxygenation of Lignin* .....97

YuYe Tong – *In Situ NMR/IR/Raman and Ab Initio DFT Investigations of Pt-Based Mono- and Bi-metallic Nanoscale Electrocatalysts: From Sulfur-Poisoning to Polymer Promoters to Surface Activity Indexes* .....98

Dionisios Vlachos – *Modern Catalytic Technologies for Converting Biomass to Renewable Fuels and Chemicals* ..... 101

Robert Bartynski – *Nanoscale Surface Chemistry and Electrochemistry of Clean and Metal-Covered Faceted Substrates: Structure, Reactivity, and Electronic Properties* ..... 107

### **Poster Presentations**

1. Radoslav Adzic – *Metal and Metal-Oxide-Supported Platinum Monolayer Electrocatalysts for Oxygen Reduction* ..... 113

2. Anastassia Alexandrova – *Catalytic Interfaces Based on Sub-nano Surface-Deposited Clusters: Why Size Matters* ..... 119

3. Eric Altman – *Structure-Reactivity Relationships in Multi-component Transition Metal Oxide Catalysts* ..... 120

4. Aravind Asthagiri –  *$\sigma$ -Complex Formation and Activation of Alkanes on the PdO(101) Surface*..... 124

5. Perla Balbuena – *Theory-Guided Design of Nanoscale Multimetallic Nanocatalysts for Fuel Cells* ..... 125

6. Matthias Batzill – *Photocatalysis of Modified Transition Metal Oxide Surfaces*.. 128

7. Alexis Bell – *Catalysis for the Selective Synthesis of Fuels and Chemical* ..... 131

8. Aditya Bhan – *Changing Selectivity of Methanol-to-Hydrocarbons Catalysis by Manipulating the Hydrocarbon Pool* ..... 134

9. Louis Bouchard – *Three Dimensional Nonequilibrium Thermochemistry Assisted by Magnetic Resonance Tomography* ..... 136

10. Donald Camaioni – *Catalytic Selective Conversion of Lignocelluloses to Transportation Biofuels* ..... 137

11. Charles Campbell – *Supported Metal Nanoparticles: Correlating Catalytic Kinetics, Energetics and Surface Structure* ..... 138

12. Jinguang Chen, Anatoly Frenkel, and Jose Rodriguez – *Dedicated Beamline Facilities for Catalytic Research: Synchrotron Catalysis Consortium (SCC)* ... 141

13. David Cox – *Hydrocarbon Dehydrogenation and Oxidation over Model Metal Oxide Surfaces*..... 144

14. Richard Crooks – *Correlation of Theory and Function in Well-Defined Bimetallic Electrocatalysts* ..... 147

15. Tanja Cuk – <i>The Water Oxidation Reaction: Transition Metal Oxide Catalysis Probed by Time Resolved Optical Spectroscopy and In Situ X-Ray Spectroscopy</i> .....	150
16. Abhaya Datye – <i>Nanostructured Catalysts for Hydrogen Generation from Renewable Feedstocks</i> .....	151
17. Paul Dauenhauer – <i>Natural Catalysts for Molten Cellulose Pyrolysis to Targeted Bio-Oils</i> .....	154
18. Robert Davis – <i>Structure and Function of Supported Base Catalysts</i> .....	155
19. Michael Deem – <i>Toward Rational, Nanoscale Control of Catalysis: A Fundamental Study of Zeolite Structure and Nucleation</i> .....	158
20. Nicholas Delgass – <i>Catalyst Design by Discovery Informatics</i> .....	161
21. Nada Dimitrijevic – <i>Photocatalytic Transformation of CO<sub>2</sub> and CH<sub>4</sub> over Titania</i> .....	167
22. David Dixon – <i>Computational Studies of Reactive Transition Metal Complexes: Critical Bond Energies</i> .....	168
23. Zdenek Dohnálek – <i>Alcohol Chemistry on (WO<sub>3</sub>)<sub>3</sub> and (MoO<sub>3</sub>)<sub>3</sub> Clusters</i> .....	169
24. Jonah Erlebacher – <i>Engineering Catalytic Nanoporous Metals for Reactions Important to the Hydrogen Economy</i> .....	170
25. Heinz Frei – <i>Monitoring the Rise of Surface Ethyl Intermediate of C<sub>2</sub>H<sub>4</sub>+H<sub>2</sub> Catalysis over Rh/Al<sub>2</sub>O<sub>3</sub> under Reaction Conditions by Step-Scan FT-IR Spectroscopy</i> .....	173
26. Cynthia Friend – <i>Molecular-Scale Understanding of Selective Oxidative Transformations of Alcohols Promoted by Au and Au-Based Alloys</i> .....	174
27. Puxiang Gao – <i>Thermal and Chemical Stability of Metal Oxide/Perovskite/ Metal Nano-interfaces: An Investigation of Modeled ZnO/(La,Sr)CoO<sub>3</sub>/Pt Nanowire Based Catalyst</i> .....	177
28. Bruce Gates – <i>Tailoring Supports as Ligands: Zeolites and Oxides as Hosts of Molecular Metal-Complex Catalysts</i> .....	178
29. Bruce Gates – <i>Supported Molecular Catalysts: Synthesis, In Situ Characterization and Performance</i> .....	184
30. Andrew Gellman – <i>Molecular-Level Design of Heterogeneous Chiral Catalysts</i> .....	190
31. Gary Haller – <i>Structured Carbon Supports for Aqueous Phase Reforming and Fuel Cell Catalysts</i> .....	196
32. Michael Henderson – <i>Fundamental Studies of Heterogeneous Photocatalysis on Model TiO<sub>2</sub> Surfaces</i> .....	199

33. Andreas Heyden – <i>Theoretical Investigation of Heterogeneous Catalysis at the Solid-Liquid Interface for the Conversion of Lignocellulosic Biomass Model Molecules</i> .....	204
34. James “Ned” Jackson – <i>Building Block Reactions for the Biomass Refinery of the Future: Aqueous Reductive Upgrading of Acids, Amides, Polyols, and Aromatics</i> .....	207
35. Thomas Jaramillo – <i>Nanostructured Electrocatalysts for Energy Conversion Reactions</i> .....	208
36. Friederike Jentoft – <i>Catching the Fish in the Hydrocarbon Pool</i> .....	209
37. John Kitchin – <i>Multifunctional Oxygen Evolution Electrocatalyst Design and Synthesis</i> .....	210
38. Harold Kung – <i>Modifying Catalysts with Functionalized Polysiloxanes</i> .....	213
39. Suljo Linic – <i>Development of Physically Transparent, Predictive Structure-Performance Relationships for Rational Design of Multi-component Catalytic Materials</i> .....	215
40. Raul Lobo – <i>Novel Photocatalysts with One-Dimensional and Two-Dimensional Nanostructures</i> .....	218
41. Raul Lobo – <i>From First Principles Design to Realization of Bimetallic Catalysts for Enhanced Selectivity</i> .....	221
42. Tobin Marks – <i>Supported Organometallic Complexes: Surface Chemistry, Spectroscopy, Catalysis, and Homogeneous Models</i> .....	227
43. Christopher Marshall – <i>The Institute for Atom-Efficient Chemical Transformations (IACT): A DOE Energy Frontier Research Center for Biomass Catalysis</i> .....	230
44. Manos Mavrikakis – <i>Atomic-Scale Design of Metal and Alloy Catalysts: A Combined Theoretical and Experimental Approach</i> .....	236
45. Will Medlin – <i>Selectivity Control through Modification of Metal Catalysts with Organic Monolayers</i> .....	242
46. Jeffrey Miller – <i>Understanding the Electronic and Chemical Modifications in Bimetallic Nanoparticle Catalysts for H<sub>2</sub> Production by In Situ XANES Spectroscopy and Density Functional Theory</i> .....	245
47. Charles Buddie Mullins – <i>Surface Chemistry of Gold Model Catalysts</i> .....	246
48. David Mullins – <i>Reactions of C<sub>2</sub>-Oxygenates on Cerium Oxide Surfaces</i> .....	249
49. Anders Nilsson – <i>Fundamental Studies of Catalysis using X-Rays</i> .....	250

50. Justin Notestein – <i>Controlling Catalyst Structures with Oxide Clusters and Oxide Nanocavities</i> .....	251
51. Ralph Nuzzo – <i>The Reactivity and Structural Dynamics of Supported Metal Nanoclusters using Electron Microscopy, In Situ X-Ray Spectroscopy, Electronic Structure Theories, and Molecular Dynamics Simulations</i> .....	252
52. Steven Overbury – <i>Fundamentals of Heterogeneous Catalysis on Surfaces and Nanostructures</i> .....	258
53. Umit Ozkan – <i>Investigation of the Nature of Active Sites on Heteroatom-Containing Carbon Nanostructures for Oxygen Reduction Reaction</i> .....	264
54. Charles Peden – <i>Alcohol Dehydration on Oxide Catalysts: Activity and Selectivity</i> .....	267
55. Charles Peden – <i>Early Transition Metal Oxides as Catalysts: Crossing Scales from Clusters to Single Crystals to Functioning Materials</i> .....	268
56. Marek Pruski – <i>Homogeneous and Interfacial Catalysis in 3D Controlled Environment</i> .....	281
57. Talat Rahman – <i>Controlling Structural, Electronic, and Energy Flow Dynamics of Catalytic Processes through Tailored Nanostructures</i> .....	288
58. Andrew Rappe – <i>Polarization-Dependence of Palladium Deposition on Ferroelectric Lithium Niobate (0001) Surfaces</i> .....	294
59. Fabio Ribeiro – <i>Fundamental Studies on the Kinetics of Oxidation Reactions</i> ...	297
60. Yuriy Román – <i>Water-Tolerant Lewis Acids for the Activation of Biomass-Derived Molecules</i> .....	300
61. Udo Schwarz – <i>Atomic Resolution Imaging and Quantification of Chemical Functionality of Surfaces</i> .....	302
62. Susannah Scott – <i>Hierarchical Design of Heterogeneous Catalysts for Hydrocarbon Transformations</i> .....	305
63. Annabella Selloni and Ulrike Diebold – <i>Towards a Molecular Scale Understanding of Surface Chemistry and Photocatalysis on Metal Oxides: Surface Science Experiments and First Principles Theory</i> .....	311
64. Carsten Sievers – <i>Increasing the Hydrothermal Stability of Heterogeneous Catalysts for Biomass Conversion</i> .....	314
65. Darío Stacchiola – <i>Catalysis and the Nature of Mixed-Metal Oxides at the Nanometer Level</i> .....	317
66. Peter Stair – <i>Institute for Catalysis in Energy Processes (ICEP)</i> .....	318
67. Steven Suib – <i>Microporous and Mesoporous Nanosize Transition Metal Oxides: Preparation, Characterization, and Applications</i> .....	324

68. Peter Sutter and Nicholas Camillone – <i>Ultrafast and Chemically Specific Microscopy for Atomic Scale Imaging of Nanophotocatalysis</i> .....	329
69. János Szanyi – <i>Chemistry on Base-Metal Oxide Nanostructures on Oxide Substrates: A Model System Approach</i> .....	332
70. Steven Tait – <i>Metal–Organic Surface Catalyst for Low-Temperature Methane Oxidation: Bifunctional Union of Metal–Organic Complex and Chemically Complementary Surface</i> .....	335
71. Franklin (Feng) Tao – <i>Integration of Operando Studies into Nanocatalysis for Efficient Energy Conversion</i> .....	336
72. Wilfred Tysoe – <i>Molecular-Level Design of Heterogeneous Chiral Catalysts</i> ...	337
73. John Vohs – <i>Fundamental Studies of the Steam Reforming of Alcohols on Pd/ZnO and Co/ZnO Catalysts</i> .....	338
74. Lai-Sheng Wang – <i>Oxide Cluster Model Studies: Toward a Molecular Level Understanding of Oxide Surfaces and Defect Structures</i> .....	341
75. Yong Wang – <i>Acid/Base and Redox Properties of Metal Oxides Catalysts</i> .....	342
76. Jason Weaver – <i>Growth and Reactivity of Oxide Phases on Crystalline Pd and Pt Surfaces</i> .....	343
77. Michael White – <i>Catalysis on the Nanoscale: Preparation, Characterization and Reactivity of Metal-Based Nanostructures</i> .....	346
78. Zili Wu – <i>Structure Dependence of CO Oxidation over Ceria Nanoshapes</i> .....	351
79. Bo Zhang – <i>Electrocatalysis at Single Metal Nanoparticles and Single Molecules</i> .....	352

### **Additional Abstracts of Funded Projects**

Uwe Burghaus – <i>Characterization of Fundamental Catalytic Properties of MoS<sub>2</sub>/WS<sub>2</sub> Nanotubes and Nanoclusters for Desulfurization Catalysis – A Surface Chemistry Study</i> .....	355
Ram Seshadri – <i>Platinum-Group Metal (PGM) Substituted Complex Oxide Catalysts</i> .....	358
Israel Wachs – <i>Fundamental Surface Structure-Photoactivity Relationships of Semiconductor Mixed Oxides for Splitting of H<sub>2</sub>O to H<sub>2</sub>/O<sub>2</sub></i> .....	361
John Yates, Jr. – <i>Spectroscopic Observation of Dual Catalytic Sites during Oxidation of CO on a Au/TiO<sub>2</sub> Catalyst</i> .....	364

<b>Participant List</b> .....	367
-------------------------------	-----

<b>Author Index</b> .....	373
---------------------------	-----

This page is intentionally blank.



# **Sunday Evening**

## **Session I**

This page is intentionally blank.

## Metal Nanocrystals: Shape Control, Assembly, Surface Chemistry and Catalysis

Peidong Yang

Department of Chemistry, University of California, Berkeley, CA 94720  
Materials Sciences Division, Lawrence Berkeley National Lab, Berkeley, CA, 94720

The ultimate goal of catalysis research is to achieve 100% selectivity for the desired products at maximum turnover rate (activity) without generating undesired byproducts. Ways to optimize activity and selectivity have been investigated on the atomic and molecular level using two-dimensional model catalysts (e.g. metal single crystals, nanoparticle arrays). It was found that key characteristics affecting both activity and selectivity are surface structure and particle size. Other features important to catalysis are site-blocking or bonding modifier additives and the metal-oxide interface. Development of a high surface area model catalyst will enable the study of the molecular ingredients which control activity and more importantly selectivity in the multifunctional (oxide / metal) composite systems. We have been developing methods for making metal nanocrystals with very narrow particle size distribution and well-defined shape.<sup>1,2,3</sup> These nanoparticles are then assembled into 2-dimensional arrays using Langmuir-Blodgett technique or embedded in mesoporous oxide supports.<sup>4,5</sup> These composites are considered as a high surface area model catalyst system as the precise control of nanocrystal size, shape, surface and interface should impart desired reaction selectivity and activity.

1. "Platonic Gold Nanocrystals", F. Kim, S. Connor, H. Song, T. Kuykendall, P. Yang, *Angew. Chem. Int. Ed.* 43, 3673, 2004
2. "Morphology control of catalytically active Pt nanocrystals", H. Lee, S. Habas, S. Kweskin, D. Butcher, G. Somorjai, P. Yang, *Angew. Chem. Int. Ed.* 45, 7824, 2006.
3. "Shaping binary metal nanocrystals through epitaxial seeded growth", S. Habas, H. Lee, V. Radmilovic, G. Somorjai, P. Yang, *Nature Mater.* 6, 692, 2007.
4. "Thermally Stable Nanocatalyst for High Temperature Reactions: Pt-Mesoporous Silica Core-Shell Nanoparticles", S. Joo, J. Park, C. Tsung, Y. Yamada, P. Yang, G. A. Somorjai, *Nature Mater.*, 8, 126, 2009.
5. "Nanocrystal Bilayer for Tandem Catalysis", Y. Yamada, C. Tsung, W. Huang, Z. Huo, S. E. Habas, T. Soejima, C. E. Aliaga, G. A. Somorjai, P. Yang, *Nature Chem.*, 3, 372, 2011.

## Catalytic and Transport Behaviors of Model Porous and Composite Nanostructures

Students: Shisheng Xiong, Ryan Molecke  
 Collaborators: Darren Dunphy (UNM), Ying-Bing Jiang (UNM)  
 Contacts: 1001 University Blvd SE Suite 100, Albuquerque, NM 87106;  
[cjbrink@sandia.gov](mailto:cjbrink@sandia.gov)

### Goal

Combine self-assembly, interfacial assembly at an air/water interface, and atomic layer deposition to create model, highly ordered porous or composite thin film nanostructures with controlled pore size, shape, and chemistry to reveal new nanoscale transport and catalytic phenomena in gas and liquid media. Prepare ordered nanoparticle (NP)/polymer or oxide composites with well-defined nanoparticle spacing and arrangement and interfacial chemistries to test collective catalytic and charge-transfer characteristics of 2D and 3D systems.

### DOE Interest

Improved membrane technologies are needed for many energy-related applications, including (but not limited to) CO<sub>2</sub> sequestration, biofuel purification, controlled oxidation, and hydrogen purification and separation. Also, new processing methods are required for producing robust 2D and 3D NP arrays on arbitrary substrates to investigate collective behavior between NPs for charge-transfer and catalytic applications (e.g. solar cells, solid-state lighting, electrocatalysis).

### Recent Progress

*Self-assembly of NP/polymer architectures with engineered structure and asymmetry:*

The fabrication of non-close packed NP array geometries over large areas is a critical step toward producing materials with anisotropic energy transfer properties and complex catalytic behavior. One prominent example of such a structure is that of oriented nanowires with side-by-side registry and high density; as the synthesis of this NP architecture has proven to be a significant challenge, we have developed a new route to oriented Au nanowire arrays by transformation and coalescence of an ordered close-packed gold NP/polymer monolayer via constrained uniaxial deformation induced by electron beam irradiation followed by room temperature sintering. This approach

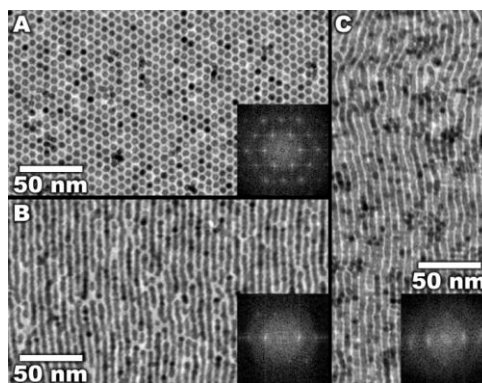


**Fig. 1:** A) A large-area hexagonal close-packed Au NP/PMMA monolayer array formed via interfacial assembly at an air/water interface, B) The chain-like nanostructure formed by e-beam irradiation of the film shown in panel A, C) The ordered Au nanowire array after further aging at RT for 7 days.

results in high densities of integrated single crystal-like nanowires that exhibit directional metallic conductivity over macroscopic length scales (Figure 1).

*Dynamic studies of NP/polymer self-assembly:* Design of routes to non-hexagonally close packed NP/polymer array geometries via interfacial assembly at an air/water requires the fundamental characterization of the NP assembly mechanism. Using grazing-incidence small-angle x-ray scattering (GISAXS) at the Advanced Photon Source, we observed the formation of NP/polymer films in real time under ambient conditions, finding the presence of a two-step process whereby an incipient loosely-packed nanoparticle phase is compressed by film drying to form a close-packed lattice (Figure 2).

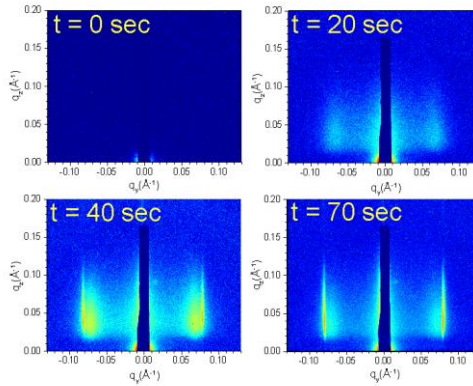


**Fig. 2:** *In-situ* GISAXS data showing the formation of a close-packed 2D NP/polymer film (scattering feature at  $q_y = 0.08 \text{ \AA}^{-1}$ ) via a less dense 2D NP array intermediate ( $q_y = \text{ca. } 0.07 \text{ \AA}^{-1}$ ).

*Ultra-thin microporous and composite membranes:* According to recent theoretical simulations, as well as studies of natural water channels (e.g. aquaporin,) asymmetric structure and alternating

molecular scale hydrophobic/hydrophilic channel surface chemistry appear to be important for fast, selective water transport through nano-structured separation membranes. Based on these findings, we have engineered a highly selective water purification membrane (Figure 3) by using an evaporation-induced self-assembly process to fabricate ultra-thin silica membranes with controlled pore network architecture, followed by subsequent atomic layer deposition (ALD) of a polypeptide to define pore size and surface chemistry, resulting in a nanostructure that mimics that of natural water channels. The resultant water desalination membrane was found to possess a 3-fold improvement in water flux, and 67% reduction in energy consumption, when compared to a commercial membrane.

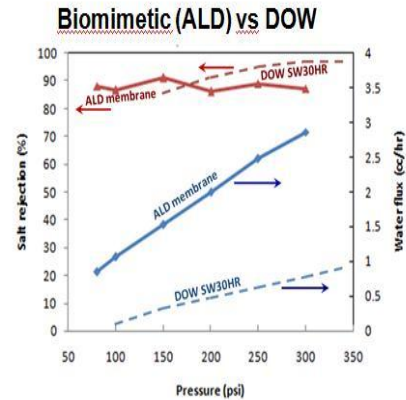
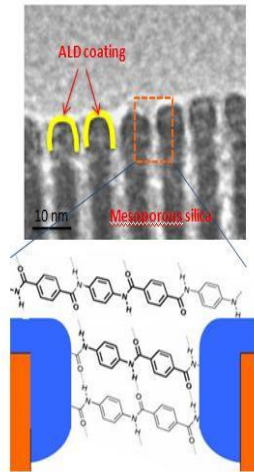


**Fig. 3:** Structure of biomimetic water purification membrane formed by a combination of self-assembly and ALD (left), and performance of the membrane vs. a commercial water purification membrane (right).

## Future Plans

*Self-assembly of NP/polymer architectures with engineered structure and asymmetry:* Recently, we have demonstrated the feasibility of synthesizing binary NP arrays with an  $AB_2$  stoichiometry through the interfacial assembly technique. Although our results so far only show local order, we are refining our assembly process to achieve long-range binary 2D lattices.

*Dynamic studies of NP/polymer self-assembly:* Our *in-situ* x-ray data suggest that NP lattice asymmetry can be induced during interfacial assembly by the presence of polymer drying stress: we will now map the assembly process across the drying film to examine this effect.

*Ultra-thin microporous and composite membranes:* We will extend our biomimetic approach to separation of other molecules of interest to the DOE, including  $CO_2$ ,  $H_2$ , and hydrocarbons. We are also studying the potential of ALD-modified nanoporous membranes for use as catalytic platforms to increase reaction selectivity. Preliminary data with  $TiO_2$ -modified films (a model catalytic system) show activity toward dye decomposition; we are now examining charge and size selectivity in these materials.

*Nanoparticle arrays as catalytic platforms:* We have also begun studies of electrocatalytic reduction behavior in ordered 2D Ag or Pt NP array/polythiophene films as compared to 3D or disordered 2D systems, with the ultimate goal of demonstrating electrocatalysis with binary 2D NP arrays (for example, Pt/CeO<sub>2</sub>  $AB_2$  structures).

## Publications (2010-2011)

1. X.M. Jiang and C. Jeffrey Brinker, "Rigid templating of high surface-area, mesoporous, nanocrystalline rutile using a polyether block amide copolymer template," *Chemical Communications* **46** (2010) 6123-6125.
2. Z. Chen, Y.B. Jiang, D.R. Dunphy, D.P. Adams, C. Hodges, N.G. Liu, N. Zhang, G. Xomeritakis, N.R. Aluru, S.J. Gaik, H.W. Hillhouse, and C.J. Brinker, "DNA translocation through an array of kinked nanopores," *Nature Materials* **9** (2010) 667-675.
3. S. Xiong, X. Miao, J. Spencer, C. Khripin, T.S. Luk, C.J. Brinker, Integration of a Close-Packed Quantum Dot Monolayer with a Photonic-Crystal Cavity Via Interfacial Self-Assembly and Transfer, *Small* **6** (2010) 2126-2129.
4. X.M. Jiang, T.L. Ward, F. van Swol, and C. J. Brinker, "Numerical Simulation of Ethanol-Water-NaCl Droplet Evaporation," *Industrial & Engineering Chemistry Research* **49** (2010), 5631-5643.
5. S. Moghaddam, E. Pengwang, Y. B. Jiang, A. R. Garcia, D. J. Burnett, C. J. Brinker, R. I. Masel, and M. A. Shannon, "An inorganic-organic proton exchange membrane for fuel cells with a controlled nanoscale pore structure," *Nature Nanotechnology* **5** (2010), 230-236.
6. C.E. Ashley, D.R. Dunphy, J. Zhang, E.C. Carnes, Z. Yuan, D.N. Petsev, P. Atanassov, O.D. Velev, M. Sprung, J. Wang, D.S. Peabody, and C.J. Brinker, "Convective Assembly of 2D Lattices of Virus-Like Particles Visualized by *In-situ* Grazing Incidence Small-Angle Scattering", *Small* **7** (2011) 1043-1050.

## Control of Heterogeneous Catalysis via Design of Organic-Inorganic Interfaces

Students: Partha Nandi, Andrew Solovyov  
Collaborators: Sonjong Hwang (California Institute of Technology), Vitaly I. Kalchenko (Ukrainian Academy of Sciences, Ukraine), Matthew Neurock (University of Virginia)

### Goal

Develop a synthetic toolkit that will enable the rational design and control of heterogeneous catalysts, using an organic-inorganic materials platform. Current research goals focus on using homogeneous and grafted Al(III)-calixarene complexes as active sites for MPV reduction catalysis. Using the requirement of MPV reduction catalysts to have open active sites (i.e. active sites possessing a labile monodentate ligand) rather than closed ones, we strive to develop general cookie-cutter-type approaches that will permit enforcing either open or closed active sites consisting of grafted Lewis-acid complexes.

### DOE Interest

This research promises to revitalize a mild and environmentally benign way of performing ketone reductions, using a sacrificial secondary alcohol as hydride source, by avoiding the aggregation and excess catalyst, which have been persistent problems when using aluminum isopropoxide. The broader context of current research is that it provides a generalizable toolkit of synthetic approaches for elucidating active site structural requirements for Lewis acid-catalyzed reactions. The fundamental insight to be had by answering this question spans many catalytic processes of interest to DOE, when requirements for either open or closed active sites are elucidated in catalysis.

### Recent Progress

The synthesis of well-defined open and closed active catalyst sites is shown below for grafted Al(III)-calixarene sites. The calixarene is the actual entity that enforces either an open or closed active site. Below recent progress in the synthesis of the required precursors and grafted calixarene materials is described. The open and closed nature of the materials is demonstrated using MPV reduction as a probe reaction.

Calix[4]arene ligand is selectively bis (1) or tris (4) alkylated at the lower rim via suitable templating cations. The resulting ligands are reacted with  $\text{Me}_3\text{Al}$  to afford corresponding monomethyl-Al complex (2) or dimethyl-Al complex (5) via evolution of methane. Finally the methyl-Al species in 2 and 5 is reacted with isolated Si-OH sites of calcined silica to obtain closed (3) and open (6) Al sites, respectively. TGA and TGA-MS analysis of (3) and (6) confirmed covalent grafting of (2) and (5) on silica.  $^{27}\text{Al}$  MAS NMR of 3 shows catalytically active tetrahedral coordination environments for Al sites centered around  $\sim 35$  ppm. Interestingly, no significant amount of catalytically unproductive octahedral site are observed in the  $^{27}\text{Al}$  MAS NMR near 0 ppm. This result is in stark contrast with what is known behavior for non-calixarene-based aluminum isopropoxide, where rampant aggregation results in a sharp increase in octahedral species during the course of time.  $^{27}\text{Al}$  MAS NMR of 6 also shows predominantly tetrahedral Al(III) sites at  $\sim 40$  ppm. Solution precursors of 3 and 6 can be synthesized by reacting 2 and 5 with

2-propanol. Both of these compounds showed exclusively tetrahedral environment by solution  $^{27}\text{Al}$  NMR. These spectra are shown below in Figure 1.

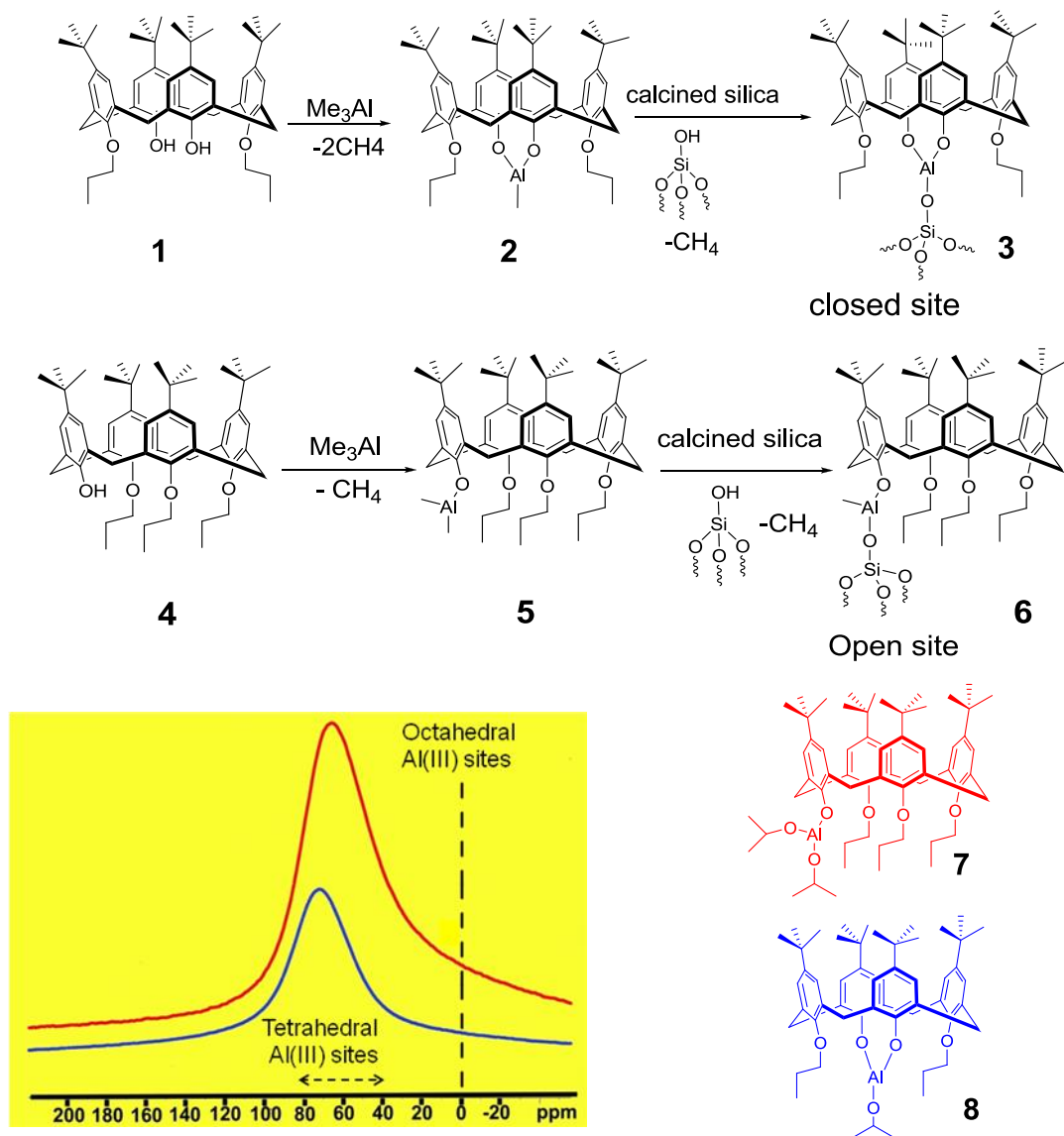


Figure 1. Solution  $^{27}\text{Al}$  NMR of the homogeneous precursors of open (**7**) and closed (**8**) heterogeneous Al-active sites

Our results show the closed Al-site catalyst **3** to be inactive for MPV reduction whereas the open MPV catalyst **6** is active for catalytic MPV reduction. These results are consistent with the critical requirement of covalent isopropoxide on Al for MPV catalysis. The catalytic heterogeneous MPV reduction results are summarized in the Figure 2 below. MPV reduction of 2-chloro-acetophenone follows a zero order kinetic regime indicating strong binding affinity of the substrate to the active site. The reduction can be performed under ambient condition and no detectable leaching of the catalyst is seen during the reduction (shown in the supporting information). The rate of catalysis is directly proportional to the loading of the catalyst and is indicative of single site nature of



this supported catalyst. The rate of the catalysis using Aerosil silica calcined at 800°C is comparable to that of the homogeneous catalyst 8.

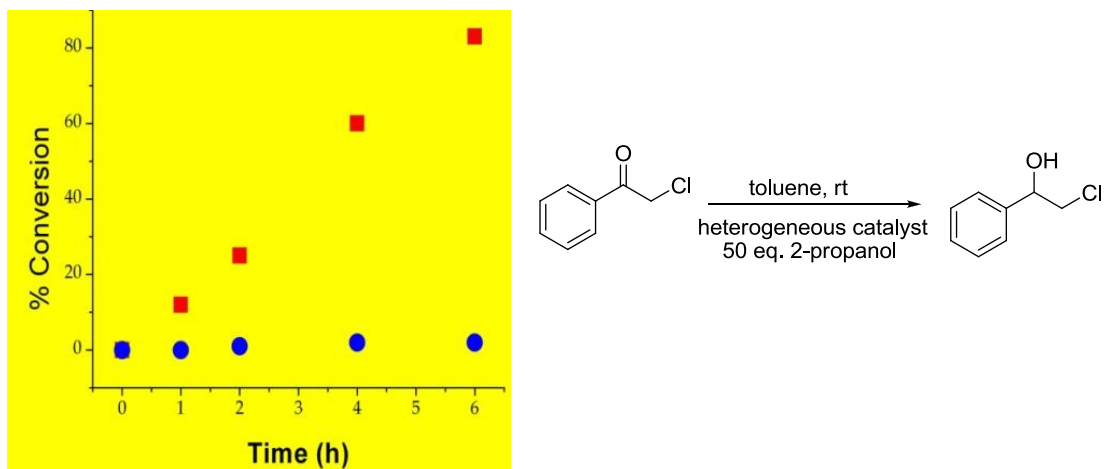


Figure 2: Heterogeneous MPV catalysis: Open (shown in red) and closed (shown in blue) sites in catalysis.

### Future Plans

Future plans include investigating enantioselective MPV catalysis using active sites based on Al(III)-calixarene complexes (preliminary results summarized in last year's report) as well as learning requirements for open and closed sites in other reacting systems such as olefin epoxidation and Bayer-Villiger oxidation. There are clear opportunities for expanding the approaches developed to other Lewis acidic metal cations.

### Publications (2009 – 2011)

Nandi, P.; Solovyov, A.; Katz, A.; *Enantioselective MPV Catalysis Using Grafted Al(III) Complexes Consisting of Vaulted Hemispherical Calix[4]arene Ligands: Bridging the Homogeneous-Heterogeneous Gap*, in preparation.

Nandi, P.; Tang, W.; Hwang, S.-J.; Neurock, M.; Katz, A.; *Catalytic Consequences of Open and Closed Sites in Grafted Al(III)-Calix[4]arene Complexes: A Comparative Study of Hydride and Oxygen Transfer Reactions*, in preparation.

Nandi, P.; Matvieiev Y. I.; Boyko, V. I.; Durkin, K. A.; Kalchenko, V. I.; Katz, A.; *MPV Reduction Using Al<sup>III</sup>-Calix[4]arene Lewis Acid Catalysts: Molecular-Level Insight Into Effect of Ketone Binding*, *J. Catal.*, submitted.

de Silva, N.; Hwang, S.-J.; Durkin, K. A. and Katz, A.; *Vanadocalixarenes on Silica: Requirements for Permanent Anchoring and Electronic Communication*, *Chem. Mater.*, **2009**, *21*, 1852-1860.

This page is intentionally blank.

**Monday Morning**

**Session II**

This page is intentionally blank.

## Surface Science goes liquid !

Hans-Peter Steinrück

Physikalische Chemie, Universität Erlangen-Nürnberg

Egerlandstraße 3, D-91058 Erlangen, Germany

e-mail: [steinrueck@chemie.uni-erlangen.de](mailto:steinrueck@chemie.uni-erlangen.de) / [www.chemie.uni-erlangen.de/steinrueck](http://www.chemie.uni-erlangen.de/steinrueck)

Ionic liquids (ILs) are a new class of materials with most interesting properties. They are liquid at room temperature, but have a negligible vapour pressure. Consequently they can, in contrast to normal liquids, be investigated by all UHV-based methods of surface science. This allows to determine their properties with the same atomic level accuracy that is presently common for solid surfaces and conventional adsorbate systems. Apart from the investigation of the specific properties of ionic liquids, which are relevant for many applications, this also opens the possibility to obtain more detailed insight in the general physical and chemical properties of liquids. In that sense it opens the door to a new chapter of surface science. In this presentation the surface and interface properties of several imidazolium-based ionic liquids will be presented, including the surface composition of non-functionalized hydrophobic ILs and PEG-functionalized hydrophilic ILs, the growth behaviour and the properties of ultrathin IL layers on various substrates and the properties of dissolved catalyst complexes. The experiments have been mainly performed using angle resolved X-ray photoelectron spectroscopy.

F. Maier, J. M. Gottfried, J. Rossa, D. Gerhard, P. S. Schulz, W. Schwieger, P. Wasserscheid, H.-P. Steinrück,  
*Surface enrichment and depletion effects of ions dissolved in an ionic liquid. An X-ray photoelectron spectroscopy study,*  
Angew. Chem. Int. Ed. 45 (2006) 7778-7780.

H.-P. Steinrück,  
*Surface Science goes liquid !,*  
Surf. Sci. 604 (2010) 481-484.

K. R. J. Lovelock, I. J. Villar-Garcia, F. Maier, H.-P. Steinrück, P. Licence,  
*Photoelectron Spectroscopy of Ionic Liquid-Based Interfaces,*  
Chem. Rev. 110 (2010) 5158-5190.

H.-P. Steinrück, J. Libuda, P. Wasserscheid, T. Cremer, C. Kolbeck, M. Laurin, F. Maier, M. Sobota, P. S. Schulz, M. Stark,  
*Surface Science and Model Catalysis with Ionic Liquid-Modified Materials,*  
Adv. Mater. (2011), DOI: 10.1002/adma.201100211

**DE-FG02-03ER15459**

**Christopher W. Jones (GT)**  
**Marcus Weck (NYU)**  
**Robert J. Davis (UVA)**

### **Developing the Science of Immobilized Molecular Catalysts**

*Additional PIs:* Marcus Weck (NYU), C. David Sherrill (GT), Peter Ludovice (GT); Robert J. Davis (UVA);

*Post-docs:* Yu Liu (NYU), Xunjin Zhu, Krishnan Venkatasubbaiah, Nicholas Brunelli, Jonathan Rawlston

*Students:* Jie Lu (NYU), Michael Kahn (NYU), Tait Takatani, Rebecca Key, Matt Kennedy, Wei Long, Yuanzhou Xi (UVA), Nina Schuchman (undergrad, NYU)

School of Chemical &  
Biomolecular Engineering  
Georgia Institute of Technology  
Atlanta, GA 30332  
[cjones@chbe.gatech.edu](mailto:cjones@chbe.gatech.edu)

Department of  
Chemistry  
New York University  
New, York, NY 10003  
[marcus.weck@nyu.edu](mailto:marcus.weck@nyu.edu)

Department of Chemical  
Engineering  
University of Virginia  
Charlottesville, VA 22904  
[rjd4f@virginia.edu](mailto:rjd4f@virginia.edu)

#### **Goals**

Cooperative catalysis, whereby two or more active sites work in concert in promoting a catalytic reaction, is ubiquitous in biological systems. Design and understanding of synthetic cooperative catalysts is the scientific target of this small team program. Past and current work has focused on the utilization of different cooperative M-Salen catalysts (where M has been Co, Al, or Ru), whereby two M-Salen catalysts work together in the rate-limiting step to catalyze the reaction. An interdisciplinary research team that can probe all aspects of catalyst synthesis, structure and properties is exploring this topic from both experimental and theoretical points of view. In particular, researchers at GT, NYU and the UVA are developing design principles for supported M-Salen catalysts that follow bimetallic (Co- and Al-Salen) reaction pathways, chiefly a family of Co-Salen catalyzed epoxide ring-opening reactions. Increasingly, other cooperative catalytic systems are being considered, including those that utilize organic active sites. Using these model systems, the fundamental principles that can be used to understand and design future classes of supported, cooperative catalysts are being elucidated.

#### *DOE Interest*

The work performed in this program elucidates fundamental principles important in the design of supported, cooperative catalysts. These catalysts have the potential of being highly active and selective while straight-forward to separate from the reaction medium. A particular focus is placed on understanding catalyst stability and deactivation mechanisms, which are critical issues that limit the current widespread use of catalysts of this type. Stable supported molecular catalysts would facilitate environmentally-benign, green chemical processing, providing a substantial energy advantage in chemical processing.

#### **Recent Progress Report**

**\* The Bigger, the Better: Ring-Size Effects of Macrocyclic Oligomeric Co-salen Catalysts.**

We have demonstrated previously that macrocyclic oligomeric Co(III)-salen complexes derived from cyclooctene salen monomers are among the most active catalysts for asymmetric epoxide

ring-opening reactions. Due to the uncontrollable feature of the ring-expanding olefin metathesis step during catalyst synthesis, the macrocyclic oligomeric Co(III)-salen complexes are produced as a mixture of oligomers with different ring sizes. Recently, we have demonstrated that increasing ring size shows a remarkable effect on reaction rates with the largest ring-size species exhibiting superior selectivities and activities. NMR studies revealed that the dimeric catalyst is strained, which is not observed for the larger ring-size catalysts. Computational modeling studies by the Ludovice group indicated that the dimer is lacking the flexibility to allow adjacent Co(III)-salen groups to interact productively in a bimetallic fashion. Further modeling studies of the dynamics and site-pairing probabilities of the different ring sizes are qualitatively consistent with the experimental results, with larger ring sizes being more active. While a quantitative agreement between experiment and modeling has not been reached, the modeling studies did suggest how the PCO-Co(III) structure can be manipulated to maximize catalytic activity. The modeling results clearly showed that the bimetallic complex was more stable for an all trans configuration in the oligomer. Thus, ring-opening metathesis polymerization catalysts that yield cyclooctene oligomers with a high fraction of trans-linked monomers should improve the catalytic activity of the system. Further catalytic tests of larger ring-size Co(III)-salen complexes (tetramer to hexamer mixture) by investigating the HKR of various racemic terminal epoxides and the asymmetric epoxide ring-opening with different nucleophiles demonstrated the superior catalytic activity of large ring-size macrocyclic catalysts.

#### **\*Shell Cross-linked Micelles (SCMs) As Nanoreactors for HKR of Epoxides.**

A theme in the overall project is cooperative catalysis, as is commonly used in biological systems. Another feature of biological systems is confinement of catalysts in different reaction zones. The research team is furthering a growing bio-inspired theme by developing shell crosslinked micelle (SCM) based nanoreactors with catalysts located in the core of the micelle. SCMs are an intriguing target for catalyst support due to their specific structure and properties. The hydrophobic core domain, which is further isolated from the micellar medium by a cross-linked layer, has its own micro-environment. It is expected that the highly confined three-dimensional arrangement of catalysts in the core could force catalysts in close proximity to each other, resulting in an enhanced reactivity for catalytic reactions following a cooperative catalytic process. Furthermore, the hydrophobic environment of the core and the degree of cross-linking of the shell may have a substantial impact on substrate selectivity because of the different permeabilities of the reactants and products through the SCMs. In addition, the hydrophilic corona and the cross-linked shell may provide a shield against catalyst poisoning and metal leaching. The stabilized core-shell structure might render an enhanced recyclability to SCMs catalyst comparing with its uncross-linked counterpart.

We initially synthesized a series of poly(norbornene)-based amphiphilic triblock copolymers containing covalently attached salen ligands in the hydrophobic block, a cinnamate group-containing middle block and a poly(ethylene glycol) methyl ether-containing repeat unit as the hydrophilic block using living ring-opening metathesis polymerization. Micellar assemblies constructed of these copolymers were stabilized by cross-linking of the cinnamate-containing middle block using UV irradiation. The catalytic activities of these SCM catalysts were investigated by hydrolytic kinetic resolution of epichlorohydrin. This first generation of Co(III)-salen SCM catalysts showed the feasibility of our approach, but the catalytic activity was low.

Our second generation SCMs with Co(III)-salen cores were synthesized from amphiphilic poly(2-oxazoline) triblock copolymers (Scheme 1) to yield micelles with a low polydispersity. The catalytic activity and selectivity of this salen-Co SCL micelle nanoreactor were investigated

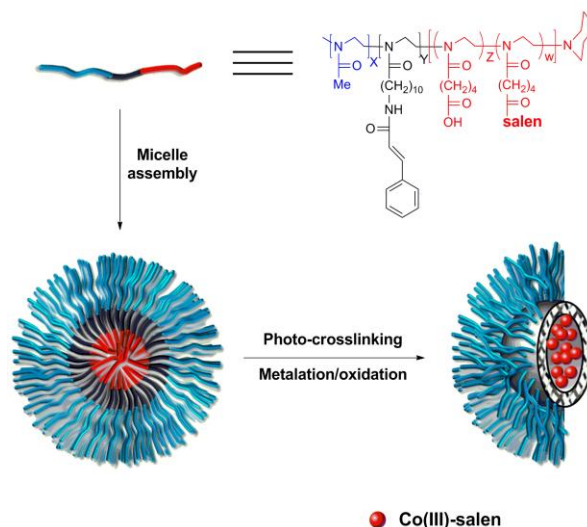
with different epoxides. An unusual substrate-selectivity was observed. First, aromatic epoxides could be resolved with excellent ee's within a short reaction time. Even the conjugated styrene oxide gave 95 % ee after one day. However, the SCM catalyst showed poor catalytic activities towards small epoxides ( $\leq 5$  carbons), like epichlorohydrin and allyl epoxide. When the side-chain was increased, some differences were observed. The less hindered cyclic hexyl epoxide and the least hindered linear epoxyhexane gave excellent reactivities. These HKR results clearly show that this SCM Co(III)-salen nanoreactor shows significantly better performance towards medium sized and medium hydrophobic epoxides. This is the first time substrate selectivity in HKR has been observed.

One aim to develop SCM supported catalysts is to increase the stability of the supported catalyst and also to provide additional shielding from catalyst leaching and poisoning. We tested the recyclability of the SCMs Co(III)-salen catalyst by HKR of epoxyhexane. From cycle one to cycle five, the catalyst was directly used for the HKR reaction without re-activation and could be recycled with marginal decreases in activity, thus suggesting the SCM catalysts are recyclable.

Our new SCMs catalysts have their own micro-catalytic environments and the hydrophilic corona and the cross-linked layer provides additional screening for substrates. The unusual substrate selectivity of these SCM Co(III)-salen catalyst shows the potential of these materials to mimic the substrate selectivity of biological catalysts in the future. Our long term goal is to develop SCL micelle nanoreactors containing multiple catalysts to perform tandem reactions.

### \*Regioselective Ring-Opening of Terminal Epoxides with Alcohols and Phenols using Co(III)-complexes.

Whereas our previous work on Co(III)-salen catalysis has focused on enantioselective ring-opening of epoxides, it was noted that the reactions are also highly regioselective, yielding ring-opened products only via nucleophilic attack at the C1 position. Regioselective ring-opening of alcohols and phenols is an important and challenging reaction and often requires elevated temperature and (or) catalyst loading. We evaluated the utility of different quasi-planar Co-complexes based on tetradentate ligands for the ring-opening of epoxyhexane with methanol as a nucleophile. Since enantioselectivity was not targeted, we evaluated Co complexes using various non-enantiopure ligands, including *trans*-Co-salen (**1**), *cis* and *trans*-Co-salen (**2**), Co-Salphen (**3**) and Co-porphyrin (**4**) (Figure 1). We also compared the activity of different counterions using *trans*-salen as the ligand system; the results are presented in Figure 2. All **1-X** catalysts showed regioselectivity above 90%. With the exception of **1-Cl**, all other **1-X** catalysts showed nearly similar activities. Among the **1-X** catalysts, **1-SbF<sub>6</sub>** showed superior activity and **1-OTs** gave better selectivity (99% selectivity (Figure 2, left)). The high activity of **1-SbF<sub>6</sub>** led us to evaluate



**Scheme 1.** Schematic description of the synthesis of poly(2-oxazoline) SCMs supported Co(III)-salen catalyst.



other ligand systems, viz. **2**, **3** and **4** with  $^-$  **SbF<sub>6</sub>** as the counter ion. To our surprise, **4-SbF<sub>6</sub>** displayed higher activity (twice) and superior selectivity (Figure 2, right) compared to other catalysts, **1-SbF<sub>6</sub>**, **2-SbF<sub>6</sub>** and **3-SbF<sub>6</sub>**. Kinetic analysis of **4-SbF<sub>6</sub>** suggested that the ring-opening reaction was kinetically higher order (1.6) in catalyst compared to **1-SbF<sub>6</sub>** (1.1). This indicated that **4-SbF<sub>6</sub>** was also a cooperative catalyst. Thus, there appear to be elements of cooperative catalysis in epoxide ring-opening with alcohols as nucleophiles, although there also appear to be mechanistic differences compared to HKR.

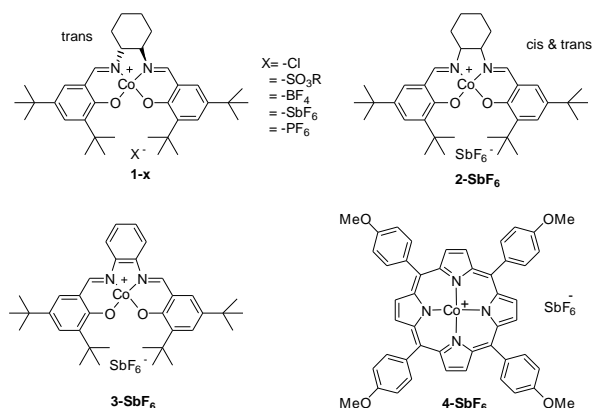


**Figure 1.** Co-complexes synthesized for alcohol ring-opening reaction.

### \*Systematic Studies of M-Salen Electronic Structure

We recently completed our series of systematic studies on the electronic structure of bare M-Salen complexes. The final paper in this series examined d<sup>4</sup> M-Salen complexes including metals Cr(II), Mn(III), Fe(IV), Mo(II), Tc(III), and Ru(IV). As in our previous studies, we performed very high quality computations using complete-active-space self-consistent-field (CASSCF) in conjunction with third-order perturbation theory corrections (CASPT3). With these results as benchmarks, we evaluated density functional theory (DFT) predictions for these systems, as DFT is the method of choice for computational studies of large catalyst systems. In agreement with our previous studies on d<sub>0</sub>, d<sub>2</sub>, and d<sub>6</sub> M-Salens, DFT (as tested using the popular BP86 and B3LYP functionals) does well at predicting geometries of these systems, but performs poorly at predicting the energy gaps between the low-lying electronic states, suggesting that energetic properties are unreliable when using these functionals. This indicates that extreme caution should be used when employing these popular functionals in mechanistic studies of M-Salen systems. In hopes of finding a robust approach, we also tested the newer M06 and M06-L functionals, which have been recommended for computations of organometallic complexes. Unfortunately, the newer functionals did not perform statistically better than B3LYP for spin-state energy gaps.

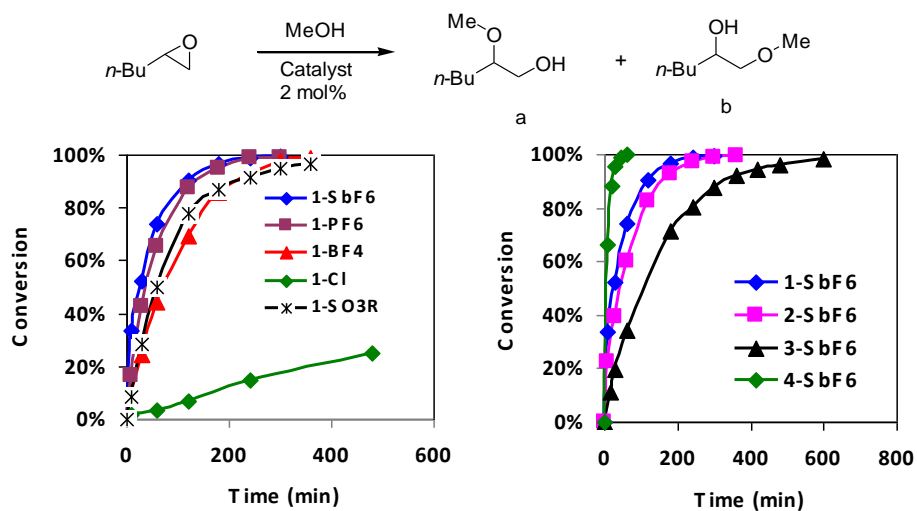


**Figure 2.** Ring-opening of epoxyhexane with methanol. (Left) Counterion study. (Right) Comparison of activity using different Co-complexes.

### **\*Reaction Mechanisms involving Cooperative Al-Salen Catalysis**

Fortunately, the Al atom does not feature the low-lying electronic states that hamper DFT studies. Hence, alongside previous and concomitant experimental work, we are exploring the Al(Cl)-Salen catalyzed addition of CN to an  $\alpha,\beta$ -unsaturated imide. At present, we have mapped out a plausible and complete reaction mechanism using BP86-D, with single-points computed using SCS-MP2/aug-cc-pVTZ (using dual-basis and density-fitting approximations to speed up the MP2 computations). Four major reaction steps, each consisting of multiple sub-steps (comprising about 15 local minima and 12 transition states) have been determined. As this mechanism involves cooperation between two Al-Salen catalysts, the chemical species involved are very large (up to 84 atoms) for such a detailed study. Our proposed mechanism is consistent in its major points with proposals by Jacobsen: namely, (a) cooperative catalysis; (b) involvement of an Al-Salen-imidate intermediate; (c) reduced reactivity for conjugated substituents in the  $\beta$ -position (leads to reduced positive partial charges at the  $\alpha$ -position that attracts the CN-nucleophile). This is one of the first complete theoretical catalytic cycles for a M-salen catalyst.

### **\* Asymmetric Henry Reactions as Reactions Requiring Acid-Base Bifunctional Catalysis**

The addition of a nitroalkane to a carbonyl compound, namely the Henry (or nitroaldol) reaction, is an important C-C bond formation reaction that produces  $\beta$ -nitroalcohols with up to two adjacent chiral carbons. Reduction of the nitro group in  $\beta$ -nitroalcohols can lead to the formation of aminoalcohols, which occur widely as natural and synthetic products as well as chemical intermediates. Many different metal complexes have been reported to be effective for chiral Henry reactions. Heterogeneous catalysts for the Henry reaction, whether chiral or achiral, are much less studied. Literature reports suggest that nanocrystalline MgO modified with the chiral ligand (S)-BINOL is an effective and reusable catalyst for the Henry reaction with comparable ee to homogeneously-catalyzed systems. However, the nature of the active sites on the modified MgO surfaces is unknown at this time. Over the past year, we have examined nanocrystalline MgO particles of about 3 nm as catalysts for the Henry reaction between benzaldehyde and nitromethane at 273 K. The surface area of nanocrystalline MgO was greater than 600 m<sup>2</sup>/g except after thermal treatment in N<sub>2</sub> at 823 K, which reduced the surface area to 359 m<sup>2</sup>/g. The areal rate of the Henry reaction over nanocrystalline MgO at 273 K was 0.015  $\pm$  0.002  $\mu\text{mol}/\text{m}^2 \text{ s}$  and was independent of pretreatment temperature over the range of 523-823 K. As mentioned above, addition of (S)-BINOL to nanocrystalline MgO has been reported previously to favor the production of one enantiomer of the Henry reaction. In the current work, negligible enantiomeric excess was observed on (S)-BINOL-modified nanocrystalline MgO catalysts, regardless of the source of nanocrystalline MgO, the MgO activation temperature, the reaction temperature, the sequence of reactant addition or the loading of (S)-BINOL. Adsorption of L-proline onto nanocrystalline MgO catalyst induced a small enantiomeric excess in the Henry reaction products, but the catalytic activity of the catalyst was low. Our studies of this system were unable to produce any useful enantioselectivity in these reactions.

### **Journal Publications - 2009-2011 (PIs underlined)**

1. Takatani, T.; Sears, J. S.; Sherrill, C. D., Assessing the Performance of Density Functional Theory for the Electronic Structure of Metal-Salens: The d6-Metals. *J. Phys. Chem. A* **2009**, *113*, 9231-9236.
2. Richardson, J. M.; Jones, C. W., Leached Nickel Promotes Catalysis Using Supported Ni(II) Complex Precatalysts in Kumada-Corriu Reactions. *J. Mol. Catal. A. Chem.* **2009**, *297*, 127-134.

3. Venkatasubbaiah, K.; Gill, C. S.; Takatani, T.; Sherrill, C. D.; Jones, C. W., A Versatile Co(bisalen) Unit for Homogeneous and Heterogeneous Cooperative Catalysis in the Hydrolytic Kinetic Resolution of Epoxides. *Chem. Eur. J.* **2009**, *15*, 3951-3955.
4. Gill, C. S.; Long, W.; Jones, C. W., Magnetic Nanoparticle Polymer Brush Catalysts: Alternative Hybrid Organic/Inorganic Structures to Obtain High, Local, Catalyst Loadings for Use in Organic Transformations. *Catal. Lett.* **2009**, *131*, 425-431.
5. Gill, C. S.; Venkatasubbaiah, K.; Jones, C. W., Recyclable Polymer and Silica Supported Ruthenium(II)-Salen Bis-Pyridine Catalysts for the Asymmetric Cyclopropanation of Olefins. *Adv. Synth. Catal.* **2009**, *351*, 1344-1354.
6. Madhavan, N.; Takatani, T.; Sherrill, C. D.; Weck, M. Macrocyclic Cyclooctene-Supported AlCl<sub>3</sub>-Salen Catalysts for Conjugated Addition Reactions: Effect of Linker and Support Structure on Catalysis. *Chem. Eur. J.* **2009**, *15*, 1186-1194.
7. Jain, S.; Venkatasubbaiah, K.; Jones, C. W.; Davis, R. J. Factors Influencing Recyclability of Co(III)-Salen Catalysts in the Hydrolytic Kinetic Resolution of Epichlorohydrin. *J. Mol. Catal. A. Chem.* **2010**, *316*, 8-15. [Editor's Choice Paper](#)
8. Ping, E. W.; Venkatasubbaiah, K.; Fuller, T. F.; Jones, C. W., Oxidative Heck Coupling using Pd(II) Supported on Organosilane-Functionalized Silica Mesocellular Foam. *Top. Catal.* **2010**, *53*, 1048-1054.
9. Venkatasubbaiah, K.; Zhu, X.; Weck, M.; Jones, C. W. Effect of Counter-ion on Recycle of Polymer Resin Supported Co(III)-Salen Catalysts in the Hydrolytic Kinetic Resolution of Epichlorohydrin. *Top. Catal.* **2010**, *53*, 1063-1065.
10. Jones, C. W. On the Stability and Recyclability of Supported Molecular Catalysts: Myths, Misconceptions and Critical Research Needs. *Top. Catal.* **2010**, *5*, 942-952.
11. Zhu, X.-J.; Venkatasubbaiah, K.; Weck, M.; Jones, C. W. Kinetic Evaluation of Cooperative Co(salen) Catalysts in the Hydrolytic Kinetic Resolution of rac-Epichlorohydrin. *ChemCatChem* **2010**, *2*, 1252-1259.
12. Zhu, X.-J.; Venkatasubbaiah, K.; Weck, M.; Jones, C. W. Highly Active Oligomeric Co(Salen) Catalysts for the Asymmetric Synthesis of  $\alpha$ -Aryloxy or  $\alpha$ -Alkoxy Alcohols via Kinetic Resolution of Terminal Epoxides. *J. Mol. Catal. A. Chem.*, **2010**, *329*, 1-10. [Editor's Choice Paper](#)
13. Xi, Y.; Davis, R. J.; "Nanocrystalline MgO Catalysts for the Henry Reaction of Benzaldehyde and Nitromethane" *J. Mol. Catal. A. Chem.*, **2011**, *341*, 22-27.
14. Takatani, T.; Sears, J. S.; Sherrill, C. D. Assessing the Performance of Density Functional Theory for the Electronic Structure of Metal-Salens: The M06 Suite of Functionals And the d4-Metals. *J. Phys. Chem. A* **2010**, *114*, 11714-11718.
15. Liu, Y.; Rawlston, J.; Swann, A.T.; Takatani, T.; Sherrill, C. D.; Ludovice, P.J.; Weck, M. The Bigger, the Better: Ring-size Effects of Macrocyclic Oligomeric Co(III)-salen Catalysts. *Chem. Sci.* **2011**, *2*, 429-438.
16. Madhavan, N.; Sommer, W.; Weck, M. Supporting Multiple Metallic Catalysts on Poly(norbornene) for Cyanide Addition to  $\alpha,\beta$ -Unsaturated Imides. *J. Mol. Catal. A. Chem.* **2011**, *334*, 1-7. [Editor's Choice Paper](#)
17. Long, W.; Jones, C. W. Hybrid Sulfonic Acid Catalysts based on Silica-Supported Poly(Styrene Sulfonic Acid) Brush Materials and their Application in Ester Hydrolysis. *ACS Catal.*, **2011**, *1*, 674-681.
18. Liu, Y.; Wang, Y.; Wang, Y.F.; Lu, J.; Piñón III, V.; Weck, M.; Shell Cross-linked Micelle-Based Nanoreactors for the Substrate-Selective Hydrolytic Kinetic Resolution of Epoxides. *J. Am. Chem. Soc.* **2011**, ASAP article.

## Structure/Composition/Function Relationship in Supported Nanoscale Catalysts for Hydrogen

Additonal PIs: Larry Curtiss, Jeff Elam, Chris Marshall, Jeff Miller  
Postdocs: James Enterkin, Hao Feng, Neng Guo, Sungsik Lee, Faisal Mehmood, Neil Schweitzer  
Collaborators: Peter Chupas, Jeffrey Greeley, Hack-Sung Kim, Randy Winans  
Contacts: P. Stair, Dept. Of Chemistry, Northwestern University, Evanston, IL 60208; [pstair@northwestern.edu](mailto:pstair@northwestern.edu)  
L. Curtiss, CSE Division, Argonne National Laboratory, 9700 S. Cass Ave., Argonne, IL 60439; [curtiss@anl.gov](mailto:curtiss@anl.gov)  
J. Elam, ES Division, Argonne National Laboratory, 9700 S. Cass Ave., Argonne, IL 60439; [jelam@anl.gov](mailto:jelam@anl.gov)  
C. Marshall, CSE Division, Argonne National Laboratory, 9700 S. Cass Ave., Argonne, IL 60439; [marshall@anl.gov](mailto:marshall@anl.gov)  
J. Miller, CSE Division, Argonne National Laboratory, 9700 S. Cass Ave., Argonne, IL 60439; [millerjt@anl.gov](mailto:millerjt@anl.gov)

### Goal

The objective of the research is to improve our fundamental understanding of composition/structure/function relationships in supported, heterogeneous catalysts for reactions that produce hydrogen from hydrogen-rich molecules. The particular focus of this project is supported metal and alloy particles with nanometer or sub-nanometer dimensions. The influence of size, composition, support and structure on the catalytic properties of metal and alloy nanoparticles and their properties under reaction conditions is a subject of intensive, ongoing interest. This project is a highly integrated effort in: 1) Novel catalyst synthesis, using advanced techniques, of highly uniform supported sub-nanometer to nanometer catalytic metal and alloy particles, 2) Measurements of catalyst atomic and nanoscopic structure and composition under synthesis, pretreatment and operating catalytic reaction conditions, 3) Experimental elucidation of kinetics and mechanisms for selected, model catalytic reactions and surface chemical reactions involving catalytic intermediates, and 4) Computational studies designed to facilitate interpretation of experimental measurements and understanding of the relationships between catalyst properties and catalytic chemistry.

### DOE Interest

The understanding and control of reactions catalyzed on solid surfaces *at the molecular-level* is a “grand challenge” for 21<sup>st</sup> Century catalysis science. The development of fundamental understanding of structure-function relationships between catalytically active sites and the chemical reactions they catalyze that are at the heart of this challenge. This project brings together a team of national laboratory researchers who develop methods for the controlled design and synthesis of active catalytic metal sites and tailored supporting oxides at the atomic scale, diverse spectroscopy, and x-ray scattering techniques for detailed characterization (both ex-situ and in-situ) of catalyst structure and dynamics, elucidation of catalytic reaction mechanisms, and theory applied to catalytic processes.

## Recent Progress

• **Development of supported metal nanoparticle synthesis by atomic layer deposition:** We have explored the use of atomic layer deposition (ALD) to prepare size-controlled metal particles and supports as a tool to advance our fundamental understanding of structure-property relationships in supported, heterogeneous catalysts capable of producing hydrogen from hydrogen-rich molecules. A series of Pd ALD catalyst samples were prepared on high surface area silica gel substrates by first depositing ALD catalyst support layers, e.g. ZnO and Al<sub>2</sub>O<sub>3</sub>. Monodispersed palladium nanoparticle catalysts were synthesized by atomic layer deposition (ALD) using alternating exposures of Pd hexafluoroacetylacetonate (Pd(hfac)<sub>2</sub>) and formalin. X-ray fluorescence and inductively coupled plasma atomic emission spectroscopy were used to quantify the Pd loading. These measurements showed that the Pd loading could be controlled precisely by the number of Pd ALD cycles as well as the precursor exposure times. Cross-sectional scanning electron microscopy and energy dispersive X-ray analysis were used to evaluate the degree of infiltration of the ALD Pd into the porous silica gel particles. Transmission electron microscopy (TEM) and high angle annular dark field (HAADF) scanning transmission electron microscopy (STEM) were performed on ALD Pd nanoparticles prepared on alumina (see **Fig. 1**).

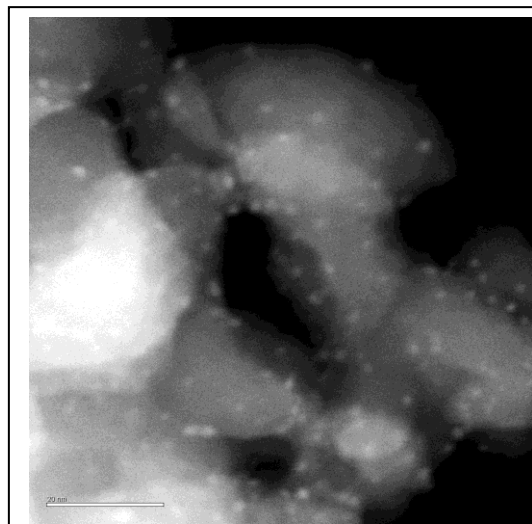


**Figure 1.** ALD Pd nanoparticles on silica gel support (20 nm scale bar).

• **Controlled nanoparticle size:** Typical ALD synthesis produced Pd particles with an average size of 1.4 nm. Removal of surface hydroxyls from the alumina support by a chemical treatment using trimethyl aluminum (TMA) before performing Pd ALD led to nanoparticles larger than 2 nm. Ultrasmall (subnanometer) Pd particles were synthesized using low-temperature metal precursor exposures. The ALD Pd particles were characterized by transmission electron microscopy, extended X-ray absorption fine structure, and diffuse reflectance infrared Fourier transform spectroscopy techniques. The catalytic performance of ALD Pd particles of different sizes was compared in the methanol decomposition reaction. The specific activity (normalized by Pd loading) of the ultrasmall Pd particles was higher than those of the larger particles. Considering the metal dispersion factor, the turnover frequency (TOF) of the ultrasmall Pd particles is comparable to that of the medium-sized (1.4 nm, on average) Pd particles synthesized under standard ALD conditions. The larger Pd particles (>2 nm) are a factor of 2 less active than the smaller Pd particles.

• **Stabilizing Supported Metal Nanoparticles:** The stability of small particles against sintering has been a serious problem restraining the applications of metal nanoparticles. This problem is prominent for supported noble metal catalysts in which NP sintering at high temperature is a major contributor to catalyst deactivation. ALD alumina was utilized as a protective layer to inhibit the sintering of supported nano-sized ALD Pd catalysts in the methanol decomposition reaction carried out at elevated temperatures. The protective ALD alumina layers were synthesized on Pd nanoparticles (1–2 nm) supported on high surface area alumina substrates. Up

to a certain over-coat thickness, the alumina protective layers preserved or even slightly enhanced the catalytic activity and prevented sintering of the Pd nanoparticles up to 500 °C.

• **Preparation of alloy nanoparticle catalysts by ALD:** ALD was used to deposit ruthenium-platinum nanostructured catalysts using 2,4-(dimethylpentadienyl)(ethylcyclopentadienyl) ruthenium, trimethyl(methylcyclopentadienyl) platinum, and oxygen as precursors. Transmission electron microscopy shows discrete 1.2 nm nanoparticles decorating the surface of the spherical alumina support. The Ru-Pt particles are crystalline with a structure similar to pure platinum. X-ray fluorescence measurements show that the nanoparticle composition is controlled by the ratio of metal precursor ALD cycles. X-ray absorption spectroscopy at the Ru K-edge indicates a nearest neighbor Ru-Pt interaction consistent with a bimetallic composition. Methanol decomposition reactions further confirm a Ru-Pt interaction and show enhanced methanol conversion for the bimetallic nanoparticles when compared to catalysts comprised of a mixture of pure Pt and Ru nanoparticles of similar loading. These results demonstrate that ALD is a viable technique for synthesizing mixed-metal nanostructures suitable for catalysis and other applications.

• **Role of support in metal nanoparticle catalysis:** Uniform, size-controlled Pt nanoparticles (1-5 nm) supported on crystalline SrTiO<sub>3</sub> nanocuboids were synthesized by ALD. The materials display exceptionally high activity for propane oxidation with TOF x1000 higher than conventional Pt catalysts and better resistance to deactivation. The increased performance is attributed to the stabilization of a Pt/PtO core/shell structure by the strong epitaxy between the Pt and the SrTiO<sub>3</sub> support.

• **Electronic and structural properties of metal and alloy nanoparticle catalysts:** The structure and electronic properties of supported metal and alloy nanoparticles are expected to depend on the particle size and composition. Direct determination of this dependence has been obtained using XANES and EXAFS. For example, EXAFS spectra of supported reduced Pt catalysts in He show a contraction of the Pt-Pt bond distance as particle size is decreased below 3 nm. The bond length decreased as much as 0.13 Å for 1 nm Pt particles. There is also a shift in the XANES to higher energy at the L<sub>3</sub> edge, a decrease in intensity near the edge and an increase in intensity beyond the edge. We suggest these features correspond to effects of coordination (the decrease at the edge) and lattice contraction (the increase beyond the edge). At the L<sub>2</sub> edge, there are only small shifts to higher energy at the edge. However, beyond the edge, there are large increases in intensity with decreasing particle size. At the L<sub>1</sub> edge there are no changes in position or shape of the XANES spectra. Adsorption of CO and H<sub>2</sub> also lead to changes in the L<sub>3</sub> and L<sub>2</sub> edges, however, no changes are observed at the L<sub>1</sub> edge. Density Functional Theory and XANES calculations show that the trends in the experimental XANES can be explained in terms of the states available near the edge. Both CO and H<sub>2</sub> adsorption result in a depletion of states at the Fermi level but the creation of anti-bonding states. Interesting bond length changes and electronic effects are also seen as a consequence of alloying in supported nanoparticles.

• **Operando adsorbate coverage determination using x-ray absorption:** Operando XAFS experiments at both the Au and Pt L<sub>3</sub> edges reveal that under WGS reaction conditions, the catalysts are fully metallic. Adsorption of H<sub>2</sub> or CO on the Pt catalysts leads to significant lengthening of the Pt-Pt bond distances; while there is little change in Au-Au bond distance with adsorbates. Adsorption of CO, H<sub>2</sub> and H<sub>2</sub>O leads to changes in the XANES spectra that can be used to determine the surface coverage of each adsorbate under reaction conditions. During

WGS, the coverage of CO, H<sub>2</sub>O, and H<sub>2</sub> are obtained by the linear combination fitting of the difference XANES, or  $\Delta$ XANES, spectra. Pt catalysts adsorb CO, H<sub>2</sub>, and H<sub>2</sub>O more strongly than the Au, in agreement with the lower CO reaction order and higher reaction temperatures.

• **DFT studies of methanol decomposition on Pd<sub>4</sub>, Cu<sub>4</sub>, and Co<sub>4</sub> clusters:** We have extended our initial analyses on Pd clusters to four-atom clusters of Cu and Co. On both types of clusters, we find that dehydrogenation of methanol is kinetically preferred to C-O bond activation. On Cu<sub>4</sub>, there is a slight preference for initial C-H bond activation, while on Co<sub>4</sub>, initial O-H bond scission is preferred. Analysis of the full dehydrogenation pathways on each of these elements, beginning with methanol and ending with CO and H<sub>2</sub>, suggests that the overall reactivity of the clusters involves a balance between the effective dehydrogenation barriers and the poisoning effect of carbon monoxide. The effective

methanol dehydrogenation barrier on Cu<sub>4</sub> clusters is relatively high, but CO binds sufficiently weakly that poisoning is unlikely to be a problem. On Co<sub>4</sub>, on the other hand, the effective dehydrogenation barriers are low, but CO binds much more strongly, implying that poisoning will be a concern. The energetics on Pd<sub>4</sub> lie between these two extremes (Fig. 2). The complete set of kinetic and thermodynamic data for Co<sub>4</sub>, Cu<sub>4</sub>, and Pd<sub>4</sub> can also be expressed in terms of a Brønsted-Evans-Polanyi (BEP) relationship.

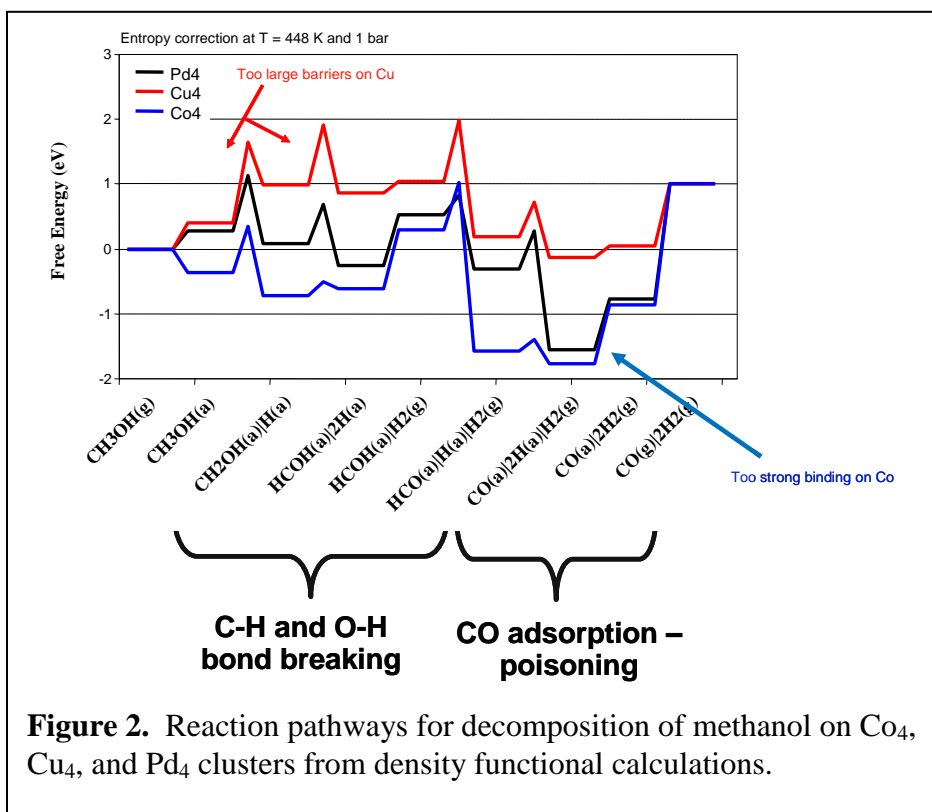


**Figure 2.** Reaction pathways for decomposition of methanol on Co<sub>4</sub>, Cu<sub>4</sub>, and Pd<sub>4</sub> clusters from density functional calculations.

methanol dehydrogenation barrier on Cu<sub>4</sub> clusters is relatively high, but CO binds sufficiently weakly that poisoning is unlikely to be a problem. On Co<sub>4</sub>, on the other hand, the effective dehydrogenation barriers are low, but CO binds much more strongly, implying that poisoning will be a concern. The energetics on Pd<sub>4</sub> lie between these two extremes (Fig. 2). The complete set of kinetic and thermodynamic data for Co<sub>4</sub>, Cu<sub>4</sub>, and Pd<sub>4</sub> can also be expressed in terms of a Brønsted-Evans-Polanyi (BEP) relationship.

### Future Plans

- The capability and flexibility of ALD to synthesize supported metal nanoparticle catalysts will be used to advantage for investigating the relationships between nanoparticle size, composition, and shape along with the nature of the support and the electronic, chemical, and catalytic properties. Particular emphases will be on understanding the role of the support and overcoats in stabilizing nanoparticle size, shape, and crystallographic orientation and on the role of the metal-support interface in catalysis.
- HAADF STEM and in-situ EXAFS will be used to study nanoparticle size and structure. In-situ XANES measurements will probe nanoparticle electronic structure and the coverage of adsorbed species under reaction conditions (see above).

- Catalytic reaction studies of hydrogen-rich molecules, primarily methanol and water, will continue. In-situ and operando FTIR and Raman spectroscopies will be carried out to identify surface reaction intermediates. A series of molecules with the potential to adsorb selectively at the metal-support interface will be investigated to probe this interface by in-situ Raman spectroscopy.
- Development will continue on a series of linear scaling relationships that correlate the binding energies of possible reaction intermediates with the corresponding binding energies of atomic carbon and oxygen. These relationships, when combined with the BEP correlations alluded to above, permit the approximate determination of full reaction potential energy surfaces, for a given metal or alloy cluster, from a simple calculation of the binding energies of C, O, and H on the corresponding clusters.

### Publications 2009-2011:

1. Vajda, S.; S. Lee, K. Sell, I. Barke, A. Kleibert, V. von Oeynhausen, K.-H. Meiwes-Broer, A.F. Rodríguez, J.W. Elam, M.J. Pellin, B. Lee, S. Seifert, R.E. Winans, *Combined temperature-programmed reaction and in situ x-ray scattering studies of size-selected silver clusters under realistic reaction conditions in the epoxidation of propene*, J. Chem. Phys., 2009. **131**: p. 121104-4.
2. Vajda, S., M.J. Pellin, J.P. Greeley, C.L. Marshall, L.A. Curtiss, G.A. Ballentine, J.W. Elam, S. Catillon-Mucherie, P.C. Redfern, F. Mehmood, and P. Zapol, *Subnanometre platinum clusters as highly active and selective catalysts for the oxidative dehydrogenation of propane*. Nat. Mater., 2009. **8**(3): p. 213-216.
3. Mehmood, F., J. Greeley, and L.A. Curtiss, *Density Functional Studies of Methanol Decomposition on Subnanometer Pd Clusters*. J. Phys. Chem. C, 2009. **113**(52): p. 21789-21796.
4. Feng, H., J.W. Elam, J.A. Libera, W. Setthapun, and P.C. Stair, *Palladium Catalysts Synthesized by Atomic Layer Deposition for Methanol Decomposition*. Chemistry of Materials, 2010. **22**(10): p. 3133-3142.
5. Setthapun, W., W.D. Williams, S.M. Kim, H. Feng, J.W. Elam, F.A. Rabuffetti, K.R. Poepelmeier, P.C. Stair, E.A. Stach, F.H. Ribeiro, J.T. Miller, and C.L. Marshall, *Genesis and Evolution of Surface Species during Pt Atomic Layer Deposition on Oxide Supports Characterized by in Situ XAFS Analysis and Water-Gas Shift Reaction*. J. Phys. Chem. C, 2010. **114**(21): p. 9758-9771.
6. Lee, S., B. Lee, F. Mehmood, S. Seifert, J.A. Libera, J.W. Elam, J. Greeley, P. Zapol, L.A. Curtiss, M.J. Pellin, P.C. Stair, R.E. Winans, and S. Vajda, *Oxidative Decomposition of Methanol on Subnanometer Palladium Clusters: The Effect of Catalyst Size and Support Composition*. J. Phys. Chem. C, 2010. **114**(23): p. 10342-10348.
7. Christensen, S.T., H. Feng, J.L. Libera, N. Guo, J.T. Miller, P.C. Stair, and J.W. Elam, *Supported Ru-Pt Bimetallic Nanoparticle Catalysts Prepared by Atomic Layer Deposition*. Nano Lett., 2010. **10**(8): p. 3047-3051.
8. Mehmood, F., J. Greeley, P. Zapol, and L.A. Curtiss, *Comparative Density Functional Study of Methanol Decomposition on Cu<sub>4</sub> and Co<sub>4</sub> Clusters*. Journal of Physical Chemistry B, 2010. **114**, 14458-66.



9. Lei, Y., F. Mehmood, S. Lee, J. Greeley, B. Lee, S. Seifert, R.E. Winans, J.W. Elam, R.J. Meyer, P.C. Redfern, D. Teschner, R. Schloegl, M.J. Pellin, L.A. Curtiss, and S. Vajda, *Increased Silver Activity for Direct Propylene Epoxidation via Subnanometer Size Effects*. *Science* (Washington, DC, U. S.), 2010. **328**(5975): p. 224-228.
10. N. Guo, B.R. Fingland, W.D. Williams, V.F. Kispersky, J. Jelic, W.N. Delgass, F.H. Ribeiro, R.J. Meyer, J.T. Miller, *Determination of CO, H<sub>2</sub>O and H<sub>2</sub> Coverage by XANES and EXAFS on Pt and Au During Water Gas Shift Reaction*, *PCCP*, **12**, 5678 - 5693 (2010).
11. C.S. Polster, R. Zhong, M.T. Cyb, J.T. Miller, C.D. Baertsch, *Selectivity Loss of Pt/CeO<sub>2</sub> PROX Catalysts at Low CO Concentrations: Mechanism and Active Site Study*, *J. Catal.*, **273**, 50-58 (2010).
12. W.D. Williams, M. Shekhar, W.-S. Lee, V. Kispersky, W.N. Delgass, F.H. Ribeiro, S.M. Kim, E.A. Stach, J.T. Miller, L.F. Allard, *Metallic Corner Atoms in Gold Clusters Supported on Rutile are the Dominant Active Site during Water-Gas Shift Catalysis*, *JACS*, **132**, 14018-14020 (2010).
13. Wyrzgol, S.A., S. Schaefer, S. Lee, B. Lee, M.D. Vece, X. Li, S. Seifert, R.E. Winans, M. Stutzmann, J.A. Lercher, and S. Vajda, *Combined TPRx, in situ GISAXS and GIXAS studies of model semiconductor-supported platinum catalysts in the hydrogenation of ethene*. *Physical Chemistry Chemical Physics*, 2010. **12**(21): p. 5585-5595.
14. Feng, H., J.A. Libera, P.C. Stair, J.T. Miller, and J.W. Elam, *Sub-nanometer Palladium Clusters Synthesized by Atomic Layer Deposition*. *ACS Catalysis*, 2011. **1**(6): p. 665-673.
15. Feng, H., J.L. Lu, P.C. Stair, and J.W. Elam, *Alumina Over-coating on Pd Nanoparticle Catalysts by Atomic Layer Deposition: Enhanced Stability and Reactivity*. *Catalysis Letters*, 2011. **141**(4): p. 512-517.
16. Stair, P.C., *Where the action is*. *Nat. Chem.*, 2011. **3**(5): p. 345-346.
17. Enterkin, J.A., W. Setthapun, J.W. Elam, S.T. Christensen, F.A. Rabuffetti, L.D. Marks, P.C. Stair, K.R. Poeppelmeier, and C.L. Marshall, *Propane Oxidation over Pt/SrTiO<sub>3</sub> Nanocuboids*. *ACS Catal.*, 2011. **1**(6): p. 629-635.
18. J. Kugai, J.T. Miller, N. Guo, C. Song, *Oxygen-Enhanced Water Gas Shift on Ceria-supported Pd-Cu and Pt-Cu Bimetallic Catalysts*, *J. Catal.*, **277**, 46-53 (2011).
19. Lei, Y., Jelic, J., Nitcher, L., Meyer, R.J., Miller, J.T., *The Effect of Particle Size and Adsorbates on L<sub>3</sub>, L<sub>2</sub> and L<sub>1</sub> X-Ray Absorption Near-Edge Spectra of Supported Pt Nanoparticles* *Top Catal.* **54**, 334-248 (2011).
20. Kugai, J., Miller, J.T., Guo, N., Song, C., *Role of Metal Components in Pd-Cu Bimetallic Catalysts Supported on CeO<sub>2</sub> for the Oxygen-Enhanced Water Gas Shift*. *Appl. Catal. B: Environ.*, **105**, 306-316 (2011).
21. J. Guo, C. Xie, K. Lee, N. Guo, J.T. Miller, M.J. Janik, C. Song, *Improving the Carbon Resistance of Ni-based Steam Reforming Catalyst by Alloying with Rh. A Computational Study Coupled with Reforming Experiments and EXAFS Characterization*, *ACS Catalysis*, **1**, 574-582 (2011).

**Catalysis: Reactivity and Structure**

Additional PIs: Jonathan C. Hanson, Ping Liu, Dario Stacchiola

Post-docs: Fan Yang, Sanjaya Senanayake, Wen Wen

Contact: The PI and Co-PIs are at the Chemistry Department of Brookhaven National Laboratory, Upton, NY 11973  
Jose A. Rodriguez; [rodriguez@bnl.gov](mailto:rodriguez@bnl.gov)  
Jonathan C. Hanson, [hanson1@bnl.gov](mailto:hanson1@bnl.gov)  
Ping Liu, [pingliu3@bnl.gov](mailto:pingliu3@bnl.gov)  
Dario Stacchiola, [djs@bnl.gov](mailto:djs@bnl.gov)

**Goal:**

The goal of this program is to provide an improved understanding of chemical catalysis by elucidating details of the fundamental properties of molecules, surfaces, and their reactions that are critical to catalysis and energy conversion. Reactivity-structure correlations explored and unraveled by utilization of synchrotron radiation are a key aspect of these studies. Complexities stemming from the inherent multi-component aspects of heterogeneous catalysis are explored using both ultra-high-vacuum surface science investigations of well-defined model systems, and powder diffraction and x-ray absorption studies of "real-world" systems. Quantum-chemical calculations based on density-functional theory are performed to help in interpretation of experimental results and to study basic aspects of catalytic reactions.

**DOE interest:**

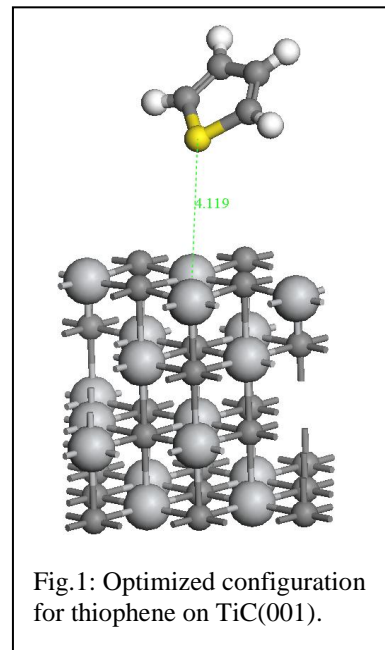
We are engaged in fundamental studies examining the behavior of catalysts used for the production of clean fuels and the prevention of environmental pollution. Basic correlations between surface structure and chemical reactivity, necessary for a rational design of heterogeneous catalysts, are being explored. The program is heavily involved in the development of new techniques for the characterization of heterogeneous catalysts and in the operation of the Synchrotron Catalysis Consortium (SCC). Proximity to the National Synchrotron Light Source (NSLS) and Center for Functional Nanomaterials (CFN) greatly enhances program impact and scope. Our work greatly influences other programs in the areas of catalysis and surface science through collaborative research. The project contributes to the DOE long term goal of understanding and controlling chemical processes for energy-related applications.

**Recent Progress**

**Desulfurization processes**

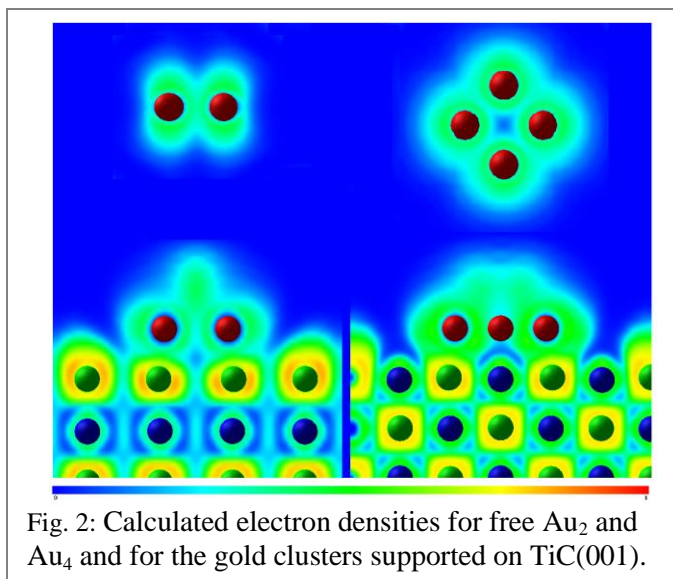
The search for better desulfurization catalysts is a major issue nowadays. In the last three years, we have investigated the interaction of S-containing molecules with surfaces of metal carbides (MoC, Mo<sub>2</sub>C, TiC) and phosphides (Ni<sub>2</sub>P). In these

compounds, the C and P sites cannot be considered as simple spectators. They moderate the reactivity of the metal centers and provide bonding sites for adsorbates. In general, the metal carbides and phosphides were able to break the S-O bonds in SO<sub>2</sub> and the C-S bond in CH<sub>3</sub>SH at temperatures below 300 K. On the other hand, a lower reactivity was observed towards thiophene. The aromatic ring in thiophene makes its C-S bonds quite stable, and for this molecule the desulfurization reactions are much more difficult than those for other sulfur containing molecules such as thiols or SO<sub>2</sub>. The reactivity of the investigated surfaces towards thiophene increases following the sequence: TiC(001) ~ MoC(001) < Ni<sub>2</sub>P(001) < Mo<sub>2</sub>C(001). Thiophene dissociates on Ni<sub>2</sub>P(001) and Mo<sub>2</sub>C(001) at room temperature. On the other hand, the interactions with TiC(001) and MoC(001) are rather weak. The thiophene molecule binds through its S-lone pair (see Figure 1) at ~ 100 K and desorbs intact upon heating to 200 K. The desulfurization activity of TiC(001) and MoC(001) increased after the deposition of metals such Fe, Co, Ni or Au. Fe, Co and Ni are frequently added to enhance the reactivity of MoS<sub>2</sub>-based HDS catalysts. On the TiC(001) and MoC(001) surfaces, these admetals became partially sulfided upon interaction with SO<sub>2</sub>, CH<sub>3</sub>SH and thiophene.



### The adsorption of gold on metal-carbide surfaces: Au-C interactions and charge polarization

Recently, gold has become the subject of a lot of attention due to its unusual catalytic properties when dispersed on some oxide supports (TiO<sub>2</sub>, CrO<sub>x</sub>, MnO<sub>x</sub>, Fe<sub>2</sub>O<sub>3</sub>, Al<sub>2</sub>O<sub>3</sub>, MgO). Bulk metallic gold typically exhibits a very low chemical and catalytic activity. Several models have been proposed for explaining the activity of gold supported on oxides: From special chemical properties resulting from the limited size of the active gold particles (usually less than 5 nm), to the effects of charge transfer between the oxide and gold, and to cooperative interactions between the metal and support. What happens when Au is deposited on a substrate which has physical and chemical properties different from those of an oxide? Carbides of the early-transition metals, like TiC, exhibit chemical and catalytic properties that in many aspects are very similar to those of expensive noble metals and quite different from those of metal oxides. We have performed a



What happens when Au is deposited on a substrate which has physical and chemical properties different from those of an oxide? Carbides of the early-transition metals, like TiC, exhibit chemical and catalytic properties that in many aspects are very similar to those of expensive noble metals and quite different from those of metal oxides. We have performed a

systematic study investigating the electronic properties of Au on different metal carbide surfaces. The results of photoemission and DFT calculations point to the formation of Au-C bonds with a substantial polarization of electrons around the gold (see Figure 2) that affects its chemical properties. The largest electronic perturbations are observed for the deposition of Au on TiC(001), ZrC(001) and TaC(001). The polarization of charge around gold facilitates bonding of the adatoms with electron-acceptor molecules (CO, O<sub>2</sub>, C<sub>2</sub>H<sub>4</sub>, SO<sub>2</sub>, etc) and helps to explain the high chemical activity that Au/TiC(001) exhibits for the oxidation of CO, the destruction of SO<sub>2</sub> and HDS of thiophene. For the case of the dissociation of SO<sub>2</sub> on Au/TiC(001), Au and C sites work in a cooperative way during the cleavage of the S-O bonds. The polarization of charge induced by the Au-C interactions maximizes the flow of electrons from Au into the LUMO of the SO<sub>2</sub>, which has S-O anti-bonding character, facilitating in this way the dissociation of the molecule.

### Initial studies on ethanol reforming and oxidation

#### - Steam reforming of ethanol on Ce<sub>1-x</sub>Ni<sub>x</sub>O<sub>2-y</sub> catalysts

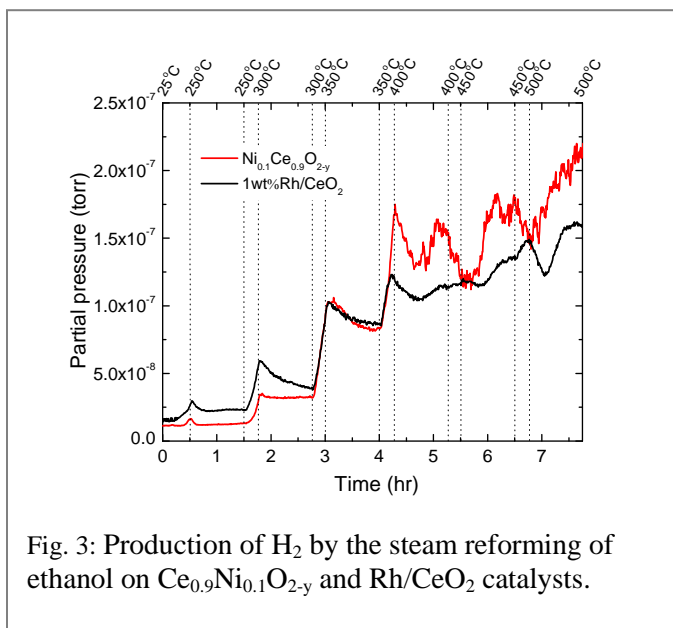


Fig. 3: Production of H<sub>2</sub> by the steam reforming of ethanol on Ce<sub>0.9</sub>Ni<sub>0.1</sub>O<sub>2-y</sub> and Rh/CeO<sub>2</sub> catalysts.

Hydrogen production from the steam reforming of ethanol (C<sub>2</sub>H<sub>5</sub>OH + 3H<sub>2</sub>O → 2CO<sub>2</sub> + 6H<sub>2</sub>) has received significant attention because ethanol can be easily obtained from renewable energy sources and is environmental friendly. There is also a strong interest in using ethanol as a fuel for mobile fuel cell applications. The process is usually carried out over expensive Rh/CeO<sub>2</sub> catalysts. In the last year, we have found that the Ce<sub>1-x</sub>Ni<sub>x</sub>O<sub>2-y</sub> mixed-metal oxide (x < 0.2) is an excellent catalyst for the steam reforming of ethanol. In the Ce<sub>1-x</sub>Ni<sub>x</sub>O<sub>2-y</sub> systems, the nickel cations are replacing cerium

cations in the lattice sites of a fluorite structure. Under the reaction conditions of ethanol steam reforming, the ethanol attacks the mixed-metal oxide inducing the partial reduction of nickel and cerium cations. This system exhibited catalytic activity with production of H<sub>2</sub> and CO<sub>2</sub> at temperatures above 300 °C. We found that the catalyst was stable, i.e. no deactivation by carbon deposition, after periods of 20 hours of operation. The catalytic activity of Ce<sub>1-x</sub>Ni<sub>x</sub>O<sub>2-y</sub> was comparable or better than that of Rh/CeO<sub>2</sub>, see Figure 3. In Ce<sub>1-x</sub>Ni<sub>x</sub>O<sub>2-y</sub>, one has a highly efficient non-expensive catalyst for ethanol reforming.

#### Development of techniques for *in-situ* characterization of powder catalysts: Time-resolved XDR, PDF, XAFS, XAFS/XRD and XAFS/IR

The development of techniques for characterizing the structural properties of catalysts under the high-pressure conditions of industrial processes is widely recognized as a top priority in the area of heterogeneous catalysis. Under reaction conditions a catalyst can undergo chemical transformations that drastically modified its composition

with respect to that obtained during the synthesis of the material. Investigations at BNL have established the feasibility of conducting sub-minute, time-resolved *in-situ* x-ray diffraction (XRD) experiments under a wide variety of temperature and pressure conditions ( $80\text{ K} < T < 1200\text{ K}$ ;  $P < 50\text{ atm}$ ). Using time-resolved XRD, one can get information about phase identification and composition of catalysts under reaction conditions, kinetics of crystallization of bulk solids and nanoparticles, crystallite size as a function of time/temperature, and structure changes during the processes.

Examples of problems studied at the NSLS in the last two years with *in-situ* time-resolved XRD include: (1) the activation of metal/oxide water-gas shift catalysts, (2) operando studies of  $\text{NO}_x$  removal on supported Pt/BaO catalysts, (3) synthesis of water splitting ZnO/GaN photocatalysts, (4) studies of nickel-based layered cathode materials for Li-ion batteries, (5) structural changes in  $\text{Ce}_{1-x}\text{Ni}_x\text{O}_{2-y}$  and Rh/CeO<sub>2</sub> catalysts under the steam reforming of ethanol, and (6) intermediate phases observed during the decomposition of  $\text{LiBH}_4$  and other hydrogen storage materials. All these studies together show how powerful is time-resolved XRD for the *in-situ* characterization of catalysts. Recently, we have acquired detectors that reduce the acquisition time of the diffraction data by a factor of 10-100, and new instrumentation is being developed to combine the technique with XAFS and IR measurements that will allow us to obtain simultaneous information about the structural, electronic and chemical properties of powder catalysts.

XRD is effective when dealing with crystalline materials, while PDF and XAFS provide short range order structural features in less ordered or amorphous catalysts. In addition, XAFS also provides information about the electronic properties of the catalysts. With the help of the NSLS staff, our group upgraded the monochromator and optics at beamline X7B, and now the facility can be used to obtain PDF data of catalysts under reaction conditions. Several studies illustrate the usefulness of this technique (see Figure 4 for an example). The Catalysis Group is a key member in the Synchrotron Catalysis Consortium, being very active in the planning of new beamlines for XRD, PDF, quick XAFS, and XAFS/XRD at the NSLS-II. In the near future, these facilities will become state-of-the-art tools for the *in-situ* characterization of catalysts.

The Catalysis Group is a key member in the Synchrotron Catalysis Consortium, being very active in the planning of new beamlines for XRD, PDF, quick XAFS, and XAFS/XRD at the NSLS-II. In the near future, these facilities will become state-of-the-art tools for the *in-situ* characterization of catalysts.

### Future plans

In the future, the focus of this research program will be on obtaining a fundamental understanding of catalytic processes associated with the cleaning of fossil-derived fuels (desulfurization), the activation and utilization of  $\text{CO}_2/\text{CO}$  (alcohol synthesis) and the use of ethanol as fuel (partial oxidation and reforming of the molecule). We will take advantage of the knowledge and expertise of the PI's for the preparation of well-defined model catalysts, the development of techniques for *in-situ* characterization, and the implementation on quantum-chemical methods for the study of

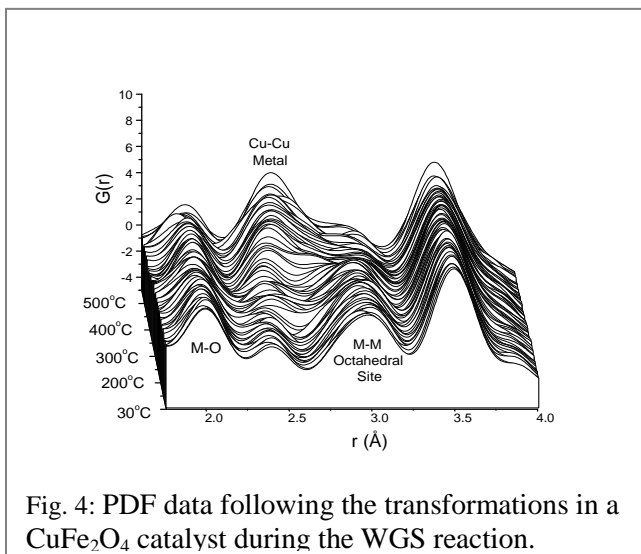


Fig. 4: PDF data following the transformations in a  $\text{CuFe}_2\text{O}_4$  catalyst during the WGS reaction.

reaction mechanisms. In a comprehensive research program, we will examine the effects of size, morphology and chemical environment, providing a truly atomistic view for explaining/predicting catalytic activity.

## **Publications (2009-2010)**

### **2010**

1. A. Hornes, A.B. Hungria, P. Bera, A. Lopez-Camara, M. Fernández-García, A. Martinez-Arias, L. Barrio, M. Estrella, G. Zhou, J.J. Fonseca, J.C. Hanson and J.A. Rodriguez, Inverse CeO<sub>2</sub>/CuO catalyst as an alternative to classical direct configurations for preferential oxidation of CO in hydrogen-rich streams *J. Am. Chem. Soc.*, **132**, 34-35 (2010).
2. J.A. Rodriguez, L. Feria, T. Jirsak, Y. Takahashi, K. Nakamura and F. Illas, Role of Au-C interactions on the catalytic activity of Au nanoparticles supported on TiC(001) towards molecular oxygen dissociation *J. Am. Chem. Soc.*, **132**, 3177-86 (2010).
3. S. Khalid, W. Caliebe, P. Siddons, I. So, B. Clay, T. Lenhard, J. Hanson, Q. Wang, A.I. Frenkel, N. Marinkovic, N. Hould, M. Ginder-Vogel, G.L. Landrot, D.L. Sparks and A. Ganjoo, Quick extended x-ray absorption fine structure instrument with millisecond time scale, optimized for in situ applications *Review of Scientific Instruments*, **81**, 015105 (2010).
4. J.A. Rodriguez, P. Liu, Y. Takahashi, K. Nakamura, F. Viñes and F. Illas, Desulfurization Reactions on Surfaces of Metal Carbides: Photoemission and Density-Functional Studies *Topics in Catal.*, **53**, 393-402 (2010).
5. J.A. Rodriguez, P. Liu, M. Pérez, G. Liu and J. Hrbek, Destruction of SO<sub>2</sub> on Au and Cu Nanoparticles Dispersed on MgO(100) and CeO<sub>2</sub>(111) *J. Phys. Chem. A*, **114**, 3802-10 (2010).
6. T. Gómez, E. Florez, J.A. Rodriguez and F. Illas, Theoretical Analysis of the Adsorption of Late Transition Metal Atoms on the (001) Surface of Early Transition Metal Carbides, *J. Phys. Chem. C*, **114**, 1622-1626 (2010).
7. H. Chen, L. Wang, J. Bai, J.C. Hanson, J.B. Warren, J.T. Muckerman, E. Fujita and J.A. Rodriguez, In Situ XRD Studies of ZnO/GaN Mixtures at High Pressure and High Temperature: Synthesis of Zn-rich (Ga<sub>1-x</sub>Zn<sub>x</sub>)(N<sub>1-x</sub>O<sub>x</sub>) Photocatalysts *J. Phys. Chem. C*, **114**, 1809-14 (2010).
8. J.A. Rodriguez and D. Stacchiola, Catalysis and the Nature of Mixed-Metal Oxides at the Nanometer Level: Special Properties of MO<sub>x</sub>/TiO<sub>2</sub>(110) {M= V, W, Ce} Surfaces *Phys. Chem. Chem. Phys.*, **12**, 9557-9565 (2010) (**invited**).

### **2009**

9. D.H. Kim, J. Szanyi, J.H. Kwak, X.Q. Wang, J.C. Hanson, M. Engelhard and C.H.F. Peden, Effects of Sulfation Level on the Desulfation Behavior of Presulfated Pt-BaO/Al<sub>2</sub>O<sub>3</sub> Lean NO<sub>x</sub> Trap Catalysts: A Combined H-2 Temperature-Programmed Reaction, *In-situ* Sulfur K-Edge X-ray Absorption

- Near-Edge Spectroscopy, X-ray Photoelectron Spectroscopy, and Time-Resolved X-ray Diffraction Study *Journal of Physical Chemistry C*, **113**, 7336-7341 (2009).
10. D.H. Kim, J.H. Kwak, J. Szanyi, X.Q. Wang, G.S. Li, J.C. Hanson and C.H.F. Peden, Characteristics of Desulfation Behavior for Presulfated Pt-BaO/CeO<sub>2</sub> Lean NO<sub>x</sub> Trap Catalyst: The Role of the CeO<sub>2</sub> Support *Journal of Physical Chemistry C*, **113**, 21123-21129 (2009).
  11. J.A. Rodriguez, J.C. Hanson, W. Wen, J.L. Brito, A. Martinez-Arias and M. Fernández-García, In-situ characterization of water-gas shift catalysts using time-resolved x-ray diffraction *Catal. Today*, **145**, 188-94 (2009).
  12. P. Liu, J.A. Rodriguez, Y. Takashi and K. Nakamura, Water-gas shift reaction on a Ni<sub>2</sub>P(001) catalyst: Formation of oxy-phosphides and highly active reaction sites *J. Catal.*, **262**, 294-301 (2009.)
  13. H. Chen, W. Wen, Q. Wang, J.C. Hanson, J.T. Muckerman, E. Fujita, A.I. Frenkel and J.A. Rodriguez, Preparation of (Ga<sub>1-x</sub>Zn<sub>x</sub>)(N<sub>1-x</sub>O<sub>x</sub>) Photocatalysts from the Reaction of NH<sub>3</sub> with Ga<sub>2</sub>O<sub>3</sub> / ZnO and ZnGa<sub>2</sub>O<sub>4</sub>: *In-situ* Time-Resolved XRD and XAFS Studies *J. Phys. Chem. C*, **113**, 3650-59 (2009).
  14. S. Hore, R. Dinnebier, W. Wen, J. Hanson and J. Maier, Structure of Plastic Crystalline Succinonitrile: High-Resolution in situ Powder Diffraction *Zeitschrift Fur Anorganische Und Allgemeine Chemie*, **635**, 88-93 (2009).
  15. E. Florez, F. Viñes, J.A. Rodriguez and F. Illas, Adsorption and Diffusion of Au Atoms on the (001) Surface of Ti, Zr, Hf, V, Nb, Ta, and Mo Carbides *J. Chem. Phys.*, **130**, 2444706-1,7 (2009).
  16. E. Florez, L. Feria, F. Viñes, J.A. Rodriguez and F. Illas, Effect of the Support on the Electronic Structure of Au Nanoparticles Supported on Transition Metal Carbides: Choice of the best substrate for Au activation *J. Phys. Chem. C*, **113**, 19994-20001 (2009).
  17. S. Senanayake, D. Stacchiola, P. Liu, C.B. Mullins, J. Hrbek and J.A. Rodriguez, Interaction of CO with OH on Au(111): HCOO, CO<sub>3</sub>, and HOCO as key Intermediates in the water-gas shift reaction *J. Phys. Chem. C*, **113**, 19536-44 (2009).
  18. J.A. Rodriguez, F. Viñes, P. Liu and F. Illas, Role of C and P sites on the Chemical Activity of Metal Carbides and Phosphides: From Clusters to Single-Crystal Surfaces, in *Model Systems in Catalysis*, R. Rioux (Editor), Springer: Berlin, 2009 (**invited**).
  19. Y. Choi and P. Liu, Mechanism of ethanol synthesis from syngas on Rh(111), *J. Am. Chem. Soc.* **131**, 13054 (2009).

### SISGR - Design and Characterization of Novel Photocatalysts With Core-Shell Nanostructures

Additional PIs: Christopher J. Bardeen (UCR)  
Yadong Yin (UCR)  
Post-docs: Dharma Kurunthu (UCR)  
Ilkeun Lee (UCR)  
Ji Bong Joo (UCR)  
Chuanbo Gao (UCR)  
Graduate Students: Robert Dillon (UCR)  
Qiao Zhang (UCR)  
Michael Dahl (UCR)  
Zhenda Lu (UCR)  
Contact: Francisco Zaera  
Department of Chemistry  
University of California, Riverside, CA 92521  
email: zaera@ucr.edu  
Phone: (951) 827-5498, Fax: (951) 827-3962

#### Goals

The overall goal of this project is to develop new photocatalysts for the production of hydrogen from water. Specifically, we aim to develop a new and novel class of well-characterized nanostructured Metal@TiO<sub>2</sub> yolk@shell photocatalysts to address two fundamental issues presently limiting this field: (1) the fast recombination of electron-hole pairs once generated by light absorption, and (2) the recombination of H<sub>2</sub> and O<sub>2</sub> on the metal surface once produced.

#### DOE Interest

Our proposed research fits squarely with several of the Grand Science Challenges recently identified by the U. S. Department of Energy in its "Directing Matter and Energy: Five Challenges for Science and the Imagination" report. Specifically, it attempts to provide answers to the following questions in that report:

- How do we control materials processes at the level of electrons? The dimensions of the core and shell of the photocatalysts will be tuned to optimize electron and hole transfer to maximize solar energy harvesting while minimizing electron-hole recombination.
- How do we design and perfect atom- and energy-efficient syntheses of revolutionary new forms of matter with tailored properties? Our photocatalysts will be designed at the nanoscale to achieve very specific properties, namely, maximum oxide-metal electron transfer and minimal H<sub>2</sub>+O<sub>2</sub> recombination.
- How do remarkable properties of matter emerge from the complex correlations of atomic or electronic constituents and how can we control these properties? Enhanced photocatalytic activity is to be attained by combining the light-absorbing properties of the oxide shell with the high electron affinity and reducing capability of the metal core.



## Recent Progress

Our project involves three directions of research:

- The development of synthetic strategies for the making of the yolk@shell nanostructures,
- The photophysical characterization of the electronic properties of those samples, with emphasis on the recombination of electron-hole pairs and electron transfer to the metal,
- The chemical characterization of our catalysts in terms of diffusivity of gases through the shells and access of the metal and in terms of photocatalytic activity.

### 1. *Synthesis.*

The most progress to date has been achieved on the synthetic front of this project. Our first accomplishment has been to develop a procedure for the synthesis of hollow TiO<sub>2</sub> nanostructures containing small anatase grains based on silica-protected calcination steps. As shown in Figure 1a, our basic strategy includes the following steps: (1) preparation of silica spheres (which may contain Au nanoparticles); (2) coating the silica surface with a TiO<sub>2</sub> layer through a sol-gel process; (3) coating the TiO<sub>2</sub> surface with an additional silica layer; (4) calcination at high temperatures (>500 °C); and (5) selective dissolution of inner and outer SiO<sub>2</sub> layer. The XRD analyses demonstrate that the TiO<sub>2</sub> shells produced in this way remain as pure anatase even after calcination at 800 and 900 °C. We believe the outer silica layer may act as a barrier to suppress the growth of anatase grains during crystallization by limiting the mobility of TiO<sub>2</sub> layers, and also that the resulting small grain size (typically < 4 nm) significantly delays the phase transition from anatase to rutile, thus producing phase pure anatase nanoshells; the limited mobility and localized crystallization also create mesoscale porosity in the TiO<sub>2</sub> shell. BET measurement of a typical sample of TiO<sub>2</sub> shells shows an average pore size of ~2.6 nm and a surface area of ~314 m<sup>2</sup>/g. For comparison, the commercially used TiO<sub>2</sub>-P25 photocatalyst typically has a surface area of ~50-60 m<sup>2</sup>/g. When used in the photocatalytic decomposition of Rhodamine B under UV light irradiation, the mesoporous shells produced at higher calcination temperatures show enhanced catalytic activity (Figure 1b). These are the catalysts being used for the characterization studies.

Additional synthetic studies are being carried out to expand on our initial concept for these photocatalysts. In one direction, we developed a general self-assembly strategy for the fabrication of novel porous nanostructured materials where nanocrystals of various compositions can be organized into colloidal clusters in emulsion and then calcined at high temperatures. For photocatalytic applications, there are a number of unique features about these materials,

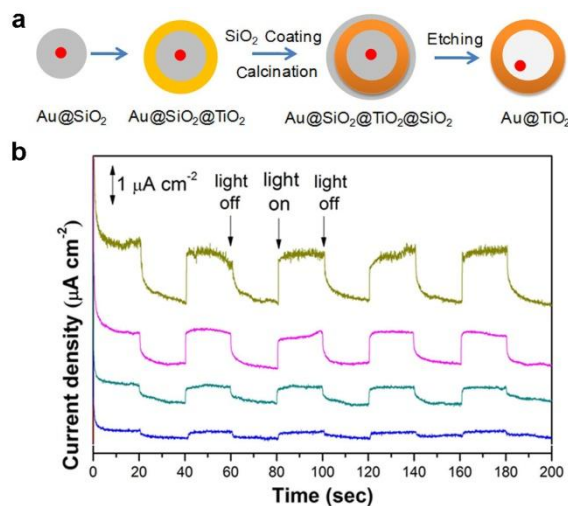


**Fig. 1.** (a) Schematic illustration of the silica-protected calcination method used for the fabrication of mesoporous hollow anatase shells. (b) Photoelectrochemical chrono-amperometry results of TiO<sub>2</sub> shells prepared by the silica-protected calcination method. From bottom to top, the calcination temperatures are: 500 °C, 650 °C, 800 °C, and 900 °C.

including clean surface, high crystallinity, small grain size and large surface area (up to  $\sim 420 \text{ m}^2/\text{g}$ ) even after high-temperature treatment, good water dispersity, and controllable pore size distribution by simply tuning the initial nanocrystal size and shape. We have demonstrated their use as highly efficient and stable photocatalysts by using anatase  $\text{TiO}_2$  nanocrystal clusters as an example. The degradation of rhodamine B under UV, visible light and direct sunshine with this mesoporous photocatalysts demonstrates improved catalytic activity. N-doping process was further done successfully to make the clusters be visible light active.

We have also found that small grain size and high crystallinity would be desirable for enhancing charge separation efficiency due to the reduced migration distance of charges and consequently lower recombination rate. To overcome the main drawback that pristine  $\text{TiO}_2$  only absorbs UV light, much effort has been devoted to developing visible-light-active  $\text{TiO}_2$  photocatalysts that can make use of both UV and visible radiation. We thus designed and synthesized a highly efficient, stable and cost-effective photocatalyst by combining simple sol-gel and calcination processes. The new catalyst has a sandwich structure that composes of a  $\text{SiO}_2$  core, a layer of gold nanoparticles (AuNPs), and a doped- $\text{TiO}_2$  nanoparticle shell (Figures 2a and 2b). The sol-gel process affords convenient incorporation of AuNPs into the catalyst with precisely controlled loading and location. Unlike many conventional methods for non-metal doping, both N and C are doped in  $\text{TiO}_2$  by introducing 3-aminopropyl-triethoxysilane (APTES), which originally acts as ligands for immobilization of AuNPs to the surface of  $\text{SiO}_2$  support but later, upon decomposition at high temperature, serves as sources of N and C for doping. The sandwich structures developed in this work have some unique advantages. For instance, embedding AuNPs inside  $\text{TiO}_2$  matrix protects them from moving and coagulation, maintaining their high specific surface area. The encapsulation also increases the contact area between AuNPs and the  $\text{TiO}_2$  matrix and therefore allows for a more efficient electron transfer than the when the nanoparticles are only loosely attached to support surface. The pre-contact of Au with  $\text{TiO}_2$  surface can significantly increase the N loading via stabilization within the oxide, and the doped N in turn can enhance the adhesion of AuNPs on the oxide surface through an electron transfer process. Only a relatively small amount ( $\sim 0.1 \text{ wt}\%$ ) of AuNPs is required for optimal catalytic performance, making it feasible for large-scale practical applications. The unique sandwich structure not only provides the ideal condition for interfacial non-metal doping and plasmonic metal decoration but also offers tunable crystal grains of  $\text{TiO}_2$  nanoparticles ( $\sim 8\text{-}15 \text{ nm}$ ) in the outer shell, all of which are beneficial to the photocatalytic efficiency. We have demonstrated the excellent performance of the new photocatalysts in a number of degradation reactions of organic pollutants, including Rhodamine B, Rhodamine 6G, methylene blue, and 2,4-dichlorophenol, under UV, visible light and direct sunlight (Figure 2c).

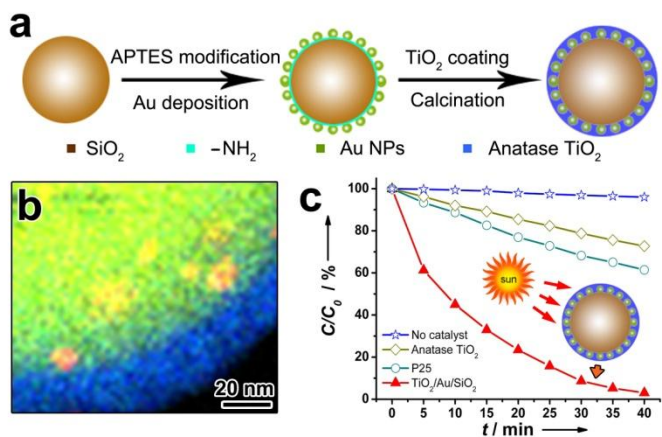


**Fig. 2.** (a) Schematic illustration of the fabrication process of sandwich-structured  $\text{SiO}_2/\text{Au}/\text{TiO}_2$  photocatalyst. (b) Elemental mapping of a single  $\text{SiO}_2/\text{Au}/\text{TiO}_2$  particle. (c) Photodegradation of RhB without catalyst and with anatase  $\text{TiO}_2$ , P25, and  $\text{SiO}_2/\text{Au}/\text{TiO}_2$  as the photocatalysts under direct sunlight illumination. Similar photocatalytic performance has been achieved for various organic dyes, including RhB, rhodamine 6G, methylene blue, and 2,4-dichlorophenol.

## 2. Photophysical Characterization.

Regarding the photophysical characterization of the electronic processes involved, we have begun performing spectroscopic measurements on the hollow spherical TiO<sub>2</sub> shells, both with and without a gold nanoparticle incorporated on the inside. The first goal has been to determine whether the addition of the Au particle creates new electronic states that could affect the photochemical activity of the TiO<sub>2</sub>. Our first measurements have involved using time-resolved luminescence to detect the presence of such states. Our preliminary experiments indicated that luminescence originating from the Au plasmon band might indicate the existence of hybrid electronic states, but subsequent experiments did not result in reproducible data. It is our opinion that the luminescence of the TiO<sub>2</sub> shells is so weak that any emission we observed must be due to minority trap states and impurities that are very sensitive to sample preparation and contamination, and thus we have abandoned this method for TiO<sub>2</sub>.

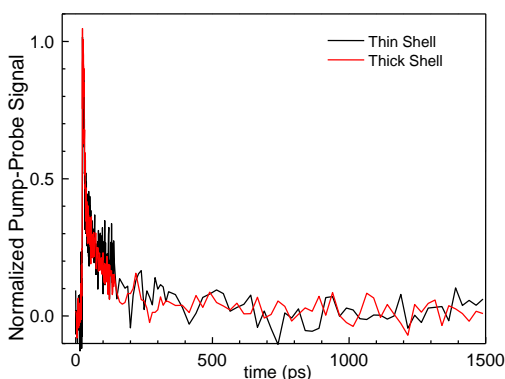


**Fig. 3.** Transient absorption decays at 620 nm for Au@TiO<sub>2</sub> nanoparticles with 20 and 50 nm shell thicknesses. Complete recovery to baseline with identical decay kinetics was observed.

Next we turned our attention to looking at charge dynamics in the Au@TiO<sub>2</sub> yolk@shell particles. Figure 3 shows some preliminary data after excitation into the gold plasmon band at 530 nm. Consistent with results from previous workers, we see very fast electron injection from Au into the amorphous TiO<sub>2</sub> shell. But unlike the bulk samples studied previously, our samples show a complete recovery of the absorption within 500 picoseconds. This is much more rapid than what was observed previously for larger particles with gold nanoparticles randomly adsorbed onto the surface. The thickness of the shell had no effect on the rapid recombination time, suggesting that local traps close to the gold particle limit the

ability of the injected electron to range over the full volume of the surrounding shell. Excitation at 530 nm is not expected to result in water splitting, since one must excite the TiO<sub>2</sub> directly using high-energy photons at about 380 nm to generate a hole in the oxide. Nevertheless, this experiment provides a way to probe charge transfer and recombination in these materials, and our data show that these dynamics are considerably more rapid for the core-shell nanoparticles than for the more random bulk powders usually studied. Future work includes exploring how the crystallinity of the TiO<sub>2</sub> shell (amorphous versus anatase versus rutile) affects the recombination dynamics, how direct excitation of TiO<sub>2</sub> affects the charge dynamics, and whether using Pt instead of Au makes a difference.

## 3. Adsorption and catalytic characterization.

The accessibility of the gold nanoparticles in our Au@TiO<sub>2</sub> nanostructures by reactants for catalysis was assessed by in-situ diffuse-reflectance infrared absorption spectroscopy (DRIFT) using carbon monoxide as a probe. IR spectra as a function of temperature for the adsorption of CO in equilibrium with 200 Torr of gas-phase CO displays two peaks, at 2090-2145 cm<sup>-1</sup> and at 2145-2210 cm<sup>-1</sup>, from CO adsorption on gold and on titania, respectively. The evolution of the coverages of the two types of CO as a function of temperature was followed. Adsorption on gold was seen even at low temperatures, suggesting that the nanoparticles are easily accessible.

The performance of the Au@TiO<sub>2</sub> catalyst was also tested for the promotion of the oxidation of CO with O<sub>2</sub> at room temperature (Figure 4). Both the CO coverages on the gold surface and the yields of the gas-phase CO<sub>2</sub> produced were followed as a function of reaction time in after adding the CO and the O<sub>2</sub> sequentially either in that order or in the reverse O<sub>2</sub>+CO sequence. Data are also reported from experiments with a reference Au/TiO<sub>2</sub>-P25 catalyst for comparison. The integrated DRIFT intensities are reported in arbitrary units, but were normalized to the value for the steady-state coverage of CO on the gold surface. The main observation from these data is that our Au@TiO<sub>2</sub> catalyst is indeed quite active in promoting the oxidation of carbon monoxide, displaying comparable reaction rates, relative to the exposed surface of the gold nanoparticles, to those obtained with the traditional Au/TiO<sub>2</sub>-P25 catalyst.

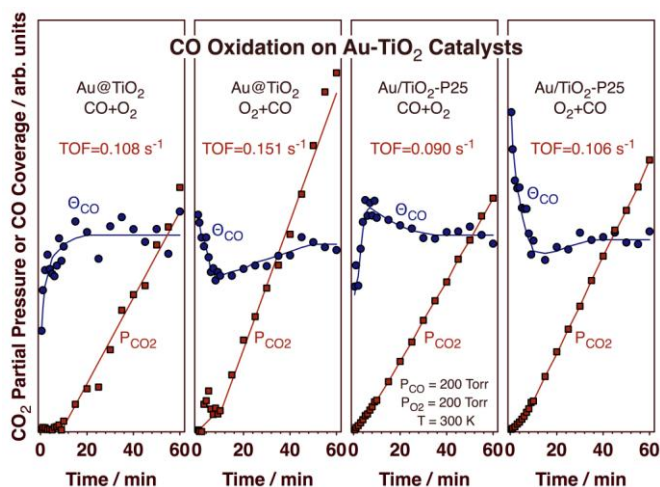


**Fig. 4.** Time dependence of the carbon monoxide coverage on gold ( $\Theta_{CO}$ , blue circles) and the carbon dioxide partial pressure ( $P_{CO_2}$ , red squares) during the room-temperature oxidation of CO with O<sub>2</sub> on gold/titania catalysts. The two left panels correspond to our Au@TiO<sub>2</sub> yolk@shell catalyst, the two right panels to a reference Au/TiO<sub>2</sub>-P25 sample. The first and third panels were obtained by first introducing 200 Torr of CO into the cell and then adding 200 Torr of O<sub>2</sub>; in the second and fourth panels the sequence was reversed. The coverage of CO on Au and the gas-phase CO<sub>2</sub> pressure were estimated from the integrated intensities of the DRIFT signals in the 2090-2145 and 2300-2400 cm<sup>-1</sup> regions, respectively.

One interesting observation here is that, with the Au@TiO<sub>2</sub>, an induction period of approximately 10 min is seen before CO conversion commences. This suggests that the reaction may be initially limited by diffusion of the reactants to the void volume inside of the titania shells (although the time appears quite long for that). A transient is also observed in the CO coverage on gold, but that occurs in a shorter time frame and is also seen with the conventional Au/TiO<sub>2</sub>-P25 catalyst, where no induction time for reaction is observed. The fact that the induction period is more noticeable in the experiment where oxygen is added last to the gas mixture suggests that oxygen diffusion through the titania shell may be slower than CO diffusion. This diffusion of gases through the titania shells needs further characterization.

### Future Plans

We plan to continue our work along the lines of the main objectives of the original plan. In terms of the synthesis of yolk@shell structures, further improvements will be needed to get better quality titania shells. We are also developing new ways to add and anchor more than one metal nanoparticle inside each titania shell, and to modify their interfacial properties. Moreover, we are looking into alternative synthetic procedures for building up shells of mixed and doped oxides in order to be able to affect their electronic structure to facilitate more light absorption.

In terms of the spectroscopic measurements, we propose to look into the effect of the properties of the titania (crystallinity, nature, size, thickness) and the metal (gold, platinum) on the dynamics of electron-hole recombination. Another factor to control is the direct excitation of titania; so far our studies have focused on indirect excitation mechanisms.

Regarding the characterization of the surfaces and the evaluation of their catalytic activity, diffusion rates will be evaluated for different gases as a function of temperature by following the time dependence of their uptake on the surface of the metal nanoparticles placed inside the shells. Their catalytic activity will be probed as well, initially by following the oxidation of CO with molecular oxygen. These properties need to be mapped out as a function of the characteristics of the yolk@shell samples, namely, the size, thickness, and crystallinity of the titania shells and the size and nature (Au, Pt) of the metal nanoparticle yolk.

Finally, we have started testing the photocatalytic performance of some of the titania based catalysts toward water splitting. A reactor has been designed and built for this, with GC gas detection. No reference catalyst has been found yet that can split pure water in our system, not even Pt/TiO<sub>2</sub>-P25, the typical reference used in many other laboratories. This search will continue, and proper calibration of the instrument will be performed before characterizing the yolk@shell samples. Additional measurements with sacrificial reactants such as methanol or silver ions will also be performed to treat each half reaction, the reduction of hydrogen and the oxidation of OH<sup>-</sup> groups, respectively.

### Representative Publications

1. Y. Hu, Q. Zhang, J. Goebel, T. Zhang, and Y. Yin, Control over the Permeation of Silica Nanoshells by Surface-Protected Etching with Water, *Phys. Chem. Chem. Phys.*, **12**, 11836-11842 (2010).
2. Qiao Zhang, Ilkeun Lee, Jianping Ge, Francisco Zaera, and Yadong Yin, Surface-Protected Etching of Mesoporous Oxide Shells for Stabilization of Metal Nanocatalysts, *Adv. Funct. Mater.*, **20(14)**, 2201–2214 (2010). INVITED
3. Ilkeun Lee, Jianping Ge, Qiao Zhang, Yadong Yin, and Francisco Zaera, Encapsulation of Supported Pt Nanoparticles with Mesoporous Silica for Increased Catalyst Stability, *Nano Research*, **4(1)**, 115-123 (2011). INVITED (Special Issue)
4. Ilkeun Lee, Manuel A. Albitar, Qiao Zhang, Jianping Ge, Yadong Yin, and Francisco Zaera, New Nanostructured Heterogeneous Catalysts with Increased Selectivity and Stability, *Phys. Chem. Chem. Phys.*, **13(7)**, 2449-2456 (2011). INVITED PERSPECTIVE (Themed Issue) COVER ART, p. 2425
5. Q. Zhang, J. B. Joo, Z. Lu, M. Dahl, D. Q. L. Oliveira, M. Ye, and Y. Yin, Y. Self-Assembly and Photocatalysis of Mesoporous TiO<sub>2</sub> Nanocrystal Clusters, *Nano Res.*, **4**, 103-114 (2011).
6. Ilkeun Lee, Ji Bong Joo, Yadong Yin and Francisco Zaera, A New Yolk@Shell Nanoarchitecture for Au/TiO<sub>2</sub> Catalysts, *Angew. Chem., Int. Ed.*, DOI:10.1002/anie.201007660 (2011). INVITED
7. R. J. Dillon and C. J. Bardeen, The effects of photochemical and mechanical damage on the excited state dynamics of charge-transfer molecular crystals composed of tetracyanobenzene and aromatic donor molecules. *J. Phys. Chem. A* **115**, 1627-1633 (2011).
8. Z. Zhang, Q. Lin, D. Kurunthu, T. Wu, F. Zuo, S.-T. Zheng, C. J. Bardeen and P. Feng, Synthesis and photocatalytic properties of a novel heteropolyniobate compound: K<sub>10</sub>[Nb<sub>2</sub>O<sub>2</sub>(H<sub>2</sub>O)<sub>2</sub>][SiNb<sub>12</sub>O<sub>40</sub>]·12H<sub>2</sub>O. *J. Am. Chem. Soc.*, submitted for publication.

This page is intentionally blank.

**Monday Afternoon**

**Session III**

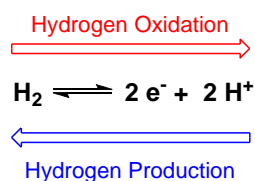
This page is intentionally blank.



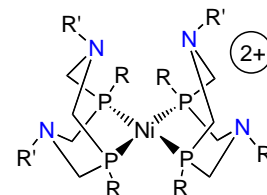
# Design and Development of Molecular Electrocatalysts for Energy Conversions

R. Morris Bullock  
Chemical and Materials Sciences Division  
Pacific Northwest National Laboratory  
Richland, Washington 99352  
morris.bullock@pnnl.gov

Solar and wind power are attractive carbon-neutral, sustainable energy sources, but their intermittent nature requires a reliable method of storing energy. Catalysts that efficiently interconvert between electrical energy and chemical bonds (fuels) are needed for a sustainable and flexible energy supply in the future. Reactions that involve transfer of multiple protons and electrons are pervasive in energy science, as exemplified by the two-proton, two-electron oxidation of H<sub>2</sub> and the reverse, production of H<sub>2</sub> by reduction of protons. Reduction of CO<sub>2</sub> to fuels such as methanol also requires controlled delivery of protons from metal catalysts. Pendant amines incorporated into the second coordination sphere of metal complexes function as proton relays. The proton relays facilitate intramolecular proton mobility, as well as the movement of protons between the metal complex and acids or bases in solution.



Electrocatalysts based on inexpensive, earth-abundant metals<sup>1</sup> (“Cheap Metals for Noble Tasks”) are needed since most fuel cells are based on platinum, an expensive, precious metal. Cobalt complexes with pendant amines on the diphosphine ligand catalyze the reduction of protons to produce H<sub>2</sub>.<sup>2</sup> Pendant amines functioning as proton relays are effective in Mn and Fe complexes that cleave H<sub>2</sub> heterolytically under mild conditions (1 atm, 22 °C). Nickel complexes with pendant amines catalyze the oxidation of H<sub>2</sub> at 1 atm.<sup>3</sup> A related series of Ni complexes have been studied in detail for electrocatalytic production of H<sub>2</sub>, with turnover frequencies over 1000 s<sup>-1</sup>.<sup>4</sup>



We thank the Division of Chemical Sciences, Biosciences and Geosciences, Office of Basic Energy Sciences, Office of Science of the U.S. Department of Energy, for support. Research carried out in the Center for Molecular Electrocatalysis, an Energy Frontier Research Center, is funded by the U.S. Department of Energy, Office of Science, Office of Basic Energy Sciences. Pacific Northwest National Laboratory is operated by Battelle for the U.S. Department of Energy.

## References

1. Bullock, R. M. (Editor), *Catalysis Without Precious Metals*. Wiley-VCH: Weinheim, 2010.
2. Wiedner, E. S.; Yang, J. Y.; Dougherty, W. G.; Kassel, W. S.; Bullock, R. M.; DuBois, M. R.; DuBois, D. L., *Organometallics* **2010**, *29*, 5390-5401.
3. Yang, J.; Chen, S.; Dougherty, W. G.; Kassel, W. S.; Bullock, R. M.; DuBois, D.; Raugei, S.; Rousseau, R.; Dupuis, M.; Rakowski DuBois, M., *Chem. Commun.* **2010**, *46*, 8618-8620.
4. Kilgore, U.; Roberts, J.; Pool, D. H.; Appel, A.; Stewart, M.; Rakowski DuBois, M.; Dougherty, W. G.; Kassel, W. S.; Bullock, R. M.; DuBois, D. L., *J. Am. Chem. Soc.* **2011**, *133*, 5861-5872.

**SISGR: Theoretically relating the surface composition of Pt alloys to their performance as the electrocatalysts of low-temperature fuel cells**

Additional PIs: None  
Postdoc: Yuhua Zhang, Sachin S. Terdalkar, Jun Zhong  
Students: Chan Xiao, Zhiyao Duan  
Collaborators: Vojislav R. Stamenkovic (Argonne Lab), Nenad M. Markovic (Argonne Lab), Rongrong Chen (IUPUI)  
Contacts: University of Pittsburgh, 3700 O'Hara Street, 538B Benedum Hall, Pittsburgh, PA 15261; guw8@pitt.edu

**Goal**

Obtain fundamental knowledge about the relation between surface composition and catalytic activity of Pt alloy catalysts for oxygen reduction reaction (ORR).

Specific objective 1: Develop and improve a first-principles based multiscale computation approach to simulating surface segregation phenomena in Pt alloy surfaces.

Specific objective 2: Predict the surface electronic structure, molecule adsorption, transition states of elementary reactions, and catalytic activity of Pt alloy catalysts for ORR.

Specific objective 3: Relate the surface composition to the surface electronic structure and further to the catalytic performance of Pt alloy catalysts for ORR.

**DOE Interest**

A fundamental understanding of the relation between the surface composition and the catalytic activity for ORR of Pt alloys is important for developing low-cost, high-performance, and long-durability electro-electrodes for polymer electrolyte membrane fuel cells. This theoretical investigation is capable of providing guiding principles for the design and synthesis of multi-component Pt alloy catalysts. Moreover, the computational techniques developed in this project and the insights gained into the correlation of surface composition and surface electronic structures are applicable to study alloy catalysts for other chemical reactions and energy applications.

**Recent Progress**

*Monte Carlo Simulation of Surface Segregation:* The surface segregation phenomena in a series of Pt binary alloys (including Pt-Ni, Pt-Co, Pt-Re, Pt-Mo, Pt-Ti, Pt-Fe, Pt-V, and Pt-Pd alloys) have been simulated using the Monte Carlo (MC) method and the developed modified embedded atom method (MEAM) potentials. Our theoretical predictions agree well with available experimental data. Moreover, our simulation results revealed that the fashion of the surface segregation (Figure 1 displays three examples) was correlated with the heat of formation of the Pt binary alloys.

*Surface Segregation in Pt Ternary Alloys:* We have used density functional theory (DFT) method to calculate the Pt surface segregation energy in the Pt<sub>3</sub>Ni, Pt<sub>3</sub>Co, and Pt<sub>3</sub>Fe (111) surfaces doped with a third transition metal M and thus investigated the influence of component M on the extent of Pt segregation to the outermost layer of the Pt<sub>3</sub>Ni/M, Pt<sub>3</sub>Co/M, and Pt<sub>3</sub>Fe/M

(111) surfaces. Furthermore, we found that the surface energy effect, strain effect, and heat of solution effect induced by the doped element M would collectively affect the Pt surface segregation energy in the  $\text{Pt}_3\text{Ni}/\text{M}$ ,  $\text{Pt}_3\text{Co}/\text{M}$ , and  $\text{Pt}_3\text{Fe}/\text{M}$  (111) surfaces. An analytical model to quantify the three effects in determining the surface segregation process is under development.

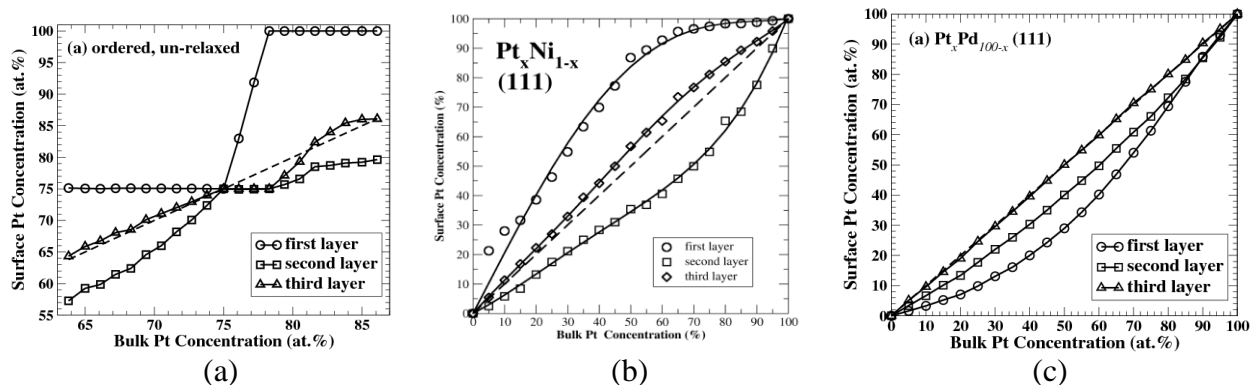


Figure 1: Calculated resultant surface composition profiles due to surface segregation process for (a) Pt-Ti alloy (showing dramatically different surface segregation processes below and above the composition of 75 at% Pt), (b) Pt-Ni alloy (showing oscillatory Pt surface segregation as a function of surface layers), and (c) Pt-Pd alloy (showing monotonically decreasing Pd surface segregation as a function of surface layers).

*Electronic Structure Calculation of Pt Alloy Surfaces:* We employed the DFT calculation method to determine the lowest-energy adsorption configuration of O, H,  $\text{O}_2$ , OH, OOH, and  $\text{H}_2\text{O}_2$ , find the minimum energy path and locate the transition states for various elementary steps of ORR on pure Pt (111) surface and Pt/M (111) surface modified by subsurface transition metal M=Ni, Co, or Fe. Our study suggested that ORR would follow hydrogen peroxide dissociation mechanism with a rate-determining step of  $\text{O}_2$  protonation reaction on the Pt/M (111) surfaces but assume peroxy dissociation mechanism with a rate-determining O protonation reaction on the pure Pt (111) surface.

## Future Plans

*Monte Carlo Simulation of Surface Segregation in Pt Ternary Alloys:* Develop the MEAM potentials for more Pt binary alloys (such as, Pt-Au and Pt-Mn) and Pt ternary alloys. Apply these MEAM potentials to simulate the surface segregation phenomena in these alloy systems using the Monte Carlo method.

*Kinetic Monte Carlo Method:* Develop kinetic MC method specifically for the ORR on pure Pt (111) and Pt/M (111) surfaces. The inputs to the kinetic MC algorithm are the reaction activation energies calculated with DFT method. The output of the kinetic MC algorithm is the reaction rate of ORR on these surfaces.

*Surface Segregation Theory:* Based on our theoretical predictions of the surface segregation in Pt binary and ternary alloys, we will develop generalized theory to describe (1) the relation between

the fashion of surface segregation (see Fig. 1) and the property of alloys, and (2) how the surface segregation process is impacted when more components are added into the alloy systems.

### **Publications (2009-2011)**

1. Z. Duan, J. Zhong, and G.F. Wang, "Modeling Surface Segregation Phenomena in the (111) Surface of Ordered Pt<sub>3</sub>Ti Crystal", *J. Chem. Phys.* 133 (2010) 114701.
2. C. Wang, G.F. Wang, D. van der Vliet, K.C. Chang, N.M. Markovic, and V. R. Stamenkovic, "Monodisperse Pt<sub>3</sub>Co Nanoparticles As Electrocatalyst: the Effect of Particle Size and Pretreatment On Electrocatalytic Reduction of Oxygen", front cover, *Phys. Chem. Chem. Phys.* 12 (2010) 6933-6939.
3. Y. Zhang, Z. Duan, C. Xiao, and G.F. Wang, "Density Functional Theory Calculation of Platinum Surface Segregation in Pt<sub>3</sub>Ni (111) Surface Doped with A Third Transition Metal", *Surf. Sci.* *in press* (2011).
4. Y. Yang, G.F. Wang, and X.D. Li, "Water Molecule-Induced Stiffening in ZnO Nanobelts", *Nano Lett.* *in press* (2011).

## Understanding the Effects of Surface Chemistry and Microstructure on the Activity and Stability of Pt Electrocatalysts on Non-Carbon Supports

Graduate Students: Sujan Shrestha and Ying Liu

Undergraduate Students: Sasha Asheghi, Jonathan Goldman, Tulsi Patel, Jeff Timbro and John Varconda

Contact Information: University of Connecticut; Department of Chemical, Materials and Biomolecular Engineering; 191 Auditorium Rd, Unit 3222; Storrs, CT 06269-3222; Phone: 860-486-2756; E-mail: [mustain@engr.uconn.edu](mailto:mustain@engr.uconn.edu)

### Goal

The objective of this project is to elucidate the effects of the chemical composition and microstructure of the electrocatalyst support on the activity, stability and utilization of supported Pt clusters. In this work, four hypotheses will be tested:

1. The electrocatalytic activity of nanosized Pt clusters can be enhanced by tailoring the metal-support interaction between the Pt catalyst and the catalyst support material
2. Increasing the interaction between the nanosized Pt clusters and the support material will increase Pt cluster stability
3. The microstructure of non-carbon catalyst supports can be tailored to increase both the electrochemically active area and reactant mass transport
4. An electrochemically modified Thiele modulus can be used as a predictive design tool for supported Pt electrocatalysts.

### DOE Interest

Advances in fundamental understanding of the influence of the electrocatalyst support on Pt activity and stability has the potential to have a significant impact on the performance and durability of several devices. In this work, the PI will focus on electrochemical applications, most notably the electrocatalyst systems for the oxygen reduction reaction (ORR) in the proton exchange membrane fuel cell (PEMFC). The PEMFC is a promising next generation energy conversion device for both portable and stationary applications. Using this new fundamental knowledge, the long term goal is to develop future catalysts with ultra-low platinum loading, high performance and low degradation rates. Though this work will focus on electrochemical systems, the findings of this study have the potential to impact heterogeneous catalysis in general, where catalyst-support interactions are of great interest.

### Recent Progress

The first reporting period (FY11) has been used to develop enabling technologies that will allow the team to test the four hypotheses, develop testing protocols for both physical and electrochemical characterization, train the graduate and undergraduate researchers and begin

testing two of the four proposed electrocatalyst supports: WC and carbon. The major outcomes of this work have been:

- I. *Synthesis and characterization of WC as an electrocatalyst support.* In this task, we have successfully synthesized single phase WC with very high surface area ( $> 140 \text{ m}^2/\text{g}$ ), demonstrated good electrochemical dispersion of Pt particles, shown that Pt/WC catalysts have higher initial activity than Pt/C catalysts, and characterized changes in the WC and Pt structures during ORR.
- II. *Precise microstructural control over the synthesis of mesoporous carbon.* In this task, we have developed a hard templating method to prepare functionalized highly ordered mesoporous carbon (HOMC) supports, successfully synthesized templates with a wide range of pore sizes with very narrow distribution, demonstrated excellent Pt dispersion compared to commercial Pt/C and performed a full suite of physical and electrochemical characterization techniques both in three-electrode measurements and in-situ.
- III. *Development of a synthesis procedure for TiAlN and assembly of a dedicated CVD reactor.* In this task, we have designed and setup a custom-built CVD reactor for our first FY12 electrocatalyst support, TiAlN.

### **Future Plans**

The work performed during the past budget period not only helped to develop a baseline for future work and assisted us in meeting the objectives of the original proposal, it has also yielded several interesting observations and opportunities for deeper study and understanding into the activity and stability of Pt clusters on our support materials. Therefore, over the next year, we plan to not only follow our proposal, but also expand our effort to pursue new issues that have come up. There are several objectives for FY12 that are listed below:

1. Deposit nanosized Pt clusters onto  $\text{WO}_3$  and investigate the interaction between  $\text{WO}_3$  and Pt clusters and its effect on Pt activity and stability. This will help us to decouple the chemical and structural effects on the performance degradation of Pt/WC catalyst that we observed during the current budget period.
2. Synthesize and electrochemically characterize raw TiAlN. As discussed in Section A.3, this is expected to be completed by the end of Summer 2011.
3. Platinize and investigate Pt/TiAlN electrocatalysts using both physical characterization and electrochemical techniques. This will include investigating the initial and time-dependent ex-situ activity, investigating the surface chemistry of the support during operation and the stability of size and structure of supported Pt clusters.
4. Investigate the kinetic response for all platinized supports for the ferri/ferrocyanide reaction. This will give us a measure of the intrinsic electron transferability of the catalyst without needing to consider the complex ORR reaction mechanism.

5. PEMFC testing of high surface area platinized supports. This will give us in-situ data and allow us to correlate the in-situ and ex-situ findings.
6. Develop improved practices for filling ultra-small pore templates. Improved pore filling will allow us to make supports with precisely controlled pore structures and improved mass transport in the catalyst layer
7. Investigate the role of surface functionalization of the HOMC template on Pt ORR activity.
8. Correlate the observed performance of carbon-based supports with structural parameters.

**Publications (FY 2011)**

1. Y. Liu and W.E. Mustain, “Structural and Electrochemical Studies of Pt Clusters Supported on High surface Area Tungsten Carbide for Oxygen Reduction”, ACS Catalysis, 1 (2011) 212.
2. S. Shrestha, Y. Liu and W.E. Mustain, “Electrocatalytic Activity and Stability of Pt Clusters on State-of-the-Art Supports: A Review”, Catalysis Reviews, Accepted.

**Thermodynamic Properties of Supported Catalysts**

Students: Kevin Bakhmutsky, Ivan Baldychev  
Collaborators: J. M. Vohs (Penn), P. Fornasiero (Trieste), Michael Smith (Villanova)  
Contact: Department of Chemical & Biomolecular Engineering, 311 Towne Building,  
220 S. 33rd Street, University of Pennsylvania, Philadelphia, PA 19104 Ph:  
215-898-4439; Fax: 215-573-2093, gorte@seas.upenn.edu

**Goals:**

Understand how support and composition affect the thermodynamic properties for oxidation and reduction of various oxide and metal catalysts. Understand how redox properties at a surface differ from that of bulk materials.

**DOE Interest:**

The thermodynamic properties for oxidation and reduction of bulk materials are well known. However, typical catalytic materials are in the form of nano-particles, supported on high-surface-area oxides, and often in the form of a mixed oxide or solid solution. The redox properties of these types of materials are not usually known in detail. For selective oxidation reactions which proceed by a Mars-Van Krevelen mechanism, understanding the redox properties of the catalyst is critical to a fundamental understanding of the reaction and to the development of new and improved catalysts. For reactions involving steam or CO<sub>2</sub>, the thermodynamic properties of the catalyst affect the oxidation state of the catalyst under steady-state reaction conditions, thereby affecting the activity and selectivity of the reaction.

**Recent Progress:**

*Supported Co:* It has been suggested that the Co catalysts used in Fischer-Tropsch Synthesis (FTS) can be oxidized under FTS conditions, even though bulk thermodynamics would suggest that Co should remain metallic. Using coulometric titration, we have demonstrated that the redox properties of Co particles as small as 4.5 nm are indistinguishable from that found for bulk Co. However, there is evidence for interactions with zirconia that shift the equilibrium  $P(O_2)$  to lower values. These interactions can be removed by the addition of dopant levels of Pd, perhaps because the precious metals segregate to the interface between the Co and the support.

*Supported MoO<sub>x</sub>:* The equilibrium properties of bulk MgMoO<sub>4</sub>, Zr(MoO<sub>4</sub>)<sub>2</sub>, Al<sub>2</sub>(MoO<sub>4</sub>)<sub>3</sub>, SrMoO<sub>4</sub>, and Cr<sub>2</sub>(MoO<sub>4</sub>)<sub>3</sub> were characterized by coulometric titration in order to understand the effect of the mixed-cation environment on the Mo<sup>+6</sup>-Mo<sup>+4</sup> equilibrium and how this in turn affects catalytic activity. For MgMoO<sub>4</sub>, Zr(MoO<sub>4</sub>)<sub>2</sub>, Al<sub>2</sub>(MoO<sub>4</sub>)<sub>3</sub>, and Cr<sub>2</sub>(MoO<sub>4</sub>)<sub>3</sub>, removal of one O/Mo occurs at a  $P(O_2)$  of 10<sup>-6</sup> atm at 873 K, corresponding to a  $\Delta G$  of oxidation of -100 kJ/mol O<sub>2</sub>; however, the equilibrium between SrMoO<sub>4</sub> and SrMoO<sub>3</sub> occurs at 10<sup>-26</sup> atm O<sub>2</sub>, corresponding to a  $\Delta G$  of oxidation equal to -375 kJ/mol O<sub>2</sub>. These thermodynamic properties differ significantly from oxidation of MoO<sub>2</sub> to MoO<sub>3</sub>. All of the mixed oxides were essentially inactive for the selective oxidation of methanol, with specific rates that were at least 100 times lower than that observed for bulk MoO<sub>3</sub>.



*Supported VO<sub>x</sub>*: The effects of a second oxide and of support composition on vanadia catalytic properties were studied using coulometric titration and methanol-oxidation rates. The redox properties for the bulk oxides V<sub>2</sub>O<sub>5</sub>, ZrV<sub>2</sub>O<sub>7</sub>, AlVO<sub>4</sub>, Mg<sub>3</sub>(VO<sub>4</sub>)<sub>2</sub>, and CeVO<sub>4</sub> were dramatically different, showing that the environment surrounding the V cations affects redox properties. However, the redox properties of isolated, mono-vanadates on zirconia, titania, and alumina were similar and very different that of the corresponding bulk oxides. Specific rates for methanol oxidation were virtually identical on all of the bulk vanadates and supported vanadia catalysts, implying that the redox properties of vanadia do not affect rates for this reaction.

#### **Future Work:**

*Co catalysts*: We are continuing to investigate the redox properties of supported Co catalysts in order to understand the effect of support and of promoters.

*Core-shell catalysts*: We have recently demonstrated the preparation of highly uniform, 2.0-nm Pd (or Pt) particles with a thin, porous shell of variable-thickness oxide (ceria, titania, or zirconia) (“Synthesis of dispersible Pd@CeO<sub>2</sub> nanostructures by self-assembly”, M. Cargnello, N. Wieder, T. Montini, R. J. Gorte, and P. Fornasiero, *Journal of the American Chemical Society*, 132 (2010) 1402-9.). These particles are prepared in solution and can be adsorbed onto a hydrophobic support in monolayer form. We are investigating the redox properties and the catalytic properties of these materials in order to quantify the influence of the support on the metal catalysts.

#### **Publications Acknowledging DE-FG02-85ER13350, from 1/1/2009 to present.**

1. “Synthesis and oxygen storage capacity of 2-D ceria nanocrystals”, Dianyuan Wang, Yijin Kang, Vicky Doan-Nguyen, Jun Chen, Rainer Kungas, Noah L. Wieder, Kevin Bakhmutsky, Raymond J. Gorte, and Christopher B. Murray, *Angewante Chemie*, accepted.
2. “A Thermodynamic Study of the Redox Properties of Supported Co particles”, K. Bakhmutsky, N. L. Wieder, T. Baldassare, M. A. Smith, and R. J. Gorte, *Applied Catalysis A*, 397 (2011) 266-271.
3. “A Comparison of Redox Properties of Molybdenum-Based Mixed Oxides”, I. Baldychev, A. Javadekar, D. J. Buttrey, J. M. Vohs, and R. J. Gorte, *Applied Catalysis A*, 394 (2011) 287-93.
4. “The Effect of Support on Redox Properties and Methanol-Oxidation Activity of Vanadia Catalysts”, I. Baldychev, J. M. Vohs, and R. J. Gorte, *Applied Catalysis A*, 391 (2011) 86-91.
5. “Ceria in Catalysis: From Automotive Applications to the Water-Gas Shift Reaction”, R. J. Gorte, *AIChE Journal*, 56 (2010) 1126-35.
6. “The Impact of Redox Properties on the Reactivity of V<sub>2</sub>O<sub>5</sub>/Al<sub>2</sub>O<sub>3</sub> Catalysts”, I. Baldychev, R. J. Gorte, and J. M. Vohs, *Journal of Catalysis*, 269 (2010) 397-403.
7. “Comparison of Redox Isotherms for Vanadia Supported on Zirconia and Titania”, P. R. Shah, I. Baldychev, J. M. Vohs, and R. J. Gorte, *Applied Catalysis A*, 361 (2009) 13-17.
8. “The Water-Gas-Shift Reaction on Pd/Ceria-Praseodymia: The Effect of Redox Thermodynamics”, K. Bakhmutsky, G. Zhou, S. Timothy, and R. J. Gorte, *Catalysis Letters*, 129 (2009) 61-65.
9. “The Effect of Thermodynamic Properties of Zirconia-Supported Fe<sub>3</sub>O<sub>4</sub> on Water-Gas Shift Activity”, I. Baldychev, J. M. Vohs, and R. J. Gorte, *Applied Catalysis A*, 356 (2009) 325-30.

This page is intentionally blank.

**Monday Evening**

**Session IV**

This page is intentionally blank.

# Enhanced Catalysis by Nano Confinements

Xinhe Bao

*State Key Laboratory of Catalysis, Dalian Institute of Chemical Physics,  
Chinese Academy of Sciences, Dalian 116023, China;*

[xhbao@dicp.ac.cn](mailto:xhbao@dicp.ac.cn); [www.fruit.dicp.ac.cn](http://www.fruit.dicp.ac.cn)

In the present talk, the unique characters of the catalysis with the nano-confined system will be demonstrated, and the emphasis will be laid on the differences of the electron properties, which derived from a so-called effect of the quantum well states in the 2D nano-systems and the effects of the interface confinement between the nano-islands and the surfaces of the substrates.

The effect of electron quantum confinement on the catalytic activities of 2D ultra-thin metal films is explored by comparing the work function change and the initial reaction rate of atomically flat films of different thickness on silicon surfaces, using complementary microscopy and spectroscopy techniques. The obvious oscillations of the oxidation rate of lead films are observed, which are attributed to be a manifestation of the Fabry-Pe´rot interference modes of electron de Broglie waves (quantum well states) in the films. The modulation of the electron density of states near the Fermi level opens a new demission for tuning the catalytic performance of metal systems via size- and thickness-dependent quantum size effects, which will be illustrated through two examples.

Coordinatively unsaturated ferrous (CUF) sites confined in nanosized matrices are active centers in a wide range of enzyme and homogeneous catalytic reactions. Preparation of the analogous active sites at supported catalysts is of great importance in heterogeneous catalysis but remains a challenge. On the basis of surface science measurements and density functional calculations, in the present talk, I will show that the interface confinement effect can be used to stabilize the CUF sites by taking advantage of strong adhesion between ferrous oxides and metal substrates. The interface-confined CUF sites together with the metal supports are active for dioxygen activation, producing reactive dissociated oxygen atoms. The structural ensemble was highly efficient for carbon monoxide oxidation at low temperature under typical operating conditions of a proton-exchange membrane fuel cell.

Carbon materials have properties different from conventional oxides in catalysis, in particular as catalyst supports. Recently, carbon nanotubes (CNTs) interest us with their well defined tubular morphology and their electron structure in the graphene walls, where  $\pi$  electrons shift from the inside to the outside due to the curvature. This provides

an intriguing confinement environment for nanocatalysts and catalytic reactions inside such small cavities. In the present talk, the unique effects of the electron confinement with CNT's and the resulted modulating in catalysis will be illustrated. The techniques to introduce metal nanoparticles homogeneously inside the CNT channels have been developed and the effects of confined metal catalysts on their physio-chemical properties, as well as their catalytic activities have been studied systematically. Using Fe as a probe, it is found that the redox properties of iron oxide and metallic iron are modified when they are confined inside the CNT channels. For example, the reduction of the CNT confined iron oxide is facilitated compared to that dispersed on the outer surface of CNTs. In this way, a distinct enhancement of the CNT encapsulated Fe species to the F-T process has also been revealed, which is attributed the favourable formation of the reduced iron species, e.g. iron carbides, inside the channel of CNTs. A striking enhancement of the catalytic activity of Rh particles confined inside nanotubes for the conversion of CO and H<sub>2</sub> to ethanol has been found. The overall formation rate of ethanol inside nanotubes exceeds that on the outside of the nanotubes by more than an order of magnitude, although the latter is much better accessible.

#### **Selected Publications:**

1. The effects of confinement inside carbon nanotubes on catalysis, Xiulian Pan, Xinhe Bao\*, *Accounts of Chemical Research*, DOI 10.1021/ar100160t (2011)
2. Interface-Confined Ferrous Centres for Catalytic Oxidation, Qiang Fu, Wei-Xue Li1, Yunxi Yao, Hongyan Liu, Hai-Yan Su1, Ding Ma, Xiang-Kui Gu, Limin Chen, Zhen Wang, Hui Zhang, Bing Wang and Xinhe Bao\*, *Science*, 328(2010)1141-1144
3. Effect of Confinement in Carbon Nanotubes on the Activity of Fischer-Tropsch Iron Catalyst, Wei Chen, Zhongli Fan, Xiulian Pan,\* and Xinhe Bao\*, *J. Am. Chem. Soc.*, 130(2008)(29)9414-9419
4. Reactions over catalysts confined in carbon nanotubes, Xiulian Pan, Xinhe Bao, *Chem. Commun., (Invited Feature Article)* (2008)6271-6281
5. Textural Manipulation of Mesoporous Materials for Hosting of Metallic Nanocatalysts, Junming Sun and Xinhe Bao, *CHEMISTRY-A EUROPEAN JOURNAL (Invited Concept article)*, (2008)(14)7478-7488
6. Enhanced Ethanol Production inside Carbon Nanotube Reactors Containing Catalytic Particles, Xiulian Pan, Zhongli Fan, Wei Chen, Yunjie Ding, Hongyuan Luo, Xinhe Bao\*, *Nature Materials*, 6(2007)507-511
7. Tuning of redox properties of iron and iron oxides via encapsulation within carbon nanotubes, Wei Chen, Xiulian Pan, Xinhe Bao\*, *J. Am. Chem. Soc.*, 129(2007)(23)7421-7426

8. Reactivities, Xucun Ma, Peng Jiang, Yun Qi, Jinfeng Jia, Yu Yang, Wenhui Duan, Wei-Xue Li, Xinhe Bao, S. B. Zhang and Qi-Kun Xue, *P NATL ACAD SCI USA (PNAS)*, **104(2007)(22)9204-9208**
9. Towards Monodispersed Silver Nanoparticles with Unusual Thermal Stability, Junming Sun, Ding Ma, He Zhang, Xiumei Liu, Xiuwen Han, Xinhe Bao\*, Gisela Weinberg, Norbert Pfaender, Dangsheng Su, *J. Am. Chem. Soc.*, **128 (49) (2006) 15756-15764**
10. Facile Autoreduction of Iron Oxide/Carbon Nanotube Encapsulates, Wei Chen, Xiulian Pan, Marc-Georg Willinger, Dang Sheng Su, and Xinhe Bao\*, *J. Am. Chem. Soc.*, **128 (10) (2006) 3136-3137**

**Dynamics at a Surface:  
Understanding Fundamental Surface Processes as an Approach to Tailored Surface  
Activity**

Ludwig Bartels,<sup>1,\*</sup> Talat S. Rahman,<sup>2</sup> Donna Chen,<sup>3</sup> Tony F. Heinz<sup>4</sup>

1: Dept. of Chemistry, U. of California, Riverside, CA 92506; email: [ludwig.bartels@ucr.edu](mailto:ludwig.bartels@ucr.edu)

2: Dept. of Physics, University of Central Florida, Orlando, FL 32816;

3: Dept. of Chemistry, U. of South Carolina, Columbia, SC 29208;

4: Dept. of Physics, Columbia University, New York, NY, 10027;

The dynamics of molecules at surfaces (and of the surface itself as a consequence of molecular processes) has been investigated with an array of techniques focusing on scanning tunneling microscopy and DFT modeling. We studied means of controlling the motion of larger molecular species (such as pentacene derivatives), allowing insight into the pathways and mechanisms employed in surface diffusion. Addressing the diffusion and desorption of CO molecules on terraces and in lateral confinement on the nanoscale, we found marked differences that suggest that confinement by itself (i.e. irrespective of e.g. the change in electronic structure of nanoclusters as compared to macroscopic ones) increases surface activity. Moreover, adsorption of species as small as CO was found to be capable of inducing a change of the surface composition of alloy nanoparticles. Finally, we elucidated theoretical origins of molecular diffusion that constitute a marked departure from an Arrhenian behavior. Variation of prefactors with temperature and the relevance of tunneling will be discussed. In conjunction, these findings suggest significantly higher mobility of adsorbates on realistic catalytic systems than expected from measurements of isolated molecules on large terraces.



**Influence of the oxidation state of supported size-selected Pt nanoparticles on catalytic decomposition and oxidation of high-order alcohols: activity, selectivity and lifetime**

Students: Jason R. Croy, Simon Mostafa, Farzad Behafarid, Jeronimo Matos  
Post docs: Luis K. Ono, Kristof Paredis, Ahmed Naitabdi  
Collaborators: Anatoly I. Frenkel, Judith C. Yang  
Contacts: University of Central Florida, Department of Physics, 4000 Central Florida Blvd., PSB430, Orlando, FL 32816; [roldan@ucf.edu](mailto:roldan@ucf.edu)

**Goal**

Obtain a qualitative and quantitative understanding of the oxidation state of structurally well-defined nanoparticle (NP) catalysts under reaction conditions, systematically tune such state by changing the NP size, composition, and oxide support, and investigate its influence on catalytic activity and selectivity.

**DOE Interest**

Chemical reactions of significant interest in the field of energy generation are being targeted, namely, the oxidation and decomposition of methanol and high-order alcohols such as 2-propanol and 2-butanol. Some byproducts from the latter reactions such as acetone and butanone are also valuable to the chemical synthesis industry. Catalytic reforming of gasoline additives (e.g. methanol, ethanol, and potentially butanol), may serve as an on-board source of hydrogen. Additionally, the design of efficient catalysts for the dehydrogenation of high-order alcohols may also contribute to improvements in chemical heat pumps, such as those based on the 2-propanol/acetone/hydrogen cycle.

**Recent Progress**

In order to engineer the next generation of nanocatalysts, a thorough understanding of the correlation between their size, shape, NP/support interactions, oxidation state, and catalytic activity is needed. In this study, the structure of small ( $0.7\text{nm} < d < 1.5\text{nm}$ ) size-selected Pt NPs synthesized by inverse micelle encapsulation has been resolved by a synergistic combination of microscopic (transmission electron microscopy-TEM, atomic force microscopy-AFM and scanning tunneling microscopy-STM), spectroscopic tools (X-ray absorption fine-structure spectroscopy, XAFS), and NP shape modeling. The model shapes were selected based on their agreement with the coordination numbers extracted by EXAFS, the NP diameters obtained by TEM, and their resemblance to real cluster shapes observed by STM on similarly synthesized samples, Fig. 1.

Using micellar Pt NPs of similar size ( $\sim 1\text{ nm}$  for S1, S2, and S4 and  $\sim 0.8\text{ nm}$  for S3) but different shape supported on  $\gamma\text{-Al}_2\text{O}_3$  as model system, the oxidation of 2-propanol was investigated in a packed-bed mass flow reactor, Fig. 1(a). The lowest onset reaction temperature for the partial oxidation of 2-propanol was obtained for S1, which is the only sample studied containing flat (2D-like) NPs. This result suggest that the NP support ( $\gamma\text{-Al}_2\text{O}_3$ ) might play a positive role in the reactivity of these NPs either by inducing strain, by providing catalytically active reaction sites at the NP/support interface, or via NP/support charge transfer processes. Nevertheless, a clear correlation between the average number of low coordinated atoms in our samples and their catalytic activity was also observed, Fig. 1(b), with lower activation reaction barriers measured for the

samples with the highest fraction of steps, kinks and corner atoms, such as S1. Furthermore, it was observed that the NPs in S1 (best catalyst) were able to easily dissociate O<sub>2</sub> at RT, while those in S4 (worst catalyst) remained metallic at RT.

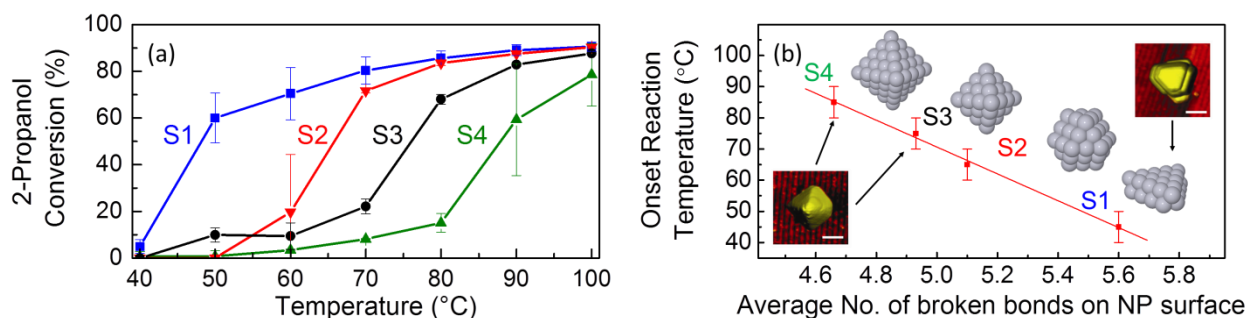
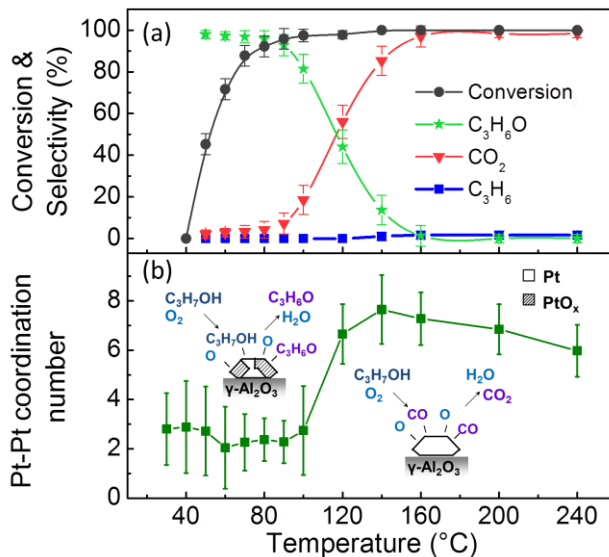


**Fig. 1** (a) Partial oxidation of 2-propanol over ~0.8-1 nm micellar Pt NPs supported on  $\gamma$ -Al<sub>2</sub>O<sub>3</sub>. (b) Onset reaction temperature displayed versus the number of broken bonds at the NP surface normalized by the total number of surface atoms. The insets show model NP shapes representative of each of the samples obtained together with STM images from larger but similarly prepared Pt NPs on TiO<sub>2</sub>(110). The scale bars in STM images are 5 nm.

The role of the oxidation state of the NP catalysts on their activity and selectivity for the partial and complete oxidation of 2-propanol was investigated under *operando* conditions via EXAFS and mass spectrometry, Fig. 2. Our *in situ* EXAFS data revealed that PtO<sub>x</sub> species are the active phase for the partial oxidation of 2-propanol to acetone. In the complete oxidation regime, the catalysts are initially metallic, but with the surface covered by chemisorbed oxygen. With increasing reaction temperature, the NPs showed signs of re-oxidation, possibly due to the desorption of passivating carbonaceous species (reaction intermediates). The decomposition of the Pt oxides in the intermediate reaction regime, where partial and total oxidation processes coexist, is attributed to the reducing effect of the hydrogen released in the dehydrogenation of 2-propanol, to carbonaceous intermediate species available at the onset of the complete oxidation reaction, as well as to the competition of CO and O<sub>2</sub> for adsorption sites on the NP surface.

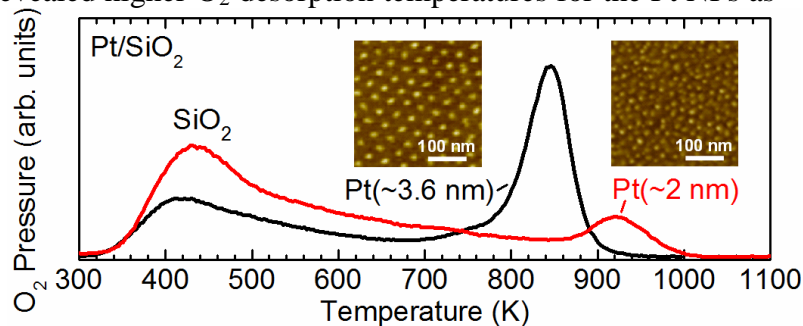
**Fig. 2** (a) Steady-state conversion and selectivity data as a function of temperature during the oxidation of 2-propanol over Pt NPs (0.7 nm)/ $\gamma$ -Al<sub>2</sub>O<sub>3</sub>. (b) Dependence of the first nearest-neighbor metallic Pt-Pt coordination number (CN) on the reaction temperature obtained from *in situ* EXAFS spectra. From the low initial Pt-Pt CN and the presence of Pt-O bonds (not shown here) it could be concluded that PtO<sub>x</sub> species are present below 100°C. The change in the selectivity from partial to complete oxidation occurs at the onset of Pt oxide decomposition (~110°C).



The effect of the NP size, support, and oxygen coverage on the formation and thermal stability of oxide species on Pt NPs deposited on SiO<sub>2</sub>, ZrO<sub>2</sub> and TiO<sub>2</sub> was also studied via *in situ* X-ray photoelectron spectroscopy (XPS) and temperature-programmed desorption (TPD). For low atomic oxygen exposures, chemisorbed O<sub>2</sub> species were detected on Pt/SiO<sub>2</sub> samples. Exposure to higher atomic oxygen coverages at RT lead to the formation and stabilization of PtO<sub>x</sub> species (PtO<sub>2</sub> and PtO). On all samples, a two-step thermal decomposition process was observed upon

annealing in UHV:  $\text{PtO}_2 \rightarrow \text{PtO} \rightarrow \text{Pt}$ . For NPs in the 2–6 nm range, the NP size was found to affect the strength of the O-binding. Contrary to the case of Pt(111), where no oxides were detected above 700 K, 10–20 % PtO was detected on the NP samples via XPS at the same temperature, suggesting the presence of strongly bound oxygen species. In addition, for identical atomic oxygen exposures, decreasing the NP size was found to favor their ability to form oxides. Interestingly, regardless of whether the desorption of chemisorbed oxygen species or that of oxygen in  $\text{PtO}_x$  species was considered, our TPD data revealed higher  $\text{O}_2$  desorption temperatures for the Pt NPs as compared to the Pt(111) surface. Furthermore, a clear size-dependent trend was observed, with an increase in the strength of the oxygen bonding with decreasing NP size, Fig. 3.

**Fig. 3**  $\text{O}_2$  TPD data from micellar Pt NPs with different sizes supported on  $\text{SiO}_2/\text{Si}(001)$ .



## Future Plans

Improve the stability, activity, and selectivity of nanocatalysts through the optimization of their size, shape, and support, and the addition of secondary metals. Since the former parameters influence the oxidation state of the nanocatalysts, the proposed investigations will shed light into the relationship between structure, chemical state and catalytic performance of industrially relevant catalysts. Target chemical reactions will include CO and  $\text{CO}_2$  hydrogenation and  $\text{CH}_4$  reforming.

## Publications (2009-2011)

1. Paredis, K.; Ono, L. K.; Mostafa, S.; Li, L.; Zhang, Z. F.; Yang, J. C.; Barrio, L.; Frenkel, A. I.; **Roldan Cuenya, B.**, Structure, Chemical Composition, and Reactivity Correlations during the In Situ Oxidation of 2-Propanol. *J. Am. Chem. Soc.* 2011, 133, 6728-6735.
2. Ono, L. K.; Croy, J. R.; Heinrich, H.; **Roldan Cuenya, B.**, Oxygen Chemisorption, Formation, and Thermal Stability of Pt Oxides on Pt Nanoparticles Supported on  $\text{SiO}_2/\text{Si}(001)$ : Size Effects. *J. Phys. Chem. C* 2011, 115, 16856-16866.
3. Mostafa, S.; Behafarid, F.; Croy, J. R.; Ono, L. K.; Li, L.; Yang, J. C.; Frenkel, A. I.; **Roldan Cuenya, B.**, Shape-Dependent Catalytic Properties of Pt Nanoparticles. *J. Am. Chem. Soc.* 2010, 132, 15714-15719
4. **Roldan Cuenya, B.**; Croy, J. R.; Mostafa, S.; Behafarid, F.; Li, L.; Zhang, Z. F.; Yang, J. C.; Wang, Q.; Frenkel, A. I., Solving the Structure of Size-Selected Pt Nanocatalysts Synthesized by Inverse Micelle Encapsulation. *J. Am. Chem. Soc.* 2010, 132, 8747-8756.
5. **Roldan Cuenya, B.**, Synthesis and catalytic properties of metal nanoparticles: Size, Shape, Support, Composition, and Oxidation State Effects. *Thin Solid Films* 2010, 518, 3127-3150.
6. Ono, L. K.; Yuan, B.; Heinrich, H.; **Roldan Cuenya, B.**, Formation and Thermal Stability of Platinum Oxides on Size-Selected Platinum Nanoparticles: Support Effects. *J. Phys. Chem. C* 2010, 114, 22119-22133
7. Mostafa, S.; Croy, J. R.; Heinrich, H.; **Roldan Cuenya, B.**, Catalytic Decomposition of Alcohols over Size-Selected Pt nanoparticles supported on  $\text{ZrO}_2$ : a study of activity, selectivity, and stability. *Appl. Catal. A* 2009, 366, 353-362.
8. Croy, J. R.; Mostafa, S.; Heinrich, H.; **Roldan Cuenya, B.**, Size-selected Pt Nanoparticles Synthesized via Micelle Encapsulation: Effect of Pretreatment and Oxidation State on the Activity for Methanol Decomposition and Oxidation. *Catal. Lett.* 2009, 131, 21-32.
9. Naitabdi, A.; Behafarid, F.; **Roldan Cuenya, B.**, Enhanced Thermal Stability and Nanoparticle-Mediated Surface Patterning: Pt/ $\text{TiO}_2(110)$ , *Appl. Phys. Lett.* 2009, 94, 083102.

This page is intentionally blank.

**Tuesday Morning**

**Session V**

This page is intentionally blank.

# Molecular mechanism, kinetics, and dynamics of metal cluster catalyzed reactions in an ion trap

Thorsten M. Bernhardt

*Institute of Surface Chemistry and Catalysis, University of Ulm, Albert-Einstein-Allee 47,  
89069 Ulm, Germany, thorsten.bernhardt@uni-ulm.de*

Practical interest in the catalytic activation and conversion of methane into valuable products, such as methanol, formaldehyde, or light olefins, and in particular ethylene, is driven by industrial and economical considerations, and has motivated extensive research aimed at the identification and development of heterogeneous catalyst materials for these processes. However, the required high reaction temperatures and/or the use of highly active reactants to activate the stable C-H bond of methane (bond dissociation energy  $440 \text{ kJmol}^{-1}$ ) renders a selective synthesis of the desired products difficult. Consequently, the selective catalytic functionalization of methane poses a longstanding central problem in organometallic chemistry.

Employing ion trap mass spectrometry,<sup>2</sup> our experiments aim to discover new selective catalytic methane activation reactions employing small mass-selected clusters of gold. In addition, even more importantly, a molecular understanding of the involved size-dependent catalytic reaction mechanism is aspired. Toward this goal the combination of our gas phase reaction kinetics measurements with first principle calculations performed by U. Landman and coworkers are an essential prerequisite.<sup>1,3,4</sup>

Following this approach it was possible to demonstrate the selective activation of methane on free  $\text{Au}_2^+$  (see Figure 1). In this catalytic reaction, coadsorption effects were found particularly important. This applied also to the hydrogen promoted activation of molecular oxygen on  $\text{Au}_n^+$  clusters.<sup>4,5</sup> Ion trap mass spectrometry in conjunction with theoretical simulations provided comprehensive insight into the mechanistic details of the  $\text{O}_2$  activation. Furthermore, most recent experiments demonstrate that free gold clusters are also able to coadsorb  $\text{CH}_4$  and  $\text{O}_2$  eventually leading to formaldehyde formation at cryogenic temperatures.<sup>6</sup> Finally, we compare the selectivity of  $\text{O}_2$  activation and methane oxidation properties of gold to free palladium cluster cations and provide an outlook on new experimental prospects to monitor the molecular dynamics of cluster catalyzed reactions in an ion trap in real time.<sup>7</sup>

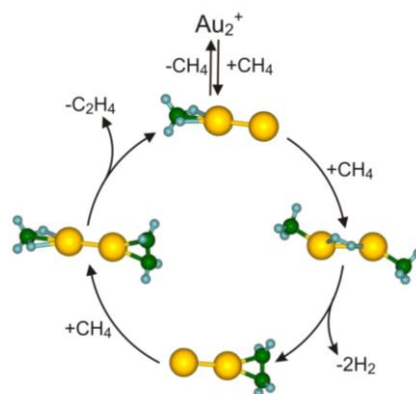


Figure 1: Catalytic reaction cycle for the selective conversion of methane to ethylene by  $\text{Au}_2^+$  determined by gas phase reaction kinetics measurements and first principles calculations.<sup>1</sup>

- (1) Lang, S. M.; Bernhardt, T. M.; Barnett, R. N.; Landman, U. *Angew. Chem. Int. Ed.* **2010**, *49*, 980.
- (2) Lang, S. M.; Popolan, D. M.; Bernhardt, T. M. In *Atomic Clusters: From Gas Phase to Deposited*; Woodruff, P., Ed.; Elsevier: Amsterdam, 2007; Vol. 12, p 53.
- (3) Socaciu, L. D.; Hagen, J.; Bernhardt, T. M.; Wöste, L.; Heiz, U.; Häkkinen, H.; Landman, U. *J. Am. Chem. Soc.* **2003**, *125*, 10437; Lang, S. M.; Bernhardt, T. M.; Barnett, R. N.; Landman, U. *Chem. Phys. Chem.* **2010**, *11*, 1570.
- (4) Lang, S. M.; Bernhardt, T. M.; Barnett, R. N.; Yoon, B.; Landman, U. *J. Am. Chem. Soc.* **2009**, *131*, 8939.
- (5) Lang, S. M.; Bernhardt, T. M. *J. Chem. Phys.* **2009**, *131*, 024310.
- (6) Lang, S. M.; Bernhardt, T. M.; Barnett, R. N.; Landman, U. *J. Phys. Chem. C* **2011**, *115*, 6788.
- (7) Popolan, D.; Bernhardt, T. M. *Chem. Phys. Lett.* **2009**, *470*, 44.

## Single-Molecule Sub-Diffraction Imaging of Nanoscale Catalysis

Peng Chen

Department of Chemistry and Chemical Biology, Cornell University, Ithaca, NY  
14853

E-mail: pc252@cornell.edu

Nanoparticles catalyze a multitude of chemical transformations important for energy conversion, petroleum processing, and pollutant removal. Understanding their structure-activity correlation is paramount for developing better catalysts, but hampered by their inherent inhomogeneity: individual nanoparticles differ from one to another, and for every nanoparticle, it can change from time to time, especially during catalysis. Furthermore, each nanoparticle presents on its surface various types of sites, which are often unequal in catalytic reactivity. To overcome these challenges, my group has been developing single-molecule fluorescence imaging methods to study the catalytic activity and dynamics of metal nanoparticles at the single-particle level, in situ, and with real-time single-turnover resolution. I will present how we interrogate the catalytic activity, mechanism, heterogeneous reaction pathways, selectivity, and surface-restructuring-coupled temporal dynamics of individual Au nanoparticles (1-6). I will also present our latest achievements in imaging and resolving catalytic reactions on a single nanocatalyst at nanometer resolution, which uncovers diverse spatial patterns of reactivity at the nanoscale.

### References

1. W. Xu, J. S. Kong, Y.-T. E. Yeh, P. Chen, Single-Molecule Nanocatalysis Reveals Heterogeneous Reaction Pathways and Catalytic Dynamics. *Nature Mater.* **7**, 992 (2008).
2. W. Xu, J. S. Kong, P. Chen, Probing the Catalytic Activity and Heterogeneity of Au-Nanoparticles at the Single-Molecule Level. *Phys. Chem. Chem. Phys.* **11**, 2767 (2009).
3. W. Xu, J. S. Kong, P. Chen, Single-Molecule Kinetic Theory of Heterogeneous and Enzyme Catalysis. *J. Phys. Chem. C* **113**, 2393 (2009).
4. P. Chen, W. Xu, X. Zhou, D. Panda, A. Kalininskiy, Single-Nanoparticle Catalysis at Single-Turnover Resolution. *Chem. Phys. Lett.* **470**, 151 (2009).
5. X. Zhou, W. Xu, G. Liu, D. Panda, P. Chen, Size Dependent Catalytic Activity and Dynamics of Gold Nanoparticles at the Single-Molecule Level. *J. Am. Chem. Soc.* **132**, 138 (2010).
6. P. Chen *et al.*, Single-Molecule Fluorescence Imaging of Nanocatalytic Processes. *Chem. Soc. Rev.* **39**, 4560 (2010).



**Nanostructured, metal-ion modified oxide catalysts for the water-gas shift and methanol steam reforming reactions**

Co-PIs: Howard Saltsburg (Tufts); George Flynn (Columbia); Irving Herman (Columbia); Siu-Wai Chan (Columbia)

Post-docs: Rui Si (Tufts); Kwang Toer Rim (Columbia); Youjin Lee (Columbia); Joan Raitano (Columbia)

Graduate Students: Yanping Zhai (Tufts); Matthew Boucher (Tufts); Nan Yi (Tufts)

Undergrad Students: Forrest Gittleston; Glenn Ferreira; Joseph Lessard (Tufts)

Collaborators: Anatoly Frenkel (Yeshiva); Jose Rodriguez (BNL); Jon Hanson (BNL), Syed Kalid (BNL); Steven Overbury (ORNL); Larry Allard (ORNL); Lihua Zhang (BNL)

Contact: M. Flytzani-Stephanopoulos, Department of Chemical and Biological Engineering, Tufts University, 4 Colby St., Medford, MA 02155; [maria.flytzani-stephanopoulos@tufts.edu](mailto:maria.flytzani-stephanopoulos@tufts.edu)  
Irving P. Herman, Department of Applied Physics and Applied Mathematics, Columbia University, New York, NY 10027; [iph1@columbia.edu](mailto:iph1@columbia.edu)

**Goal**

The overall goal of this project is to elucidate the role of metal ions anchored on oxide supports, and the role of oxide structures in stabilizing the metal ions in their active state for catalyzing reactions of interest to fuel reforming for hydrogen generation. The low-temperature water-gas shift and methanol steam reforming reactions are studied on Au, Pt, Cu on nanoscale ceria, iron oxide, and zinc oxide. Alkali promotion was added to the program objectives last year. The concentration and types of oxygen defects are strong functions of the size, shape, and composition of the oxide nanoparticles. Novel chemical synthesis techniques are employed to control the size and shape of oxide nanoparticles, which in turn controls metal ion stabilization and catalytic activity for the two reactions under study in the project.

**DOE Interest**

The project was motivated by the original reports<sup>1,2</sup> by the PI's group that the activity of ceria-supported gold or platinum catalysts for the water-gas shift reaction is not due to the presence of the metal nanoparticles. Rather, a sub-structure of oxidized metal atoms and ceria, i.e. Au-O-Ce and Pt-O-Ce ensembles, contains the active sites for this reaction. While the metal particle size distribution is not important, the particle size, shape, and oxygen defect density of the host oxide (ceria) are crucial for an active water-gas shift catalyst. These results have a major impact on catalyst design and development. The extension of these findings to other fuel processing reactions, such as methanol steam reforming, is of interest. Also, under investigation in this project are other nanoscale oxide hosts, such as zirconia, iron oxide, and zinc oxide. Since the last report, we have identified that alkali addition can enable the use of silica and alumina supports on which Pt in low amounts (<1 wt%) is rendered as active as Pt on ceria. These findings are exciting and of interest to DOE in that they free the choice of catalyst support from the rare earth oxides to cheap and abundant oxide supports. Lower-cost catalysts for hydrogen generation and purification are critical to the development and market penetration of fuel cells.

**Recent Progress**

Earlier in the project, in an effort to understand whether the oxide support effect was direct or indirect through the stabilization of active metal sites, we prepared ceria single crystals at the nanoscale and

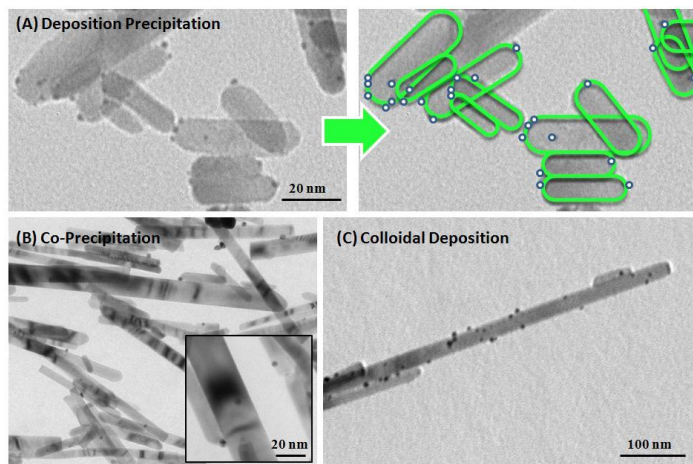
examined the effect of using Au/CeO<sub>2</sub> nanoshapes (cubes, rods, polyhedra) for the water-gas shift reaction in a first-of-a-kind study that was published in 2008.<sup>3</sup> We recently used the same approach to examine the structure sensitivity of the methanol steam reforming reactions on Au/CeO<sub>2</sub><sup>4,5</sup> and extended the study to ZnO and Fe<sub>3</sub>O<sub>4</sub> nanoshapes.<sup>6,7</sup> The findings from this part of the work are summarized in the following sections. Our catalysis and characterization results have pointed consistently to the importance of single atoms or few atom-clusters of Au<sup>8,9</sup> or Pt<sup>10</sup> strongly bound to the oxide as the active sites for the water-gas shift reactions. To further probe this, a model catalyst, namely Au adatoms on a Fe<sub>3</sub>O<sub>4</sub> (111) single crystal surface, was used by the co-PI George Flynn's group at Columbia to image Au adatoms and examine CO adsorption on these surfaces using STM/STS.<sup>11</sup> Furthermore, we collaborated with researchers at Oak Ridge National Lab (Larry Allard and Steven Overbury) to image Au atoms on real iron oxide catalysts using HAADF/ac-STEM and evaluate their thermal stability.<sup>12,13</sup> A remarkable stability in oxygen-rich WGS was demonstrated catalytically.<sup>14</sup> Throughout the project, we have had a fruitful interaction with our collaborators at Brookhaven National Lab.

Since last year, we have taken a new direction in the project to evaluate alkali metals as promoters of the WGS activity of monometallic catalysts on oxide supports. We stumbled upon a large promotion effect of Na and K on otherwise inert Pt/SiO<sub>2</sub> catalysts, as a result of preparation of core-shell Pt@SiO<sub>2</sub> nanoparticles via a reverse microemulsion synthesis that used NaOH as base. Substituting NH<sub>4</sub>OH for NaOH resulted in inert Pt@SiO<sub>2</sub> particles. This prompted us to evaluate the alkali promotion effect in open silica supports, and resulted in a recently published report<sup>15</sup> which describes new possibilities for the design of very active WGS catalysts on any oxide support, including the low-cost, abundant silica and alumina. The experimental work was complemented by new computational work carried out by our collaborator Manos Mavrikakis at Wisconsin in which the stability and good thermochemical properties of alkali-promoted Pt(OH)<sub>x</sub> species for the low-temperature water-gas shift reactions was demonstrated.<sup>15</sup> These findings have motivated us to focus part of our on-going work and the proposed future scope of the project to the investigation of potential alkali promotion of other metals, as well as other reactions, e.g. the methanol steam reforming reaction.

Highlights from last year's findings of the project are presented below.

### Methanol Conversion to Hydrogen over Au/ZnO Nanoshapes

During the past year, we examined oxide carriers of gold other than ceria for the WGS and SRM reactions. We reported for the first time on the latter reaction on Au/ZnO nanoshapes.<sup>6,7</sup> By using structure-controlled ZnO supports we are able to examine "shape effects" among ZnO crystals with varying ratios of exposed {0001} surfaces to the bulk.



Gold was added to the ZnO nanostructures by various techniques; the one that worked the best was deposition precipitation (DP).<sup>7</sup> The samples were dried under vacuum at 80 °C for 12 h, and calcined in static air at 280°C for 4 h. When Au is added by DP, it is apparent that gold binds selectively to the {0001} surfaces or the ends of the ZnO nanorods (Fig. 1A).

**Figure 1.** TEM images of Au-ZnO prepared by different Au deposition methods.

Methanol- (methanol + O<sub>2</sub>)- and (methanol + H<sub>2</sub>O)- TPSR measurements were conducted ramping the temperature at 2°C/min to 400°C at an overall flowrate of 50 cc/min. From CH<sub>3</sub>OH-TPSR we found that the decomposition of methanol proceeds through methyl formate at temperatures below 250°C, and produces H<sub>2</sub> and CO<sub>2</sub> rather than CO. There is also a small amount of methyl formate produced below 100 °C; this can be attributed to Au interacting with weakly bound surface oxygen supplied by ZnO. If the proposed mechanism is true, then the addition of oxygen to the system should increase the amount of low temperature methylformate produced; this is in fact the case and can be viewed in Fig. 2, showing (CH<sub>3</sub>OH+O<sub>2</sub>)- TPSR. It will be interesting to evaluate how the availability of surface oxygen differs among different ZnO nanoshapes in future work.

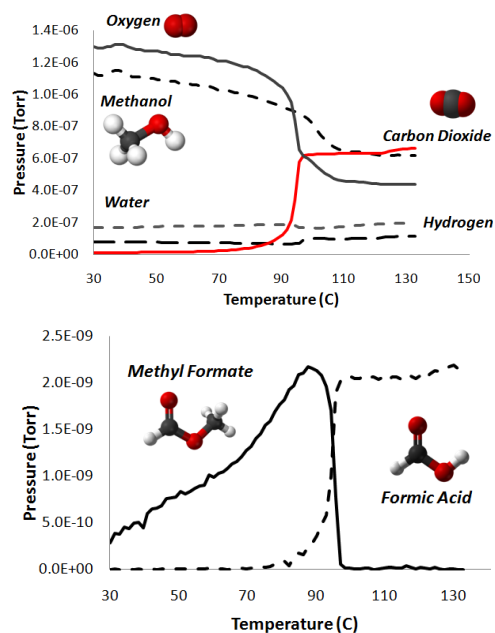


**Figure 2.** (Methanol + O<sub>2</sub>)- TPSR over Au-ZnO.

In conclusion, we have shown the merits of atomically dispersed Au on either CeO<sub>2</sub> or ZnO as a highly selective catalyst for the low-temperature SRM reaction.<sup>4,7</sup> Especially attractive is the Au/CeO<sub>2</sub> system which shows the highest activity and stability in this reaction, along with the highest H<sub>2</sub> yield below 250°C; hence it merits further development for applications to fuel processing and fuel cell systems.

### Scanning Tunneling Microscopy (STM) of CO and H<sub>2</sub>O adsorption on Au/Fe<sub>3</sub>O<sub>4</sub> (111)

STM/STS work conducted by the Flynn group in this project has shown that Au adatoms on the Fe<sub>3</sub>O<sub>4</sub>(111) surface preferentially bind over the uncoordinated O atoms, and when dosed with CO at 260K, adsorption of CO molecules normal to the surface takes place atop the gold adatom sites.<sup>11</sup> Last year, the work was extended to determine the behavior of water adsorption on this surface. Water species were observed only on Fe-terminated Fe<sub>3</sub>O<sub>4</sub>(111) domains at 235 K and 245 K. At 235 K dissociated hydroxyl groups OH and loosely bound physisorbed water molecules were observed on the Fe-terminated Fe<sub>3</sub>O<sub>4</sub>(111) domains while no evidence was found for the existence of water species on the O-terminated FeO(111) domains. When the sample temperature was raised to 245 K, only hydroxyl groups atop the surface terminating Fe<sup>+3</sup> cations are observed. It is to be noted that CO molecules are adsorbed atop the oxygen sites of an Fe<sub>3</sub>O<sub>4</sub>(111) surface via catalytic Au adatoms. Thereby CO molecules are adjacent to hydroxyls atop surface terminating Fe<sup>+3</sup> cations, hence activation of the CO + OH (key step in the WGS reaction) is feasible.<sup>16</sup> These findings have direct implications to the design of Au/FeOx catalysts for the low-temperature water-gas shift reaction.

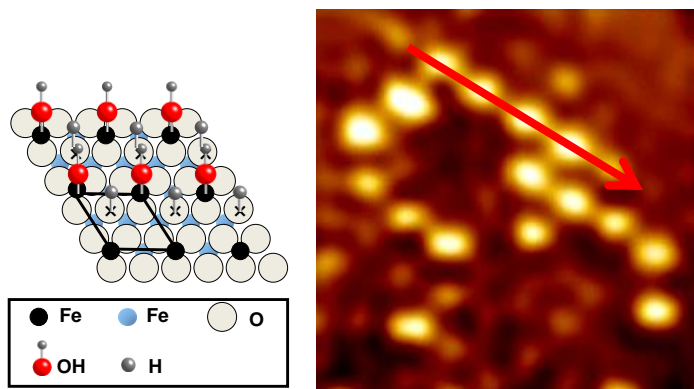


**Figure 4.** a) Model for adsorbed water species on  $\text{Fe}_3\text{O}_4$  (111). Dissociative adsorption of water, with hydroxyl groups (OH) bound to the surface iron cations and hydrogen atoms (H) bound to the uncapped oxygen; b) A topographic STM image,  $5.35 \text{ nm} \times 4.03 \text{ nm}$ , obtained at +1.2 V (sample positive), 1.0 nA and 235 K. The bright features atop the surface terminating Fe atoms are hydroxyl groups.

### In situ Raman scattering of Au-doped $\text{CeO}_2$ nanoshapes in CO gas flow

In work conducted last year, the Herman group has investigated the Au/ $\text{CeO}_2$  nanoshapes used catalytically at Tufts by in situ Raman scattering experiments using CO gas flow and a wide range of temperatures. Oxygen vacancy levels were monitored during the oxidation of CO by  $\text{CeO}_{2-\delta}$  nanorods and Au- $\text{CeO}_{2-\delta}$  nanorods, nanocubes, and nanopolyhedra by using Raman scattering. The first-order  $\text{CeO}_2$   $F_{2g}$  peak near  $460 \text{ cm}^{-1}$  decreases when this reaction is fast (fast reduction and relatively slow re-oxidation of the surface), because of the lattice expansion that occurs when  $\text{Ce}^{3+}$  replaces  $\text{Ce}^{4+}$  during oxygen vacancy creation. This shift correlates with reactivity for CO oxidation. Increases in the oxygen deficit  $\delta$  as large as  $\sim 0.04$  were measured relative to conditions when the ceria sample was not reduced.<sup>17</sup>

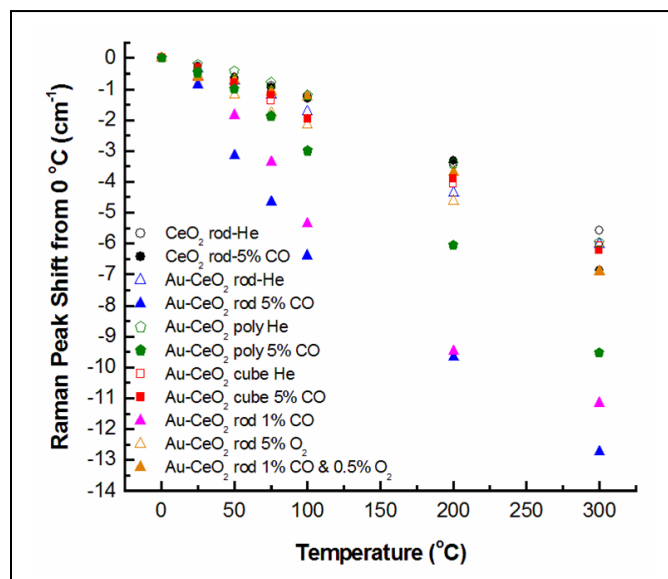


**Figure 5.** The main  $\text{CeO}_2$  Raman peak ( $F_{2g}$ ) shifts (relative to the shifts at  $0 \text{ }^\circ\text{C}$ ) as a function of temperature over  $\text{CeO}_2$  nanorods, Au- $\text{CeO}_2$  nanorods, Au- $\text{CeO}_2$  nanopolyhedra, and Au- $\text{CeO}_2$  nanocubes exposed to various gas flows (in situ). CO indicates 5% CO, 1% CO, and 1% CO/0.5%  $\text{O}_2$  flows carried in He, and  $\text{O}_2$  indicates 5%  $\text{O}_2/\text{N}_2$  flow.<sup>17</sup>

### Stabilizing and activating $\text{Pt}(\text{OH})_x$ groups on inert supports

It is highly desirable to devise new ways to maximize the number of active Pt- or Au-O sites on supports to improve the overall WGS activity of the catalyst. We recently showed this to be possible for Pt by the addition of alkali promoters.<sup>15</sup> Indeed, alkali ions (Na, K) added in small amounts activate platinum adsorbed on any oxide support, but in our recent work we focused on inert alumina or silica supports to unambiguously demonstrate the promotion. The alkali ion-associated surface -OH groups are activated by CO at low temperatures ( $\sim 100^\circ\text{C}$ ) in the presence of atomically dispersed Pt. Both experimental evidence, and density-functional theory (DFT) calculations conducted by the Mavrikakis group at Wisconsin,

suggest that a partially oxidized Pt-alkali-O<sub>x</sub>(OH)<sub>y</sub> species is the active site for the low-temperature Pt-catalyzed WGS reaction.<sup>15</sup> The catalytic site is support-independent; same on Al<sub>2</sub>O<sub>3</sub> and on SiO<sub>2</sub>. The apparent activation energy is similar, E<sub>app</sub> = 70±5 kJ/mol, for Pt on any support, including ceria. In situ XANES found no change in the oxidation state of Pt with time-on-stream and no activity loss was observed.<sup>15</sup> These findings are useful for the design of highly active and stable WGS catalysts that contain only trace amounts of a precious metal without the need for a reducible oxide support such as ceria.

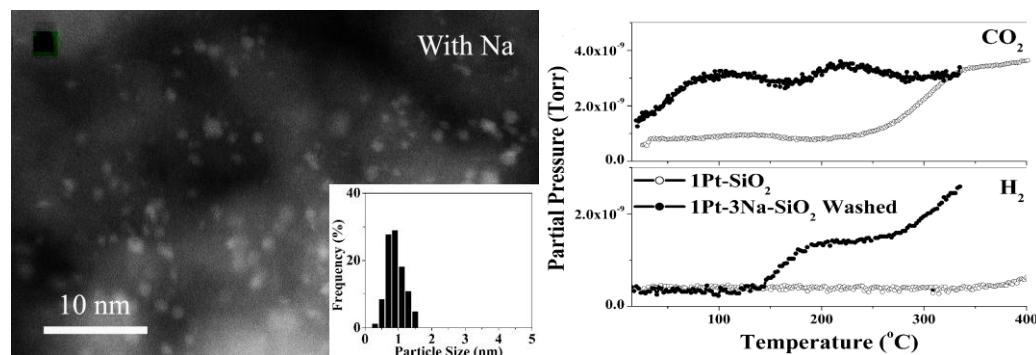


**Figure 6.** HAADF/aberration corrected-STEM image and Pt particle size distribution of 1Pt-3Na-SiO<sub>2</sub> washed sample and its corresponding CO-TPR; 5% CO-He, 20 cm<sup>3</sup>/min, 5°C/min. WGS reaction light off is at ~120°C. By comparison, the Na-free 1Pt-SiO<sub>2</sub> sample is inactive.<sup>15</sup>

### Future Directions

All the activities highlighted above are continuing in the near future. A comprehensive and complementary approach is followed in the project to elucidate the metal-oxide interaction at the atomic scale. A new task in next year's plan is the evaluation of alkali promotion of gold for the WGS and of other metals for the SRM reaction. Synthesis, characterization and evaluation of surface alloys for the reactions of methanol under study in the project will also continue. The desired outcome is a good mechanistic understanding of the chemistries under investigation, and of the stabilization of the key catalyst structures.

### References and Refereed Publications (since 2008) acknowledging this DOE Grant

Note: a reference in italics also belongs to the 'publications' list. Publications 18-21 were not referenced in this report.

1. "Active nonmetallic Au and Pt species on ceria-based water-gas shift catalysts", Q. Fu, H. Saltsburg, M. Flytzani-Stephanopoulos, *Science* 301(2003) 935-938.
2. "Activity and stability of low-content gold-cerium oxide catalysts for the water-gas shift reaction", Q. Fu, W. Deng, H. Saltsburg, M. Flytzani-Stephanopoulos, *Appl. Catal. B* 56 (2005) 57-68
3. "Shape and crystal-plane effects of nanoscale ceria on the activity of Au-CeO<sub>2</sub> catalysts for the water-gas shift reaction", R. Si, M. Flytzani-Stephanopoulos, *Angew. Chem. Int. Ed.* 47 (2008) 2884-2887.
4. "Steam reforming of methanol over ceria and gold-ceria nanoshapes", N. Yi, R. Si, H. Saltsburg, M. Flytzani-Stephanopoulos, *Appl. Catal. B* 95 (1-2) (2010) 87-92.
5. "Active gold species on cerium oxides nanoshapes for methanol steam reforming and the water-gas shift reactions", N. Yi, R. Si, H. Saltsburg, M. Flytzani-Stephanopoulos *Energy Environ. Sci.* 3 (2010) 831-837.

6. "Hydrogen Production from Methanol over Gold Supported on ZnO and CeO<sub>2</sub> Nanoshapes", M. B. Boucher, N. Yi, F. Gittleson, B. Zugic, H. Saltsburg, M. Flytzani-Stephanopoulos, *J. Phys. Chem. C* 115 (2011) 1261-1268.
7. "Shape effect in metal oxide supported nanoscale gold catalysts", M. Boucher, S. Goergen, N. Yi, M. Flytzani-Stephanopoulos, *Phys. Chem. Chem. Phys.* 115 (2011) 1261-1268.
8. "Comparison of the activity of Au/CeO<sub>2</sub> and Au/Fe<sub>2</sub>O<sub>3</sub> catalysts for the CO oxidation and the water-gas shift reactions", W. Deng, C. Carpenter, N. Yi, M. Flytzani-Stephanopoulos, *Top. Catal.* 44 (2007) 199-208.
9. "Reaction-relevant gold structures for the water-gas shift reaction on Au-CeO<sub>2</sub>", W. Deng, R. Si, A. Frenkel, M. Flytzani-Stephanopoulos, *J. Phys. Chem. C* 112 (2008) 12834-12840.
10. "The importance of strongly bound Pt-CeO<sub>x</sub> species for the water-gas shift reaction: catalyst activity and stability evaluation", D. Pierre; W. Deng, M. Flytzani-Stephanopoulos, *Top. Catal.* 46 (2007) 363-373.
11. "Charging and chemical reactivity of gold nanoparticles and adatoms on the (111) surface of single-crystal magnetite: A scanning tunneling microscopy/spectroscopy study", K.T. Rim, D. Eom, L. Liu, E. Stolyarova, J. M. Raitano, S.-W. Chan, M. Flytzani-Stephanopoulos, G. W. Flynn, *J. Phys. Chem. C* 113 (2009) 10198-10205.
12. "Evolution of gold structure during thermal treatment of Au/FeO<sub>x</sub> catalysts revealed by aberration-corrected electron microscopy", L.F. Allard, A. Borisovich, W. Deng, R. Si, S.H. Overbury, M. Flytzani-Stephanopoulos, *J. Electr. Micr.* 58 (2009) 199-212.
13. "Behavior of Au Species in Au/Fe<sub>2</sub>O<sub>3</sub> catalysts characterized by novel in situ heating techniques and aberration-corrected STEM imaging", L. F. Allard, S. H. Overbury, M. Flytzani-Stephanopoulos, *Micros. Microanal.* 16 (2010) 375-385.
14. W. Deng and M. Flytzani-Stephanopoulos, *Angew. Chem. Int. Ed.* 4 (2006) 2285-2289.
15. "Alkali-Stabilized Pt-OH<sub>x</sub> Species Catalyze Low-Temperature Water-Gas Shift Reactions", Y. Zhai, D. Pierre, R. Si, W. Deng, P. Ferrin, A. U. Nilekar, G. Peng, J. A. Herron, D. C. Bell, H. Saltsburg, M. Mavrikakis, M. Flytzani-Stephanopoulos, *Science* 329 (2010) 1633-1636.
16. "Scanning tunneling microscopy study of water adsorption on the reduced surface of a natural single Hematite  $\alpha$ -Fe<sub>2</sub>O<sub>3</sub> crystal: Implications for catalysis", K.T. Rim, D. Eom, S.W. Chan, M. Flytzani-Stephanopoulos, G.W. Flynn, *J. Phys. Chem. C*, submitted.
17. "Raman Analysis of Mode Softening in Nanoparticle CeO<sub>2-x</sub> and Au-CeO<sub>2-x</sub> during CO Oxidation", Y. Lee, G. He, A.J. Akey, R. Si, M. Flytzani-Stephanopoulos, I.P. Herman, *JACS*, in review.
18. "Controlled Synthesis of Co<sub>3</sub>O<sub>4</sub> Nanopolyhedra and Nanosheets at Low Temperature", H. Liang, J. M. Raitano, L. Zhang, S.-W. Chan, *Chem. Commun.* 48 (2009) 7569-7571.
19. "Cubic phase stabilization in nanoparticles of hafnia-zirconia oxides: Particle-size and annealing environment effects", C.-H Lu, J.M. Raitano, S. Khalid, L. Zhang, S.-W. Chan, *J. Appl. Phys.* 103 (2008) 124303/1-7.
20. "In situ ultra-small-angle X-ray scattering study of the solution-mediated formation and growth of nanocrystalline ceria", A. J. Allen, V.A. Hackley, P.R. Jemian, J. Ilavsky, J. M. Raitano, S.-W. Chan, *J. Appl. Crystal.* 41 (2008) 918-929.
21. "Structure Sensitivity of the Low-temperature Water-Gas Shift Reaction on Cu-CeO<sub>2</sub> Catalysts", R. Si, J. M. Raitano, N. Yi, H. Y. Liang, S.W. Chan, M. Flytzani-Stephanopoulos, *Catal. Today*, in press.

**Theoretical studies in heterogeneous catalysis and electrocatalysis**

Lead PIs: Jose A. Rodriguez (BNL), Michael G. White (BNL/SBU), Radoslav R. Adzic (BNL)

Postdocs: Alba Vidal (BNL), YongMan Choi (BNL)

Student: Yixiong Yang (SBU)

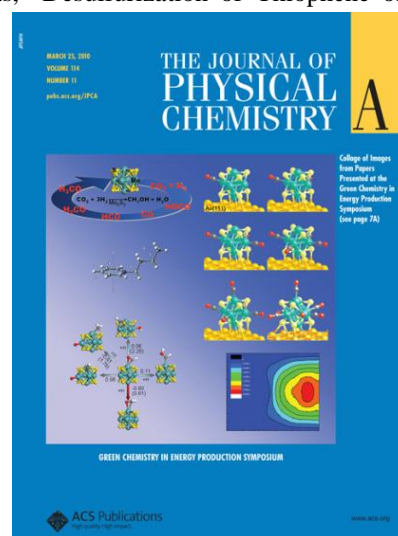
Contact: Chemistry Department, Brookhaven National Laboratory, Upton, NY11973;

[pingliu3@bnl.gov](mailto:pingliu3@bnl.gov)

Understanding the mechanisms and dynamics of catalyzed transformations and rational design on the basis of understanding have been the grand challenges for catalysis in energy. To accomplish this task requires not only enough knowledge of catalytic processes, which cannot be well characterized experimentally. This talk will focus on establishing a molecular level understanding of heterogeneous catalysis and electrocatalysis, and on developing, in strong interaction with experiments, new catalysts using combined density functional theory (DFT), kinetic modeling and sensitivity analysis. Such theoretical studies were implemented into four projects funded by DOE-BES: Catalysis: reactivity and structure (FWP: CO-09) [1,2], Catalysis on the nanoscale (FWP: CO-019) [3,4], In-situ studies of active sites and mechanism for the water-gas shift reaction on metal/oxide nanocatalysts (FWP: CO-027) [5,6] and Metal and Metal oxide-supported platinum monolayer electrocatalysts for oxygen reduction (FWP: MA-510-MAEA) [7,8]. The performed theoretical calculations not only well describe and understand the working catalysts observed experimentally, but also identify the key factors that control activity and provide guidance for discovery of better catalysts.

## References

1. Y. Choi, P. Liu, "Understanding of Ethanol Decomposition on Rh(111) from Density Functional Theory and Kinetic Monte Carlo Simulations", *Catalysis Today*, **165**, 64 (2011).
2. Y. Choi, P. Liu, "Mechanism of Ethanol Synthesis from Syngas on Rh(111)", *Journal of the American Chemical Society*, **131**, 13054 (2009).
3. P. Liu, Y. Choi, Y. Yang, M.G. White, "Methanol Synthesis from H<sub>2</sub> and CO<sub>2</sub> on a Mo<sub>6</sub>S<sub>8</sub> Cluster: a Density Functional Study", *Journal of Physical Chemistry A*, **114**, 3888 (2010).
4. J.A. Rodriguez, P. Liu, Y. Takahashi, K. Nakamura, F. Viñes, F. Illas, "Desulfurization of Thiophene on Au/TiC(001): Au-C Interactions and Charge Polarization", *Journal of the American Chemical Society*, **131**, 8595 (2009).
5. P. Liu, "Water-Gas Shift Reaction on Oxide/Cu(111): Rational Catalyst Screening from Density Functional Theory", *Journal of Chemical Physics*, **133**, 204705 (2010).
6. J. A. Rodríguez, J. Graciani, J. Evans, J. B. Park, F. Yang, D. Stacchiola, S. D. Senanayake, S. Ma, M. Pérez, P. Liu, J. F. Sanz, J. Hrbek, "Water-Gas Shift Reaction on a Highly Active Inverse CeO<sub>x</sub>/Cu(111) Catalyst: Unique Role of Ceria Nanoparticles", *Angewandte Chemie International Edition*, **48**, 8047 (2009).
7. K. Sasaki, H. Naohara, Y. Cai, Y. Choi, P. Liu, M. Vukmirovic, J. Wang, R. R. Adzic, "Core-Protected Platinum Monolayer Shell High-Stability Electrocatalysts for Fuel-Cell Cathodes", *Angewandte Chemie International Edition*, **47**, 8602 (2010).
8. J. X. Wang, H. Inada, L. Wu, Y. Zhu, Y. Choi, P. Liu, W.P. Zhou, R. R. Adzic, "Oxygen Reduction on Well-Defined Core-Shell Nanocatalysts: Particle Size, Facet, and Pt Shell Thickness Effects", *Journal of the American Chemical Society*, **131**, 17298 (2009).



### Modeling catalyzed growth of single-wall carbon nanotubes

Graduate Students: Diego A. Gómez-Gualdrón and Juan C. Burgos  
 Undergrad. students: Humberto Reyna, Gilbert McKenzie, Mariano Forti, and Erick Jones.  
 Collaborators: Boris Yakobson, Rice University, Houston, TX; Prof. Javier Alvarado, Instituto Tecnológico de Celaya, Mexico; Prof. Jie Liu, Duke University, NC  
 Contacts: Texas A&M University, 3122 TAMU, College Station, TX 77843, phone : 979-845-3375, e-mail: [balbuena@tamu.edu](mailto:balbuena@tamu.edu)

#### Goal

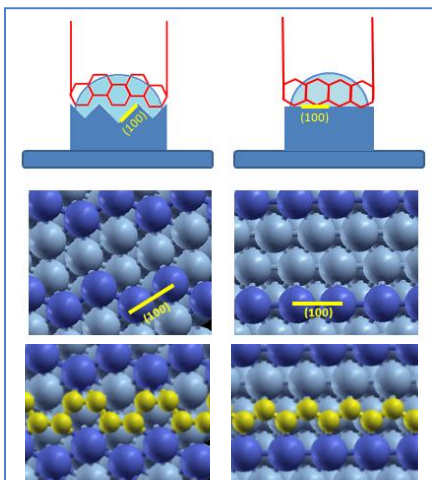
First principles computational methods are used to determine a) the role of morphology, size, and chemical composition of supported metal nanoparticles on the catalyzed synthesis of single-walled carbon nanotubes; b) role of the cluster-substrate interactions to establish a given nanocluster morphology; c) effect of the nanoparticle morphology and chemical composition on the selective growth of specific chiralities.

#### DOE Interest

Understanding selective nanotube growth is one of the current outstanding challenges for the development of technological applications using single-walled carbon nanotubes, especially for nanoelectronics, nanosensing, and biomedical uses. In addition, fundamental studies of carbon nucleation and growth on transition metal nanoparticles, as well as the dynamic evolution of the catalyst during growth provide new insights for rational design and control of many related catalytic processes where carbon is an undesired subproduct.

#### Recent Progress

*Influence of the surface pattern on the growth of specific structures:* Our density functional



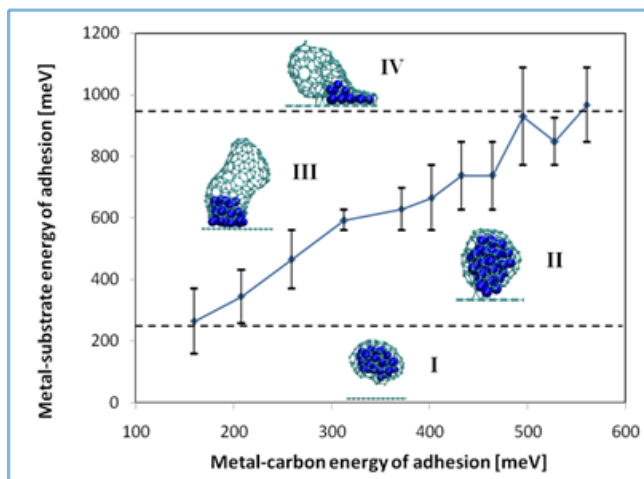
theory (DFT) studies demonstrated the existence of an inverse template effect during growth of carbon nanotubes using floating catalysts. Classical molecular dynamics (MD) simulations using a reactive force field proved the influence of a strongly interacting substrate on the structure of a metal nanocatalyst and illustrated how such interaction may help preserve catalyst crystallinity. DFT optimizations of carbon structures on stepped (211) and (321) cobalt surfaces showed the template effect imparted by the nanocatalyst surface on the growing carbon structure at early stages of nucleation. It was found that depending on the step structure and type of building block (short chains, single atoms, or hexagonal rings) thermodynamics

favor arm-chair or zig-zag termination, which provides guidelines for a chirality-controlled process based on tuning the catalyst structure and the type of precursor gas. Additional MD studies were used to prove the existence of a surface template for intermediate chiralities (between arm-chair and zig-zag).



*Effect of catalyst composition.* We investigated the effect of bimetallic and trimetallic compositions on C adsorption and absorption. The surfaces investigated belong to the group of  $\text{Fe}_2\text{Al-X}$  (with  $X = \text{Nb, Ti, and V}$ ) that have technological interest because of their anticorrosive properties.

*Effects of catalyst size and metal-substrate interactions on the growth of single-walled carbon nanotubes.* We developed a simple model combining thermodynamic and kinetic



effects to identify regions of single-wall carbon nanotube growth in the phase space defined by work of adhesion, temperature, and catalyst size. We constructed a growth diagram in the space of metal-substrate vs. metal-carbon strengths of adhesion, defining regions of nanotube growth and encapsulation. In the growth region we identify zones of higher or lower quality of the nanotubes grown. This theoretical characterization is very useful to guide a controlled synthesis.

## Future Plans

*Model of quartz substrates as templates for selective growth:* The morphology of Co and Fe clusters on  $\text{SiO}_2$  surfaces is studied using DFT methods. The results are used for the development of force fields to be used in classical MD simulations for assessing the surface template effect at realistic synthesis conditions. Specifically we are interested in determining the range of conditions (substrate and catalyst geometry) where horizontal nanotubes can grow, their growth mechanism, and the reasons for selective formation of semiconducting or metallic nanotubes (but not their mixture).

*Effect of adsorption of inert gases and water vapor on the growth.* We are also working on modifications to our reactive MD program to incorporate new features such as the presence of inert species (like  $\text{H}_2$ , He, steam) that increase the gas pressure but do not contribute to growth. However, higher gas pressures can modify the catalyst shape and occupy adsorption sites, thus modifying the nanotube growth behavior.

## Publications (2009-2011)

1. D. A. Gómez-Gualdrón, J. Zhao, and P. B. Balbuena, "Nanocatalyst structure as a template to define chirality of nascent single-wall carbon nanotubes," *J. Chem. Phys.* **134** (2011) 014705.
2. J. C. Burgos, E. Jones, and P. B. Balbuena, "Effect of the metal-substrate interaction strength on the growth of single-walled carbon nanotubes," *J. Phys. Chem. C.* **115** (2011) 7668-7675.
3. J. C. Burgos, H. Reyna, B. I. Yakobson and P. B. Balbuena, "Interplay of Catalyst Size and Metal-Carbon Interactions on the Growth of Single-Wall Carbon Nanotubes," *J. Phys. Chem. C* **114** (2010) 6952-6958.

4. M. A. Ribas, D. Feng, P. B. Balbuena, and B. I. Yakobson, "Nanotube nucleation versus carbon-catalyst adhesion: Probed by molecular dynamics simulations," *J. Chem. Phys.* **131** (2009) 224501.
5. D. A. Gómez-Gualdrón and P. B. Balbuena, "Effect of metal cluster-cap interactions on the catalyzed growth of single-wall carbon nanotubes," *J. Phys. Chem. C* **113** (2009) 698-709.
6. D. A. Gómez-Gualdrón and P. B. Balbuena, "Growth of chiral single-walled carbon nanotubes in the presence of a cobalt cluster," *Nanotechnology* **20** (2009) 215601.
7. G. E. Ramirez-Caballero, J. C. Burgos, and Perla B. Balbuena, "Growth of carbon structures on stepped (211) cobalt surfaces," *J. Phys. Chem. C* **113** (2009) 15658-15666.
8. G. E. Ramirez-Caballero, P. B. Balbuena, P. R. Alonso, P. H. Gargano, and G. H. Rubiolo "Carbon adsorption and absorption in  $L1_2$   $Fe_3Al$  surfaces," *J. Phys Chem. C.* **113** (2009) 18321-18330.

**Tuesday Afternoon**

**Session VI**

This page is intentionally blank.

## **In-situ Spectroscopy of Catalytic Solids at the Single Particle Level**

Bert M. Weckhuysen\*

Debye Institute for Nanomaterials Science, Utrecht University,  
Universiteitsweg 99, 3584 CG Utrecht, The Netherlands  
e-mail: b.m.weckhuysen@uu.nl

Heterogeneous catalysis is a fascinating, but complex multidisciplinary science, which is core business to our energy, automotive, chemical and pharmaceutical industries as most chemical reactions are catalyzed by at least one material containing a multitude of often distinct catalytic functionalities. Although progress has been made in our understanding of catalytic solids, their functioning under realistic reaction conditions represents still a very important scientific challenge to both academia and industrial scientists. Deep mechanistic insight in the fundamentals of heterogeneous catalysis can only be acquired by using advanced characterization methods as well as proper in-situ reaction cells and related measurement protocols. In recent years we have seen the development of space-resolved and tomographic characterization approaches, ultimately allowing performing single molecule-single catalyst particle in-situ studies.

In this lecture, such advanced spatiotemporal characterization methods for the characterization of individual zeolite crystals will be discussed. First, the intergrowth structure of zeolite H-ZSM-5 crystals is elucidated in great detail. For this purpose, a template burning method has been developed with confocal fluorescence microscopy, whereas the pore orientation of the individual building blocks can be assessed with Electron Back-Scattering Diffraction and Focused Ion Beam milling (EBSD-FIB). By analyzing a large set of various morphological distinct large H-ZSM-5 crystals a unifying view on the intergrowth structure of these materials could be obtained. Furthermore, by using TEM lamelling, electron diffraction studies in combination with AFM and XPS, it was possible to reveal outer and inner surface molecular diffusion boundaries affecting the overall performance of the crystals. In a second step, UV-Vis, synchrotron IR and fluorescence microscopy has been employed to map the formation of reaction products and the absorption spectra obtained allow for a kinetic analysis of the reaction products formed. In a third step, 3-D maps of the reactant and product molecules within the crystal are visualized with Coherent Anti-Stokes Raman Scattering (CARS) and confocal fluorescence microscopy. We have shown the capabilities of this multi-technique approach by using the styrene oligomerization as probe reaction for mapping Brønsted acidity in H-ZSM-5 crystals. Furthermore, we have extended this methodology to study the effect of mesoporosity in H-ZSM-5 crystals on their acidity, Al distribution and catalytic reactivity. In a final part of the lecture, in-situ nanoscale chemical imaging of zeolites will be presented by making use of the recently developed Scanning Transmission X-ray Microscopy (STXM) method.

**Structure-Property Relationship in Metal Carbides and Bimetallic Alloys**

**Graduate Students:** Daniel Esposito, Thomas Kelly, Michael Humbert (graduated in 2009), Carl Menning (graduated in 2009), Alan Stottlemeyer (graduated in 2010)

**Collaborators:** Dr. Anatoly Frenkel (Yeshiva Univ.)

**Contact:** Department of Chemical Engineering, University of Delaware, jgchen@udel.edu; telephone: 302-831-0642

**Goals:**

The objective of the current project is to use selected metal carbides and bimetallic alloys as model systems to unravel the relationship between the electronic/geometric structures and the chemical/catalytic properties to assist the rational design of alternative catalytic materials.

**DOE Interest:**

Metal carbides and bimetallic alloys are alternative catalysts that can either replace Pt or substantially reduce the amount of Pt in a wide range of catalytic and electrocatalytic applications. The proposed research, using a combination of surface science experiments, DFT calculations, and catalytic/electrocatalytic evaluations, should help in predicting and controlling the catalytic and electrocatalytic properties of transition metals in general and carbide/bimetallic catalysts in particular.

**Recent Progress:****A. ML Pt/WC as Low-Cost, Active and Stable Electrocatalysts**

Fuel cells, electrolyzers, and photoelectrochemical cells are electrochemical devices that are commonly touted as core technologies in a clean energy future. Central to the operation of all of these devices are electrocatalysts that assist the electrochemical reactions at the anode and cathode. Unfortunately, many state-of-the-art catalysts used in the aforementioned technologies are comprised of expensive Pt-group metals (Pt, Ru, Rh, Ir, and Pd). The high price and limited supplies of these precious metals create potentially prohibitive barriers to market penetration and scale-up production of devices requiring large catalyst loadings for efficient operation. Our effort in the past year was to take advantages of the Pt-like properties of transition metal carbides, such as tungsten monocarbide (WC), and use them as substrates to support one monolayer (ML) of Pt for use in electrochemical applications, including alcohol oxidation, oxygen reduction, and hydrogen evolution reactions. By using a low cost support substrate such as WC, the ML Pt-WC structure offers great potential to drive down catalyst costs for various electrochemical and photoelectrochemical applications.

In order to probe the similarities between ML Pt-WC and bulk Pt catalysts, DFT calculations were used to determine the binding energies of reactant molecules that are relevant to key electrochemical applications. For example, DFT calculations confirm that the hydrogen binding energy, a descriptor for hydrogen evolution reaction (HER) activity, is similar on ML Pt-WC(0001) and bulk Pt(111), suggesting that the two systems should have similar HER activity.

Such prediction has been verified experimentally on both Pt-WC thin films and powder catalysts. As shown in the Tafel curves in Figure 1a and the exchange current density in Figure 1b, the HER activity of the WC surface is far less than that of the Pt foil, but the addition of one ML of Pt to WC results in a surface with HER activity comparable to the bulk Pt foil. Furthermore, Figure 1c illustrates that the WC substrate is electrochemically stable under HER operation conditions. These discoveries were highlighted in a front cover in *Angewandte Chemie International Edition*. The opportunities and limitations of ML Pt-WC electrocatalysts for various electrochemical applications were described in an Invited Perspective in *Energy and Environmental Science*.

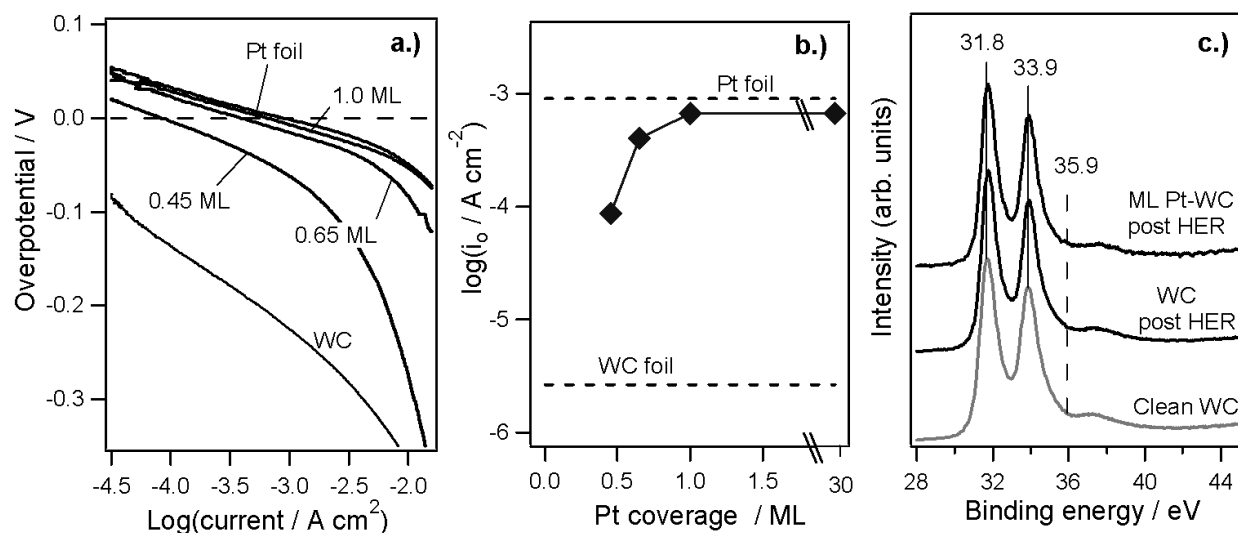


**Figure 1.** a.) Tafel curves comparing HER activity for ML amounts of Pt deposited on PVD WC thin film compared to unmodified WC and polycrystalline Pt foil in 0.5 M H<sub>2</sub>SO<sub>4</sub>. b.) HER exchange current density ( $i_0$ ) as a function of Pt coverage on WC thin film. Data have been modified from. c.) XPS W 4f peaks of WC and 1 ML Pt-WC following HER measurements compared to that of a clean WC surface.

## B. Controlling O-H, C-H, C-C and C-O Bond Scission on Ni/Pt and Ni/WC Surfaces

The motivation for investigating the thermal decomposition of alcohols on metal-modified WC is to replace Pt with less expensive metals. Using a combined experimental and theoretical approach, we demonstrated the general similarity between monolayer Ni/Pt and Ni/WC for the reforming of ethanol to produce syngas (H<sub>2</sub> and CO). Our results indicate that the monolayer Ni can be supported on a WC substrate instead of Pt, and that the electronic and chemical properties of the monolayer Ni are essentially identical, demonstrating the feasibility to use Pt-free catalysts for the reforming of oxygenate molecules.

## C. Extending Model Surfaces to Supported Catalysts

We continue our efforts in bridging the “materials gap” and “pressure gap” between UHV studies on model surfaces and catalytic evaluations on supported catalysts. For the latter we continue to utilize a wide range of characterization techniques, including in-situ EXAFS to confirm the formation of bimetallic structures in the supported catalysts. The hydrogenation of C=C and/or C=O bonds were then evaluated using both batch and flow reactors, which confirmed the strong correlation between model surfaces and supported catalysts.

## Selected Publications Acknowledging Current Grant during 2010-2011:

- D.V. Esposito and J.G. Chen\*, “Monolayer Platinum Supported on Tungsten Carbides as Low-Cost Electrocatalysts: Opportunities and Limitations”, *Energy and Environmental Science*, (**Invited Perspective**), accepted (2011). DOI: 10.1039/c1ee01851e
- M.P. Humbert, A.L. Stottlemeyer, C.A. Menning, and J.G. Chen\*, “Bridging the Materials Gap between Single Crystal and Polycrystalline Surfaces: Hydrogen Adsorption and Cyclohexene Hydrogenation on Ni/Pt Bimetallic Surfaces”, *Journal of Catalysis*, 280 (2011) 96-103.
- H. Ren, D.A. Hansgen, T.G. Kelly, A.L. Stottlemeyer and J.G. Chen\*, “Replacing Platinum with Tungsten Carbide (WC) for Reforming Reactions: Similarities in Ethanol Decomposition on Ni/Pt and Ni/WC Surfaces”, *ACS Catalysis*, 1 (2011) 390-398.
- R. Zheng, M.P. Humbert, Y. Zhu\* and J.G. Chen\*, “Low-temperature hydrogenation of the C=O bond of propanal over Ni-Pt bimetallic catalysts: From model surfaces to supported catalysts”, *Catalysis Science & Technology*, 1 (2011) 638-643.
- T.G. Kelly, A.L. Stottlemeyer, H. Ren and J.G. Chen\*, “Comparison of O-H, C-H and C-O Bond Scission Sequence of Methanol on Tungsten Carbide Surfaces Modified by Ni, Rh and Au”, *Journal of Physical Chemistry C*, 115 (2011) 6644-6650.
- I.J. Hsu, D.V. Esposito, E.G. Mahoney, A. Black, and J.G. Chen\*, “Electrodeposition of shape controlled Pt particles for methanol electrooxidation”, *Journal of Power Sources*, 196 (2011) 8307-312.
- S. Qi, W. Yu, W.W. Lonergan, B. Yang, and J.G. Chen\*, “General Trend in the Partial and Complete Hydrogenation of 1,4-Cyclohexadiene over Pt/Co, Pt/Ni and Pt/Cu Bimetallic Catalysts”, *ChemCatChem*, 2 (2010) 625-628.
- A.L. Stottlemeyer, P. Liu and J.G. Chen\*, “Controlling Bond Scission Sequence of Adsorbed Methanol by Modifying Surface Properties: Theoretical Predictions and Experimental Verification”, *Journal of Chemical Physics*, 133 (2010) 104702.
- M.C. Weidman, D.V. Esposito, I.J. Hsu and J.G. Chen\*, “The Electrochemical Properties of Tungsten and Tungsten Monocarbide (WC) Over Wide pH and Potential Ranges”, *Journal of the Electrochemical Society*, 157 (2010) F179-F188.
- C.A. Menning and J.G. Chen\*, “Regenerating Pt-3d-Pt Model Electrocatalysts through Oxidation-Reduction Cycles Monitored at Atmospheric Pressure”, *Journal of Power Sources*, 195 (2010) 3140-3144.
- M.P. Humbert, C.A. Menning, and J.G. Chen\*, “Replacing Bulk Pt in Pt-Ni-Pt Bimetallic Structures with Tungsten Monocarbide (WC): Hydrogen Adsorption and Cyclohexene Hydrogenation on Pt-Ni-WC”, *Journal of Catalysis*, 271 (2010) 132-139.
- J.P. Bosco, K. Sasaki, M. Sadakane, W. Ueda and J.G. Chen\*, “Synthesis and Characterization of Three-Dimensionally Ordered Macroporous (3DOM) Tungsten Carbide: Application to Direct Methanol Fuel Cells”, *Chemistry of Materials*, 22 (2010) 966-973.
- D.A. Hansgen, D.G. Vlachos\* and J.G. Chen\*, “First Principles-Based Bimetallic Catalyst Selection: An Application to the Ammonia Decomposition Reaction”, *Nature Chemistry*, 2 (2010) 484-489.
- D.V. Esposito, S.T. Hunt, A.L. Stottlemeyer, K.D. Dobson, B.E. McCandless, R.W. Birkmire and J.G. Chen\*, “Low-Cost Hydrogen Evolution Catalysts Based on Monolayer Platinum on Tungsten Monocarbide (WC) Substrates”, *Angewandte Chemie International Edition*, (**Journal Cover**, VIP) 49 (2010) 9859-9862.



**Tuesday Evening**

**Session VII**

This page is intentionally blank.

## Understanding activity and selectivity in syngas reactions

Additional PIs: Anders Nilsson, Felix Studt, Frank Abild-Pedersen, Thomas Bligaard  
Postdocs: Aleksandra Vojvodic, Jens Hummelshøj  
Students: Andrew J Medford,  
Collaborators: S. Dahl (Technical University of Denmark),  
Contact: SLAC National Accelerator Laboratory,  
Menlo Park, CA 94025, USA  
[norskov@stanford.edu](mailto:norskov@stanford.edu)

### Goal

The goal of the present project is to develop an understanding of the factors determining the rate and selectivity of syngas reactions, the conversion of a mixture of CO, CO<sub>2</sub> and H<sub>2</sub> into methane, methanol, higher alcohols and higher hydrocarbons. The work is part of the SLAC-based SUNCAT Center for Interface Science and Catalysis, which is formed to study the electronic and structural factors determining the catalytic properties of solid surfaces as a basis for the design of new catalysts. Syngas conversion is one class of reactions studied in the Center.

### DOE Interest

Syngas reactions form a good testing ground for the development of a quantitative understanding of catalytic processes. In spite of the simple reactants, syngas reactions process great complexity by having many different possible products. At present, it is still not understood in detail why some catalysts give some products while other give different ones. It is also not understood why no viable catalyst exists for the direct synthesis of higher alcohols. Syngas reactions are of immediate importance in the sustainable production of fuels. They can be used to convert solar hydrogen[1] into liquid fuels (by reducing CO<sub>2</sub>) or as an avenue in the conversion of biomass into liquid fuels (through gasification of biomass). The work addresses the fundamental challenges associated with the atomic-scale design of catalytic materials.

### Recent Progress

*Development of scaling relations:* By performing a series of density functional theory calculations of reaction energies and activation energies of a large number of elementary reactions involving C-C, C-O, C-H and O-H bond breaking (or formation) on a series of metal and oxide surfaces, we have shown how the activation energies scale with reaction energies and reaction energies scale with the adsorption energies of the atoms bonding to the surface[2,3].

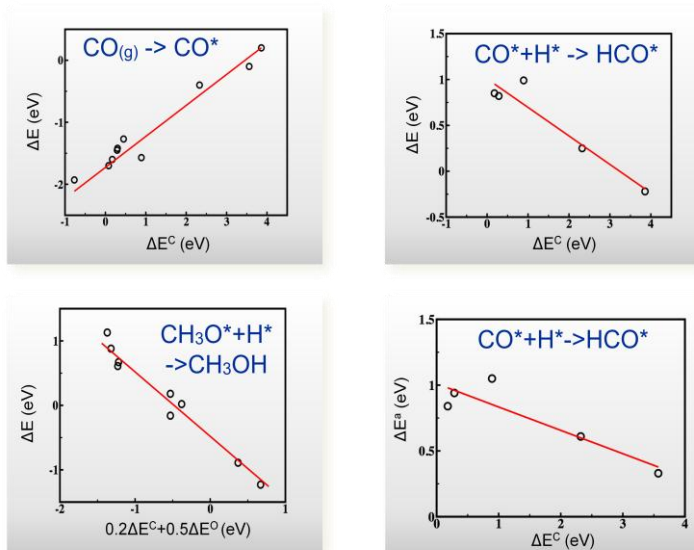


**Figure 1.** Scaling of calculated reaction energies and activation energies of elementary reactions of relevance to methanol synthesis with the oxygen and carbon adsorption energy on different stepped transition metal surfaces.

*Describing trends in methanol synthesis:* The scaling relations can be used to reduce the number of independent variables characterizing a surface[4]. For the case of methanol synthesis there are 18 reaction energies and activation energies in the problem (just for CO hydrogenation). The scaling relations provide a first estimate of all 18 relevant energies characterizing the full reaction based on knowledge of only the C and the O adsorption energies. This means, that we can calculate the variations in the methanol synthesis rate as a function of these variables, see in Figure 2.

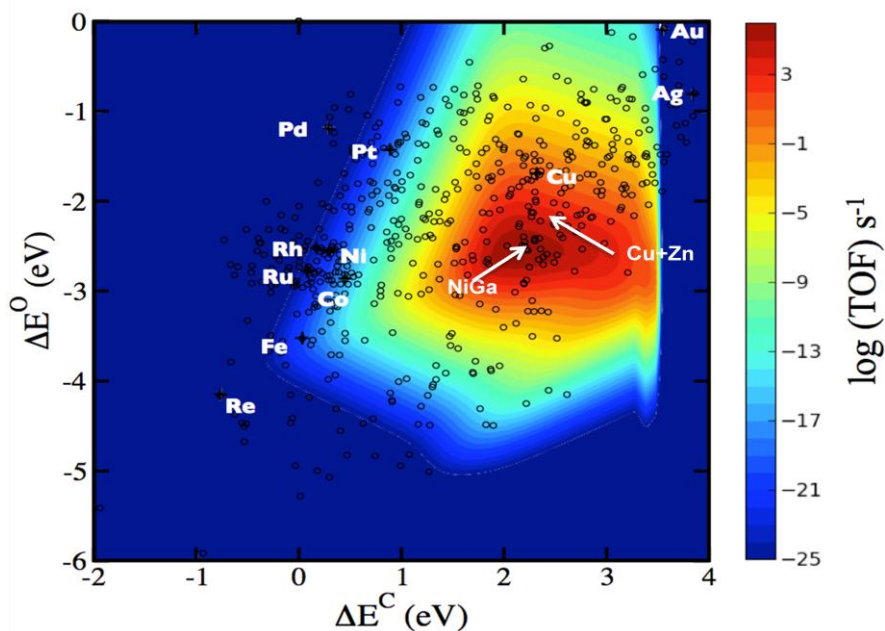


**Figure 2.** Calculated rate of methanol synthesis (513 K, 40 bar CO, 40 bar H<sub>2</sub>) as a function of the carbon and oxygen adsorption energy. The position of the elemental metals is indicated. The open circles signify values for binary alloys and values for Zn doped Cu and a NiGa alloy are marked.

*Identifying the active site of the Cu/ZnO/Al<sub>2</sub>O<sub>3</sub> catalyst for methanol synthesis.* One of the conclusions that have been reached from the theoretical studies is that a very active site in CO and CO<sub>2</sub> hydrogenation on Cu surfaces consists of a step with Zn atoms alloyed into the step, see Figure 2. Detailed experiments in the group of Robert Schlögl at the Fritz Haber Institute have led to the same conclusion, and together the theoretical and experimental studies provide a compelling model of the active site in the commercial catalyst.

*A new class of interesting alloy catalysts for methanol synthesis:* Once the descriptors of the activity have been identified (the C and O adsorption energies for methanol synthesis) it is simple to screen a number of alloys as potential catalysts (if they can be made and are stable). Figure 2 shows a number of such alloys included. Several have been tested in collaboration with the experimental group of Søren Dahl at the technical University of Denmark. An example of a very active Ni-Ga alloy is shown in Figure 3.

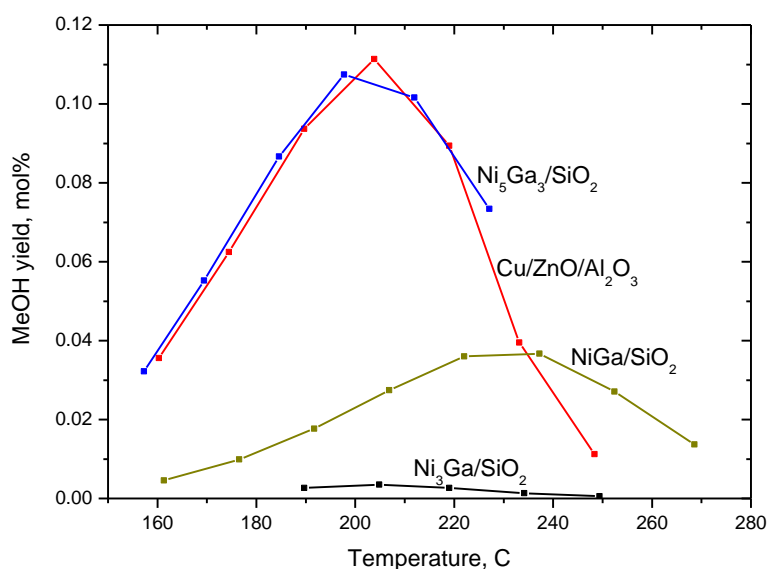


**Figure 3.** Measured methanol synthesis rate (1 bar) for different Ni-Ga alloys as compared with a Cu/ZnO(Al<sub>2</sub>O<sub>3</sub>) catalyst. Data from S. Dahl et al., DTU.

## Future Plans

*Development of a kinetic model including all possible reaction products.* We intend to further develop the DFT-based kinetic models to describe trends in selectivity towards different products.

*Studying C-C coupling on transition metal carbides.* The scaling relations give rise to specific bounds to the activity of the class of materials that obey them. Different structures have different scaling relations. The same is true for different types of oxides[3]. We will study carbides for C-C coupling in Fischer Tropsch synthesis and higher alcohol synthesis to see if we can find new, more active and selective classes of materials.

*Development of a detailed model of Fischer-Tropsch synthesis* . We plan to study the selectivity trends for C-C coupling in detail. We will develop models of adsorbate-adsorbate interactions and will apply them to a study of descriptors and trends in selectivity of the transition metals.

*Building up data-bases*: Catalyst design is based on identifying descriptors and using data bases to identify interesting leads. We will develop this formalism further to include several syngas reactions.

### **Publications (2010-2011)**

1. Y. Hou, B. L. Abrams, P. C.K. Vesborg, M. E. Björketun, K. Herbst, L. Bech, A. M. Setti, C. D. Damsgaard, T. Pedersen, O. Hansen, J. Rossmeisl, S. Dahl, J. K. Nørskov, I. Chorkendorff: *Bioinspired molecular co-catalysts bonded to a silicon photocathode for solar hydrogen evolution*, Nature Materials **10**, 434(2011)
2. S. Wang, B. Temel, J. Shen, Glenn Jones, L. C. Grabow, F. Studt, T. Bligaard, F. Abild-Pedersen, C. H. Christensen, J. K. Nørskov: *Universal Brønsted-Evans-Polanyi Relations for C-C, C-O, C-N, N-O, N-N, and O-O Dissociation Reactions*, Catal Lett **141**, 370 (2011)
3. A. Vojvodic, F. Calle-Vallejo, W. Guo, S. Wang, A. Toftelund, F. Studt, J. I. Martínez, J. Shen, I. C. Man, J. Rossmeisl, T. Bligaard, J. K. Nørskov, and F. Abild-Pedersen: *On the behavior of Brønsted-Evans-Polanyi relations for transition metal oxides* J. Chem. Phys. **134**, 244509 (2011)
4. J. K. Nørskov, F. Abild-Pedersen, F. Studt, T. Bligaard, *Density functional theory in surface chemistry and catalysis*, PNAS **108**, 937 (2011)

## Towards Realistic Reaction Environments in Catalysis Simulation

Students: Jason Bray  
Post-docs: Dr. Zhengzheng Chen, Dr. Jean-Sabin McEwen  
Collaborators: Fabio Ribeiro (Purdue)  
Contact: W. F. Schneider, 182 Fitzpatrick Hall, Notre Dame, IN 46556;  
Phone: (574) 631-8754; Email: [wschneider@nd.edu](mailto:wschneider@nd.edu)  
Web page: [www.nd.edu/~wschnei](http://www.nd.edu/~wschnei)

### Goal

Develop a theoretical framework to incorporate the effects of adsorbate coverage on the rates of reaction steps and their manifestation in observed reaction kinetics. Apply these models in the context of catalytic oxidations.

### DOE Interest

First-principles models have enabled a revolution in catalyst materials by design, by identifying descriptors or reactivity. To forge even tighter connections between experiment and simulation, it is important to develop simple yet reliable models that connect computed properties, like adsorption energies and reaction rates, to experimental observables, and to understand how these properties depend on details of catalyst structure and composition. This work will enhance the utility of computational methods for catalyst development.

### Recent Progress

*“Basis site” model of catalytic oxidations over Pt(111)*: The observed rate of reaction over a catalytic surface is a sum over the rates at individual reactions “sites”:

$$r = \sum_i \tilde{r}_i \tilde{s}_i \quad (1)$$

Sites might be distinguished by local structural features of a catalyst particle, such as steps or edges, by local variations in composition, as in an alloy catalyst, or by the local coverage of adsorbates. We have been focusing on this last case, in the context of catalytic oxidations over Pt. We have developed carefully validated representations of an O-covered Pt(111) surface, used these representations to characterize surface reaction sites, developed a Brønsted-Evans-Polyani type relationship for the dependence of a representative reaction rate, O<sub>2</sub> dissociation, on the site type, and constructed rate averages using equation (1) as a function of reaction conditions. The approach lends itself to calculating rate derivatives for comparison with experiment, to analysis of the most kinetically relevant sites in a surface reaction, and guidance on how to best incorporate site-specific information into DFT calculations of surface reactions.

*Reaction kinetics at a low symmetry surface*: The work described above has focused on the high-symmetry, Pt(111) surface, which provides a number of computational and conceptual simplifications. To take the next step towards something more representative of a high surface area catalyst particle, we are carrying out a similar analysis on the stepped, kinked Pt(321) surface. This facet presents a variety of reaction sites solely due to its low symmetry, which we

have characterized and correlated with experimental observation. Further, adsorbate coverage effects the type and distribution of sites in distinct ways, which we are capturing through the use of a “cluster expansion,” which represents the energy of a configuration of adsorbates in terms of pair, triplet, ..., interactions with other adsorbates.

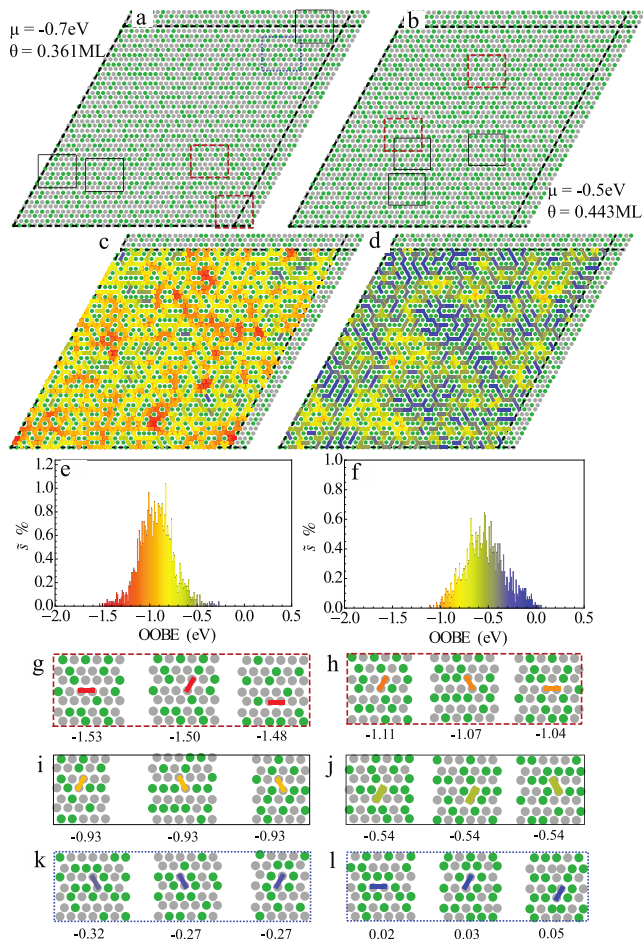


Figure 1. Equilibrium distributions of O adsorbates on a Pt(111) surface under two conditions (a,b), color coded to identify “hot” and “cold” regions of reactivity (c,d), density distributions of sites (e,f), and zoom ins on configurations.

*Transition from chemisorption to surface oxidation:* Both models described above consider the particle surface to be a static backdrop atop which reactions occur. But particles can respond to their reaction environments in more complicated ways, for instance by reconstructing. In this part of this project, we are examining the oxygen-induced reconstruction of the Pt(111) surface and its effects on local reaction sites and rates. Work to date has identified the conditions necessary to induce a reconstruction on this surface, and the structural and energetic evolution that accompanies reconstruction. We intend to generate a cluster expansion that spans the non-reconstructed and reconstructed regimes, enabling us to calculate reaction rates using an approach like that in equation (1).

### Future Plans

With this general framework in place, we intend to expand in several directions: to use results for several types of surface structures to build a model for catalyst particles that would allow the effect of particle size on reactivity to be predicted; to explore metals other than Pt and in



particular to explore surface alloying as another discriminator of reaction sites; and to consider reactions beyond NO oxidation whose rates depend on different types of descriptors.

**Publication (2009-2011)**

1. J. M. Bray and W. F. Schneider, "Potential Energy Surfaces for Oxygen Adsorption, Dissociation, and Diffusion at the Pt(321) Surface," *Langmuir*, **2011**, in press
2. H. Wang and W. F. Schneider, "Adsorption and Reactions of NO<sub>x</sub> on RuO<sub>2</sub>(110)," *Catal. Today*, **2011**, *165*, 49-55.
3. L. Xiao and W. F. Schneider, "Influence of  $\alpha$ -Alumina Supports on Oxygen Binding to Pd, Ag, Pt, and Au," *Chem. Phys. Lett.* **2010**, *484*, 231-236.
4. Wang, H.; Schneider, W. F., Nature and role of surface carbonates and bicarbonates in CO oxidation over RuO<sub>2</sub>. *Phys. Chem. Chem. Phys.* **2010**, *12*, 6367-6374.
5. Wang, H.; Schneider, W. F., Molecular origins of surface poisoning during CO oxidation over RuO<sub>2</sub>(110). *Surf. Sci.* **2009**, *603* (16), L91-L94.
6. Getman, R. B.; Schneider, W. F., DFT-Based Coverage-Dependent Model of Pt-Catalyzed NO Oxidation. *ChemCatChem* **2010**, *2*, 1450-1460.
7. Getman, R. B.; Schneider, W. F.; Smeltz, A. D.; Delgass, W. N.; Ribeiro, F. H., Oxygen-Coverage Effects on Molecular Dissociations at a Pt Metal Surface. *Phys. Rev. Lett.* **2009**, *102* (7), 076101-4.

## Investigations of C-X Bond Activation on Doped Metal Oxide Catalysts

Postdocs: Sudhanshu Sharma, Zhenpeng Hu, Bo Li

Graduate Students: Alan Derk, Lauren Misch

Undergraduate Students: George Moore, Ross Brunson

**Contacts:** Professor Eric McFarland (805-8934343, mcfar@engineering.ucsb.edu), Dept. of Chemical Engineering, Professor Horia Metiu (805-8932256, metiu@chem.ucsb.edu), Dept. of Chemistry and Biochemistry, University of California, Santa Barbara, CA 93106

### Overall Goals:

To synthesize and characterize the activity of new substitutionally doped metal oxide catalysts, predicted by density functional theory, capable of activating C-x bonds. This project is a joint experimental-theoretical effort aimed at the controlled activation of the C-H bond for the partial oxidation and oxidative dehydrogenation of methane, ethane, propane, and propene.

### DOE Interest:

Understanding and controlling hydrocarbon reactivity is essential for developing technical strategies to improve and optimize existing processes and develop new routes for the production and utilizations of hydrocarbon containing fuels and chemicals. Doped oxides, in which a few cations in a host oxide are replaced with heteroatoms, are interesting new catalysts for alkane activation. Very few have been studied and it is very likely that among so many possible dopant/oxide combinations there are some dopant-host pairs that can break efficiently the C-H bond in methane, ethane, or propane to initiate and control partial oxidation or oxidative dehydrogenation chemistry useful for the conversion of U.S. natural gas and shale gas resources.

### Recent Progress:(1-15)

1. We have used a combination of theory and experiments to show that ZnO substitutionally doped with Ti or Al oxidizes CO by several parallel reaction pathways that differ from the traditional Mars-van Krevelen (MVK) mechanism. In one, the dopant atoms at the surface of the doped oxide adsorb and activate O<sub>2</sub> so that it reacts with CO. In the other, a surface oxygen atom from the lattice next to the dopant, D, moves onto the dopant and creates an O-D group and an oxygen vacancy. The O-D group is capable of oxidizing a reductant. To test these predictions made by theory, we prepared Ti- and M-doped ZnO and have shown that these compounds oxidize CO at temperatures at which pure-phase ZnO, Al<sub>2</sub>O<sub>3</sub>, or TiO<sub>2</sub> do not. The plausibility of the proposed mechanisms was tested by studying CO oxidation with isotopically labeled oxygen.
2. Density functional theory has led us to document two rules. (1) The presence of a low-valence dopant makes the oxide a better oxidant. (2) A chemical compensation effect which shows that adsorbing an electron donor on the surface of an oxide activated by low-valence dopant, counteracts strongly the effect of the dopant. We have found the potential for both local and global effects of the dopant on catalytic chemistry. We have tested these rules and other predictions in our experimental studies.

3. We extended our understanding of the impact of specific dopants and the vacancy energetics in C-O oxidation to activation and transformation of the C-H bond. We have found that the choice of dopant strikes a fine balance between the ability to dissociate the C-H bond on the dopant and oxidize the reactant, with the ability to form surface oxygen vacancies. We have examined electrophilic Pt and Ru as atomic dopants in ceria hosts to regulate and utilize changes in the energy to make oxygen vacancies and therefore the ability of the surface to act as an oxidant. We have studied catalytic activity of Pt-doped CeO<sub>2</sub> for the combustion and partial oxidation and for the dry reforming of methane. The catalyst was prepared by three methods resulting in ceria containing different ratios of ionic Pt versus Pt. We show that these materials have different catalytic activity for methane oxidation and dry reforming and that they are more active when the fraction of ionic Pt is increased. Density functional theory was used to help understand the role of Pt dopant. It was found that the presence of Pt activates the oxygen atoms next to it in the surface layer and this decreases the activation energy for dissociative adsorption of methane (which is the rate-limiting step in the reaction). Whereas complete combustion of methane in oxygen occurs preferentially on traditionally supported Pt catalysts, high selectivity for the partial oxidation of methane to CO and H<sub>2</sub> was achieved on Pt-doped CeO<sub>2</sub>. The critical step in facilitating the synthesis gas formation is the decrease in the energy of oxygen-vacancy formation caused by the Pt doping.

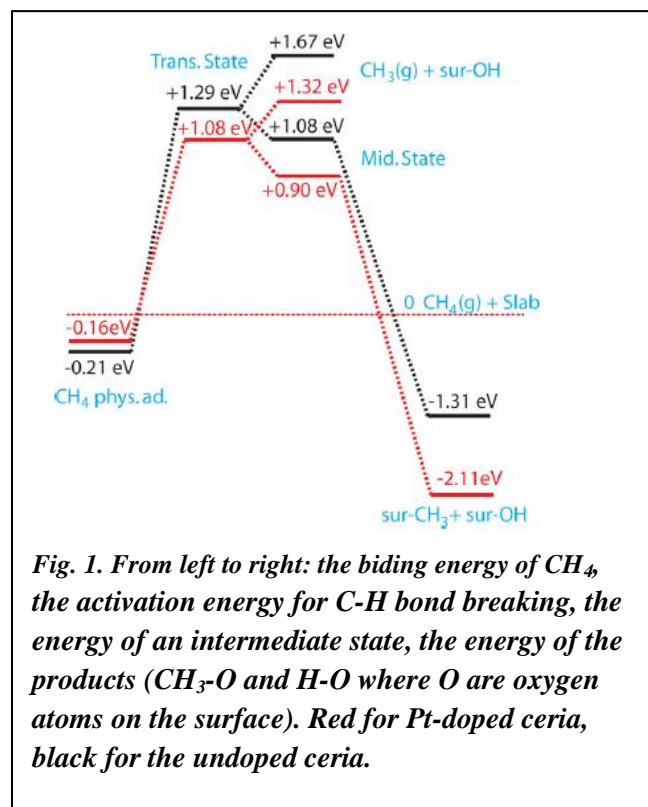


**Fig. 1.** From left to right: the binding energy of CH<sub>4</sub>, the activation energy for C-H bond breaking, the energy of an intermediate state, the energy of the products (CH<sub>3</sub>-O and H-O where O are oxygen atoms on the surface). Red for Pt-doped ceria, black for the undoped ceria.

4. Reduction of CO<sub>2</sub> by hydrogen traditionally follows the FT mechanism pathway where CO<sub>2</sub> is reduced to CO via formate ion intermediate. CO thus formed is hydrogenated further to eventually give methane. We have studied the methanation of CO<sub>2</sub> catalyzed by ceria doped with Ni, Co, Pd, or Ru. Ce<sub>0.96</sub>Ru<sub>0.04</sub>O<sub>2</sub> and Ce<sub>0.95</sub>Ru<sub>0.05</sub>O<sub>2</sub> perform best, converting 55% of CO<sub>2</sub> with a 99% selectivity for methane, at a temperature of 450 C. This is comparable to the best catalysts found previously for this reaction. Ce<sub>0.95</sub>Ru<sub>0.05</sub>O<sub>2</sub> was characterized by XRD, electron microscopy, BET, XPS, IR spectroscopy, and temperature-programmed reaction with Ar, H<sub>2</sub>, CO, and CO<sub>2</sub> + H<sub>2</sub>. Steady-state methanation was studied at several temperatures between 100 and 500 degrees C. We find that the methanation reaction takes place on the reduced Ce<sub>0.95</sub>Ru<sub>0.05</sub>O<sub>2</sub>, and the role of the dopant is to make the reduction

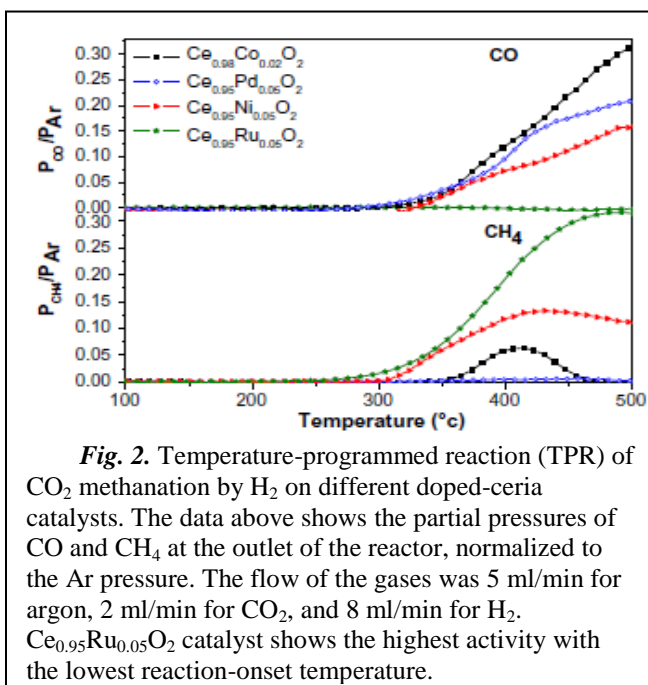


**Fig. 2.** Temperature-programmed reaction (TPR) of CO<sub>2</sub> methanation by H<sub>2</sub> on different doped-ceria catalysts. The data above shows the partial pressures of CO and CH<sub>4</sub> at the outlet of the reactor, normalized to the Ar pressure. The flow of the gases was 5 ml/min for argon, 2 ml/min for CO<sub>2</sub>, and 8 ml/min for H<sub>2</sub>. Ce<sub>0.95</sub>Ru<sub>0.05</sub>O<sub>2</sub> catalyst shows the highest activity with the lowest reaction-onset temperature.

possible at lower temperature than on pure ceria. We found that if Ru is doped in the CeO<sub>2</sub> matrix (rather than dispersed as nano particles) the mechanism is significantly different than previously thought. CO and hydrogen do not react, whereas CO<sub>2</sub> and hydrogen give methane at high selectivity. Bicarbonates are found to be essential for methanation. Ce<sub>0.95</sub>Ru<sub>0.05</sub>O<sub>2</sub> shows long time stability without being deactivated by the deposition of carbonaceous species. Activity is maintained because of the ionic nature of dopant Ru in CeO<sub>2</sub>.

## Future Plans

1. Continue DFT based calculations of cation and anion doped oxides with emphasis on C-H bond activation and use of CO<sub>2</sub> as a source of surface active oxygen utilizing other transition metal and lanthanide hosts.
2. In addition to relative activities, characterize quantitatively the catalytic properties of the most interesting doped oxide catalysts for C-H and C-O bond activation under steady-state and transient conditions in differential reactor configurations and examine the dependencies of reactivity on temperature and reactant compositions.
3. Examine the performance of doped oxides as regenerable solid reactants in chemical looping oxidation/reduction reactions.
4. Continue the development of consistent methods to synthesize and demonstrate that true “doped oxides” are achieved and not mixed phases.

## List of Publications Funded by this Grant (2008-2011)

1. Sharma S, Hu ZP, Zhang P, McFarland EW, Metiu H. CO<sub>2</sub> methanation on Ru-doped ceria. *Journal of Catalysis*. 2011;278(2):297-309.
2. Zhang P, Chi MF, Sharma S, McFarland E. Silica encapsulated heterostructure catalyst of Pt nanoclusters on hematite nanocubes: synthesis and reactivity. *Journal of Materials Chemistry*. 2010;20(10):2013-2017.
3. Tang W, Hu ZP, Wang MJ, Stucky GD, Metiu H, McFarland EW. Methane complete and partial oxidation catalyzed by Pt-doped CeO<sub>2</sub>. *Journal of Catalysis*. 2010;273(2):125-137.
4. Park JN, Zhang P, Hu YS, McFarland E. Synthesis and characterization of sintering-resistant silica-encapsulated Fe<sub>3</sub>O<sub>4</sub> magnetic nanoparticles active for oxidation and chemical looping combustion. *Nanotechnology*. 2010;21(22).
5. Forman AJ, Park JN, Tang W, Hu YS, Stucky GD, McFarland EW. Silica-Encapsulated Pd Nanoparticles as a Regenerable and Sintering-Resistant Catalyst. *Chemcatchem*. 2010;2(10):1318-1324.
6. Tang W, Jayaraman S, Jaramillo TF, Stucky GD, McFarland EW. Electrocatalytic Activity of Gold-Platinum Clusters for Low Temperature Fuel Cell Applications. *Journal of Physical Chemistry C*. 2009;113(12):5014-5024.
7. Park JN, McFarland EW. A highly dispersed Pd-Mg/SiO<sub>2</sub> catalyst active for methanation of CO<sub>2</sub>. *Journal of Catalysis*. 2009;266(1):92-97.
8. Pala RGS, Tang W, Sushchikh MM, et al. CO oxidation by Ti- and Al-doped ZnO: Oxygen activation by adsorption on the dopant. *Journal of Catalysis*. 2009;266(1):50-58.

9. Tang W, Lin HF, Kleiman-Shwarsstein A, Stucky GD, McFarland EW. Size-dependent activity of gold nanoparticles for oxygen electroreduction in alkaline electrolyte. *Journal of Physical Chemistry C*. 2008;112(28):10515-10519.
10. Sushchikh M, Cameron L, Metiu H, McFarland EW. Size and Pressure Independent Kinetics of CO Oxidation on Alumina-Supported Iridium Nanoparticles. *International Journal of Chemical Kinetics*. 2008;40(12):826-830.
11. Park JN, Forman AJ, Tang W, et al. Highly Active and Sinter-Resistant Pd-Nanoparticle Catalysts Encapsulated in Silica. *Small*. 2008;4(10):1694-1697.
12. Hu Z, Metiu H. Choice of U for DFT+U calculations for titanium oxides. *J. Phys. Chem. C*. 2011;115(13):5841-5845.
13. Hu Z, Li B, Sun X, Metiu H. Chemistry of doped oxides: The activation of surface oxygen and the chemical compensation effect. *J. Phys. Chem. C*. 2011;115(7):3065-3074.
14. Chrétien S, Metiu H. Electronic structure of partially reduced rutile TiO<sub>2</sub>(110) surface: Where are the unpaired electrons located? *J. Phys. Chem. C*. 2011;115(11):4696-4705.
15. Li B, Metiu H. DFT studies of oxygen vacancies on undoped and doped La<sub>2</sub>O<sub>3</sub> surfaces. *J. Phys. Chem. C*. 2010;114(28):12234-12244.

This page is intentionally blank.

**Wednesday Morning**

**Session VIII**

This page is intentionally blank.



## **Catalytic depolymerization and hydrodeoxygenation of lignin**

Johannes A. Lercher

Pacific Northwest National Laboratory, Institute for Integrated Catalysis,  
Richland WA 99352

e-mail: [johannes.lercher@pnl.gov](mailto:johannes.lercher@pnl.gov)

TU München, Department of Chemistry and Catalysis Research Center,  
Garching 85748, Germany

e-mail: [johannes.lercher@ch.tum.de](mailto:johannes.lercher@ch.tum.de)

Lignin, but also byproducts of the primary conversion such as substituted phenols are interesting niche alternatives as raw materials for energy carriers and chemicals. The lecture will outline the successful strategies to produce phenol monomers and oligomers from lignin, as well as stopping the re-polymerization of the primary products. The main reaction route utilized is hydrolysis, but radical reactions occurring at lower solvent densities will also be discussed. The key elementary steps involved in the hydrogenation and hydrodeoxygenation of the intermediate products need dual (i.e., metal and acid-base) catalytic functions. It will be shown that the elementary steps during hydrodeoxygenation in aqueous phase are drastically different from those in gas phase reactions. The boundary conditions for full hydrogenation, hydrodeoxygenation and ring opening reactions of the primary products will be discussed to indicate the potential for synthesizing fuel components.

**In Situ NMR/IR/Raman and ab initio DFT Investigations of Pt-Based Mono- and Bi-metallic Nanoscale Electrocatalysts: from Sulfur-Poisoning to Polymer Promoters to Surface Activity****Indexes**

Postdocs: In-Su Park, Bolian Xu  
Ph. D Students: Dianne Atienza, Augusta M. Hofstead-Duffy, Dejun Chen  
Undergraduates: Thomas Hsu-Yao, Brian McCuire, Steven M. Ryckbosch, Ashley Zacca, Jessica Lucas, Bao Nguyen  
Contact: Department of Chemistry, Georgetown University, 37<sup>th</sup> & O Streets, NW, Washington, DC 20057; yyt@georgetowntown.edu

**Goal**

The long-term objectives of our research effort are two folds: 1. Advance significantly our fundamental understanding of sulfur poisoning of Pt-based mono- and bi-metallic nanoscale electrocatalysts through careful interrogation of long and short range electronic effects caused by the poisonous sulfur-metal bonding. 2. Investigate and establish correlations among the surface d band center, the frontier orbitals of the metal surface as represented by the surface local density of states at the Fermi level ( $E_f$ -LDOS), and the associated electrochemical reactivity.

**DOE Interest**

Lack of detailed molecular level information on how sulfur-metal interaction poisons heterogeneous catalysts in general and electrocatalysts in particular impedes significantly the pace of developing practically viable sulfur-tolerant catalysts. Achieving the aforementioned objectives should help in a significant way the development of sulfur-tolerant catalysts by providing much needed molecular level electronic/geometric structure – functionalities relationships.

**Recent Progress**

**1. Chemical state of adsorbed sulfur on Pt nanoparticles:** Chemical state and structure of adsorbed sulfur on Pt surface in general have been an outstanding subject of debate (monolayer vs multilayer and zero valence vs negative charged) and no consent has been reached until very recently. In our study, we first carried out rather detailed EC study (left low corner of Figure 1) of the problem but could not answer these outstanding questions based solely on the EC data obtained on commercial Pt black and Pt/C nanoparticles (NPs). The accumulative oxidation charges seemed to suggest a multi-layer structure. We then carried out in situ sulfur-coverage-dependent SERS

study of sulfur-covered Pt surface (as shown at the left and right up corners in Figure 1). Still, the in situ SERS could only indicate that there probably existed only one dominant sulfur species but was unable to provide a definitive answer. Finally, with the assistance of detailed *ab initio* DFT calculation, we were able to pinpoint that the dominant sulfur species most likely adsorbed on Pt in a monolayer structure with S<sup>2-</sup> as the chemical state. This combined approach is illustrated by Figure 1. Accordingly, we proposed the following reaction stoichiometry for the electro-oxidation of the adsorbed sulfur species:



Additionally, we have also observed an interesting hysteresis for blocking the hydrogen adsorption

sites by a given S coverage generated by S adsorption or by S desorption (S-EO stripping), attributed to the different S partition patterns on the Pt NP surfaces. Although differences do exist, the general effect of the S<sub>ads</sub> observed in Pt/C and Pt black was remarkably similar. It is therefore expected that the clear identification of the chemical state of the S<sub>ads</sub> on Pt NPs and of the different S partition patterns depending on the adsorption or desorption process, will have important ramifications in terms of understanding the chemistry of sulfur poisoning as well as promotion of catalytic activity of the underlying metals.

**2. An in situ SERS Investigation of the Chemical States of Sulfur Species Adsorbed onto Pt from Different Sulfur Sources.** The study focused on in situ SERS spectroelectrochemistry investigation of sulfur adsorption and electro-oxidation on highly roughened polycrystalline Pt surface. It was intended to address a specific question: Does the final chemical state of the adsorbed sulfur species depend on the initial chemical state of the sulfur in deposition sources? Three different sulfur deposition sources were used: Na<sub>2</sub>S solution, electrochemically reductive SO<sub>2</sub> solution, and S<sup>0</sup> suspension. In all cases, the same dominant vibrational band at 300 cm<sup>-1</sup> was observed on the freshly prepared S-adsorbed Pt electrode, indicating the same chemical state of the adsorbed sulfur which was recently assigned as the Pt-S<sup>2-</sup> (see Sect. 1 above). Possible spill-over sulfur adsorption from the deposited solid polymeric S<sup>0</sup><sub>8</sub> was observed. The three sharp peaks at 150 cm<sup>-1</sup>, 220 cm<sup>-1</sup>,

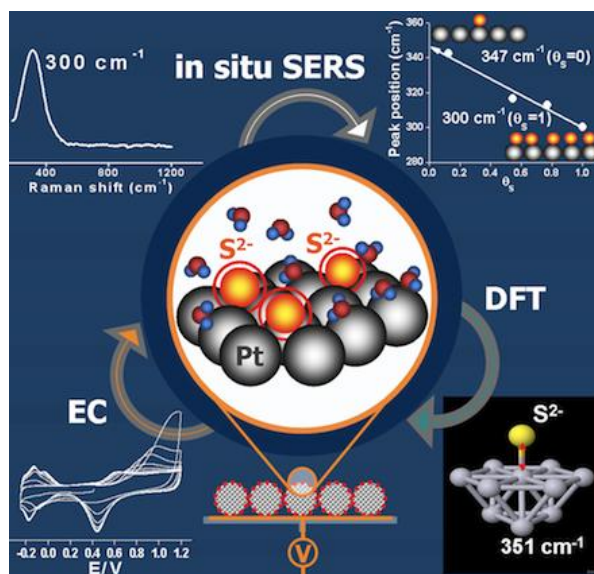


**Figure 1.** A combination of electrochemistry (left low corner), *in situ* SERS (left and right up corners), and *ab initio* DFT (right low corner) studies has pinpointed the adsorbed sulfur species on Pt NPs as a negatively charged sulfide S<sup>2-</sup> (carton in the middle).

and  $470\text{ cm}^{-1}$  in the SERS spectra are characteristic to the polymeric  $\text{S}_8$  species. As can be seen, their amplitude became constant after the 1<sup>st</sup> oxidative CV, indicating that a substantial amount of  $\text{S}_8$  could stay on the electrode surface without being electro-oxidized. Such  $\text{S}_8$  could be one of the sources for S spill-over that flattened the CV profile in region more positive than  $\sim 0.7\text{V}$  after the stable CV was reached, i.e., no clear current hump at  $\sim 0.7\text{V}$  was observed. Indeed, the band at  $300\text{ cm}^{-1}$ , although its intensity decreased, still exists even after the 21<sup>st</sup> CV. We speculate that a constant (steady-state) small amount of S diffuse out of the spill-over source (probably solid polymeric  $\text{S}_8$ ) and adsorb onto the Pt electrode that would be electro-oxidized during the subsequent CV scan.

Overall, this work yielded important information on sulfur adsorption and electro-oxidation on roughened, polycrystalline platinum surfaces and demonstrated clearly the applicability and usefulness of the in situ SERS spectroelectrochemistry in investigating the chemistry of sulfur adsorption/poisoning on platinum surfaces.

#### **Publications (2009-2011)**

1. Thomas Hsu-Yao, Kevin P. Browne, Nicole Honesty, YuYe J. Tong, "Polyoxometalate-Stabilized Pt Nanoparticles and Their Electrocatalytic Activities", *Phys. Chem. Chem. Phys.*, **2011**, *13*, 7433-7438.
2. De-Jun Chen, Augusta M. Hofstead-Duffy, In-Su Park, Dianne O. Atienza, Ceren Susut, Shi-Gang Sun, and YuYe J. Tong, "Identification of the most active sites and surface water species: A comparative study of CO and methanol oxidation reactions on core-shell M@Pt (M=Ru, Au) nanoparticles by in situ IR spectroscopy", *J. Phys. Chem. C*, **2011**, *115*, 8735–8743.
3. Thomas C. Allison and YuYe J. Tong, "Evaluation of Methods to Predict Reactivity of Gold Nanoclusters", *Phys. Chem. Chem. Phys.*, **2011**, *13*, 12858-12864
4. Ceren Susut, YuYe J. Tong, "Size Dependent Methanol Electro-oxidation Activity of Pt Nanoparticles with Different Shapes", *Electrocatalysis*, **2011**, *2*, 75-81.
5. Ceren Susut, De-Jun Chen, Shi-Gang Sun, YuYe J. Tong, "Capping Polymer-Enhanced Electrocatalytic Activity on Pt Nanoparticles: A Combined Electrochemical and in situ IR Spectroelectrochemical Study", *Phys. Chem. Chem. Phys.*, **2011**, *13*, 7467-7474.
6. Bingchen Du, Oksana Zaluzhna, YuYe J. Tong, "Electrocatalytic properties of Au@Pt nanoparticles: effects of Pt shell packing density and Au core size", *Phys. Chem. Chem. Phys.*, **2011**, *13*, 11568-11574.
7. In-Su Park, Bolian Xu, Dianne O. Atienza, Augusta M. Hofstead-Duffy, Thomas C. Allison, and YuYe J. Tong, "Chemical State of Adsorbed Sulfur on Pt Nanoparticles", *ChemPhysChem*, **2011**, *12*, 747-752.
8. Bolian Xu, In-Su Park, Ying Li, De-Jun Chen, YuYe J. Tong, "In situ Surface-Enhanced Raman Scattering Spectroscopic Study of Sulfur Adsorption on Polycrystalline Platinum Electrode Surface", *Electrochemistry* (Chinese Chemical Society), **2010**, *16*, 255-262.
9. Bingchen Du, S. A. Rabb, C. Zangmeister, YuYe Tong, "A Volcano Curve: Optimizing Methanol Electro-oxidation on Pt-decorated Ru Nanoparticles", *Phys. Chem. Chem. Phys.* **2009**, *11*, 8231 - 8239.

**Modern Catalytic Technologies for Converting Biomass to Renewable Fuels and Chemicals**

- Additional PIs:** Mark Barteau, Jingguang Chen, Doug Buttrey, Doug Doren, Feng Jiao, Mike Klein, Kelvin Lee, Raul Lobo, Stan Sandler, Yushan Yan (Univ. of Delaware); Scott Auerbach, Paul Dauenhauer, Wei Fan, George Huber (Univ. of Massachusetts); Aditya Bhan, Michael Tsapatsis (Univ. of Minnesota); Mark Davis (California Institute of Technology); Ray Gorte, John Vohs (Univ. of Pennsylvania); Bruce Koel (Princeton University); Mark Snyder (Lehigh University); Phil Westmoreland (Univ. of North Carolina); Anatoly Frenkel (Brookhaven National Lab)
- Post-docs:** Phuong Do, Samir Mushrif, Yulin Huang, Ana Belen Pinar (Univ. of Delaware); Sounak Roy (Univ. of Delaware and Univ. of Pennsylvania); Do-Young Hong, Nafiseh Rajabbeigi (Univ. of Minnesota); Zhuopeng Wang (Univ. of Minnesota and Univ. of Massachusetts); Eranda Nikolla (California Institute of Technology); Won Cheol Yoo (Univ. of Minnesota and Lehigh Univ.); Xiaofang Yang (Princeton University, University of Delaware, Lehigh University)
- Graduate Students:** Yu-Ting Cheng, Jechan Lee, Julian Santander (Univ. of Massachusetts); Vinit Choudhary, Tim Courtney, Ashay Javadekar, Bill Lonergan, Matt Mettler, Hui Ren, Michael Saliccioli, Dallas Swift, Sarah Tupy, Ke Xiong, Weiting Yu (Univ. of Delaware); Patrick Fahey, Vikram Seshadri (North Carolina State University); Daniel Gregory, Qianying Guo (Lehigh University); Abhimanyu Jayakumar, Jesse McManus (University of Pennsylvania); Rajiv Ranjan, Xueyi Zhang (Univ. of Minnesota)
- Collaborators:** Vladimiro Nikolakis, Stavros Caratzoulas, Weihua Deng, Ying Chen, Tiefeng Wang (Univ. of Delaware); Hai Wang (Univ. of Southern California)

**Contact:**

Dion Vlachos, Catalysis Center for Energy Innovation, University of Delaware  
Newark, DE 19716, (302) 831-2830, vlachos@udel.edu

## Goals

The mission of CCEI is threefold, namely to:

- (1) develop the enabling science leading to improved or radically new heterogeneous catalytic technologies for viable and economic operation of biorefineries from various lignocellulosic biomass feedstocks;
- (2) enable technology transfer; and
- (3) educate the workforce needed to develop and implement these new technologies.

To realize cost-efficient biorefineries, CCEI's research has three major goals, namely to:

- (1) transform biomass and/or its derivatives into valuable chemicals, fuels and electricity through a fundamental understanding of the chemistry and catalyst performance;
- (2) design novel multiscale hierarchical materials with nanoscale resolution suitable for processing derivatives from the complex, multiphase media of biomass to ensure efficient, highly selective, and benign processes; and
- (3) promote catalyst design and technology advancement through novel theoretical and multiscale simulation platforms and cutting-edge characterization tools.

## DOE Interest

Our thrusts address the grand challenges in the *Basic Research Needs (BRN): Catalysis for Energy* report of designing materials with controlled specificity and developing computational tools and multiscale models. Specific areas of focus include “catalysis; nanostructured materials; characterization and measurement techniques; theory, modeling, and simulation” and “[synthesis of] new, more effective catalyst structures that exploit multifunctionality and versatility to guide reactions through highly selective pathways”. For example, understanding the chemistry of biomass processing at low temperatures in the liquid phase has been identified as a key direction of catalysis research and is a key to the chemicals thrust. CCEI also addresses the following *BES* long-term program measures: “By 2015, demonstrate progress in understanding, modeling, and controlling chemical reactivity and energy transfer processes in the gas phase, in solutions, at interfaces, and on surfaces for energy-related applications, employing lessons from inorganic, organic, self-assembling, and biological systems.”

## Recent Progress

### \* *Reforming technology:*

Our goal is to achieve the selective scission of O-H, C-H, C-O and C-C bonds of alcohols, polyols, and furans through catalysis. Our experimental efforts include several parallel research approaches: surface science measurements on well-defined single crystal surfaces, synthesis and characterization of supported catalysts, and catalytic evaluation in vapor phase and liquid phase using batch and flow reactors. We develop computational methods that can guide rational catalyst design for reforming of biomass derivatives to syngas and/or hydrogen, and to value-added chemicals by correlating activity and selectivity to electronic properties of metals and supports. Current efforts focus on vapor phase processing.

Using Ni/Pt(111) as a model bimetallic surface, we investigated the reaction mechanism of ethylene glycol (Figure 1) and glycolaldehyde on Pt(111), Ni(111), and Ni/Pt(111). The Ni/Pt(111) surface monolayer structure shows the highest reforming activity for both reactants, indicating that the presence of a C=O bond in oxygenates does not affect the reforming pathway.

In parallel, we have developed a group additivity method for various biomass derivatives on various metals, along with microkinetic models for polyols. In addition, we have designed

isotopic labeling experiments (Figure 1) for validation of model predictions and identification of key reaction steps reforming chemistry.

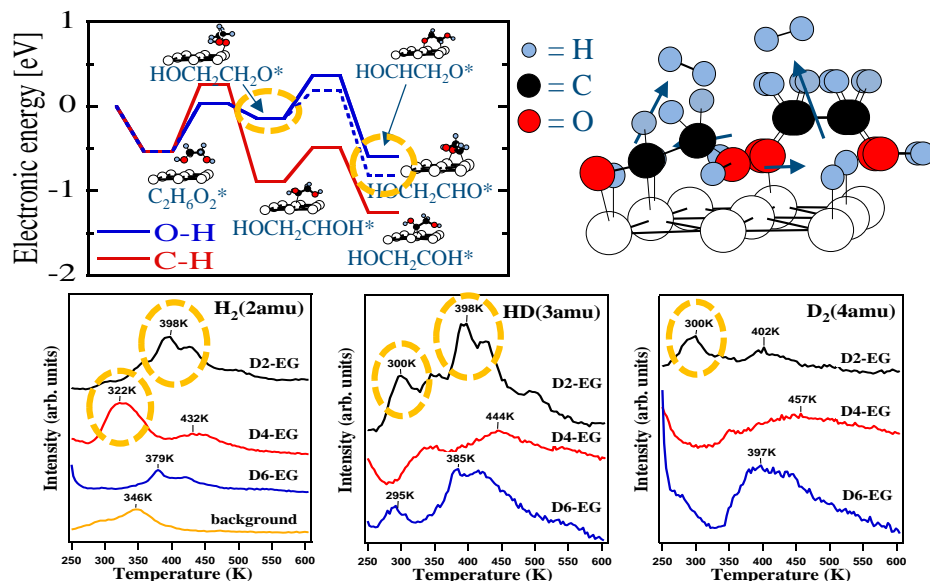


**Figure 1.** Top: DFT predicted energy surfaces for ethylene glycol decomposition on Pt(111). Bottom: TPD experiments of deuterated ethylene glycol.

**\* Selective transformation of sugars to furans:**

We focus on the catalytic conversion of biomass derived sugars to chemicals. We aim at novel catalyst discovery and design through fundamental understanding of catalytic and mass transport processes accomplished by integrating experiments on catalyst synthesis, reaction kinetics, mass transport and in situ characterization.

We discovered that a large pore zeolite that contains tin (Sn-Beta synthesized in the presence of hydrofluoric acid) is able to isomerize glucose to fructose in aqueous media with high activity and selectivity. The Sn-Beta catalyst is able to perform the isomerization reaction in highly acidic, aqueous environments with equivalent activity and product distribution as in media without added acid. This enables Sn-Beta to couple isomerization with other acid-catalyzed

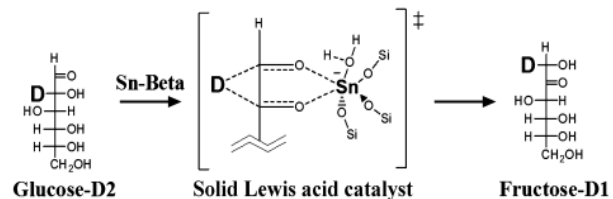


**Figure 2.** Glucose isomerization mechanism via intramolecular hydride shift.

reactions, including hydrolysis/isomerization or isomerization/dehydration reaction sequences. Coupling of glucose isomerization with acid catalyzed starch to glucose and fructose to HMF was demonstrated. We have performed NMR

spectroscopy on isotopically labeled glucose which revealed that the reaction of glucose in water proceeds by an intramolecular hydride shift rather than proton transfer, providing the first mechanistic demonstration of Sn-Beta acting as a Lewis acid in a purely aqueous medium (Figure 2). Preliminary assessments indicate that the Sn-beta catalyst is stable and robust in aqueous environment.

In parallel, we studied the glucose to fructose isomerization and fructose dehydration to HMF using hybrid quantum mechanics/molecular mechanics (QM/MM) and *ab initio* Molecular Dynamics (Car-Parrinello) free energy calculations. We completed a QM/MM MD study on the dehydration of fructose to HMF and proposed a 10-step mechanism proceeding via a series of intramolecular hydride and proton transfer steps. We showed that solvent re-organization is responsible for high activation free energies during hydride transfers and that water-mediated proton transfer is faster than direct intramolecular proton transfer.

**\* Biomass depolymerization and bio-oil upgrade:**

Our goal is to study the conversion of biomass into fuel blend components (including aromatics and alkanes) starting with pyrolysis of solid biomass followed by hydrodeoxygenation and deoxygenation of the pyrolysis vapors. We focus on the condensed phase chemical pathways. Cellulose pyrolysis produces a range of smaller oxygenated intermediates including levoglucosan and hydroxylacetaldehyde. We study the hydrodeoxygenation and



**Figure 4.** High speed photography image of aerosol formation during cellulose pyrolysis.

deoxygenation of these intermediates with zeolites. Deoxygenation with zeolites involves the direct production of aromatics and olefins, as shown in.

**\*Direct carbon fuel cells:**

We study the direct, electrochemical oxidation of biomass using molten-metal anodes in solid oxide fuel cells (SOFC) in order to produce electricity without first reforming the biomass. The work is aimed towards developing a fundamental understanding of the processes that limit the performance of these electrodes. One aspect of the work involves understanding oxygen transfer at the metal-electrolyte interface and determining what properties affect the impedance of this reaction. Another aspect of the work deals with the oxidation of biomass in the molten-metal electrodes.

We identified the melting temperature of the oxide as the important parameter in affecting the impedance of the molten-metal anodes. We showed that the impedance for molten Pb electrodes dropped dramatically when the temperature was raised just above the melting temperature of PbO (1161 K). Because Sb and Sb<sub>2</sub>O<sub>3</sub> are liquids at 973 K, we investigated the properties of molten-Sb electrodes. We demonstrated that the impedance of molten-Sb anodes was less than 0.1 ohm-cm<sup>2</sup> at 973 K. Fuel cells with molten-Sb electrodes exhibited an open-circuit potential

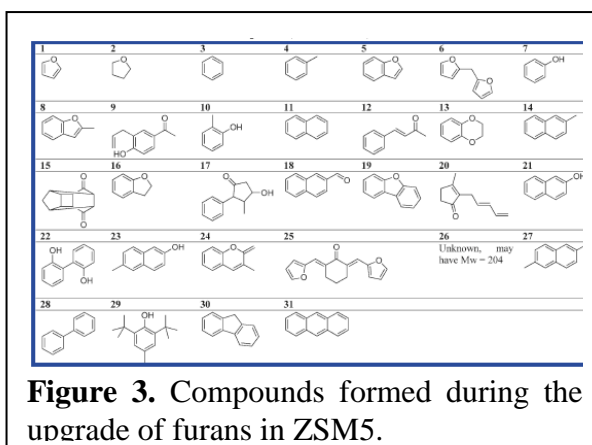


**Figure 3.** Compounds formed during the upgrade of furans in ZSM5.

Hydrodeoxygenation involves the addition of hydrogen to remove oxygen. By combining insights from catalytic kinetics with detailed catalyst characterization we synthesize new catalysts. We use *ab initio* chemistry to calculate molecular structures, compute thermochemistry and kinetics. We have developed experimental capabilities to study the condensed-phase chemistry, under isothermal conditions, and successfully identified and quantified all pyrolysis products (permanent gases, volatiles and char). Figure 4 shows an image of cellulose pyrolysis and the formation of aerosols from the condensed phase.



of 0.75 V, the Nernst potential for equilibrium between Sb and Sb<sub>2</sub>O<sub>3</sub>. We operated a fuel cell on sugar at a constant power density of 300 mW/cm<sup>2</sup> and 0.5 V at 973 K for a period of more than 12 hours, the time required to consume 0.5 g of sugar char (formed by heating sugar to 873 K in a covered container).

### Publications (2010-2011)

1. A. J. Foster and R. F. Lobo, Identifying reaction intermediates and catalytic active sites through in situ characterization techniques, *Chemical Society Reviews* **39**(12), 4783-4793 (2010).
2. A. Jayakumar, S. Lee, A. Hornes, J. M. Vohs, and R. J. Gorte, A Comparison of Molten Sn and Bi for Solid Oxide Fuel Cell Anodes, *Journal of the Electrochemical Society* **157**(3), B365-B369 (2010).
3. A. Jayakumar, J. M. Vohs, and R. J. Gorte, Molten-Metal Electrodes for Solid Oxide Fuel Cells, *Industrial & Engineering Chemistry Research* **49**(21), 10237-10241 (2010).
4. R. F. Lobo, Synthetic Glycolysis, *Chemsuschem* **3**(11), 1237-1240 (2010).
5. M. Moliner, Y. Roman-Leshkov, and M. E. Davis, Tin-containing zeolites are highly active catalysts for the isomerization of glucose in water, *Proceedings of the National Academy of Sciences of the United States of America* **107**(14), 6164-6168 (2010).
6. Y. Roman-Leshkov, M. Moliner, J. A. Labinger, and M. E. Davis, Mechanism of Glucose Isomerization Using a Solid Lewis Acid Catalyst in Water, *Angewandte Chemie-International Edition* **49**(47), 8954-8957 (2010).
7. M. Saliccioli, Y. Chen, and D. G. Vlachos, Density Functional Theory-Derived Group Additivity and Linear Scaling Methods for Prediction of Oxygenate Stability on Metal Catalysts: Adsorption of Open-Ring Alcohol and Polyol Dehydrogenation Intermediates on Pt-Based Metals, *Journal of Physical Chemistry C* **114**(47), 20155-20166 (2010).
8. D. G. Vlachos and S. Caratzoulas, The roles of catalysis and reaction engineering in overcoming the energy and the environment crisis, *Chemical Engineering Science* **65**(1), 18-29 (2010).
9. D. G. Vlachos, J. G. G. Chen, R. J. Gorte, G. W. Huber, and M. Tsapatsis, Catalysis Center for Energy Innovation for Biomass Processing: Research Strategies and Goals, *Catalysis Letters* **140**(3-4), 77-84 (2010).
10. H. Y. Wang, M. Stamatakis, D. A. Hansgen, S. Caratzoulas, and D. G. Vlachos, Understanding mixing of Ni and Pt in the Ni/Pt(111) bimetallic catalyst via molecular simulation and experiments, *Journal of Chemical Physics* **133**(22), (2010).
11. I. Baldychev, A. Javadekar, D. J. Buttrey, J. M. Vohs, and R. J. Gorte, A study of the redox properties and methanol oxidation rates for molybdenum-based mixed oxides, *Applied Catalysis A: General* **394**(1-2), 287-293 (2011).
12. S. Caratzoulas and D. G. Vlachos, Converting fructose to 5-hydroxymethylfurfural: A quantum mechanics/molecular mechanics study of the mechanism and energetics, *Carbohydrate Research* **346**, 664-672 (2011).
13. T. R. Carlson, Y. T. Cheng, J. Jae, and G. W. Huber, Production of green aromatics and olefins by catalytic fast pyrolysis of wood sawdust, *Energy & Environmental Science* **4**(1), 145-161 (2011).
14. Y.-T. Cheng and G. W. Huber, Chemistry of Furan Conversion into Aromatics and Olefins over HZSM-5: A Model Biomass Conversion Reaction, *ACS Catalysis* **1**, 611-628 (2011).

15. T. Courtney, G. Mpourmpakis, J. Chen, D. G. Vlachos, and S. Caratzoulas, Glycerol Dehydration Mechanisms in the Presence of Explicit Solvent Molecules, *J. Chem. Phys.*, Submitted (2011).
16. A. I. Frenkel, A. Yevick, C. Cooper, and R. Vasic, Modeling the Structure and Composition of Nanoparticles by Extended X-Ray Absorption Fine-Structure Spectroscopy, *Annual Review of Analytical Chemistry* **4**(1), null (2011).
17. H. Jobic, J. E. Santander, W. C. Conner, G. Wittaker, G. Girit, A. Harrison, J. Ollivier, and S. M. Auerbach, Experimental Evidence of Selective Heating of Molecules Adsorbed in Nanopores under Microwave Radiation, *Physical Review Letters* **106**(15), 157401 (2011).
18. W. W. Lonergan, X. Xing, R. Zheng, S. Qi, B. Huang, and J. G. Chen, Low-Temperature 1,3-Butadiene Hydrogenation over Supported Pt/3d/Al<sub>2</sub>O<sub>3</sub> Bimetallic Catalysts, *Catalysis Today* **160**, 61-69 (2011).
19. N. S. Marinkovic, Q. Wang, L. Barrio, S. N. Ehrlich, S. Khalid, C. Cooper, and A. I. Frenkel, Combined in Situ X-ray absorption and diffuse reflectance infrared spectroscopy: An attractive tool for catalytic investigations, *Nuclear Instruments and Methods in Physics Research A*, In press (2011).
20. G. Mpourmpakis and D. G. Vlachos, Computational-based catalyst design for thermochemical transformations, *MRS Bulletin* **36**, 211-215 (2011).
21. E. Nikolla, Y. Roman-Leshkov, M. Moliner, and M. E. Davis, "One-Pot" Synthesis of 5-(Hydroxymethyl)furfural from Carbohydrates using Tin-Beta Zeolite, *ACS Catalysis* **1**, 408-410 (2011).
22. S. T. Qi, B. A. Cheney, R. Y. Zheng, W. W. Lonergan, W. T. Yu, and J. G. G. Chen, The effects of oxide supports on the low temperature hydrogenation activity of acetone over Pt/Ni bimetallic catalysts on SiO<sub>2</sub>, gamma-Al<sub>2</sub>O<sub>3</sub> and TiO<sub>2</sub>, *Applied Catalysis A-General* **393**(1-2), 44-49 (2011).
23. M. Saliccioli, W. Yu, M. A. Barteau, J. G. Chen, and D. G. Vlachos, Differentiation of O-H and C-H Bond Scission Mechanisms of Ethylene Glycol on Pt and Ni/Pt Using Theory and Isotopic Labeling Experiments *Journal of American Chemical Society*, Accepted (2011).
24. G. D. Stefanidis and D. G. Vlachos, Low cost, small scale processing technologies for production applications in various environments: Part 4. Distributed biofuel production *Engineering & Processing: Process Intensification J.*, Submitted (2011).
25. H. Zhang, Y. T. Cheng, T. P. Vispute, R. Xiao, and G. W. Huber, Catalytic Conversion of Biomass-derived Feedstocks into Olefins and Aromatics with ZSM-5: The Hydrogen to Carbon Effective Ratio, *Energy & Environmental Science*, In press (2011).

**Nanoscale surface chemistry and electrochemistry of clean and metal-covered faceted substrates: Structure, reactivity, and electronic properties**

Postdocs: Wenhua Chen  
Quantong Shen  
Undergraduate: Grant Junno  
Collaborators: Timo Jacob (U. Ulm, Germany); Jingguang Chen (U. Delaware); Bruce Koel (Lehigh/Princeton)  
Contacts: Rutgers University, 136 Frelinghuysen Rd, Piscataway, NJ 08854;  
[bart@physics.rutgers.edu](mailto:bart@physics.rutgers.edu)

### **Goal**

The goal of this work is to explore new aspects of nanoscale phenomena in surface chemistry and electrochemistry with the aim to characterize the relationships between nanoscale surface features (facets and clusters) and catalytic reactivity/selectivity. A long-term goal is to improve reactivity and selectivity by controlling the shape and size distribution of nanoscale surface features. Our emphasis is on atomically rough and morphologically unstable surfaces that undergo nanoscale faceting when covered by adsorbate (gas or metal) and annealed to elevated temperatures. There are three parts of the project: faceting of model catalytic surfaces, growth of metallic nanoparticles on the faceted surfaces, and reactivity/selectivity of the nanoscale facets in catalytic reactions.

### **DOE Interest**

Recent work has demonstrated that reactivity and selectivity in catalysis can be tuned by controlling the nanoparticle size and shape. However, highly dispersed supported catalysts used in industry usually have a wide distribution of sizes and shapes of nanoparticles. Great progress has been recently made in controlling shape and size of nanoparticles. To elucidate the reaction mechanism, which is in turn beneficial to the design and development of new catalysts, macroscale model catalysts (planar single crystals) and nanoscale model catalysts are usually used to catalyze the reactions. These structures can exhibit new phenomena in heterogeneous catalysis, as well as in electrochemical reactions.

### **Recent Progress**

*Faceting of Re and electrochemistry of Pt/Re:* C-induced faceting of Re(11-21) has been discovered. Upon annealing in C<sub>2</sub>H<sub>2</sub>, initially planar Re(11-21) becomes nano-faceted and covered by three-sided nanopyramids. This nano-faceted surface is then utilized as a nanotemplate to synthesize a Pt monolayer electrocatalyst. We have found that the monolayer of Pt on the C/Re nanotemplate exhibits higher activity for the hydrogen evolution reaction compared to pure Pt.

*Faceting of Ir and surface chemistry on faceted Ir(210):* Clean planar Ir(210) and clean faceted Ir(210) with tailored sizes of three-sided nanopyramids have been prepared to investigate reactions of NO+CO and NO+C<sub>2</sub>H<sub>2</sub>. Evidence is found for structure sensitivity in both reactions on faceted Ir(210) versus planar Ir(210). In addition, NO+CO reactions exhibits size effects on faceted Ir(210) for average facet size ranging from 5 to 14nm. Moreover, when planar Ir(210) is pre-covered by 1ML CO and then exposed to NO, “explosive” evolution of N<sub>2</sub> and CO<sub>2</sub> has been observed.

*Faceting of Ru and application of faceted O/Ru surfaces:* O-induced nano-faceting of Ru(11-20) and Ru(11-21) has been found. By depositing gold onto the faceted O/Ru(11-20) surface held at room temperature, gold nanoparticles with regular spacings are fabricated. Gold nanoparticles are found to nucleate preferentially within valleys of the faceted surface.

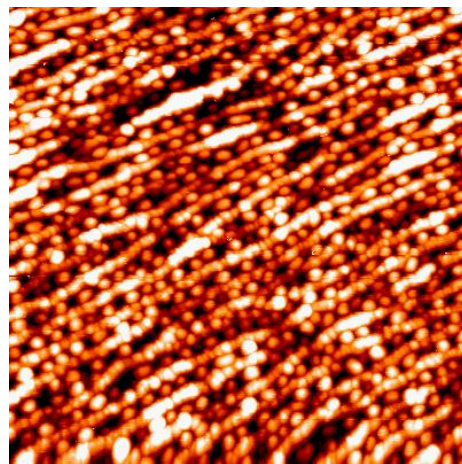


Fig. 1: STM image (100nm × 100nm) showing Au nanoclusters on a faceted O/Ru(11 $\bar{2}$ 0) surface.

#### **Future Plans:**

*Identifying new faceted surfaces as model nanocatalysts:* To search for and to characterize (with atomic resolution) nanoscale faceting of adsorbate (gas or metal)-covered metallic (fcc Cu, hcp Re and Ru) and bimetallic (FeAl) surfaces; to identify factors that cause faceting of surfaces with different crystal structures; to develop procedures to generate clean faceted surfaces.

*Use faceted surfaces as templates for nanoparticle growth:* To search for growth of metallic nanoparticles on oxygen-covered faceted surfaces (Ir, Re, Ru, and FeAl) with a narrow size distribution and regular spacing at specific sites.

*Explore surface and electrochemistry of faceted surfaces:* To correlate surface morphology with catalytic reactivity and selectivity in surface reactions over clean and metal-covered faceted surfaces; to search for special kinetic phenomena associated with nanometer-scale size effects.

#### **Publication (2009-2011)**

1. P. Kaghazchi, T. Jacob, H. Wang, W. Chen and T.E. Madey, "First principles studies on adsorbate-induced faceting of Re(11-21)", *Phys. Rev. B (Brief Reports)*, **79** (2009) 132107-4.
2. W. Chen, A.L. Stottlemyer, J.G. Chen, P. Kaghazchi, T. Jacob, T.E. Madey and R.A. Bartynski, "Adsorption and decomposition of NO on O-covered planar and faceted Ir(210)", *Surf. Sci.*, **603** (2009) 3136-3144.
3. Govind, W. Chen, H. Wang and T.E. Madey, "Growth of oxygen induced nanoscale-pyramidal facets on Rh(210) surface", *Phys. Rev. B*, **81** (2010) 085415-9

4. Q. Shen, W. Chen, H. Wang, Govind, T.E. Madey and R.A. Bartynski, "Nano-faceting of the Ru(11-20) surface", *Surf. Sci.*, **604** (2010) L12-15.
5. W. Chen, Q. Shen, R.A. Bartynski, P. Kaghazchi and T. Jacob, "Reduction of NO by CO on unsupported Ir: Bridging the materials gap", *ChemPhysChem*, 11 (2010) 2515-2520. (**featured on the front cover of Issue 12/2010 and highlighted in the news section of ChemPhysChem**)
6. B.V. Yakshinskiy, Q. Shen, R.A. Bartynski, "Interaction of benzene and toluene vapors with Ru(0001) surface: Relevance to MLM contamination", *Proc. SPIE*, 7969 (2011) 796922-10.
7. Q. Shen, W. Chen, R.A. Bartynski, "Growth of gold nanoparticles on faceted O/Ru(11-20) nanotemplate", *Surf. Sci.*, **605** (2011) 1454-1458.

This page is intentionally blank.

# Poster Presentations

This page is intentionally blank.



## Metal and Metal Oxide-Supported Platinum Monolayer Electrocatalysts for Oxygen Reduction

Additional PIs: Jia Wang, Miomir Vukmirovic, Kotaro Sasaki, Ping Liu

Post-docs: Yun Cai, Stoyan Bliznakov

Graduate Students: Meng Li, Kurian Kuttiyiel, Yu Zhang (Stony Brook U); Lijun Yang, Beijing U.China

Contact: Radoslav Adzic; Brookhaven National Laboratory; Upton, NY 11973-5000

Phone: 631-344-4522, Fax: 631 344-5815; [adzic@bnl.gov](mailto:adzic@bnl.gov)),

Collaborators: M. Mavrikakis, U. Wisconsin; Y. Zhu, Brookhaven National Laboratory; K. Moore, Oak Ridge National Laboratory

### Goals

This program involves studies of basic problems of electrocatalysis of fuel cell reactions while focusing on platinum monolayer electrocatalysts for the O<sub>2</sub> reduction reaction (ORR) and ternary electrocatalysts for ethanol oxidation to CO<sub>2</sub>. The goals include developing ultimately low Pt content electrocatalysts with high activity and high stability facilitated by the second generation of core-shell nanoparticles with surface and sub-surface modified cores, using cores with smooth surfaces, nanorods, nanowires, hollow nanoparticles and those having predominantly (111) facets. Kinetic modeling and theoretical calculations are carried out for a deeper insight into the kinetics of the (ORR) and ethanol oxidation. Studies using well-defined surfaces are carried out to gain understanding of the atomic-scale phenomena involved in the interactions of Pt monolayers with supports as well as developing new catalysts for ethanol oxidation.

### DOE Interest

The project is focused at developing several Pt monolayer catalysts that are likely to have the highest Pt mass activity, and excellent potential to overcome the obstacles hindering the broad application of fuel cells. The results will enhance our understanding of the metal monolayer-support interactions for a viable approach for controlling chemical reactivity in the top atomic layer. They will also provide insights into catalytic behavior of core-shell nanoparticles and possibilities for designing their properties. In addition, we explore the catalyst capable of C – C bond splitting at low overpotentials in the oxidation of small organic molecules.

### Progress Report

#### Improving activity and stability of Pt monolayer electrocatalysts

Several methods for improving Pt ML catalysts have been developed based, *inter alia*, on the understanding of the factors affecting the ORR kinetics and the behavior of nanoparticles and a Pt monolayer (ML). The new strategies used to design Pt monolayer electrocatalysts include fine-tuning of the Pt-support interaction to enhance their activity and stability based on:

- i) Pd or other metal ML placed between a Pt ML and a core, and
- ii) Sub-surface modification of cores to tune the interaction with a Pt ML
- iii) Tetrahedral nanoparticles as the cores,
- iv) Hollow Pd nanoparticles as the cores.

The systems i)-ii) we termed the second generation of core-shell electrocatalysts that can use the cores not suitable as a direct support for a Pt monolayer. Adverse effects can be avoided by surface or sub-surface modification using an “interlayer”, for example, a Pd monolayer. This approach was demonstrated by modifying the Pt<sub>ML</sub>-IrCo/C and Pt<sub>ML</sub>-Ru/C interaction by a Pd interlayer. Similar improvements can be achieved by the sub-surface modification of cores, for example an Ir ML at a sub-surface of a Pd nanoparticle.

Below we describe several illustrations of the recent results.

### Bimetallic IrNi core Pt ML shell electrocatalysts for the ORR

To further decrease the noble metal content we synthesized noble metal-non noble metal core in which segregation of noble metal, Ir, is induced by thermal treatment. Thus, inner Ni core is covered by Ir outer core consisting of ca. 2MLs of Ir (Fig. 1). Thermally treated IrNi core-shell nanoparticles are covered by a Pt ML using galvanic displacement of a Cu monolayer deposited at underpotentials. The Pt mass activity of the Pt<sub>ML</sub>/IrNi/C electrocatalyst from a scale-up synthesis is approximately

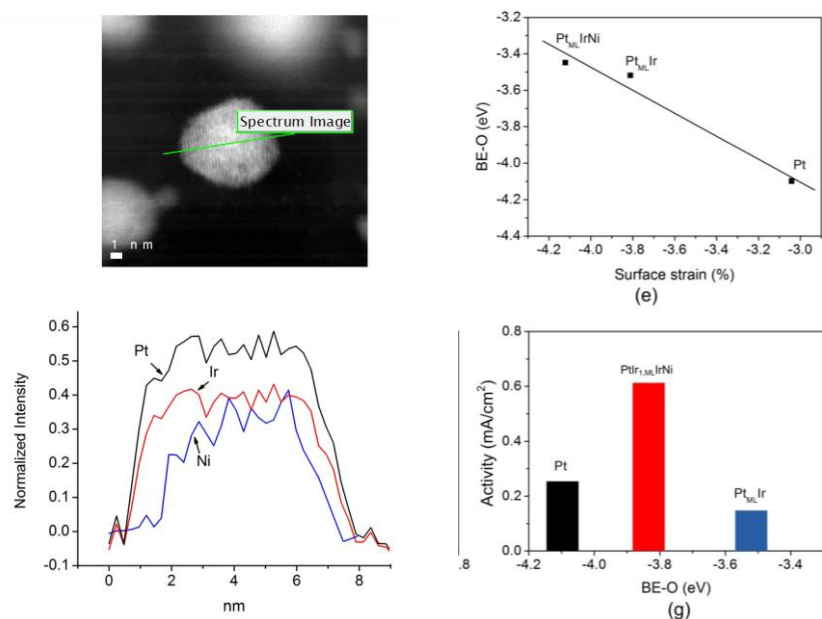


Fig. 1 HAADF- STEM image of a PtIrNi nanoparticle, and comparison of the EELS intensities for the Pt and Ir M-edge and Ni L-edge along the scanned line (left panels); Right panels (e) Predicted binding energy of oxygen (BE-O) as a function of strain on Pt<sub>ML</sub>IrNi, Pt<sub>ML</sub>Ir and Pt using the nanoparticle models. (g) Pt specific activity against BE-O on PtIr<sub>1,ML</sub>IrNi, Pt<sub>ML</sub>Ir and Pt.

3 times higher than that of the commercial Pt/C electrocatalyst. The electronic, geometrical and segregation affects of Pt monolayer by the IrNi substrates results in a catalytic activity different from that of pure Pt. The structure and composition of the

core-shell nanoparticles were verified using transmission electron microscopy and *in situ* X-ray absorption spectroscopy, while potential cycling test of 50,000 cycles confirmed the stability of the electrocatalyst. DFT computations show that adding Ni to Ir makes BE-O weaker as a function of strain that results in higher activity of a Pt ML on Ir-Ni core than on Ir, or that of Pt/C. Interaction of O and Ir can cause segregation of Ir to the surface, which further enhance the activity (Fig. 1).

### Synthesis and the catalytic activity of Pt monolayer on Pd tetrahedral nanocrystals

A small number of low-coordination sites and defects, and high content of the (111)-oriented facets on Pt nanoparticles is required for an active ORR electrocatalyst. Such is the case of tetrahedral nanoparticles (Fig.2). They can be prepared in the presence Poly(vinylpyrrolidone) (PVP), used as a protecting and reducing agent, which is difficult to remove. We developed a noninvasive method involving a CO adsorption-induced removal of surfactants. PVP removal was achieved upon CO stripping at a high potential (1.0 V vs RHE). It played a decisive role in improving the activity of the Pt<sub>ML</sub>/TH Pd electrocatalyst for the ORR in addition to the (111) orientation of Pd. (Fig. 2)

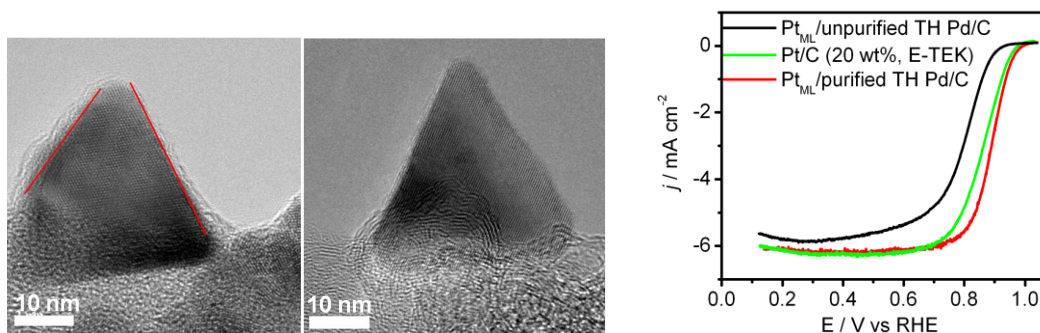


Fig. 2. High-resolution TEM image of the TH Pd before (left panel) and after CO treatment; Polarization curves of the commercial Pt/C (green) and Pt<sub>ML</sub>/TH Pd/C with (red) and without CO treatment (black); 0.1M HClO<sub>4</sub>; sweep rate 20mV/s.(right panel)

### Pt hollow nanoparticles and Pt ML on hollow Pd nanoparticles electrocatalysts for the ORR

A hollow core is an interesting structure because it may induce a desirable lattice contraction in a Pt shell without engendering the instability caused by dissolution of core materials. We synthesized compact Pt hollow nanoparticles using Ni templates (Figure 3), which could be expected on the basis of Kirkandall effect. Their sufficient thermal stability for PEM fuel cell application (operate at 80 °C) is demonstrated by *in situ* TEM images. The Pt hollow particles, denoted by the red bar in Fig. 3b, had lost about 33% of their initial ORR activity after 50 hours, but exhibited no further loss thereafter. The ORR activity of solid Pt nanoparticles is much more modest. We attribute the highly sustainable ORR activity on Pt hollow nanospheres partly to the hollow-induced lattice contraction, and to the oxidation-resistant surface morphology.

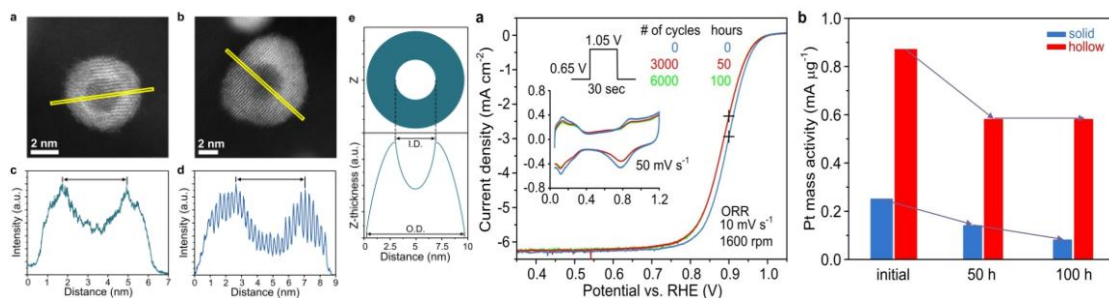


Fig. 3 a,b, High-resolution STEM images of Pt hollow particles, c,d, line-scans of the intensity profile nearly parallel (c) and perpendicular (d) to the direction of the lattice plane. (e) Calculated z-thickness versus x-distance at the  $y=0$  position for a hollow sphere. (left three panels); a, Sequential ORR polarization and voltammetry (inset) curves for Pt hollow nanocatalysts, b, Pt mass activity as a function of potential cycling time for Pt hollow and solid nanoparticles. (right two panels).

Hollow Pd nanoparticles were synthesized in a similar way as Pt counterparts described above. The electrocatalyst consisting of a Pt ML on hollow Pd nanoparticles has very high specific and mass activities, as a consequence of the hollow-induced lattice contraction, and to the oxidation-resistant surface morphology

### The stability mechanism of core-shell nanoparticles – shell protected by the core

On the basis of accelerated stability fuel cell tests of Pt/Pd/C and Pt/Pd<sub>9</sub>Au/C catalysts we proposed the mechanism explaining stability of Pt ML, which remains unchanged in tests up to 200,000 potential cycled, while some dissolution of Pd occurs. The stability is ascribed to: i) PtOH formation shifted positively, ii) Contraction of Pt and Pd lattices induced by some loss of Pd (hollow may form) and iii) Cathodic protection effect.

### Electrocatalysts for ethanol oxidation

Further studies of the ternary Pt-Rh-SnO<sub>2</sub>/C electrocatalysts capable of splitting the C-C bonds at room temperature involved optimizing the content of Rh in the catalyst. The highest activity was found for the 1:1/2:1 atomic ratio of Pt:Rh:Sn. The catalysts composed of random PtRh alloy on SnO<sub>2</sub> nanoparticles with the average particle size around 2-3 nm and a narrow size distribution. (Fig. 4) The role of constituents is as follows, **SnO<sub>2</sub>**: precludes the Rh and Pt sites to form M-OH caused by the lateral repulsion of MOH and hydroxyl species on SnO<sub>2</sub>, so they can react with ethanol; provides OH to oxidize CO; **Pt**: helps ethanol dehydrogenation, modifies Rh for moderate bonding to ethanol, **Rh**: accomplishes the C-C bond breaking. DFT calculations show that the oxametallacycle intermediate undergoes the C-C bond splitting.

Given the similar oxidation behavior of Rh and Ir, we checked the possibility to replace expensive Rh with inexpensive Ir. The catalyst PtIrSnO<sub>2</sub> can indeed split the C-C bond at low potential (Fig. 5). The reaction rate is lower than that of PtRhSnO<sub>2</sub>. Inducing

the C-C bond splitting on Ir in PtIrSnO<sub>2</sub> supports the mechanism of repulsive interaction of MOH with SnO<sub>2</sub>, which provide a guideline for further research in this area.

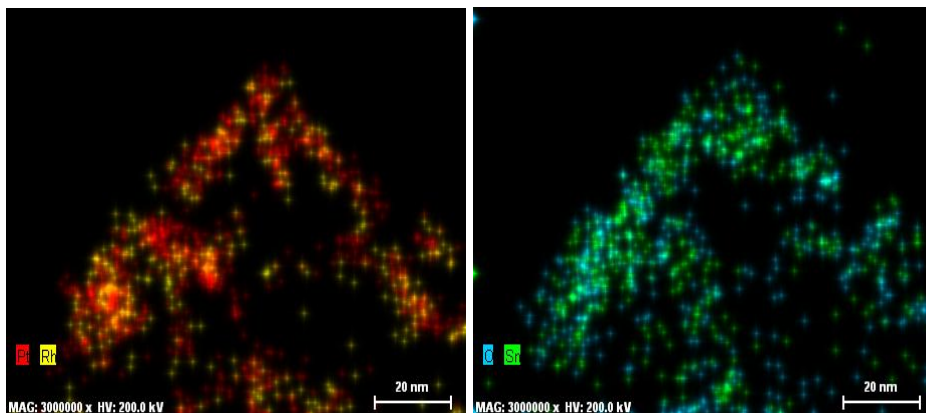


Fig. 4 EDS elemental mapping of PtRhSnO<sub>2</sub> catalyst. The Pt-Rh map suggests that a random alloyed has been formed (left panel). The O-signal associated with Sn confirms that broad rafts are amorphous SnO<sub>2</sub>. (right panel); The Pt-Sn map show that PtRh particles are decorating the broader SnO<sub>2</sub> rafts (not shown) With K. Moore and D. Cullen, Oak Ridge National Laboratory.

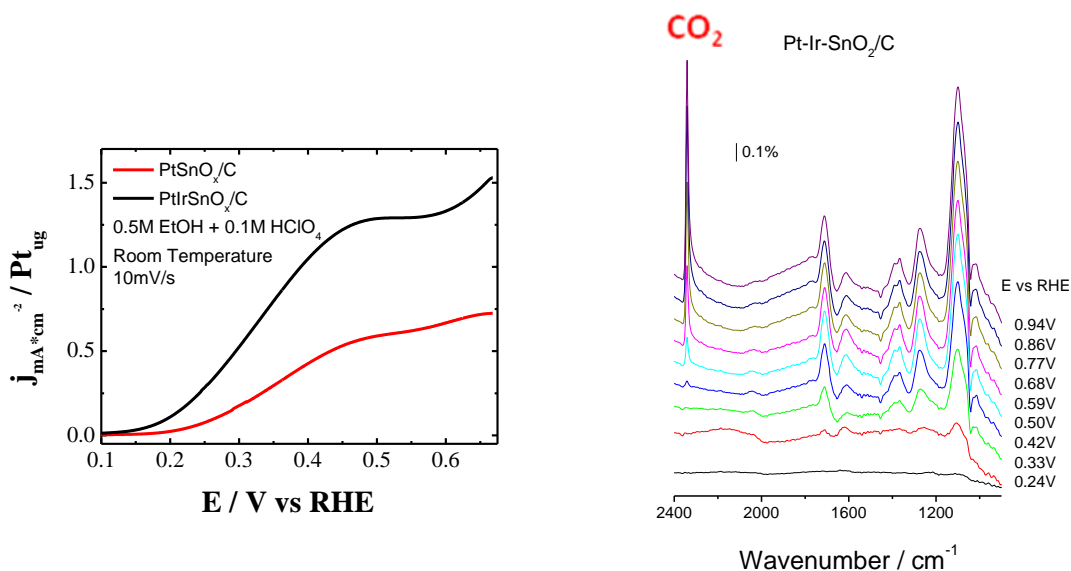


Fig. 5 Oxidation of ethanol on PtSnO<sub>2</sub> and PtIrSnO<sub>2</sub> (left panel) and the FTIR in situ measurements with PtIrSnO<sub>2</sub>. CO<sub>2</sub> generation is observed (right panel).

### Future studies

The proposed future work is aimed to improve the most promising results obtained so far, to address the open basic questions of the interaction of Pt monolayer with supports and their effects on the kinetics of the ORR, to explore the possible solution to the barrier imposed by the low open circuit potential of the ORR, to increase our understanding of the mechanism of cores protecting the shells in core-shell catalysts, to design and synthesize the second generation of core-shell catalysts, particularly using a sub-surface core modifications. The supports will be based on Pd and Pd alloys, but also

on Ir and Re, refractory metals, and selected oxides. CeO<sub>2</sub>, NbO<sub>2</sub> and Magneli phases oxides.

We will study Pt monolayers on surfaces with predominant highly coordinated atoms in the form of nanorods, nanowires, smooth nanoparticles, hollow Pd spheres, single crystalline nanoparticles with predominantly (111) facets. We will address two important problems of the kinetics of the ORR by exploring new approach to their solution. These are: i) Further studies of the mechanism of core-protecting monolayer-shell and ii) Addressing the challenge of the low open circuit potential of the ORR.

The low open circuit potential of the ORR and the inability to reach the thermodynamic potential of 1.23 V is a major problem of the ORR kinetics and the cause of the inefficiency of the H<sub>2</sub>/O<sub>2</sub> fuel cells. We propose to explore the concept of the “dry cave effect” by applying Pt surface modifications by fluorinated organics to reduce water activity. Considerable effort will be focused on the electrocatalysts for ethanol oxidation.

We will continue with theoretical studies to determine What are the geometries and energetics of reactants, possible intermediates and transition states? On which sites does the reaction take place? How are the ORR activities of metal in the extended surface and in the form of supported-nanoparticles related? To address these questions, theoretical calculations will be coordinated with our experiments on well-defined model catalysts. DFT calculations will be combined with micro-kinetic modeling, kinetic Monte Carlo (KMC) and molecular dynamic (MD) simulations to study the ORR on core-shell nanoparticles and oxide-supported nanoparticles.

## Publications

- J. X. Wang, H. Inada, L. Wu, Y. Zhu, Y. Choi, P. Liu, W-P. Zhou, R. R. Adzic, *Oxygen reduction on well-defined core-shell nanoparticles: Size, facet, and Pt shell thickness effects* *J. Am. Chem. Soc.*, **131**(2009) 17298 ( **JACS Select**).
- A. Kowal, M. Li, M. Shao, K. Sasaki, M.B. Vukmirovic, J. Zhang, N. S. Marinkovic, P. Liu, A.I. Frenkel, R. R. Adzic, Ternary Pt/Rh/SnO<sub>2</sub> Electrocatalysts for Oxidizing Ethanol to CO<sub>2</sub> *Nature Materials*, **8** (2009) 325.
- J. X. Wang, F. Uribe, T. E. Springer, J. Zhang, R. R. Adzic, Intrinsic kinetic equation for O<sub>2</sub> reduction reaction in acidic media: The double Tafel slope and fuel cell applicat”, *Faraday Discuss.* 140 347 (2009).
- Peter A. Ferrin, Shampa Kandoi, Junliang Zhang, Radoslav Adzic, Manos Mavrikakis, Molecular and Atomic Hydrogen Interactions with Au-Ir Near-Surface Alloys, *J. Phys. Chem. C* 2009, **113**, 1411–1417
- K. Sasaki, R.R. Adzic, XAS of Platinum Monolayer Fuel Cell Electrocatalysts – Unambiguous, Direct Correlation of Spectroscopy Data with Catalytic Properties, *Synchrotron Radiation News*, **22**(1) (2009) 17.
- Tanushree Ghosh, Miomir B. Vukmirovic, Francis J. DiSalvo, Radoslav R. Adzic, *Intermetallics as Support for Pt Monolayer O<sub>2</sub> Reduction Electrocatalysts: Potential for Significantly Improving Properties*, *J. Am. Chem. Soc.*, **132**(2010) 906.
- Zhou, W.-P.; Sasaki, K.; Su, D.; Zhu, Y.; Wang, J. X.; Adzic, R. R., *Gram-Scale-Synthesized Pd<sub>2</sub>Co-Supported Pt Monolayer Electrocatalysts for Oxygen Reduction Reaction*, *J. Phys. Chem. C*, **114**(2010) 8950.
- , K. Sasaki, J.X. Wang, H. Naohara, N. Marinkovic, K. More, H. Inada, R.R. Adzic, *Recent advances in platinum monolayer electrocatalysts for oxygen reduction reaction: Scale-up synthesis, structure and activity of Pt shells on Pd cores* *Electrochimica Acta*, **55**(2010) 2645.
- Seth L. Knupp, Miomir B. Vukmirovic, Pradeep Haldar, Jeffrey A. Herron, Manos Mavrikakis, and Radoslav R. Adzic, *Platinum Monolayer Electrocatalysts for O<sub>2</sub> Reduction: Pt Monolayer on Carbon-Supported PdIr Nanoparticles*, *Electrocatal.*, **1**(2010) 213.
- , Kotaro Sasaki, Hideo Naohara, Yun Cai, Yong Man Choi, Ping Liu, Miomir B. Vukmirovic, Jia X. Wang and Radoslav R. Adzic, *High-Stability Electrocatalysts for Fuel-Cell Cathodes* *Angew. Chem. Int. Ed.*, **49**(2010) 8602.
- , Yangchuan Xing, Yun Cai, Miomir Vukmirovic, Wei-Ping Zhou, Jia Wang, Radoslav Adzic, Hiroko Karan, *Enhancing Oxygen Reduction Reaction Activity via Pd-Au Alloy Sublayer Mediation of Pt Monolayer Electrocatalysts* *J. Phys. Chem. Lett.*, **1**(2010) 3238.
- Kuanping Gong, Dong Su, and Radoslav R. Adzic, *Platinum-Monolayer Shell on AuNi<sub>0.5</sub>Fe Nanoparticle Core Electrocatalyst with High Activity and Stability for the Oxygen Reduction Reaction*, *J. Am. Chem. Soc.*, **132**(2010), 14364. *Platinum Monolayer Electrocatalysts: Improving Structure and Activity*, Kotaro Sasaki, Miomir B. Vukmirovic, Jia X. Wang, Radoslav R. Adzic, *Fuel Cell Science: Theory, Fundamentals, and Bio-Catalysis*. Andrzej Wieckowski and Jens K. Nørskov (Eds.), John Wiley & Sons, Inc., Hoboken, New Jersey, 2010, pp. 215 –236

## Catalytic interfaces based on sub-nano surface-deposited clusters: why size matters

Anastassia N. Alexandrova

Department of Chemistry and Biochemistry, University of California, Los Angeles

e-mail: [alexandrova@chem.ucla.edu](mailto:alexandrova@chem.ucla.edu)

Surface-deposited clusters formed by only a few atoms are a new and fascinating catalytic machinery, whose catalytic properties are highly tunable through cluster size and composition. A seemingly erratic dependence of catalytic proficiency of Pd<sub>n</sub> clusters deposited on titania on cluster size has been observed experimentally, and the reason for it was eluded to be electronic. Here, we explicate this dependence. The global and local minima of Pd<sub>n</sub> on stoichiometric and defected titania have been identified, and the preference for the shape and binding sites has been explained based on the chemical bonding in these systems. Mobility of the clusters on titania also has been investigated. We elucidate the mechanism of the catalyzed reaction of CO oxidation, and reproduce the experimental trend. In addition to unique electronic properties of clusters of different size, the catalytic apparatus appears to employ clusters' anisotropic mobility and surface defects.

Preliminary results will be presented on modeling small surface deposited clusters in the presence of explicit solvent and at finite temperatures and pressures.

**Structure-Reactivity Relationships in Multi-Component Transition Metal Oxide Catalysts**

Postdocs, Researchers: Dr. Min Li, Dr. Todd Schwendemann

Students:

Collaborators: A. Boothroyd (Oxford University), C.H. Ahn (Yale), V.E. Henrich (Yale), C.A.F. Vaz (Yale).

Contact: Prof. Eric I. Altman, Department of Chemical and Environmental Engineering, Yale University, PO Box 208260, New Haven, CT 06520; Phone (203) 432-4375; E-mail [eric.altman@yale.edu](mailto:eric.altman@yale.edu)

**Goal**

Transition metal oxide catalysis is governed by a complex interplay between structure and composition. As a result, subtle changes in catalyst formulation and preparation can dramatically affect catalytic activity and selectivity. These effects are often ascribed to modifications of the local structure or electron density around the active metal cation. Synergistic effects between cations in an oxide matrix have also been suggested as drivers for increased activity and selectivity. It has been difficult to isolate these effects as compositional changes are generally accompanied by structural changes. The goal of this project has been to determine the relative importance of geometric and electronic effects by creating well-defined surfaces where the electron density and local structural environment can be varied independently.

**DOE Interest**

Transition metal oxides play key roles in a wide range of processes central to efficient utilization of scarce resources with minimal environmental impact. Combinations of vanadium, tungsten, and titanium oxides are currently used to eliminate nitrogen oxides emitted from power plants, while other oxides show activity for nitrogen oxide reduction at a fraction of the cost of the Pt-group metals currently used to catalyze this reaction in automotive applications. Transition metal oxides have also been the most promising candidates for selective oxidative dehydrogenation and coupling reactions that show promise for efficiently converting plentiful light alkanes to liquid transportation fuels and more valuable chemicals. The fundamental research in this project aims to put design of catalysts that enable new efficient processes on a more systematic, rational basis. Advances in these areas will enable more efficient use of scarce resources while also potentially reducing the environmental impact of power generation and chemical transformations.

**Recent Progress**

Over the last couple of years we have focused on the complementary areas of creating and characterizing the structure and reactivity of oxide heterostructures in which the influences of structural and chemical effects in supported oxides are distinguished; and on characterizing the surface structure and chemistry of prototypical oxide structures in



which the cations can be varied without changing the structural environment of the active cation.

In the latter area we have investigated prototypical scheelite-, spinel-, and perovskite-structured catalytic materials using a range of surface science methods including electron diffraction, scanning tunneling microscopy, photoelectron spectroscopy, molecular beam epitaxial growth (MBE), ion scattering, and thermal desorption. We have characterized the non-polar (100) surface of  $\text{CaWO}_4$ , the base member of the scheelite class of materials which includes many important oxidation catalysts. We found that  $\text{CaWO}_4$  behaves vastly differently from  $\text{WO}_3$  which we have extensively studied: unlike  $\text{WO}_3$ ,  $\text{CaWO}_4$  is extremely difficult to reduce and alcohols that readily dehydrate on  $\text{WO}_3$  only physisorb on  $\text{CaWO}_4(100)$ . Ion scattering results indicated that the coordinatively unsaturated W sites that strongly adsorb alcohols on  $\text{WO}_3$  are not accessible on the  $\text{CaWO}_4(100)$  surface. We used adsorption of the Lewis acid  $\text{BF}_3$  to characterize the basicity of surface oxygens on the  $\text{CaWO}_4$  surface; although Ca is considered to impart basic character, there was no evidence of strong basic sites on the  $\text{CaWO}_4$  surface. The results highlight the difficulty in predicting the behavior of complex oxides based on the behavior of the simpler constituent oxides.

For the perovskites we have investigated  $\text{LaCoO}_3$  (100) and (110) surfaces. This material was chosen as prototypical perovskite because of the distinct functionality of Co as a redox center and La as a basic oxide; the interesting properties of this material as both a catalyst support and active phase; and because of fundamental interest in modifications of polar perovskite surfaces that can influence structure and reactivity. Regarding the latter, in contrast to our prior findings for  $\text{LaAlO}_3$ , we found no evidence of reconstructions of the polar  $\text{LaCoO}_3$  surfaces. Photoelectron spectroscopy data indicate that the material is metallic and so we suggest that the polar surfaces are compensated by redistribution of the conduction electrons rather than atomic rearrangements as in insulating  $\text{LaAlO}_3$ . We have characterized the reactivity of the  $\text{LaCoO}_3(100)$  surface using alcohol thermal desorption which thus far shown mostly molecular desorption. As the (100) surface may terminate in either  $\text{LaO}$  or  $\text{CoO}_2$ , we are investigating the role of the surface termination in determining the reactivity.

We have studied  $\text{Co}_3\text{O}_4$  and orthovanadates of the form  $\text{M}_3\text{V}_2\text{O}_8$  as examples of spinel-structured catalytic oxides (the latter is a cation-deficient spinel). The former has recently attracted attention because of the observation of low temperature CO oxidation and NO reduction activity, while the latter are candidate oxidative dehydrogenation catalysts. In the orthovanadates, M can be divalent cations including Mg, Ni and Co. This group of materials forms a bridge to our prior work on epitaxial vanadia catalysts where the interface with the support affects the structure and reactivity of the vanadium cations as opposed to vanadium ions in a well-defined crystal structure where the secondary cation can be varied without changing the structure. For  $\text{Co}_3\text{O}_4$ , we have found interesting changes in the termination of (110)-oriented epitaxially grown thin films depending on the environment, as well as an interaction with  $\alpha\text{-Al}_2\text{O}_3(0001)$  that enables the formation of thin  $\text{Co}_2\text{O}_3$ , a material that is not otherwise stable. Meanwhile, we have characterized the structural, electronic, and chemical properties of stoichiometric  $\text{Ni}_3\text{V}_2\text{O}_8$  (010) surfaces. As summarized in the figure below, the surface terminates in an unreconstructed spinel "A" plane that exposes both Ni and V cations. It is an

insulator that only weakly adsorbs 1-propanol. We are currently investigating the effect of oxidation and reduction on the reactivity of this surface. Moving forward, we plan on investigating Co orthovanadate which will offer an interesting comparison to our parallel efforts on  $\text{LaCoO}_3$  and  $\text{Co}_3\text{O}_4$ .

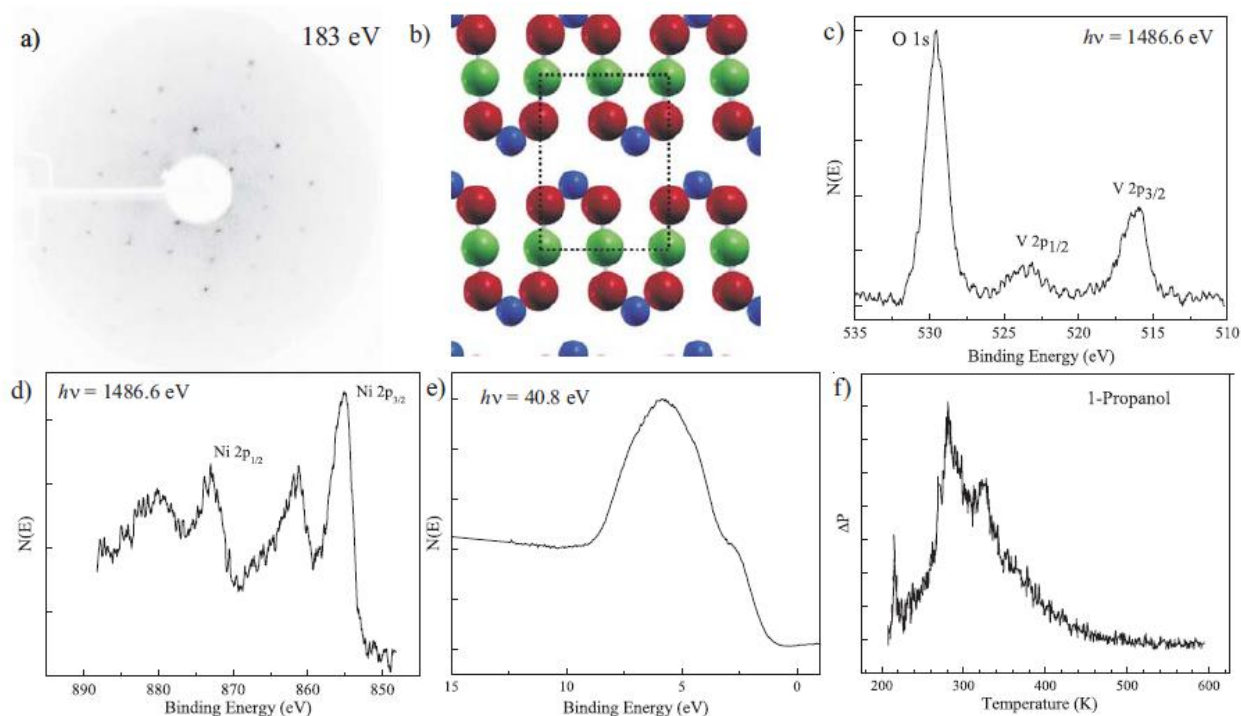


**Fig. 1. Summary of  $\text{Ni}_3\text{V}_2\text{O}_8$  (010) results. a) Rectangular LEED pattern consistent with spinel (010) A termination pictured in (b) where the red ball represent oxygen, the blue vanadium, and the green nickel atoms. c) V 2p and O 1s and d) Ni 2p XPS core level spectra consistent with  $\text{V}^{5+}$  and  $\text{Ni}^{2+}$ . d) He II UPS spectrum illustrating the insulating character of the material. f) TPD curve for 1-propanol molecular desorption.**

### Future Plans

Future work will focus on the Co and Co-containing oxides with the objective of understanding the nature of the reactive sites on these surfaces and how they can be stabilized to create efficient catalysts. The work is combining local scanning probe measurements that elucidate the details of the reactive sites with more macroscopic thermal desorption and oxygen titration measurements.

### Recent Publications

J.H. Ngai, T.C. Schwendemann, A.E. Walker, Y. Segal, F.J. Walker, E.I. Altman and C.H. Ahn, "Achieving A-site Termination on  $\text{La}_{0.18}\text{Sr}_{0.82}\text{Al}_{0.59}\text{Ta}_{0.41}\text{O}_3$  Substrates," *Advanced Materials* **22** (2010) 2945.

E.I. Altman and U.D. Schwarz, "Mechanisms, Kinetics and Dynamics of Oxidation and Oxide Surfaces Investigated by Scanning Probe Microscopy," *Advanced Materials* **22** (2010) 2854.

C.A.F. Vaz, D. Prabhakaran, E.I. Altman and V.E. Henrich, "Experimental Studies of the Interfacial Cobalt Oxide in  $\text{Co}_3\text{O}_4/\text{Al}_2\text{O}_3(0001)$  Epitaxial Films," *Physical Review B* **80** (2009) 1555457.

C.A.F. Vaz, C.H. Ahn, V.E. Henrich and E.I. Altman, "Growth and Characterization of Thin Epitaxial  $\text{Co}_3\text{O}_4(111)$  Thin Films," *Journal of Crystal Growth* **311** (2009) 2648.

**$\sigma$ -complex formation and activation of alkanes on the PdO(101) surface**

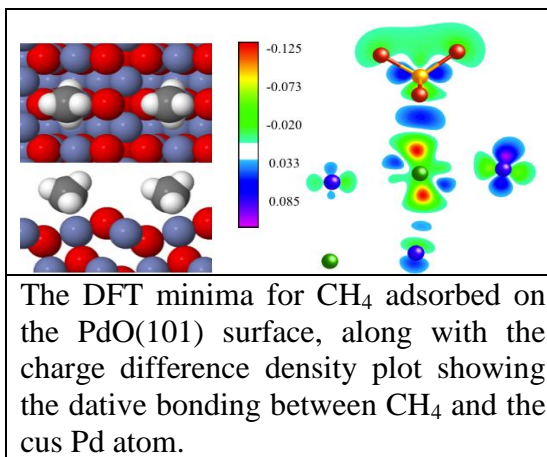
Lead PI: Jason F. Weaver (University of Florida)

Additional PIs: Aravind Asthagiri (The Ohio State University)

Students: Heywood H. Kan, Can Hakanoglu, Jose A. Hinojosa Jr., Jeffery Hawkins, Abbin Antony

Contact: William G. Lowrie Department of Chemical & Biomolecular Engineering, The Ohio State University, Columbus, OH 43210, Tel. 614-688-8882, [asthagiri@chbmeng.ohio-state.edu](mailto:asthagiri@chbmeng.ohio-state.edu)

For Pd-based catalysts used in the combustion of methane in lean gas turbines, several catalyst studies suggest that the PdO phase is critical to high activity but there is still a lack of a fundamental understanding of the nature of this observed activity. As part of our DOE project, we have used density functional theory (DFT) to explore the adsorption and activation of a series of n-alkanes on the PdO(101) surface. Experimental surface science studies in the Weaver group of alkanes from methane to n-pentane show an increase in binding energy of ~20-25 kJ/mol on the PdO(101) surface versus the Pd(111) surface. Our DFT calculations demonstrated that this enhanced binding was associated with  $\sigma$ -complexes that form between the alkanes and the coordinatively unsaturated (cus) Pd atoms at the surface. The dative bonding leads to a weakening of the C-H bonds, which reduces the barrier for C-H activation. One issue with DFT for this system is the failure to incorporate dispersion interactions accurately. To address this issue we have applied Grimme's empirical DFT-D3 approach to determine the adsorption energies of n-alkanes from methane to pentane on both the PdO(101) and Pd(111) surface. The DFT-D3 adsorption energies give excellent agreement with the experimental values for both surfaces. Incorporation of dispersion into our DFT studies of the activation barriers is ongoing and we will report these results in the poster. Finally, to explore strategies to enhance alkane binding and decrease the barrier to C-H activation we performed DFT calculations of the adsorption and activation of methane on a series of doped PdO(101) surfaces. The doping consisted of replacing the Pd cus atom with the metals Ru, Rh, Ag, Os, Ir, Pt and Au. We find a Bronsted-Evans-Polanyi correlation for the activation barriers for the doped surface. The activation barrier is correlated to the final dissociated state and charge analysis shows that C-H activation is heterolytic. The barrier for C-H activation is lowered from 64 to ~49 kJ/mol upon doping the PdO(101) surface with Pt. We are currently exploring strategies to grow Pt-PdO(101) structures experimentally to test the DFT predictions.



**Theory-guided design of nanoscale multimetallic nanocatalysts for fuel cells**

Additional PIs: Jorge M. Seminario  
Graduate Students: Rafael Callejas-Tovar, Pussana Hirunsit (graduated August 2010), Gustavo Ramirez-Caballero, Julibeth M. Martinez de la Hoz  
Undergrad. students: Santosh Koirala, Birendra Adhikari, Diego F. Leon, Diego A. Guio, Wenta Liao, Hilda Mera, Ashish Mathkari  
Postdocs: Yuguang Ma and Juan Sotelo  
Contacts: Texas A&M University, 3122 TAMU, College Station, TX 77843, phone 979-845-3375, e-mail: [balbuena@tamu.edu](mailto:balbuena@tamu.edu)

**Goal**

First-principles analyses of oxygen reduction catalysts are carried out to answer these questions: 1) How the catalytic surface and its environment change as the reaction takes place, and how these changes affect the activity and stability of the catalyst; 2) What are the effects of the dynamics of the catalyst and that of the surrounding medium on the catalytic activity and stability; 3) What is the effect of important side reactions on the catalytic process. We use a concerted multiscaled theoretical analysis of nanoscale multimetallic catalysts including their environment. Our ab initio approach is directly applicable to other catalytic reactions taking place on nanoscale particles. Proof of concept experiments are planned as complement to our theoretical studies.

**DOE Interest**

This research facilitates the rational design of catalysts for the oxygen reduction reaction with improved activities and durabilities. Such reaction is important not only in fuel cell electrocatalysts but also in water splitting (its reverse process) which is a key reaction for solar cells. Simultaneously, this research advances fundamental and applied aspects of catalytic reactions such as the physics, chemistry, methods, and development of accurate guidelines for rational design.

**Recent Progress**

*Surface segregation effects in alloy nanoparticles:* Analysis of core-shell and ordered alloys showed segregation trends to be dependent on three main factors: atomic size, surface energies, and heat of formation of the alloy. However, the segregation trend in most cases changes substantially when oxygen is adsorbed on the surface, and is then dominated by the tendency of the most oxyphilic species to migrate to the surface. Low coordination sites such as steps and kinks usually enhance the segregation trend. One interesting exception is the case of Ir cores covered by one monolayer of Pt, where Ir (in spite of its oxyphilicity) does not segregate to the surface even in the presence of up to 0.5 monolayer of oxygen. To complement our thermodynamic analysis, we developed a new model to investigate the kinetics of metal segregation for an infinitely diluted solute in bimetallic alloys.

*Reactivity of low-coordinated sites in acid medium.* Using a combined density functional theory and Green's function approach we studied the reduction of oxygen on small supported clusters in aqueous acid medium, modeled by hydronium and dihydrated

hydronium ( $\text{H}_7\text{O}_3^+$ ). In particular, we showed that a locally neutral neighborhood of an active site in the bimetallic cluster assists in the protonation reaction, and is equally effective to that of a complex hydronium hydration.

*Correlation of surface segregation and dissolution trends in core-shell alloy surfaces:* A systematic study as a function of core composition starting with monometallic cores of the 3d, 4d, and 5d groups revealed that all the 4d and 5d pure cores may serve as stable cores, and their beneficial effect on the Pt monolayer may be further tuned by alloying the core to another element, here chosen from 3d or 5d groups. The  $\text{Pd}_3\text{X}$  cores enhance the stability of the surface Pt atoms both in vacuum and under adsorbed oxygen; however the high oxygen-philicity of some of the X elements induces their surface segregation causing surface poisoning with oxygenated species and dissolution of the X metals in acid medium.

*Design of a new dissolution-resistant catalyst material:* Based on our DFT studies, we formulated and evaluated a new catalytic material both for activity and for stability of the surface atoms against dissolution in acid medium. The significant stability improvement predicted for the new material is due to the addition of a small-radius species that locates in the interstitial sites of the top subsurface layers locking the core transition metal atoms in their positions, thus avoiding their segregation to the surface and posterior dissolution, which is driven by the oxidative acid environment. We demonstrated the durability and activity enhancement for the platinum/iron-carbon/iridium system. We also investigated alternative core and alternative anchor materials. Experiments are being conducted to validate the theoretical predictions.

*Surface oxidation and reconstruction effects on pure Pt and Pt-skin surfaces.* Buckling of surface Pt atoms is known to occur at high oxygen coverage on pure Pt and alloy surfaces. We developed a novel multi-scale modeling approach where we mimic the oxidation process of extended surfaces of pure Pt and Pt-alloys as a function of increasing oxygen coverage, yielding the time evolution of the surface at a given extent of oxidation.

## **Future Plans**

*Evolution of nanocatalyst surface under oxidation and reduction conditions.* Our multiscale theoretical method is applied to investigate how nanocatalyst particles evolve as a function of the extent of oxidation. Such oxidation is given by various oxygenated species such as atomic oxygen and water dissociation products. The pH effect is also incorporated. Important features such as the migration of oxygen to the subsurface, segregation of the non-noble atoms and buckling effects as precursors of dissolution are investigated.

*Effects of geometric and electronic confinement on catalytic reactions.* We investigate the origins of the enhanced catalytic activity found in nanoporous structures after dealloying. We suggest that such activity enhancement is originated by the geometric and electronic confinement resulting from the nanoporous structure originated after the dealloying process. We have defined a systematic plan to verify our hypothesis and investigate additional details that can be applied to a more general class of catalytic processes.

## **Publications (2009-2011)**

1. G. E. Ramírez-Caballero and P. B. Balbuena, "Confinement-induced changes in magnetic behavior of a Ti monolayer on Pt" *Chem. Phys. Lett.*, **507** (2011) 117-121.

2. R. Callejas-Tovar, W. Liao, J. Martinez de la Hoz, and P. B. Balbuena, "Molecular dynamics simulations of surface oxidation on Pt(1 1 1) and Pt/PtCo/Pt<sub>3</sub>Co(1 1 1)" *J. Phys. Chem C.* **115** (2011) 4104-4113.
3. G. E. Ramirez-Caballero, A. Mathkari, and P. B. Balbuena, "Confinement-induced polymerization of ethylene," *J. Phys. Chem C.* **115** (2011) 2134-2139.
4. J. M. Martinez de la Hoz, D. F. Leon-Quintero, P. Hirunsit, and P. B. Balbuena, "Evolution of a Pt(111) surface at high oxygen coverage in acid medium," *Chem. Phys. Lett.* **498** (2010) 328-333.
5. G. E. Ramirez-Caballero, P. Hirunsit, and P. B. Balbuena, "Shell-anchor-core structures for enhanced stability and catalytic oxygen reduction activity," *J. Chem. Phys.* **133** (2010) 134705.
6. P. Hirunsit and P. B. Balbuena, "Stability of Pt monolayers on Ir-Co cores with and without a Pd interlayer," *J. Phys. Chem. C* **114** (2010) 13055-13060.
7. G. E. Ramirez-Caballero and P. B. Balbuena, "Confinement effects on alloy reactivity," *Phys. Chem. Chem. Phys.* **12** (2010) 12466-12471.
8. G. E. Ramirez-Caballero and P. B. Balbuena, "Dissolution-resistant core-shell materials for acid medium oxygen reduction electrocatalysts," *J. Phys. Chem. Lett.* **1** (2010) 724-728..
9. K. Gong, W-F Chen, K. Sasaki, D. Su, M. B. Vukmirovic, W. Zhu, E. L. Izzo, C. Perez-Acosta, P. Hirunsit, P. B. Balbuena, and R. R. Adzic, "Platinum monolayer electrocatalysts: Improving the activity for the oxygen reduction reaction with palladium interlayer on IrCo alloy core," *J. Electroanal. Chem.* **649** (2010) 232-237.
10. Y. Ma and P. B. Balbuena, "Surface adsorption and stabilization effect of Iridium in Pt-based alloy catalysts for PEM fuel cell cathodes," *ECS Transactions* **25** (2009) 1037-1044.
11. Y. Ma and P. B. Balbuena, "Role of Iridium in Pt-based Alloy Catalysts for the ORR: Surface Adsorption and Stabilization Studies," *J. Electrochem. Soc.* **157** (2010) B959-B963.
12. G. E. Ramirez-Caballero, Y. Ma, R. Callejas-Tovar, and P. B. Balbuena, "Surface segregation and stability of core-shell alloy catalysts for oxygen reduction in acid medium," *Phys. Chem. Chem. Phys.* **12** (2010) 2209-2218.
13. P. Hirunsit and P. B. Balbuena, "Effects of water and electric field on atomic oxygen adsorption on PtCo alloys," *Surf. Sci.* **603** (2009) 3239-3248.
14. G. E. Ramirez-Caballero and P. B. Balbuena, "Effect of confinement on oxygen adsorbed between Pt(111) surfaces," *J. Phys. Chem. C* **113** (2009) 7851-7856.
15. J. M. Martinez De La Hoz, R. Callejas-Tovar and P. B. Balbuena, "Size effect on the stability of Cu-Ag nanoalloys," *Mol. Sim.* **35** (2009) 785-794.
16. P. Hirunsit and P. B. Balbuena, "Surface atomic distribution and water adsorption on PtCo alloys," *Surf. Sci.* **603** (2009) 911-919.
17. Y. Ma and P. B. Balbuena, "Surface segregation in bimetallic Pt<sub>3</sub>M (M=Fe, Co, Ni) alloys with adsorbed oxygen," *Surf. Sci.* **603** (2009) 349-353.
18. J. C. Sotelo and J. M. Seminario "Protonation of O<sub>2</sub> adsorbed on a Pt<sub>3</sub> island supported on transition metal surfaces," *J. Chem. Phys.* **131**(2009) 044709.
19. K. Salazar-Salinas, L. A. Jauregui; C. Kubli-Garfias, and J. M. Seminario "Molecular biosensor based on a coordinated iron complex," *J. Chem. Phys.* **130** (2009) 105101-1-9.

**Photocatalysis of Modified Transition Metal Oxide Surfaces**

Postdoc: Junguang Tao

Students: Tim Luttrell

Collaborators: Xueqing Gong (ECUST, Shanghai)

Contacts: University of South Florida, Tampa, FL 33620- [mbatzill@usf.edu](mailto:mbatzill@usf.edu)

**Goal:**

To establish a cause-effect relationship for structurally and compositionally modified photocatalysts. Gaining molecular scale understanding of how surface and bulk modifications alter the photocatalytic reactivity to aid the design for next generation photocatalysts.

**DOE Interest:**

Efficient clean up of organic pollutants and direct production of chemical fuels from sun light by photocatalytic processes is of interest for clean, renewable energy production. A better fundamental understanding of the interplay between (surface) structure, (hetero) interfaces and composition on the one hand, and the (photo) catalytic properties on the other hand will enable a better understanding and controlled design of complex photocatalyst materials.

**Recent Progress:**

*Face dependent surface properties:* It is well established that the photocatalytic properties depend on the surface orientation<sup>1</sup> of the material. Our studies aim at understanding the fundamental surface properties of different surface-orientation of the prototypical photocatalyst TiO<sub>2</sub>. In particular we address the difference of the surface properties of the TiO<sub>2</sub>(011) surface compared to the frequently studied (110) surface. We found differences in the binding energy of defect induced band gap states for the two rutile surfaces<sup>2</sup> which we attributed to a crystal field effect as a consequence of the surface reconstruction of the (011)-2x1 surface. Such a change in the binding energy of surface trapped electrons has consequences for charge transfer processes in photocatalytic reactions. Furthermore, the adsorption properties of (011)-2x1 surface was found to be dramatically different from that of the (110) surface probed by carboxylic acid adsorption<sup>3</sup>. The role the surface reconstruction plays for the surface reactivity is of continuing interest and is discussed in the 'future plans' section.

*Novel narrow band gap surface phases:* While studying the properties of TiO<sub>2</sub>(011) surfaces an exciting discovery has been made that indicates the presence of meta-stable pure TiO<sub>2</sub> surface phases with a much reduced band gap as shown in Fig. 1. We thoroughly characterized the electronic properties of this surface phase by scanning tunneling spectroscopy and resonant photoemission spectroscopy and found that the surface phase induces an oxygen derived state on top of the bulk valence band of TiO<sub>2</sub><sup>4</sup>. This surface state may enable visible light absorption and/or hole-trapping at the surface which both could have potential importance for photocatalytic



applications. The structural and (photo)chemical properties of this new phase of  $\text{TiO}_2$  will be studied further in the future.

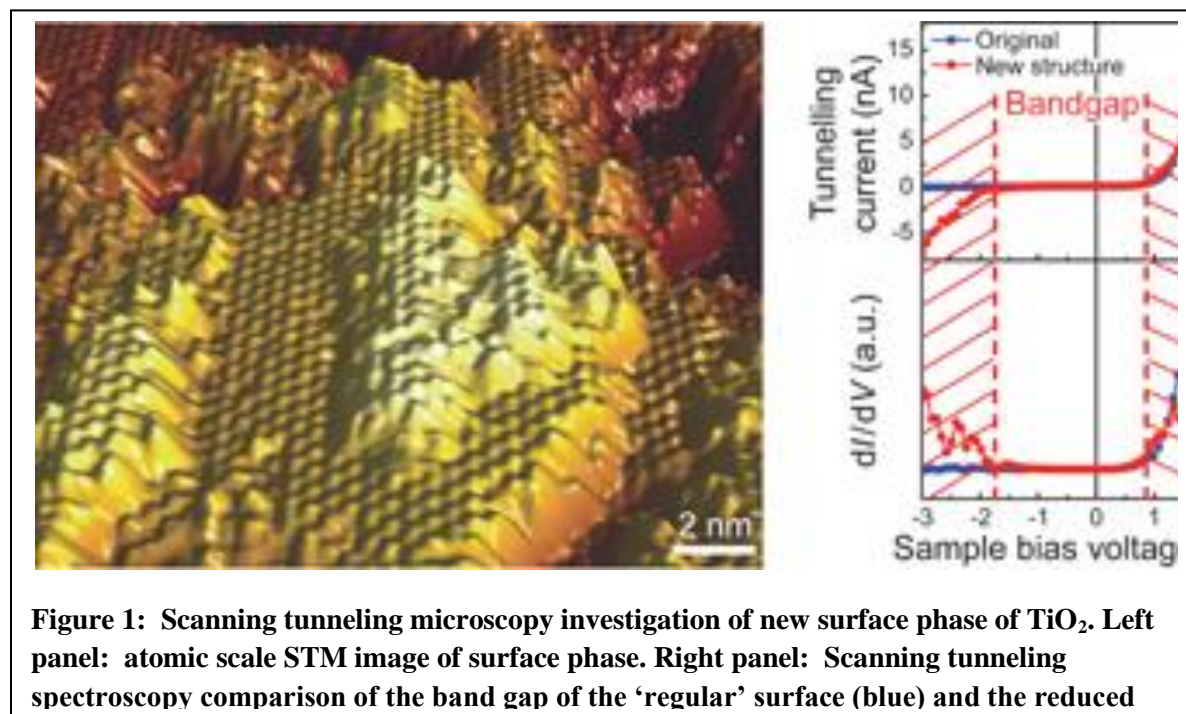


**Figure 1: Scanning tunneling microscopy investigation of new surface phase of  $\text{TiO}_2$ . Left panel: atomic scale STM image of surface phase. Right panel: Scanning tunneling spectroscopy comparison of the band gap of the ‘regular’ surface (blue) and the reduced**

*Surface nanostructuring:* In our quest to better understand the influence of nanoscale surface morphology on the photocatalytic properties we enhanced our understanding of surface nano-patterning by a newly developed grazing incidence ion sputtering approach. The formation mechanisms of nanoripple structures that exhibit defined step edge orientations have been investigated<sup>5</sup>. This novel sample preparation procedure will enable us to correlate surface photoactivity with surface nanostructures in the near future.

### **Future Plans:**

All the above outlined research thrusts are ongoing and critical questions remain to be answered:

*Face dependent surface properties:* How stable is the surface reconstruction of the  $\text{TiO}_2(011)\text{-}2\times 1$  surface in different environments? Our initial adsorption studies appear to indicate that the surface/interface structure may change for different adsorbates. This will be further investigated by STM and in collaboration with computational theorists.

*Novel narrow band gap surface phases:* What is the structure of the narrow band gap surface phase on  $\text{TiO}_2(011)$ ? From theoretical predictions it appears possible that the narrowed band gap is due to formation of titanyl-oxygen at the surface. We will investigate this, through collaborations with other experimentalists with appropriate equipment (FTIR, HREELS).

*Surface nanostructuring:* How do the photocatalytic properties change for different surface morphologies? In an initial experiment we plan to use photocatalytic degradation of organic dyes in aqueous solution to measure the relationship between surface morphology and photoreactivity.

*Growth of model photocatalyst epitaxial films:* An important medium term goal of this project is to prepare photocatalyst samples with well defined surface properties that can be modified in order to investigate the role of bulk and surface modification on the photocatalytic properties. In the first half of this research project we have been setting up a laser MBE system to grow epitaxial metal oxide films and are now in the process of optimizing the growth of SrTiO<sub>3</sub> photocatalysts on LaAlO<sub>3</sub> substrates as the initial model system. In the second part of this project the goal is to modify these films with N-doping and investigate the effect of charge-compensating co-dopants for increasing N-concentration and minimizing defect formation. Surface modifications with monolayers will be studied subsequently.

### **Publications:**

---

<sup>1</sup> **Invited Perspective:** “Fundamental aspects of surface engineering of transition metal oxide photocatalysts” M. Batzill, Energy & Environmental Science **submitted**

<sup>2</sup> “Role of Surface Structure on the Charge Trapping in TiO<sub>2</sub> Photocatalysts” J. Tao, T. Luttrell, M. Batzill, **J. Phys. Chem. Lett.** **1**, 3200-3206 (2010).

<sup>3</sup> “Adsorption of Acetic Acid on Rutile TiO<sub>2</sub>(110) vs. (011)-2x1 Surfaces” J. Tao, T. Luttrell, J. Bylsma, M. Batzill, **J. Phys. Chem. C** **115**, 3434-3442 (2011).

<sup>4</sup> “A Two-dimensional phase of TiO<sub>2</sub> with a reduced band gap” J. Tao, T. Luttrell, M. Batzill, **Nature Chem.** **3**, 296-300 (2011).

<sup>5</sup> “Nanoripple Formation on TiO<sub>2</sub>(110) by low-energy grazing incidence ion sputtering” T. Luttrell, M. Batzill, **Phys. Rev. B** **82**, 35408 (2010).

### Catalysis for the Selective Synthesis of Fuels and Chemical

Postdocs: Anastasia Grigorieva, Vladimir Shapovalov, Jennifer Strunk  
Students: Andrew Getsoian, William C. Vining, Zheng Zhai  
Collaborators: Martin Head-Gordon (UC Berkeley)  
Contacts: Department of Chemical Engineering, University of California, Berkeley,  
CA 94720-1462; [bell@cchem.berkeley.edu](mailto:bell@cchem.berkeley.edu)

#### Goal

The goal of this program is to develop a molecular understanding of catalytically active centers and to use this knowledge to in order to synthesize unusual chemical and physical environments at such centers. The program involves a synergistic combination of efforts in the areas of catalyst synthesis, characterization, and evaluation. Quantum chemical simulations of catalytically active centers are used guide the interpretation of experimental findings and suggest novel structures to be attempted synthetically.

#### DOE Interest

Understanding the fundamental relationships between catalyst composition and structure and catalyst activity and selectivity is one of the primary goals of the DOE Chemical Energy program. Work done on this project contributes to an atomic and molecular understanding of catalysis, and in particular to the definition of the structure of a catalytically active site, the mechanism by which chemical transformations occur at such sites, and the means by the activity and selectivity of a site can increased.

#### Recent Progress

*Methanol Oxidation at Isolated Vanadate Centers:* The structure and properties of isolated vanadate centers deposited on two-dimensional, submonolayer deposits of  $\text{TiO}_x$ ,  $\text{ZrO}_x$ , and  $\text{CeO}_x$  deposited on  $\text{SiO}_2$  have been characterized experimentally and theoretically and investigated for the oxidation of methanol. As shown in Fig. 1, the specific activity of isolated vanadate species increases by nearly two orders of magnitude with increasing surface density of promoting oxide. Application of 51V NMR has shown that the fraction of the vanadate species interacting with the promoter oxide can be determined quantitatively.

The strong effect of titania on the rate of methanol oxidation to formaldehyde is attributed to the formation of oxygen defects in titania-containing catalysts. Evidence for such defects obtained by EPR and DFT calculations has shown that the occurrence of defects adjacent to isolated vanadates can explain the strong enhancement in the rate of methanol oxidation observed for titania-containing catalysts.

*Hydrocarbon Oxidation on Mixed Metal Oxides:* The selective oxidation of hydrocarbons over mono- and multi-metallic oxides is widely used to produce commodity and specialty products (e.g., aldehydes, alcohols, carboxylic acids). However, despite the importance of such processes, catalyst selection is largely based on empiricism and attempts to define

the optimal properties for a given reaction based on one or more quantitative descriptor of catalyst properties have not proven successful. We have, therefore, initiated an effort aimed at developing a fundamental understanding of how the composition and structure of mixed metal oxides are related to their activity and selectivity. The system chosen for investigation is the oxidation of propene to acrolein on oxides containing a mixture of Bi, V, and Mo ( $\text{Bi}_{(1-x)/3}\text{V}_{1-x}\text{Mo}_x\text{O}_4$ ) they can be prepared with values of  $x$  from 0 to 1.0, while maintaining a  $\alpha$ -scheelite crystal structure. Systematic characterization of the physical and chemical properties of these catalysts have been carried out using UV-Vis and Raman spectroscopy, as well as XPS and XAS. These studies have been paralleled by DFT calculations of the effects of composition on the electrophilic and nucleophilic properties of the O atoms exposed at the oxide surface. Measurements have also been made of the activity and selectivity of  $\text{Bi}_{(1-x)/3}\text{V}_{1-x}\text{Mo}_x\text{O}_4$  for the oxidation of propene to acrolein. This work has shown that both nucleophilic and electrophilic surface oxygen atoms are required, together with exposed  $\text{Mo}^{6+}$  cations in order to achieve high activity and selectivity for the formation of acrolein.

### **Future Plans**

*Catalysis by Vanadate Species on Tailored Supports:* Work will continue on the synthesis and characterization of monolayer and bilayer coatings of titania, zirconia, and other oxides on silica, as part of an effort to prepare tailored supports. These model structures will be compared with those proposed on the basis of quantum mechanical calculations. Isolated metal oxo species, e.g., vanadates and molybdates will then be deposited onto these tailored supports and investigated with the aim of identifying the role of the deposited layer on the activity and selectivity of the oxo species for a variety of test reactions. The importance of the interlayer on processes such as oxygen transport and reactant adsorption will be explored.

*Hydrocarbon Oxidation on Mixed Metal Oxides:* We plan to continue our efforts on multmetallic oxide catalysts with the aim of establishing the relationship between the activity and selectivity of these materials for partial oxidation of hydrocarbons and oxygenated organic products. Experiments using UV-Visible spectroscopy and XANES will be implemented to follow changes in oxidation state of the bulk, and high-pressure XPS used to probe the oxidation states of the catalyst surface, as functions of the reaction temperature and gas composition. We will continue our efforts on  $\text{Bi}_{(1-x)/3}\text{V}_{1-x}\text{Mo}_x\text{O}_4$  and initiate new studies on  $\text{Mo}_3\text{Nb}_{2-x}\text{V}_x\text{O}_{14}$ . The latter catalyst has been identified as a good candidate for the oxidation of ethene to acetaldehyde and acetic acid. Experimental characterization of catalysts will be complemented by DFT calculations of the nucleophilic and electrophilicity of O atoms present at the oxide surface. Efforts to use DFT in order to identify reaction pathways from reactants to products initiated recently will be continued. The results of such calculations will be used to identify which O atoms are most likely to be involved in the oxidation of ethene and propene, and to determine the dependence of activation energies on the surface composition of mixed metal oxides.

### **Publications (2009-2011)**

1. J. L. Bronkema and A. T. Bell, "Mechanistic studies of methanol oxidation to formaldehyde on isolated vanadate sites supported on high surface area zirconia," J.

Phys. Chem. C, 112, 6404-6412 (2008).

2. J. Bronkema and A. T. Bell, "An investigation of the reduction and reoxidation of isolated vanadate sites supported on MCM-48," *Catal. Lett.* 122, 1-8 (2008).
3. B. Kilos, A. T. Bell, and E. Iglesia, "Mechanism and site requirements for ethanol oxidation on vanadium oxide domains," *J. Phys. Chem. C* 113, 2830-2836 (2009).
4. A. Dinse and R. Schomacker, "The role of lattice oxygen in the oxidative dehydrogenation of ethane on alumina-supported vanadium oxide," *Phys. Chem. Chem. Phys.*, 11, 6119-6124 (2009).
5. A. Goodrow, M. Head-Gordon, and A. T. Bell, "Are spin-forbidden crossings a bottleneck in methanol oxidation," *J. Phys. Chem. C*, 113, 19361-19364 (2009).
6. W. Vining, A. Goodrow, J. Strunk, and A. T. Bell, "An experimental and theoretical investigation of the structure and reactivity of bilayered  $\text{VO}_x/\text{TiO}_x/\text{SiO}_2$  catalysts for methanol oxidation," *J. Catal.*, 270 163-171 (2010).
7. J. Strunk, W. C. Vining, and A. T. Bell, "A Study of oxygen vacancy formation and annihilation in submonolayer coverages of  $\text{TiO}_2$  dispersed on MCM-48," *J. Phys. Chem., C* 114, 16937-16945 (2010).
8. J. Strunk, W. C. Vining, and A. T. Bell, "Synthesis of different  $\text{CeO}_2$  structures on mesoporous silica and characterization of their reduction properties," *J. Phys. Chem. C* 115, 4114-4126 (2011).
9. W. C. Vining, and A. T. Bell, *J. Catal.* "Investigation into the nature and activity of  $\text{VO}_x/\text{ZrO}_2/\text{SiO}_2$  catalysts in methanol oxidation to formaldehyde," *J. Catal.*, 281, 222-230 (2011).
10. W. C. Vining, and A. T. Bell, *J. Catal.* "Investigation of the structure and activity of  $\text{VO}_x/\text{CeO}_2/\text{SiO}_2$  catalysts for methanol oxidation to formaldehyde," *J. Catal.*, in press.

# Changing Selectivity of Methanol-to-Hydrocarbons Catalysis by Manipulating the Hydrocarbon Pool

Aditya Bhan

University of Minnesota, Department of Chemical Engineering and Materials Science,  
Minneapolis, MN 55455

email: [abhan@umn.edu](mailto:abhan@umn.edu)

The dehydrative condensation of methanol on zeolites is unique in its ability to form carbon-carbon bonds and concurrently restrict the carbon-chain length based on the shape selective characteristics of the molecular sieve. Mechanistic,<sup>[1]</sup> spectroscopic,<sup>[2]</sup> and theoretical computational chemistry<sup>[3]</sup> based studies have confirmed that carbon-carbon bond formation in methanol-to-hydrocarbons (MTH) occurs via an indirect route, known as the “hydrocarbon pool” mechanism. In this hypothesis, organic species, specifically, olefins and arenes, contained inside the zeolite pore act as scaffolds for C-C bond formation. Therefore, the catalytic behavior in MTH systems is determined not only by the structural and compositional features of the inorganic molecular sieve, but also by the organic co-catalyst that comprises the hydrocarbon pool.<sup>[4-6]</sup> The effects of zeolite structure and topology on MTH chemistry have been extensively studied, however, the role of the organic co-catalyst in controlling rate and selectivity remain largely unexplored.

We report that by co-feeding olefin and aromatic compounds with dimethyl ether (DME), we can control the composition of the organic hydrocarbon pool and thereby modulate the relative contribution of olefin and arene methylation cycles in MTH resulting in systematic variations in MTH selectivity at iso-conversion (Figure 1). These effects of changing the organic co-catalyst in MTH catalysis persist at varying temperatures, conversion, and space velocity. Therefore, changing the hydrocarbon pool provides a simple and specific strategy to tune selectivity for carbon-carbon bond formation reactions in MTH in a way that can be both predicted and controlled. Kinetic and isotopic studies that probe the identity and reactivity of specific olefin and arene components of the hydrocarbon pool, and an assessment of the relative propagation of olefin and arene methylation cycles as a function of zeolite topology will be presented.

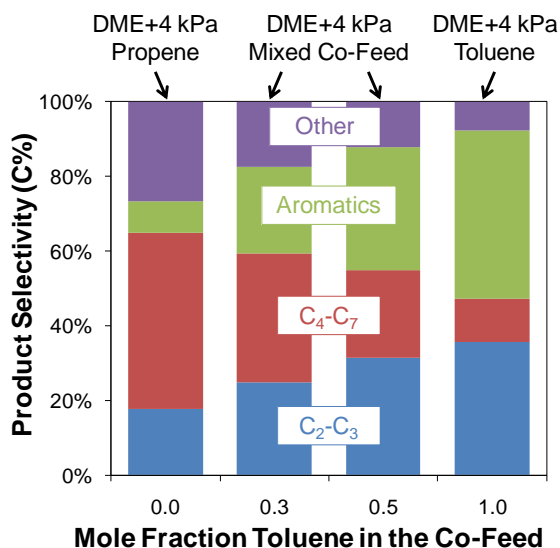


**Figure 1.** Measured selectivity for MTH on HZSM-5 at 548 K, 70 kPa DME, 4 kPa co-feed, DME WHSV = 20 g (g catalyst)<sup>-1</sup> h<sup>-1</sup>, 14-19% carbon conversion.

## References

- [1] I. M. Dahl, S. Kolboe, *Catalysis Letters* 1993, 20, 329.
- [2] W. Song, J. F. Haw, J. B. Nicholas, C. S. Heneghan, *Journal of the American Chemical Society* 2000, 122, 10726.
- [3] D. Lesthaeghe, V. Van Speybroeck, G. B. Marin, M. Waroquier, *Chemical Physics Letters* 2006, 417, 309.
- [4] R. M. Dessau, R. B. LaPierre, *Journal of Catalysis* 1982, 78, 136.
- [5] M. Bjørgen, S. Svelle, F. Joensen, J. Nerlov, S. Kolboe, F. Bonino, L. Palumbo, S. Bordiga, U. Olsbye, *Journal of Catalysis* 2007, 249, 195.
- [6] M. Bjørgen, F. Joensen, K.-P. Lillerud, U. Olsbye, S. Svelle, *Catalysis Today* 2009, 142, 90.

## Three dimensional nonequilibrium thermochemistry assisted by magnetic resonance tomography

L.-S. Bouchard, R. Sharma

University of California, Dept. of Chemistry and Biochemistry, Los Angeles, CA 90095

e-mail: [bouchard@chem.ucla.edu](mailto:bouchard@chem.ucla.edu)

Three dimensional tomography techniques such as magnetic resonance imaging (MRI) and micro computed tomography ( $\mu$ -CT) are combined together with the formalism of linear nonequilibrium thermodynamics (NET) (de Groot and Mazur, 1961) to provide a new set of tools for the study of *in situ* heterogeneous catalytic reactions in an operating reactor. Phase-encoded nuclear magnetic resonance (NMR) spectra yield local temperature, density and chemical potentials of the fluid phase whereas velocity-encoded MRI enables us to derive local pressures. The  $\mu$ -CT images provide density of the solid phase catalyst, which is used to compute effective-medium properties such as the volume-averaged heat capacity. These quantities are obtained in a non-invasive manner and therefore do not perturb the reaction. The local entropy inside the catalytic reactor is derived from these quantities using the Gibbs-Duhem equation. The Gibbs equation is used to produce maps of the entropy production, which can then be analyzed and related to the lost work. This integrated formalism could be used as a means to optimize the topology of catalytic reactors. We then use the equations for conservation of total mass, momentum, energy and species mass for a steady state flow to derive a number of thermodynamically relevant quantities: reaction rate constant, activation energy, heat capacity, thermal conductivity and surface reactivity. These parameters are spatially-resolved, measured in an operating reactor, and therefore include the effects of the transport processes and catalyst distribution. Reactions we have studied using these techniques are olefin hydrogenation on metal surfaces (Pt, Pd) (from nanocluster to bulk) as well as metal-organic framework (MOF) catalysts. The latter system presents unique transport and storage properties which are readily obtained from the measurement.

### References

S.R. de Groot, P. Mazur, Non-equilibrium thermodynamics, North-Holland (1963)



**Catalytic selective conversion of lignocelluloses to transportation biofuels**

Lead PI: Johannes A. Lercher

CoPIs: Yong Wang, Donghai Mei, Jianzhi Hu and John Fulton

Student(s): Baoxiang Peng and Jiayue He

Collaborators: Chen Zhao, Catalysis Research Center, Technische Universität München

Contact: Chemical and Materials Sciences Division, Pacific Northwest National

Laboratory, PO Box 999, Richland, WA 99352; donald.camaioni@pnl.gov

While lignocellulosic biomass is a potential green and sustainable energy-resource, the production of clean hydrocarbon-based energy carriers from biomass requires new catalytic approaches to transform the wide variety of substrates into a more uniform pool of hydrocarbons. The fundamental challenges for this effort are designing novel catalytic systems for selective cleavage of chemical bonds in biomass and controlling the properties of liquids and liquid/solid interfaces for catalysis. Recent results obtained from Technische Universität München show that the dual functionality of metal and acid is indispensable for the efficient aqueous-phase hydrodeoxygenation (HDO) of bio-derived phenols and alcohols.<sup>1-4</sup> Furthermore, new results open the possibility of C-C bond coupling in tandem with HDO of substituted phenols over the dual functional catalysts, producing high yields of saturated C<sub>12</sub>-C<sub>18</sub> hydrocarbons. The kinetics of the elementary reactions in the overall hydrodeoxygenation will be analyzed to elucidate reaction mechanisms, and the surface chemistry and state of the catalyst materials will be characterized under reaction conditions by in-situ spectroscopic methods together with theoretical and modeling studies.

**References**

1. C. Zhao, J. He, A. A. Lemonidou, X. Li, J. A. Lercher, Aqueous-phase hydrodeoxygenation of bio-derived phenols to cycloalkanes. *Journal of Catalysis* **280**, 8 (2011).
2. C. Zhao, Y. Kou, A. A. Lemonidou, X. Li, J. A. Lercher, Hydrodeoxygenation of bio-derived phenols to hydrocarbons using RANEY<sup>®</sup> Ni and Nafion/SiO<sub>2</sub> catalysts. *Chemical Communications* **46**, 412 (2010).
3. C. Zhao, Y. Kou, A. A. Lemonidou, X. Li, J. A. Lercher, Highly selective catalytic conversion of phenolic bio-oil to alkanes. *Angewandte Chemie International Edition* **48**, 3987, (2009).
4. A. Wawrzetz, B. Peng, A. Hrabar, A. Jentys, A. A. Lemonidou, J. A. Lercher, Towards understanding the bifunctional hydrodeoxygenation and aqueous phase reforming of glycerol. *Journal of Catalysis* **269**, 411 (2010).

**Supported Metal Nanoparticles:  
Correlating Catalytic Kinetics, Energetics and Surface Structure**

Postdoc: Dr. Yong Yang  
Students: Jason Farmer, Jason Sellers, Eric Karp, Trent Silbaugh,  
Collaborators: Prof. Hajo Freund and Dr. Svetlana Schauermann, Fritz Haber Institute, Berlin;  
Dr. Chuck Peden, PNNL, Prof. Chuck Mims, University of Toronto.  
Contacts: Chemistry Department, Box 351700, University of Washington,  
Seattle, WA 98195-1700, [campbell@chem.washington.edu](mailto:campbell@chem.washington.edu)

**Goals**

To provide the basic understanding of surface structure-function relationships needed to develop new and improved catalyst materials involving metal nanoparticles supported on oxide and carbon surfaces for reactions of importance in energy conversion and environmental protection. To clarify the geometric, energetic and dynamic factors which control the atomic-level structure of certain metal / support interfaces, and the interplay between this structure and the chemical / catalytic reactivity of metal-on-support surfaces.

**DOE Interest**

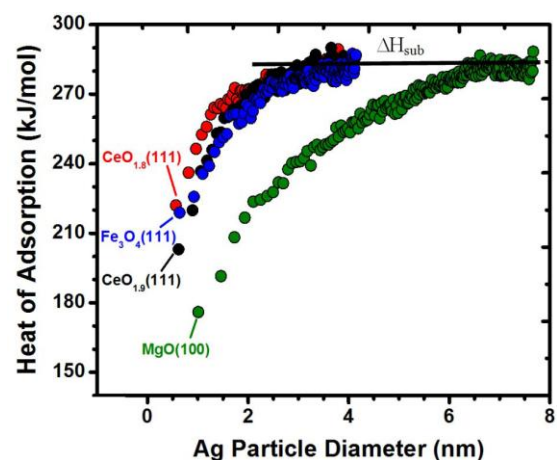
Transition metal nanoparticles dispersed across the surfaces of oxide and carbon support materials form the basis for most solid catalysts used for industrial chemical reactions that produce fuels and clean up pollution associated with the generation and use of fuels. They also serve as the best electrocatalysts for fuel cells and photocatalysts for solar energy use. If we are to provide the energy needed for sustained economic development using alternate energy sources (biomass, solar or nuclear) and avoid serious environmental problems, we must develop new and improved solid catalysts, electrocatalysts and photocatalysts for a variety of reactions. This experimental research provides the basic understanding needed to do this. Also, the energy measurements performed in this program (which are unique in the world) will serve as important benchmarks for developing more accurate computational tools for surface science and materials science, which could favorably impact this and many other technologies of importance to DOE.

**Recent Progress**

We have studied several well-defined model catalysts consisting of metal nanoparticles supported on single-crystalline oxide surfaces, structurally characterized using a variety of ultrahigh vacuum surface science techniques. We have used calorimetry techniques invented here and unique in the world to measure the energies of the metal atoms in these particles and the energy of adsorbed intermediates on these particles, and to determine how these energies depend on the size of the particles and the nature of the oxide support upon which they sit. We have started to see correlations between these energies (which reflect the bonding strengths of these metal nanoparticles to their support and to catalytic intermediates) with each other and with their catalytic properties (sintering kinetics, elementary-step rates and net catalytic reaction rates), specifically how these vary with particle size and the nature of the support surface. We believe that when this correlation is better developed, it will prove crucial to understanding how and why specific structural properties of catalysts determine their catalytic properties. By assessing this interplay between industrially important rates (of sintering and catalytic steps or net reactions)

and their thermodynamic driving forces, we expect to provide a deeper fundamental understanding of oxide- and carbon-supported metal catalysts particles. This understanding will facilitate development of better catalyst materials for clean, sustainable energy technologies.

**Metal Adsorption Energetics:** The adsorption energies and growth morphology of silver on reduced  $\text{CeO}_2(111)$  thin films on  $\text{Pt}(111)$  at 300 K was studied using adsorption microcalorimetry in combination with  $\text{He}^+$  ISS, AES, XPS, electron energy loss spectroscopy (EELS), sticking probability measurements, low LEED and STM<sup>6-7</sup>. Similar measurements were made for Ag on 4 nm thick  $\text{Fe}_3\text{O}_4(111)$  films<sup>13</sup>. The energies of Ag atoms in Ag nanoparticles on  $\text{CeO}_2(111)$ ,  $\text{Fe}_3\text{O}_4(111)$  and  $\text{MgO}(100)$ , were analyzed versus particle size (see Fig. 1)<sup>7,13</sup>. We found that their stability increases with particle size below 5000 atoms per particle. Silver nanoparticles of any given size below 1000 atoms have much higher stability (30 to 70 kJ per



mole of silver atoms) on  $\text{Fe}_3\text{O}_4(111)$  and reduced  $\text{CeO}_2(111)$  than on  $\text{MgO}(100)$ . We showed that this effect is the result of the very large adhesion energy ( $\sim 2.3$  joules per square meter) of Ag nanoparticles to  $\text{CeO}_{2-x}(111)$  and  $\text{Fe}_3\text{O}_4(111)$ . These results explain the unusual sinter resistance of late transition metal catalysts on ceria supports.

**Figure 1:** The measured adsorption energy of Ag atoms versus the average Ag particle diameter to which they add, for Ag particles on different 4-nm-thick oxide film surfaces grown on metal crystals.

**Molecule Adsorption Energetics on Size-selected Metal Nanoparticles:** In collaboration with Hajo Freund's group at the Fritz Haber Institute, we made the first ever *direct* measurements of adsorption heats of small molecules on size-controlled metal nanoparticles on any single-crystal oxide surface. Specifically, we reported that the adsorption enthalpy of CO on Pd clusters on  $\text{Fe}_3\text{O}_4(111)$  increases with particle size from 120 to 5000 Pd atoms per particles<sup>5,14</sup>. This was done on a unique new single crystal adsorption calorimeter apparatus we helped build in Freund's lab in Berlin following our heat detector design, whose design we have published<sup>10</sup>.

**Studies of Catalytic Reaction Kinetics and Mechanisms:** We reported a new and very powerful kinetics concept called the "generalized degree of rate control", which can be applied to any microkinetic model of any multistep chemical process (catalytic or not) to quantify the extent to which each transition state and each intermediate controls the net reaction rate<sup>2</sup>. We elucidated the mechanism of methanol synthesis from syngas over Cu-based catalysts using fast transient kinetics and isotopic tracing, probing both the gas phase and adsorbed species with mass spectroscopy and FTIR<sup>3,8</sup>. This was done in collaboration with scientists at the Institute for Interfacial Catalysis at Pacific Northwest National Lab and Prof. Chuck Mims (U.Toronto).

### Future plans

Metal-support interfacial bond strengths will be measured for several specific metal-on-oxide and metal-on-graphite systems chosen to reveal how this strength depends on the choice of metal and support surface. We will test some of these systems for sintering kinetics to verify our microkinetic models that predict sintering rates based on these same energies and surface

structural properties. We will determine how these same structural properties affect the energy of the key adsorbed intermediates for two important catalytic reactions for energy technology: the steam reforming of a liquid oxygenates to make H<sub>2</sub> and the water-gas shift reaction. We will also determine how the particle size and support affect the elementary-step and net reaction rates for these reactions, and correlate these effects with (1) the energy of the surface metal atoms, as measured by calorimetry, and (2) the strength with which these metal atoms bond the key adsorbed intermediates, as measured by calorimetry and reflected in their enthalpies.

### **Publications acknowledging this grant's support (2009-11)**

1. Experimental measurements of the energetics of surface reactions, C. T. Campbell and O. Lytken, *Surface Science* 603, 1365-1372 (2009) (issue in honor of Gerhard Ertl's Nobel Prize).
2. The degree of rate control: how much the energies of intermediates and transition states control rates, C. Stegelmann, A. Andreasen, C. T. Campbell, *Journal of the American Chemical Society* 131, 8077-82 (2009) (Cover Article, highlighted in *Science* and web: *Nature Chemistry*).
3. Simultaneous MS-IR studies of surface formate reactivity under methanol synthesis conditions on Cu/SiO<sub>2</sub>, Y. Yang, C. Mims, R. Disselkamp, C. H. F. Peden and C. T. Campbell, *Topics in Catalysis* 52, 1440-47 (2009).
4. Lithium Adsorption on MgO(100): Calorimetric Energies and Structure, J. A. Farmer, N. Ruzycki, J. F. Zhu and C. T. Campbell, *Physical Review B* 80, art. no. 035418 (2009), 8 pages.
5. Particle size dependent heats of adsorption of CO on supported Pd nanoparticles as measured with a single crystal microcalorimeter, J. H. Fischer-Wolfarth, J. A. Farmer, J. M. Flores-Camacho, A. Genest, I. V. Yudanov, N. Rösch, C. T. Campbell, S. Schauermaun and H. J. Freund, *Physical Review B (Rapid Communication)* 81, 241416(R) (2010), 4 pages.
6. Ag Adsorption on Reduced CeO<sub>2</sub>(111) Thin Films, J. A. Farmer, J. H. Baricuatro and C. T. Campbell, *Physical Chemistry C* (invited for D. W. Goodman issue) 114, 17166-72 (2010).
7. Ceria Maintains Smaller Metal Catalyst Particles by Strong Metal - Support Bonding, J. A. Farmer and C. T. Campbell, *Science* 329, 933-936 (2010).
8. The (non) formation of methanol by direct hydrogenation of formate on copper catalysts, Y. Yang, C.A. Mims, R.S. Disselkamp, J-H. Kwak, C.H.F. Peden and C.T. Campbell, *Physical Chemistry C* 114, 17205-11 (2010).
9. Surface chemistry: Key to control and advance myriad technologies, J. T. Yates Jr. and C. T. Campbell, *Proc. National Academy of Sciences* 108, 911-916 (2011).
10. An improved single-crystal adsorption calorimeter for determining gas adsorption and reaction energies on complex model catalysts, J-H. Fischer-Wolfarth, J. Hartmann, J. A. Farmer, J. M. Flores-Camacho, C. T. Campbell, S. Schauermaun and H-J. Freund, *Review of Scientific Instruments* 82, art. No. 024102 (2011) (15 pages).
11. Adsorption Microcalorimetry: Recent Advances in Instrumentation and Application, M. C. Crowe and C. T. Campbell, *Annual Rev. Analytical Chemistry*, Vol. 4, 41-58 (2011).
12. Growth, structure and stability of Ag on CeO<sub>2</sub>(111): synchrotron radiation photoemission studies, D. Kong, G. Wang, Y. Pan, S. Hu, J. Hou, H. Pan, C. T. Campbell and Junfa Zhu, *J. Phys. Chem. C* 115, 6715-25 (2011).
13. Insights into Catalysis by Gold Nanoparticles and their Support Effects through Surface Science Studies of Model Catalysts, C. T. Campbell, J. C. Sharp, Y. X. Yao, E. M. Karp and T. L. Silbaugh, *Faraday Discussions* (invited), (in press).
14. Adsorption energetics of CO on supported Pd nanoparticles as a function of particle size by single crystal microcalorimetry, J. M. Flores-Camacho, J.-H. Fischer-Wolfarth, M. Peter, C. T. Campbell, S. Schauermaun and H.-J. Freund, *Phys. Chem. Chem. Phys.* (submitted).

**Dedicated Beamline Facilities for Catalytic Research:  
Synchrotron Catalysis Consortium (SCC)**

**Co-PIs:** Radoslav Adzic, Brookhaven National Laboratory  
Simon R. Bare, UOP LLC, a Honeywell Company  
Jonathan Hanson, Brookhaven National Laboratory  
Steve L. Hulbert, Brookhaven National Laboratory  
David R. Mullins, Oak Ridge National Laboratory  
Steve Overbury, Oak Ridge National Laboratory

**Research Staff:** Nebojsa Marinkovic, University of Delaware

**Postdoctoral Fellow:** Adele Wang, University of Delaware

**Contact:** Department of Chemical Engineering, University of Delaware,  
jgchen@udel.edu; telephone: 302-831-0642

**Goals:**

Since its establishment in 2005, the Synchrotron Catalysis Consortium (SCC) has coordinated significant efforts to promote the utilization of cutting-edge catalytic research under *in-situ* conditions. The main goals of the SCC are to provide assistance and develop new sciences/techniques to the catalysis community through the following concerted efforts:

- Dedicated beamtime on two X-ray Absorption Fine Structure (XAFS) beamlines and one additional beamline combining XAFS and X-ray Diffraction (XRD)
- Dedicated *in-situ* reactors for a variety of catalytic and electrocatalytic studies
- A research staff and a postdoctoral fellow to assist experimental set-up and data analysis
- Training courses and help sessions by the PIs and co-PIs
- Development of new techniques for catalytic and electrocatalytic research
- Design and coordinating the implementation of a suite of beamlines for catalysis studies at the new light source, NSLS-II

**DOE Interest:**

The availability of well-maintained, user-friendly and state-of-the-art synchrotron facilities should help a large number of catalysis and electrocatalysis groups. Our synchrotron catalysis consortium continues to provide a new model for operating synchrotron facilities. We believe such model provides a closer interaction between funding agencies, beamline scientists and catalysis users. The closer interaction should lead to the more efficient utilization of the synchrotron facilities, which ultimately benefits the nation as a whole by increasing the return on the investments made in our national laboratory system. The consortium represents a critical

step for the catalysis community in the United States to remain competitive in *in-situ* catalytic and electrocatalytic research using synchrotron-based techniques.

### **Recent Progress:**

#### **A. Assistance to Catalysis Users**

The SCC members have made significant progress in setting up dedicated facilities for the catalysis community on three beamlines, X18A, X18B and X19A. The dedicated SCC beamline staff and postdoctoral fellow provided assistance to the catalysis user groups in many ways, including training the users on beamline operation and safety, setting up dedicated reactors and gas-handling systems, and providing experimental assistance when needed. Since its establishment SCC has helped many catalysis groups, including a large percentage of first-time new catalysis groups who would otherwise not be able to start synchrotron research. The catalysis user groups are from academic, industry, and national laboratories. They include Argonne National Lab, BNL, Boston College, Case Western Univ., Colorado State Univ., Columbia Univ., Duracell Technical Center, GE Global, General Motors, Georgia Tech, George Washington Univ., Hunter College, Kent State Univ., MIT, NJIT, Northeastern Univ., NRL, Ohio State Univ., ORNL, Penn State Univ., PNNL, Stony Brook Univ., Texas A&M Univ., Univ. Central Florida, Tufts Univ., Univ. Alberta, UC Berkeley, UC Davis, UC Santa Cruz, Univ. Delaware, Univ. Kansas, Univ. Kentucky, Univ. Illinois, Univ. Madrid, Univ. Minnesota, Univ. New Hampshire, Univ. New Mexico, Univ. South Carolina, Univ. Tennessee, Univ. Texas at Austin, Univ. Vermont, Univ. Virginia, Univ. Washington, Univ. Waterloo, Univ. Wisconsin, UOP, UTC Powers, Virginia Tech, Yale Univ., and Yeshiva Univ.

#### **B. Development of New instrumentation for Catalysis Research**

In addition to maintaining and improving dedicated XAFS capabilities for the catalysis users, the SCC team also led R&D efforts on commissioning, testing and operating new techniques tailored to catalysis and electrocatalysis research. Below are two examples of facilities recently developed by SCC members during the past funding cycle:

***Combined Quick EXAFS/XRD instrument:*** The XAFS and XRD techniques give complementary information about the structure of catalytic materials: XRD is effective in crystalline materials while XAFS provides short range order structural features in disordered, amorphous and/or low dimensional materials. In addition, XAFS also gives very valuable information about the electronic properties of the catalysts. These two methods have been developed and advanced *independently* from each other at synchrotron sources in the US and abroad. To analyze catalysts under their operating conditions, a new approach is needed, namely, the simultaneous collection of the XRD and quick-XAFS (QEXAFS) data under *in-situ* conditions together with online product analysis (RGA). The SCC and NSLS teams have finished building the first instrument in the US for combined, time-resolved Quick XRD/XAFS experiments at beamline X18A. Such a combination allows the measurement of changes in the actual structure (in the short, medium and long range order), electronic properties and chemical activity of heterogeneous catalysts simultaneously, coupled with online gas analysis for *in-situ* chemical transformations.

***DRIFTS/XAFS/MS measurements:*** Together with the researchers from Harrick Scientific, the SCC team designed and built Diffuse Reflectance Infrared Fourier Transform Spectroscopy

(DRIFTS) cell for transmission XAFS. The cell can be used for *in-situ* measurement at temperatures up to 800 °C in a gaseous environment. The design allows the identification of the surface intermediates using DRIFTS, the detection of the reaction products using on-line gas detection by mass spectrometry (RGA), and at the same time the characterization of the catalysts using XAFS.

### **C. Workshops, On-Site Help and Training Courses Offered by SCC**

In order to promote the utilization of synchrotron facilities in the catalysis and electrocatalysis communities, it is critical to train graduate students, postdoctoral fellows, and research staff on data collection and data analysis. The SCC PIs and staff have provided training to all new catalysis users working on the SCC beamlines. For example, Dr. Frenkel gave on-site help 2-3 days a week, and consulted visiting groups on issues ranging from data analysis to planning XAFS experiments. In addition, SCC members have organized several training courses and workshops, **which were over-subscribed and received very positive feedback**. Many of the SCC catalysis users attended one of the training courses. Below is a brief description of two short courses.

### **D. Coordinating with NSLS-II Facilities**

NSLS-II is a new state-of-the-art medium energy storage ring designed to deliver world leading brightness and flux with top-off operation for constant output. The facility will be able to produce X-rays up to 10,000 times brighter than those produced at the NSLS today, enabling 1nm-size focusing and 0.1 meV energy resolution. Due to its uniquely high brightness and flux, these capabilities will allow researchers to undertake several types of measurements for catalysis, electrochemistry and energy sciences:

- Nanometer scale understanding of activity, selectivity, stability, performance and degradation mechanisms of catalysts
- Design of model catalysts that aim to provide perhaps indirect but nonetheless important information on the more complex commercial catalysts
- Development of combined, multi-technique methodologies and instrumentation for real time, *in-situ* catalysis studies
- Development of instrumentation that simulates laboratory and industrial conditions for energy release, storage, and generation where the catalytic process can be followed in a time resolved manner.

Expanding the range of SCC-supported beamlines will not only enable an enhanced temporal and spatial resolution in characterization methodology (combined, quick XAFS/XRD at X18A) but also serve as a necessary link in transitioning existing NSLS-based catalysis research to the new, much more advanced NSLS-II. The construction of the new light source is well underway, with a target date for first operations in 2015. Multi-technique characterization with simultaneous reaction product analysis will undoubtedly remain a flagship technique at NSLS-II. **The SCC team will continue to play a leadership role to ensure that the needs by the catalysis community are adequately addressed in the NSLS-II facilities.**

### **Publications Acknowledging Current Grant during 2009-2011:**

Over 120 publications have acknowledged the SCC beamline supports during this period.

**Hydrocarbon Dehydrogenation and Oxidation over Model Metal Oxide Surfaces**

Students: John D. Brooks, Yujung Dong, Xu Feng  
Collaborators: G.V. Gibbs, (Virginia Tech), David R. Mullins (ORNL)  
Contacts: Department of Chemical Engineering, Virginia Tech, Blacksburg, VA 24061;  
dfcox@vt.edu

**Goal**

Develop an understanding of structure/function relationships determining selectivity in metal oxide catalytic surface chemistry related to alkane oxidation and dehydrogenation.

**DOE Interest**

Process chemistries for the conversion of alkanes to alkenes or selectively-oxygenated products can utilize lower-cost feedstocks and offer a more versatile usage of petrochemical resources. Industrial reaction processes for ethane dehydrogenation are driven by nonselective free-radical gas-phase reactions which could be improved with the development of selective heterogeneous catalysts. Studies of the reaction of C<sub>1</sub> and C<sub>2</sub> hydrocarbon fragments on materials like chromia which are useful for dehydrogenation of larger alkanes provide insight into fundamental chemical processes effecting selectivity in these catalytic systems.

**Recent Progress**

Our recent efforts have focused on examining the reaction of the C<sub>1</sub> hydrocarbon fragments methyl and methylene on a sequence of three surfaces of corundum-structured transition metal oxides – Cr<sub>2</sub>O<sub>3</sub> (10 $\bar{1}$ 2), Cr<sub>2</sub>O<sub>3</sub> (0001) and Fe<sub>2</sub>O<sub>3</sub> (10 $\bar{1}$ 2) – chosen to help separate the effects of structural and electronic properties on reactivity. Stoichiometric Cr<sub>2</sub>O<sub>3</sub> (10 $\bar{1}$ 2) and (0001) surfaces expose nominally Cr<sup>3+</sup> cations in different local coordination environments with one and three coordination vacancies, respectively, compared to the bulk. Stoichiometric Cr<sub>2</sub>O<sub>3</sub> (10 $\bar{1}$ 2) and Fe<sub>2</sub>O<sub>3</sub> (10 $\bar{1}$ 2) maintain the same nominal structure but with cation 3d<sup>3</sup> and 3d<sup>5</sup> electronic configurations, respectively, allowing a direct examination of the influence of the d electron density on the surface chemistry.

*CH<sub>3</sub> Reactions on  $\alpha$ -Cr<sub>2</sub>O<sub>3</sub>*: The reaction of CH<sub>3</sub>I (CD<sub>3</sub>I) has been used to generate CH<sub>3</sub> fragments on both the (10 $\bar{1}$ 2) and (0001) stoichiometric surfaces of  $\alpha$ -Cr<sub>2</sub>O<sub>3</sub>. On both surfaces, methyl dehydrogenation to methylene is rate-limiting, and observed near 500 K. The results indicate that methyl dehydrogenation is structure insensitive, and does not depend significantly on the coordination of the surface Cr cation or the local structure of nearest neighbor oxygen anions at the reaction site. On both surfaces, methane, ethylene and hydrogen gas are observed as products in the same temperature range. Methane is formed by H addition to methyl fragments, and ethylene is formed primarily by the coupling (C-C bond formation) of two methylene groups. Halogen deposition in an amount corresponding to one halogen atom per surface cation shuts down the chemistry of both surfaces. On the (0001) surface where cations on the clean surface expose multiple coordination vacancies, this result was unexpected. The



loss of reactivity on the (0001) surface for halogen coverages of one atom per surface cation is attributed to the formation of a stable, tetrahedrally-coordinated  $\text{Cr}^{4+}$  center. DFT confirms a lifting of the inward relaxation of the cation center known for the clean surface to give a tetrahedral-like  $\text{CrO}_3\text{X}$  center. Additionally, DFT shows that the dehalogenation of multiply-halogenated surface Cr sites is exothermic with a low barrier for halogen diffusion to form singly halogenated Cr centers.

*CH<sub>2</sub> Reactions on  $\alpha\text{-Cr}_2\text{O}_3$ :* The reaction of  $\text{CH}_2\text{Cl}_2$  has been used to generate surface methylene species. The principle reaction of  $\text{CH}_2$  fragments on both the  $(10\bar{1}2)$  and (0001) stoichiometric surfaces of  $\alpha\text{-Cr}_2\text{O}_3$  is coupling to ethylene. On the  $(10\bar{1}2)$  surface where Cr cations on the clean surface expose only a single coordination vacancy, the rate-limiting step in methylene coupling is the surface diffusion of methylene. Two reaction channels are observed (~280 and 400K), and attributed to two diffusion paths across the surface. On the (0001) surface, one primary reaction-limited channel to ethylene is observed near 400 K, and again attributed to a rate-limiting surface reaction step.

Computational results for  $\text{CH}_2$  on  $\text{Cr}_2\text{O}_3$  are mixed. XPS suggests a metal-only bound  $\text{CH}_2$  species on  $\alpha\text{-Cr}_2\text{O}_3(10\bar{1}2)$  as does DFT assuming a ferromagnetic  $\text{Cr}_2\text{O}_3$  ground state, and two diffusion routes matching the experimental barriers are found. If an antiferromagnetic ground state is assumed, a minimum energy methylene species bridged between a surface cation and anion is predicted, and only one barrier to diffusion is correctly matched. Since the chemistry occurs near or above the Néel temperature of antiferromagnetic  $\text{Cr}_2\text{O}_3$ , a diamagnetic solution (not readily accessible with DFT) should be most appropriate.

*Chemistry on  $\alpha\text{-Fe}_2\text{O}_3(10\bar{1}2)$ :* This work is ongoing.

### **Future Plans**

*Experimental Investigation of  $\text{Fe}_2\text{O}_3$  Surface Chemistry:* In addition to the  $\text{C}_1$  chemistry being investigated with TPD, synchrotron based NEXAFS and high-resolution photoemission will be used to characterize the reaction intermediates on  $\alpha\text{-Fe}_2\text{O}_3(10\bar{1}2)$ .

*Computational Investigation of  $\text{Fe}_2\text{O}_3$  Surface Chemistry:* DFT will be used to examine the same reaction chemistry for the antiferromagnetic ground state of  $\alpha\text{-Fe}_2\text{O}_3(10\bar{1}2)$  currently being investigated experimentally. Since the Néel temperature of hematite (955 K) is significantly higher than the temperatures observed for the surface chemistry, there is no ambiguity regarding the proper choice of ground state for the calculation.

### **Publications (2009-2011)**

1. J.D. Brooks, T.L. Chen, D.R. Mullins and D.F. Cox, Reactions of ethylidene on a model chromia surface: 1,1-dichloroethane on stoichiometric  $\alpha\text{-Cr}_2\text{O}_3(10\bar{1}2)$ , *Surface Science*, **605** (2011) 1170-1176.

2. G.V. Gibbs, A.F. Wallace, R.T. Downs, N.L. Ross, D.F. Cox and K.M. Rosso, Thioarsenides: van der Waals bonded Interactions and bond paths, *Physics and Chemistry of Minerals*, **38** (2011) 267-291.
3. G.V. Gibbs, A.F. Wallace, R. Zallen, R.T. Downs, N.L. Ross, D.F. Cox and K.M. Rosso, Bond Paths and van der Waals Interactions in Orpiment,  $\text{As}_2\text{S}_3$ , *The Journal of Physical Chemistry A*, **114** (2010) 6550-6557.
4. G.V. Gibbs, A.F. Wallace, D.F. Cox, R.T. Downs, N.L. Ross and K.M. Rosso, Si-O Bonded Interactions, Silica Polymorphs and Siloxane Molecules, *American Mineralogist*, **94** (2009) 1085-1102.
5. J.D. Brooks, Q. Ma and D.F. Cox, Reactions of ethyl groups on a model chromia surface: ethyl chloride on stoichiometric  $\alpha\text{-Cr}_2\text{O}_3$  ( $10\bar{1}2$ ), *Surface Science*, **603** (2009) 523-528.
6. M.A. McKee, Q. Ma, D.R. Mullins, M. Neurock and D.F. Cox, Reactions of vinyl groups on a model chromia surface: vinyl chloride on stoichiometric  $\alpha\text{-Cr}_2\text{O}_3$  ( $10\bar{1}2$ ), *Surface Science*, **603** (2009) 265-272.
7. G.V. Gibbs, A.F. Wallace, D.F. Cox, P.M. Dove, R.T. Downs, N.L. Ross and K.M. Rosso, The role of directed van der Waals bonded interactions in the determination of the structures of molecular arsenate solids, *The Journal of Physical Chemistry A*, **113** (2009) 736-749.

**Correlation of Theory and Function in Well-Defined Bimetallic Electrocatalysts**

Additional PIs: Graeme Henkelman  
Postdocs: Hyun You Kim, Daniel Sheppard  
Students: Emily Carino, Nathan Froemming, V. Sue Myers, Wenjie Tang  
David Yancey, Liang Zhang, Sam Chill, Chun-Yuang Lu  
Collaborators: Anatoly Frenkel (Yeshiva University)  
Contacts: Department of Chemistry and Biochemistry, 1 University Station,  
A5300, The University of Texas at Austin, Austin, TX 78712-0165  
Email: crooks@cm.utexas.edu

**Goal**

The objective of this research project is to correlate the structure of nanoparticles that are comprised of ~100 atoms to their catalytic function. The project is based on a growing body of evidence suggesting that catalytic properties can be tailored through controlled synthesis of nanoparticles. What is missing from many of these studies, and what we are contributing, is a model catalyst that is sufficiently small and well-characterized that its function can be directly predicted by theory. Specifically, our work seeks to develop a fundamental and detailed understanding of the relationship between the structure of nanoscopic oxygen-reduction catalysts and their function. We have assembled a team with expertise in theory, synthesis, and advanced characterization methods to address the primary objective of this project. We anticipate the outcomes of the study to be: (1) a better theoretical understanding of how nanoparticle structure affects catalytic properties; (2) the development of advanced, *in-situ* and *ex-situ*, atomic-scale characterization methods that are appropriate for particles containing about 100 atoms; and (3) improved synthetic methods that produce unique nanoparticle structures that can be used to test theoretical predictions.

**DOE Interest**

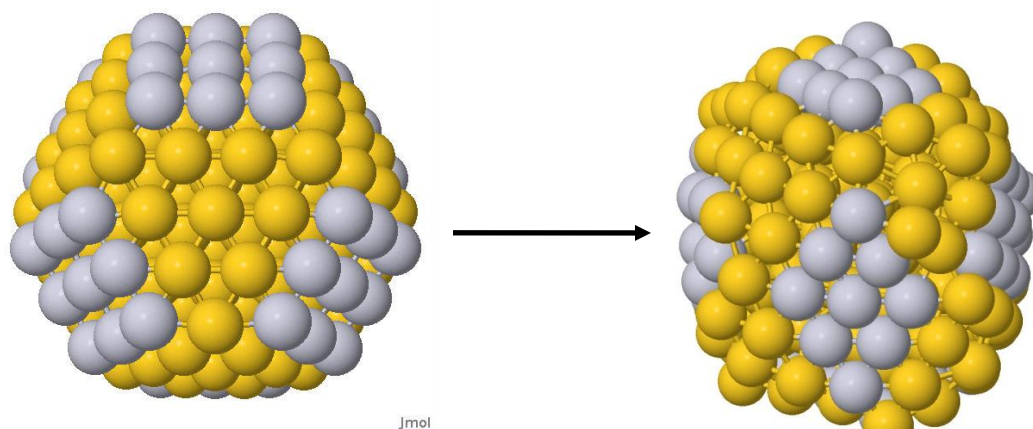
Our proposed research directly addresses two of the DOE Grand Challenges for Basic Energy Sciences. Specifically, we endeavor to use synthesis and theory to develop first-principles rules for predicting the structure of new forms of matter that have programmable catalytic functions. The rules and principles discovered during this project will likely be useful for designing other (nonsynthetic) materials as well. Within this broader context, our proposal specifically addresses the Hydrogen Fuel Initiative and Catalysis for Energy components of the DOE BES Use-Inspired Discovery Science research thrusts discussed in the announcement for this new DOE BES program.

**Recent Progress**

*Pt@Cu DENs*: The synthesis of Pt@Cu DENs by UPD of Cu onto 3 differently sized Pt cores was described. The voltammograms indicate that Cu UPD is a two-step deposition and stripping process which is believed to correspond to Cu deposition on the (100) and (111) facets of cubooctahedral Pt DENs. The core@shell configuration was confirmed by in-situ EXAFS. The Cu UPD process was modeled on Pt DENs consisting of 147 atoms. The results of DFT indicate that Cu shell decorates just the facets, not the edges and

corners that adjoin the facets and the first part of the Cu shell selectively deposits on the (100) facet. The findings from recent electrochemical and EXAFS studies of Pt@Cu DENs with just partial shell coverage are in good agreement with the DFT models.

*Au@Pb and Au@Pt DENs:* Au nanoparticles consisting of 147 atoms have been synthesized within PAMAM dendrimer templates. The surface structure of these particles has been determined using Pb UPD and suggests that Au DENs have (100) and (111) facets. UPD Pb is also used as a sacrificial monolayer for galvanic exchange for Pt. The amount of Pt surface decoration on the Au DENs can be controlled by the extent of Pb UPD. Certain surface features of the Au nanoparticles are decorated with Pt by only forming UPD Pb on particular facets of the particles. Au<sub>147</sub>@Pt particles were then tested for their activity toward the oxygen reduction reaction (ORR). The structures of Au@Pb and Au@Pt particles have been modeled using DFT as well as the binding energies of oxygen to the surface of Au@Pt particles having varying amounts of surface Pt. While Au@Pb structures are structurally stable, the Au@Pt structure undergoes a surface reorganization, shown below, such that the Pt atoms all align in a (111) orientation. These calculations indicate very good agreement to the experimental system.



### Future Plans

*Site-specific catalysis:* We plan to use Au@Pt and Pt@Cu DENs to examine site-specific catalysis of CO oxidation, water-gas shift, and the ORR by blocking particular catalyst sites with UPD metals.

*Au@Bi DENs:* Au surfaces having Bi UPD layers have shown activity for the ORR. We have observed similar trends on Au@Bi DENs. We plan to determine the structure of the Bi UPD layer on Au DENs. Preliminary results indicate that Bi forms an alloy with Au<sub>147</sub> DENs upon Bi UPD.

### Publications (2010-2011)

- D. F. Yancey; E. V. Carino; R. M. Crooks "Electrochemical Synthesis and Electrocatalytic Properties of Au@Pt Dendrimer-Encapsulated Nanoparticles" *J. Am. Chem. Soc.* **2010**, *132*, 10988-10989.

- M. G. Weir; V. S. Myers; A. I. Frenkel; R. M. Crooks "In-situ X-ray Absorption Analysis of ~1.8 nm Dendrimer-Encapsulated Pt Nanoparticles During Electrochemical CO Oxidation" *ChemPhysChem* **2010**, *11*, 2942-2950 (invited, special issue on electrochemistry).
- D. Sheppard, G. Henkelman, O. Anatole von Lilienfeld "Alchemical Derivatives of Reaction Energetics", *J. Chem. Phys.* **2010**, *133*, 084104.
- W. Tang, L. Zhang, and G. Henkelman "Catalytic Activity Improvement in Pd/Cu Random Alloy Nanoparticles" *J. Phys. Chem. Lett.* **2011**, *2*, 1328-1331.
- C.-Y. Lu and G. Henkelman "The Role of Geometric Relaxation in Oxygen Binding to Metal Nanoparticles" *J. Phys. Chem. Lett.* **2011**, *2*, 1328-1331.
- M. Welborn, W. Tang, J. Ryu, V. Petkov, and G. Henkelman "A Combined Density Functional and X-ray Diffraction Study of Pt Nanoparticle Structure" *J. Chem. Phys.* (in press, 2011).
- V. S. Myers; M. G. Weir; E. V. Carino; D. F. Yancey; R. M. Crooks "Dendrimer-encapsulated Nanoparticles: New Synthetic and Characterization Methods and Catalytic Applications" *Chem. Sci.* (submitted, 2011).
- H.-Y. Kim, G. Henkelman, and H.-M. Lee "Oxygen Vacancies Facilitate CO Oxidation by CeO<sub>2</sub> Supported Au Nanoparticles" (submitted, 2011).
- H.-Y. Kim, J.-N. Park, G. Henkelman, and J.-M. Kim "Design of Highly-Nanodispersed Pd-MgO/SiO<sub>2</sub> Composite Catalyst with Multifunctional Activity for CH<sub>4</sub> Reforming" (submitted, 2011).
- W. Tang, G. Henkelman "How the Size of Pt Nanoparticles Effects the Oxygen Reduction Reaction (in preparation).
- E. V. Carino; H. Y. Kim; G. Henkelman; R. M. Crooks "Site-Selective Cu Deposition at Pt Dendrimer-Encapsulated Nanoparticles: Correlations Between Theory and Experiment" (in preparation).

## **The Water Oxidation Reaction: Transition metal oxide catalysis probed by time resolved optical spectroscopy and in-situ x-ray spectroscopy**

**Tanja Cuk**

Chemistry Department, UC Berkeley  
Faculty Scientist, Chemical Sciences Division, LBNL

Sunlight to fuel systems rely on robust water oxidation catalysts with high turnover rates (product evolution/s) and quantum efficiencies (product evolution/light absorbed) under visible light irradiation. While these macroscopic properties generally benchmark catalysts, they have yet to be related to tunable, microscopic properties defining a mechanistic cycle in photodriven, thermodynamically uphill reactions. We explore these microscopic properties for the water oxidation half-reaction on transition metal oxides in two different ways: 1) optical pump-probe techniques using a unique sample configuration to map out the spectrum of excited states that carry a hole to the catalyst-liquid interface, creating a molecular change at the interface equivalent to a surface-trapped state in the electronic spectrum 2) using x-ray techniques, we compare the valence band structure among a number of different oxides for similarities in the local d-p hybridization relevant to robust water oxidation catalysis. In the future, we plan to carry out time-resolved infrared and x-ray experiments to understand how the excited state electronic spectrum corresponds to new vibrational modes and oxidation state changes.

**Nanostructured Catalysts for Hydrogen Generation from Renewable Feedstocks**

Additional PIs: Yong Wang (Washington State University & Pacific Northwest National Lab),  
Post-docs: Barr Halevi (UNM), He Zhang(PNNL).  
Graduate Students: Eric Petersen, Patrick Burton (UNM).  
Undergrad Students Aaron Roy, Lisa Lowery (UNM).  
Collaborators: Robert Schloegl, Fritz Haber Institute, Berlin, Germany, John Vohs (Univ. of Pennsylvania)  
Contacts: Abhaya Datye, University of New Mexico, Dept. of Chemical & Nuclear Engineering, MSC 01 1120, Albuquerque, NM, 87131-0001; [datye@unm.edu](mailto:datye@unm.edu)  
Yong Wang, Pacific Northwest National Laboratory, 902 Battelle Boulevard, P.O. Box 999, Richland, WA 99352; [yongwang@pnl.gov](mailto:yongwang@pnl.gov)

**Goal**

This is a collaborative effort involving the research groups at the University of New Mexico (Datye) and Pacific Northwest National Labs (Wang). The research program is directed towards the development of highly active and selective catalysts for the production of hydrogen from renewable alcohols. The initial work has focused on the fundamental understanding of methanol conversion to hydrogen, and on associated reactions such as the water gas shift, with the ultimate goal of designing advanced catalysts for converting renewable feedstocks such as bioethanol to hydrogen.

**DOE Interest**

The proposed project directly addresses one of the BES long-term program measures, namely to demonstrate progress in understanding, modeling, and controlling chemical reactivity and energy transfer processes in the gas phase, at interfaces, and on surfaces for energy-related applications. The robust and integrated approaches developed will lead to new discoveries in catalyst synthesis, characterization, mechanistic understanding of reforming reactions and control of surface sites, all of which will have a broad impact on the design of catalysts at the nanoscale. The results of the proposed work will impact chemical reactivity at the level of elementary surface reactions for a wide range of bimetallic catalyzed chemical transformations. The applications of the tools will lead to new fundamental understanding of the science underlying hydrogen fuels and to discovery of principles for rational design of new processes relevant to a Hydrogen Economy. The project addresses basic research needs to assure a secure energy future.

**Recent Progress****Aerosol-Derived Unsupported Bimetallic Model Catalysts**

We have developed a unique platform for studying the contribution of the metal phase to multifunctional supported catalysts. Unsupported multimetallic aerosol-derived alloy powders are homogeneous and phase-pure and can have surface areas ranging 1-10 m<sup>2</sup>/g, making them suitable for use in conventional flow reactors. We have illustrated the utility of aerosol-derived alloy powders via synthesis of single phase PdZn (see Fig. 1) which was used to determine the

intrinsic Methanol Steam Reforming reactivities of the different components of the Pd/ZnO system.

PdZn aerosol-derived catalysts were made using high purity palladium and zinc nitrate dissolved in 10% nitric acid. The nitrate salt mixture was atomized to produce droplets that dried as they passed through a furnace, and the droplets were collected on a filter (Fig. 2). The collected powder was reduced at 500 C in flowing 5% H<sub>2</sub> for 4 h.

The aerosol-processing approach produces 1-5m<sup>2</sup>/g powders composed of 20-60nm crystallites sintered into 400nm spherical agglomerates. The material is homogeneous in both phase and composition on the nano- and micro-meter scale, with surface composition matching the bulk. While the phase diagram of PdZn shows multiple phases (Fig. 3), in

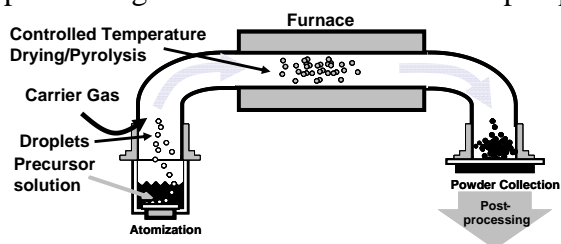


**Figure 2** Setup used to generate unsupported PdZn

practice we are only able to make the following phases: Zn alloyed in fcc Pd, which is the PdZn<sub>α</sub> phase, the tetragonal PdZn<sub>β1</sub>, and hexagonal ZnO. These phase pure materials were used to measure the intrinsic reactivity via vacuum TPD as well as in a flow reactor operating at atmospheric pressure. The intrinsic reactivity measurements demonstrate the utility of these model catalysts for use across many experimental regimens.

These homogeneous multimetallic model catalyst materials can be used to bridge the materials and pressure gap between UHV surface science studies (which rely on single

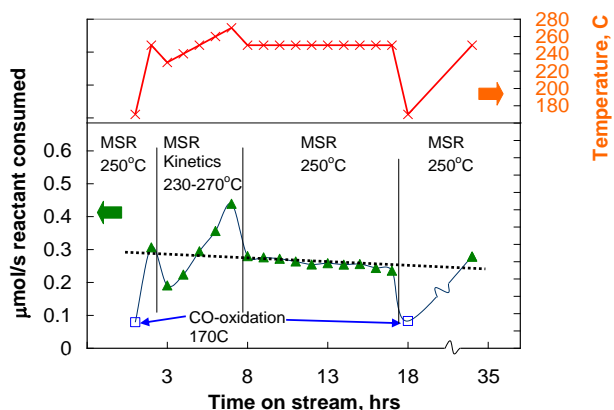


**Figure 4** Illustrative reactivity study for PdZn<sub>β</sub>

crystals, surface alloys and batch reactions) and flow reactors (which make use of supported metal catalysts that can contain nanoparticles but often with multiple phases of differing size and composition). The surface areas and composition of the aerosol derived powders were measured via H<sub>2</sub> and CO chemisorption and compared to BET surface area and used to determine the

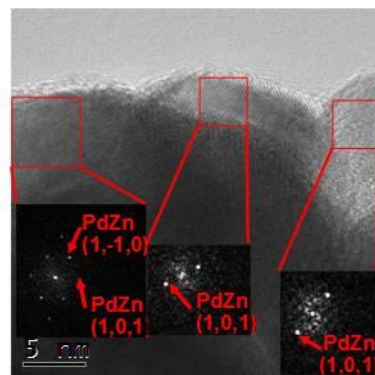


**Figure 1** HRTEM micrographs illustrating nanophase homogeneity of unsupported PdZn<sub>β</sub> sample made via aerosol processing of Pd and Zn nitrates

the following phases: Zn alloyed in fcc Pd, which is the PdZn<sub>α</sub> phase, the tetragonal PdZn<sub>β1</sub>, and

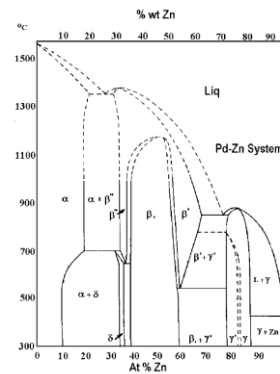


**Figure 3** Binary phase diagram for PdZn

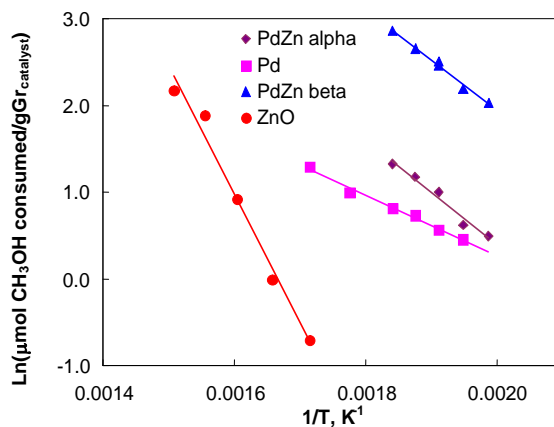


**Figure 5** Methanol Steam Reforming



number of surface sites, which were confirmed by CO oxidation used as a probe of surface sites. SEM/EDS, STEM/EDS, and Ambient Pressure-XPS measurements showed that bulk composition of the unsupported PdZn powders was similar to the surface composition, indicating these powders are good models. Using this powders we were able to independently measure the reactivity of the major phases of the Pd/ZnO catalyst system. The measurements of inherent catalytic activity showed that the PdZn<sub>β1</sub> phase accounted for most if not all the catalytic activity previously reported for Pd/ZnO.

## Future Work

### Formation and Stabilization of Single Atom Pd Species on ZnO (1 0 1 0) – a Novel Mechanism for Metal-Support Interactions

We have found that Pd/ZnO catalysts reduced at high temperatures exhibit improved reactivity for MSR, greater than the reference PdZn<sub>β1</sub> phase. Examination of Pd/ZnO catalysts by Aberration Corrected STEM (AC-STEM) revealed that catalysts reduced at 500 °C exhibit an abundance of bright objects whose contrast was consistent with dispersed single atom species of Pd. We have explored the conditions that favor the formation and stabilization of these single atom species on the non-polar ZnO (1 0 1 0) surface, which is the dominant facet exposed in ZnO powders. The reactivity of these atomically Pd species for CO oxidation and for Methanol Steam Reforming will be studied in future work.

## Publications (2010-2011)

- (1) P.D. Burton, E.J. Peterson, T.J. Boyle, and A.K. Datye, *Synthesis of High Surface Area ZnO(0001) Plates as Novel Oxide Supports for Heterogeneous Catalysts*. Catalysis Letters, 2010. 139(1-2): p. 26-32.
- (2) Vanessa Lebarbier, Ron Dagle, Abhaya Datye and Yong Wang, *The effect of PdZn particle size on reverse-water-gas-shift reaction*, Applied Catalysis A: General 379 (2010) 3–6.
- (3) B. Halevi, E.J. Peterson, A. Delariva, E. Jeroro, V.M. Lebarbier, Y. Wang, J.M. Vohs, B. Kiefer, E. Kunkes, M. Havecker, M. Behrens, R. Sehlogl, and A.K. Datye, *Aerosol-Derived Bimetallic Alloy Powders: Bridging the Gap*. Journal of Physical Chemistry C, 2010. 114(40): p. 17181-17190.
- (4) A.M.Karim, Y.Su, J.Sun, C.Yang, J.J.Strohm, D.L.King, and Y.Wang, “A comparative study between Co and Rh for steam reforming of ethanol”, Appl. Catal.B: Environmental 96 (2010) 441-448.
- (5) B. Roy, K. Loganathan, H.N. Pham, A.K. Datye, and C.A. Leclerc, Surface modification of solution combustion synthesized Ni/Al<sub>2</sub>O<sub>3</sub> catalyst for aqueous-phase reforming of ethanol. International Journal of Hydrogen Energy, 2010. 35(21): p. 11700-11708.
- (6) P. D. Burton, T. J. Boyle and A. K. Datye, Facile, Surfactant-free synthesis of Pd nanoparticles for heterogenous catalysts, J. Catalysis. 2011. 280(2): p. 145-149.
- (7) E.J. Peterson, B. Halevi, B. Kiefer, M.N. Spilde, A.K. Datye, J. Peterson, L. Daemen, A. Llobet, and H. Nakotte, *Aerosol synthesis and Rietveld analysis of tetragonal (β1) PdZn*. Journal of Alloys and Compounds, 509 (2011) 1463–1470.
- (8) G.K. Smith, S. Lin, W.Z. Lai, A. Datye, D.Q. Xie, and H. Guo, Initial steps in methanol steam reforming on PdZn and ZnO surfaces: Density functional theory studies. Surface Science, 2011. 605(7-8): p. 750-759.

## Natural Catalysts for Molten Cellulose Pyrolysis to Targeted Bio-Oils

Additional PIs: None  
Students: Alex Paulsen, Andrew Teixeira  
Contacts: University of Massachusetts Amherst, 686 North Pleasant Street,  
Amherst, MA 01003; Dauenhauer@ecs.umass.edu

### Goal

Develop a fundamental understanding of the role of inorganic catalysts naturally occurring within high temperature molten cellulose chemistry.

### DOE Interest

The chemistry of thermal degradation of cellulose and biomass biopolymers ultimately dictates the performance of numerous energy-related technologies including gasification, wood combustion, and fast pyrolysis of biomass. Development of kinetic models based on a fundamental understanding of the molecular-level pyrolysis chemistry will ultimately lead to improved reactor design for energy applications. This research will specifically focus on the chemistry of the inorganic catalysts within biomass which significantly alter the products produced from cellulose pyrolysis.

### Future Plans

The utilization of lignocellulosic biomass as an alternative reduced-carbon feedstock processed within high temperature thermo-chemical catalytic reactors is hindered by a limited fundamental understanding of the role of catalysts that naturally exist within biomass. The natural catalysts of biomass including the inorganic ions necessary for biological function as well as the oxides obtained from soils have been shown to exhibit significant influence during pyrolysis. The objective of this project is to study the catalytic chemistry of naturally occurring inorganic materials within high-temperature molten carbohydrates to understand their effect on the selection of volatile organics and gases produced during pyrolysis. The role of inorganic catalysts on biopolymer decomposition within the high temperature ( $> 400$  °C), intermediate condensed phase will be interpreted through a targeted study of specific molten carbohydrate reactions including ether hydrolysis, retro-aldol condensation, and dehydration which select for the competing catalytic pathways of product formation. The reaction intermediates and oxidation state of natural catalysts within the molten liquid will be characterized with the use of a new experimental liquid sampling technique capable of extracting and quenching molten carbohydrate/catalyst mixtures.

**Structure and Function of Supported Base Catalysts**

Postdoc: Makarand Gogate  
Graduate Students: Yuanzhou Xi (graduated), Joseph Kozlowski, Theodore Birkey  
and Bhushan Zope  
Undergrad Student: Matthew Aronson  
Contact: Chemical Engineering, University of Virginia, 102 Engineers Way,  
Charlottesville, VA 22911; [rjd4f@virginia.edu](mailto:rjd4f@virginia.edu)

**Goal**

Solid bases are heterogeneous catalysts that have not been broadly exploited compared to solid acids. Thus, we have focused our efforts on understanding how a variety of solid bases, including metal oxides, mixed metal oxides and zeolites, function in catalytic transformations. Over the last few years, we probed the reactivity of layered double hydroxides for transesterification reactions that are important for conversion of biorenewable resources to fuels and chemicals. The synthesis of biodiesel fuel from plant oils (triglycerides) and methanol currently employs homogeneous base catalysts to facilitate transesterification although these liquid base catalysts need to be removed and neutralized in the process. In particular, the role of water in the transesterification of tributyrin (a model triglyceride) with methanol over the hydroxyl form of hydrotalcite was explored. Our most recent work has focused on the coupling of short chain alcohols, such as ethanol coupling to butanol, over solid base catalysts.

**DOE Interest**

Solid base catalysts exhibit high activities and selectivities for many kinds of reactions important for fuels and chemicals production, including transesterifications, condensations, alkylations, cyclizations, and isomerizations; however, many of these processes are carried out industrially using liquid bases as catalysts. These applications can require nearly stoichiometric amounts of the liquid base for conversion to the desired product. Replacement of liquid bases with solid base catalysts allows for easier separation from the product as well as possible regeneration and reuse. Basic solids also have the added advantages of being non-corrosive and environmentally friendly, which allows for easier disposal.

A molecular-level understanding of solid basicity is required before structure/function properties of new materials can be effectively predicted. A significant fraction of previous research on solid bases therefore involves the correlation of base strength to catalyst composition. However, since strong bases are also poisoned by carbon dioxide and water, common side products in catalytic reactions, new base catalysts that are more resistant to deactivation by these molecules need to be developed. The search for novel solid bases that catalyze transformations with high product selectivity, high reaction rate, and low deactivation rate is an ongoing process.

Research in this program addresses at least two long term measures relevant to the BES. For example our project involves designing, modeling, fabricating, characterizing, analyzing,

assembling and using new materials and structures, particularly at the nanoscale, for energy-related applications. Moreover, the project will advance the understanding, modeling, and controlling of chemical reactions on surfaces for energy-related applications, employing lessons from inorganic, organic and self-assembling systems.

### Recent Progress

A co-precipitated Mg-rich mixed oxide catalyst with Mg:Zr 11:1 was approximately 300% more active than MgO on a surface area basis, whereas pure ZrO<sub>2</sub> was inactive for the transesterification of tributyrin with methanol (see Table 1). (The rate constant  $k_1$  is associated with the first step in the transesterification sequence.) To explore the nature of the activity enhancement, samples were characterized by X-ray diffraction, N<sub>2</sub> adsorption, CO<sub>2</sub> adsorption microcalorimetry and DRIFTS of adsorbed CO<sub>2</sub> and CH<sub>3</sub>OH. Although the sol-gel synthesis method provided better atomic-level mixing of Mg and Zr, the resulting catalysts were not as effective as mixed oxides prepared by co-precipitation. The most active mixed oxide (Mg:Zr 11:1) exhibited a high initial heat of CO<sub>2</sub> adsorption and modified modes of methanol adsorption compared to MgO. However, the CO<sub>2</sub> adsorption capacity did not correlate to catalyst activity.

**Table 1. Reactivity comparison of Mg-Zr mixed oxides for transesterification of tributyrin with methanol.**

Catalyst	Surface Area (m <sup>2</sup> g <sup>-1</sup> )	$k_1$ (x10 <sup>6</sup> ) <sup>(c)</sup> (Lmol <sup>-1</sup> m <sup>-2</sup> s <sup>-1</sup> )
Mg:Zr 1:1 (1.4) <sup>(a)</sup>	176	0.37 ± 0.12
Mg:Zr 5:1 (5.6) <sup>(a)</sup>	223	0.50 ± 0.03
Mg:Zr 8:1 (8.2) <sup>(a)</sup>	256	0.73 ± 0.07
Mg:Zr 11:1 (11.1) <sup>(a)</sup>	173	3.00 ± 0.30
Mg:Zr 11:1 (11.1) <sup>(a)(d)</sup>	212	3.19 ± 0.35
MgO	292	0.70 ± 0.02
MgO from Mg(OH) <sub>2</sub> <sup>(b)</sup>	22	1.16 ± 0.34
ZrO <sub>2</sub>	123	0

(a) Values in parentheses indicate Mg/Zr molar ratio from elemental analysis

(b) Mg(OH)<sub>2</sub>, nanopowder (Aldrich, 99.9%)

(c) Errors represent 95% confidence intervals on fitted reaction rate constants

(d) Made using Labmax synthesis method at FHI

These intriguing results suggested that we needed better synthesis methods and characterization techniques if we were ever going to understand the fundamental nature of the promotional effect of Zr on MgO surfaces. Therefore, graduate student Joseph Kozlowski spent the summer of 2010 at the Fritz Haber Institute in the group of Prof. Dr. Robert Schlogl. A material prepared at the FHI is included in Table 1 for comparison.

Part of the research funded by this grant also involved exploratory studies on how an oxophilic

promoter like iron affects alcohol synthesis over supported rhodium nanoparticles. In particular, the influences of support (silica or titania) and loading of Fe promoter on the activity and selectivity of Rh-based catalysts for the direct synthesis of ethanol from syngas were investigated. Specifically, The hydrogenation of CO, CO+CO<sub>2</sub>, and CO<sub>2</sub> over titania-supported Rh, Rh-Fe, and Fe catalysts was carried out in a fixed-bed microreactor system nominally operating at 543 K and 20 atm. A comparative study of CO and CO<sub>2</sub> hydrogenation showed that while Rh and Rh-Fe/TiO<sub>2</sub> catalysts exhibited appreciable selectivity to ethanol during CO hydrogenation, they functioned primarily as methanation catalysts during CO<sub>2</sub> hydrogenation. The Fe/TiO<sub>2</sub> sample was primarily a reverse water gas shift catalyst. The interface between Rh and FeO<sub>x</sub> is thought to play a key role in the alcohol synthesis reaction.

### **Future Plans**

The enhancement of transesterification rates by adding Zr to MgO has been repeated multiple times, but no satisfactory explanation of the phenomenon has been discerned. Thus, we propose to study the mixed oxide materials as catalysts for alcohol coupling reactions. Solid bases are known to couple ethanol to butanol, a potentially important reaction for transportation energy streams, whereas solid acids dehydrate ethanol to ethylene. The selectivity patterns of the ethanol reactions will be used together with isotopic labeling studies to determine the role of added Zr on the surface reactivity of MgO.

### **Publications (2009-2011)**

- Y. Xi and R.J. Davis, "Influence of Textural Properties and Trace Water on the Reactivity and Deactivation of Reconstructed Layered Hydroxide Catalysts for Transesterification of Tributyrin with Methanol" *J. Catal.*, **268** (2009) 307-317.
- M.A. Haider, M.R. Gogate and R.J. Davis, "Fe-Promotion of Supported Rh Catalysts for Direct Conversion of Syngas to Ethanol" *J. Catal.* **216** (2009) 9-16.
- J.T. Kozlowski, M.T. Aronson and Robert Davis, "Transesterification of tributyrin with methanol over basic Mg:Zr mixed oxide catalysts" *Appl. Catal. B: Environ.*, **96** (2010) 508-515.
- Y. Xi and R.J. Davis, "Intercalation of Ethylene Glycol into Yttrium Hydroxide Layered Materials" *Inorg. Chem.* **49** (2010) 3888-3895.
- Y. Xi and R.J. Davis, "Glycerol Intercalated Mg-Al Hydrotalcite as a Potential Solid Base Catalyst for Transesterification" *Clays and Clay Minerals* **58** (2010) 475-485.
- M.R. Gogate and R.J. Davis, "Hydrogenation of CO<sub>2</sub> over supported Rh-Fe catalysts," *Catal. Commun.* **11** (2010) 901-906.

**DE-FG02-03ER15456**

**Michael W. Deem**

**Toward Rational, Nanoscale Control of Catalysis: A Fundamental Study of Zeolite Structure and Nucleation**

Student: Man Chen

Postdoc: Ramdas Pophale

Collaborators: Mark E. Davis (Caltech), Yushan Yan (Delaware),  
Berend Smit (UC Berkeley)

Rice University, 6100 Main Street – MS 142, Houston, TX 77005-1892

[mwdeem@rice.edu](mailto:mwdeem@rice.edu)

<http://www.mwdeem.rice.edu>

Period: 9/15/2009 – 9/14/2012

### **Goal**

Develop the database of zeolite-like materials, solve structures of new zeolite materials, and predict barriers to zeolite nucleation in the presence of structure directing agents.

### **Recent Progress**

*Zeolite-Like Structure Generation:* We have constructed a database of computationally-predicted zeolite-like structures. To date, we have roughly 2.7 million structures in this database, with roughly 10% within the 30kJ/mol Si energetic band above  $\alpha$ -quartz in which the known zeolites lie. This number is to be compared to the roughly 190 structures of known zeolites. Predicted structures within this band have geometric and topological characteristics similar to that of known zeolites. Known zeolites were shown to lie on the low-density edge of the distribution of predicted structures. Dielectric constants and X-ray powder diffraction patterns were calculated. The structures were deposited in two publicly available databases. This work was featured on the cover of *J. Chem. Phys. C* [2].

We have further refined this database, to fix the SLC and BKS forcefields so that they obey the Pauli exclusion principle. This massive effort resulted in a database of 2.6M structures, with roughly 15% within the 30kJ/mol Si energetic band above  $\alpha$ -quartz in which the known zeolites lie. The agreement with known zeolite structures is even more satisfactory now, as both the SLC and BKS structures appear zeolite-like. These structures are freely available at [www.hypotheticalzeolites.net/database/deem/](http://www.hypotheticalzeolites.net/database/deem/) and in the PCOD database of Armel Le Bail. This work was featured on the cover of *Phys. Chem. Chem. Phys.* [3].

Structures in the database include both oxygen and silicon atoms and have been energy minimized by GULP using both the polarizable SLC interatomic potential, with modified oxygen shell charge, and the non-polarizable BKS interatomic potential. There are 2.7M topologically unique, energy-refined structures in the database. Of these, 314k are within 30 kJ/mol Si of quartz as judged by the SLC interatomic potential (and 585k are within 65 kJ/mol Si of quartz as judged by the BKS interatomic potential) and, thus, thermodynamically accessible as aluminosilicates. The remainder of the structures may be accessible via elemental substitutions, which allow a greater range of bond lengths and angle values. These energy-minimized structures may be screened for physical or

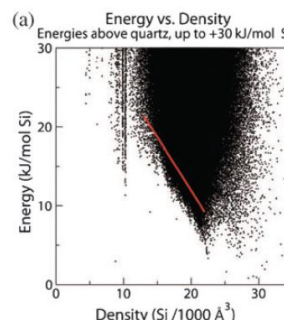
chemical applications. In addition, there is a database of 4.4M Si-only framework configurations, guaranteed to be unique within each space group. These silicon framework structures are interesting for coarse-grained searching. All of these structures have been deposited with the hypothetical zeolite network database and the predicted crystallographically open database (PCOD).

It is anticipated that further use of the present database may be useful to answer a number of technological and scientific questions. For example, searching the database for specific physiochemical functions may allow structures for particular applications to be identified. While direct use of zefsaII is likely to be more efficient, the database may also be searched to identify newly-synthesized materials with unknown structures. Ideas for continued development of rational solid-state synthesis may be explored. For example, which of the structures can be synthesized, and how?

It is our long-term goal that structures from this database will be identified by their predicted material properties and become the subject of targeted synthesis by our experimental colleagues. We also look forward to collaboration with our theoretical colleagues to screen the database for interesting and useful physiochemical functions. For example, in collaboration with Berend Smit, we will begin to address the calculation of catalytic materials properties. The strategy we will follow when considering a set of industrially interesting transformations is to list all known mechanisms with intermediate states for performing the transformation. By examining the physical constraints that the zeolite places upon the reactions, we can determine which are feasible. In this way, we can rank the hypothetical frameworks for likely performance on the transformation.

The known zeolites lie at the low-density edge of the distribution of zeolite-like materials (red line). This placement of the knowns within the distribution of possibilities may be a result of limitations of current solution-phase synthetic techniques, whereby zeolites condense from Si-rich solution. Perhaps different synthetic routes will allow synthesis of a broader range of zeolitic materials.

An interesting mechanistic feature is the “feasibility factor” line. This line, in red in the figure, had previously been identified as a least-squares fit to zeolite destabilization energies (over that of  $\alpha$ -quartz) as a function of density. We now see that this line is the low-density edge of the distribution of possible zeolite structures. As such, this suggests a mechanistic explanation: zeolites are crystallized from low-density solution, and the first zeolite that can be made as density is increased nucleates. This low-density edge suggests that currently feasible zeolites lie on the low-density edge of all possible zeolites. Perhaps new synthetic techniques will be able to access zeolites in the interior of the distribution of possible structures.



This database is now being screened by colleagues at Georgia Tech (David Scholl), Berkeley (Berend Smit), Northwestern (Randy Snurr), BASF, Chevron, and others. As

example properties, we have calculated low and high frequency dielectric constants. We have also calculated elastic moduli. And we have calculated density, coordination sequences, and ring distributions.

*Low-k Dielectric Materials:* Although there are many different types of zeolite framework structures, only a few (e.g., MFI and MEL) have been investigated because measurement of the dielectric constant requires the preparation of a high quality thin film. The development of a simple measurement method for powdered zeolite samples is essential to accelerate the screening process for zeolites. In [7], time-domain reflectometry (TDR) coupled with the use of a transmission line is introduced for the first time for measuring low-k powdered materials. The technique can quickly measure the dielectric constants of powdered samples over a large frequency range using less than 0.5 g of sample with high reliability and accuracy. Successful measurements on quartz and high-k materials (e.g., HfO<sub>2</sub>) indicated that this method can be applied to powdered samples in general.

Deem was awarded the Professional Progress Award of the AIChE and elected to fellowship of AAAS.

### **DOE Interest**

Even just in the area of carbon capture materials, zeolites show a tremendous potential for improve throughput and selectivity versus polymeric systems. A very limited subset of the database of new zeolite-like materials has been screened, with already a number of better-performing materials found. It goes without saying that zeolites are currently used on a massive scale in energy-related applications. Understanding zeolite nucleation is important not only scientifically for the discovery and synthesis of new materials, but also in an engineering sense for improving the performance of existing materials that are not performing as well as they could due to poor “crystallinity.” Considerations include catalysts with improved catalytic properties for improving refining economics and for reducing environmentally-unfriendly by-products, design of better, smarter, and more energy-efficient separation processes, and design of zeolites that are more effective for radioactive waste cleanup and stewardship purposes. Parallel tempering and biased Monte Carlo are general materials simulation methods now in use.

### **Related Publications (2009-2011)**

- 1) Y. Yan, M. Sun, W. Maichen, R. Pophale, Y. Liu, R. Cai, C. M. Lew, H. Hunt, M. W. Deem, and M. E. Davis “Dielectric Constant Measurement of Zeolite Powders by Time Domain Reflectometry,” *Micropor. Mesopor. Mater.* **123** (2009) 10-14 [2: joint funding DOE and other federal (Deem’s contribution was solely BES/DOE)].
- 2) M. W. Deem, R. Pophale, P. A. Cheeseman, and D. J. Earl, “Computational Discovery of New Zeolite-Like Materials,” with cover image, *J. Phys. Chem. C* **113** (2009) 21353-21360 [1: solely funded by BES/DOE].
- 3) M. W. Deem, R. Pophale, P. A. Cheeseman, and D. J. Earl, “A Database of New Zeolite-Like Materials,” with cover image, *Phys. Chem. Chem. Phys.* (2011) doi: 10.1039/c0cp02255a, [1: solely funded by BES/DOE].



**CATALYSIS SCIENCE INITIATIVE: Catalyst Design by Discovery Informatics**

Co-PIs: J. M. Caruthers, M. Abu-Omar (Chemistry), F. H. Ribeiro, K. T. Thomson, W. F. Schneider (Notre Dame University)

Research Associate: G. Medvedev

Postdoc: J. Wang

Students: J. Clay (Notre Dame), M. Jones (Chemistry), W.-S. Lee, J. H. Pazmiño, K. Sabnis, M. Shekhar, S. Stamatias, J. Switzer, E. Smith (Chemistry), K. Steelman (Chemistry), N. Travia (Chemistry), D. Williams, S. Xiong

Collaborators: J. T. Miller, Argonne National Laboratory; E. A. Stach, Materials Engineering, Purdue and Brookhaven National Laboratory.

Contact: W. N. Delgass, Forney Hall of Chemical Engineering, 480 Stadium Mall Drive, Purdue University, West Lafayette, IN 47907-2100, [delgass@ecn.purdue.edu](mailto:delgass@ecn.purdue.edu)

**Goal**

The goal of this research is development of a new paradigm for catalyst discovery and optimization through a model-based approach to catalyst design. While the approach is general, issues specific to heterogeneous catalysis are addressed in studies of the water gas shift reaction and those for homogeneous systems in studies of single site olefin polymerization.

**DOE Interest**

In this catalyst design approach, rate constants from modeling detailed kinetic data are combined with chemical insights from density functional theory to identify descriptors of the catalyst system, and those descriptors are used in a quantitative model to design improved catalysts. Validation of this new design concept has the potential to change the catalysis research landscape by dramatically shortening hypothesis testing and new discovery cycles for virtually any catalyst system. Applications with energy impact include generation of hydrogen for fuel, production of fuels and chemicals from coal or biomass, engine after-treatment via NO<sub>x</sub> removal, and the development of environmentally friendly chemical processes.

**Recent Progress**

**Water Gas Shift Reaction** - The water gas shift (WGS) reaction has clear impact on energy issues as a central pathway to clean hydrogen, but it also serves here as an excellent test bed for discovery of catalyst descriptors and development of our model-based approach to catalyst design that we call *Discovery Informatics*. Specific objectives for the WGS program are to build a database with sufficient chemical and information diversity to allow identification of active sites, to model the kinetics, to identify descriptors of the kinetic parameters, and ultimately to use those descriptors to create a predictive model for WGS activity. A combination of accurate steady state and transient kinetic measurements with detailed catalyst characterization using TEM, EXAFS, XANES, and IR, often in the *operando* mode, for catalysts synthesized on model supports to facilitate the TEM analysis has led us to the working hypothesis that, for supported Au, the coordinatively unsaturated corner and perimeter atoms at the metal support interface are the dominant active sites, while for Pt, all the surface atoms participate. In spite of this

substantial difference in behavior, we find that the support plays a deciding role in water activation for both metals and may do so by providing support-specific sites. We have developed a microkinetic model that accounts for these trends but have not fully addressed the need to incorporate the coverage dependence of the CO binding energy to the surface. We focus here on identifying and quantifying active sites, understanding the dramatic role that the support plays, promotion by alkali metals, and modeling.

**Active Sites:** The strong dependence of the WGS reaction rate with Au nanoparticle size in the range of 1 nm to 7 nm has been studied in detail. The WGS reaction rate per total mole of Au for Au/Al<sub>2</sub>O<sub>3</sub> catalysts varies with the average Au particle size (*d*) as  $d^{-2.2 \pm 0.2}$ .<sup>[1]</sup> Changes in reaction order with *d*, however, show that these catalysts have more than 1 active site. Modeling of the kinetic data has allowed us determine that the dominant active sites are the low coordinated corner Au atoms, which are 3 and 7 times more active than the perimeter Au atoms for Au/Al<sub>2</sub>O<sub>3</sub> and Au/TiO<sub>2</sub> catalysts respectively. *Operando* Fourier transform infrared spectroscopy (FTIR) experiments show that the CO adsorbed on Au<sup>0</sup> is an active intermediate. In contrast, all the surface Pt sites exhibit the same rate and are also metallic in nature.

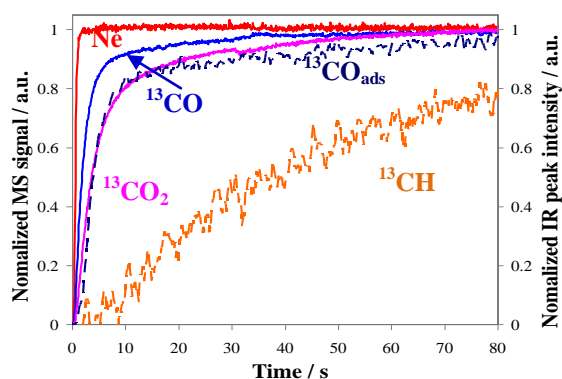


**Figure 1:** Normalized MS signal and IR peak intensity of Pt/CeO<sub>2</sub> (solid line: MS signal, dot line: IR peak intensity).

SSITKA, and Br poisoning experiments were also used to confirm the assignment of active sites for Au/TiO<sub>2</sub>.

**Support Effect:** The H<sub>2</sub>O order for Au catalysts exhibited the following trend: Au/Al<sub>2</sub>O<sub>3</sub> (~0.6) > Au/Al<sub>2</sub>O<sub>3</sub>-WGC (~0.5) > Au/CeO<sub>2</sub> (~0.3) > Au/ZrO<sub>2</sub> (~0.0) > Au/TiO<sub>2</sub> (~-0.3). On Pt catalysts, the H<sub>2</sub>O order followed a different trend: Pt/Al<sub>2</sub>O<sub>3</sub> (0.93) > Pt/SiO<sub>2</sub> (0.84) > Pt/La<sub>2</sub>O<sub>3</sub> ~ Pt/TiO<sub>2</sub> ~ Pt/ZrO<sub>2</sub> ~ Pt/CeO<sub>2</sub> (0.66 – 0.72). For both Au and Pt catalysts, the apparent activation energies varied with the support. We interpret these data to show that the support plays a direct role in activating H<sub>2</sub>O and conclude that more active supports have higher coverages of hydroxyl species.

**Alkali Promoted Pt catalysts:** In light of recent literature [Zhai, et al., *Science*, 329 (2010) 1633] that reports a strong promotional effect of adding sodium to Pt/Al<sub>2</sub>O<sub>3</sub>, we studied a series of catalysts prepared by consecutive impregnation of Pt and different amounts of alkali (Li, Na, K, Cs). The WGS rate per mol of Pt is shown in Figure 2. From EXAFS, we observed that the Pt in all fresh Pt/Na/Al<sub>2</sub>O<sub>3</sub> samples was oxidized when the samples were exposed to air. Upon

*Operando FTIR with Steady State Isotopic Transient Kinetic Analysis (SSITKA):* In order to confirm our site assignments, we have performed *Operando* FTIR simultaneously with SSITKA, Figure 1. From SSITKA, the total amount of surface intermediates, N<sub>CO<sub>x</sub></sub>, was found to be comparable to the CO surface coverage on Pt measured under WGS reaction conditions. Furthermore, the normalized IR peak intensities of <sup>13</sup>CO adsorbed on Pt (<sup>13</sup>CO<sub>ads</sub>) best correlate with the normalized MS response of <sup>13</sup>CO<sub>2</sub>. These results are strong evidence that metallic surface Pt atoms are the dominant active sites for WGS reaction on Pt/CeO<sub>2</sub> catalysts. *Operando* FTIR,

reduction in 3.5% H<sub>2</sub>/He at 300°C, no oxidized Pt was detected at any level of Na loading (including Na-free, Pt/Al<sub>2</sub>O<sub>3</sub>). More importantly, the same result was obtained under WGS reaction conditions. Kinetic measurements on the alkali-modified Pt catalysts showed an increase in H<sub>2</sub>O order to values closer to 1 and -0.2 order for CO<sub>2</sub>. For comparison, Pt/Al<sub>2</sub>O<sub>3</sub> tested at the same temperature exhibits a H<sub>2</sub>O order of 0.68 and zero order in CO<sub>2</sub>. No changes in the CO or H<sub>2</sub> order were observed. Interestingly, orders of ~1 and -0.2 for H<sub>2</sub>O and CO<sub>2</sub> were also observed for Pt/Na/P25, where the rate promotion was equal to a factor of 6 (at 300°C) with respect to unpromoted Pt/P25, a catalyst which is already 10 times more active than Pt/Al<sub>2</sub>O<sub>3</sub>. These data suggest the creation of a new type of active site, which we are in the process of identifying.

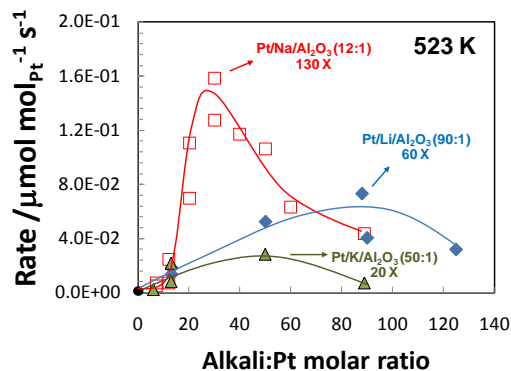


Figure 2: Rate per total mole Pt vs. alkali:Pt

**Kinetic Modeling:** Construction of a forward model for use in our concept for model-based catalyst design requires a microkinetic model for the kinetic behavior. We have developed a suite of kinetic modeling tools and continue to tune these tools for use with our water gas shift (WGS) catalyst library. We first recreated the model from the the paper of Grabow et al., *J. Phys. Chem. C*, 112 (2008) 4608 using their data for WGS on Pt/Al<sub>2</sub>O<sub>3</sub> and then validated that the code was able to simulate the kinetics of the Pt/Al<sub>2</sub>O<sub>3</sub> data collected at Purdue. Bayesian parameter estimation<sup>[2]</sup> was then performed on a simplified model, with and without CO coverage dependencies of the different binding energies. The results indicate that (1) adsorbed CO, OH, and free Pt sites are the most abundant surface species, (2) dissociation of the carboxyl group formed from CO and OH is a rate controlling step, and (3) coverage dependence of the CO binding energy is necessary. Our current work suggests that a single microkinetic model can explain trends for a large number of catalysts.

**Density Functional Theory:** Development of descriptors needs support from computational chemistry. We rely on theory to supply some of the constants needed, particularly for equilibrated steps and to provide a formalism for scaling parameters across families of materials. To this end, the focus of efforts to date has been on a complete, consistent set of DFT-based parameters for Pd that can be used for parameterization of a kinetic model. The overall picture that is emerging is a surface dominated by CO, upon which water dissociation is rate limiting and may occur via multiple pathways depending on co-adsorbate coverage. Given the high CO coverage, CO\* + OH\* → COOH\* → CO<sub>2</sub> + H\* is the most likely route to CO<sub>2</sub>, similar to that proposed on Cu and Pt by the Mavrikakis group.

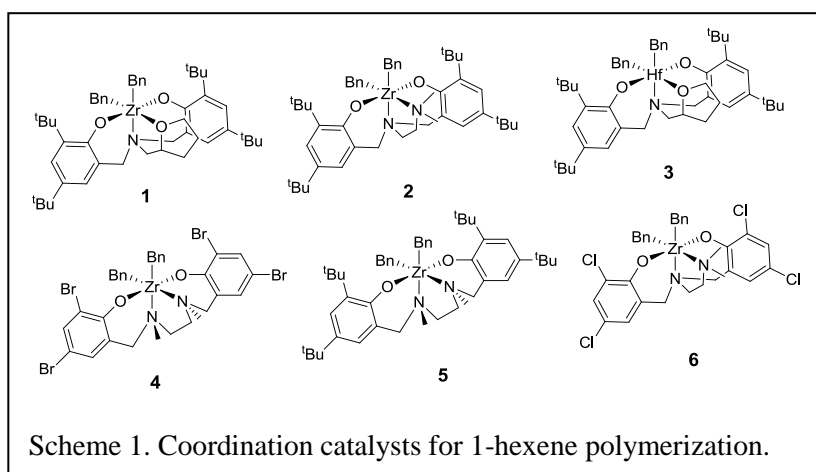
**Single Site Olefin Polymerization** - While the majority of polyolefins is produced using heterogeneous catalysts, single site homogeneous catalysts are increasingly gaining ground because they can afford polymers with precisely engineered physical properties. Additionally, homogeneous catalysts hold promise for designing systems from first principles. A major challenge in the field is the lack of reliable/robust values for the relevant rate constants for initiation ( $k_i$ ), propagation ( $k_p$ ), misinsertion ( $k_{mis}$ ), chain transfer ( $k_{CT}$ ), etc. In this research, we have made significant advances in establishing a standard for how to obtain robust and reliable rate constants for single-site olefin polymerization catalysts. The most stringent requirement is

satisfying the MWDs at different monomer conversions, in addition to monomer consumption, end group analysis, and active site counting. This approach of fitting multi-response data sets guarantees a well defined kinetic mechanism and meaningful rate constants for all the relevant steps, allowing true structure-function understanding. During this past year, we have demonstrated the viability of our method and corrected the literature on Brintzinger's catalyst. In addition, using non-Cp coordination catalysts, we have discovered that the pendant ligand, NMe<sub>2</sub> versus THF, has a large effect on  $k_{CT}$ , and shown quantitatively that  $k_p$  for Hf is 20 times slower than that for Zr, resulting in more chain termination. Finally, we are expanding our kinetics toolkit to other systems with colleagues in the community

**Brintzinger's Catalyst:** The first application of our multi-response formalism was to the batch polymerization of 1-hexene by *rac*-C<sub>2</sub>H<sub>4</sub>(1-Ind)<sub>2</sub>ZrMe<sub>2</sub> activated with B(C<sub>6</sub>F<sub>5</sub>)<sub>3</sub>.<sup>[3]</sup> We showed it is possible to predict the entire multi-response data set (including the MWDs) using a kinetic model featuring 57% of the catalyst as the active form responsible for polymerization. This finding has significant implications regarding the behavior of the catalyst and the polymer produced and is potentially relevant to other single-site polymerization catalysts, where it would have been undetected because of incomplete kinetic modeling.

**Non-Cp Coordination Catalysts** – To expand our library of catalyst structures and corresponding rate constants, we have prepared a number of salan-type coordination catalysts, Scheme 1[Cohen, et al., *Organometallics*, 28 (2009) 1391]. Quantitative kinetic analysis for 1-hexene polymerization in the condensed phase is carried out by (1) following monomer consumption via <sup>1</sup>H NMR, (2) quenching the reaction and acquiring the MWD at 20-40% conversion and at the end of reaction (≥ 90% conversion), (3) counting active sites by quenching the reaction at different conversions with CH<sub>3</sub>OD and analyzing the resulting polymer by <sup>2</sup>H NMR, (4) analyzing vinylene and vinylidene end groups by <sup>1</sup>H NMR, and (5) determining the initiation rate constant ( $k_i$ ) independently by measuring the kinetics at low monomer to catalyst ratio, 5:1.

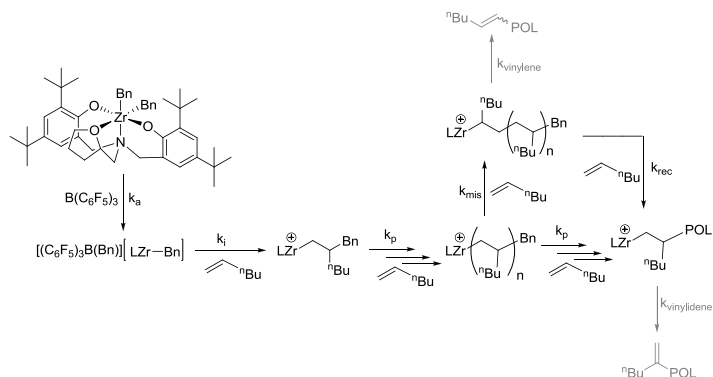
A single kinetic model was used to fit the entire data set for catalyst **1** including the GPC curves, where the initial amount of activated catalyst and the rate of deactivation were allowed to vary in each experiment, Scheme 2. While the values for  $k_{CT}$  can be obtained from end group analysis of the polymer, they are small enough not to be needed to predict the MWDs.



A significant amount of the catalyst undergoes 2,1-mis-insertion and recovers at a much slower rate than that of propagation.

Analysis of the experimental data for catalyst **2** showed that the same kinetic mechanism observed for **1** could also fit the behavior of **2**, as illustrated in Figure 3, but here the chain transfer rate constants to give vinylidene and vinylene cannot be ignored. The rate constants are very similar for the two systems except for the two chain transfer rate constants, which are 100-

fold different. We suspect that the bonding strength of the pendent ligand to the metal plays a key role in the chain transfer pathway—which we hypothesize occurs by  $\beta$ -hydride elimination—and we have begun a series of DFT calculations that will provide further insight.



Scheme 2. Kinetic mechanism for 1-hexene polymerization with catalyst 1.

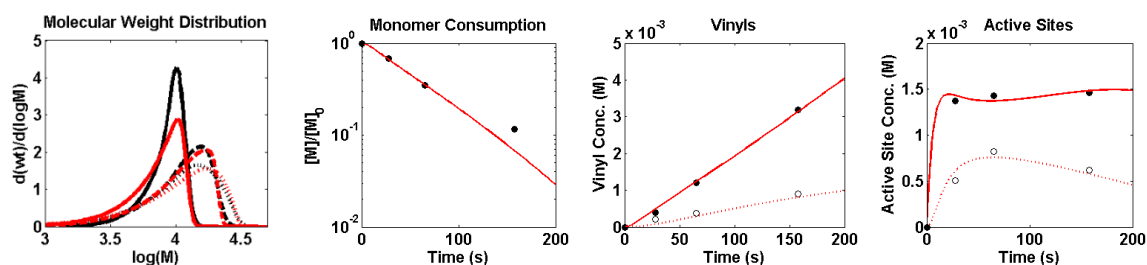


Figure 3. Best-fit model prediction (red) for 2/ $B(C_6F_5)_3$  polymerization of 1-hexene. The molecular weight distributions are given at 32% (—), 65% (---), 88% (|||) monomer conversion. The vinyl data are vinylidene (●) and vinylene (○). The active site data are primary C–Zr (○) and secondary C–Zr (●).

**Hf versus Zr:** The literature is void of a direct and quantitative comparison between Hf and Zr to provide decisive insight on what rate constants vary and by how much. We prepared catalyst 3, which is the structural analog of 1. Furthermore, we established by metal analysis (ICP-MS) that complex 3 contains less than 0.1% Zr. We find the Hf catalyst to produce significantly more vinyl end groups, primarily as consequence of 23 times lower  $k_p$  for Hf versus Zr.

**Expansion of our microkinetics toolkit to a wider class of polymerization reactions:** Our current software for single-site polymerization kinetics is based on population balance (PB) equations and, thus cannot be used to describe several practically and fundamentally important systems, such as the co-polymerization of different monomer species. In batch co-polymerization, the molecular weight distribution as well as the microstructure of chains i.e. co-monomer sequence distribution are of interest and are available experimentally, provided one of the co-monomers is UV active. Unfortunately, keeping track of chain microstructure within the standard PB framework is combinatorially prohibitive. Reaction between two growing chains resulting in a growing chain of combined length is another event that requires extension of the PB approach.

An alternative to the PB method is the use of a stochastic approach based on the dynamic Monte Carlo (DMC) algorithm for chemically reacting systems pioneered by D.T. Gillespie [Gillespie, D.T. *J. Phys. Chem.* **1977**, *81*, 2340]. An original version of the DMC method has been developed allowing treatment of co-polymerization and combination reactions. To speed the computation, the size of the system is rescaled in the course of the simulation depending on the current monomer conversion and the MWD. In collaboration with the Waymouth group at Stanford the new DMC solver is being applied to describing kinetics of the synthesis of cyclic polylactide.

### Future Plans

In the *water gas shift* area the emphasis will be on refining and integrating our microkinetic models for the wide varieties of catalysts we have studied experimentally. Progress with the Au and Pt systems will be expanded to the Pd and mixed metal results. We will also be working with Bill Schneider to use DFT to develop descriptors associated with the various metal and support sites we have identified.

In the *single site olefin polymerization* area, we have data and modeling results for two non-Cp Salen systems. We are nearing completion of data sets for two other catalysts. These successes are validating our multi-response data analysis approach. We expect to continue to expand our catalyst library and put ourselves in a position to create models with sufficient diversity to allow testing of the inverse search for new, more active, catalysts. We will continue to look for opportunities to interact with other groups to expand the impact of our experimental protocol and modeling tools on the community.

### Publications 2009-2011

1. Williams, W. D., M. Shekhar, W.-S. Lee, V. F. Kispersky, W. N. Delgass, F. H. Ribeiro, S. M. Kim, E. A. Stach, J. T. Miller, L. F. Allard, "Metallic Corner Atoms in Gold Clusters Supported on Rutile are the Dominant Active Site during Water-Gas Shift Catalysis", *J. Am. Chem. Soc., Commun.*, *132* (40), 14018-14020 (2010).
2. Hsu, Shuo-Huan, Stephen D. Stamatias, James M. Caruthers, W. Nicholas Delgass, Venkat Venkatasubramanian, Gary E. Blau, Michael Lasinski, Seza Orcun, "A Bayesian Framework for Building Kinetic Models of Catalytic Systems," *Industrial and Engineering Chemistry Research*, *48*, 4768-4790 (2009).
3. Novstrup, Krista A., Nicholas E. Travia, Grigori A. Medvedev, Cornel Stanciu, Jeffrey M. Switzer, W. Nicholas Delgass, Mahdi M. Abu-Omar, and James M. Caruthers, "Insights from Kinetic Modeling of Rich Multi-Response Data in [*rac*-(C<sub>2</sub>H<sub>4</sub>(1-Indenyl)<sub>2</sub>)Zr(Me)<sub>2</sub>]-Catalyzed 1-Hexene Polymerization," *J. Am. Chem. Soc.*, *132*, 558–566 (2010).
4. Krishnamurthy, Gowri, Aditya Bhan and W. Nicholas Delgass, "Identity and Chemical Function of Gallium species inferred from Microkinetic Modeling Studies of Propane Aromatization over Ga/HZSM-5 Catalysts," *J. Catal.*, *271*, 370-385 (2010).
5. Phatak, Abhijit A., W. Nicholas Delgass, Fabio H. Ribeiro, and William F. Schneider," DFT Comparison of Water Dissociation Steps on Cu, Au, Ni, Pd and Pt," *J. Phys. Chem. C*, *113*, 7269-7276 (2009).

## Photocatalytic transformation of CO<sub>2</sub> to CH<sub>4</sub> over titania

Nada M. Dimitrijevic,\* Kimberly A. Gray

Chemical Sciences and Engineering Division, Argonne National Laboratory, Argonne, IL 60439, and Department of Civil & Environmental Engineering, Northwestern University, Evanston, IL 60208

e-mail: dimitrijevic@anl.gov

Important elementary steps in photocatalytic conversion of CO<sub>2</sub> into fuels (methanol and methane) occur on the surface of semiconductor nanocrystallites and require both understanding of the structural properties of photocatalyst that direct electron movement across the interface, and mechanistics of the multistep reaction pathways of CO<sub>2</sub> conversion. Synergy of synthesis, characterization and testing allows identifications of those features and pathways that selectively facilitate CO<sub>2</sub> reduction. We synthesized titania nanotubes having diameter of 8-12 nm and length of 50-300 nm using hydrothermal method with calcination. Electron paramagnetic resonance spectroscopy (EPR) was used to interrogate the effects of nanotube structure on the charge separation and trapping, and has revealed that five-coordinated Ti sites at the surface of nanotubes calcined at 400 °C are associated with maximum CO<sub>2</sub> reduction.[1] Isolated metallic (Pt) clusters,[2] or Fe(III)-oxo centers,[3] on the surface of titania not only affect morphology of the nanotubes and nanoparticles, but alter optical and electronic properties of nanocomposites allowing for visible light CO<sub>2</sub> photocatalysis. The mechanism of CO<sub>2</sub> reduction on TiO<sub>2</sub> was examined using an EPR technique.[4] It was found that water, both dissociated on the surface of TiO<sub>2</sub> and in subsequent molecular layers, has a threefold role: (i) stabilization of charges (preventing electron-hole recombination), (ii) as electron donor (reaction of water with photogenerated holes to give OH radicals) and (iii) as electron acceptor (formation of H atoms in a reaction of photogenerated electrons with protons on the surface). Dissolved CO<sub>2</sub> in a form of carbonates/bicarbonates competes with water for photogenerated holes, acting as hole scavenger. Detection of H atoms, ·OCH<sub>3</sub> and ·CH<sub>3</sub> radicals as reaction intermediates, and first-principles calculations suggest a concerted two-electron, one-proton transfer to adsorbed carbon dioxide molecules, and demonstrates the importance of hydrogen/water management on the photocatalyst surface.

### References

1. B. K. Vijayan, N. M. Dimitrijevic, T. Rajh, K. A. Gray, *J. Phys. Chem. C* **114**, 12994 (2010)
2. B. K. Vijayan, N. M. Dimitrijevic, J. Wu, K. A. Gray, *J. Phys. Chem. C* **114**, 21262 (2010)
3. J. A. Libera, J. W. Elam, N. F. Sather, T. Rajh, N. M. Dimitrijevic, *Chem. Mater.* **22**, 409 (2010)
4. N. M. Dimitrijevic, B. K. Vijayan, O. G. Poluektov, T. Rajh, K. A. Gray, H. He, P. Zapol, *J. Am. Chem. Soc.* **133**, 3964 (2011)

**Computational Studies of Reactive Transition Metal Complexes: Critical Bond Energies**

Lead PI: Dr. Charles Peden, Pacific Northwest National Laboratory  
Postdocs: Dr. S. Li, Dr. M. Vasiliu  
Graduate Student: R. Craciun

Contact information: Department of Chemistry, The University of Alabama, Shelby Hall, Box 870336, Tuscaloosa AL 35487-0336; [dadixon@bama.ua.edu](mailto:dadixon@bama.ua.edu)

Olefin metathesis by transition metal complexes can be used to manipulate C–C bonds catalytically and is broadly applicable. Heats of formation of the parent Schrock-type metal complexes  $M(NH)(CRR')(OH)_2$  ( $M = Cr, Mo, W$ ;  $CRR' = CH_2, CHF, CF_2$ ) and  $MO_2(OH)_2$  compounds were predicted at a reliable computational level (CCSD(T)/CBS + corrections).  $M=O$ ,  $M-O(H)$ ,  $M=CRR'$  ( $CRR' = CH_2, CHF, CF_2$ ) and  $M=N(H)$  adiabatic and diabatic bond dissociation energies (BDEs) were predicted. The BDEs for the  $M=Cr$  complexes are predicted to be the smallest and for  $M=W$ , the largest. For the  $M(NH)(CRR')(OH)_2$  complexes, the order of BDEs is generally  $M=N(H) > M-O(H) > M=CRR'$ . The  $M=CRR'$  BDEs increase in the order  $CF_2 < CHF < CH_2$ ; the  $CF_2$  and  $CHF$  Schrock-type complexes are much less stable than  $CH_2$  complexes. The  $\sigma$ -withdrawing and  $\pi$ -donating substituent F substantially stabilizes the singlet ground state of the carbene so that the metal-carbene BDE becomes much weaker. The weaker  $M=CRR'$  bond when R and/or R' are a  $\sigma$ -withdrawing and  $\pi$ -donating substituent will not readily form in either the starting catalyst or the metal product generated by the retro [2+2] cycloaddition; this type of catalyst cannot readily be used for olefin metathesis reactions involving carbenes and/or olefins with such substituents. The singlet-triplet splitting in the carbene is a critical component in the design of effective olefin metathesis catalysts in terms of the parent catalyst and the groups on the olefins being transferred. The results show that the carbene centers involved in the metathesis reactions need to have triplet ground states or a small singlet-triplet splitting for a singlet ground state in order to form good  $M=C$  bonds. The weaker  $Cr=C$  bonds make it unlikely that Cr compounds will be good catalysts for such reactions using these catalysts. The  $M(NH)(CH_2)(OH)_2$  and  $MO_2(OH)_2$  model compounds are predicted to be medium to weak Brønsted acids and modest Lewis acids. The moderate Lewis acidity coupled with the steric constraints present in the parent  $M(NH)(CH_2)(OH)_2$  with no substituents on N, C, or O is not large enough for  $C_2H_4$  to form more than a very weak van der Waals type complex. The formation of the metallacycle proceeds via a direct addition of the olefin to the catalyst without the formation of a pre-complex. For  $M(NH)(CH_2)(OH)_2$  plus ethylene, distorted trigonal bipyramidal (TBP) or square pyramidal (SP) metallacycles are formed as intermediates with the SP geometry preferred with the  $=NH$  in the axial position. The energies of the SP and TBP complexes are reasonably close in the unsubstituted metallacycle so that substituents on O, N or C can change the relative energies of the conformers as found experimentally. The Brønsted acidity calculations show the carbene hydrogens on the  $CH_2$  on the complex are not very acidic so that it may be possible to design such catalysts for aqueous solution. A clear similarity between these types of homogeneous catalysts and heterogeneous catalysts such as the transition metal oxides is observed. The  $M-PH_3$  bond energy (BE) for the 0 and + 2 oxidation states for  $M = Ni, Pd, \text{ and } Pt$  for  $M(PH_3)_2$  and  $MCl_2(PH_3)_2$  for the design of new C-C cross-coupling catalysts were predicted using this approach. A wide range of DFT functionals failed to give good results.



**Alcohol chemistry on (WO<sub>3</sub>)<sub>3</sub> and (MoO<sub>3</sub>)<sub>3</sub> Clusters**

Lead PI: Charles H. F. Peden  
Postdocs: Zhenjun Li, Yeohoon Yoon.

Contact: Zdenek Dohnálek, Fundamental and Computational Sciences Directorate and Institute for Integrated Catalysis, Pacific Northwest National Laboratory, P.O. Box 999, MS K8-88, Richland, WA 99352; [Zdenek.Dohnalek@pnnl.gov](mailto:Zdenek.Dohnalek@pnnl.gov)

The catalytic conversion of C1-C4 aliphatic alcohols on cyclic (WO<sub>3</sub>)<sub>3</sub> and (MoO<sub>3</sub>)<sub>3</sub> clusters was studied experimentally and theoretically using temperature-programmed desorption, infrared reflection-absorption spectroscopy and density functional theory. Three reaction channels, dehydration, dehydrogenation, and condensation, are observed on WO<sub>3</sub> while only dehydration and dehydrogenation are seen on (MoO<sub>3</sub>)<sub>3</sub>. Additionally, a significant decrease in the alcohol conversion yield is also observed on (MoO<sub>3</sub>)<sub>3</sub>. The lower product yield is attributed to the lower deprotonation yield resulting from the lower Lewis acidity of Mo(VI) as compared to W(VI). The lack of condensation channel on (MoO<sub>3</sub>)<sub>3</sub> is also a consequence to the lower deprotonation yield as it leads to a negligible concentration of the Mo(VI) centers coordinated with two alkoxy species required for this reaction. Dehydrogenation occurs for both primary and secondary alcohols on (MoO<sub>3</sub>)<sub>3</sub> but only for primary alcohols on (WO<sub>3</sub>)<sub>3</sub>. This is likely due to easier reducibility of Mo(VI). On both clusters, the dehydration temperature decreases with increasing alkyl chain length and chain number. DFT calculations provide further insight into the reaction mechanisms and relative selectivity among the reaction channels on W(VI) and Mo(VI) metal centers.

This work is a part of Transition Metal Oxide BES/Catalysis Science program at PNNL. Research was performed in the Environmental Molecular Sciences Laboratory, a national scientific user facility sponsored by the Department of Energy's Office of Biological and Environmental Research and located at Pacific Northwest National Laboratory.

## Engineering Catalytic Nanoporous Metals for Reactions Important to the Hydrogen Economy

Students: Josh Snyder

Contacts: Johns Hopkins University, 102 Maryland Hall, 3400 N. Charles St., Baltimore, MD 21218; [Jonah.Erlebacher@jhu.edu](mailto:Jonah.Erlebacher@jhu.edu)

### Goal

Explore the properties of dealloyed nanoporous metals as catalysts for fuel cell reactions, particularly for oxygen reduction, taking advantage of their high surface areas, tunable surface and bulk composition, and the ability to absorb secondary phases in the pores that enhance chemical reactivity.

### DOE Interest

The use of precious metal catalysts for electrochemical oxygen reduction plays a central role in many energy conversion technologies including fuel cells and batteries. This reaction is currently the bottleneck in fuel cell catalysis, and reduction of the amount of precious metals required to generate enough power is a central problem. To improve oxygen reduction in fuel cells, strategies include fundamental understanding of the details of the chemical reactions involved as they vary with surface composition and development of new form factors for the catalyst (other than traditional nanoparticles) that can leverage the architecture of nanoscale environment to improve reactivity. Toward this end nanoporous metals made by dealloying (selective electrochemical dissolution) is emerging as an important class of materials, as they are useful in functional fuel cells, and are also convenient platforms with which to study the fundamental electrochemistry of chemical reactions important to the hydrogen economy.

### Recent Progress

*Fundamental electrochemistry of porosity evolution in dealloyed Ni/Pt nanoporous metals:* Synthesis of highly porous (pore/ligament size ~3 nm) Ni/Pt from dealloyed nickel-rich precursor alloys has been successful. The structural characterization of this material has been complemented by electrochemical characterization that shows self-assembly of a core-shell structure, with similar activity and composition to the Pt<sub>3</sub>Ni system. The activity of nanoporous NiPt toward oxygen reduction has been studied as a function of depth of porosity and potential, and we have developed methods to deconvolute the effects of mass transport of reactants within the pore and intrinsic surface activity.

*Development of nanoporous metal/ionic liquid composite catalysts:* We have taken advantage of the high porosity of nanoporous NiPt to make a novel catalyst that may be the most active yet discovered for oxygen reduction. By filling the pores with an ionic liquid with particular properties – hydrophobicity, electrochemical stability, protic, and

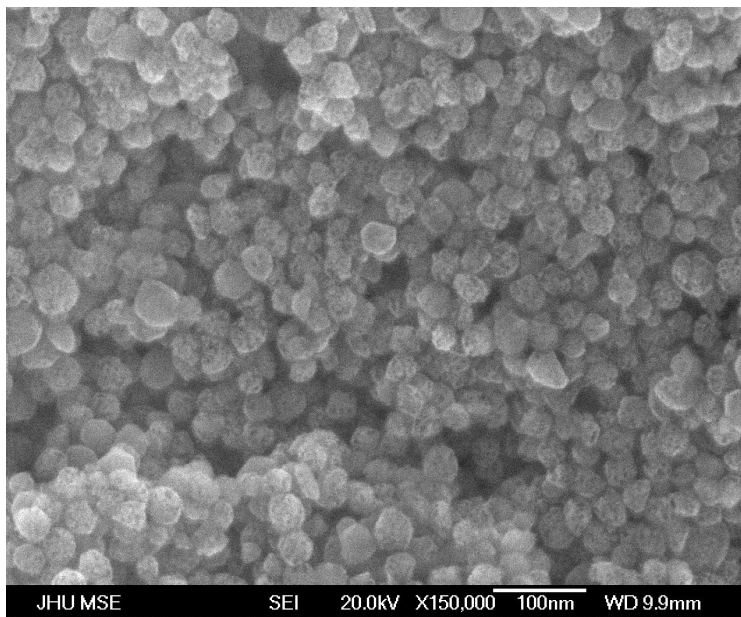


Figure 1. Nanoporous nanoparticles made by dealloying Ni/Pt precursor particles.

higher oxygen solubility than water – oxygen is biased to remain in the pores until it is reduced. A particular ionic liquid was found to increase activity at 0.9 V vs. RHE by a factor of nearly 2.5.

*Fabrication of nanoporous nanoparticles:* Rotating disk electrochemistry of nanoporous NiPt + ionic liquid composites suggests a nanoporous nanoparticle composite catalyst may have mass activities at 0.9 V vs. RHE well over 1 mA/microgram. We have developed methods to synthesize such particles, Figure 1, and are working to characterize their activity.

### **Future Plans**

*Characterize of the reaction kinetics of nanoporous metal/IL composites:* In an effort to gain understanding of reactions at metal/electrolyte interfaces, we will characterize the kinetics of oxygen reduction on NPMs as it depends on proton concentration, oxygen partial pressure, temperature, potential, and how these kinetics are convolved with effects of porosity and/or an IL phase in the pores. This test will clarify the role of changes in the reaction barriers at the surface (due to adsorbates and/or surface composition) and increases in attempt frequency (due to confinement of oxygen at this interface, and repulsion of water from it).

*Development of new nanoporous metals and composites:* We will make nanoporous metals with ultra-low Pt loading by dealloying new binary and ternary alloy precursors, particularly Ni/Pd(Pt), driven by intelligent materials design strategies that will drive trace amounts of Pt in the precursor alloys to the surface during dissolution. We will explore methods to improve the oxygen solubility of the hydrophobic secondary phase in the porous metal. And we will continue to develop synthesis strategies to make

nanoporous nanoparticles, with and without IL, with an eye toward integration of these materials into operational fuel cells.

### **Publications and Patents (2008-2011)**

1. J. Snyder, T. Fujita, M.W. Chen, J. Erlebacher, "Enhanced Oxygen Reduction in Nanoporous Metal/Ionic Liquid Composite Electrocatalysts," *Nature Materials* **9** (2010), 904-907.
2. J. Erlebacher, "Materials Science of Proton Exchange Membrane Fuel Cell Catalysts," *Solid State Physics* **61** (2009), 77-141.
3. J. Erlebacher, R. Seshadri, "Hard Materials with Tunable Porosity," *MRS Bulletin* **34** (2009), 561-568.
4. A. Mathur, J. Erlebacher, "Effects of Substrate Shape, Curvature and Roughness on Thin Heteroepitaxial Films of Pt on Au(111)," *Surface Science* **602** (2008) 2863-2875.
5. J. Snyder, P. Asanithi, A.B. Dalton, J. Erlebacher, "Stabilized nanoporous metals by dealloying ternary alloy precursors," *Advanced Materials* **20** (2008) 4883-4886.
6. R. Zeis, T. Lei, K. Sieradzki, J. Snyder, J. Erlebacher, "Catalytic reduction of oxygen and hydrogen peroxide by nanoporous gold," *J. Catalysis* **253** (2008) 132-138.
7. J. Erlebacher, J. Snyder, "Composite Nanoporous Metal/Ionic Liquid Catalysts", Provisional Application for Patent, #61299672, 2010.
8. J. Erlebacher, J. Snyder, "Porous Metal Catalysts for Oxygen Reduction," U.S. Patent Application No. 61/181,795, 2009.

## Monitoring the Rise of Surface Ethyl Intermediate of $C_2H_4 + H_2$ Catalysis over $Rh/Al_2O_3$ under Reaction Conditions by Step-Scan FT-IR Spectroscopy

Miao Zhang and Heinz Frei

Physical Biosciences Division, Lawrence Berkeley National Laboratory  
Berkeley, CA 94720  
e-mail: HMFrei@lbl.gov

The initial step of important heterogeneous catalytic reactions over noble metal catalysts such as ethylene hydrogenation to ethane or hydroformylation of ethylene to propionaldehyde is the reaction of weakly  $\pi$ -bonded  $C_2H_4$  with surface hydrogen to form surface ethyl species ( $C_2H_5Rh$ ). In our previous work, we have reported the direct observation of the surface ethyl by the rapid-scan FT-IR method under reaction conditions (time resolution  $\geq 20$  millisecond)[1]. The catalysis was initiated by an ethylene gas pulse released from a fast valve. While surface ethyl was detected and reaction of subsequent intermediates and final product temporally resolved, the growth of  $C_2H_5Rh$  is too fast for this method. Using step-scan FT-IR spectroscopy at 100 microsecond resolution, we have been able to monitor the rise of  $C_2H_5Rh$  on 2 nm Rh nanoparticles supported on  $Al_2O_3$  and found it to be essentially complete within 30 milliseconds (300 K, 1 atm). Interestingly, the spectroscopy revealed that growth occurs at early times at a few preferred Rh surface sites as indicated by the appearance of narrow bands in the 1170-1220  $cm^{-1}$  region. These ultimately merge into a broad absorption of the  $CH_2$  wagging mode centered at 1200  $cm^{-1}$ .

In order to monitor elementary steps of heterogeneous catalysis on the early microsecond time scale, we are developing a method that initiates catalysis with a nanosecond laser pulse for heating of the metal nanoparticle catalyst coupled with step-scan FTIR monitoring (capable of time resolution up to 10 nanosecond). The laser heating pulse generates hot electrons and lattice vibrations that may activate adsorbed reactants or intermediates. In order to maximize reactant surface coverage prior to arrival of the laser heating pulse, the latter is preceded by a gas pulse from a fast valve for reactant loading (two pulse method). Recent results with this method using hydrogenation of ethylene over supported  $Rh/Al_2O_3$  nanoparticles will be presented.

- [1] N. Sivasankar and H. Frei. Direct Observation of Kinetically Competent Surface Intermediates upon Ethylene Hydroformylation over  $Rh/Al_2O_3$  under Reaction Conditions by Time-Resolved FT-IR Spectroscopy. *J. Phys. Chem. C* **115**, 7545-7553 (2011).

## Molecular-scale Understanding of Selective Oxidative Transformations of Alcohols Promoted by Au and Au-based Alloys

Postdoctoral Associates: Dr. Derek Butcher

Graduate Students: Mr. Bingjun Xu, Ms. Cassandra Freyschlag, Mr. Joshua Klobas

Collaborators: Prof. Katharina Al-Shamery; Mr. Peter Clawin (Oldenburg University, Germany); Prof. Marcus Bäumer, Dr. Arne Wittstock, Dr. Volkmar Zielasek (Bremen University, Germany); Dr. Juergen Biener (Lawrence Livermore Laboratories); Prof. Hans-Joachim Freund, Prof. Robert Schloegl (Fritz Haber Institute, Berlin) Prof. Efthimios Kaxiras, Prof. Robert J. Madix (Harvard University); Prof. John Gleaves (Washington University)

Contacts: Harvard University, CCB, 12 Oxford St., Cambridge, MA 02138;  
E-mail: [cfriend@seas.harvard.edu](mailto:cfriend@seas.harvard.edu)

**Goal:** Develop a molecular-scale mechanistic framework for complex selective oxidation processes on gold and gold-based alloys as a means of understanding how to improve selectivity and activity of catalyst materials that can operate at low temperature by bridging model studies on extended gold surfaces and working gold catalysts.

**DOE Interest:** Heterogeneous catalysis is a key technology for securing our future because most major chemical syntheses rely on heterogeneous catalysis to control activity and selectivity. Fundamental understanding of reaction mechanisms is an important first step to designing new materials and processes for important catalytic reactions.

### Recent Progress:

We have combined theory and experiment to understand selective oxidation reactions on Au because of the intense recent interest in using gold to promote reactions with high selectivity and at low temperature. Our recent significant accomplishments (i) to bridge the gap between model surface chemistry investigations and a catalytic process at atmospheric pressure for selective oxidation of alcohols catalyzed by gold; (ii) to build on our understanding of the molecular-scale mechanisms for alcohol and olefin oxidation, to understand how to control selectivity for complex cross coupling reactions promoted by metallic gold; and, (iii) to discover and demonstrate new classes of reactions promoted by O-covered metallic Au that will motivate the study of new catalytic processes. We have made an unprecedented connection between our fundamental mechanism at low pressure and implementation under catalytic conditions (Figure 1).

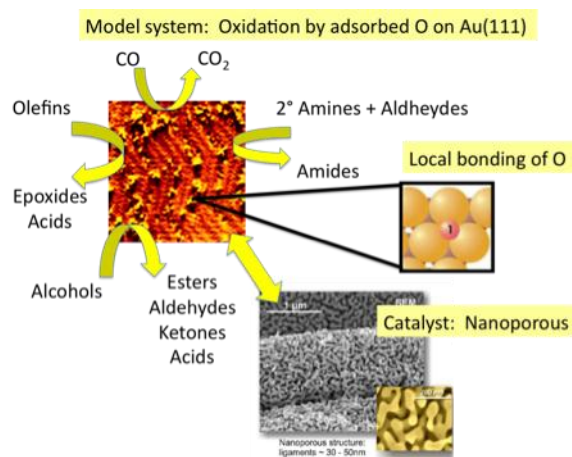


**Figure 1:** Schematic showing the reactions investigated and the bridge between model studies and a working catalyst (nanoporous Au). The local bonding of O was determined using a combination of density functional theory (DFT) and vibrational spectroscopy.

*Bridging model studies and catalytic processes: Selective oxidative coupling of alcohols over Au.* Recently, gold has also been intensely studied as a catalyst for key synthetic reactions. Gold is an attractive catalyst because it is highly active and very selective for partial oxidation processes suggesting promise for energy-efficient “green” chemistry. We established a direct parallel between model studies of methanol oxidation on O-covered Au(111) and a working catalyst, nanoporous Au.

Model studies show that atomic oxygen bound to metallic Au in 3-fold sites has high activity the oxidation of methanol. Our model studies showed that: (a) adsorbed O is required for O-H dissociation to form methoxy; (b) dissociation of the C-H bond to form formaldehyde occurs subsequently in the rds and can be promoted by adsorbed O, OH or another methoxy; (c) reaction between residual methoxy and formaldehyde to form  $\text{CH}_3\text{OC}(\text{H}_2)=\text{O}$  is essential barrierless and diffusion of these reactants on the surface is facile; and, (d) elimination of H yields methyl formate, the selective oxidation product.

In parallel studies of methanol oxidative coupling on nanoporous gold we achieved near 100% selectivity for methyl formate production using  $\text{O}_2$  as an oxidant and a total pressure of 1 atm (Figure 2). Selective oxidative coupling was promoted even at room temperature, although the conversion increases to ~60% at higher, yet moderate (~60 °C), temperature. The nanoporous Au retained its activity for at least 14 days. The trends in selectivity control as a function of  $\text{O}_2$  partial pressure are in agreement with our model studies—at higher concentrations of oxygen and at higher temperature, there is more combustion.

*Selectivity control of complex oxidative processes.* We have built on our understanding of the molecular-scale steps for for complex, selective olefin oxidation and alcohol oxidative coupling over oxygen-covered Au(111) to establish fundamental principles governing selectivity in complex systems. Recent focus has been on oxidative coupling of mixtures of alcohols and the selective oxidation of substituted olefins that contain allylic C-H bonds.

Controlling the selectivity towards production of specific esters in cross-coupling is a long-sought goal in designing efficient synthetic routes. Mixtures of different alcohols react efficiently on Au to produce esters that result from cross coupling. We identified two key factors that determine selectivity in the oxidative *cross-coupling* of alcohols on oxygen-covered Au(111). (1) The surface concentration of alkoxys is skewed toward the higher molecular weight alcohol in the mixture exposed to the surface due to displacement reactions. (2) The relative activation energies for  $\beta$ -H cleavage of alkoxys are:  $E_{\text{methoxy}} > E_{\text{ethoxy}} > E_{\text{butoxy}}$ . Accordingly, we achieved a selectivity of ~70% for methyl acetate from oxidation of a mixture of methanol and ethanol.

*Discovering new reactions via molecular-scale understanding.* A significant accomplishment of our work is the generalization to predict new synthetic pathways promoted by oxygen-covered Au. The general framework for reaction is that an electron deficient carbon in, e.g. a C=O bond in an aldehyde, can be attacked by an electron rich species, e.g an alkoxide. This paradigm led to predictions of new pathways for important reactions with the potential to be catalyzed by gold.

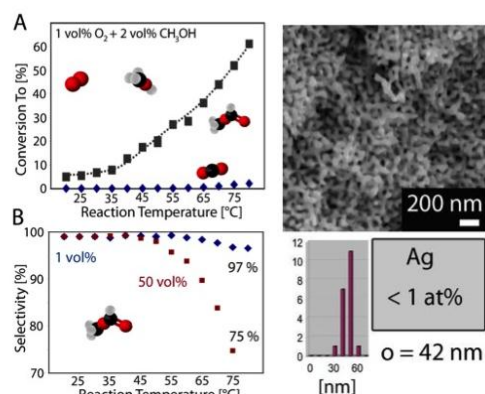


**Figure 2:** Selective oxidative coupling of methanol to yield methyl formate occurs (A) with nearly 100% selectivity near room temperature for a 1:2  $\text{O}_2$ : methanol mixture at atmospheric pressure; whereas (B) the selectivity is lower for higher (50% volume) of  $\text{O}_2$ . Nanoporous Au has ligaments (mainly 40-50 nm) shown on the right SEM image and it contains <1% Ag.

Two classes of reactions were predicted and experimentally confirmed in our lab: (1) the low-temperature activation of the N-H bond in secondary amines to yield  $R_2N_{(ads)}$  which attacks the C in formaldehyde when it is introduced to the surface affording the amide,  $R_2NC(H)=O$ ; and (2) carbonylation of methoxy to yield a stable surface intermediate,  $CH_3OC=O$ , that reacts with other electron rich species to form carbonylated products, e.g.  $CH_3O-C(=O)OCH_3$ . These examples illustrate the value of fundamental understanding of reaction mechanisms as a means of rationally predicting new classes of reactions. Carbonylation processes, in particular, are an important class of reactions to produce commodity chemicals as well as methylation agents used in chemical synthesis. This reaction has heretofore not been tested or reported in a gold catalyzed process. We plan to test nanoporous Au for activity for this process.

#### Future Work:

Our future work will focus on studies of planar Au-Ag, Au-Cu, and Au-Pd alloy surfaces. Our objective is to increase the rate of  $O_2$  dissociation via alloying and modification of surface structure. We will study oxidative processes, especially oxidation of alcohols, . In parallel, we will perform fundamental studies of nanoporous Au in vacuum in order to better understand the reactions that occur catalytically on this material.

#### Publications, 2010-2011

1. Bingjun Xu, Efthimios Kaxiras, Cynthia M. Friend, "Theoretical Study of O-assisted coupling of methanol on Au(111), *J. Phys. Chem. C*, **2011**, 115 (9) 3703-3708; DOI: 10.1021/jp110835w.
2. Thomas A. Baker, Xiaoying Liu, and C.M. Friend, "The Mystery Of Gold's Chemical Activity: Local Bonding, Morphology And Reactivity Of Atomic Oxygen", *Physical Chemistry-Chemical Physics* **2011**, 13, 34-46. (DOI: 10.1039/C0CP01514H).
3. Bingjun Xu, R.J. Madix, and C.M. Friend, "Achieving Optimum Selectivity in Oxygen Assisted Alcohol Cross-Coupling on Gold", *J. Am. Chem. Soc.* 2010, 132, 16571-16580. (DOI: 10.1021/ja106706v)
4. Xiaoying Liu, Thomas A. Baker, and C.M. Friend, "Effect of Molecular Structure on the Epoxidation of Allylic Olefins by Atomic Oxygen on Au." *Dalton Trans.* **2010**, 39 8521-8526, DOI: 10.1039/C0DT00047G.
5. Xiaoying Liu and C.M. Friend, "Selective Oxidation of Cyclohexanol and 2-Cyclohexen-1-ol on O/Au(111): The Effect of Molecular Structure", *Langmuir*, **2010**, 16552-16557. DOI: 10.1021/la1015302.
6. Baker, T.A.; Kaxiras, E.; Friend, C. M., "Insights from Theory on the Relationship Between Surface Reactivity and Gold Atom Release", *Topics in Catalysis*, 2010, 53 (5-6): 365-377.
7. X. Liu, C.M. Friend, "Competing Epoxidation and Allylic Hydrogen Activation: trans- $\beta$ -Methylstyrene Oxidation on Au(111)," *J. Phys. Chem. C*, 2010, 26(4) 2445-2451.
8. Wittstock, V. Zielasek, J. Biener, C. M. Friend, and M. Baeumer, "Nanoporous gold catalysts for selective gas-phase oxidative coupling of methanol at low temperature," *Science*, 2010, 327, 319-322.
9. B. Xu, L. Zhou, R. J. Madix, and C. M. Friend, "Highly selective acylation of dimethylamine mediated by oxygen atoms on metallic gold surfaces," *Angew. Chem. Int. Ed.*, 2010, 49, 394-398.
10. R. G. Quiller, X. Liu, and C. M. Friend, "Mechanistic insights into selectivity control for heterogeneous olefin oxidation: Styrene oxidation on Au(111)," *Chemistry—An Asian Journal*, 2010, 5, 78-86.
11. L. Zhou, C. G. Freyschlag, B. Xu, C. M. Friend, and R. J. Madix, "Direct selective oxygen-assisted acylation of amines driven by metallic silver surfaces: dimethylamine with formaldehyde" *Chem. Comm.* 2010, 46, 704-706.
12. T. A. Baker, C. M. Friend, and E. Kaxiras, "Local bonding effects in the oxidation of CO on oxygen-covered Au(111) from ab initio molecular dynamics simulations," *J. Chem. Theor. Comput.*, 2010, 6, 279-287.
13. B. Xu, X. Liu, J. Haubrich, and C. M. Friend, "Vapour-phase gold-surface-mediated coupling of aldehydes with methanol," *Nature Chem.*, 2010, 2, 61-65.



## Thermal and chemical stability of metal oxide/perovskite/metal nano-interfaces: An investigation of modeled ZnO/(La,Sr)CoO<sub>3</sub>/Pt nanowire based catalyst

P.X. Gao,<sup>1,\*</sup> W.J. Cai,<sup>1</sup> P. Shimpi,<sup>1</sup> H.Y. Chen,<sup>2</sup> J.M. Bai,<sup>2</sup> Q. Wang,<sup>2</sup> Y.B. Guo,<sup>1</sup> Z.H. Zhang,<sup>1</sup>  
H.Y. Gao,<sup>1</sup> S. Glod,<sup>1</sup> Z. Ren<sup>1</sup>

<sup>1</sup> Department of Chemical, Materials and Biomolecular Engineering & Institute of Materials Science, University of Connecticut, Storrs, CT 06269-3136

<sup>2</sup> Brookhaven National Laboratories, Upton, New York, 11973

\*E-mail: puxian.gao@ims.uconn.edu

Heterogeneous composite nanowire arrays, with semiconductor ZnO nanowire as the core and perovskite (La,Sr)CoO<sub>3</sub> (LSCO) mesoporous film as the shell, have been synthesized through a two-step fabrication process. The loading of dispersive Pt nanoparticles onto the composite nanowires enables a new type of mobile emission control catalysts. A systematic comparative study has been carried out on the chemical and physical thermal stability of these composite nanowires, upon subjected to ambient and reducing thermal aging at high temperature. An array of structure/morphology characterization (SEM, TEM, XRD, and XAS) and chemical and thermal analyses (TPR, TGA, and DSC) has been conducted for unraveling the interface structure variation and phase interactions before and after the thermal aging tests. ZnO nanowire arrays have been observed to degrade significantly in terms of physical morphology and orientation after thermal annealing at temperature up to 800 °C. On the contrary, much better thermal stability have been revealed in the mesoporous perovskite shelled ZnO nanowire arrays at temperature up to 1000 °C, possibly due to the strong oxide-perovskite interaction and ‘stabilizing’ effect from the LSCO nanoshell. Furthermore, the loaded Pt nanoparticles on ZnO/LSCO seemed to be more stable than those in ZnO/Pt nanowires at high temperature, which may be due to a bi-fold effect from physical blocking of mesoporous LSCO nanocrystals and strong LSCO/Pt perovskite/metal interaction. The mesoporous perovskite shelled nanowire composite strategy for stabilizing the chemical and physical structures of nanowire based catalysts could be of important implication on improving and expanding nanomaterials utilization in high temperature catalysis, fuel cell, and sensor applications.

**Abbreviation:** SEM: scanning electron microscopy; TEM: transmission electron microscopy; XAS: X-ray absorption spectroscopy; XRD: X-ray diffractometry; TPR: temperature-programmed reduction; TGA/DSC: thermo-gravimetric analysis/differential scanning calorimetry;

### References

1. D.L. Jian, P.X. Gao, W.J. Cai, B.S. Allimi, S.P. Alpay, Y. Ding, Z.L. Wang, C. Brooks, *J. Mater. Chem.*, **2009**, *19*, 970.
2. H.Y. Gao, W.J. Cai, P. Shimpi, H.-J. Lin, and P.X. Gao, *J. Phys. D: Appl. Phys.*, **2010**, *43*, 272002.
3. H.Y. Gao, M. Staruch, M. Jain, P.X. Gao, P. Shimpi, Y.B. Guo, W.J. Cai, and H.-J. Lin, *Appl. Phys. Letts*, **2011**, *98*, 123105.
4. W.J. Cai, P. Shimpi, H.Y. Gao, C. Brooks, P.X. Gao, *submitted*, **2011**.
5. P. Shimpi, C.C. Chung, P. Alpay, P.X. Gao, *submitted*, **2011**.

**TAILORING SUPPORTS AS LIGANDS: ZEOLITES AND OXIDES AS HOSTS OF  
MOLECULAR METAL-COMPLEX CATALYSTS**

PI: Bruce C. Gates

Students: Veronica Aguilar-Guerrero, Yalin Hao, Jing Lu, Isao Ogino, Jacob Wolf (all PhD students; Aguilar-Guerrero, Hao, and Ogino have finished) and Suppatra Khabuanchalad (working for a PhD at Suranaree University of Technology in Thailand). Collaborators include David Britt (University of California, Davis; Nigel Browning, University of California, Davis; C. Y. Chen (Chevron), and David Dixon (University of Alabama).

**Contact:** Bruce C. Gates: Department of Chemical Engineering and Materials Science, University of California, Davis, CA 95616, Phone: (530) 752-3953, Email: bcgates@ucdavis.edu

**Yearly budget:** \$560,000 for three years

**Period of execution:** 2/16/2009 to 6/1/11 (including continuing work from prior grant)

**Year started:** 2009

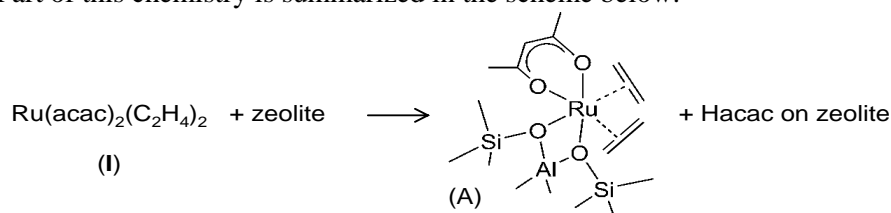
Understanding of the chemistry of oxide-supported metal complexes is hindered by the complexity of their structures, which is linked to the intrinsic non-uniformity of the support surfaces. But when the support is crystalline, the bonding sites may be essentially uniform and open up the opportunity for precise characterization of the supported species. Consequently we used a family of crystalline supports, zeolites, to make such species in one-step reactions of metal acetylacetonate (acac) compounds with the supports; these metal acac precursors are  $\text{Rh}(\text{C}_2\text{H}_4)_2(\text{acac})$ ,  $\text{Ir}(\text{C}_2\text{H}_4)_2(\text{acac})$ , and *cis*- $\text{Ru}(\text{acac})_2(\eta^2\text{-C}_2\text{H}_4)_2$ . Data obtained with these zeolite-supported metal complexes demonstrate how simultaneous characterization of well-defined supported species by complementary spectroscopic methods and theory can lead to detailed structural information about the ligand sphere of supported metal complexes and the genesis of catalytically active species.

When samples were made from *cis*- $\text{Ru}(\text{acac})_2(\eta^2\text{-C}_2\text{H}_4)_2$  and dealuminated zeolite HY, IR and EXAFS spectra indicated that when the ruthenium loading was 1.0 wt%, the surface species were mononuclear ruthenium complexes,  $\text{Ru}(\text{acac})(\text{C}_2\text{H}_4)_2^{2+}$ , bonded to the surface by two Ru–O bonds at  $\text{Al}^{3+}$  sites of the zeolite. A high degree of uniformity of the chemisorbed species was demonstrated by sharp bands in the  $\nu_{\text{CO}}$  IR spectrum characteristic of ruthenium dicarbonyls, formed by reaction of the complex with CO. In the presence of ethene and  $\text{H}_2$ , the surface-bound  $\text{Ru}(\text{acac})(\text{C}_2\text{H}_4)_2^{2+}$  entered into a catalytic cycle for ethene dimerization and operated stably. IR data show that at the start of the catalytic reaction an acac ligand of the  $\text{Ru}(\text{acac})(\text{C}_2\text{H}_4)_2^{2+}$  species was dissociated and captured by a zeolite  $\text{Al}^{3+}$  site. Catalytic ethene dimerization proceeded approximately 600 times faster with a co-feed of ethene and  $\text{H}_2$  than with just ethene. The data provide evidence of the importance of the cooperation of  $\text{Al}^{3+}$  sites in the zeolite and  $\text{H}_2$  in the feed for the genesis of the catalytically active species.

The maximum loading of the anchored ruthenium complexes was one per two  $\text{Al}^{3+}$  sites; at higher loadings, the excess *cis*- $\text{Ru}(\text{acac})_2(\text{C}_2\text{H}_4)_2$  was physisorbed. Investigation of supported samples with systematically varied ratios of chemisorbed to physisorbed species indicate that the catalytic ethene dimerization reaction proceeded much faster on the chemisorbed species than on the physisorbed species,

which had negligible activity under our conditions. IR and EXAFS data characterizing the supported samples indicate that (1) the Ru center in the chemisorbed species was more electropositive than that in the physisorbed species and (2) Ru–ethene bonds in the chemisorbed species were less symmetric than those in the physisorbed species, suggesting that ethene ligands in the chemisorbed species were in a configuration appropriate for dimerization. Transient IR spectra and Ru K edge XANES and EXAFS spectra characterizing the supported ruthenium complex were obtained with flow reactors as the complex was converted into a form that catalyzes ethene conversion to butene in the presence of H<sub>2</sub> (Fig 1). The formation of the catalytically active species resulted from the removal of acac ligands from the ruthenium (as shown by IR and EXAFS spectra) and the simultaneous decrease in the symmetry of the ruthenium complex, with ruthenium remaining mononuclear and the formal oxidation of the ruthenium remaining essentially unchanged. The removal of anionic acac ligands from the ruthenium was evidently compensated by the bonding of other anionic ligands—such as hydride formed from H<sub>2</sub> in the feed stream. Removal of the acac ligands must have led to coordinatively unsaturated ruthenium complexes, suggested to be Ru(H)(C<sub>2</sub>H<sub>4</sub>)<sub>2</sub><sup>+</sup>, which reacted with ethene, ultimately forming butene.

Part of this chemistry is summarized in the scheme below:



Thus, the data show that the zeolite plays multiple roles: (1) that of a ligand to anchor the electropositive ruthenium complex with uniform structure (A), (2) that of a ligand to activate ethene ligands in the chemisorbed species, and (3) that of a support to aid in the removal of acac ligands for genesis of the catalytically active species. The data demonstrate the unique value of dealuminated Y zeolite—and in prospect many other zeolites—as nearly uniform supports to allow precise synthesis of supported catalysts and detailed elucidation of structure and function.

Thus, these results open the door to a potentially large class of well-defined zeolite-supported metal complex catalysts that can be understood in a depth rivaling that of well-characterized molecular catalysts in solution, and results obtained with supported complexes of rhodium and of iridium on various zeolites bear out this expectation. The work has led to a general method for synthesis of supported metal complexes having a high degree of uniformity, whereby organometallic precursors incorporating acac ligands react with zeolites incorporating OH groups near Al sites. The method is illustrated by the reactions of Rh(acac)(CO)<sub>2</sub> and of *cis*-Ru(acac)<sub>2</sub>(η<sup>2</sup>-C<sub>2</sub>H<sub>4</sub>)<sub>2</sub> with zeolites slurried in *n*-pentane at room temperature. The zeolites used in addition to dealuminated HY were H-Beta, H-SSZ-42, H-Mordenite, and HZSM-5. IR and EXAFS spectra of the zeolites incorporating rhodium complexes indicate the formation of Rh(CO)<sub>2</sub><sup>+</sup> bonded near Al sites; similar results have been obtained for the formation of zeolite-supported Rh(η<sup>2</sup>-C<sub>2</sub>H<sub>4</sub>)<sub>2</sub> from Rh(acac)(η<sup>2</sup>-C<sub>2</sub>H<sub>4</sub>)<sub>2</sub>. IR spectra of the supported rhodium *gem*-dicarbonyls include sharp, well-resolved ν<sub>CO</sub> bands, demonstrating that the sites surrounding each metal complex are nearly equivalent. The frequencies of the ν<sub>CO</sub> bands show how the composition of the zeolite influences the bonding of the supported species, demonstrating subtle differences in the roles of the zeolite as ligands. When the zeolite has pore openings larger than the critical diameter of the precursor organometallic compound, the latter undergoes facile transport into the interior of the zeolite, so that a uniform distribution of the supported species results, but when the precursors barely fit through the zeolite apertures, the mass transport resistance is significant and the supported metal complexes are concentrated near the pore mouths.

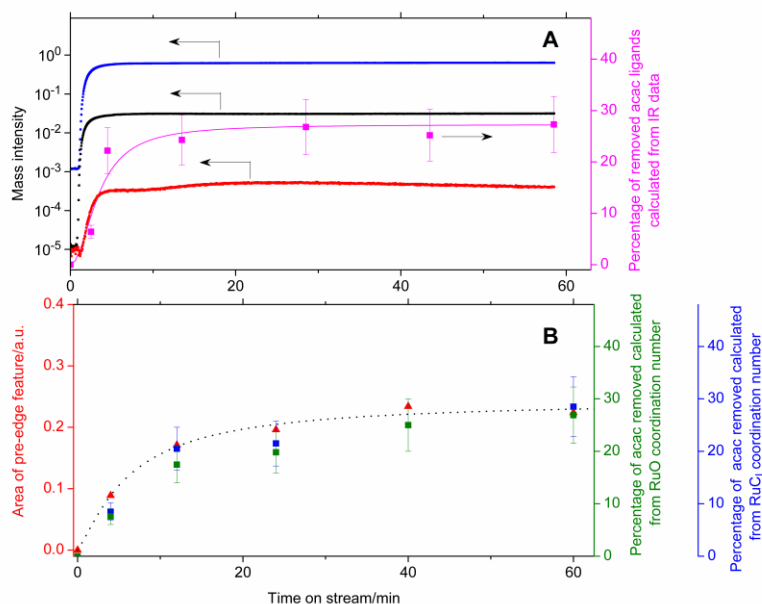
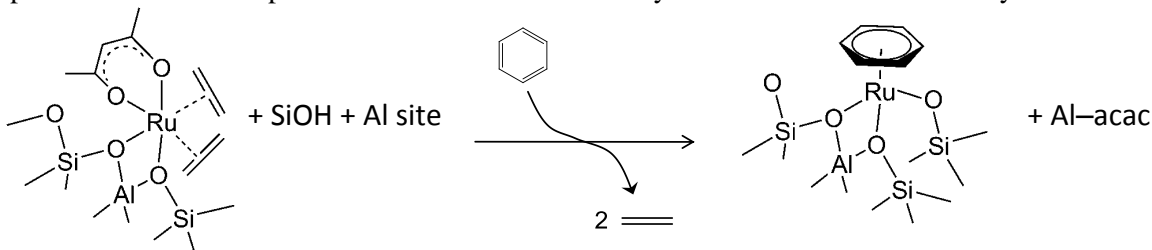


**Fig. 1.** Activation of zeolite-supported ruthenium complex catalyst for ethene dimerization reaction performed in an IR cell (A) and in an XAS cell (B). (A) Mass spectra characterizing effluent gas from the IR cell containing the sample (left ordinate-axis, C<sub>2</sub>H<sub>4</sub> ( $m/z = 26$ , C<sub>2</sub>H<sub>4</sub><sup>+</sup>, black), H<sub>2</sub> ( $m/z = 2$ , blue), and C<sub>4</sub>H<sub>8</sub> ( $m/z = 55$ , C<sub>4</sub>H<sub>7</sub><sup>+</sup>, red)), and approximate percentage of acac ligands removed from ruthenium in the supported sample determined from the deconvolution of IR spectra characterizing the supported sample. The reactant mixture entered the IR cell approximately 30 s after the start of the flow of reactant ethene + H<sub>2</sub>. (B) Change in peak area in the pre-edge region (red ▲); approximate percentage of acac ligands removed from ruthenium calculated from the decrease of the Ru–C<sub>1</sub> coordination number (blue ■); and percentage of acac ligands removed determined from decrease of the Ru–O coordination number (green ■) relative to value characterizing the initial supported sample in flowing helium. The time lags in the two systems differed by about 30 s, and therefore the time-on-stream axis of Figure 1B was shifted to align the starts of the changes. The IR cell contained a wafer of sample, whereas the XAS cell was a tubular reactor packed with catalyst and characterized by a different residence time distribution, which accounts for the different shapes of the curves in parts A and B.

Benzene reacted cleanly with the supported ruthenium complex that gave a structure with benzene  $\pi$ -bonded to the Ru center; calculations done by the group of David Dixon show good agreement between the predictions and the experimental results. The chemistry is summarized schematically below:



The essentially molecular ruthenium benzene complex anchored at the aluminum sites of dealuminated zeolite Y was formed by the reaction of the zeolite-supported mononuclear ruthenium complex, [Ru(acac)( $\eta^2$ -C<sub>2</sub>H<sub>4</sub>)<sub>2</sub>]<sup>+</sup>, with <sup>13</sup>C<sub>6</sub>H<sub>6</sub> at 413 K. IR, <sup>13</sup>C<sub>6</sub>H<sub>6</sub> NMR, and EXAFS spectra of the sample demonstrate replacement of two ethene ligands and one acac ligand in the original complex with one <sup>13</sup>C<sub>6</sub>H<sub>6</sub> ligand, with the formation of adsorbed protonated acac, Hacac. The EXAFS results indicate that the supported [Ru( $\eta^6$ -C<sub>6</sub>H<sub>6</sub>)]<sup>2+</sup> incorporates an oxygen atom of the support to balance the charge, being

bonded the zeolite via three Ru–O bonds. The supported ruthenium benzene complex is analogous to such complexes with polyoxometalate ligands, consistent with a high structural uniformity of the zeolite-supported species, which led to good agreement of the spectra with calculations at the level of density functional theory. The calculations show that the interaction of the zeolite with the Hacac formed on reaction of the original complex with  $^{13}\text{C}_6\text{H}_6$  drives the reaction forming the ruthenium benzene complex.

The zeolite H- $\beta$ -supported mononuclear rhodium diethene complex ( $\text{Rh}(\text{C}_2\text{H}_4)_2\{\text{O}_2\text{Al}\}$ ), where the braces indicate a part of the zeolite, was characterized in transient experiments with XANES and IR spectroscopies (combined with mass spectrometry of the effluent gas) while the sample was in contact with flowing CO. The data indicate a simple stoichiometric conversion of the supported metal complex into another species, identified by the spectra as the zeolite-supported rhodium *gem*-dicarbonyl ( $\text{Rh}(\text{CO})_2\{\text{O}_2\text{Al}\}$ ). The sharpness of the  $\nu_{\text{CO}}$  bands in the IR spectrum indicates a high degree of uniformity of the supported rhodium *gem*-dicarbonyl, and isosbestic points in the XANES spectra as the transformation was occurring imply that the rhodium diethene complex was also highly uniform. Spectra similarly show that treatment of the supported rhodium *gem*-dicarbonyl with flowing  $\text{C}_2\text{H}_4$  resulted in another stoichiometrically simple transformation, giving a species suggested to be  $\text{Rh}(\text{C}_2\text{H}_4)(\text{CO})_2\{\text{O}_2\text{Al}\}$ . The intermediate was ultimately transformed when the sample was purged with helium into another highly uniform supported species, inferred on the basis of IR spectra to be  $\text{Rh}(\text{C}_2\text{H}_4)(\text{CO})\{\text{O}_2\text{Al}\}$ . EXAFS spectra characterizing the supported rhodium diethene complex and the species formed from it show how the Rh–O bond distance at the Rh–support interface varied in response to the changes in the ligands bonded to the rhodium.

We also prepared structurally well-defined manganese complexes on high-area MgO powder by vapor deposition of  $\text{Mn}_2(\text{CO})_{10}$ . The supported species were treated under  $\text{O}_2$  at 673 K and evacuated at the same temperature and then characterized by infrared (IR), electron paramagnetic resonance (EPR), and X-ray absorption spectroscopies. The results show that when the manganese loading of the sample was 3.0 wt%, most of the  $\text{Mn}_2(\text{CO})_{10}$  was physisorbed, but when the loadings were less, chemisorbed species predominated, being formed by adsorption of  $\text{Mn}_2(\text{CO})_{10}$  with hydroxyl groups on the MgO surface. Treatment of samples containing 1.0 wt% Mn with  $\text{O}_2$  at room temperature resulted in oxidation of the manganese and the formation of surface species that are well represented as the  $d^4$  complex  $\text{Mn}(\text{CO})_3(\text{O}_s)_3$  (where  $\text{O}_s$  is surface oxygen of MgO), as indicated by IR and extended X-ray absorption fine structure (EXAFS) spectra. The EXAFS data show Mn–C, C $\equiv$ O, and Mn– $\text{O}_s$  bond lengths as 1.90, 1.43, and 1.98 Å, respectively.

Complexes of numerous transition metals catalyze C–C bond formation, and an enormous industrial production of oligomers and polymers from alkenes is carried out with complexes of early transition metals such as Cr, Ti, and Zr, some of them supported. Late transition metals such as Ni, Pd, or Rh also catalyze these reactions, typically relying on halides, which allow the metal to shuttle between oxidation states in the catalytic cycle. Active alkene oligomerization catalysts have also been prepared from complexes of late transition metals by incorporation of ligands such as those with neutral multidentate nitrogen-donor groups.

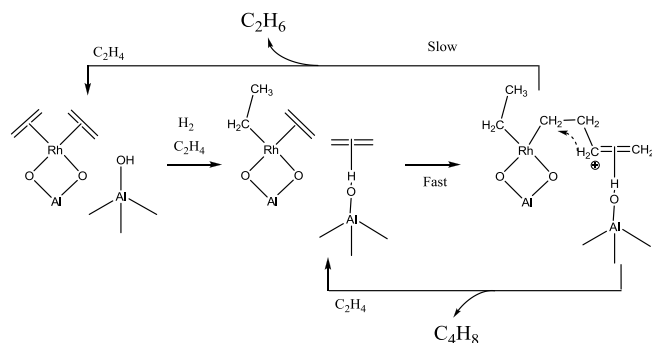
The formation of C–C bonds by dimerization of small alkenes such as ethene can take place on supported catalysts including reduced cobalt oxides, nickel oxides, and ruthenium clusters in the presence of  $\text{H}_2$ , provided that the ratio of the  $\text{H}_2$  to alkene partial pressures is low—but only with poor selectivities to *n*-butenes, typically <1% (the dominant reaction is hydrogenation of the C=C bond). We have shown that site-isolated rhodium complexes supported on dealuminated zeolite HY, prepared from  $\text{Rh}(\text{C}_2\text{H}_4)_2(\text{acac})$ , catalyze the dimerization of ethene in the absence of halides, with high selectivities to *n*-butenes (~75%) even when high partial pressures of  $\text{H}_2$  are employed ( $\text{H}_2/\text{C}_2\text{H}_4 = 4$ ). The selective performance of this catalyst for C–C bond formation in the absence of

labile ligands such as halides is a new and unanticipated result.

Characterization of the catalyst in the working state by IR and EXAFS spectroscopies (even during catalysis with flowing mixtures of  $C_2H_4 + H_2$  at 303 K and 1 bar) coupled with H/D exchange reaction experiments demonstrated that the catalysis involves a cooperation between mononuclear rhodium complexes and Brønsted acid sites of the zeolite support.  $H_2$  promotes the dimerization reaction, which is accompanied by a slower hydrogenation of the C=C bond, and we infer that the ethyl species expected to be intermediates in the hydrogenation reaction are not involved in the formation of the C–C bonds. Thus, the mode of action of the new dimerization catalyst differs both from that pertaining to halide-containing rhodium complexes and that pertaining to strongly Brønsted acidic solids.

The observation that site-isolated rhodium complexes supported on zeolite HY, initially present as  $Rh(C_2H_4)_2$ , catalyze the dimerization of ethene in a once-through plug-flow reactor at 1 bar and 303 K (with or without  $H_2$  in the feed—the reaction is faster with  $H_2$ ) is contrasted with our observation that the isostructural rhodium complexes supported on highly dehydroxylated MgO are 100% selective for hydrogenation of the C=C bond in the presence of  $H_2$  and inactive under our conditions when  $C_2H_4$  is used in the absence of  $H_2$ . The behavior of the MgO-supported catalyst agrees with reports demonstrating that Rh(I) species require the participation of ligands such as halides to catalyze the alkene oligomerization. For example,  $Rh(C_2H_4)_2(acac)$ , the precursor used to synthesize our zeolite- and MgO-supported catalysts, can be transformed into an active alkene dimerization catalyst by treatment with HCl.

On the basis of the catalytic data and IR and EXAFS spectra of the functioning catalysts, we propose a mechanism (Scheme 1) for the dimerization of ethene on the zeolite incorporating the rhodium complex. In this scheme, an ethene molecule weakly adsorbed on an Al–OH site of the zeolite (which is not reactive enough to couple with another ethene from the gas phase as occurs with stronger Brønsted acids) reacts with a second ethene molecule activated on a nearby rhodium site. To account for the observed high selectivity to butenes, we infer that the interaction between two adsorbed ethene molecules is faster than the hydrogenation of the C=C bond. The data indicate that the formation of the C–C bond, which is the rate determining step when the reaction is catalyzed by rhodium halide complexes and is quite slow on acidic zeolites, is facilitated by a cooperation between the Rh(I) species and the acid sites of the support. In contrast, the accumulation of relative large amounts of hydrocarbons on the surface of the catalyst during reaction (evidenced by intense IR bands in the range  $2960\text{--}2875\text{ cm}^{-1}$ , together with the observed deactivation of the catalyst over time, suggests that product desorption might be rate determining (notwithstanding the deactivation, more than 2000 turnovers of the catalyst were achieved in 5 h on stream, demonstrating that the reaction is catalytic). This observation, together with the fact that  $H_2$  accelerates the dimerization reaction (Table 2) without being incorporated into the product butenes, suggests that the role of hydrogen is to facilitate the regeneration of the active sites by accelerating the desorption of the products.



Scheme 1. Simplified reaction scheme for the conversion of ethene on a zeolite-supported rhodium complex catalyst in the presence of  $H_2$ . The reaction intermediates are proposed on the basis of IR and EXAFS data, results of  $H_2/D_2$  exchange experiments, and catalyst performance data.

To our knowledge, these results provide the first evidence of a cooperation between metal complexes and solid Brønsted acids in the formation of C–C bonds, giving the first evidence of the activity of the zeolite-supported rhodium complexes for alkene dimerization in the absence of halides, even with high selectivity to *n*-butenes in an excess of H<sub>2</sub>. The EXAFS and IR spectra and the results of the H/D exchange experiments indicate that the mode of action of the zeolite-supported rhodium complexes acting in concert with the adjacent acidic sites differs fundamentally from that observed for halide-containing rhodium complexes and strong Brønsted acids alone.

Other results are summarized in the publications listed below.

### **Publications: 2009 -2011**

- "CO Oxidation Catalyzed by Gold Supported on MgO: Spectroscopic Identification of Carbonate-like Species Bonded to Gold during Catalyst Deactivation," Y. Hao, M. Mihaylov, E. Ivanova, K. Hadjiivanov, H. Knözinger, and B. C. Gates, *Journal of Catalysis*, **261**, 137 (2009).
- "Genesis of a Cerium Oxide-Supported Gold Catalyst for CO Oxidation: Transformation of Mononuclear Gold Complexes into Clusters as Characterized by X-Ray Absorption Spectroscopy," V. Aguilar-Guerrero, R. J. Lobo-Lapidus, and B. C. Gates, *Journal of Physical Chemistry C*, **113**, 3259 (2009).
- "Activation of Dimethyl Gold Complexes on MgO for CO Oxidation: Removal of Methyl Ligands and Formation of Catalytically Active Gold Clusters," Y. Hao and B. C. Gates, *Journal of Catalysis*, **263**, 83 (2009).
- "Kinetics of CO Oxidation Catalyzed by Supported Gold: A Tabular Summary of the Literature," V. Aguilar-Guerrero and B. C. Gates, *Catalysis Letters*, **130**, 108 (2009).
- "Role of the Support in Catalysis: Activation of a Mononuclear Ruthenium Complex for Ethene Dimerization by Chemisorption on Dealuminated Zeolite Y," I. Ogino and B. C. Gates, *Chemistry—a European Journal*, **15**, 6827 (2009).
- "Imaging Gold Atoms in Site-isolated MgO-Supported Mononuclear Gold Complexes," A. Uzun, V. Ortalan, Y. Hao, N. D. Browning, and B. C. Gates, *Journal of Physical Chemistry C*, **113**, 16847 (2009).
- "Nanoclusters of Gold on a High-Area Support: Almost Uniform Nanoclusters Imaged by Scanning Transmission Electron Microscopy," A. Uzun, V. Ortalan, Y. Hao, N. D. Browning, and B. C. Gates, *ACS Nano*, **3**, 3691 (2009).
- "Transient Spectroscopic Characterization of the Genesis of a Ruthenium Complex Catalyst Supported on Zeolite Y," I. Ogino and B. C. Gates, *Journal of Physical Chemistry C*, **113**, 20036 (2009).
- "Reactions of Highly Uniform Zeolite H- $\beta$ -Supported Rhodium Complexes: Transient Characterization by Infrared and X-ray Absorption Spectroscopies," I. Ogino and B. C. Gates, *Journal of Physical Chemistry C*, **114**, 8405 (2010).
- "A Zeolite-Supported Molecular Ruthenium Complex with  $\eta^6$ -C<sub>6</sub>H<sub>6</sub> Ligands: Chemistry Elucidated by Using Spectroscopy and Density Functional Theory," I. Ogino, M. Chen, J. Dyer, P. W. Kletnieks, J. F. Haw, D. A. Dixon, and B. C. Gates, *Chemistry—a European Journal*, **16**, 7427 (2010).
- "Zeolite-supported metal complexes of rhodium and of ruthenium: a general synthesis method influenced by molecular sieving effects," I. Ogino, C.-Y. Chen, and B. C. Gates, *Dalton Transactions*, **39**, 8423 (2010).
- "Prototype Supported Metal Cluster Catalysts: Ir<sub>4</sub> and Ir<sub>6</sub>," A. Uzun, D. A. Dixon, and B. C. Gates, *ChemCatChem*, **3**, 95 (2011).
- "A Bifunctional Mechanism for Ethene Dimerization: Catalysis by Rhodium Complexes on Zeolite HY in the Absence of Halides," P. Serna and B. C. Gates, *Angewandte Chemie International Edition*, in press (on web).

**Supported Molecular Catalysts: Synthesis, in-situ Characterization and Performance**

**PIs:** James F. Haw (PI),<sup>1</sup> Bruce C. Gates, (Co-PI),<sup>2</sup> David A. Dixon (Co-PI)<sup>3</sup>

**Students:** A. J. Liang (graduate),<sup>2</sup> R. J. Lobo-Lapidus,<sup>2</sup> A. Uzun,<sup>2</sup> M. Chen (graduate),<sup>3</sup> J. Dyer (graduate),<sup>3</sup> T. Glenn Kelly (undergraduate),<sup>3</sup> Désirée Picone (undergraduate)<sup>3</sup>

University of Southern California,<sup>1</sup> University of California Davis,<sup>2</sup> The University of Alabama<sup>3</sup>

**Contact:** Bruce C. Gates: Department of Chemical Engineering and Materials Science, University of California, Davis, CA 95616, Phone: (530) 752-3953, Email: bcgates@ucdavis.edu

**Yearly budget:** \$300,000

**Period of execution:** 12/15/2007 to 12/14/10

**Year started:** 2004

**Overview**

The complexity of typical supported metal catalysts used in industry, incorporating clusters or particles of differing size and shape on nonuniform surfaces, hinders the development of fundamental understanding of how they work. To understand this class of catalysts better and to lay a foundation for the prediction of properties leading to improved catalyst designs, we strive to make supported metal catalysts with well-defined structures and to vary them systematically—not just the structures and compositions of the metal frames, but also the ligands bonded to the metals. The technological advantages of solid catalysts (robustness for operation at high temperatures, lack of corrosion, and ease of separation of products) can be combined with the advantages of soluble catalysts (e.g., selectivity) by the synthesis of structurally discrete, nearly uniform catalysts on supports. Our goal is to synthesize, characterize, test, and model such catalysts and their reactions, thereby opening a door to unprecedented fundamental understanding of the properties of such materials as well as providing a link between heterogeneous and homogeneous catalysis. We have employed molecular chemistry in nano-scale cages of zeolites and on surfaces of porous solids for the precise synthesis of catalysts with discrete, uniform, well-defined sites, primarily mononuclear metal complexes. We have characterized them (sometimes in the functioning state) with complementary experimental techniques including EXAFS, STEM, vibrational spectroscopy (including isotopic substitution), and NMR spectroscopy. We used computational chemistry to interpret the results, map out reaction paths, provide bases for the design of new catalysts, improve methods of data analysis, and identify key experiments.

**Selected research highlights**

A significant advance emerging from our collaborative research is the demonstration of how strongly spectroscopy, imaging, and theory/computation reinforce each other in the characterization of well-defined samples. We have used computational chemistry approaches to characterize the structures described above, including the zeolite-supported  $\text{Rh}(\text{C}_2\text{H}_4)_2$  complexes. Besides facile, reversible ligand exchange reactions, this complex reacted to form  $\text{C}_2\text{H}_5$  ligands and ethane by reverse spillover of hydrogen from support hydroxyl groups. The combined experimental and computational results provide clear evidence of a new rhodium monohydride species incorporating a CO ligand or possibly a  $\text{C}_2\text{H}_4$  ligand. The use of isotopic labeling in combination with DFT electronic structure calculations of the



frequencies was critical to analyzing the experimental spectra and the observation of new intermediates. The combination of all the results provides a detailed picture of catalytic intermediates on the surface and unique insights into the behavior of such site-isolated catalysts. LBDEs characteristic of the model acidic site of zeolite-supported metal complexes  $LL'M\text{-Al(OH)}_4$  were calculated for  $M = \text{Ir, Rh, and Co}$ , and  $L =$  combinations of  $\text{C}_2\text{H}_2, \text{C}_2\text{H}_4, \text{C}_2\text{H}_5, \text{CO, H, H}_2, \text{ and N}_2$ . These results show that the Ir complexes gain more stability than the Rh or Co complexes by incorporation of a second ligand. The average LDEs for the first ligand dissociation exhibit the trend  $\text{Ir} > \text{Rh} > \text{Co}$ .

A Ru-benzene complex anchored at the acidic aluminum sites of the zeolite was formed by the reaction of  $\text{C}_6\text{H}_6$  (or  $^{13}\text{C}_6\text{H}_6$ ) with the supported Ru complex  $[\text{Ru}(\text{acac})(\eta^2\text{-C}_2\text{H}_4)_2]^+$ .

IR,  $^{13}\text{C}$  NMR, and EXAFS spectra of the sample demonstrate replacement of two ethylene ligands and one acac ligand in the original complex with one  $^{13}\text{C}_6\text{H}_6$  ligand. EXAFS results indicate that the supported  $[\text{Ru}(\eta^6\text{-C}_6\text{H}_6)]^{2+}$  incorporates an anionic oxygen atom from a silanol group in the complex that is not directly bonded to the Al sites, providing a -1 formal charge, which balances the  $\text{Ru}^{+2}$  charge, corresponding to three Ru–O bonds to the zeolite. The average calculated chemical shifts characterizing the  $\text{C}_6\text{H}_6$  in our complexes range from 84 to 86 ppm, enabling assignment of the observed 93-ppm resonance to a benzene molecule bonded to Ru at the acid site. The LBDEs for the set of ligands given above (for the Ir, Rh, Co complexes) bonded to Ru were calculated for both the neutral complex (Ru(II)) and a cationic complex in which the +2 charge is not balanced by an additional anionic oxygen of the zeolite. These calculations have been extended to  $\text{Os}^{2+}$ . To better understand the actual reaction process, we calculated the energetics of a variety of reactions and showed that the inclusion of entropy terms and the interaction of the Hacac with the zeolite are sufficient to provide the energy needed for the displacement reaction to proceed. This investigation is one of the most thorough characterizing the reactivity of a site-isolated surface metal site.

We have calculated the binding of all singly charged metal ions in models of the acidic site of a zeolite at the CCSD(T)/CBS (complete basis set) level. There is a significant decrease in the binding energy of the high-spin metal ion  $\text{Tc}^+$  for the second row transition metals. As the metal ion spin decreases after  $\text{Tc}^+$  (filling up the d shell), the M–O bond distance decreases and the binding energy increases. This work provides the first reliable metal ion binding scale for transition metal ions in zeolites. These calculations opened the way to calculations of the activation of  $\text{CH}_4$  on  $\text{MO}^{2+}$  for  $M = \text{V, Cr, Mn, Nb, Mo, Tc, Ta, W, and Re}$  substituted in a model of the acid site of a zeolite at the B3LYP and CCSD(T) levels. The barriers are all substantially less than the C–H bond energy in  $\text{CH}_4$ , increase with increasing atomic number in a row, and decrease with increasing atomic number in a column. The lowest predicted barrier is for  $M = \text{Ta}$

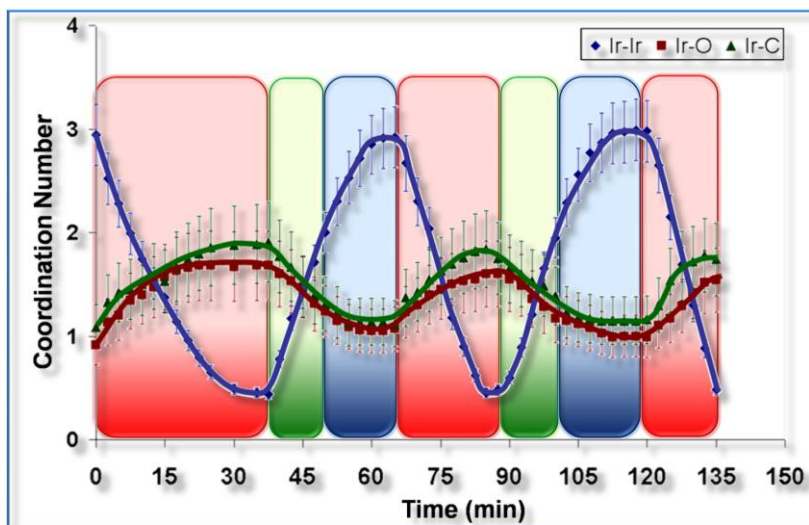


Fig. 1. EXAFS analysis characterizing changes in the coordination numbers of a working catalyst formed from  $\text{Ir}(\text{C}_2\text{H}_4)_2(\text{acac})$  and dealuminated zeolite Y showing the conversion of clusters approximated as  $\text{Ir}_4$  to predominantly mononuclear iridium complexes, following a step-change in the feed to the flow reactor/EXAFS cell from  $\text{H}_2$  to a mixture with  $\text{C}_2\text{H}_4:\text{H}_2 = 4$  (molar, indicated with a red background). After 35 min, the feed composition was switched to equimolar  $\text{C}_2\text{H}_4 + \text{H}_2$  (indicated with a green background). Later the feed ratio was switched to  $\text{C}_2\text{H}_4:\text{H}_2 = 0.3$  (molar, indicated with a dark blue background). Subsequent changes are indicated by the color coding.

and is only 12 kcal/mol. These results show that C–H bond activation is possible with low barriers on such complexes and suggest new experiments to test the predictions.

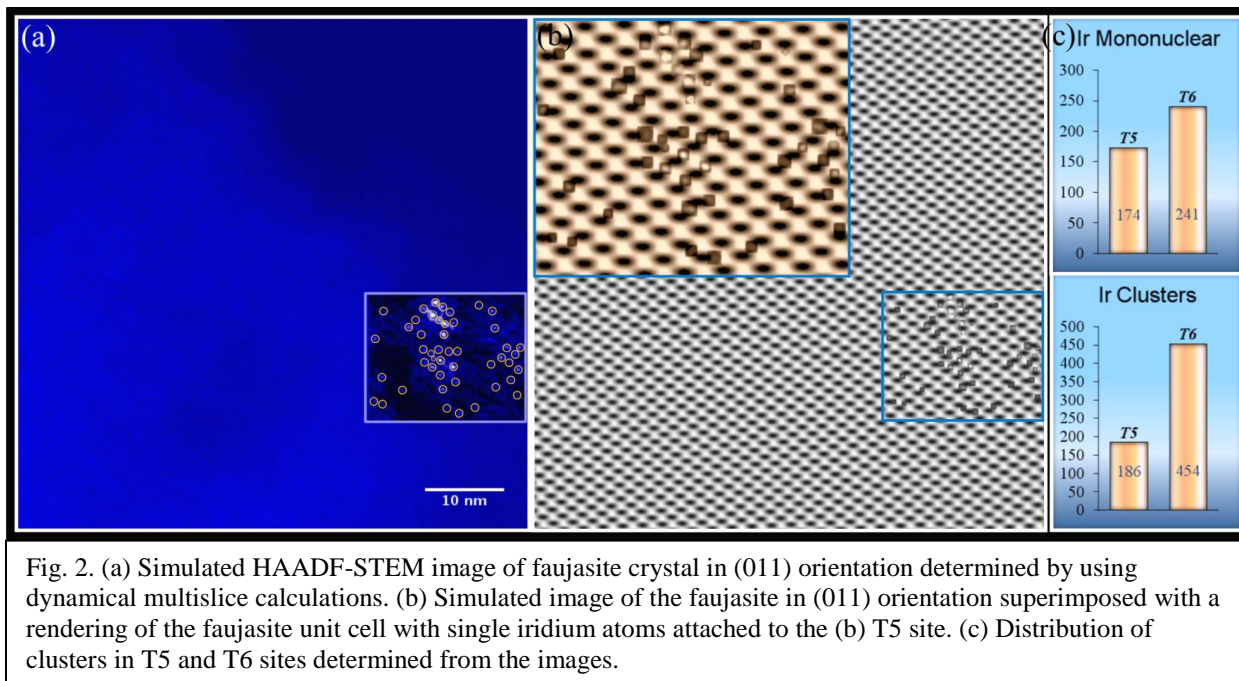
Extending the research to metal clusters on supports, we investigated  $\text{Ir}(\text{C}_2\text{H}_4)_2$  complexes bonded to the zeolite (via two Ir–O bonds) as they were converted into tetrairidium clusters in the presence of  $\text{H}_2$ . There was no evidence of intermediates in the conversions, leading to the hypothesis that they were converted rapidly as mononuclear iridium fragments migrated facilely on the zeolite surface. Cluster formation was reversible and was followed in real time by transient XANES, EXAFS, and IR spectroscopies. The sharp isosbestic points in the XANES spectra as the cluster formed indicated that the clusters were unique, and the EXAFS Ir–Ir coordination number of nearly 3 indicated that they were  $\text{Ir}_4$  (these clusters have stable tetrahedral metal frameworks). The process was cleanly reversed by treatment of the supported clusters in ethylene. The results indicate that the ratio of clusters to mononuclear Ir complexes in the zeolite was determined by the ratio of ethylene to  $\text{H}_2$  partial pressures. Thus, the data implied that we could tune the structure of the catalyst at the molecular level by control of this ratio. Our transient XANES, EXAFS, and IR spectra demonstrated this tuning capability.<sup>Error! Bookmark not defined.</sup> By varying the ratio of ethylene to  $\text{H}_2$  in the feed stream to a flow reactor that was either an EXAFS or an IR cell, we demonstrated that this ratio determined the proportion of the catalyst that was in the form of mononuclear species and clusters during ethylene hydrogenation catalysis (Fig. 1). For more complex catalysts and reactions, these results point to new approaches to tuning catalyst structure and performance. To the best of our knowledge, this is the *first example of the tuning of the structure of a solid catalyst at the molecular level using a reactive environment*.

By extending the development of STEM techniques to characterize supported metal catalysts by using low-dose imaging with aberration correction (and handling the samples with rigorous air-exclusion methods), we imaged isolated Ir atoms and clusters approximated as  $\text{Ir}_4$  within the pores of dealuminated Y zeolite (Fig. 2). These are the *first images of metal atoms and metal clusters within the interior pore structure of a zeolite*; the methods allowed us to overcome the inherent difficulties of using TEM to characterize zeolites, which are highly susceptible to beam damage.

These results demonstrate the value of state-of-the-art STEM (done at ORNL) used in concert with state-of-the-art transient XANES and EXAFS spectroscopies (determined at the MRCAT beamline at the APS). In addition, they demonstrate the importance of simplicity in structure for the precisely synthesized supported catalysts (essentially molecular in nature), allowing precise determination of the structure and chemistry and rigorous application of theory in concert with spectroscopy. We propose to use these techniques to characterize more complex (but still nearly uniform) structures in the next phase of the research.

Similarly, the mononuclear Rh complexes described above, incorporating two ethylene ligands and anchored to dealuminated zeolite Y by two Rh–O bonds, were characterized by transient EXAFS spectroscopy and IR spectroscopy as they were converted into clusters in the presence of  $\text{H}_2$ . EXAFS spectra indicate reduction of the Rh in the complex at 298 K to form Rh clusters less than 3 Å in average diameter. Contacting the resultant clusters with  $\text{C}_2\text{H}_4$  led to their oxidative fragmentation, and the process was reversible. In these aspects, the results match those mentioned above for Ir. But when the  $\text{H}_2$  treatment was carried out at a higher temperature (373 K), larger clusters formed, but they were nonuniform. The reduction and oxidation of the rhodium were confirmed by XANES spectra. During the ethylene treatments, ethyl groups formed on the Rh, as indicated by IR spectra; treatment in  $\text{H}_2$  led to hydrogenation of these groups to form ethane, and the ethyl groups are inferred to be intermediates in the catalytic hydrogenation of ethylene. Ethylene in the gas phase helps stabilize rhodium in the form of mononuclear complexes on the zeolite during catalysis, hindering the cluster formation. In summary, *the Rh chemistry is similar to that described above for Ir in the same zeolite, but it was not as simple and well defined as the Ir chemistry; the uniqueness of Ir for*

the investigation of cluster formation may be related to the high stability of the tetrairidium framework.



Clusters of the oxophilic metal Re, which are resistant to reduction to form zerovalent metal clusters, also present unique opportunities for investigation of the catalytic properties of small supported metal clusters at much higher temperatures than supported clusters such as Ir<sub>4</sub> will tolerate without aggregating. We investigated cationic Re clusters as catalysts for *n*-butane hydrogenolysis at 533 K. The samples incorporated clusters of similar average size, approximated as Re<sub>3</sub> (indicated by EXAFS data), but having Re in significantly different average oxidation states, as indicated by the XANES edge positions. Re<sub>3</sub> clusters with Re in the lower oxidation state were more active than clusters with Re in the higher oxidation state. We also investigated larger clusters (approximately Re<sub>10</sub>, on average, as determined by EXAFS spectroscopy) having Re in essentially the same oxidation state as in the Re<sub>3</sub> clusters in one of the aforementioned samples. The data show that the catalytic activity for *n*-butane hydrogenolysis increased with increasing cluster size. Thus, both cluster size and metal oxidation state are important in catalysis, and these are *the first data to allow clear resolution of the separate effects of cluster size and metal oxidation state in catalysis by supported metal clusters.*

Similarly, samples made from H<sub>3</sub>Re<sub>3</sub>(CO)<sub>12</sub> were tested as catalysts for conversion of methylcyclohexane in the presence of H<sub>2</sub> at 773 K. The catalyst was active for dehydrogenation, isomerization, ring opening, and hydrocracking; the catalytically active species were inferred on the basis of EXAFS data to be Re<sub>3</sub>; *the stability of the small supported oxophilic metal clusters could portend the more widespread application of such materials as catalysts.*

We also used Re carbonyl clusters as probe molecules to help elucidate the surface chemistry of TiO<sub>2</sub>. Anatase-phase TiO<sub>2</sub> was treated under vacuum to create Ti<sup>3+</sup> surface-defect sites and surface O<sup>-</sup> and O<sup>2-</sup> species (indicated by EPR spectra), accompanied by the disappearance of bridging surface OH groups and the formation of terminal Ti<sup>3+</sup>-OH groups (indicated by IR spectra). EPR spectra showed that the probe molecule H<sub>3</sub>Re<sub>3</sub>(CO)<sub>12</sub> reacted preferentially with the Ti<sup>3+</sup> sites, forming Ti<sup>4+</sup> sites with OH groups as the H<sub>3</sub>Re<sub>3</sub>(CO)<sub>12</sub> was adsorbed. EXAFS spectra showed that these clusters were deprotonated upon

adsorption, with the triangular metal frame remaining intact; EPR spectra demonstrated the simultaneous removal of surface O<sup>-</sup> and O<sup>2-</sup> species. The data determined by the three complementary techniques form the basis of a schematic representation of the surface chemistry. According to this picture, during evacuation at 773 K, defect sites are formed on hydroxylated titania as a bridging OH group is removed, forming two neighboring Ti<sup>3+</sup> sites, or, when a Ti<sup>4+</sup>-O bond is cleaved, forming a Ti<sup>3+</sup> site and an O<sup>-</sup> species, with the Ti<sup>4+</sup>-OH group being converted into a Ti<sup>3+</sup>-OH group. When H<sub>3</sub>Re<sub>3</sub>(CO)<sub>12</sub> is adsorbed on a titania surface with Ti<sup>3+</sup> defect sites, it reacts preferentially with these sites, becoming deprotonated, removing most of the oxygen radicals, and healing the defect sites. *The value of metal cluster carbonyls as surface probes is associated with the rich structural information that results from their characterization by IR and EXAFS spectroscopies.*

Extending the work on clusters formed from Rh complex precursors into new territory, we collaborated with Randall Meyer and Mike Trenary (University of Illinois-Chicago), who use planar surfaces as supports. The Al<sub>2</sub>O<sub>3</sub>/Ni<sub>3</sub>Al(111) surface was used as a template for the nucleation and growth of Rh clusters from the precursor Rh(CO)<sub>2</sub>(acac). When the complex was deposited on Al<sub>2</sub>O<sub>3</sub>/Ni<sub>3</sub>Al(111) from the gas phase, it was observed to bind preferentially to specific sites associated with the film superstructure and appeared to be stable at temperatures up to 473 K, at which point some sintering and aggregation processes began. Annealing the sample to 673 K resulted in further sintering of the metal as well as an apparent loss in the surface coverage by rhodium species, possibly as a consequence of a combination of desorption and deligation. After annealing of the sample to 873 K, the coverage by Rh species decreased by about 50% with respect to the initial coverage. Our results suggest that using a more bulky organometallic precursor to form deposited metal particles on oxide substrates may result in increased resistance to sintering processes. This work is just a first step, but it may be regarded as *significant in beginning to bridge our approach with high-area supports such as zeolites and the classical surface-science approach with planar supports.*

To understand the functionality of nanostructures, it is desirable to examine individual nanostructures by observation of every atom in its 3D location with chemical sensitivity. By working with supported bimetallic clusters that are extremely small, we have shown how aberration-corrected STEM can be used to identify the individual atoms, map the full nanocluster structure in three dimensions with atomic resolution, and observe the rearrangements of the atoms under the influence of the electron beam. We determined the structure of supported Rh-Ir clusters dispersed on the surface of porous MgO at atomic scale in three dimensions in images recorded sequentially by using an aberration-corrected STEM, coupled with full dynamical multi-slice image simulations.

We have written an invited review of the chemistry of supported metal clusters as a Feature Article in *Chemical Communications*. We have also been exploring the chemistry of the lanthanide metals relevant to the design of new catalysts for C-H bond activation.

### **Publications resulting from the project in the preceding 2 years**

1. "Zeolite-Supported Organorhodium Fragments: Essentially Molecular Surface Chemistry Elucidated with Spectroscopy and Theory," A. J. Liang, R. Craciun, M. Chen, T. G. Kelly, P. W. Kletnieks, J. F. Haw, D. A. Dixon, and B. C. Gates, *J. Am. Chem. Soc.*, **2009**, *131*, 8460-8473.
2. "Dynamic Structural Changes in a Zeolite-Supported Iridium Catalyst for Ethene Hydrogenation," A. Uzun and B. C. Gates, *J. Am. Chem. Soc.*, **2009**, *131*, 15887-15894.
3. "Rhenium Complexes and Clusters Supported on  $\gamma$ -Al<sub>2</sub>O<sub>3</sub>: Effects of Rhenium Oxidation State and Nuclearity on Catalytic Activity for Conversion of *n*-Butane," R. J. Lobo-Lapidus and B. C. Gates, *J. Catal.*, **2009**, *268*, 89-99.

4. Transient Spectroscopic Characterization of the Genesis of a Ruthenium Complex Catalyst Supported on Zeolite Y Isao Ogino and Bruce C. Gates *J. Phys. Chem. C*, **2009**, *113*, 20036–20043
5. "A Site-Isolated Mononuclear Iridium Complex Catalyst Supported on MgO: Characterization by Spectroscopy and Aberration-Corrected Scanning Transmission Electron Microscopy," A. Uzun, V. Ortalan, N. D. Browning, and B. C. Gates, *J. Catal.*, **2010**, *269*, 318-328.
6. "Atomic-Scale Direct Imaging of Single Metal Atoms and Metal Clusters in the Pores of Dealuminated HY Zeolite," V. Ortalan, A. Uzun, B. C. Gates, and N. D. Browning, *Nature Nanotech.*, **2010**, *5*, 506-510. (highlighted in *C&EN* and *Nature Chem*)
7. "A Zeolite-Supported Molecular Ruthenium Complex with  $\eta^6$ -C<sub>6</sub>H<sub>6</sub> Ligands: Chemistry Elucidated with Spectroscopy and Density Functional Theory," I. Ogino, M. Chen, J. Dyer, P. W. Kletnieks, J. F. Haw, D. A. Dixon, and B. C. Gates, *Chem. Eur. J.*, **2010**, *16*, 7427-7436. (cover)
8. "Adsorption and Reaction of Rh(CO)<sub>2</sub>(acac) on Al<sub>2</sub>O<sub>3</sub>/Ni<sub>3</sub>Al(111)," Y. Lei, A. Uhl, J. Liu, C. Becker, K. Wandelt, B. C. Gates, R. Meyer, and M. Trenary, *Phys. Chem. Chem. Phys.*, **2010**, *12*, 1264-1275.
9. A. Kulkarni, R. J. Lobo-Lapidus, and B. C. Gates, "Metal Clusters on Supports: Synthesis, Structure, Reactivity, and Catalytic Properties," *Chem. Commun.*, **2010**, *46*, 5997-6015. (invited Feature Article).
10. "Towards full-structure determination of bimetallic nanoparticles with an aberration-corrected electron microscope," V. Ortalan, A. Uzun, B. C. Gates, and N. D. Browning *Nature Nanotech.* **2010**, *5*, 843-847
11. "Prototype Supported Metal Cluster Catalysts: Ir<sub>4</sub> and Ir<sub>6</sub>," A. Uzun, D. A. Dixon, and B. C. Gates, *ChemCatChem*, **2011**, *3*, 95-107
12. "Matrix Infrared Spectroscopic and Computational Investigations of the Lanthanide Metal Atom-Methylene Fluoride Activation Products CH<sub>2</sub>LnF<sub>2</sub>," X. Wang, H-G. Cho, L. Andrews, M. Chen, D.A. Dixon, H.-S. Hu, and J. Li, *J. Phys. Chem. A*, **2011**, *115*, 1913-1921
13. "Matrix Infrared Spectroscopic and Electronic Structure Investigations of the Lanthanide Metal Atom-Methyl Fluoride Reaction Products CH<sub>3</sub>-LnF and CH<sub>2</sub>-LnHF. The Formation of Single Carbon-Lanthanide Metal Bonds," M. Chen, D. A. Dixon, X. Wang, H.-G. Cho, and L. Andrews *J. Phys. Chem. A*, **2011**, *115*, 5609–5624.

**Molecular-level Design of Heterogeneous Chiral Catalysts**

PI: Andrew J. Gellman (Carnegie Mellon University)

Additional PIs: Davis S. Sholl (Georgia Tech)  
Wilfred T. Tysoe (U. of Wisconsin – Madison)  
Francisco Zaera (U. of California – Riverside)

Post-docs: Luke Burkholder (U. of Wisconsin – Madison)  
Yun Bai (U. of Wisconsin – Madison)  
Ilkeun Lee (U. of California – Riverside)  
Karakalos Stavros-Georgios (U. of California – Riverside)  
Xuerong Shi (Georgia Tech)

Grad Students: Zhenjun Li (U. of Wisconsin – Madison)  
Michael Garvey (U. of Wisconsin – Madison)  
Mausumi Mahapatra (U. of Wisconsin – Madison)  
Anibal Boscoboinik (Graduate Student)  
Xin Yang (U. of California – Riverside)  
Xiao Xiao (U. of California – Riverside)  
Junghyun Hong (Visiting Scholar)  
Brian Holsclaw (Carnegie Mellon University)  
Bharat Mahtre (Carnegie Mellon University)  
Yongju Yun (Carnegie Mellon University)  
Vladimir Pushkarev (Carnegie Mellon University, Graduated 2010)  
Wai-Yeng Cheong (Carnegie Mellon University, Graduated 2010)

Visiting Scholar: Junghyun Hong (U. of California – Riverside)

Collaborators: Prof. Giorgio Zgrablich (National University of San Luis, Argentina)  
Michael Weinert (Department of Physics, UW-Milwaukee)

Contact Info: Andrew J. Gellman, Department of Chemical Engineering, Carnegie Mellon University, 5000 Forbes Ave., Pittsburgh, PA 15213, [gellman@cmu.edu](mailto:gellman@cmu.edu)  
David S. Sholl, School of Chemical & Biomolecular Engineering, Georgia Tech, 311 Ferst Drive, N.W., Atlanta, GA 30332-0100, [David.Sholl@chbe.gatech.edu](mailto:David.Sholl@chbe.gatech.edu)  
Wilfred Tysoe, Department of Chemistry, University of Wisconsin-Milwaukee, 3210 N. Cramer Street, Milwaukee, WI 53211, [wtt@uwm.edu](mailto:wtt@uwm.edu)  
Francisco Zaera, Department of Chemistry, University of California at Riverside, 501 Big Springs Road, Chemical Sciences #146 Riverside, CA 92521, [francisco.zaera@ucr.edu](mailto:francisco.zaera@ucr.edu)

## Goal

Understanding and controlling selectivity is one of the key challenges in heterogeneous catalysis. Among problems in catalytic selectivity enantioselectivity is perhaps the most the most challenging. The primary goal of the project on “Molecular-level Design of Heterogeneous Chiral Catalysts” is to understand the origins of enantioselectivity on chiral heterogeneous surfaces and catalysts. The efforts of the project team include preparation of chiral surfaces, characterization of chiral surfaces, experimental detection of enantioselectivity on chiral surfaces and computational modeling of the interactions of chiral probe molecules with chiral surfaces.

## DOE Interest

Controlling selectivity in catalysis is one of the key challenges to improving the efficiency of many chemical transformation processes conducted on an enormous scale. It is also critical to reducing waste streams generated by these processes and thus, to minimizing the environmental impact of catalytic chemical transformations. The development of highly selective catalysts requires an understanding of the catalyst characteristics and the reaction parameters that determine selectivity. Catalyst selectivity is determined by the influence of catalyst surface structure and adsorbate-adsorbate interactions that influence the energetics of competing elementary reaction pathways. The ongoing effort on “Molecular-level Design of Heterogeneous Chiral Catalysts” addresses the most challenging form of catalytic selectivity. It has made significant strides in understanding the origins of enantioselectivity and in the design of enantioselective catalytic materials; accomplishments that will have broad impact on the development of highly selective catalysts for various processes.

## Recent Progress

### One-to-one chiral surfaces

**NEA on Pd(111).** 2-Butanol and methyl lactate adsorb enantioselectively on a Pd(111) surface modified by NEA. In addition, NEA-modified surfaces enantioselectively hydrogenate methyl pyruvate to methyl lactate. The distribution and structure of NEA on Pd(111) surfaces has been determined using STM. Molecular-resolution images of NEA molecules were obtained at low coverages and temperatures (Figure 1), and are imaged as a dim elongated part with a smaller, but brighter, protrusion adjacent to it. Two conformations were found for the NEA molecules differing in the position of the small-bright part with respect to the long axis of the molecule and two distinct image shapes that are assigned to an *endo* and *exo* conformer.

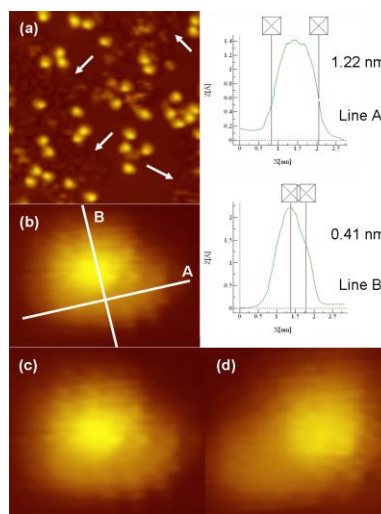


Figure 1. 20 nm  $\times$  20 nm STM image of NEA on Pd(111) at low coverage (relative coverage  $\theta = 0.057$  ML) taken at 100 K. The line profiles along the white lines are shown on the right and correspond to a molecule along its long axis (top) and perpendicular to it (bottom). Imaging conditions:  $V_b = -101$  mV; current set point  $I_t = 19.3$  pA.

**Cinchonidine on silica.** A synthetic effort has been initiated to tether cinchona alkaloid modifiers to high-surface-area silica supports, with the ultimate goal of combining them with Pt nanoparticles to obtain the same enantioselective behavior as when the cinchona is used as a chiral modifier in solution. Cinchonidine was tethered to a xero-gel silica substrate in order to create a new solid chiral catalyst. Two synthetic routes were explored for this grafting, relying on the use of an intermediate linker and so-called "click" chemistry (Figure 2). The activity of the supported cinchonidine proved comparable to that of the free molecule, but tethering does lead to a significant loss in enantioselectivity. The reasons for this impact on enantioselectivity are being explored.

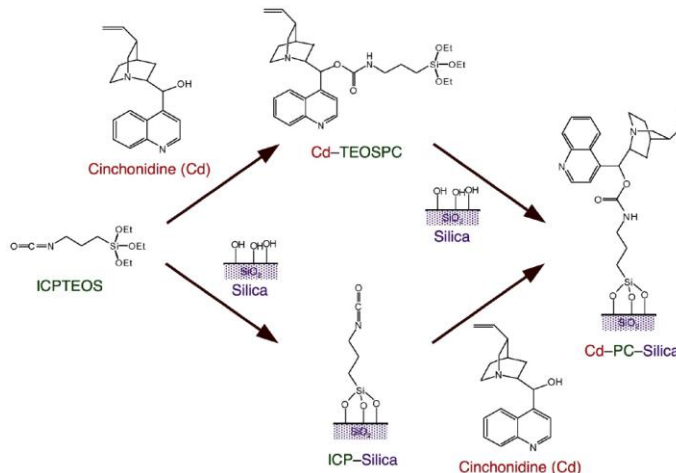


Figure 2. Schematic representation of the strategy followed in this research for the tethering of cinchonidine (Cd) on high-surface-area silica supports. An intermediate linker, 3-isocyanatopropyltriethoxysilane (ICPTEOS), was used as part of a "click" chemistry approach, and the system assembled sequentially by following either of the two routes shown in this figure.

### Chiral Templates

**Amino Acids on Pd(111).** Propylene oxide (PO) adsorbs enantioselectively on amino acid modified surfaces, where the amino acid structures can be varied in a systematic way by varying the functional group. Amino acids with *n*-alkyl groups (alanine, 2-aminobutanoic acid and norvaline) show enantioselectivity, while branching at the  $\alpha$ -carbon (valine, leucine) leads to non-enantioselective chemisorption of PO. Branching at the  $\beta$ -carbon (isoleucine) leads to intermediate enantioselectivity. Scanning tunneling microscope (STM) images of some selected amino acids adsorbed on Pd(111) at 290 K reveal that modifiers which render the surface enantioselective (alanine and 2-aminobutanoic acid) form tetramers, while valine, which has an  $ER = 1$ , does not. It is postulated that the tetramers act as chiral templates, and valine and

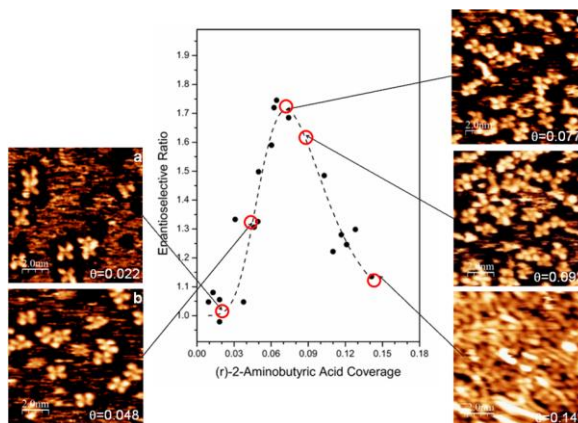


Figure 3. Plot of  $ER$  of propylene oxide on a Pd(111) surface modified by 2-aminobutanoic acid versus modifier coverage.



leucine, which form only dimers, do not form enantioselective surfaces. This is the first direct evidence for the formation on chiral templates on metal surfaces. The correlation between enantiospecific adsorption and the formation of the tetramers at different coverages of 2-amino butyric acid is demonstrated in Figure 3.

**L-lysine on Cu(100).** While templating of Pt(111) and Pd(111) with various chiral molecules leads to enantioselective adsorption of chiral probes such as PO, the same is not so commonly true on Cu single crystal surfaces. An extensive set of experiments using a number of combinations of chiral templates and chiral probes failed to observe enantiospecific adsorption. The exception to this is the templating of the Cu(100) surface with D- and L-lysine. The desorption kinetics of R- and S-PO adsorbed on the L- and D-lysine modified Cu(100) surfaces is enantiospecific. The peak desorption temperatures of R- and S-PO observed during TPD experiments exhibit a diastereomeric relationship. One possible explanation is the potential for lysine adsorbed on Cu to form a zwitterion and thus, expose an  $-\text{NH}_3^+$  group for hydrogen bonding interactions with the adsorbed PO. A second possibility is that lysine adsorbed on Cu(100) is known to form naturally chiral  $(3,1,17)^{\text{R}\&\text{S}}$  microfacets and it may be that it is the presence of these chiral microfacets that induces the enantiospecific interactions with adsorbed R- and S-PO.

### Imprinted chiral surfaces

The Cu(100) surface can be chirally imprinted by adsorption of L-lysine. Previous literature has reported the reconstruction of Cu(100) surfaces to form homochiral  $(3,1,17)^{\text{R}}$  facets upon adsorption of L-lysine at high coverage and after annealing to 430 K (*J. Am. Chem. Soc.* 122, **2000**, 12584). We have demonstrated using TPD experiments that the adsorption energetics of D- and L-lysine on the chiral  $\text{Cu}(3,1,17)^{\text{R}\&\text{S}}$  and achiral Cu(100) surfaces are consistent with this chiral imprinting (Figure 4). The implication of this work is that the adsorption energy of L-lysine on  $\text{Cu}(3,1,17)^{\text{R}}$  is greater than on  $\text{Cu}(3,1,17)^{\text{S}}$  and Cu(100), thereby driving the homochiral reconstruction. The desorption energies of D- and L-lysine on the Cu(100) surface are significantly lower than on either of the  $\text{Cu}(3,1,17)^{\text{R}\&\text{S}}$  surfaces. Furthermore, large enantiospecific differences in desorption kinetics were observed for D- and L-lysine on the  $\text{Cu}(3,1,17)^{\text{R}\&\text{S}}$  surfaces. This observed enantiospecificity is believed to originate from the enantiospecific interactions of lysine with the chiral kinked steps on these surfaces. The

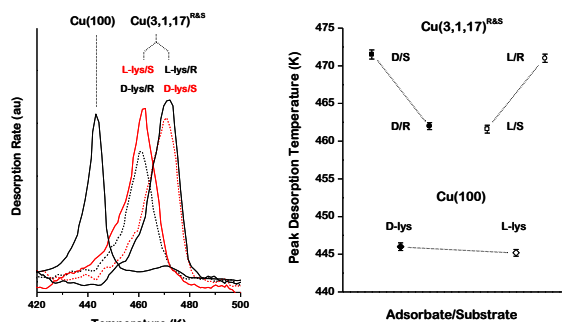


Figure 4. Left-hand panel. TPD of L-lysine from the  $\text{Cu}(3,1,17)^{\text{R}\&\text{S}}$  surfaces following exposure to L-lysine for 800 sec. The highest temperature desorption features from the  $\text{Cu}(3,1,17)^{\text{R}\&\text{S}}$  surfaces reveals a difference in peak desorption temperatures of  $9.5 \pm 0.8$  K. TPD spectra were collected at a heating rate of 1 K/sec while monitoring the signal at  $m/q = 30$ . Right-hand panel. Plot of peak desorption temperatures of L-lysine and D-lysine on the  $\text{Cu}(3,1,17)^{\text{R}}$ ,  $\text{Cu}(3,1,17)^{\text{S}}$  and Cu(100) surfaces. Error bars correspond to one standard deviation in the temperature measurements and have been determined from six repetitions of each TPD spectrum. The results on the  $\text{Cu}(3,1,17)^{\text{R}}$  and  $\text{Cu}(3,1,17)^{\text{S}}$  surfaces reveal a clear and significant diastereomeric effect.

observation that adsorption of L-lysine on  $\text{Cu}(3,1,17)^{\text{R}}$  is energetically preferred over adsorption on  $\text{Cu}(3,1,17)^{\text{S}}$  is consistent with the formation of homochiral  $(3,1,17)^{\text{R}}$  facets during L-lysine adsorption on  $\text{Cu}(100)$ .

### Naturally chiral surfaces

Surface explosions are a class of surface reaction mechanisms that have extremely non-linear kinetics.

These are decomposition reactions that require the presence of empty sites on surfaces in order for adsorbate decomposition to occur. The need for an empty site for the decomposition reaction results in kinetics that are described using rate laws such as  $r = k \cdot \theta \cdot (1 - \theta)$ , where  $\theta$  represents the coverage of adsorbed species. As the coverage approaches the saturations value, the reaction has the characteristics of an autocatalytic explosion. Once nucleated, the reaction is self-accelerating because each decomposition event uses one empty site but creates two more. These extremely non-linear reaction kinetics result in high enantiospecificity, if observed on chiral surfaces. The decomposition of tartaric acid,  $\text{CO}_2\text{HCH}(\text{OH})\text{CH}(\text{OH})\text{CO}_2\text{H}$ , is extremely enantiospecific on several naturally chiral surfaces:  $\text{Cu}(531)$ ,  $\text{Cu}(17,5,1)$ ,  $\text{Cu}(643)$ , and  $\text{Cu}(653)$ . Figure 5 shows the TPR spectra obtained following the adsorption of racemic, R- and S-tartaric acids on  $\text{Cu}(531)^{\text{R\&S}}$  and  $\text{Cu}(17,5,1)^{\text{R\&S}}$ . The explosive decomposition kinetics results in extremely enantiospecific decomposition kinetics and the very high resolution of the decomposition peaks on the chiral surfaces. Over the course of the past year we have continued to collect data on the explosion kinetics of tartaric acid on several Cu surfaces in order to ultimately model the explosion process with a view to understanding the origins of the enantioselectivity.

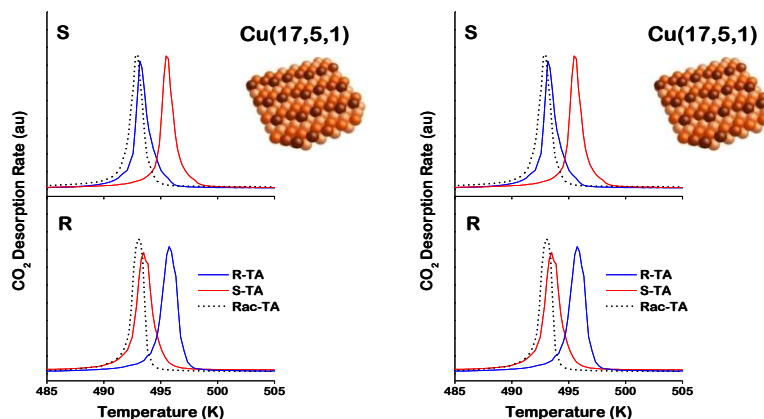


Figure 5. TPR spectra of tartaric acid decomposition at saturation coverage on the  $\text{Cu}(17,5,1)^{\text{R\&S}}$  surfaces and on  $\text{Cu}(531)^{\text{R\&S}}$  surfaces. The explosive reaction mechanism results in the reaction occurring over a very narrow temperature range and yielding extremely high enantiospecificity.

### Publications 2009-2011

1. JW Han, JN James, DS Sholl, "Chemical speciation of adsorbed glycine on metal" *surfaces Journal of Chemical Physics* 135(3), No. 034703
2. JW Han, JN James, DS Sholl, "Enantiospecific adsorption of amino acids on hydroxylated quartz (1,0,-1,0)" *Physical Chemistry Chemical Physics* 12(28), 8024-8032
3. DS Sholl, AJ Gellman, "Developing Chiral Surfaces for Enantioselective Chemical Processing" *AICHE J.* 55(10), (2009), 2484-2490
4. JW Han, DS Sholl, "Enantiospecific Adsorption of Amino Acids on Hydroxylated Quartz (0001)" *Langmuir* 25(18), (2009), 10737-10745

5. JW Han, DS Sholl, JR Kitchin “Step decoration of chiral metal surfaces” *J. Chem. Phys.* 130(12), (2009), 124710
6. V Bustos, D Linares, A Gil Rebaza, WT Tysoe, D Stacchiola, L Burkholder, G Zgrablich, “Monte Carlo Theory Analysis of Thermal Programmed Desorption of Chiral Propylene-Oxide from Pd(111) Surfaces” *J. Phys. Chem. C* 113, (2009) 3254-3258
7. L Burkholder, D Stacchiola, JA Boscoboinik, WT Tysoe, “Enantioselective Chemisorption on Model Chirally Modified Surfaces: 2-Butanol on  $\alpha$ -1-(1-Naphthylethylamine)/Pd(111)”, *J. Phys. Chem C.*, 113, (2009), 13877-13885
8. L Burkholder, WT Tysoe “Structure and Reaction Pathways of Methyl Pyruvate on Pd(111)” *J. Phys. Chem. C.* 113, (2009), 15298-15306
9. L. Burkholder, WT Tysoe, “Structure and Reaction Pathways of Methyl Lactate on Pd(111)”, *Surf. Sci.*, 603, (2009), 2714-2720
10. Z Li, WT Tysoe, “The Adsorption and Reaction of 2-butanol on Clean and Oxygen-covered Pd(100)”, *Surf. Sci.*, 604, (2010), 1377-1387
11. L Burkholder, M Weinert, M Garvey, WT Tysoe, “Structure of Methyl Pyruvate and  $\alpha$ -(1-Naphthyl)ethylamine on Pd(111)”, *J. Phys. Chem. C.*, 115, (2011), 8790–8797
12. JA Boscoboinik, Y Bai, L Burkholder, WT Tysoe, “Structure and Distribution of S- $\alpha$ -(1-Naphthyl)-Ethylamine on Pd(111)”, *J. Phys. Chem C.*, 33, (2011), 16488-16494
13. Z Ma, F Zaera, “Chiral Modification of Catalytic Surfaces”, in *Design of Heterogeneous Catalysts: New Approaches based on Synthesis, Characterization, and Modelling*, edited by U.S. Ozkan, Wiley-VCH, Weinheim, pp 113-140 (2009).
14. J Lai, Z Ma, L Mink, LJ Mueller, F Zaera, “Influence of Peripheral Groups on the Physical and Chemical Behavior of Cinchona Alkaloids”, *J. Phys. Chem. B.*, 113(34), (2009), 11696–11701.
15. F Zaera, “Regio, Stereo, and Enantio-Selectivity in Hydrocarbon Conversion on Metal Surfaces”, *Acc. Chem. Res.*, 42(8), (2009), 1152–1160
16. F Zaera, “The New Materials Science of Catalysis: Toward Controlling Selectivity by Designing the Structure of the Active Site”, *J. Phys. Chem. Lett.*, 1(3), (2010), 621-627.
17. JL Sales, V Gargiulo, I Lee, F Zaera, G Zgrablich, “Monte Carlo Modeling of the Enantioselective Adsorption of Propylene Oxide on 1-(1-Naphthyl)ethylamine-Modified Pt(111) Surfaces”, *Catal. Today*, 158(1-2), (2010), 186-196.
18. F Zaera, “Surface Chemistry at the Liquid/Solid Interface”, *Surf. Sci.*, 605(13/14), (2011), 1141-1145
19. J Hong, I Lee, F Zaera, “Cinchona Alkaloids Anchored on Porous Silica as Enantioselective Heterogeneous Catalysts, *Top. Catal.*, in press (2011)
20. AJ Gellman “Enantioselectivity on naturally chiral metal surfaces” Ch. 4 in Model Systems in Catalysis: From Single Crystals and Size Selected Clusters to Supported Enzyme Mimics, ed. R.M. Rioux, (2010), p. 75-95, Springer Publ.
21. N Shukla, MA Bartel, AJ Gellman “Enantioselective separation on chiral Au nanoparticles” *J Amer. Chem. Soc.*, 132(25), (2010), 8575–8580
22. WY Cheong, Y Huang, N Dangaria, AJ Gellman “Probing Enantioselectivity on Chirally Modified Cu(110), Cu(100) and Cu(111) Surfaces” *Langmuir* 26(21), (2010), 16412-16423
23. WY Cheong, AJ Gellman “Energetics of chiral imprinting of Cu(100) by lysine” *Journal of Physical Chemistry C* 115, (2011), 1031-1035
24. Y Huang, AJ Gellman, “Enantiospecific adsorption of (R)-3-methylcyclohexanone on naturally chiral surfaces vicinal to Cu(110)” *Topics in Catalysis*, in press (2011)
25. AJ Gellman, DS Sholl “Chemical processing with one hand” *Chemical Engineering Progress*, Oct. 2009, 16
26. AJ Gellman, “Chiral Surfaces: Accomplishments and Challenges” *ACS Nano* 4(1), (2010) 5-10

**Structured Carbon Supports for Aqueous Phase Reforming and Fuel Cell Catalysts**

Postdoc: Sungchul Lee  
Students: Xiaoming Wang, Zhiteng Zhang, Changchang Lee  
Collaborators: Lisa Pfefferle (Yale), Steven Suib (U. of Conn.) Johannes Lercher (Technical University of Munich)  
Contacts: Yale University, 9 Hillhouse Ave, P. O. box 208286, New Haven, CT 06520-8286; gary.haller@yale.edu

**Goal**

Develop the fundamental science of nanoparticles of oxides covalently bonded to carbon nanotubes (CNT) with specific reference to ZrO<sub>2</sub>, sulfated ZrO<sub>2</sub> and TiO<sub>2</sub> and to develop methods of directing the deposit of metals, e.g, Pt, on the oxide and/or the CNT support.

**DOE Interest**

Renewable energy sources of the future will require catalysts to produce fuels from biomass. This project proposes to investigate the fundamental science of catalysts for conversion of biomass to hydrogen and for producing useful power from alcohols in fuel cells. The extraction of hydrogen is accomplished in water from soluble, biomass derived, oxygenated hydrocarbons by aqueous phase reforming (APR, the catalytic, high pressure reaction between water and oxygenated hydrocarbons to produce hydrogen and carbon dioxide). The direct alcohol fuel cell electrodes require catalysts for the oxidation of alcohol. Catalysts for APR and direct alcohol fuel cells use catalysts which have the active component dispersed on a support, a high area material that stabilizes small metal particles of metal, such as Pt. Carbon supports are advantageous for APR because they are stable in the aqueous phase (do not dissolve as common oxide supports do) and are advantageous for catalyst used in fuel cells because of the necessary electrical conductivity.

**Recent Progress**

*Single-walled carbon nanotube (CNT) synthesis catalysts:* CNT diameter selectivity depends on a narrow metal particle distribution because the metal particle size determines the CNT diameter. Different strategies have been used to design metal particle anchors for the catalyst, e.g., unreduced Co<sup>2+</sup> in MCM-41 (our standard approach) and carburized Mo (the CoMoCat® approach of SouthWest Nano Technologies). We have explored a combination of the two where Mo is incorporated into the MCM-41 matrix and anchors Co metal particles but is not carburized and requires much less Mo than the commercial CoMoCat®.

*CNT as catalyst support for metals:* While functionalized (oxidized) CNT are effective supports for Pt, e.g., provide stable support in aqueous reactions such as fuel cells or aqueous phase reforming, in some cases increased dispersion resulting from functionalization does not result in increased activity. We have elucidated the phenomena for CNT supported Pt and Pt-Co and demonstrated that the oxygen functional groups on

CNT can also affect the supply of reactant when reactants of different hydrophobicity compete for adsorption on the CNT support. This may have a positive effect on activity, e.g., water gas shift reaction, or a negative effect, e.g., aqueous phase reforming, depending on the reaction and reaction conditions.

*Covalently bonded oxide nanoparticles on CNT:* Many oxide particle CNT composites have been explored for a variety of applications, including catalytic applications, but most of these do not involve covalent bonding between the oxide particle and CNT. Covalent bonding can stabilize the oxide particle against sintering, and improve electronic coupling between the oxide and the CNT (where that is needed, e.g., in fuel cell electrode catalysts). We have used C and O NEXAFS to demonstrate C–O–Zr bonding between ZrO<sub>2</sub> nanoparticles and multi-walled CNT.

### **Future Plans**

*Covalently bonded oxide nanoparticles on CNT:* We plan to demonstrate the usefulness of covalently bonded ZrO<sub>2</sub>/MWCNT for acid catalyzed reactions (sulfated ZrO<sub>2</sub>/MWCNT), and to explore the extension of this catalyst synthesis to other oxides, e.g., TiO<sub>2</sub>.

*CNT as catalyst support for metals:* The measurement of the point of zero charge (PZC) of CNT has already been explored; manipulation of the PZC and varying precursor (anion or cation at various pH) will be used to selectively ion exchanged Pt on the oxide or CNT portion of a composite support such as ZrO<sub>2</sub>/MWCNT. These catalysts will allow the exploration and contrast of bifunctional catalysis with the same overall catalyst composition but different structure on the molecular level.

### **Publications (2009-2011)**

1. S. Lee, Z. Zhang, X. Wang, L. D. Pfefferle, and G. L. Haller, "Characterization of multi-walled carbon nanotubes catalyst supports by point of zero charge," *Catalysis Today* **164** (2011) 68-73.
2. S. Lee, C. Zoican Loebick, L. D. Pfefferle, and G. L. Haller, "High-Temperature Stability of Cobalt Grafted on Low-Loading Incorporated Mo-MCM-41 Catalyst for Synthesis of Single-Walled Carbon Nanotubes," *J. Phys. Chem. C* **115** (2011) 1014-1024.
3. X. Wang, N. Li, J. A. Webb, L. D. Pfefferle, and G. L. Haller, "Effect of surface oxygen containing groups on the catalytic activity of multi-walled carbon nanotube supported Pt catalyst," *Appl. Catal. B*, **101** (2010) 21-30.
4. X. Wang, N. Li, L. D. Pfefferle, and G. L. Haller, "Effect of surface oxygen containing groups on carbon nanotube supported catalyst," *ACS Division of Fuel Chemistry Preprints* **55** (2010) 40-41.
5. X. Wang, N. Li, L. D. Pfefferle, and G. L. Haller, "Carbon nanotube supported Pt and Pt-Co bimetallic catalyst: Structure and aqueous phase reforming activity," *ACS Division of Fuel Chemistry Preprints* **55** (2010) 193-194.
6. X. Wang, N. Li, L. D. Pfefferle, and G. L. Haller, "Pt-Co bimetallic Catalyst supported on Single-walled carbon nanotubes: Effect of alloy formation and oxygen containing groups," *J. Phys. Chem. C* **114** (2010) 16996 -17002.

7. X. Wang, N. Li, L. D. Pfefferle, and G. L. Haller, "Pt-Co bimetallic catalyst supported on single walled carbon nanotube: XAS and aqueous phase reforming activity studies." *Catalysis Today* **146** (2009) 160-165.
8. C. Wang, S. Lim, G. Du, C. Zoican Loebicki, N. Li, S. Derrouiche, and G. L. Haller, "Synthesis, Characterization, and Catalytic Performance of Highly Dispersed Co-SBA-15." *J. Phys. Chem. C* **113** (2009) 14863-14871.
9. N. Li, X. Wang, F. Ren, G. L. Haller, and L. D. Pfefferle, "Diameter Tuning of Single-Walled Carbon Nanotubes with Reaction Temperature Using a Co Monometallic Catalyst." *J. Phys. Chem. C* **113** (2009) 10070-10078.

**Fundamental Studies of Heterogeneous Photocatalysis on Model TiO<sub>2</sub> Surfaces**

Additional PIs: Zdenek Dohnálek, Igor Lyubinetsky, Greg Kimmel, Nick Petrik  
Post-docs: N. Aaron Deskins\*, Dong J. Kim\*, Mingmin Shen, Zhitao Wang, Yeohoon Yoon, Robert T. Zehr\* (\* - no longer at PNNL)  
Graduate Students: none  
Undergrad Students: none  
Collaborators: D.A. Dixon (U. Alabama),  
Contact: M.A. Henderson, Pacific Northwest National Laboratory, PO Box 999, MS K8-80, Richland, WA 99352; phone: (509) 376-2192; Email: [ma.henderson@pnl.gov](mailto:ma.henderson@pnl.gov);

**Goal**

The goal of this project is to provide the field of heterogeneous photocatalysis with fundamental insights into the molecular-level properties of photocatalytic transformations through study of photochemical reactions on model TiO<sub>2</sub> materials. In this project, molecular-level expertise at PNNL in surface science, photodynamics and scanning probe microscopy is being used to study three areas of importance to heterogeneous photocatalysis on TiO<sub>2</sub>. These are: (1) detailed reaction mechanisms, (2) mechanisms of charge transfer, charge trapping and energy redistribution, and (3) surface structure and material dependences, each as they relate to photochemical reactions. These issues are explored using a variety of model TiO<sub>2</sub> systems including single crystal surfaces, surfaces with additives, and surfaces prepared with controlled structural and electronic defects.

**DOE Interest**

Heterogeneous photocatalysis on TiO<sub>2</sub> has received considerable attention of late due to increased interest in using light to promote chemical transformations in remediation and energy technologies. Fundamental questions remain unaddressed, e.g., reaction and charge transfer mechanisms, specific surface reaction sites, selectivity, and interplay between thermal and non-thermal processes. The vast majority of research effort in the literature has been phenomenological, resulting in conflicting explanations for crucial issues such as the performance differences between the polymorphs of TiO<sub>2</sub> (anatase and rutile). Work in this project is of direct relevance to DOE's mission of increasing fundamental scientific understanding of heterogeneous catalysis and of light-to-chemical energy conversions.

**Recent Progress (FY09 to FY11)**

*Choices in Charge Transfer Initiated Bond Breaking* During photocatalysis on TiO<sub>2</sub>, charge transfer to or from adsorbates results in unstable states that lead to bond breaking. Generally speaking, the charge transfer state associated with hole activity is toward neutralization (e.g., in the case of hole-mediated reactions with carboxylates) and that with electron activity it is toward ionization (e.g., electron scavenging of O<sub>2</sub> to form O<sub>2</sub><sup>-</sup> species). In either case, the 'excited' adsorbate can be viewed from a thermodynamic perspective in which the system chooses the lowest energy pathway in response to the charge transfer event. In some cases, dynamics in the 'excited' state may cause thermodynamically unfavorable pathways to open up. Organic carbonyl molecules adsorbed on the TiO<sub>2</sub>(110) surface offer a unique opportunity to explore the

interplay between dynamics and thermodynamics during charge transfer. Figure 1 shows a schematic reaction mechanism that we have found to apply to a wide variety of organic carbonyls (e.g., acetone, butanone, acetaldehyde, etc.) adsorbed on TiO<sub>2</sub>(110). The first step involves a thermal process that converts carbonyl ((R<sub>1</sub>)(R<sub>2</sub>)CO) into diolate species ((R<sub>1</sub>)(R<sub>2</sub>)CO<sub>2</sub>) via reaction with a surface oxygen species. The second step involves photodecomposition of this diolate, via radical ejection, to adsorbed carboxylate. Looking at a variety of R<sub>1</sub> and R<sub>2</sub> groupings, comparing experimental observations and theoretical bond energy assessments, we find that the thermodynamic pathway is chosen (i.e., the weaker C-R bond breaks) in all cases except those involving highly halogenated substituents (e.g., trifluoroacetone). In the latter cases, there is a partitioning of the charge transfer energy between the weaker and stronger bonds allowing both channels to be observed. These results suggest that a deeper understanding of the dynamics of the ‘excited’ state is needed in order to predict (and control) the mechanistic directions of photochemical reactions on surfaces.

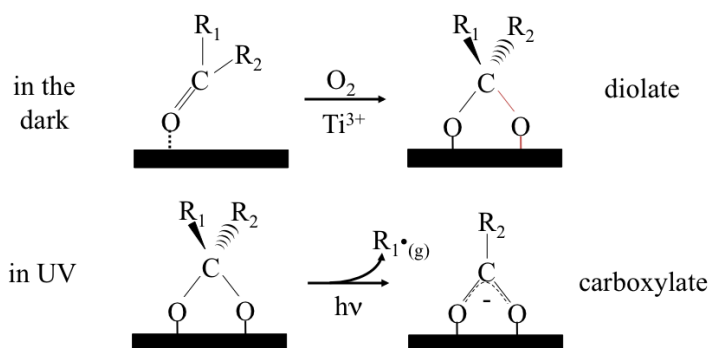


Figure 1 With dissimilar substituents, photoactivation of adsorbed diolates on TiO<sub>2</sub>(110) generally involves breaking the weaker of the two C-R bonds.

Identifying Reactive Oxygen Species on TiO<sub>2</sub> Surfaces As often is the case, species that are easily identifiable on surfaces tend to be those that are most stable (hence, least reactive), while those that are the most active are both difficult to detect and more likely to be the key reactants/intermediates. In the case of photocatalysis on TiO<sub>2</sub>, identifying and characterizing reactive oxygen species is a challenge because these species are difficult to differentiate from lattice oxygen with most spectroscopic tools (e.g., photoemission or vibrational spectroscopy). We have employed scanning tunneling microscopy to investigate the details of O<sub>2</sub> chemistry on rutile TiO<sub>2</sub>(110) that leads to the formation of oxygen adatom (O<sub>a</sub>) pairs at terminal Ti sites. An intermediate, metastable O<sub>a</sub>-O<sub>a</sub> configuration with two nearest-neighbor O atoms is observed immediately after O<sub>2</sub> dissociation at 300 K, however the nearest-neighbor O<sub>a</sub> pair configuration is destabilized by Coulomb repulsion between the O<sub>a</sub>'s leading to separation further along the Ti row into the stable second-nearest neighbor configuration. This is illustrated in the three STM frames (and their accompanying surface models) of

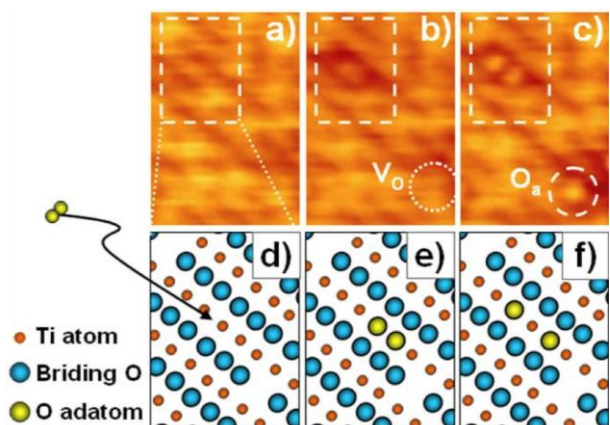


Figure 2 (a-c) Consecutive time-lapse STM images (126 s between frames) of the (3.5 × 5.1) nm<sup>2</sup> area taken during O<sub>2</sub> dosing at 300 K; (d-f) schematic models of the rectangular region



Figure 2. In ‘a’, an O<sub>2</sub> molecule approaches the clean TiO<sub>2</sub>(110) surface leading to adsorption and dissociation (‘b’). The metastable state in which the two O<sub>a</sub>’s reside at neighboring sites is promptly stabilized by movement of one O<sub>a</sub> away (‘c’). In contrast, the dissociation of an O<sub>2</sub> at a vacancy (V<sub>O</sub>) results in only one O<sub>a</sub> state (see bottom right of ‘b’ and ‘c’). The potential energy surface calculated for O<sub>2</sub> dissociation on Ti rows and following O<sub>a</sub>’s separation strongly supports the experimental observations. Furthermore, our results show that the delocalized electrons associated with the O vacancies are being utilized in the O<sub>2</sub> dissociation process on the Ti row, whereas two oxygen vacancies (four electrons) per O<sub>2</sub> molecule are required in order for this process to become viable. These results provide a window into a metastable configuration of two O<sub>a</sub>’s on TiO<sub>2</sub>(110) that might possess chemistry uniquely different from that of an isolated O<sub>a</sub>. For example, this metastable configuration may be important in O<sub>2</sub> formation reactions important in water photooxidation reactions.

### *Angular Dependence in the Photodesorption of CO and CO<sub>2</sub> During CO Photooxidation on TiO<sub>2</sub>*

One of the unexplored aspects of heterogeneous photocatalysis is that of energy partitioning as a result of charge transfer chemistry. Charge carriers generated by photon absorption possess (essentially) the energy difference between the band edges of the photocatalyst absorbing the light. In the case of TiO<sub>2</sub>, this amounts to ~3 eV per electron-hole pair. While some of this energy can be viewed as being invested in bond forming and bond breaking events that result from transfer events to adsorbates, much of this potential energy becomes unaccounted for in the aftermath of the transfer event. Being able to ‘follow the energy’ is a critical in obtaining a fundamental understanding of heterogeneous charge transfer catalysis and in develop photocatalytic systems that optimally utilize energy in photoconversion processes. We have employed the rutile TiO<sub>2</sub>(110) surface to explore the subject of energy partitioning during photocatalysis of a model photochemical reaction: CO oxidation. Figure 3 provides detailed angular profiles from photon stimulated desorption (PSD) measurements resulting from UV irradiation of coadsorbed mixtures of CO and O<sub>2</sub> on TiO<sub>2</sub>(110). Inspection of the profiles parallel (<001> direction) and perpendicular to the surface rows shows that the angular dependence of O<sub>2</sub> PSD is quite different from that of CO<sub>2</sub> PSD, but that of CO resembles the product CO<sub>2</sub>. (No CO PSD is observed in the absence of coadsorbed O<sub>2</sub>.) But perhaps most notable is that the CO<sub>2</sub> and CO PSD signals are highly oriented away from the surface normal, titled at ~±50° in directions perpendicular to the surface rows. In a situation in which the photoproduct (CO<sub>2</sub>) were allowed to reach energy accommodation with the surface, we would expect

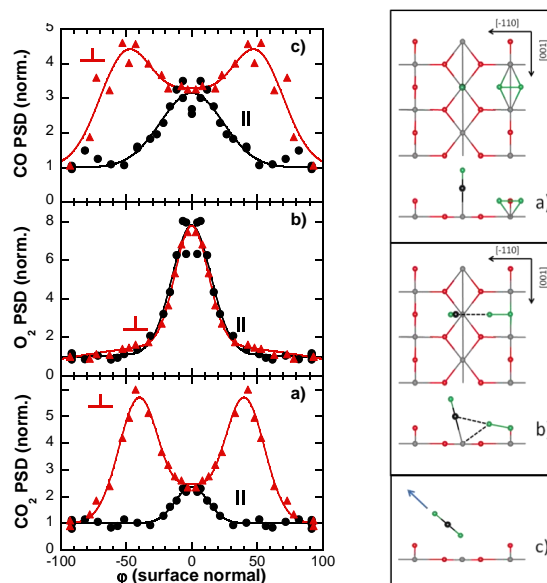


Figure 3 (Left: a-c) Angular dependence of CO<sub>2</sub>, O<sub>2</sub> and CO PSD signals, respectively, during photoreaction of coadsorbed CO and O<sub>2</sub> on rutile TiO<sub>2</sub>(110). The ‘0’ point in each plot is the surface normal, and angular deviation in the PSD signals from this point are shown in directions parallel and perpendicular to the rows on the TiO<sub>2</sub>(110) surface. (Right: a-c) Proposed mechanism for the angular dependence in CO<sub>2</sub> PSD.

only PSD peaked normal to the surface. Observations of strong angular dependence in both the product *and* the reactant suggests that the PSD of both are accompanied with non-thermal energy distributions. Also, given that the reactant possesses the same profile as the product suggests that the reactant PSD results from exiting a transition state in the photooxidation reaction. Based on these observations, we proposed the photoreaction depicted on the right in Figure 3 in which PSD of both the successful and unsuccessful photoreaction follows a trajectory of the attempted C-O bond formation. Extension of this concept to other photoreactions, as well as the reverse reactions (e.g., CO<sub>2</sub> photodecomposition) will provide fundamental insights into how energy is distributed among products and reactants during photocatalysis on TiO<sub>2</sub>.

### Future Plans

- Studies on the proximity effects in heterogeneous photochemistry; for example, examining with STM the rates of photodecomposition or photodesorption of a probe molecule in relation to surface structural features (steps, point defects) or other adsorbed species.
- Examinations of the photocatalytic properties of highly dispersed Ti<sup>4+</sup> centers in microporous structures (e.g., mesoporous silica or zeolites) with development of similar model photocatalysts supported on photocatalytically inert single crystal oxide surfaces (e.g.,  $\alpha$ -Al<sub>2</sub>O<sub>3</sub>(0001)).
- Exploration of the chemical and photochemical properties of non-TiO<sub>2</sub> single crystal surfaces, such as ZnO, PdO and RuO<sub>2</sub>.
- Photoreduction of CO<sub>2</sub> and photooxidation of H<sub>2</sub>O on single crystal oxide surfaces.

### Publications (FY09-FY11)

1. Deskins, N.A. and M. Dupuis (2009). "Intrinsic Hole Migration Rates in TiO<sub>2</sub> from Density Functional Theory." *Journal of Physical Chemistry C* 113(1): 346.
2. Deskins, N.A., R. Rousseau and M. Dupuis (2009). "Localized Electronic States from Surface Hydroxyls and Polarons in TiO<sub>2</sub>(110)." *Journal of Physical Chemistry C* 113(33): 14583.
3. Deskins, N.A., R. Rousseau and M. Dupuis (2010). "Defining the Role of Excess Electrons in the Surface Chemistry of TiO<sub>2</sub>." *Journal of Physical Chemistry C* 114(13): 5891.
4. Deskins, N.A., R. Rousseau and M. Dupuis (2011). "Distribution of Ti<sup>3+</sup> Surface Sites in Reduced TiO<sub>2</sub>." *Journal of Physical Chemistry C* 115(15): 7562.
5. Dohnálek, Z., I. Lyubinetsky and R. Rousseau (2010). "Thermally-driven processes on rutile TiO<sub>2</sub>(110)-(1x1): A direct view at the atomic scale." *Progress in Surface Science* 85(5-8): 161.
6. Du, Y., N.A. Deskins, Z. Zhang, Z. Dohnálek, M. Dupuis and I. Lyubinetsky (2009). "Two Pathways for Water Interaction with Oxygen Adatoms on TiO<sub>2</sub>(110)." *Physical Review Letters* 102(9): 096102.
7. Du, Y., N.A. Deskins, Z. Zhang, Z. Dohnálek, M. Dupuis and I. Lyubinetsky (2009). "Imaging Consecutive Steps of O<sub>2</sub> Reaction with Hydroxylated TiO<sub>2</sub>(110): Identification of HO<sub>2</sub> and Terminal OH Intermediates." *Journal of Physical Chemistry C* 113(2): 666.
8. Du, Y., N. A. Deskins, Z.R. Zhang, Z. Dohnálek, M. Dupuis and I. Lyubinetsky (2010). "Formation of O adatom pairs and charge transfer upon O<sub>2</sub> dissociation on reduced TiO<sub>2</sub>(110)." *Physical Chemistry Chemical Physics* 12(24): 6337.

9. Du, Y., N.A. Deskins, Z.R. Zhang, Z. Dohnálek, M. Dupuis and I. Lyubinetsky (2010). "Water Interactions with Terminal Hydroxyls on TiO<sub>2</sub>(110)." *Journal of Physical Chemistry C* 114(40): 17080.
10. Henderson, M.A. (2010). "Oxygen plasma activation of Cr(CO)<sub>6</sub> on α-Fe<sub>2</sub>O<sub>3</sub>(0001)." *Surface Science* 604(17-18): 1502.
11. Henderson, M.A. (2010). "Low temperature oxidation of Fe<sup>2+</sup> surface sites on the (2x1) reconstructed surface of α-Fe<sub>2</sub>O<sub>3</sub>(01(-1)2)." *Surface Science* 604(13-14): 1197.
12. Henderson, M.A. (2010). "Photochemistry of methyl bromide on the α-Cr<sub>2</sub>O<sub>3</sub>(0001) surface." *Surface Science* 604(19-20): 1800.
13. Henderson, M.A. (2011). "A Surface Science Perspective on TiO<sub>2</sub> Photocatalysis." *Surface Science Reports* 66: 185.
14. Henderson, M.A., N.A. Deskins, R.T. Zehr and M. Dupuis (2011). "Generation of organic radicals during photocatalytic reactions on TiO<sub>2</sub>." *Journal of Catalysis* 279(1): 205.
15. Henderson, M.A. and K.M. Rosso (2011). "Oxidation of H<sub>2</sub>S by coadsorbed oxygen on the α-Cr<sub>2</sub>O<sub>3</sub>(0001) surface." *Surface Science* 605(5-6): 555.
16. Lyubinetsky, I., N.A. Deskins, Y. Du, E.K. Vestergaard, D.J. Kim and M. Dupuis (2010). "Adsorption states and mobility of trimethylacetic acid molecules on reduced TiO<sub>2</sub>(110) surface." *Physical Chemistry Chemical Physics* 12(23): 5986.
17. Petrik, N.G. and G.A. Kimmel (2009). "Nonthermal Water Splitting on Rutile TiO<sub>2</sub>: Electron-Stimulated Production of H<sub>2</sub> and O<sub>2</sub> in Amorphous Solid Water Films on TiO<sub>2</sub>(110)." *Journal of Physical Chemistry C* 113(11): 4451.
18. Petrik, N.G. and G.A. Kimmel (2010). "Photoinduced Dissociation of O<sub>2</sub> on Rutile TiO<sub>2</sub>(110)." *Journal of Physical Chemistry Letters* 1(12): 1758-1762.
19. Petrik, N.G. and G.A. Kimmel (2010). "Off-Normal CO<sub>2</sub> Desorption from the Photooxidation of CO on Reduced TiO<sub>2</sub>(110)." *Journal of Physical Chemistry Letters* 1: 2508.
20. Petrik, N.G. and G.A. Kimmel (2011). "Electron- and Hole-Mediated Reactions in UV-Irradiated O<sub>2</sub> Adsorbed on Reduced Rutile TiO<sub>2</sub>(110)." *Journal of Physical Chemistry C* 115(1): 152.
21. Petrik, N.G., Z.R. Zhang, Y. Du, Z. Dohnálek, I. Lyubinetsky and G.A. Kimmel (2009). "Chemical Reactivity of Reduced TiO<sub>2</sub>(110): The Dominant Role of Surface Defects in Oxygen Chemisorption." *Journal of Physical Chemistry C* 113(28): 12407.
22. Shen, M. and M.A. Henderson (2011). "Impact of Solvent on Photocatalytic Mechanisms: Reactions of Photodesorption Products with Ice Overlayers on the TiO<sub>2</sub>(110) Surface." *Journal of Physical Chemistry C* 115(13): 5886.
23. Wang, T.H., D.A. Dixon and M.A. Henderson (2010). "C-C and C-Heteroatom Bond Dissociation Energies in CH<sub>3</sub>R'C(OH)<sub>2</sub>: Energetics for Photocatalytic Processes of Organic Diolates on TiO<sub>2</sub> Surfaces." *Journal of Physical Chemistry C* 114(33): 14083.
24. Zehr, R.T., N.A. Deskins and M.A. Henderson (2010). "Photochemistry of 1,1,1-Trifluoroacetone on Rutile TiO<sub>2</sub>(110)." *Journal of Physical Chemistry C* 114: 16900.
25. Zehr, R.T. and M.A. Henderson (2010). "Thermal chemistry and photochemistry of hexafluoroacetone on rutile TiO<sub>2</sub>(110)." *Physical Chemistry Chemical Physics* 12(28): 8084.

## Theoretical Investigation of Heterogeneous Catalysis at the Solid-Liquid Interface for the Conversion of Lignocellulosic Biomass Model Molecules

Students: Mian M. Faheem

Contacts: University of South Carolina, 301 S. Main, Columbia, SC 29208;  
[heyden@cec.sc.edu](mailto:heyden@cec.sc.edu)

### Goals

Develop and validate a highly efficient and accurate computational method for predicting elementary reaction rates at the solid-liquid interface that is based on a novel subtraction scheme for metal surfaces and QM/MM minimum free energy path methods recently developed in the enzyme and homogeneous catalysis communities. Furthermore, identify the importance of an aqueous phase on the reaction mechanism, activity, and selectivity for C-O versus C-C bond cleavage in glycerol and reductive deoxygenation versus hydrogenation of guaiacol over Pt (111) catalyst surfaces.

### DOE Interest

Our desire to better understand chemical reactions at the solid-liquid interface is motivated by the fact that various recently proposed catalytic processes for the conversion of oxygenated hydrocarbons into fuels or chemicals occur in a liquid-phase environment. A key advantage of liquid-phase catalytic processing is that thermally unstable reactant molecules, such as carbohydrates, can be processed at relatively low temperatures at which undesirable thermal degradation reactions are slow and targeted product selectivities are high. In particular, the aqueous-phase processing (APP) of biomass-derived oxygenated hydrocarbons, recently introduced by Dumesic and coworkers, represents a promising catalytic liquid-phase technology for the renewable production of fuels and chemicals. At the same time, our understanding of heterogeneous catalysis in the liquid phase is very limited. And while it is generally known that solvent effects can dramatically change a catalyst's activity and selectivity by changing the free energies of reactants, products, and transition states by stabilizing or destabilizing charged intermediates and transition states (other often less important effects are of dynamical nature such as cage effects or solvent effects on reactant diffusion and energy accumulation and relaxation), it is currently hardly possible to predict the specific effects of a complex liquid environment on a catalyst's activity and selectivity. This again severely inhibits the rational design of heterogeneous catalysts for the conversion of lignocellulosic biomass into chemicals and fuels.

Next, glycerol constitutes a relatively small (i.e., computationally accessible) model molecule for various sugars and is one of the top twelve building block chemicals that can be derived from sugar and converted to high-value bio-based chemicals. As a result, it is an ideal model in the

study of selectivity descriptors that point to catalytic materials that selectively break C-O versus C-C bonds under APP conditions.

Finally, guaiacol is a model molecule with significant resemblance to eugenol, a primary C9 building block of lignin that has been selected for this study because of the potential importance of the lignin-to-chemical conversion, i.e., the conversion of lignin building blocks into renewable benzene and phenol, for the viability of a future biorefinery.

## Recent Progress

Figure 1 illustrates that our QM/MM methodology (PBE functional, TZVP basis set, and TIP3P water model) together with the subtraction scheme and at least two layer thick cluster models is able to compute the heat of reaction of the C-C bond scission of dehydrogenated ethylene glycol in the presence of seven (quasi-randomly oriented) hydrogen bonded water molecules (in TIP3P geometry) on a Pt (111) surface to within 2 kcal/mol of full DFT (VASP) calculations. In other words, even without any force-field parameterization the QM/MM approach with subtraction scheme seems accurate enough for the study of various bond cleavage reactions at the Pt (111)-water interface.

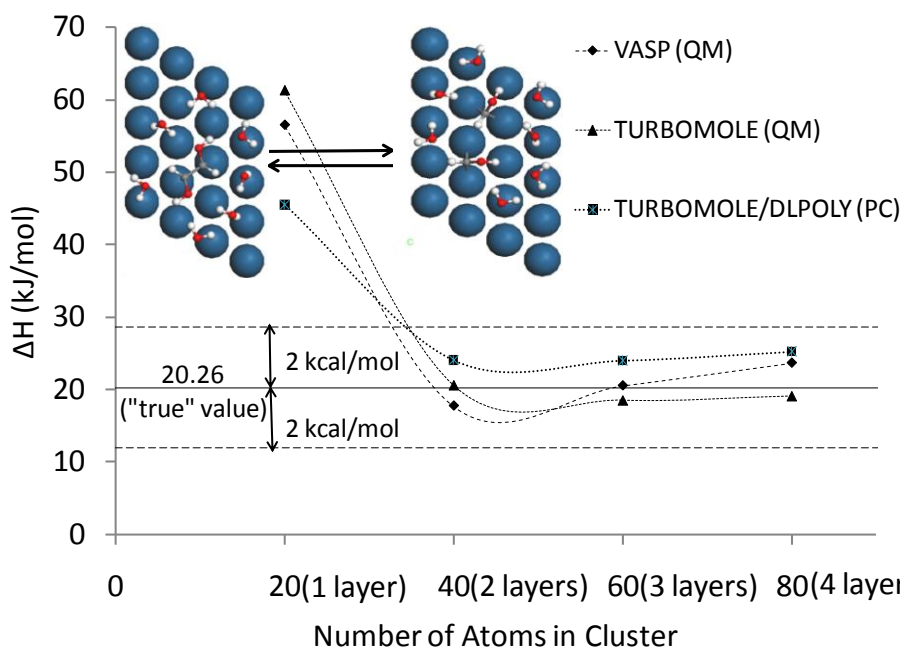


**Fig. 1:** Calculated heat of reaction of C-C bond scission of dehydrogenated ethylene glycol on a Pt (111) surface in the presence of 7 water molecules using the subtraction scheme with various cluster models, electronic structure codes, and water models (QM = all quantum, PC = electrostatic embedding with TIP3P water model). On a 8x8x4 surface model (full DFT with VASP) we calculate  $\Delta H = 20.26$  kJ/mol.

## Future Plans

*Method development and validation:* The focus is on developing a QM/MM force field (electrostatic embedding plus Lennard-Jones potential) for the Pt-H<sub>2</sub>O and adsorbed

glycerol/guaiacol-H<sub>2</sub>O interactions and implementing this force field together with the QM/MM-minimum free energy path method into the ChemShell environment. Furthermore, we plan to continue validating the subtraction scheme and generate water configurations characteristic for the catalyst surface-liquid water interphase. Next, we test free energy convergence with system size and simulation time.

*Reductive deoxygenation of glycerol and guaiacol:* Calculate for both the gas- and aqueous-phase systems reaction free energies for various processes in the conversion of glycerol and guaiacol on the Pt (111) catalyst surface. Calculate the most relevant free energy barriers, develop a microkinetic reactor model, and identify activity and selectivity descriptors. Finally, identify the importance/role of an aqueous phase on the reaction mechanism, activity, and selectivity of various catalytic biomass conversion processes.

## **Publications**

None to report yet.

# Building Block Reactions for the Biomass Refinery of the Future: Aqueous Reductive Upgrading of Acids, Amides, Polyols, and Aromatics

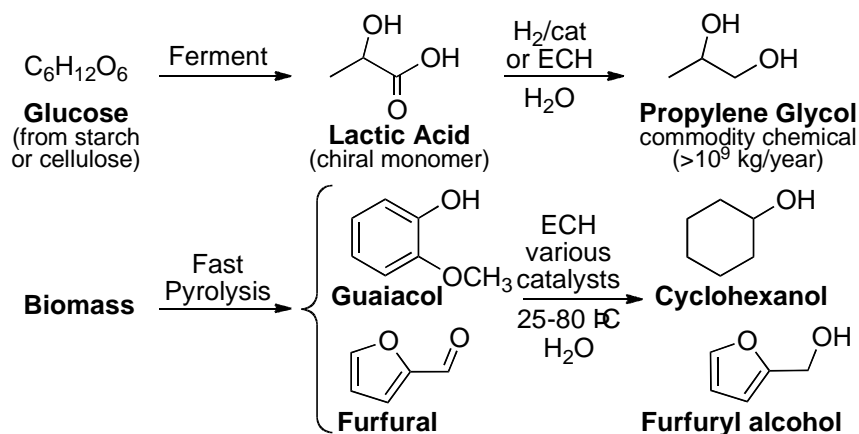
James E. “Ned” Jackson

Department of Chemistry, Michigan State University, East Lansing, Michigan 48824

As fossil resources grow rarer and more expensive, and the impacts of rising atmospheric CO<sub>2</sub> starkly emerge, it is critical to shift the world’s chemical and energy industries to a renewable, carbon-neutral basis. This large-scale challenge is ultimately one of economies—of money, energy, and carbon—and the chemical pathways needed to practically enable the shift.

The scope, boundary conditions, and chemistry of the energy and fuels problem have led our team (NJ + Profs. Dennis Miller, Chem. Engg. and Chris Saffron, Biosys. Engg. & Forestry, MSU) to a three-step approach: (a) use plants to efficiently capture carbon; (b) liquefy the resulting biomass via fast pyrolysis; and (c) use solar-derived electricity to upgrade the “bio-oil” via electrocatalytic reduction, minimizing steps and cost while maximizing energy content and carbon retention in the products. By storing electrical energy as fuels, this capability will also address the timing mismatch between environmental energy capture and electricity usage.

The project draws on our work to develop pathways for the future “biomass refinery.” Our focus—catalytic reductions (hydrogenation/hydrogenolysis, electrolysis) by which organic acids,<sup>1-3</sup> carbohydrates,<sup>4</sup> aromatics, and related feedstocks can be converted to useful chemicals and fuels—is illustrated below with a few examples. Kinetics, isotopic labeling, substituent effects, stereochemistry, catalyst surface adsorption, reactor performance, and process economics have been studied for a variety of substrates and mixtures. Though begun with practical aims, these efforts have turned up a novel C-H activation, modest insights into catalytic mechanisms, and some promising, simple conversions of possible value to the liquid fuels problem.



1. Dalavoy, T. S.; Jackson, J. E.; Swain, G. M.; Miller, D. J.; Li, J.; Lipkowski, J. “Mild electrocatalytic hydrogenation of lactic acid to lactaldehyde and propylene glycol” *J. Catal.* **2007**, *246*, 15-28.
2. Xi, Y.; Jackson, J. E.; Miller, D. J. “Characterizing Lactic Acid Hydrogenolysis Rates in Laboratory Trickle Bed Reactors” *Ind. Eng. Chem. Res.*, **2011**, *50*, 5440–5447.
3. Pimparkar, K.; Jackson, J. E.; Miller, D. J. “Hydrogenation of Amino Acid Mixtures to Amino Alcohols” *Ind. Eng. Chem. Res.* **2008**, *47*, 7648-7653.
4. Peereboom, L.; Jackson, J. E.; Miller, D. J. “Interaction of Polyols with Ruthenium Metal Surfaces in Aqueous Solution” *Green Chem.*, **2009**, *11*, 1979-1986.

## **Nanostructured electrocatalysts for energy conversion reactions**

Thomas F. Jaramillo, Stanford University, Chem. Eng. Dept.

This paper will focus on our efforts to develop catalytic materials for low-temperature, electron-driven production and consumption of chemical fuels. The reactions we seek to catalyze include: (1) H<sub>2</sub> generation from water, (2) the synthesis of alcohols and hydrocarbons from CO<sub>2</sub>, (3) the oxidation of water to O<sub>2</sub>, and (4) the oxygen reduction reaction (ORR). The first three reactions are relevant to the synthesis of chemical fuels from renewable resources (e.g. wind and solar), while reaction (4) is a major technical obstacle at the cathode in fuel cells. Common catalysts for each of these reactions face challenges in terms of activity, selectivity, stability, and/or cost and earth-abundance. Our research group seeks to tailor the surface chemistry of materials through control of morphology, stoichiometry, and surface structure in order to overcome performance barriers, particularly for low-cost, earth-abundant materials.



## Catching the Fish in the Hydrocarbon Pool

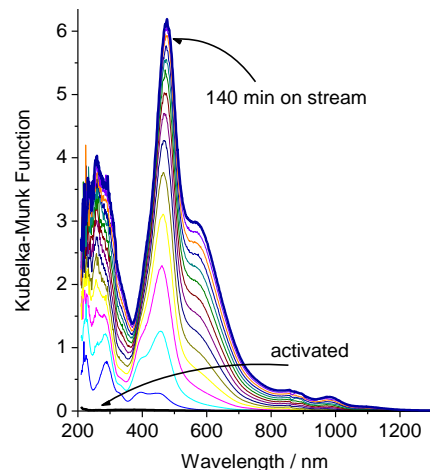
Friederike C. Jentoft

Chemical, Biological, and Materials Engineering, University of Oklahoma  
Norman, OK 73019, USA, Email: fcjentoft@ou.edu

In some catalytic processes, the turnover of the reactant is believed to proceed not on an intrinsic site of the catalyst but on a complex consisting of a surface site and a reactant- or impurity-derived organic co-catalyst. Examples are the conversion of methanol to olefins on molecular sieves via the “hydrocarbon pool mechanism” [1], the dehydrogenation of ethylbenzene on “oxidative condensation products” [2], and the isomerization of alkanes after creation of an “olefin pool” on promoted sulfated zirconia [3]. In these cases, the catalyst has a dual role; it generates the appropriate co-catalyst and provides an adequate environment for interaction of the active complex with further reactant molecules. Disjoining these functions would be advantageous; one reason is that the presence of a pool of molecules will always limit selectivity. An essential element of our strategic approach towards a designed inorganic-organic catalyst is the identification of the relevant organic surface species.

The core of our methodology consists of the characterization of the operating catalyst by various spectroscopies and kinetic measurements. To detect the co-catalyst on the surface amongst spectators and poisons, we correlate spectroscopic information with simultaneously collected performance data. This approach will be illustrated with the help of two examples.

1. Skeletal isomerization of alkanes proceeds on the surface of solid acids over a surprisingly wide temperature range; for example, *n*-butane isomerizes at room temperature on sulfated zirconia, whereas more than 200°C are needed to observe conversion on H-Mordenite. We analyze the surface species during isomerization using primarily in situ UV–vis–NIR spectroscopy, which is highly sensitive towards unsaturated compounds, and IR spectroscopy. Olefins are known to promote alkane isomerization [4,5]; and, interestingly, even addition of ethylene or propylene will enhance conversion of *n*-butane [4]. However, olefins also instigate deactivation. Spectroscopic data (exemplified in figure) allow the identification of surface species; moreover, with suitable experiments the formation of such species (from feed or additives), their reactivity, their location and their function can be ascertained.



Formation of unsaturated surface species on H-Mordenite during *n*-butane isomerization at 683 K.

2. Initial results on the conversion of methanol to olefins on various molecular sieves show interesting correlations between certain surface species and catalyst performance.

1. I. M. Dahl, S. Kolboe, *J. Catal.* **149**, 458–464 (1994).
2. A. E. Lisovskiia, C. Aharonia, *Catal. Rev. - Sci. & Engr.* **36**, 25–74 (1994).
3. M. A. Coelho, D. E. Resasco, E. C. Sikabwe, R. L. White, *Catal. Lett.* **32**, 253–262 (1995).
4. N. Lohitharn, J. G. Goodwin, Jr., E. Lotero, *J. Catal.* **234**, 199–205 (2005).
5. K. B. Fogash, Z. Hong, J. A. Dumesic, *J. Catal.* **173**, 519–529 (1998).

**Multifunctional Oxygen Evolution Electrocatalyst Design and Synthesis**

Students: James Landon, Nilay Inoglu, Ethan Demeter  
Collaborators: Jan Rossmeisl (DTU), Jens Nørskov (Stanford), Israel Wachs (Lehigh)  
Contacts: Carnegie Mellon University, 5000 Forbes Ave, Doherty Hall A207F,  
Pittsburgh, PA 15208; [jkitchin@andrew.cmu.edu](mailto:jkitchin@andrew.cmu.edu)

**Goal**

To use an integrated computational and experimental approach to identify cost-effective oxide-based materials for oxygen evolution electrocatalysis.

**DOE Interest**

Oxygen plays a crucial role in determining the efficiency of many energy technologies. For example in water electrolysis, oxygen is a byproduct in the production of hydrogen, yet it is the efficiency of the oxygen evolution reaction that determines the efficiency of the whole operation. At a scale that is relevant for energy applications, oxygen evolution catalysts must be cheap, active and stable. Oxide-based materials are one of the most promising materials for oxygen evolution electrocatalysis that has already been established in large-scale industrial applications.

**Recent Progress**

*Mixed oxide oxygen evolution electrocatalyst synthesis:* A series of mixed Ni-Fe oxide electrocatalysts at different compositions have been synthesized by three different methods; an evaporation induced self-assembly method that produced powders with surface areas around 10 m<sup>2</sup>/gm, a hard template synthesis that produced powders about 100 m<sup>2</sup>/gm, and dip-coated Ni wire mesh electrodes. The electrocatalysts show a maximum in activity at approximately 10 mol% Fe, independent of the synthesis method (Figure 1). X-ray diffraction shows the Fe is not incorporated into the Ni oxide lattice, implicating surface Fe oxide sites in the enhanced activity. EXAFS shows evidence that the Fe sites experience an increased oxidation state when oxygen evolution potentials are applied (Figure 2).

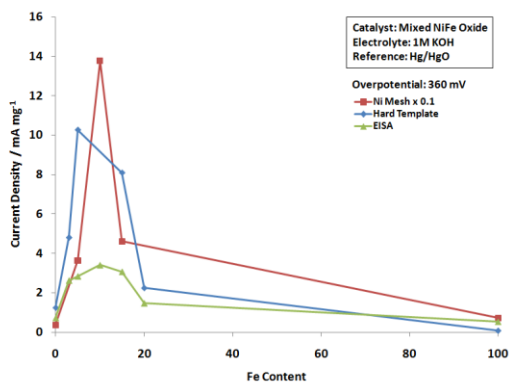


Figure 1. A peak in catalytic activity is observed as a function of Fe content with 10 mol% Fe content having the highest activity. There exists a synergistic effect between Ni and Fe which leads to an increase in the oxygen evolution activity, this effect is shown using three synthesis methods.

#### *Computational modeling of oxide reactivity:*

A key goal in this work is to develop computational models for the electronic structure and reactivity of oxides, in analogy with our understanding of transition metal electronic structure and reactivity. We have recently showed that the *d*-band properties of bulk perovskites such as the *d*-band center and width are correlated (Figure 3) similarly as they are in metals. The significance of this finding is that the electronic structure, specifically the *d*-band properties of the transition metal atom, of perovskites can be easily estimated using a simple tight binding method. Equally significantly, we have shown that some chemical properties of perovskite oxide surfaces are correlated with the surface electronic structure (Figure 4). The significance of these results is that they suggest oxide surfaces can be designed with specific reactivity by choosing a composition that provides a particular average lattice constant and oxidation state.

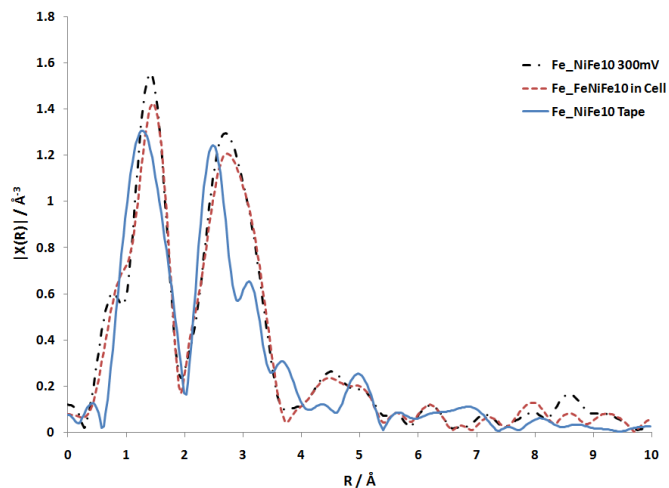


Figure 2. in situ EXAFS data shows that under oxygen evolution conditions, the oxide phases present in the 10 mol% Fe mixed Ni-Fe oxide catalyst become more oxidized. This oxidation increases as a function of applied potential. Small increases in the Fe-Fe bond intensity around 3 Å was also seen.

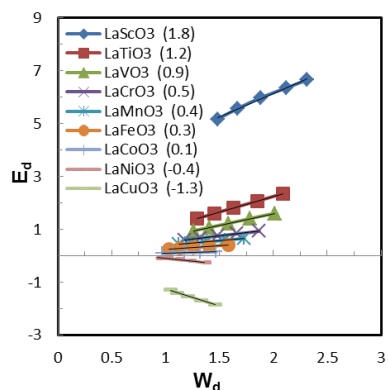


Figure 3. Correlation of d-band width and d-band center for bulk perovskites.

### Future Plans

*in situ vibrational and synchrotron spectroscopy:* We will use these methods to probe the surface state of oxide electrocatalysts under electrochemical control.

*Impact of hybrid functionals on trends of oxide reactivity:* Oxides have complex electronic structures that are not captured accurately with standard functionals. We are planning to reexamine the trends we have observed with standard functionals using newer hybrid functionals to ensure the trends are still valid.

### Publications

1. Isabela C. Man, Hai-Yan Su, Federico Calle-Vallejo, Heine A. Hansen, José I. Martínez, Nilay G. Inoglu, John Kitchin, Thomas F. Jaramillo, Jens K. Nørskov, Jan Rossmeisl, *Universality in Oxygen Evolution Electro-Catalysis on Oxide Surfaces*, ChemCatChem, 3, (2011).
2. Sneha A. Akhade and John R. Kitchin\*, *Effects of strain, d-band filling and oxidation state on the bulk electronic structure of cubic 3d perovskites*, accepted, J. Chem. Phys. Aug. 2011.

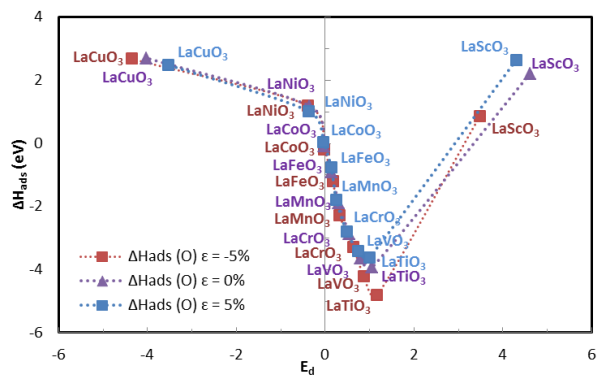


Figure 4. Correlation of adsorption energies of oxygen on (001) perovskite surfaces with the surface d-band center.

### Modifying Catalysts with Functionalized Polysiloxanes

PhD Students: Michael Missaghi, Neema Mashayekhi, John Galloway  
Visiting student: Baosong Fu  
Collaborators: Linda Broadbelt (Northwestern), Mayfair Kung (Northwestern), Jeff Miller (ANL)  
Contacts: Chemical and Biological Engineering Department, Northwestern University, Evanston, IL 60208-3120; hkung@northwestern.edu

#### Goal

Explore the use of polysiloxanes as a versatile platform to form molecules that contain specific functional groups at designated positions, so as to permit design of specific ligands for transition metal complex catalysts and to form precursor molecules in the synthesis of catalysts of designed structures.

#### DOE interest

There is increasing evidence that non-covalent bonding interaction can play an important role in affecting selectivities in a catalytic reaction. However, the spatial orientation and nature of the interaction are essential features that need to be controlled before beneficial effects can be realized, as evidenced by the conformational requirements of enzymes. Successful demonstration of control at the atomic level, via fundamental understanding of the interaction involved and synthesis requirements to generate the desired catalytic structure will enable realization of energy and material-efficient catalytic transformations essential in fuels and chemicals production, including efficient utilization of biomass resources.

#### Recent progress

A series of methylsiloxane compounds of various chain lengths that are functionalized with pyridyl groups at the terminal positions was synthesized successfully and used as ligands in the aerobic Pd(OAc)<sub>2</sub>-catalyzed oxidation of benzyl alcohol to benzaldehyde at 353 K. The effect of lengths of the linear siloxanes was systematically investigated, as was the effect of the attachment point of the pyridine ring (*meta* or *para*). It was found that *meta*-substituted pyridylsiloxanes were generally more effective in protecting the catalyst against Pd agglomeration. For this purpose, the optimal *meta*-pyridylsiloxane ligands had 4 to 6 silicon atoms or 10 silicon atoms for *para*-pyridylsiloxane ligands. The effect could be explained by the different metal-ligand binding affinity and ring-chain and ring size distributions as a function of ligand structure, particularly the ability of the bis-pyridyl ligand to form a mononuclear cyclic complex with Pd.

Polysiloxanes can be designed to contain different ratios of reducing and anchoring functionalities in close proximity. When they are used to aid the synthesis of Pd nanoparticles, the ratio of the Pd loading to the density of anchoring functionality can be used to tune the metal particle size in the nanometer range, permitting independent control of metal particle size and metal loadings. A third functionality, Si-OH, on the same polysiloxane, can be used to connect the polymer to an oxidic support, such as Al<sub>2</sub>O<sub>3</sub>, via condensation with a metal alkoxide

followed by calcination. These silanol groups can be used to anchor oxo-titanium substituents onto the polysiloxanes chain. When this polysiloxanes was used to synthesize supported Au nanoparticles, samples containing Au particles with varying amount of isolated oxo-titanium species at the periphery could be prepared. These catalysts are shown to be able to oxidize propane selectively to acetone, and the activity correlates with the amount of oxo-titanium at the proximity of the Au particles.

### Future plans

New polysiloxanes possessing multiple functional groups will be synthesized to effect region-specific catalytic transformation.

Utilizing the ability to synthesize oxo-metal clusters adjacent to metal nanoparticles, the importance of such oxo-metal-metal interface in catalysis will be elucidated.

### Publications (2009-2011)

1. "Use of Dendrimers in Catalyst Design," Bert D. Chandler, Jeong-Kyu Lee, Harold H. Kung and Mayfair C. Kung, in *Design of Heterogeneous Catalysts, New Approaches based on Synthesis, Characterization and Modeling*, U. Ozkan ed., Wiley-VCH publ., 2009, p.59-81.
2. "Synthesis of Organofunctional Silicon Hydride Halides from Methylchlorosilane," Michael N. Missaghi, Christopher M. Downing, Mayfair C. Kung, and Harold H. Kung, *Organometallics*, **2008**, 27 (23), pp 6364–6366.
3. "Striking Confinement Effect:  $\text{AuCl}_4^-$  Binding to Amines in a Nanocage Cavity," Juan D. Henao, Young-Woong Suh, Jeong-Kyu Lee, Mayfair C. Kung and Harold H. Kung, *J. Amer. Chem. Soc.* **2008**, 130 (48), pp 16142–16143.
4. "Synthesis Strategies to Design Structures for Catalytic Applications," Harold H. Kung and Mayfair C. Kung, *Cuihua Xuebao (Chin. J. Catal.)*, 29(11) (2008) 1187-1192.
5. "Nature-Inspired Design and Synthesis of Heterogeneous and Macromolecular Catalysts," Harold H. Kung and Mayfair C. Kung, *Catalysis Today*, 148 (2009) 2–5.
6. "Aqueous phase epoxidation of 1-butene catalyzed by suspension of Au/TiO<sub>2</sub> +TS-1," Jian Jiang, Harold H. Kung, Mayfair C. Kung, Jiantai Ma, *Gold Bulletin*, 42 (2009) 280-287.
7. "A Engineered Polymer for Controlled Metal Nanoparticle Synthesis," Baosong Fu, Michael N. Missaghi, Christopher M. Downing, Mayfair C. Kung, Harold H. Kung, Guomin Xiao, *Chem Mater.* 2010. **22**(7): p. 2181-2183.
8. "Isotope Labelling Study of CO Oxidation-Assisted Epoxidation of Propene. Implication on Oxygen Activation on Au Catalysts," Jian Jiang, Sean M. Oxford, Baosong Fu, Mayfair C. Kung, Harold H. Kung, Jiantai Ma, *Chem Commun.* 46 (2010) 3791 - 3793.
9. "Bis(pyridyl)siloxane-Pd(II) Complex Catalyzed Oxidation of Alcohol to Aldehyde: Effect of Ligand Tethering on Catalytic Activity and Deactivation Behavior," Michael N. Missaghi, John M. Galloway, and Harold H. Kung, *Applied Catalysis A: General*, **391** (2011) 297–304; 10.1016/j.apcata.2010.09.008.
10. "Bis(pyridyl)siloxane Oligomeric Ligands for Palladium(II) Acetate: Synthesis and Binding Properties," Michael N. Missaghi, John M. Galloway, and Harold H. Kung, *Organometallics*, 29 (2010) 3769-3779.

**Development of physically transparent, predictive structure-performance relationships for rational design of multi-component catalytic materials**

Student: Hongliang Xin, Adam Holewinski, Eranda Nikolla

Contact: Department of Chemical Engineering, University of Michigan,  
[linic@umich.edu](mailto:linic@umich.edu)

Goals

Develop physically transparent, predictive models relating the perturbations of metallic surfaces, by chemical promotion (for example promotion by alkali adsorbates), poisoning, or alloying, and the chemical and catalytic behavior of those surfaces.

DOE Interest

Identical surface sites of neighboring metals in the periodic table of elements bind various adsorbates by up to  $\sim 1$  eV ( $\sim 100$  KJ/mol) difference in adsorption energies, which means that while one metal might be chemically inert for a particular chemical transformation, its first neighbor in the periodic table might be overly chemically active (it gets poisoned by adsorbates) and equally catalytically inefficient. Obviously, the optimal material would be somewhere in between these two extremes. Rapid identification of optimal metal catalysts (for example, alloys or promoted metals) has been hampered by the lack of predictive models that would guide us in the discovery of these catalysts. For example, reliable models to predict how the adsorption energy of an adsorbate on a metal surface changes as the local chemical environment of the adsorption site is changed by the formation of an alloy or intermetallic compound are lacking. The lack of these models, along with the immense size of the phase space of available promoter, poisons, and alloys, makes it almost impossible to identify optimal catalytic materials. The central question we attempt to answer in this project is the following: how does a perturbation of a metal surface (by promotion, poisoning, alloying) affect the chemical activity of the surface? The ultimate objective is to develop simple predictive theories that can guide us in the discovery of novel, more efficient multi-component catalysts. This objective is critical for accomplishing a long-term DOE goal of “heterogeneous catalysis by design”.

Recent ProgressMain accomplishments:

1. We have developed a very general and physically transparent model, based on DFT methodology, which allows us to identify underlying physical mechanisms that govern the changes in the chemical activity of a metal surface as this surface is perturbed. This framework can be used to study various perturbations, including chemical promotion and alloying.
2. This model was utilized to examine the effect of Cs adsorbates (promoters) on the O<sub>2</sub> dissociation reaction on Ag(111). These studies revealed that the main mode by which Cs affects the dissociation of O<sub>2</sub> on Ag(111) is a long-range

electrostatic/polarization interaction between Cs and relevant reaction intermediates. These interactions stabilize the transition state involved in the dissociation of O<sub>2</sub>, therefore lowering the activation barrier. It was shown that these conclusions in general apply for any combination of electronegative adsorbates and electropositive promoters on metal surfaces.

3. We have also studied how a working state of an alkali promoter changes as a function of external conditions, i.e., pressure and temperature of reactants. In this context, we have examined possible formation of Cs-oxide complexes as a function of the chemical potential of gas-phase O<sub>2</sub> (pressure and temperature). We employed ab-initio statistical mechanics and ab initio kinetic Monte Carlo simulations to show that finite temperature and pressure of reactants can significantly affect the mechanism and extent of alkali promotion.
4. We have studied the effect of alkali promoters on the working state of promoted metal surface. The studies showed that alkali promoters can affect not only the kinetic of surface reactions but also the working state of the promoted catalytic material by affecting the on- and sub-surface steady state concentration of adsorbates. More specifically, we found that Cs affects the uptake of oxygen by Ag (and therefore change in the oxidation state of Ag).
5. We have also employed the model, developed under Accomplishment 1, to analyze mechanisms associated with the changes in the chemical activity of metal surfaces in response to the formation of alloys. In this context, we developed a predictive framework that can relate the geometric structure of an alloy to its chemical activity using only measurable physical characteristics of the constitutive metals in their pure unalloyed form. This framework opens up avenues for a very rapid screening for optimal alloys for various chemical transformations.
6. We performed a number of experimental studies verifying and validating the predictive capacity of the proposed framework.
7. The model was used to screen for novel Pt-based catalyst for the electrochemical oxygen reduction reaction (ORR). The model many promising alloy compositions that perform the ORR reaction with lower over-potential losses than pure Pt. Some of the predictions were validated experimentally. The model was also used to outline general strategies for the synthesis of optimal ORR electro-catalysts.
8. The model was also use to identify Ni-based alloy catalysts that show improved resistance to carbon-induced deactivation compared to pure Ni.

#### Publications (2009-2011)

1. H. Xin, S. Linic, Exceptions to the d-band Model of Chemisorption on Metal Surfaces: the Dominant Role of Repulsion between Adsorbate States and Metal d-states, *J. Chem. Phys.*, **132**, 221101, 2010. (Selected to the 2010 Editors' Choice list, highlighting “notable JCP articles published in 2010 that present ground-breaking research”)
2. H. Xin, N. Schweitzer, E. Nikolla, Suljo Linic, Developing Relationships between the Local Chemical Reactivity of Alloy Catalysts and Physical Characteristics of Constituent Metal Elements, *J. Chem. Phys.*, **132**, 111101, 2010.
3. N. Schweitzer, H. Xin, E. Nikolla, Suljo Linic\*, “Establishing relationships between the geometric structure and chemical reactivity of alloy catalysts based on their measured electronic structure“, *Topic in Catalysis*, 2010, **53**, 348,



4. E. Nikolla, J. Schwank, S. Linic, Improving the tolerance of Ni electro-catalysts to carbon-induced deactivation in direct electrochemical oxidation of hydrocarbons on SOFCs by alloying, **Journal of Electro-chemical Society**, 156(11), B1312-B1316, 2009
5. E. Nikolla, J. Schwank, and S. Linic\*, “Measuring and Relating the Electronic Structures of Nonmodel Supported Catalytic Materials to Their Performance, **Journal of the American Chemical Society**, 2009, 131 (7), pp 2747–2754
6. E. Nikolla, J. Schwank, and S. Linic\*, “Comparative study of the kinetics of methane steam reforming on supported Ni and Sn/Ni alloy catalysts: the impact of the formation of Ni alloy on chemistry”, **Journal of Catalysis**, 2009, 263, 220–227
7. D. Ingram, S. Linic, "First-Principles Analysis of the Activity of Transition and Noble Metals in the Direct Utilization of Hydrocarbon Fuels at Solid Oxide Fuel Cell Operating Conditions", **Journal of Electrochemical Society**, 156, B1457, 2009.
8. P. Christopher, H. Xin, S. Linic, Visible light enhanced catalytic oxidation reactions on plasmonic silver nanostructures, **Nature Chemistry**, 3, 467. 2011
9. D. B. Ingram, S. Linic, ‘Water splitting on composite plasmonic-metal/semiconductor photo-electrodes: Evidence for selective plasmon induced formation of charge carriers near the semiconductor surface”, **Journal of the American Chemical Society**, 133, 5202, 2011
10. N. Schweitzer, J. Schaidle, E. Obiefune, X. Pan, S. Linic, L. Thompson, High Activity Carbide Supported Catalysts for Water Gas Shift, **Journal of the American Chemical Society**, 133, 2378, 2011
11. S. Linic\*, P. Christopher, “Overcoming limitation for the design of selective heterogeneous catalysts by manipulating shape and size of catalytic particles: Epoxidation reactions on silver (Ag)”, **ChemCatChem**, 2, 1061, 2010.
12. P. Christopher, D. B. Ingram, S. Linic, Enhancing photo-chemical activity of semiconductor nanoparticles with optically active Ag nano-structures: Photo-chemistry mediated by Ag surface plasmons, **J. Phys. Chem. C**, 114, 9173, 2010.

**Novel Photocatalysts with One-Dimensional and Two-Dimensional Nanostructures**

**Additional co-PIs:** Douglas Doren, University of Delaware, Chemistry and Biochemistry.

**Students:** Bharat Bhopana, Heather Schmidt

**Contacts:** Center for Catalytic Science and Technology, Department of Chemical Engineering and Department of Chemistry and Biochemistry, University of Delaware, Newark, DE 19716. 302-831-1261, [lobo@udel.edu](mailto:lobo@udel.edu)

**Collaborators:** Prof. Tatyana Polenova, Department of Chemistry and Biochemistry, University of Delaware

**Goal**

To develop novel photocatalytic materials capable of using a portion of the visible light spectrum to facilitate the partial and total oxidation of organic compounds in the gas and liquid phase.

**DOE Interest**

Semiconductor photocatalysis is one of the most promising approaches for the destruction or transformation of hazardous chemicals. A major emphasis has been centered on TiO<sub>2</sub> photocatalysis as TiO<sub>2</sub> is abundant, inexpensive, and useful in the destruction of many types of substances. Despite its many advantages, TiO<sub>2</sub> has the serious disadvantage that its bandgap (~3.2 eV) is relatively high and only a small fraction of the photons from sunlight are used efficiently (<10%). We are developing novel photocatalyst compositions that have bandgaps below 3.0 eV following evidence by the Domen's group that bimetallic oxy nitrides (and related compounds) have lower bandgaps than their oxide counterparts while maintaining most of their photocatalytic activity.

**Recent Progress**

*Structure-Property Relations of Spinel Zn-Ga oxy-nitrides:* Sol-gel methods have been used to synthesize high surface area spinel ZGON photocatalysts with controllable band gaps (**Figure 1**). The band gap decrease to less than 3 eV with increasing nitrogen content (< 3 wt%) and these photocatalysts are active in visible light ( $\lambda > 420$  nm) for the degradation of cresol and rhodamine B. Density functional theory calculations show that this band gap reduction is associated with hybridization between the dopant N 2p states with Zn 3d orbitals at the top of the valence band. The incorporation of nitrogen reduces the uniformity of the local structure of the spinel ZGONs, as reflected in X-ray absorption spectra and Raman measurements relative to zinc gallate, suggesting the presence of defects. The oxynitrides exhibit faster photocatalytic rates of reaction than the oxide precursor. The degradation mechanisms were determined to be via the attack by hydroxyl radicals and holes for rhodamine B and cresol, respectively. Addition of Pt as a co-catalyst increased the rate of photo degradation.

*Tin(II)-doped Titania Photocatalysts:* We have demonstrated visible-light photocatalytic activity of Sn<sup>2+</sup> doped TiO<sub>2</sub>. The catalysts are prepared from the reaction of titanium butoxide and several tin precursors at 80°C in aqueous solutions. Samples synthesized with SnCl<sub>2</sub> have lower band gaps (red-shifted to the visible region) with respect to anatase TiO<sub>2</sub>. The catalysts are isostructural to anatase TiO<sub>2</sub> even at the highest loadings of Sn<sup>2+</sup>. The

majority of surface cation sites are tin, with a small fraction of tin also incorporated in the bulk particles. The experiments also indicate the presence of chlorine which also influence the optical and catalytic properties as confirmed by comparison to materials prepared using bromide precursors. These catalysts are photocatalytically active for the degradation of organic molecules with rates higher than the standards (P25 TiO<sub>2</sub>) and also evidenced from the generation of hydroxyl radicals using visible light. This protocol could be extended to incorporate Sn<sup>2+</sup> into other oxide semiconductors to prepare photocatalysts with interesting electronic properties.

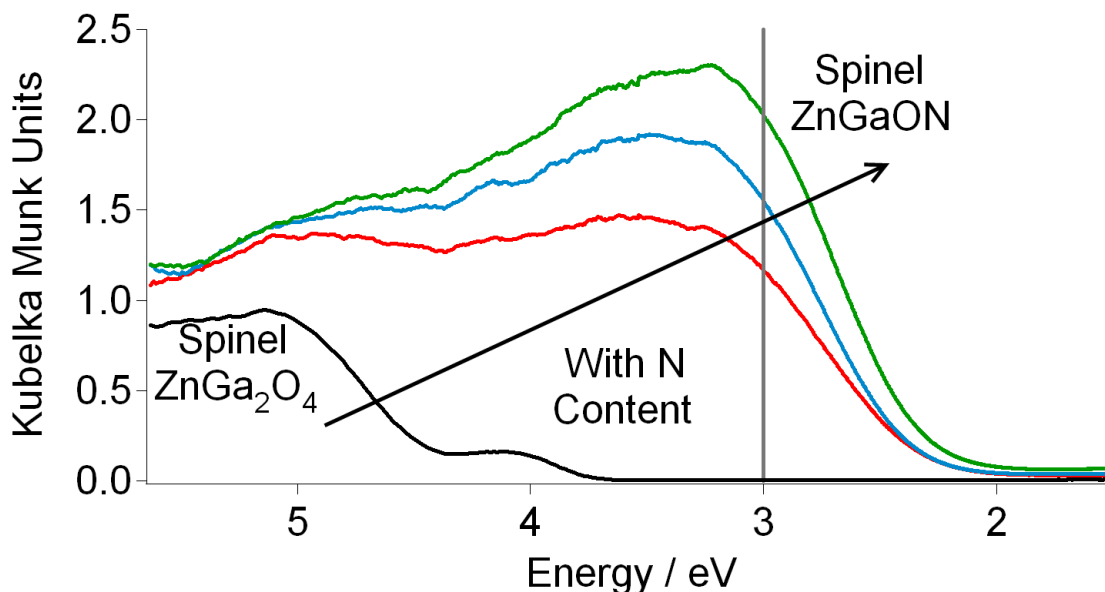


**Figure 1:** UV-vis Spectra of Zinc-Gallium Oxonitrides Prepared at Different Nitridation Temperatures.

*Photocatalytic Properties of Zinc Germanates:* We developed protocols for the hydrothermal synthesis of zinc germanate (Zn<sub>2</sub>GeO<sub>4</sub>) materials having a variety of morphologies and photochemical properties in surfactant, template and catalyst free conditions. A systematic variation of synthesis conditions and detailed characterization using X-ray diffraction, ultraviolet-visible diffuse reflectance spectroscopy, Raman spectroscopy, electron microscopy, X-ray photoelectron spectroscopy, and small angle X-ray scattering led to a better understanding of the growth of these particles from solution. At 140°C, the zinc germanate particle morphology changes with pH from flower-shaped at pH 6.0, to poly-disperse nano-rods at pH 10 when the Zn to Ge ratio in the synthesis solution is 2. When the Zn to Ge ratio is reduced to 1.25, mono-disperse nano-rods could be prepared at pH 7.5. Photocatalytic tests show that Zn<sub>2</sub>GeO<sub>4</sub> nano-rods (by weight) and flower shaped (by surface area) are the most active for methylene blue dye degradation among the synthesized zinc germanate materials.

### Future Plans

*Water Splitting and CO<sub>2</sub> Reduction Using Novel Photocatalysts:* We are investigating the application of three new materials (spinel ZGONs, SnO<sub>x</sub>-TiO<sub>2</sub> anatase and SnO<sub>x</sub>-ZGO) for water splitting using UV and visible light.

*Electronic Structure Calculations of Mixed-Metal Oxynitrides:* We are investigating the electronic structure of the novel ZGON spinel materials using cluster and periodic models to understand what is the impact of the nitrogen and gallium coordination on the bandgap and potential for photocatalytic activity.

**Publications (2009-2011)**

Sole Funding by DOE-BES (this grant)

- (1) Boppana, V.B.R., Doren, D. J., **Lobo, R. F.**, "Structure Analysis and Photocatalytic Properties of Spinel Zinc Gallium Oxy-Nitrides", *Chem. Eur. J.*, **2011**, in press.
- (2) Boppana, V.B.R., Lobo, R. F., " SnO<sub>x</sub>-ZnGa<sub>2</sub>O<sub>4</sub> Photocatalysts with Enhanced Visible Light Activity", *ACS Catal.*, **2011**, accepted.
- (3) Boppana, V.B.R., Doren, D. J., **Lobo, R. F.**, "Photocatalytic degradation of organic molecules on mesoporous visible-light-active Sn(II) doped titania", *J. Catal.*, **2011**, in press..
- (4) Boppana, V.B.R., Doren, D. J., **Lobo, R. F.**, "Analysis of Ga coordination environment in novel spinel Zinc Gallium Oxy-nitride photocatalyst", *J. Mater. Chem.*, **2010** 20 9787-9797
- (5) Boppana, V.B.R.; Hould, N.D.; Lobo, R.F.; "Synthesis, characterization and photocatalytic properties of novel zinc germanate nano-materials", *J. Sol. State Chem.* **2011**, 184, 1054-1062.
- (6) Boppana, V.B.R., Doren, D. J., **Lobo, R. F.**, "A spinel oxinitride with visible light photocatalytic activity", *ChemSusChem*, **2010**, 3, 814-817.
- (7) Ooms, K, Polenova, T., Shough, A.M., Doren, D.J., Nash, M.J., Lobo R. F., "Identification of mixed valence vanadium in ETS-10 using EPR, 51-V solid-state NMR and DFT studies", *J. Phys. Chem. C.*, **2009**, 113, 10477-10484.

**CATALYSIS SCIENCE INITIATIVE: From First Principles Design to Realization of Bimetallic Catalysts for Enhanced Selectivity**

Additional PIs: Mark Barteau, Jochen A. Lauterbach, Raul F. Lobo, Dionisios G. Vlachos (Delaware); Manos Mavrikakis, James A. Dumesic (Wisconsin), Richard Crooks (U. of Texas) and Younan Xia (Washington U.)

Postdocs and Graduate Students: Apoorva Kulkarni, Stephen Edie, Beth Cheney and Mellinger, Zachary (Delaware); Surojit Pande (Texas); Falk Einhorn, Sha Li (Wisconsin), Hui Zang (Wash. U.).

Collaborators: Radoslav Adzic (BNL), Flemming Besenbacher (U of Aarhus, Denmark), Anatoly Frenkel (Yeshiva U. and the National Synchrotron Light Source), Graeme Henkelman (UT Austin), Valeri Petkov (Central Michigan U. and the Advanced Photon Source), Jens Norskov and Jan Rossmeisl (DTU), Bryan Eichhorn (U of Maryland), Matthew Neurock (U of Virginia), Jeff Greeley (ANL).

Contact: Raul F. Lobo, Center for Catalytic Science and Technology, Department of Chemical Engineering, University of Delaware, Newark, DE 19716, [lobo@udel.edu](mailto:lobo@udel.edu), 302-831-8056.

**Goal**

The goal of this project is to demonstrate a new paradigm for design for improving catalyst selectivity. Our approach is to enhance selectivity by design via the integration of four research components: Theory and Modeling; Surface Science; Materials Synthesis, Characterization and Scale-up; and Catalyst and Reactor Dynamics and Optimization. This integrative approach is being applied to catalytic reactions where bimetallic catalysts may be advantageous.

**DOE Interest**

“Catalysis by design” has been a dream for decades. To specify the composition and structure of matter to effect a desired catalytic transformation with desired and predicted rate and selectivity remains a monumental challenge, especially in heterogeneous catalysis. Our research thrusts have been chosen not only for their practical and scientific relevance, e.g. for more efficient and sustainable chemicals and fuels production, but also because they provide a foundation for developing and exploring broadly applicable principles and strategies for catalyst design.

**Recent Progress**

*Low-Temperature Water-Gas-Shift Reaction:* Our work to date has elucidated novel catalysis for H<sub>2</sub> and alkanes production from biomass derived carbohydrates. Furthermore, we have shown that this catalytic chemistry is analogous to chemistry found at the surface science level, both with experiments and theory in collaboration with other members of this team. In addition, systematic fundamental studies of low temperature Water-Gas-Shift (WGS), central in fine-tuning selectivity to H<sub>2</sub> versus alkanes in carbohydrate reforming, have identified the main reaction path and specific reactivity descriptors.

Recently, we investigated the role of *alkali promoters* for low temperature WGS. Pt-group based catalysts are non-pyrophoric and stable, and might make ideal candidates for portable hydrogen-related applications. In particular, experimental results show that alkali ions (e.g.: sodium or

potassium) activate Pt supported on Al<sub>2</sub>O<sub>3</sub> or SiO<sub>2</sub>. Alkali promotion leads to the formation of *sub-nanometer clusters* containing partially oxidized Pt (Pt<sup>2+</sup>, Pt<sup>4+</sup>). Using DFT calculations, we sought to narrow down possibilities for the nature of the active site of this novel catalyst by screening Pt<sub>w</sub>K<sub>x</sub>O<sub>y</sub>OH<sub>z</sub> clusters to fit experimentally measured properties. Our results identified a PtK<sub>6</sub>O<sub>4</sub>(OH)<sub>2</sub> structure as the most promising active site, but there are other structures that have similar characteristics, which could be responsible for the remarkable WGS activity.

*Propylene Epoxidation over Silver Catalysts:* In the first part of our investigations we established the network of reactions that limit the selectivity of propylene epoxidation by investigating the isomerization and decomposition of PO over silver and Cs-promoted silver catalysts. The results are illustrated in Figure 2. Propylene oxide reacts under anaerobic and aerobic conditions to through the formation of oxametallacycles 1 and 2 (OMC1 and OMC2). These surface intermediates can desorb to form the epoxide, isomerize to form propanal or acetone, or dehydrogenate by loss of an allylic hydrogen.

All these secondary reaction pathways of the OMC intermediates quickly produce carbon dioxide in an aerobic environment.

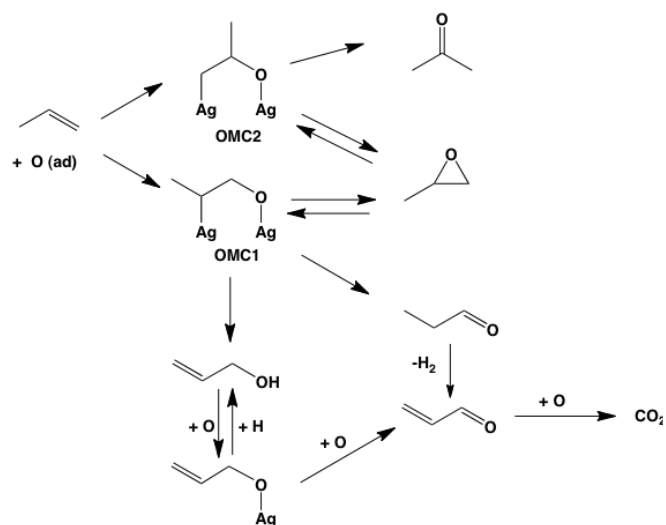


**Figure 2.** Proposed mechanism of epoxidation and decomposition of propylene over silver catalysts.

*Group-additivity scheme for thermochemical properties of reactive surface species.* To accelerate the design of improved heterogeneous catalysts for selective oxidation of ethylene and propylene, we need to model the relevant surface chemistries accurately and completely. The non-selective combustion of ethylene and propylene to CO<sub>2</sub> and water proceeds through a complex network of reactions involving potentially hundreds of surface-bound chemical intermediates. We require accurate estimates of the thermochemical properties (standard state enthalpy, entropy, and heat capacity) for these species, which can be extremely difficult and

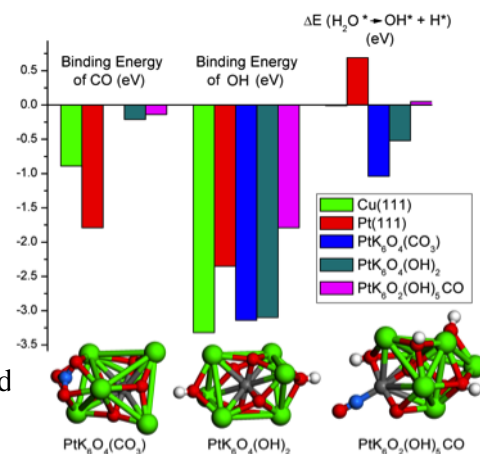


**Figure 1.** WGS thermochemical properties for active site models versus extended surfaces.

Based on the fact that to achieve high selectivity fast desorption of the OMC is required, we investigated catalysts containing metal promoters showing an ability to reduced the heat of adsorption of such intermediates. We also investigated the addition of dienes—in highly diluted form—to poison the surface such that dehydrogenation of the allylic carbon is inhibited. The combination of heavy Cs promotion and the addition of ppm levels of butadiene lead to unprecedented increases of selectivity in our catalysts to levels in excess of 35%.

costly to obtain experimentally. Instead, we obtain these properties from first principles using quantum chemistry calculations based on Density Functional Theory (DFT). Although computation of thermochemical properties from DFT is more feasible than their experimental measurement, the amount of computation required is still staggering, even for a single surface.

To reduce the computational burden, we are researching a group-additivity scheme based on the formal approach taken by Benson *et.al.*<sup>1</sup> in which thermochemical properties are estimated by summing contributions from constituent functional groups. We have extended Benson's existing scheme for gas phase molecules to include groups unique to surface-bound species. Our methods also enable us to compute the required group contributions using properties of a representative subset of species. A sample of our results is illustrated for the Pt(111) surface in Figure 5. The estimates obtained from group-additivity are in strong agreement with the originally-calculated values, giving strong confidence in the applicability of group-additivity to species not in the original fitting set. This drastically reduces the computational burden for computing surface intermediate thermochemical properties.

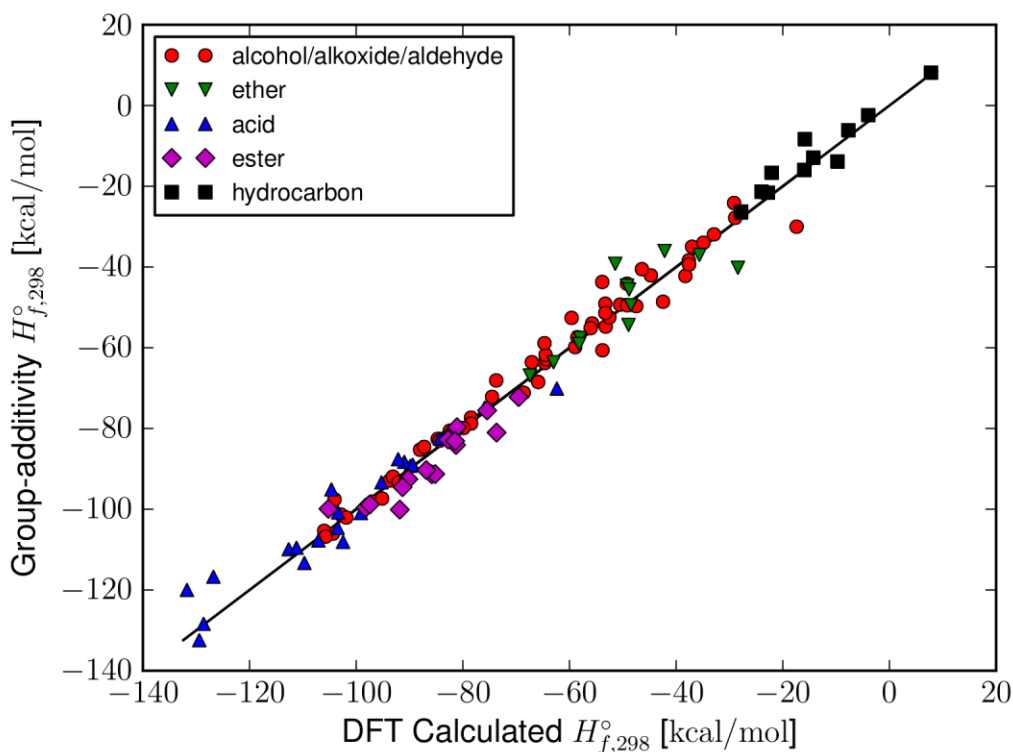


**Figure 3** Parity plot comparing DFT calculated enthalpies of Pt(111) surface-bound species to estimates from group-additivity.

*Product Distribution from Hydrogenation of Allyl Alcohol on Size-Specific Monometallic Dendrimer-Encapsulated Nanoparticles.* Our model hydrogenation reaction was the homogeneous hydrogenation of allyl alcohol (AA) catalyzed by monometallic DENs. We tested three different monometallic DENs, Pd, Pt, and Au DENs, and varied the atomic sizes (39, 55, 79, 147, 200, and 225 atoms), in the size range of 1.2 to 1.9 nm. The product distribution of hydrogenation of allyl alcohol catalyzed by the three monometallic (Pd, Pt, and Au) DENs was

<sup>1</sup> Benson, Sidney W.; *Thermochemical Kinetics, 2<sup>nd</sup> ed.*; Wiley: New York, 1976

investigated using gas chromatography (GC) and found to vary with nanoparticle metal and size. Of the catalysts studied the Pd DENs demonstrated the highest conversion rate. Specifically, Pd DENs convert ~90% of allyl alcohol into *n*-propanol while ~10% converts to propionaldehyde. With Pt DENs, only *n*-propanol is detected as a product. Au DENs demonstrated no catalytic activity towards the hydrogenation of AA.

Studies performed to check the stability of the DENs and the reaction components (ethanol, allyl alcohol, propyl alcohol, and propionaldehyde). The chromatogram shown in Figure 1A indicates complete stability under the reaction conditions used. Figure 1B shows the GC plots for hydrogenation of AA using Pd<sub>147</sub> DENs. According to these results, ~25 min is required for complete conversion of AA to *n*-propanol and propionaldehyde. A complete set of data for the three different monometallic DENs has now been obtained, and a manuscript reporting the results is in preparation.

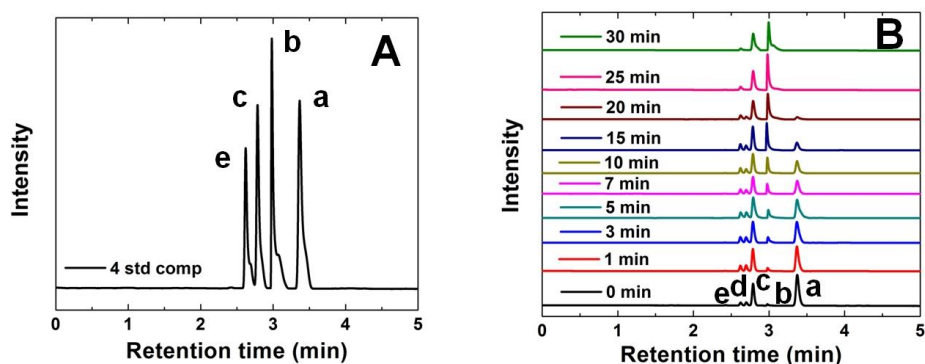


**Figure 3.** GC curve of (A) the four reaction components and (B) hydrogenation of AA using Pd<sub>147</sub> DENs. Here, a: allyl alcohol, b: *n*-propanol, c: ethanol, d: unknown, and e: propionaldehyde.

## Future Plans

*Water-Gas-Shift Reaction:* 1) elucidating structure and reactivity of metal/metal oxide interfaces by studying the model system of Pt/FeO<sub>x</sub> with various probe molecules involved in biomass conversion, and in particular the WGS reaction. This effort entails strong interactions with the group of Prof. Flemming Besenbacher in Aarhus University, Denmark, performing STM, and other surface science experiments, and DFT calculations, performed at UW.

*Propylene Epoxidation:* Analyze the energetics of selective and unselective reaction paths of propylene epoxidation on Ag(111), using a combination of DFT calculations, performed at UW, and experiments, performed at UD. We plan to focus on modifications to the existing Cs/butadiene/Ag-based catalysts to improve the selectivity of the propylene epoxidation reaction. We will investigate the addition of chlorine-containing molecules such as dichloroethane to maintain a constant concentration of chlorine on the surface of the silver catalysts. In the case of ethylene epoxidation this strategy has shown to be very effective to increase selectivity and reduce the combustion of ethylene. We will also investigate the mechanism of propylene epoxidation in the Cs/butadiene/Ag-based catalysts using propylene selectively deuterated at different positions. These investigations will quantify the importance of the 1-2 hydride shift in



OMC1 and OMC2 towards the formation of the ketone moiety, one of the important and undesirable channels for combustion of the propylene.

*Selective Hydrogenation of Allyl-Alcohol:* The focus is now on the hydrogenation of allyl alcohol and calculation of TOF (normalized to the number of moles of Pd) for this reaction. The following studies are proposed. First, the catalytic hydrogenation of allyl alcohol will be studied using different sizes of mono- and bimetallic DENs. Second, we will calculate the TOF with respect to the size and different atoms (face, surface, and edge etc.). Third, we will examine how geometrical changes to bimetallic Pd/Au and Pd/Pt DENs the nanoparticles (core-shell and alloy) affect the hydrogenation reaction. Finally, after successful completion of the reaction, the product distribution will be characterized by GC,  $^1\text{H}$ , and  $^{13}\text{C}$  NMR. Furthermore, we will use the same bimetallic DENs for selective hydrogenation of  $\alpha,\beta$ -unsaturated aldehydes and conjugated alkenes to allyl alcohols and monoalkenes, respectively.

### **Publications (2009-2011):**

- (1) Bilbao, D.; Lauterbach, J. "Gas-phase coupling of reactive surfaces by oscillating reactant clouds", *Journal of Catalysis* **2010**, 272, 309.
- (2) Cheney, B. A.; Lauterbach, J. A.; Chen, J. G. G. "Reverse micelle synthesis and characterization of supported Pt/Ni bimetallic catalysts on gamma-Al<sub>2</sub>O<sub>3</sub>", *Applied Catalysis a-General* **2011**, 394, 41.
- (3) Dellamorte, J. C.; Barteau, M. A.; Lauterbach, J. "Opportunities for catalyst discovery and development: Integrating surface science and theory with high throughput methods", *Surface Science* **2009**, 603, 1770.
- (4) Dellamorte, J. C.; Lauterbach, J.; Barteau, M. A. "Palladium-silver bimetallic catalysts with improved activity and selectivity for ethylene epoxidation", *Applied Catalysis a-General* **2011**, 391, 281.
- (5) Fickel, D. W.; D'Addio, E.; Lauterbach, J. A.; Lobo, R. F. "The ammonia selective catalytic reduction activity of copper-exchanged small-pore zeolites", *Applied Catalysis B-Environmental* **2011**, 102, 441.
- (6) Ford, D. C.; Nilekar, A. U.; Xu, Y.; Mavrikakis, M. "Partial and complete reduction of O<sub>2</sub> by hydrogen on transition metal surfaces", *Surface Science* **2010**, 604, 1565.
- (7) Huang, W.; Li, A.; Lobo, R. F.; Chen, J. G. "Effects of Zeolite Structures, Exchanged Cations, and Bimetallic Formulations on the Selective Hydrogenation of Acetylene Over Zeolite-Supported Catalysts", *Catalysis Letters* **2009**, 130, 380.
- (8) Knudsen, J.; Merte, L. R.; Grabow, L. C.; Eichhorn, F. M.; Porsgaard, S.; Zeuthen, H.; Vang, R. T.; Laegsgaard, E.; Mavrikakis, M.; Besenbacher, F. "Reduction of FeO/Pt(111) thin films by exposure to atomic hydrogen", *Surface Science* **2010**, 604, 11.
- (9) Knudsen, J.; Merte, L. R.; Peng, G. W.; Vang, R. T.; Resta, A.; Laegsgaard, E.; Andersen, J. N.; Mavrikakis, M.; Besenbacher, F. "Low-Temperature CO Oxidation on Ni(111) and on a Au/Ni(111) Surface Alloy", *Acs Nano* **2010**, 4, 4380.
- (10) Lonergan, W. W.; Vlachos, D. G.; Chen, J. G. G. "Correlating extent of Pt-Ni bond formation with low-temperature hydrogenation of benzene and 1,3-butadiene over supported Pt/Ni bimetallic catalysts", *Journal of Catalysis* **2010**, 271, 239.
- (11) Merte, L. R.; Grabow, L. C.; Peng, G.; Knudsen, J.; Zeuthen, H.; Kudematsch, W.; Porsgaard, S.; Laegsgaard, E.; Mavrikakis, M.; Besenbacher, F. "Tip-Dependent Scanning Tunneling Microscopy Imaging of Ultrathin FeO Films on Pt(111)", *Journal of*

- Physical Chemistry C* **2011**, *115*, 2089.
- (12) Merte, L. R.; Knudsen, J.; Grabow, L. C.; Vang, R. T.; Laegsgaard, E.; Mavrikakis, M.; Besenbacher, F. "Correlating STM contrast and atomic-scale structure by chemical modification: Vacancy dislocation loops on FeO/Pt(111)", *Surface Science* **2009**, *603*, L15.
- (13) Peng, G. W.; Merte, L. R.; Knudsen, J.; Vang, R. T.; Laegsgaard, E.; Besenbacher, F.; Mavrikakis, M. "On the Mechanism of Low-Temperature CO Oxidation on Ni(111) and NiO(111) Surfaces", *Journal of Physical Chemistry C* **2010**, *114*, 21579.
- (14) Saliccioli, M.; Chen, Y.; Vlachos, D. G. "Microkinetic Modeling and Reduced Rate Expressions of Ethylene Hydrogenation and Ethane Hydrogenolysis on Platinum", *Industrial & Engineering Chemistry Research* **2011**, *50*, 28.
- (15) Zhai, Y. P.; Pierre, D.; Si, R.; Deng, W. L.; Ferrin, P.; Nilekar, A. U.; Peng, G. W.; Herron, J. A.; Bell, D. C.; Saltsburg, H.; Mavrikakis, M.; Flytzani-Stephanopoulos, M. "Alkali-Stabilized Pt-OH<sub>x</sub> Species Catalyze Low-Temperature Water-Gas Shift Reactions", *Science* **2010**, *329*, 1633.
- (16) Zhang, H.; Jin, M. S.; Wang, J. G.; Li, W. Y.; Camargo, P. H. C.; Kim, M. J.; Yang, D. R.; Xie, Z. X.; Xia, Y. A. "Synthesis of Pd-Pt Bimetallic Nanocrystals with a Concave Structure through a Bromide-Induced Galvanic Replacement Reaction", *Journal of the American Chemical Society* **2011**, *133*, 6078.
- (17) Zhang, H.; Li, W. Y.; Jin, M. S.; Zeng, J. E.; Yu, T. K.; Yang, D. R.; Xia, Y. N. "Controlling the Morphology of Rhodium Nanocrystals by Manipulating the Growth Kinetics with a Syringe Pump", *Nano Letters* **2011**, *11*, 898.
- (18) Zhang, H.; Xia, X. H.; Li, W. Y.; Zeng, J.; Dai, Y. Q.; Yang, D. R.; Xia, Y. N. "Facile Synthesis of Five-fold Twinned, Starfish-like Rhodium Nanocrystals by Eliminating Oxidative Etching with a Chloride-Free Precursor", *Angewandte Chemie-International Edition* **2010**, *49*, 5296.

## Supported Organometallic Complexes: Surface Chemistry, Spectroscopy, Catalysis and Homogeneous Models

DE-FG02-86ER13511

Tobin J. Marks

Postdoc: Maximilliano Delferro, Changle Chen  
Graduate students: Linda Williams, Staci Wegener, Michael Weberski  
Collaborators: Ignazio Fragala, Alessandro Motta (U. Catania), Alceo Macchioni, Cristiano Zuccaccia (U. Perugia), Jeffery Miller, Neng Guo, Chris Marshall (Argonne Nat. Lab.), Michael Lanagan (Penn. State U.), Peter Nickias (Dow Chemical).  
Contact information: Department of Chemistry and the Center for Catalysis and Surface Science, Northwestern University, Evanston IL 60208-3113  
[t-marks@northwestern.edu](mailto:t-marks@northwestern.edu) <http://chemgroups.northwestern.edu/marks/>

Date of execution/start: November 15, 2009

### Research Goals and Specific Objectives

Model, understand, elaborate, and exploit pathways by which organometallic molecules of varying nuclearity undergo chemisorptive activation and catalytic activity enhancement on selected solid surfaces. Such processes closely connect to real-world, large-scale industrial hydrocarbon processes and to manufacturing cleaner, greener, more environmentally acceptable products, including those from renewal resources. Research combines synthesis of catalysts, chemisorptive surface chemistry, homogeneous analogue catalysis, structural analysis, and computation, and involves collaboration with national laboratories and industry. Objectives in the past year were: 1) Investigate mononuclear and binuclear organometallic chemisorption on “super Brønsted acid” oxides, 2) Synthesize and characterize mononuclear and polynuclear catalyst precursors for chemisorption and homogeneous catalysis, 3) Use this information to produce new types of efficient energy storage materials, 4) Computationally model both chemisorbed catalysts and their reactivity modes.

### DOE Interest

The present catalyst synthesis and characterization activities connect directly with the efficiency, selectivity, and “greenness” of real-world industrial processes that are currently practiced on a huge scale, and to the ability of these processes to produce cleaner, more environmentally acceptable products. This includes processes using renewable, bio-feedstocks such as polyethylene production from sugar cane, and those which produce high-capacity energy storage materials.

**Recent Progress.** *Metal Hydrocarbyl Chemisorption on Sulfated Metal Oxide Surfaces.* Electrophilic Zr surface alkyls are created in high coverages by chemisorptive protonolysis of group 4 alkyls, and these species exhibit extreme activity for arene and olefin hydrogenation as well as for olefin polymerization. Benzene hydrogenation rates exceed that of any catalyst yet discovered. The kinetics and mechanism were characterized, revealing that ~ 97% of the surface Zr species are catalytically significant--unusual for any heterogeneous catalyst. Density functional theory (DFT) analysis of the sulfated  $\gamma$ -alumina (AlS) surface as well as the pathway for  $\text{Cp}_2\text{Zr}(\text{CH}_3)_2$  (**2**; Cp =  $\eta^5\text{-C}_5\text{H}_5$ ) chemisorption on the AlS surface are reported. The surface coverage pathway to sulfate monolayer formation is first analyzed as is the subsequent thermal treatment/activation process under AlS synthetic conditions. Using the most stable configuration of the sulfated surface as the chemisorption substrate, it is found that Zr-CH<sub>3</sub> protonolysis yields cationic species which interact with the surface sulfate species to form anchored cations, electrostatically bound to surface sulfate anions. Changes in sulfate vibrational spectra on zirconocene chemisorption are in good agreement with experiment. Zr K-edge X-ray absorption fine structure spectroscopic (XAFS) characterization

of Cp<sub>2</sub>ZrH<sub>2</sub> (**1**), **2**, Cp'<sub>2</sub>ZrH<sub>2</sub> (**3**) (Cp' = η<sup>5</sup>-(CH<sub>3</sub>)<sub>5</sub>C<sub>5</sub>) and Cp'ZrMe<sub>3</sub> (**4**) and as well as their AlS-supported product catalysts **1**/AlS, **3**/AlS and **4**/AlS is used to elucidate the metrical nature of the Zr···AlS interaction. XAFS data analysis yields key structural information: the supported organozirconium centers have electrostatic interactions with the surface sulfate O atoms at average (long) Zr···O distances of 2.25 - 2.36 Å, in good agreement with the computational results. EXAFS analysis of benzene dosing experiments with **4**/AlS reveals that benzene is captured by essentially all of the Zr centers and is bound in an η<sup>6</sup> fashion, with an average Zr–C bond distance of 2.27 Å. These results are in excellent agreement with the computational and catalytic mechanistic results.

*Nuclearity Effects on Catalyst Activity and Selectivity.* The synthesis and characterization of two neutrally charged bimetallic nickel(II) ethylene polymerization catalysts, {2,7-di-[2,6-(3,5-dimethylphenylimino)methyl]-1,8-naphthalenediolato}-bis-Ni(II)(methyl)(trimethylphosphine) ((CH<sub>3</sub>)FI<sup>2</sup>-Ni<sub>2</sub>) and {2,7-di-[2,6-(3,5-di-trifluoromethylphenylimino)methyl]-1,8-naphthalenediolato}-bis-Ni(II)(methyl)(trimethylphosphine) ((CF<sub>3</sub>)FI<sup>2</sup>-Ni<sub>2</sub>) are reported. These catalysts, along with their monometallic analogues [2-*tert*-butyl-6-((2,6-(3,5-dimethylphenyl)phenylimino)methyl)phenolato]-Ni(II)-methyl(trimethylphosphine) ((CH<sub>3</sub>)FI-Ni) and [2-*tert*-butyl-6-((2,6-(3,5-ditrifluoromethylphenyl)phenylimino)methyl)phenolato]-Ni(II)-methyl(trimethylphosphine) ((CF<sub>3</sub>)FI-Ni) produce polyethylenes in the presence of Ni(COD)<sub>2</sub> ranging from low M<sub>w</sub>, highly branched oligomers, to high M<sub>w</sub> polymers with low branch densities. In the bimetallic catalysts, catalyst center–catalyst center cooperative effects are evidenced by increased product polyethylene branching in ethylene homopolymerizations, as well as by increased norbornene incorporation selectivity in ethylene-*co*-norbornene polymerizations, with bimetallic catalysts (CH<sub>3</sub>)FI<sup>2</sup>-Ni<sub>2</sub> and (CF<sub>3</sub>)FI<sup>2</sup>-Ni<sub>2</sub> enchaining ~3× and 6×, respectively, more norbornene than the monometallic catalysts (CH<sub>3</sub>)FI-Ni and (CF<sub>3</sub>)FI-Ni. Additionally, bimetallic catalysts (CH<sub>3</sub>)FI<sup>2</sup>-Ni<sub>2</sub> and (CF<sub>3</sub>)FI<sup>2</sup>-Ni<sub>2</sub> exhibit enhanced thermal stability over previously reported dinickel catalysts. The mechanism of bimetallic catalyst deactivation at 50°C was investigated and is found to involve an unexpected polymerization intermediate, {2,7-di-[2,6-(3,5-di trifluoromethylphenylimino)methyl]-1-hydroxy,8-naphthalenediolato-Ni(II)(methyl)(trimethylphosphine), (CF<sub>3</sub>)FI<sup>2</sup>-Ni(OH)}, that contributes to polyethylene formation at 50°C. The molecular structure of (CF<sub>3</sub>)FI<sup>2</sup>-Ni<sub>2</sub> is reported and reveals a Ni···Ni distance of 5.8024(5) Å.

*Heterogeneous Catalytic Synthesis of Energy Storage Materials.* Inexpensive materials combining the processability and mechanical properties of inexpensive polymers with the high dielectric constants of ferroelectric oxides are highly desirable for energy storage applications as in large-scale capacitors. To this end, a series of 0-3 metal oxide-polyolefin nanocomposites were synthesized via in-situ olefin polymerization using the single-site catalysts: C<sub>2</sub>-symmetric dichloro[*rac*-ethylenebisindenyl]zirconium (IV), Me<sub>2</sub>Si(<sup>*t*</sup>BuN)(η<sup>5</sup>-C<sub>5</sub>Me<sub>4</sub>)TiCl<sub>2</sub>, and (η<sup>5</sup>-C<sub>5</sub>Me<sub>5</sub>)TiCl<sub>3</sub> immobilized on methylaluminumoxane (MAO)-treated BaTiO<sub>3</sub>, ZrO<sub>2</sub>, 3 mol% yttria-stabilized zirconia, 8 mol% yttria-stabilized zirconia, *sphere*-shaped TiO<sub>2</sub> nanoparticles, and *rod*-shaped TiO<sub>2</sub> nanoparticles. The resulting composites were structurally characterized by X-ray diffraction, SEM, TEM, <sup>13</sup>C NMR, and DSC. TEM shows that the nanoparticles are well-dispersed in the polymer matrix, with each individual nanoparticle surrounded by polymer. Electrical measurements reveal that most of these nanocomposites have leakage current densities ~ 10<sup>-6</sup>-10<sup>-8</sup> A/cm<sup>2</sup>; relative permittivities increase as the nanoparticle volume fraction increases, with measured values as high as 6.1. At the same volume fraction, *rod*-shaped TiO<sub>2</sub> nanoparticle-isotactic-polypropylene nanocomposites exhibit significantly greater permittivities than the corresponding *sphere*-shaped TiO<sub>2</sub> nanoparticle-isotactic-polypropylene nanocomposites. The energy storage densities of these nanocomposites are as high as 9.4 J/cm<sup>3</sup>.

## Future Plans

To activate polynuclear molecule-based catalysts to new levels of activity, we will investigate more Brønsted acidic supports, seeking catalytic effects only possible via the agency of adjacent catalytic centers. We will expand our work to hydrocarbon metathesis processes. A variety of binuclear catalyst precursors will be chemisorbed and studied. Structural characterization will include solid state NMR and EXAFS/XANES at ANL, with operando studies of catalysts turning over and/or being inhibited. Here, our systems with virtually 100% active sites present a unique opportunity. We also plan investigations of cooperative effects in analogous homogeneous binuclear group 10 catalysts, focusing on transformations that are normally exceeding difficult by virtue of steric congestion and/or unfavorable substrate basicity.

## Publications (2009-2011)

1. Motta, A.; Fragala, I.L.; Marks, T.J. Proximity and Cooperativity Effects in Binuclear  $d^0$  Olefin Polymerization Catalysts. Theoretical Analysis of Structure and Mechanism, *J. Amer. Chem. Soc.*, **2009**, *131*, 3974-3984.
2. Rodriguez, B.A.; Delferro, M.; Marks, T.J. Enchainment Cooperativity Effects in Neutrally Charged Bimetallic Nickel (II) Phenoxyiminato Polymerization Catalysts, and Enhanced Selectivity for Polar Comonomer Enchainment, *J. Am. Chem. Soc.*, **2009**, *131*, 5902-5919.
3. Salata, M.R.; Marks, T.J. Catalyst Nuclearity Effects in Olefin Polymerization. Enhanced Activity and Comonomer Enchainment in Ethylene + Olefin Copolymerizations Mediated by Bimetallic Group 4 Phenoxyiminato Catalysts, *Macromolecules*, **2009**, *42*, 1920-1933.
4. Williams, L.A.; Marks, T.J. Chemisorption Pathways and Catalytic Olefin Polymerization Properties of Group 4 Mono- and Binuclear Constrained Geometry Complexes on Highly Acidic Sulfated Alumina, *Organometallics*, **2009**, *28*, 2053-2061.
5. Guo, N.; DiBenedetto, S.A.; Tewari, P.; Lanagan, M.T.; Ratner, M.A.; Marks, T.J. Nanoparticle, Size, Shape, and Interfacial Effects on Leakage Current, Permittivity, and Breakdown of Metal Oxide – Polyolefin Nanocomposites: Experiment and Theory, *Chem. Mater.*, **2010**, *22*, 1567-1578.
6. Delferro, M.; McInnis, J.P.; Marks, T.J. Synthesis, Characterization and Ethylene Homopolymerization Characteristics of an Electron-Deficient Nickel(II) Phenoxyiminato Catalyst with a Non-Innocent Intramolecular Hydrogen-Bond, *Organometallics*, **2010**, *29*, 5040-5049.
7. Delferro, M.; Marks, T.J. Multinuclear Olefin Polymerization Catalysis: Structure, Function, and Cooperativity, *Chem. Rev.* **2011**, *111*, 2450–2485.
8. Williams, L.A.; Marks, T.J. Synthesis, Characterization, and Heterogeneous Catalytic Implementation of Sulfated Alumina Nanoparticles. Arene Hydrogenation and Olefin Polymerization Properties of Supported Organo-Group 4 Complexes, *ACS Catalysis*, **2011**, *1*, 238–245.
9. Rodriguez, B.A.; Weberski, Jr., M.P.; Marks, T.J. Poisoning Radical and Coordinative Polymerization Sites in Close Proximity: Neutral Hetero-Bimetallic Aryloximinato Ni/Pd Catalysts for Ethylene-co-Methacrylate Polymerization and Block Copolymer Synthesis, submitted.
10. Weberski, M.P.; Chen, C.; Delferro, M.; Marks, T.J. Catalyst Center-Catalyst Center Cooperativity and Deactivation Mechanisms in Bimetallic Nickel(II) Phenoxyiminato-Based Ethylene Polymerization Catalysts, submitted for publication.
11. Li, Z.; Fredin, L.A.; Tewari, P.; DiBenedetto, S.A.; Lanagan, M.T.; Ratner, M.A.; Marks, T.J. *In Situ* Catalytic Encapsulation of Core-Shell Nanoparticles having Variable Shell Thickness. Dielectric and Energy Storage Properties of High-Permittivity Metal Oxide Nanocomposites, submitted.
12. Williams, L.A.; Guo, N.; Motta, A.; Fragala, I.L.; Marshall, C.L.; Miller, J.T.; Marks, T.J. Direct Visualization of a Heterogeneous Single-Site Catalyst with Nearly 100% Active Sites by Combined XAFS Spectroscopy and Quantum Chemical Analysis, submitted for publication.
13. Weberski, M.P.; Chen, C.; Delferro, M.; Zuccaccia, C.; Macchioni, A.; Marks, T.J. Suppression of  $\beta$ -H Chain Transfer in Ni(II) Catalyzed Ethylene Polymerization via Weak Secondary Ligand Interactions, submitted for publication.

**Christopher L. Marshall**

**The Institute for Atom-efficient Chemical Transformations (IACT): A DOE Energy Frontier Research Center for Biomass Catalysis**

Additional PIs: Chemistry and Chemical Engineering Departments, Northwestern University, Chemical Engineering Department, Purdue University, Chemical Engineering Department, University of Wisconsin-Madison; Material Science Division, Brookhaven National Laboratory (all 21 PI names are listed on web site <http://www.iact.anl.gov>)

EFRC Collaborators: Catalysis Center for Energy Innovation (CCEI) at the University of Delaware, Center for Atomic-level Catalyst Design (CALC-D) at Louisiana State University, Center for Direct Catalytic Conversion of Biomass to Biofuels (C3Bio) at Purdue University

Contact: Christopher L. Marshall, Chemical Sciences and Engineering Division, Argonne National Laboratory, 9700 South Cass Avenue, Argonne, IL 60439; [marshall@anl.gov](mailto:marshall@anl.gov)  
Peter C. Stair, Department of Chemistry, Northwestern University, 2137 Sheridan Road, Evanston, IL 60208-3113 & Chemical Sciences and Engineering Division, Argonne National Laboratory, 9700 South Cass Avenue, Argonne, IL 60439; [pstair@northwestern.edu](mailto:pstair@northwestern.edu)

**Goal**

Argonne National Laboratory along with its partners has established an Energy Frontier Research Center, the Institute for Atom-efficient Chemical Transformations (IACT) whose focus is to advance the science of catalysis for the efficient conversion of energy resources into usable forms. IACT is a partnership among world-class scientists at Argonne National Laboratory, Northwestern University, University of Wisconsin-Madison, Purdue University and Brookhaven National Laboratory. Using a multidisciplinary approach involving integrated catalyst synthesis, advanced characterization, catalytic experimentation, and computation, IACT is addressing key chemistries associated with clean, efficient utilization of biomass to fuels. We have identified the efficient removal of oxygen from biomass and the hydrogenation as key chemistries and unifying themes for IACT.

**DOE Interest**

To effectively advance the science and understanding of these new catalytic materials, collaborative application of a host of characterization tools is required. In many cases, the important questions about catalyst structure, composition, and function can only be answered through advances in measurement science, and this is an important aspect of IACT research. The interpretation, understanding, and optimization of experimental results by computation are also critical parts of advancing the science. Finally, the primary motivation and ultimate evaluation of synthesized, characterized, and computationally modeled catalysts is their catalytic and chemical performance. Thus, IACT can be viewed as having four distinct, but intimately interlinked tasks: 1) Catalyst Synthesis, 2) In-situ Characterization, 3) Computational Modeling, and 4) Chemical and Catalytic Reaction Science. For maximum productivity, this effort clearly requires a multidisciplinary

integrated EFRC approach. IACT is conducting a systematic investigation aimed at understanding on the atomic scale how 1) catalyst, 2) reagent, 3) method of activation, and 4) environment influence the deoxygenation of organic functional groups represented in biomass.

## Recent Progress

### \* *Nanobowl Synthesis:*

This project is developing methods for fabricating nanobowl architectures allowing the positioning of catalytic and/or chemisorption surface sites with a resolution of 0.1 nm via three strategies: templated atomic layer deposition (ALD), silsesquioxane templated synthesis (STS), and porous organic polymers (POPs). Specific accomplishments include:

- Used the BlueGene/P supercomputer to model ZrO<sub>2</sub> nanobowls (13Å diameter, 6 Å depths) for future computational studies of sugar decomposition. Developed empirical potential models of amorphous alumina nanobowls that can capture dynamics at elevated temperatures.
- Synthesized nanobowl catalysts on TiO<sub>2</sub> nanoparticles using calixarene templates and ALD Al<sub>2</sub>O<sub>3</sub> overcoats and evaluated using the photocatalytic oxidation of alcohols. Relative rates for 1- vs. 2-alcohols reached a maximum of 10x at 5 ALD cycles when the nanobowls became comparable to molecular dimensions (see Figure).
- First generation Al<sub>2</sub>O<sub>3</sub>-Ti-SiO<sub>2</sub> nanobowl catalysts were applied to glucose-to-fructose isomerization.
- Found that ALD Pd is superior for isolating ring oxidation products. Prepared ALD Pd on planar crystals for SFG studies of molecular orientation on metal and metal oxide catalysts.
- Synthesized Pt-Pd bimetallic nanoparticles. XAS measurements revealed a Pt core – Pd shell nanostructure and HRTEM demonstrated that they are ultra-fine (~1 nm) and monodispersed.
- Synthesized POPs comprising porphyrin building blocks (PPOPs) and metallated with Fe(II), Mn(II), and Pd(II) yielding M-PPOP catalysts that were active for olefin and alkane oxidation. Characterized M-PPOPs using SAXS/XAS.

### \* *Catalysts for Reforming Formic Acid and Glycerol to H<sub>2</sub>:*

This project is developing liquid-phase, biomolecule reforming catalysts for H<sub>2</sub> production. The goal is to understand which biomolecules efficiently produce H<sub>2</sub>, the mechanism of H<sub>2</sub> and by-product light alkane production and determine which catalyst properties, e.g., metal and support, result in high activity and selectivity. During the initial experimental phase testing, the kinetics and reaction products of glycerol, propanol and formic acid reforming were determined. Specific accomplishments include:

- Atomic layer deposition synthesis of ultra-fine (~1nm), uniform, mono-dispersed Pt-Pd bimetallic nanoparticles.
- Synthesis of non-porous, nano-sized (10-15nm) t-ZrO<sub>2</sub> supports with SBET = 55m<sup>2</sup>/g, which are stable over a wide range of pH (1~14).

- Density Functional Theory (DFT) studies of the reaction paths for formic acid decomposition on transition metal surfaces. The primary and secondary reaction pathways for formic acid decomposition have been identified and a microkinetic model for HCOOH decomposition and coupled WGS is under development.
- The initial product of propanol reforming is H<sub>2</sub> and propanal. The final products are ethane, CO<sub>2</sub> and 2 H<sub>2</sub>. The C-C cleavage only occurs on oxygenated C atoms. While there is little CO at the reactor outlet, under reaction, CO is the primary surface intermediate.
- Reforming of glycerol leads to cleavage of C-C and C-OH bonds; the former reactions have been investigated with detailed DFT calculations. Cleavage of C-OH bonds gives reaction intermediates with saturated C's. Mo promotion leads to a significant increase in the H<sub>2</sub> production rate, but has little effect on selectivity. Under reaction, CO and H<sub>2</sub>O are the primary surface intermediates.
- DFT studies and characterization of the conformational, energetic, and electronic aspects of CO adsorption on Pt<sub>n</sub>, Mo<sub>m</sub>, and Pt<sub>n-m</sub>Mo<sub>m</sub> (n=2-7, 13, 55, 0<m<n) nano-catalysts, demonstrate that admixing of Mo lowers the CO adsorption energy on Pt sites.

**\* Breakdown of Furfuryl Alcohol:**

Research in the conversion of furfuryl alcohol addresses both the hydrogenation of furfural to furfuryl alcohol and its subsequent conversion to levulinic acid, to understand the factors that control catalytic activity and selectivity. Research on the hydrogenation of furfural to furfuryl alcohol is elucidating the factors that control the activity and selectivity for hydrogenation of the C=O group, in contrast to the undesirable hydrogenation of the C=C bonds in the furan ring. Research dealing with the conversion of furfuryl alcohol to levulinic acid will involve a combination of theoretical studies, micro-kinetic analyses, and experimental studies involving reaction kinetics measurements, catalyst synthesis, and characterization of surface acid/base and redox properties. Specific accomplishments include:

- Predicted thermochemistry for chemical conversions for 5-hydroxy-methyl furfural using high-level quantum chemical methods. Analyzed experimental spectra and theoretical spectra of furan derivatives and levulinic acid.
- Assessed theoretical methods to predict the Raman vibrational spectrum for furan derivatives. Predicted energetics and mechanism of furfuryl alcohol polymerization using DFT.
- Predicted thermodynamics of the formation of alkyl levulinate and levulinic acid from furfuryl alcohol using high-level quantum mechanical theory.
- Identified fructosides in fructose dehydration to HMF in an alcohol solvents. Identified humin precursors in fructose dehydration in water. Identified intermediates in the conversion of furfuryl alcohol to levulinic acid in water.
- Proposed pathways for the conversion of furfuryl alcohol to levulinic acid and ethyl levulinate in both water and ethanol, respectively.
- Coated SBA-15 with TiO<sub>2</sub>/SiO<sub>2</sub> by ALD and functionalized surface with propylsulfonic acid moieties, thereby improving hydrothermal stability of the acid catalyst.



- Built an operando XAFS cell for gas phase furfuryl hydrogenation study and optimized the catalyst activation conditions on beamline (200°C and 1 hour are sufficient to reduce Cu<sup>2+</sup> to metallic copper).

**\* Breakdown of Glucose:**

This project utilizes both theory and experiments in a complementary and integrated approach to determine the mechanism(s) for the breakdown of glucose, and to develop new catalysts that efficiently accomplish desirable multi-step transformations in this process. Specific accomplishments include:

- Developed a catalytic system that cleaves etheric bonds yielding alcohols and hydrocarbons based on Ln(OTf)<sub>3</sub> (cleaves etheric bonds), and a Pd(0) hydrogenation catalyst. Effective Pd nanoparticulate catalysts were also prepared using ALD.
- Determined where <sup>13</sup>C<sub>1</sub> and <sup>13</sup>C<sub>6</sub> carbons in fructose and HMF reside in reaction products, with results consistent with theoretical predictions for HMF.
- Identified at least two intermediates for fructose to HMF. The second has a structure very similar to theoretical predictions.
- A highly dispersed Fe-SiO<sub>2</sub> catalyst has shown isomerization activity at 100°C for the isomerization of glucose to fructose and mannose.
- Nanobowl catalysts consisting of Al<sub>2</sub>O<sub>3</sub> on Ti on SiO<sub>2</sub> show selectivity patterns similar to Ti-beta but with lower rates that are more consistent with base catalysis by residual Al<sub>2</sub>O<sub>3</sub> surfaces.
- Comparison of thermodynamic estimation methods between group additivity and quantum chemical calculations on pathways for glucose to products. Comparison of group additivity and experimental values for the known glycolysis pathway and a variety of reactions involving sugars. Identified novel pathways from pyruvate to 1-butanol and developed a structure-based screening strategy for ranking pathways based on protein docking calculations. Developed a comprehensive reaction network for lactic acid hydrogenation to propylene glycol and propanoic acid and identified key reaction intermediates.
- Adsorption thermochemistry and activation energy barrier calculations and identified minimum energy paths for conversion of lactic acid to propylene glycol and propanoic acid on Pt(111).
- Studied thermochemistry trends for the elementary steps in lactic acid hydrogenation on late transition metals. A detailed microkinetic model for lactic acid hydrogenation is being developed.
- Developed detailed models of glucose, fructose, and HMF chemistry in aqueous environments. For fructose to HMF, identified an intermediate consistent with NMR observations.
- Developed Periodic Density Functional Theory models of the selective hydrogenation of furfural to furfuryl alcohol, THF, and THFA on Pd(111) and Pt(111) which includes a detailed analysis of the thermodynamics of the intermediates that result from furfural hydrogenation, and a determination of selected kinetic barriers for key elementary reactions.
- A high level, CCSD-based (G4) quantum study of the energies and reaction barriers for the fructose dehydration through fructofuranosyl intermediates to 5-

hydroxy-methyl furfural (HMF).

### **Future Plans**

- The nanobowl synthesis studies will concentrate on
  - Refinement of nanobowl models to include aqueous stability and catalytic metal centers
  - Development of advance the X-ray and microscopic methods for characterizing nanobowls
  - Synthesis of nanobowls by ALD, POP, and STS incorporating different catalytic metal centers and a diversity of sidewall/host materials
  - Demonstration of the remarkable selectivity of these nanobowls for catalyzing the chemical transformations in the other projects.
- The reforming project will concentrate on:
  - Determine through experimental and DFT modeling the fundamental catalytic properties, e.g., metal or alloy composition, support type, reaction pathway, etc., that lower the selectivity of C-OH cleavage, which yields light alkanes, while producing H<sub>2</sub>.
  - Determine through experimental and DFT modeling the fundamental catalytic properties, e.g., metal or alloy composition, support type, reaction pathway, etc., that increase the turnover rate of H<sub>2</sub> production.
  - Synthesize high performance reforming catalysts with novel supports and active phases that also show high stability under the reaction conditions.
  - Develop improved in situ analytical methods, primarily TEM and XAFS, for better understanding of the active catalyst.
- The furfuryl alcohol conversion project will concentrate on:
  - Study the effects of pressure on the conversion of furfural using a series of catalysts synthesized under Project 1.
  - Utilize fluidized bed reactor for making larger quantities of nanobowl materials originally synthesized under the nanobowl project.
  - Utilize in situ XAFS cell with DRIFT unit to study the changes in coordination, oxidation state, and bonding of furfural on catalysts.
  - Develop an effective modeling system to calculate XANES spectral changes of catalysts.
- The glucose breakdown project will concentrate on:
  - Couple aforementioned materials with acid-catalyzed dehydration to understand catalytically active sites by surface spectroscopy. Test a new class of isomerization/dehydration catalysts based on supported amines to mimic the Malliard reactions.
  - Merge some of the insights from 2011 with computational work currently being done on other selective hydrogenation reactions.
  - Compare the activity and selectivity of different monometallic catalysts to identify

the most efficient monometallic catalyst for lactic acid hydrogenation, prior to embarking on identifying promising alloy catalysts and they are performing minimum energy path calculations on Cu(111), which was identified as a promising catalyst from trends analysis.

- Quantify mass balance, identify intermediates for HMF to formic and levulinic acids, determine if the “first” intermediate observed in fructose degradation is one species.

### **Publications (2009-2011)**

1. Kaur, P.; Hupp, J. T.; and Nguyen, S. B. T.; "Porous Organic Polymers in Catalysis: Opportunities and Challenges," *ACS Catalysis*, 2011, 1, 819–835.
2. Assary, R. S.; Redfern, P. C.; Greeley, J.; and Curtiss, L. A.; "Mechanistic Insights into the Decomposition of Fructose to Hydroxy-Methyl-Furfural in Neutral and Acidic Environments Using High-Level Quantum Chemical Methods," *Journal of Physical Chemistry B*, 2011, 115 (15), pp 4341–4349.
3. Assary, R. S.; Broadbelt, L. J.; and Curtiss, L. A.; "Bronsted-Evans-Polanyi Relationships for C-C Bond Forming and C-C Bond Breaking Reactions in Thiamine-catalyzed Decarboxylation of 2-Keto Acids Using Density Functional Theory," accepted by the *Journal of Molecular Modeling* (2011).
4. Kim, T. J.; Assary, R. S.; Curtiss, L. A.; Marshall, C. L.; and Stair, P. C.; "Vibrational Properties of Levulinic Acid and Furan Derivatives: Raman Spectroscopy and Theoretical Calculations," accepted by the *Journal of Raman Spectroscopy* (2011).
5. Shultz, A. M.; Farha, O. K.; Hupp, J. T.; and Nguyen, S. B. T.; "Synthesis of Catalytically Active Porous Organic Polymers from Metalloporphyrin Building Blocks," *Chemical Science* 2011, 2, 686–689.
6. Kandoi, S.; Greeley, J.; Simonetti, D.; Shabaker, J.; Dumesic, J. A.; and Mavrikakis, M.; "Reaction Kinetics of Ethylene Glycol Reforming over Platinum in the Vapor versus Aqueous Phases," *Journal of Physical Chemistry C*, 2011, 115, 961–971.
7. Pagan-Torres, Y. J.; Pham, H. N.; Libera, J. A.; Elam, J. W.; Marshall, C. L.; Datye, A. K.; and Dumesic, J. A.; "Synthesis of Highly Ordered Hydrothermally Stable Mesoporous Silica-Niobia Catalysts by Atomic Layer Deposition," submitted to *Nature-Materials* (2010).
8. Christensen, S. T.; Feng, H.; Libera, J. L.; Guo, N.; Miller, J. T.; Stair, P. C.; and Elam, J. W.; "Supported Ru–Pt Bimetallic Nanoparticle Catalysts Prepared by Atomic Layer Deposition" *Nano Letters* 2010, 10 (8), 3047–3051.
9. Assary, R. S.; Redfern, P. C.; Hammond, J. R.; Greeley, J.; and Curtiss, L. A.; "Predicted Thermochemistry for Chemical Conversions of 5-Hydroxymethylfurfural," *Chemical Physics Letters*, 497, 123–128 (2010).
10. Assary, R. S.; Redfern, P. C.; Hammond, J. R.; Greeley, J.; and Curtiss, L. A.; "Computational Studies of the Thermochemistry for Conversion of Glucose to Levulinic Acid," *Journal of Physical Chemistry B* 2010, 114 (27), 9002–9009.

### Atomic-scale design of metal and alloy catalysts: A combined theoretical and experimental approach

Additional-PIs: R. R. Adzic (Brookhaven National Lab), B. Eichhorn (U of Maryland), J. A. Dumesic (UW-Madison)

Postdocs: F. Celik

Graduate Students: P. Ferrin, J. Herron, J. Jiao, R. Nabar, P. Nason, A. Nilekar, S. Alayoglu, Z. Liu

Undergrad Students: H. Stotz, S. Tonelli

Collaborators: F. Besenbacher (Aarhus U.-Denmark), M. Flytzani-Stephanopoulos (Tufts U.), E. Iglesia (UC-Berkeley), A. V. Ruban (KTH-Sweden)

Contact: M. Mavrikakis, Dept. Chem. & Bio. Eng., Univ. of Wisconsin – Madison, Madison, WI, 53706; [manos@engr.wisc.edu](mailto:manos@engr.wisc.edu)  
R. R. Adzic, Chem. Dept., Brookhaven National Laboratory, Upton, NY 11973; [adzic@bnl.gov](mailto:adzic@bnl.gov)  
B. Eichhorn, Dept. Chem. & Biochem., Univ. of Maryland, College Park, MD 20742; [Eichhorn@umd.edu](mailto:Eichhorn@umd.edu)  
J. A. Dumesic, Dept. Chem. & Bio. Eng., Univ. of Wisconsin – Madison, Madison, WI, 53706; [dumesic@engr.wisc.edu](mailto:dumesic@engr.wisc.edu)

#### Goal

The main objective of this combined theoretical and experimental project is to: (i) *design* from first-principles, (ii) *synthesize* using advanced *nanosynthesis* techniques, and (iii) experimentally evaluate *new metal and alloy nanoparticles*, with unique *catalytic* properties for a number of important chemical reactions. Measurable impact can be found in a number of applications, including low temperature fuel cells, hydrogen production and purification, and liquid fuels production. The importance of the atomic-scale architecture of these new theoretically-designed catalysts to their unique properties is driving the development of *new inorganic materials synthesis* approaches, which are capable of synthesizing the theoretically determined optimal, and in some cases, metastable, nanoscale catalytic architectures.

#### DOE Interest

The proposed fundamental research, using a combination of theory and experiments, should have significant impact on designing catalysts at the nanoscale. These new catalysts could, for instance, greatly facilitate the CO<sub>2</sub> chemical fixation, purification of hydrogen, and reduce costs of fuel cell electrocatalysts.

#### Recent Progress

##### 1. *Chemical capture of CO<sub>2</sub>: Methanol synthesis on Copper (Cu)<sup>1</sup>:*

Though methanol (CH<sub>3</sub>OH) has been industrially synthesized for almost 100 years over Cu/ZnO supported catalysts, the exact mechanism for this process remains controversial. Unresolved questions include: (1) the carbon source for the reaction (CO

versus CO<sub>2</sub>), (2) the nature of the active site and (3) the importance of the support. In order to provide some theoretical insight into these important questions, we have developed a comprehensive microkinetic model for methanol synthesis over a Cu catalyst, based on rigorous density functional theory (DFT) calculated thermochemical and kinetic parameters. The DFT-derived parameters are optimized to fit a database of experimental results using the industrial Cu/ZnO/Al<sub>2</sub>O<sub>3</sub> catalyst.

Without any adjustments to the rate parameters derived from DFT on Cu(111), methanol production rates were found to be 6 orders of magnitude smaller than the experimental rates. However, optimization of the DFT-derived parameters was able to fit the experimental results well ( $R^2 = 0.92$ ) over a wide-range of conditions. The optimized parameters and reaction rates provide a number of interesting insights into the nature of the active site as well as the reaction mechanism. The following intermediates required significant stabilization (by 0.3 to 0.6 eV) to fit the experimental data: OH, COOH, HCO, HCOO, HCOOH, CH<sub>3</sub>O<sub>2</sub>, CH<sub>2</sub>O, CHO, and CH<sub>3</sub>OH. For the closed-shell species (CH<sub>3</sub>OH, CH<sub>2</sub>O, and HCOOH), this increased stabilization may be due to the deficiency in standard DFT to capture van der Waals interactions. However, the fitted values for CH<sub>2</sub>O and CH<sub>3</sub>OH are similar to experimental heats of adsorption on Cu(110) and oxidized Cu(110) surfaces, respectively. This suggests that clean Cu(111) may not accurately represent the commercial Cu/ZnO/Al<sub>2</sub>O<sub>3</sub> catalyst, rather a more open (Cu(110), Cu(100), or Cu(211)) or partially oxidized surface may be the active site. Further work on more complex model sites (Cu/ZnO) would be needed to evaluate any synergistic effects provided by the ZnO support.

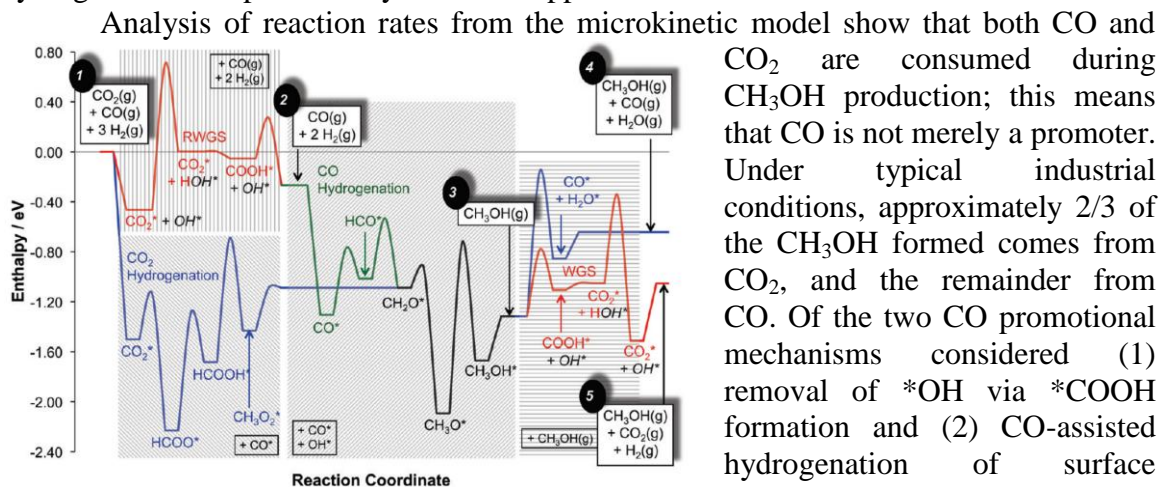


**Figure 1.** Potential energy surface for methanol synthesis. Adsorbed H\* is omitted from labeling and spectator species are shown in black boxes within shaded regions<sup>1</sup>.

Analysis of reaction rates from the microkinetic model show that both CO and CO<sub>2</sub> are consumed during CH<sub>3</sub>OH production; this means that CO is not merely a promoter. Under typical industrial conditions, approximately 2/3 of the CH<sub>3</sub>OH formed comes from CO<sub>2</sub>, and the remainder from CO. Of the two CO promotional mechanisms considered (1) removal of \*OH via \*COOH formation and (2) CO-assisted hydrogenation of surface intermediates, only the former was substantial. Yet, the overall contribution of these promotional pathways towards CH<sub>3</sub>OH formation was small compared to direct hydrogenation of CO/CO<sub>2</sub>. The reaction rates show a CO<sub>2</sub> hydrogenation mechanism proceeding through the following intermediates: CO<sub>2</sub>\* → HCOO\* → HCOOH\* → CH<sub>3</sub>O<sub>2</sub>\* → CH<sub>2</sub>O\* → CH<sub>3</sub>O\* → CH<sub>3</sub>OH\*, while CO hydrogenation follows: CO\* → HCO\* → CH<sub>2</sub>O\* → CH<sub>3</sub>O\* → CH<sub>3</sub>OH\*. These pathways are coupled by the water gas shift reaction, as shown in the potential energy surface plotted in Figure 1. In both CO and CO<sub>2</sub> hydrogenation pathways, the rate limiting step involves methoxy (CH<sub>3</sub>O\*)

hydrogenation. At low  $\text{CO}_2/(\text{CO} + \text{CO}_2)$  ratios (i.e.  $\text{CO}_2$  poor feeds),  $\text{CH}_3\text{O}^*$  formation is rate limiting, while  $\text{CH}_3\text{O}^*$  hydrogenation is rate limiting in  $\text{CO}_2$  rich feeds.

## 2. Combining scaling relationships with BEP correlations for predicting activity and selectivity<sup>16</sup>

DFT calculations have been used to rationally design catalysts with improved activity and selectivity. However, the computational cost of these calculations represents a significant barrier. In order to address this key issue, a number of correlations have been developed for minimizing computational cost while retaining the necessary design accuracy. Two prime examples of these correlations are the well-established Brønsted-Evans-Polanyi (BEP) correlation as well as linear scaling relationships between adsorbate binding strengths. Using these two linear correlations the kinetics and thermodynamics of a reaction network can be estimated by calculating only a few key binding energies on a particular surface.

As a case study in applying this approach to important catalytic systems, we utilized the above two correlations in a fundamental analysis of the ethanol decomposition reaction mechanism. The energetics of elementary steps in the ethanol decomposition reaction network were determined by combining the scaling relationships with DFT-calculated binding energies for H, O, C, and CO on the close-packed facets of Cu, Pt, Pd, Ni, Ir, Rh, Co, Os, Ru, and Re.

Using these kinetic and thermodynamic parameters, a simple mean-field kinetic model predicting production rates of various products was developed and compared to experimentally measured rates, see Figure 2. Overall, the model over-predicted the turnover frequency by approximately 2 orders of magnitude. This over-prediction is not surprising given the multitude of approximations used in the development of the kinetic model, and the choice of close-packed surfaces for the DFT calculations. However, the relative trends between metals predicted by the model agree fairly well with the experimentally determined reactivity trends.

## 3. Core-Shell alloys for electrocatalysis and heterogeneous catalysis<sup>15,6,9</sup>:

The oxygen reduction reaction (ORR) is an essential reaction occurring at the cathode of low temperature fuel cells. The slow ORR kinetics characterized by a high overpotential and requirement for expensive, platinum-based catalysts, are significant hurdles that must be overcome for practical implementation of fuel cells. In order to improve catalytic performance and reduce demands on precious metals, we have been developing alloy catalysts using a combination of theory as well as experimental synthesis, characterization, and reactivity evaluation.

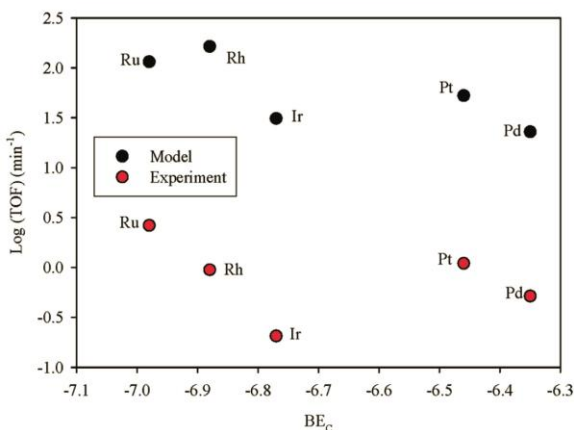


**Figure 2.** Logarithm of model-predicted and experimental turnover frequency (TOF, in  $\text{min}^{-1}$ ) for C-C bond breaking in ethanol. X-axis shows the binding energy of C on the close-packed facets of several metals. The rate on Cu is negligible<sup>16</sup>.

Using DFT methods, we have begun designing ternary alloy catalysts featuring a Pt monolayer deposited onto an annealed Pd<sub>x</sub>X<sub>z</sub> alloy. The reactivity of these ternary alloys mostly reflects that of the Pt\*/Pd structure modified through ligand and strain effects. Our experimental studies of Pt\*/Pd<sub>3</sub>Fe single crystals have demonstrated that this strategy can lead to highly active, energy efficient, and lower cost catalysts (see Figure 3)<sup>15</sup>.

We also studied the activity on core@shell nanoparticles, specifically PdIr@Pt. The PdIr@Pt nanoparticles showed 20 times and 25% higher Pt-mass activity than Pt/C and Pt\*/Pd/C, respectively<sup>6</sup>. Our DFT calculations showed that the existence of the PdIr layer beneath the Pd sublayer weakens the binding of OH on the Pt\*/Pd structure, leading to enhanced ORR activity. These two studies show that improvements of catalyst composition based on fundamental understanding can continue to improve ORR activity while simultaneously reducing the demand on precious metals.

Another area where core-shell nanoparticles (NPs) have shown improved catalytic performance is in preferential oxidation (PROX) of CO in hydrogen. This reaction is responsible for removing any residual CO contaminants remaining in H<sub>2</sub> streams after water

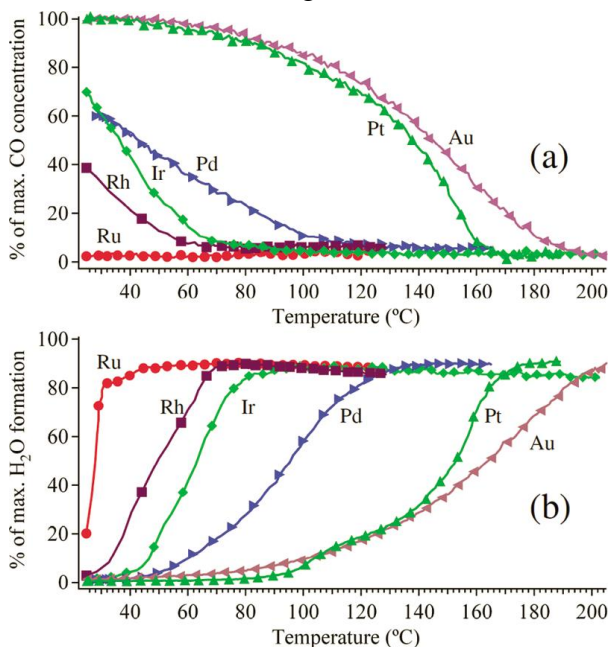


**Figure 4.** TPR plots for the PROX reaction showing (a) CO concentration and (b) H<sub>2</sub>O formation at a CO level of 1000 ppm, for the X@Pt, core@shell, NPs with ca. 1 ML thick Pt shells and the 2.5 nm Pt particle catalysts<sup>9</sup>.

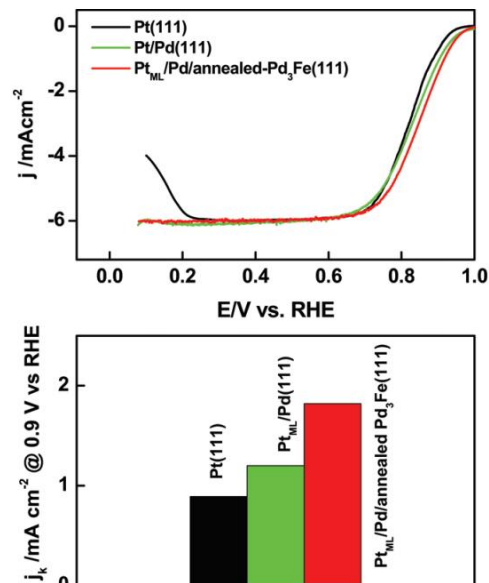


**Figure 3.** (Top) polarization curves for the ORR at 1600 rpm in oxygen-saturated 0.1 M HClO<sub>4</sub> at room temperature; scan rate: 20 mV s<sup>-1</sup>. (Bottom) comparison of ORR specific activities at 0.9 V<sub>RHE</sub><sup>15</sup>.

gas shift processing.

Recently, we published a detailed analysis of the relative PROX activity for a series of specifically synthesized X@Pt NPs (X = Ru, Rh, Ir, Pd, Pt, or Au)<sup>9</sup>. First, we evaluated the CO saturation coverage over close-packed, extended-surface analogues of these NPs (Pt\*/X) surfaces using DFT calculations. The combination of ligand and strain effects reduces the binding of CO on Ru@Pt, Rh@Pt, and Ir@Pt versus pure Pt. For Ru, in particular, this decrease leads to a reduced saturation coverage of 1/2 ML, versus 2/3 ML for Pt. Our theoretical analysis predicted the

following ranking of PROX reactivity of these alloys (from worst to best): Pt\*/Au < Pt < Pt\*/Pd < Pt\*/Ir < Pt\*/Rh < Pt\*/Ru. The core@shell NPs were

specifically synthesized and characterized, and experimentally tested for their PROX activity. Figure 4 shows experimental TPR results for the PROX reaction on these NPs which display reactivity trends in agreement with our DFT predictions. Furthermore, H<sub>2</sub> oxidation followed CO oxidation for all of the NPs studied except Au@Pt, where they occurred simultaneously, indicating enhanced selectivity to CO oxidation.

To understand the selectivity towards CO oxidation (versus H<sub>2</sub> oxidation), we calculated the activation barriers for each of the reactions in the network. Hydrogen-assisted O<sub>2</sub> dissociation, providing O\*, is facile on all these surfaces, and as a result selectivity and activity are governed by the relative difficulty of two elementary steps consuming O\*, namely CO\*+O\* and H\*+O\*. The OH formation barrier on all the aforementioned surfaces was found to be higher than the CO oxidation barrier (except on Pt\*/Au), rationalizing the observed selectivity trends. Furthermore, the calculated CO oxidation barriers exactly predict the experimentally observed relative PROX activity trends.

### Future Plans

We are currently advancing studies along two main fronts, (1) Vapor-phase catalytic reduction of NO with H<sub>2</sub> and (2) electrocatalytic oxidation of alternative fuels, including dimethyl ether and ammonia. In catalytic reduction of NO with H<sub>2</sub>, we investigate the fundamental reaction mechanism and reactivity trends, including structure sensitivity, on selected monometallic particles (Pt, Rh, Pd, Ir, and Ru). This project includes theoretical work as well as experimental evaluation of shape- and size-selected synthesized NPs. These investigations on monometallic catalysts will lay the foundations needed to start exploring the synthesis of improved alloy catalysts for this reaction, with targeted selectivity towards N<sub>2</sub> as the main reaction product. Further, we have begun studying the electrocatalytic oxidation of ammonia (NH<sub>3</sub>) and dimethyl ether (DME) on monometallic single crystals for a range of late transition metals to elucidate their fundamental reaction mechanisms, including structure sensitivity. This is the first stage of a longer-term project in electro-oxidation of NH<sub>3</sub> and DME reactions, which is geared towards eventually developing alloy catalysts with improved activity and efficiency.

### Publications (2009–2011)

1. L. C. Grabow, and M. Mavrikakis, *Mechanism of Methanol Synthesis on Cu through CO<sub>2</sub> and CO Hydrogenation*, ACS Catal. 1, 365 (2011).
2. L. R. Merte, L. C. Grabow, G. Peng, J. Knudsen, H. Zeuthen, W. Kudernatsch, S. Porsgaard, E. Lægsgaard, M. Mavrikakis, and F. Besenbacher, *Tip-Dependent Scanning Tunneling Microscopy Imaging of Ultrathin FeO Films on Pt(111)*, J. Phys. Chem. C 115, 2089 (2011).
3. Y. P. Zhai, D. Pierre, R. Si, W. L. Deng, P. Ferrin, A. U. Nilekar, G. W. Peng, J. A. Herron, D. C. Bell, H. Saltsburg, M. Mavrikakis, and M. Flytzani-Stephanopoulos, *Alkali-Stabilized Pt-OH<sub>x</sub> Species Catalyze Low-Temperature Water-Gas Shift Reactions*, Science 329, 1633 (2010).
4. L. R. Merte, G. W. Peng, R. T. Vang, A. Resta, E. Laegsgaard, J. N. Andersen, M. Mavrikakis, and F. Besenbacher, *Low-Temperature CO Oxidation on Ni(111) and on a Au/Ni(111) Surface Alloy*, J. Knudsen, ACS Nano 4, 4380 (2010).
5. G. Peng, L. R. Merte, J. Knudsen, R. T. Vang, E. Laegsgaard, F. Besenbacher, and M. Mavrikakis, *On the Mechanism of Low-Temperature CO Oxidation on Ni(111) and NiO(111) Surfaces*, J. Phys. Chem. C 114, 21579 (2010).



6. S. L. Knupp, M. B. Vukmirovic, P. Haldar, J. A. Herron, M. Mavrikakis, and R. R. Adzic, *Platinum Monolayer Electrocatalysts for O<sub>2</sub> Reduction: Pt Monolayer on Carbon-Supported PdIr Nanoparticles*, Electrocatal. 1, 213 (2010).
7. M. Ojeda, A. W. Li, R. Nabar, A. U. Nilekar, M. Mavrikakis, and E. Iglesia, *Kinetically Relevant Steps and H<sub>2</sub>/D<sub>2</sub> Isotope Effects in Fischer-Tropsch Synthesis on Fe and Co Catalysts*, J. Phys. Chem. C 114, 19761 (2010).
8. D. C. Ford, A. U. Nilekar, Y. Xu, and M. Mavrikakis, *Partial and Complete Reduction of O<sub>2</sub> by Hydrogen on Transition Metal Surfaces*, Surf. Sci. 604, 1565 (2010).
9. A. U. Nilekar, S. Alayoglu, B. Eichhorn, and M. Mavrikakis, *Preferential CO Oxidation in Hydrogen: Reactivity of Core-Shell Nanoparticles*, J. Am. Chem. Soc. 132, 7418 (2010).
10. M. Ojeda, R. Nabar, A. U. Nilekar, A. Ishikawa, M. Mavrikakis, and E. Iglesia, *CO Activation Pathways and the Mechanism of Fischer-Tropsch Synthesis*, J. Cat. 272, 287 (2010).
11. S. Kandoi, P. A. Ferrin, and M. Mavrikakis, *Hydrogen on and in Selected Overlayer near-Surface Alloys and the Effect of Subsurface Hydrogen on the Reactivity of Alloy Surfaces*, Top. Cat. 53, 384 (2010).
12. J. Knudsen, L. R. Merte, L. C. Grabow, F. M. Eichhorn, S. Porsgaard, H. Zeuthen, R. T. Vang, E. Laegsgaard, M. Mavrikakis, and F. Besenbacher, *Reduction of FeO/Pt(111) Thin Films by Exposure to Atomic Hydrogen*, Surf. Sci. 604, 11 (2010).
13. J. Rempel, J. Greeley, L. B. Hansen, O. H. Nielsen, J. K. Nørskov, and M. Mavrikakis, *Step Effects on the Dissociation of NO on Close-Packed Rhodium Surfaces*, J. Phys. Chem. C 113, 20623 (2009).
14. P. Ferrin, and M. Mavrikakis, *Structure Sensitivity of Methanol Electrooxidation on Transition Metals*, J. Am. Chem. Soc. 131, 14381 (2009).
15. W. P. Zhou, X. F. Yang, M. B. Vukmirovic, B. E. Koel, J. Jiao, G. W. Peng, M. Mavrikakis, and R. R. Adzic, *Improving Electrocatalysts for O<sub>2</sub> Reduction by Fine-Tuning the Pt-Support Interaction: Pt Monolayer on the Surfaces of a Pd<sub>3</sub>Fe(111) Single-Crystal Alloy*, J. Am. Chem. Soc. 131, 12755 (2009).
16. P. Ferrin, D. Simonetti, S. Kandoi, E. Kunkes, J. A. Dumesic, J. K. Nørskov, and M. Mavrikakis, *Modeling Ethanol Decomposition on Transition Metals: A Combined Application of Scaling and Brønsted-Evans-Polanyi Relations*, J. Am. Chem. Soc. 131, 5809 (2009).
17. P. A. Ferrin, S. Kandoi, J. L. Zhang, R. Adzic, and M. Mavrikakis, *Molecular and Atomic Hydrogen Interactions with Au-Ir near-Surface Alloys*, J. Phys. Chem. C 113, 1411 (2009).
18. L. R. Merte, J. Knudsen, L. C. Grabow, R. T. Vang, E. Laegsgaard, M. Mavrikakis, and F. Besenbacher, *Correlating STM Contrast and Atomic-Scale Structure by Chemical Modification: Vacancy Dislocation Loops on FeO/Pt(111)*, Surf. Sci. 603, L15 (2009).
19. A. U. Nilekar, A. V. Ruban, and M. Mavrikakis, *Surface Segregation Energies in Low-Index Open Surfaces of Bimetallic Transition Metal Alloys*, Surf. Sci. 603, 91 (2009).

**Selectivity Control through Modification of Metal Catalysts with Organic Monolayers**

Additional PI: Daniel K. Schwartz

Students: Carolyn Schoenbaum, Rudy Kahsar

Collaborators: Jeroen van Bokhoven (ETH-Zurich)

Contacts: University of Colorado, Dept. of Chemical and Biological Engineering  
UCB 424, ECCH 111; Boulder, CO 80309-0424; [will.medlin@colorado.edu](mailto:will.medlin@colorado.edu)

**Goal**

Investigate structure-reactivity relationships for supported metal catalysts modified by self-assembled monolayers of organic thiolates, as a method for understanding the role of the near-surface environment in controlling surface reactivity.

**DOE Interest**

By tailoring the properties of the monolayer-forming species, one can alter adsorbate-adsorbate interactions to control activity and selectivity in heterogeneous catalysis. Self-assembled monolayers represent a useful model platform for understanding how the properties of a metal-solution interface alter reactivity. A combination of catalyst screening experiments and surface characterization is being used to understand mechanisms by which monolayers can influence catalyst activity and selectivity in several probe reactions.

**Recent Progress**

*Reactivity studies.* The selective reaction of one part of a bifunctional molecule is a fundamental challenge in heterogeneous catalysis and a critically-important task for many processes including the conversion of biomass-derived intermediates. Selective hydrogenation of unsaturated epoxides to saturated epoxides (Scheme 1) is particularly difficult given the reactivity of the strained epoxide ring, and traditional platinum group catalysts show low selectivity for these reactions. We recently described a new approach for the preparation of highly selective Pd catalysts involving the deposition of n-alkanethiol self-assembled monolayer (SAM) coatings. These coatings improve the selectivity of 1-epoxybutane formation from 1-epoxy-3-butene on palladium catalysts from 11% to as high as 94% at equivalent reaction conditions and conversions. Although sulfur species are generally considered to be indiscriminant catalyst poisons, we find that the reaction rate to the desired product on a catalyst coated with a thiol having an 18 carbon aliphatic tail was 40% of the rate on an uncoated catalyst. Interestingly the activity decreased for catalysts coated with less ordered SAMs having shorter chains. The behavior of SAM-coated catalysts was compared to catalysts where surface sites were modified by carbon monoxide, hydrocarbons, or sulfur atoms. The results suggest that the SAMs restrict sulfur coverage to enhance selectivity without significantly poisoning the activity of the desired reaction.

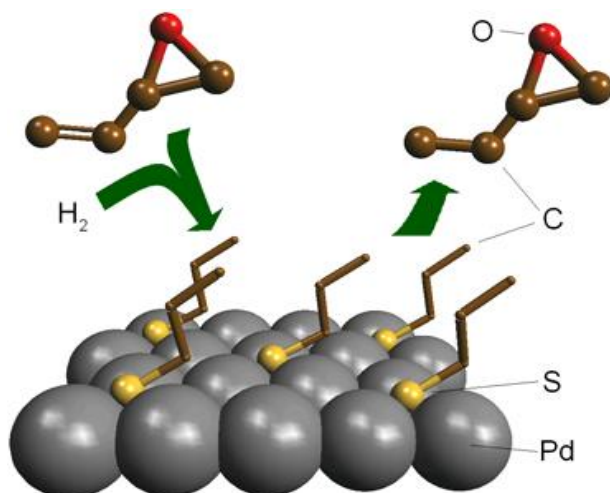
*Characterization of metal-surface interactions.* In a separate study, we conducted surface-level investigations of the adsorption of EpB and related molecules on SAM-coated Pd(111), with an aim of identifying mechanistic explanations for the observed catalytic behavior. Alkanethiol SAM-covered Pd(111) surfaces were prepared by conventional techniques and transferred to ultrahigh vacuum, where they were characterized using Auger electron spectroscopy (AES) and temperature programmed desorption (TPD) of EpB and other probe molecules. Whereas previous studies have shown that EpB undergoes rapid decomposition via epoxide ring opening on uncoated Pd(111), TPD studies show that EpB does not undergo substantial ring opening on SAM-covered surfaces, but rather desorbs intact at temperatures less than 300 K. Systematic comparisons of EpB desorption spectra to spectra for other C<sub>4</sub> oxygenates suggest that the SAM creates a kinetic barrier to epoxide ring-opening reactions that does not exist on the uncoated surface. The EpB desorption spectra as a function of exposure show behavior similar to the desorption of olefins from Pd(111), indicating that the binding of the olefin functionality, in contrast to that of the epoxide ring, is not significantly perturbed. EpB desorption spectra from surfaces with less well-ordered SAMs show the presence of weakly bound states not observed on well-ordered SAM surfaces. The lower activity observed on catalysts covered with less well-ordered SAMs is hypothesized to occur due to partial confinement of adsorbates into these weakly bound, less active states.

### **Future Plans**

*Variation of reaction chemistry.* We are investigating the hydrogenation of other probe molecules, including acetylene, ethylene, and 4-nitrostyrene on SAM-coated surfaces, as well as the oxidation of propylene and glucose.

*Variation of supported metal composition.* We are preparing and screening catalysts in which the active component is Pd, Pt, Ag, and Au. All of these surfaces are well-known to allow preparation of thiolate SAMs, with Ag and Au having been more extensively characterized as substrates for SAMs.

*Variation of SAM-forming thiolate.* A primary interest in the use of SAMs for modifying catalytic behavior is that the composition of SAMs can be finely tuned to control surface reactivity. In the first year of this project we will primarily focus on changing the length of n-alkanethiol SAMs to control film thickness and crystallinity, as well as exploring differences between the use of hydrophobic (formed from alkanethiols) and hydrophilic (formed from thioglycerol) SAMs.



**Scheme 1.** Selectivity of C=C hydrogenation from 1-epoxy-3-butene improves dramatically on SAM-coated Pd catalysts.

**Publications (2010-2011)**

S.T. Marshall, D.K. Schwartz, J.W. Medlin, “Adsorption of oxygenates on alkanethiol-functionalized Pd(111) surfaces: Mechanistic insights into the role of self-assembled monolayers on catalysis”, *Langmuir*, accepted for publication (2011).

**Understanding the Electronic and Chemical Modifications in Bimetallic Nano-particle Catalysts for H<sub>2</sub> Production by *in Situ* XANES spectroscopy and Density Functional Theory**

Lead PI: Peter C. Stair

Postdoc: Tianpin Wu, Neil Schweitzer, Neng Guo

Contact: Division of Chemical Sciences and Engineering, 9700 S. Cass Ave, Argonne National Laboratory, Argonne, IL 60439; [millerjt@anl.gov](mailto:millerjt@anl.gov)

The production of H<sub>2</sub> from MeOH decomposition, WGS or biomass reforming, for example, utilizes metallic nano-particle (NP) catalysts. Bimetallic catalysts offer superior performance for activity, selectivity and stability; however, a fundamental understanding of how the electronic structure and resulting chemistry is altered in bimetallic NP's is not fully understood. Synthesis of bimetallic Pd-M (M = Pt, Au, Cu, Zn) and single metal Pd, Pt, Au and Cu on silica catalysts were prepared by the method of electrostatic adsorption (1) to give nano-particles of less than about 5 nm in size. EXAFS, at both metal edges, reveal the nano-particle structure, which for Pd generally forms an M core and Pd shell. A low energy *in situ* XAS cell was constructed to measure the Pd L<sub>3</sub> and L<sub>2</sub> edge XANES. The bimetallic Pd-M catalysts show significant changes in the XANES spectra compared to those of Pd only indicating a significant modification of the Pd electronic structure (2). In Pd-Pt bimetallic NP's, for example, the shift in the energy of the Pt L<sub>3</sub> edge is opposite to that at the Pd L<sub>3</sub>. L edge XANES are also strongly modified upon chemisorption, for example with CO (3). By examining the adsorption of CO, changes to the Pd L edge XANES confirms that there is a significant fraction of surface Pd; although the Pt L<sub>3</sub> XANES spectra also indicate partial coverage of the NP surface by Pt. Finally, the Pd TOR and selectivity is

To better understand interaction of the two metals in a bimetallic NP and their affect on the electronic and chemical properties, in collaboration with Prof. Randall Meyer and his students from the University of Illinois at Chicago, Density Functional Theory calculations were performed using the CASTEP code to determine the d-electron density of states for Pd-M alloys (3, 4). In addition, the probability of the dipole allowed core to valence electronic transitions were calculated and agreed well with the experimental L edge XANES spectra. The DFT simulations indicate that the electron occupancy of both Pt and Pd in Pd-Pt alloys are very similar suggesting little electron transfer between the two metals; however, there are large changes in the width of the d-DOS for both metals, a narrowing of the d-band for Pt and broadening in Pd indicating significant changes in the hybridization of metal-metal bonds. The experimental and theoretical results are consistent with changes in the energy of the d-electrons in bimetallic transition metals with little electron transfer between the two (2).

**References:**

1. Miller, J.T., Schreier, M., Kropf, A.J. and Regalbuto, J.R., *J. Catal.*, 225, 203-212 (2004)
2. N. Schweitzer, H. Xin, E.Nikolla, J.T. Miller, S. Linic, *Top. Catal.*, 53, 348-356 (2010)
3. N. Guo, B.R. Fingland, W.D. Williams, V.F. Kispersky, J. Jelic, W.N. Delgass, F.H. Ribeiro, R.J. Meyer, J.T. Miller, *PCCP*, 12, 5678 - 5693 (2010)
4. Lei, Y., Jelic, J., Nitche, L., Meyer, R.J., Miller, J.T., *Top. Catal.*, 54, 334-248 (2011)

## Surface Chemistry of Gold Model Catalysts

Additional PIs: N/A  
 Postdocs: N/A  
 Students: Ming Pan, Ting Yan  
 Collaborators: J. A. Rodriguez (BNL), S. D. Senanayake (BNL), D. Stachiolla (BNL), J. Hrbek (BNL), and G. Henkelman (UT-Austin)  
 Contacts: Department of Chemical Engineering, University of Texas at Austin, 1 University Station C0400, Austin, TX 78712-0231; (512) 471-5817; [mullins@che.utexas.edu](mailto:mullins@che.utexas.edu)

## Goal

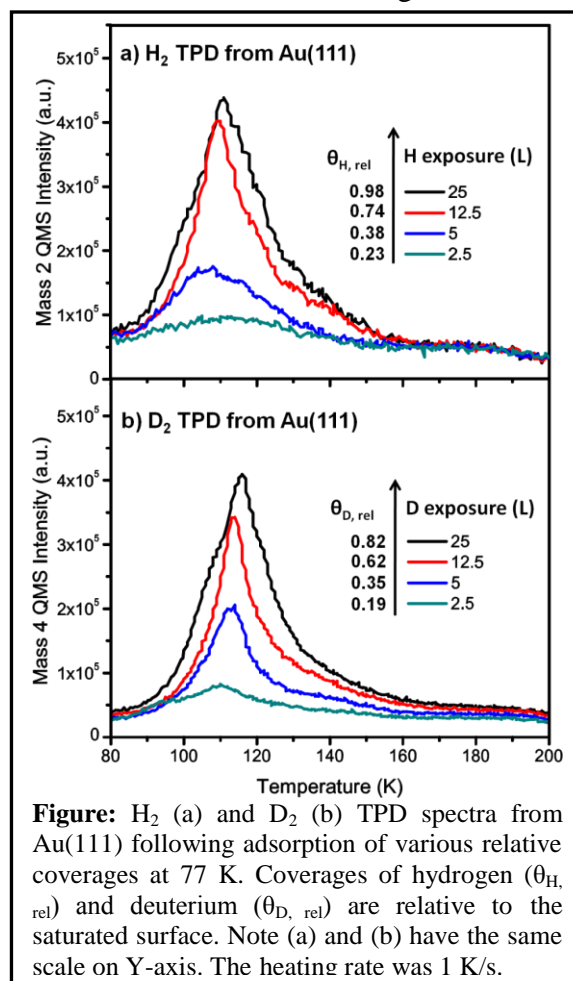
Our goals involve contributing to the understanding of issues related to gold catalysis through the study of specific surface chemical reactions on gold model catalysts in vacuum, including: What is the origin of the gold particle size effect? What is the nature and structure of the active site? What mechanisms drive the reaction [e.g., what is the role of moisture, which seems to be required for so many gold-catalyzed reactions]? What is the role of a metal oxide support?

## DOE Interest

Catalysis by metal-oxide supported gold is of interest to the Department of Energy since this catalytic system holds some promise for low-temperature one-step chemical conversions (e.g., epoxidation of propylene). Additionally, fundamental catalysis science is of interest to the DOE.

## Recent Progress

Gold-based classical high surface area catalysts have been widely investigated for hydrogenation reactions but fundamental studies on model catalysts are lacking. We have recently conducted experimental measurements of the reaction of hydrogen adatoms and adsorbed acetaldehyde on the Au(111) surface employing temperature programmed desorption. We have also shown that chemisorbed hydrogen adatoms bind weakly with desorption peaks at  $\sim 110$  K indicating an activation energy for recombinative desorption of  $\sim 28$  kJ/mol. We further demonstrate that



acetaldehyde ( $\text{CH}_3\text{CHO}$ ) can be hydrogenated to ethanol ( $\text{CH}_3\text{CH}_2\text{OH}$ ) on the H atom pre-covered Au(111) surface at cryogenic temperatures. Isotopic experiments employing D atoms indicated less hydrogenation activity.

The effect of moisture on CO oxidation on Au/TiO<sub>2</sub>(110) model catalysts has also been investigated using temperature-programmed desorption and molecular beam reactive scattering under ultrahigh vacuum (UHV) conditions. Oxygen exchange is observed between adsorbed atomic oxygen and isotopically labeled water. Coadsorbed water ( $\text{H}_2^{18}\text{O}$ ) takes part in CO oxidation on O<sub>a</sub> precovered Au/TiO<sub>2</sub>(110) model catalysts, leading to the formation of C<sup>16</sup>O<sup>18</sup>O and C<sup>16</sup>O<sup>16</sup>O. The amount of C<sup>16</sup>O<sup>18</sup>O produced increases with increasing water coverages; however, the total amount of CO<sub>2</sub> produced decreases. Although coadsorbed O<sub>a</sub> and H<sub>2</sub>O have a minimal influence on the initial adsorption probability of CO, the total uptake of CO decreases as H<sub>2</sub>O coverages increase. Interestingly, the adsorption of water induces desorption of predeposited molecularly chemisorbed O<sub>2</sub>. Thus, adsorbed water slightly inhibits CO oxidation on atomic oxygen precovered Au/TiO<sub>2</sub>(110) model catalysts under UHV conditions.

### Future Plans

We propose to study surface chemical reactions on model gold catalysts using ultrahigh vacuum surface science techniques including temperature programmed desorption and molecular beam methods. In particular, the primary model catalyst surfaces we will study include (i) planar wafers of a metal oxide [TiO<sub>2</sub>(110) and CeO<sub>2</sub>(111)] decorated with gold clusters and (ii) “inverse” model catalysts composed of metal oxide nanoparticles (ceria and titania) dispersed on a Au(111) surface [as well as simply Au(111)]. Several valuable studies investigating the physical characterization of such “inverse” surfaces have been conducted recently along with a few studies of their chemistry and we plan to build upon this previous work as well as recent research of our own. We propose two major themes regarding the surface chemistry of these model gold surfaces: (i) the hydrogenation chemistry of gold in ultrahigh vacuum, and (ii) partial oxidation reactions at near atmospheric pressure.

### Publications Crediting DOE BES Grant No. DE-FG02-04ER15587 (2008-2011)

1. C. B. Mullins and G. O. Sitz, “Taking a selective bite out of methane,” *Science* **319**, 736-737 (2008). <http://dx.doi.org/10.1126/science.1153906>
2. R. A. Ojifinni, N. S. Froemming, J. Gong, T. S. Kim, M. Pan, T. S. Kim, J. M. White, G. Henkelman, and C. B. Mullins, “Water-enhanced low-temperature CO oxidation and isotope effects on atomic oxygen covered Au(111),” *J. Am. Chem. Soc.* **130**, 6801-6812 (2008). <http://dx.doi.org/10.1021/ja800351j>
3. J. Gong, D. W. Flaherty, R. A. Ojifinni, J. M. White, and C. B. Mullins, “Surface chemistry of methanol on clean and atomic oxygen pre-covered Au(111)” *J. Phys. Chem. C* **112**, 5501-5509 (2008). <http://dx.doi.org/10.1021/jp0763735>
4. Rotimi A. Ojifinni, Jinlong Gong, Nathan S. Froemming, David W. Flaherty, Ming Pan, Graeme Henkelman, and C. B. Mullins, “Carbonate formation and decomposition on atomic oxygen pre-covered Au(111),” *J. Am. Chem. Soc.* **130**, 11250-11251 (2008). <http://dx.doi.org/10.1021/ja803482h>

5. Jinlong Gong and C. B. Mullins, "Enhanced carbonate formation on gold," *J. Phys. Chem. C* **112**, 17631-17634 (2008). <http://dx.doi.org/10.1021/jp805871j>
6. Jinlong Gong, David W. Flaherty, Ting Yan, and C. Buddie Mullins, "Selective oxidation of propanol on Au(111): Mechanistic insights into aerobic oxidation of alcohols," *ChemPhysChem* **9**, 2461-2466 (2008). <http://dx.doi.org/10.1002/cphc.200800680>
7. Jinlong Gong and C. Buddie Mullins, "Selective oxidation of ethanol to acetaldehyde on gold," *J. Am. Chem. Soc.* **130**, 16458-16459 (2008). <http://dx.doi.org/10.1021/ja805303s>
8. Jinlong Gong, Ting Yan, and C. Buddie Mullins, "Selective oxidation of propylamine to propionitrile and propaldehyde on oxygen-covered gold," *Chem. Commun.* 761-763 (2009). <http://dx.doi.org/10.1039/b821050k>
9. Rotimi A. Ojifinni, Jinlong Gong, David W. Flaherty, Tae S. Kim, and C. Buddie Mullins, "The effect of annealing on reactivity of oxygen towards water, CO, and CO<sub>2</sub> on Au(111)," *J. Phys. Chem. C* **113**, 9820-9825 (2009). <http://dx.doi.org/10.1021/jp9022019>
10. Jinlong Gong and C. Buddie Mullins, "Surface science studies of oxidative chemistry on gold," *Acc. Chem. Res.* **42**, 1063-1073 (2009). <http://dx.doi.org/10.1021/ar8002706>
11. Ming Pan, Son Hoang, Jinlong Gong, and C. Buddie Mullins, "CO dissociation triggered by adsorbed oxygen and water on Ir(111)," *Chem. Commun.* 7300-7302 (2009). <http://dx.doi.org/10.1039/b914308d>
12. Ting Yan, Jinlong Gong, and C. Buddie Mullins, "Oxygen exchange in the selective oxidation of 2-butanol on oxygen precovered Au(111)," *J. Am. Chem. Soc.* **131**, 16189-16194 (2009). <http://dx.doi.org/10.1021/ja9062986>
13. S. D. Senanayake, D. Stachiolla, P. Liu, C. Buddie Mullins, J. Hrbek, and J. A. Rodriguez, "The interaction of CO with OH on Au(111): HCOO, CO<sub>3</sub> and HOCO as key intermediates in the water-gas shift reaction," *J. Phys. Chem. C* **113**, 19536-19544 (2009). <http://dx.doi.org/10.1021/jp908169s>
14. Son Hoang, Ming Pan, and C. Buddie Mullins, "Surface chemistry of 2-propanol on clean and oxygen pre-covered Ir(111)," *J. Phys. Chem. C* **113**, 21745-21754 (2009). <http://dx.doi.org/10.1021/jp907324n>
15. Ming Pan, Son Hoang, and C. Buddie Mullins, "Interaction of water with the clean and oxygen precovered Ir(111) surface," *Catal. Today* **160**, 198-203 (2011). <http://dx.doi.org/10.1016/j.cattod.2010.05.008>
16. Ting Yan, Jinlong Gong, David W. Flaherty, and C. Buddie Mullins, "The effect of adsorbed water in CO oxidation on Au/TiO<sub>2</sub>(110)," *J. Phys. Chem. C* **115**, 2057-2065 (2011). <http://dx.doi.org/10.1021/jp109295u>
17. Ming Pan, David W. Flaherty, and C. Buddie Mullins, "Low-temperature hydrogenation of acetaldehyde to ethanol on H-precovered Au(111)," *J. Phys. Chem. Lett.* **2**, 1363-1367 (2011). <http://dx.doi.org/10.1021/jz200577n>
18. David W. Flaherty, Wen-Yueh Yu, Zachary D. Pozun, Graeme Henkelman, and C. Buddie Mullins, "Mechanism for the water-gas shift reaction on monofunctional platinum and cause of catalyst deactivation," accepted by *J. Catal.* (July 2011).



**Reactions of C<sub>2</sub> - Oxygenates on Cerium Oxide Surfaces**

Lead PI: Steven H. Overbury  
Co-PI: Ye Xu  
Postdocs: Sanjaya Senanayake, Tsung-Liang Chen and Florencia Calaza  
Contact: Chemical Sciences Division, Oak Ridge National Laboratory, Oak Ridge, TN  
37831-6201, [mullinsdr@ornl.gov](mailto:mullinsdr@ornl.gov)

A series of organic oxygenates containing two C atoms and different O-containing functional groups have been studied on oxidized and reduced CeO<sub>2</sub>(111), specifically ethanol, acetic acid, acetaldehyde and ethylene glycol. Ethanol exhibits the simplest reaction chemistry adsorbing solely as an ethoxide on both oxidized and reduced surfaces. The ethoxide reacts to produce ethylene and acetaldehyde with the ethylene pathway becoming more dominant as the ceria becomes reduced. Acetic acid adsorbs as an acetate. On the oxidized surface dehydration of the acetate leads to ketene formation. C-C bond cleavage is also evident as CO and CO<sub>2</sub> are produced. As the surface is reduced the CO and CO<sub>2</sub> pathways disappear and deoxygenation of the acetate leads to production of acetaldehyde and more extensive dehydration produces acetylene. In addition to the acetate, small amounts of an ethylene enolate are observed on the reduced surface. Acetic acid is unique among the molecules studied in that a small amount of coupling was observed to produce acetone and a substantial amount of unreactive C residue is left on the reduced surface. Acetaldehyde is unreactive on an oxidized surface. On a reduced surface acetaldehyde forms an ethylene enolate. The enolate reacts to produce mostly ethylene and a lesser amount of acetylene. The C<sub>2</sub> diol, ethylene glycol, deprotonates at both ends producing ethylenedioxy on the surface. Although it contains alcohol functional groups, the chemistry of ethylene glycol appears to have more in common with acetic acid and acetaldehyde than ethanol, however. On the oxidized surface the primary products are CO and acetaldehyde. The CO appears to be produced via a formate intermediate whereas acetaldehyde is produced by C-O bond cleavage in the ethylenedioxy. On the reduced surface C-O cleavage produces a stable ethylene enolate intermediate. This reacts to produce acetaldehyde, ethylene and acetylene.

Research sponsored by the Division of Chemical Sciences, Geosciences, and Biosciences, Office of Basic Energy Sciences, U.S. Department of Energy

## *Fundamental Studies of Catalysis Using X-rays*

Anders Nilsson

SUNCAT, SLAC National Accelerator Laboratory, Stanford, CA

I will demonstrate how electron and x-ray spectroscopy can be used to address fundamental questions regarding the reaction mechanism of the oxygen reduction reaction (ORR) on Pt and probe the electronic structure of Pt and adsorbed species of model system Pt catalysts. From time resolved x-ray photoelectron spectroscopy (XPS) we have determined the activation barrier for the O<sub>2</sub> dissociation process on Pt to be in the range around 0.25 eV [1]. Using in-situ studies under real electrochemical conditions of single crystal surfaces using high resolution Pt L-edge spectroscopy we have identified oxide growth at certain potentials that could have some major influence on the rate of the ORR reaction [2]. Recent dealloyed Pt-Cu catalysts have shown an enhanced activity in comparison to pure Pt by factor of 5 tested in a real fuel cell [3]. We demonstrate that this activity enhancement comes from compression strain of the Pt lattice that leads to modifications of the Pt electronic structure and subsequently weakens the surface bond of adsorbed oxygen species [4].

1. D. J. Miller et al. *J. Chem. Phys.* **22**, 224701 (2010)
2. D. Friebel et al. *Phys. Chem. Chem. Phys.* **13**, 262 (2011)
3. R. Srivats et al. *Angew. Chem. Int. Ed.* **46**, 8988 (2007)
4. P. Strasser et al. *Nature Chemistry* **2**, 454 (2010)

## Controlling catalyst structures with oxide clusters and oxide nanocavities

Justin M. Notestein

Department of Chemical and Biological Engineering, Northwestern University

e-mail: [j-notestein@northwestern.edu](mailto:j-notestein@northwestern.edu)

Important goals in heterogeneous catalyst development are to increase selectivity and stability, both of which can, in principle, be controlled by atom-precise design and synthesis of a catalyst active site. Imbedding active sites in zeolite cavities has long been used to impart control over the domain size of a metal catalyst, prevent it from deactivation by sintering or agglomeration, and to impart selectivity based on size discrimination. Here, we instead demonstrate two routes to controlling catalyst domains on non-microporous supports by use of pre-formed metal oxide clusters to synthesize corresponding low-nuclearity metal oxide domains, and by use of nm-cavities synthesized in nm-thick oxide films deposited the surface of another support.

In the first case, we supported mono-, di-, and tetranuclear Mn complexes synthesized from a triazacyclononane ligand. These and other low nuclearity metal oxide complexes were originally synthesized by others as potential structural mimics of the active sites in important metalloenzymes like catalase or the oxygen evolving center in photosystem II. While several of these mimics are active catalysts in their own right for low temperature oxidation, they are essentially unexplored on supports. These cationic complexes were supported on silica, titania, and alumina by non-aqueous impregnation and calcined to produce the final heterogeneous catalysts, or they were supported on carboxylate-containing surfaces such as modified silica or activated carbons and used intact. The structures of the supported catalysts were understood by NMR, diffuse reflectance UV-visible spectroscopy and XANES/EXAFS, and were consistent with retention of the structure of the original complex on bare supports and reductive coordination by carboxylates on the modified surfaces. For example, EXAFS showed no higher coordination Mn shells for the supported monomer, and 1 or 3 Mn neighbors for the dimer and tetramer, respectively. Supported on carboxylates, these complexes had epoxidation and hydroxylation reactivity dependant on the carboxylate structure, surface, nearby grafted groups, and Mn complex nuclearity. Alkane oxidation by the bare oxides was dependent on precursor nuclearity. Further correlations between precursor structure, final supported structure, hydrogen-TPR, and reactivity in alkane oxidation will be described.

In the second approach, we and collaborators utilized atomic layer deposition (ALD) to grow thin (< 2nm) oxide layers over catalyst surfaces previously modified with bulky template molecules such as *tert*-butylcalix[4]arene or adamantanecarboxylic acid. This generated ~1 nm<sup>3</sup> (1 yoctoliter) nanocavities in the oxide film as demonstrated by SAXS, QCM during synthesis, TEM, and auxiliary techniques. After template removal, nanocavities in an inert film gave shape-selective access to the underlying catalyst surface. Size selectivity of the catalysts was demonstrated through selective photooxidation of benzyl alcohol vs. more hindered alcohols over an originally non-selective titania photocatalyst that was over-coated with alumina films 0.3-0.5 nm thick and perforated with nanocavities. Additional results are described on the use of these nanocavities in other reactions and as special exchange sites for the synthesis and protection against deactivation for size-constrained metal and metal oxide clusters.

Overall, the used of these small cavities and of small oxide cluster precursors, and especially their combination, may lead to new paradigms in heterogeneous catalyst synthesis and increased selectivity for particular reactions and reactants within complex networks.

**The Reactivity and Structural Dynamics of Supported Metal Nanoclusters Using Electron Microscopy, in situ X-Ray Spectroscopy, Electronic Structure Theories, and Molecular Dynamics Simulations.**

Additional PIs: Judith Yang (U. Pittsburgh), Duane Johnson (Ames Lab and Iowa State U.), Anatoly Frenkel (Yeshiva U.)  
 Post-docs: Long Li (U. Pittsburgh), Relja Vasic (Yeshiva U.), Lin-lin Wang (Iowa State)  
 Grad. Students: Sergio Sanchez (Illinois), Matthew Small (Illinois), Evan Erickson (Illinois), Zhongfan Zhang (U. Pittsburgh), Ross Grieshaber (U. Pittsburgh)  
 Collaborators: J. Rehr (U. Washington), R. Finke (Colorado State), X. Teng (U. New Hampshire), B. Roldan Cuenya (UCF), R. Crooks (UT Austin), J. Chen (U. Delaware), R. Adzic (BNL), E. Stach (BNL), D. Nackashi (Protochips), J. Mastovich (RJ Lee Group), C. Matranga, S. Natesakhawat (DOE-NETL)

**Contact:**

R. G. Nuzzo, Chemistry Dept., Univ. of Illinois, 600 S Mathews Avenue, Urbana, IL, 61801; [r-nuzzo@illinois.edu](mailto:r-nuzzo@illinois.edu)  
 J. C. Yang, Dept. of Mech. Eng. Mat. Sci., Univ. of Pittsburgh, 3700 O'Hara St, Pittsburgh, PA 15261; [judyang@pitt.edu](mailto:judyang@pitt.edu)  
 A. I. Frenkel, Dept. of Physics, Yeshiva Univ., 245 Lexington Avenue, New York, NY 10016; [Anatoly.Frenkel@yu.edu](mailto:Anatoly.Frenkel@yu.edu)  
 D. D. Johnson, Ames Laboratory and Dept. Mat. Sci. and Eng., Iowa State Univ., Ames, Iowa 50011; [ddj@ameslab.gov](mailto:ddj@ameslab.gov)

**Goal**

This project involves the characterization of metal nanoparticle (NPs) catalysts with the goal of achieving a fundamental understanding of their dynamical and structural properties and the correlations these have with behavior seen in catalytic chemistry. Nanocatalyst materials prepared via controlled chemical syntheses are characterized using a variety of analytical techniques, highlighted by the complementary use of X-ray absorption spectroscopy (XAS) and advanced transmission electron microscopy (TEM). Theoretical calculations further augment an understanding of structures that are characteristic of the nanometer dimensions of catalyst materials or of their local environment.

**DOE Interest**

In our program of collaborative research, we seek to develop and apply integrated (experimental and theoretical) analysis methodologies to provide deep understandings of structure and mechanism in heterogeneous catalysis, with a particular focus on clusters containing less than 100 atoms. Our goals are: 1) *Describing the full 3D structural habits of supported metal clusters of interest in heterogeneous catalysis;* 2) *Clarifying the nature of the energy landscapes that lead to these structural habits;* 3) *Elucidating the atomistic nature of the dynamics mediating structural transformations and leading to enhanced reactivity of supported metal clusters in heterogeneous catalysis;* and 4) *Understanding the impacts and interplay of size, shape, elemental composition, substrate material including surface defects and electronic structure modifications on cluster properties.* We highlight our coordinated efforts to characterize heretofore poorly understood physiochemical behaviors seen in such systems and the critical role that interactions with adsorbates and supports play in mediating them. The systems explored in

this work include exceptionally well-defined metal and metal-alloy catalysts supported in diverse forms—materials that are synthesized by the collaborating team and chosen for the insights they empower into fundamental electronic, structural, and dynamical behaviors. Our work builds a significant foundation to advance what we hope will be important progress towards a fundamental grand challenge—to bridge atomic-level understandings in predictive ways to the chemical and rate-centric properties exhibited by a catalytic material.

## Recent Progress

**A. Mesoscopic amorphization of supported Pt nanoparticles: Dependency on size, support and adsorbates:** In the first year our collaborative team characterized the amorphous-to-crystalline structural behavior of supported Pt nanoparticles (NPs) as a function of the cluster size, specifically examining how these size-dependent scalings of highly anisotropic atomic strains respond to both support and adsorbate interactions. We combined synthetic and analytical methods available to Nuzzo, Yang and Frenkel for multi-technique, complementary (in situ XAFS and ex situ TEM) studies that were integrated with first-principles theoretical calculations done by Johnson. As described in our 2010 report, observations of >3000 NPs by high-resolution TEM (HRTEM) showed that NPs < 1.1 nm are disordered, and that a non-abrupt amorphous-to-ordered transition zone exists, with a narrower transition zone for Pt/ $\gamma$ -Al<sub>2</sub>O<sub>3</sub> than for that of Pt/C. The question remained, however, what is the role of hydrogen atmosphere in stabilizing the ordered structure, and it could not be answered by ex-situ TEM studies that are done in vacuum. In the second year, we were able to extend this work, and validate a quasi-thermodynamic model founded on theory by conducting environmental TEM (ETEM) experiments with the same systems in different ambient atmospheres. Our results revealed enhancement of the *fcc* crystallinity of the initially disordered Pt NPs results due to exposure to H<sub>2</sub>, which was predicted by theoretical simulations. These results are also in full agreement with in-situ EXAFS results obtained for the same samples (**Figure 1**).

First-principles calculations predicted that the energetically preferred structure of a 1.1 nm NP in an inert atmosphere on C or  $\gamma$ -Al<sub>2</sub>O<sub>3</sub> lacks crystalline order while adsorbates stabilize a truncated *fcc* structure, which is more pronounced on C supports. As shown in **Figure 1**, theory, including *ab initio* Molecular Dynamics simulations, helped identify the mesoscopic effects in the NP structure, especially in regards to effects related to size, support and adsorbates. In the past funding period, theory results showed that there are shear instabilities in (100) facets of transition-metal NP arising from the electronic effects that drive surface reconstruction in the semi-infinite bulk. We also showed that such inherent surface-energy-driven instabilities are removed by adsorbates, e.g. H. The predictions were confirmed by careful structural characterization of the Pt NPs under environmental conditions using in-situ EXAFS and recently ETEM. In support of the dramatic adsorbate effect predicted by theory, the new ETEM result also exhibit a striking effect of H adsorbates on the stabilization of the NP crystalline structure. The ETEM results agree well with the theoretical predictions; the 1.1 nm Pt in He shows greater static disorder than do larger Pt NPs, and H adsorbates presumably cause clusters to reconstruct into their crystalline TC shape, as predicted from the filling of antibonding states in the Pt NPs.

**Major Outcome:** *Our work demonstrates, and explains for the first time, how a statistical description is necessary to understand structural behaviors of nanoparticles where the atomic strains due to size and adsorbates strongly impact atomic ordering in NP catalytic materials.*

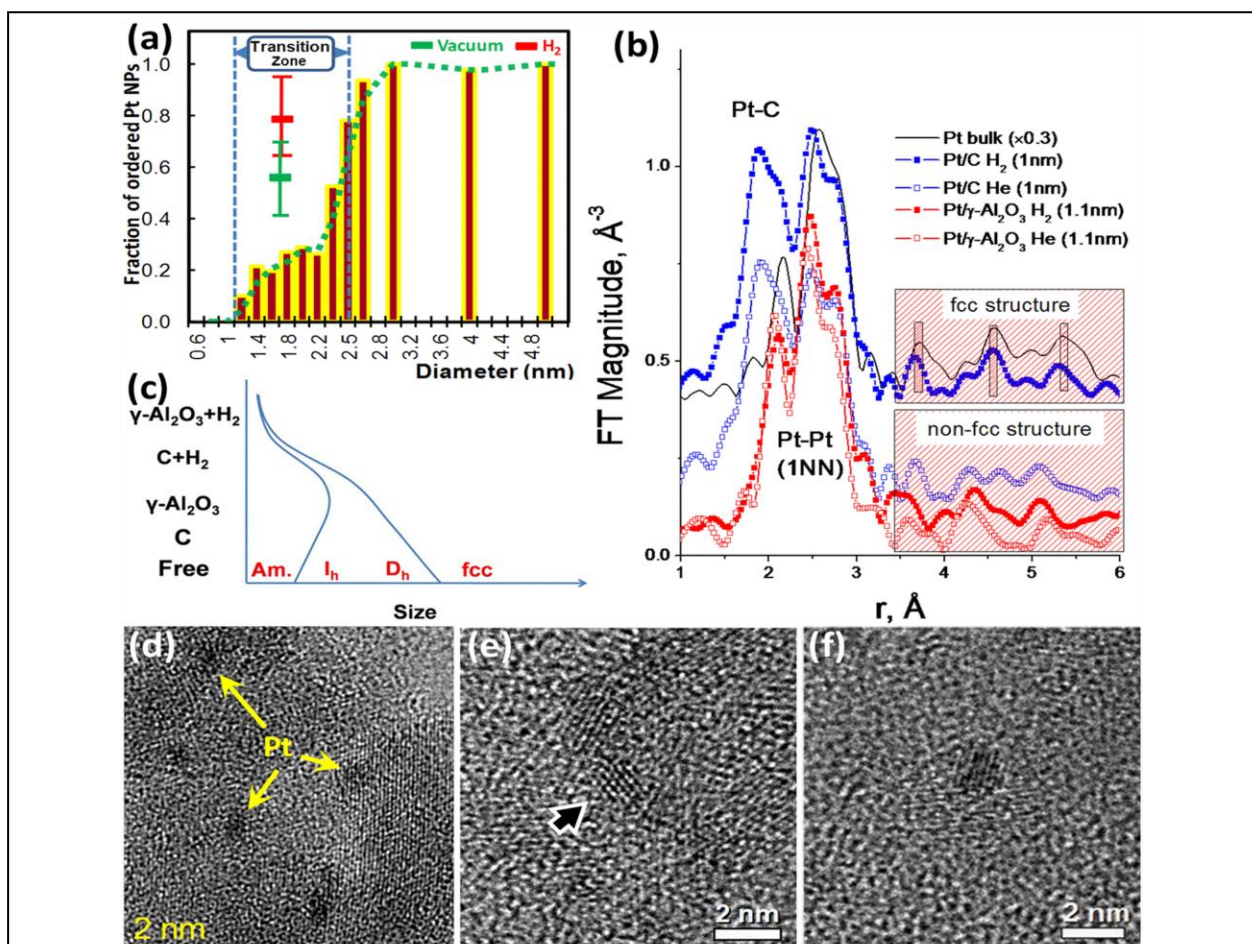
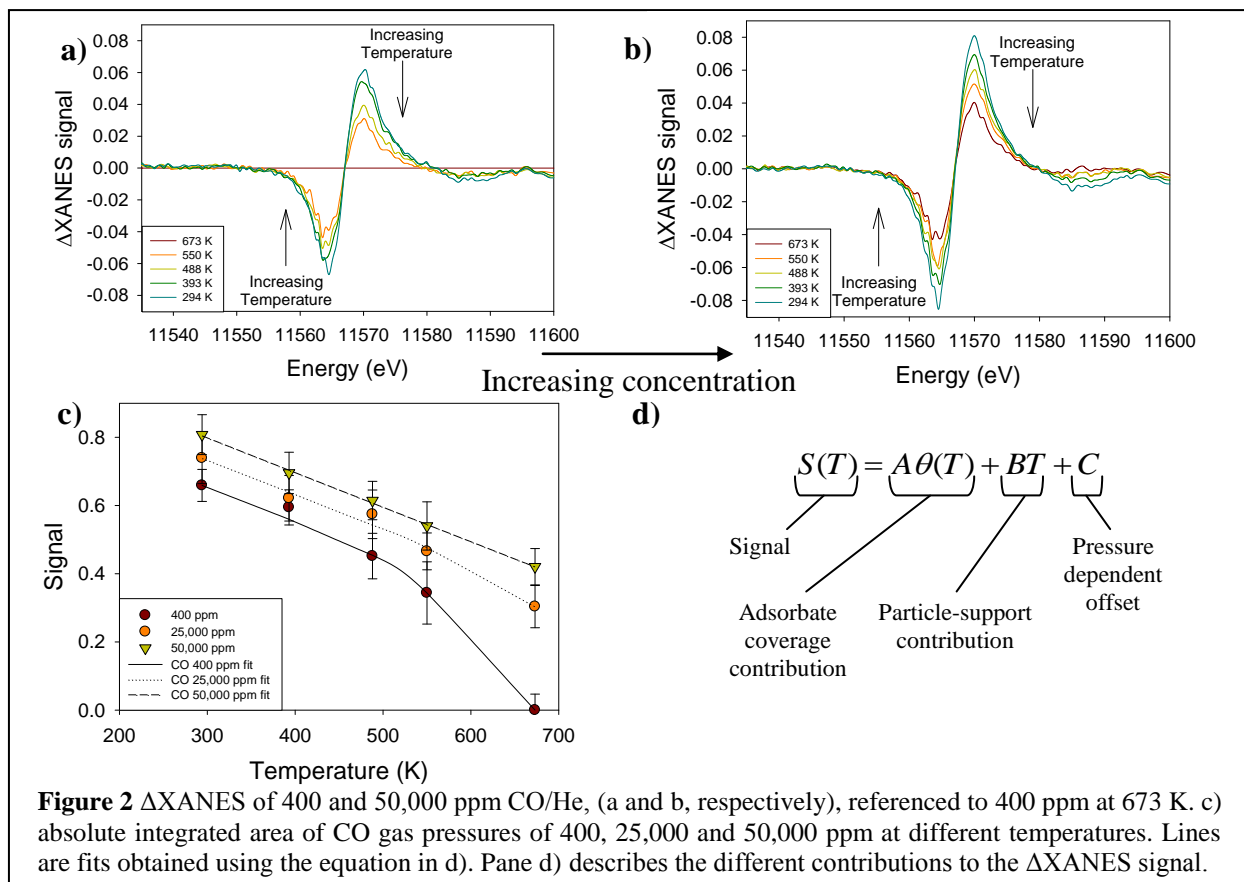


**Figure 1:** (a) The fraction of ordered Pt NPs supported on  $\gamma$ - $\text{Al}_2\text{O}_3$  as a function of size from HRTEM observations. Overlaid on (a) are ETEM results comparing as-prepared sample in vacuum, [see 1(d) a HRTEM image of disordered Pt NPs from 1.2 to 1.5nm], with the same sample exposed to 1 torr  $\text{H}_2$  after heated to 385  $^\circ\text{C}$  for > 30 min and cooled down to RT within the ETEM [see 1(e) and 1(f) - HRTEM images of ordered 1.2nm and 1.4nm Pt NPs, respectively].  $\text{H}_2$  exposure enhanced the fraction of ordered NPs. Figure 1(b) shows EXAFS data on reduced Pt/ $\gamma$ - $\text{Al}_2\text{O}_3$  and Pt/C NPs of similar average sizes. The Pt/C under  $\text{H}_2$  demonstrates a local fcc-like structure, same as in Pt foil, while the rest of the samples show different types of structural order beyond the 1<sup>st</sup> neighbor. Figure 1(c) shows schematic phase diagram of Pt NP reflecting size and chemical environment.

### B. EXAFS studies of adsorbate effects on electronic, structural, thermal properties

We very recently have acquired XAS data pertaining to the structural dynamics that result from the adsorption of CO and  $\text{H}_2$  gases on Pt/ $\gamma$ - $\text{Al}_2\text{O}_3$ , an industrially relevant catalyst, under a variety of partial pressure and temperature conditions (which in turn broadly vary the coverage and thermally responsive atomic strains). By making these measurements under steady state conditions we have managed to separate dynamic alterations to the system caused by thermally mediated changes between the particle and support from effects arising from coverage dependent electron donation. To isolate the electronic changes occurring within the system, we compare the difference spectra ( $\Delta\text{XANES}$ ) in the area of the Pt  $L_3$ -edge energy. **Figures 2a-b** shows how effecting changes in conditions of pressure and temperature under CO leads to significant perturbations in the  $\Delta\text{XANES}$  data. By plotting the absolute, integrated intensity of the  $\Delta\text{XANES}$  versus temperature (**Figure 2c**) two things can be noted: 1) even though 50,000 ppm CO should fully saturate the Pt surface across all temperatures there is a near-linear change in the signal with temperature and 2) there is a clear dependence of the absolute, integrated intensity on the

partial pressure of CO. This provides support for an empirical mathematical model grounded in physical interpretations (**Figure 2d**), where each contribution to the electronic state of Pt is separable. If one assumes that the coverage ( $\theta$ ) can be modeled by a Langmuir isotherm, we can determine the approximate heat of adsorption for both gases on Pt/ $\gamma$ -Al<sub>2</sub>O<sub>3</sub>. Comparison of these values with internal strain energies derived from the EXAFS data therefore allows for an unprecedented look at how the strength of adsorbate binding is altered by the bond relaxations that underpin nanoparticle order/disorder structural transitions.



### Future plans

*Investigation of adsorption characteristics of heterogeneous catalysts using High Energy Resolution Fluorescence Detection.* Measurements of Pt/ $\gamma$ -Al<sub>2</sub>O<sub>3</sub>, a hydrogenation catalyst, by the Nuzzo-Frenkel groups at the NSLS beamline X18B showed, for the first time, pressure-dependent, charge-transfer effects for CO and H coverage on Pt XAS. These and other observations (e.g., surface strain contributions to the heat of adsorption) require further interpretation in terms of adsorbate-binding modes' dependence on the dynamic gas coverage and temperature. High energy-resolution fluorescence detection (HERFD) has been applied by M.Tromp (Munich) to study the adsorption of CO on Pt, and has tremendous potential for coverage-dependent studies. We expect to observe – and to separate and individually interpret – systematic changes in Pt-CO bonding with changing CO pressure, the temperature, and the particle-support interaction. Interpretation of the effects in terms of cluster-adsorbate-substrate interactions will be guaranteed by our use of monodisperse (~1 nm) Pt clusters. Our team collaboration with Tromp group will allow for a deeper understanding of how the ambient

environment can alter catalytic systems and how different environmental factors contribute to optimizing a catalytic system.

*In-situ electrochemistry experiments with NP-modified electrodes for oxygen-reduction reaction.*

We have recently made a major advance that has extended the capacity of synchrotron X-ray characterization methods that, in conjunction with other probes, provide important new *in-operando* capabilities for elucidating the atomic and electronic structures of operating electrocatalysts. The most significant feature of the work is the development of a new integrated electrochemical XAS cell that can provide substantial transport fields and thus allow direct measurements across a broad range of operating potentials and currents. In our initial work, we explored with particular interest the structural dynamics and electronic properties of supported nanocluster catalysts during their active mediation of the oxygen reduction reaction. Preliminary in-situ electrochemical XAS experiments by Brookhaven (Frenkel) and Illinois (Nuzzo) have shown drastic differences in the electronic structure of platinum electrocatalysts under oxygen and nitrogen environments, over a wide range of the potential dependent operating current densities. These measurements are made possible due to a novel in-situ electrochemical XAS cell design developed at Illinois (Nuzzo) that can supply extremely high (non-depleting) oxygen flux to the working electrode (WE), while fully immersing the WE in a thin electrolyte that provides excellent X-ray transmission. Large, stable operational currents are achieved due to high oxygen permeation into the cell. This work is continuing and will be extended to establish how in the full IV scan this bonding evolves and the coverage dependences that attend it.

*Structural dynamics of supported Pt NPs on  $\gamma$ -Al<sub>2</sub>O<sub>3</sub> or C-black with environmental TEM (ETEM). Collaboration with Dr. E.A. Stach at the Center for Functional Nanomaterials, BNL.*

We employed the dedicated ETEM to visualize structures and possible structural changes leading to amorphization, and adsorbate-driving recrystallization of alumina-supported Pt nanoparticles under environmental conditions. The Pt NPs with other supports, e.g., C-black, will be examined under environmental conditions in the near future.

*Creation of model Pt NPs on  $\gamma$ -Al<sub>2</sub>O<sub>3</sub> single crystal thin film.* Single crystal  $\gamma$ -Al<sub>2</sub>O<sub>3</sub> thin film are being created by oxidation of NiAl(110) at high temperatures under ambient air. The  $\gamma$ -Al<sub>2</sub>O<sub>3</sub> support effects on the Pt NP's equilibrium shape as well as the Pt/ $\gamma$ -Al<sub>2</sub>O<sub>3</sub> atomic and electronic interfacial structures are being characterized by cross-sectional HRTEM such that a direct comparison between experiments and theoretical simulations will be feasible.

*Theoretical development.* We will investigate catalytic effects of TM NPs on different supports, especially critical surface and defect-mediated physics, with focus on desorption enthalpies and kinetic barriers. We will develop an improved algorithm to obtain kinetic barriers, as most methods that can include both surfaces and molecules or NPs cannot address catalytic dopants with varying magnetic states that alter kinetic barriers. We will continue to help interpret data from the mesoscopic amorphization collaboration. We also will address electrocatalytic behavior especially under differing environments to help assess ongoing experiments in our collaborative efforts. Short-term projects are: Complete theoretical study of the *non-ergodic behavior of supported NPs* that appears responsible for our recent experimental results on T-dependent NP bond-length effects involving varying environments (e.g., He and H), making critical direct comparison to determine whether non-ergodic behavior impacts all experimental studies; Cluster-expansion study of supported, alloyed NP, making connection to our experimental studies; Catalytic effect of small transition-metal NP on MgH<sub>2</sub>(110) surface; Create and use a valid nudged-elastic band method that addresses change in charge and/or magnetic state of an atom or adsorbate, as well as local structural changes due to local chemistry changes.



## Selected publications from PIs on this grant

1. L. Li, L.-L. Wang, D. D. Johnson, Z. Zhang, S. I. Sanchez, J. H. Kang, R. G. Nuzzo, Q. Wang, A. I. Frenkel, J. Ciston, E. A. Stach and J. C. Yang, Mesoscopic Amorphization of Supported Pt Nanoparticles: Dependency on Size, Support and Adsorbates, submitted.
2. M. W. Small, S. I. Sanchez, L. D. Menard, J. H. Kang, A. I. Frenkel and R. G. Nuzzo, The Atomic Structural Dynamics of  $\gamma$ -Al<sub>2</sub>O<sub>3</sub> Supported Ir-Pt Nanocluster Catalysts Prepared From a Bimetallic Molecular Precursor: A Study Using Aberration-Corrected Electron Microscopy and X-ray Absorption Spectroscopy, *J. Am. Chem. Soc.*, **133**, 3582-3591 (2011).
3. A. I. Frenkel, A. Yevick, C. Cooper, R. Vasic, Modeling the structure and composition of nanoparticles by EXAFS, *Ann. Rev. Anal. Chem.*, doi:10.1146/Annurev-Anchem-061010-113906.
4. M. G. Weir, V. Sue Myers, A. I. Frenkel, R. M. Crooks, In situ X-ray absorption analysis of ~1.8 nm Dendrimer-encapsulated platinum nanoparticles during electrochemical CO oxidation, *Chem. Phys. Chem.*, **11**, 2942-2950 (2010).
5. B. Roldan Cuenya, J. R. Croy, S. Mostafa, F. Behafarid, L. Li, Z. Zhang, J. C. Yang, Q. Wang, A. I. Frenkel, Solving the Structure of Size-Selected Pt Nanocatalysts Synthesized by Inverse Micelle Encapsulation, *J. Am. Chem. Soc.* **132**, 8747-8756 (2010).
6. S. Mostafa, F. Behafarid, J. R. Croy, L. K. Ono, L. Li, J. C. Yang, A. I. Frenkel, B. R. Cuenya, Shape-Dependent Catalytic Properties of Pt Nanoparticles, *J. Am. Chem. Soc.* **132**, 15714-15719 (2010).
7. L. Li, Z. Zhang, J. R. Croy, S. Mostafa, B. R. Cuenya, A. I. Frenkel, J. C. Yang, Ultra-small and Monodisperse Pt nanoparticles supported on  $\gamma$ -Al<sub>2</sub>O<sub>3</sub>, *Microsc. Microanal.* **16**, 1192-1193 (2010).
8. L. Li, Z. Zhang, J. Ciston, E. A. Stach, L.-l. Wang, D. D. Johnson, Q. Wang, A. I. Frenkel, S. I. Sanchez, M. W. Small, R. G. Nuzzo, J. C. Yang, H<sub>2</sub>-driven crystallization of supported Pt nanoparticles observed with aberration-corrected E- TEM, *Microsc. Microanal.* **17**, (2011). In press.
9. Z. Zhang, L. Li, J. C. Yang, " $\gamma$ -Al<sub>2</sub>O<sub>3</sub> Thin Film Formation via oxidation of  $\beta$ -iAl(110)", *Acta Mater.*, (2011), doi: 10.1016/j.actamat.2011.05.064.
10. Z. Zhang, L. Li, M. Shah, J-G. Wen, J. C. Yang, " $\gamma$ -Al<sub>2</sub>O<sub>3</sub> Thin Films Catalyst Model Support Preparation on  $\beta$ -NiAl(110) Alloy", *Mater. Res. Soc. Symp. Proc.* 1217 (Catalytic Materials for Energy, Green Processes, and Nanotechnology), Y05-02/1 (2010).
11. Z. Zhang, L. Li, L.-l. Wang, S. I. Sanchez, R. Grieshaber, Q. Wang, D. D. Johnson, A. I. Frenkel, R. G. Nuzzo, J. C. Yang, Preparation and characterization of Pt/ $\gamma$ -Al<sub>2</sub>O<sub>3</sub> model catalyst on NiAl alloy, *Microsc. Microanal.* **16**, 1464-1465 (2010).
12. Z. Zhang, L. Li, L.-l. Wang, S. I. Sanchez, Q. Wang, D. D. Johnson, A. I. Frenkel, R. G. Nuzzo, J. C. Yang, The Role of  $\gamma$ -Al<sub>2</sub>O<sub>3</sub> Single Crystal Support to Pt Nanoparticles Construction, *Microsc. Microanal.* **17**, (2011). In press.
13. W. M. Alley, I. K. Hamdemir, Q. Wang, A. I. Frenkel, L. Li, J. C. Yang, L. D. Menard, R. G. Nuzzo, S. Ozkar, K. A. Johnson, R. G. Finke, Iridium Ziegler-Type Hydrogenation Catalysts Made from [(1,5-COD)Ir( $\mu$ -O<sub>2</sub>C<sub>8</sub>H<sub>15</sub>)]<sub>2</sub> and AlEt<sub>3</sub>: Spectroscopic and Kinetic Evidence for the Ir<sup>III</sup> Species Present and for Nanoparticles as the Fastest Catalyst, *Inorg. Chem.* **49**, 8131-8147 (2010).
14. S. I. Sanchez, M. W. Small, J. M. Zuo, R. G. Nuzzo, Structural characterization of Pt-Pd and Pd-Pt core-shell nanoclusters at atomic resolution. *J. Am. Chem. Soc.* **131**, 8683-8689 (2009).
15. Sanchez, S. I.; Small, M. W.; Sivarmakrishnan, S.; Wen, J.; Zuo, J.-M.; Nuzzo, R. G., Visualizing materials chemistry at atomic resolution. *Analytical Chemistry* **82**, 2599-2607 (2010).
16. L. D. Menard, Q. Wang, J. H. Kang, A. Sealey, G. S. Girolami, A. I. Frenkel, R. G. Nuzzo Structural characterization of bimetallic nanomaterials with overlapping x-ray absorption edges. *Phys. Rev. B* **80**, 064111 (2009).
17. A. Kulkarni, L.-L. Wang, D. D. Johnson, D. Sholl, K. Johnson, First-Principles Characterization of Amorphous Phases of MB<sub>12</sub>H<sub>12</sub>, M=Mg, Ca; *J. Phys. Chem. C* **114**, 14601-14605 (2010).
18. A. Alam, B. Kraccek, D. D. Johnson, Structural, magnetic and defect properties of Co-Pt-type magnetic-storage alloys: a DFT study of processing effects. *Phys. Rev. B.* **82**, 024435 (2010).

**Fundamentals of Heterogeneous Catalysis on Surfaces and Nanostructures**

Co-PIs: Sheng Dai, David R. Mullins, Zili Wu, De-en Jiang, Ye Xu

Collaborators: Viviane Schwartz, Edward W. Hagaman, Larry Allard, Jane Howe, Takeshi Egami (U. Tennessee), W. Dmowski (U. Tennessee)

Postdocs: Meijun Li, Tsung-Liang Chen, Peter Albrecht, Florencia Calaza, J. Christopher Bauer, Sanjaya Senanayake, W.O. Gordon, Hongfeng Yin, Zhen Ma

Contact: Chemical Sciences Division, Oak Ridge National Laboratory, Oak Ridge, TN 37831-6201, [overburysh@ornl.gov](mailto:overburysh@ornl.gov)

**Goals**

The overarching goal of this project is to understand the interactions between metals and their supports and the crucial role that supports play in promoting or altering catalytic pathways and controlling surface chemistry and catalytic reactions involving oxygenates. Work described in this abstract focuses upon two major aspects: 1) surface chemistry and redox reactions on reducible oxide surfaces; 2) the role of support type and surface structure on the catalytic activity of Au nanoparticles.

**DOE interest**

New catalysts hold the key to technology innovation in efficient and clean production and utilization of fuels and chemicals. This work provides a research basis for preparing, testing and understanding catalysts with potential application in these technologies.

**Recent Progress***Surface chemistry on CeO<sub>2</sub>*

We have been using a combination of UHV and synchrotron based techniques to explore the surface chemistry of redox reactions on CeO<sub>2</sub> surfaces. We are exploring how the reducibility of CeO<sub>2</sub> affects its surface chemistry. We have probed adsorption of alcohols, ketones, aldehydes, and ethylene glycol to explore how these oxygenates interact with the oxidized CeO<sub>2</sub>(111) and defective reduced surface.

Our work reveals that alcohols readily adsorb by deprotonating to form alkoxides, although differences between primary and secondary alcohols occur during TPD. Primary alcohols dehydrogenate mostly to aldehydes while secondary alcohols dehydrate to alkene, although the competition between dehydration and dehydrogenation depend upon extent of reduction of the ceria. Ketone and aldehyde functionalities, lacking the weakly acidic proton behave quite differently as we find in studies of acetone and acetaldehyde. Although both molecules weakly bind to oxidized CeO<sub>2</sub>(111), on the reduced surface they interact more strongly in an η<sub>1</sub>-

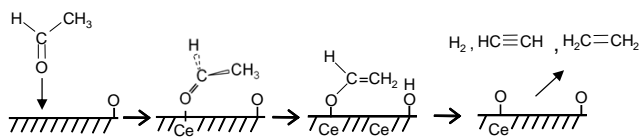


**Fig. 1** Adsorption and reaction of acetaldehyde on reduced CeO<sub>2-x</sub>(111)

configuration, a portion of which dehydrogenates to form an enolate type species (Fig. 1). The compelling experimental evidence is C1s binding energies (which in acetone show three distinguishable carbon types), NEXAFS evidence indicating C-O and CH<sub>x</sub>

surrounding a C=C bond, FTIR spectra and DFT calculations. In acetaldehyde the enolate intermediate reacts along three competing pathways: recombination with the surface hydroxyls to produce the original molecule; nucleophilic attack by surface H resulting in deoxygenation to ethylene; and dehydration to produce acetylene. Dimethyl and diethyl ethers were also examined. Being unable to deprotonate or rehybridize, the adsorption is weak. However, the existence of hydroxyls on the reduced surface is found to weaken the ether linkages and lead to formation of alkoxide. Ethylene glycol, the smallest di-alcohol, adsorbs through a single deprotonation at low temperature, but the second deprotonation occurs at elevated temperatures to form a stable dioxethylene. The oxygenate chemistry and desorption products are altered in each case described above by variation in the oxidation state of the CeO<sub>2</sub> surface, and, in turn, the molecular transformations alter the oxidation state of the surface. These results point to the participation and exchange of surface lattice oxygen.

### Structure sensitivity

Studies described above were completed on a (111) surface of CeO<sub>2</sub>. We hypothesized that surface chemistry will be altered by variation in the atomic structure of the CeO<sub>2</sub> surface, which in turn can affect adsorption and oxygen availability. We are exploring this hypothesis by two approaches. The first approach, in progress, is to prepare and study the corresponding surface chemistry on CeO<sub>2</sub>(100) surfaces. The second approach is based upon the use of monofaceted nanocrystals as tools to explore structure-function relation.

Following the literature, nanoparticles of CeO<sub>2</sub> shaped as octahedra, cubes and rods have been prepared. The octahedra and cubes correlate to crystallites terminated on (111) and (100) surfaces, respectively, while microscopic evaluation of the surfaces of rods indicates these are a more complicated mix of defective surfaces with terminations near (110) orientation. Conventional characterization techniques such as *operando* DRIFTS and Raman, TPR/TPD, isotope exchange and packed-bed catalytic measurements have been carried out to compare these different, high surface area nanoshapes to learn about the effect of structure upon surface chemistry and catalytic performance. We have examined the defect sites on these surfaces using O<sub>2</sub> adsorption. On oxidized surfaces, rods have the most abundant intrinsic defect sites, followed by cubes and octahedra. When reduced, the induced defect sites are more clustered on rods than on cubes, although similar amounts are produced on the two surfaces. The different defect sites on ceria lead to different types of surface dioxygen. Superoxide on one-electron defect sites and peroxide on two-electron defect sites with different clustering degree are identified, and their stability and reactivity are found to be structure dependent.

The behavior toward catalytic CO oxidation was investigated to learn how CO interacts with the different ceria nanoshapes and its ability to incorporate lattice oxygen from each surface (Fig. 2). CO adsorption at room temperature leads to strongly bonded carbonate on rods and cubes but weakly bonded carbonate on octahedra. CO-TPR reveals that the reducibility of these ceria nanoshapes is in line with their CO oxidation activity, i.e., rods > cubes > octahedra. The ability of adsorbed O<sub>2</sub> to exchange with lattice oxygen at reaction temperature also shows similar dependence. It is suggested

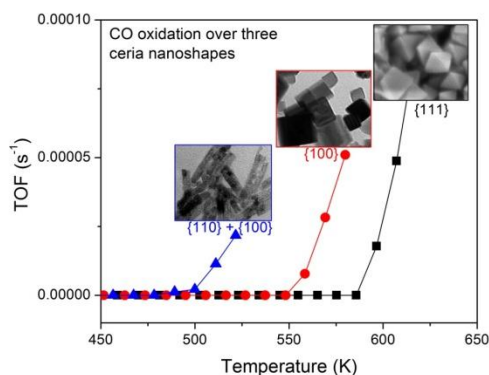


**Fig. 2** Effect of surface structure on CO oxidation.

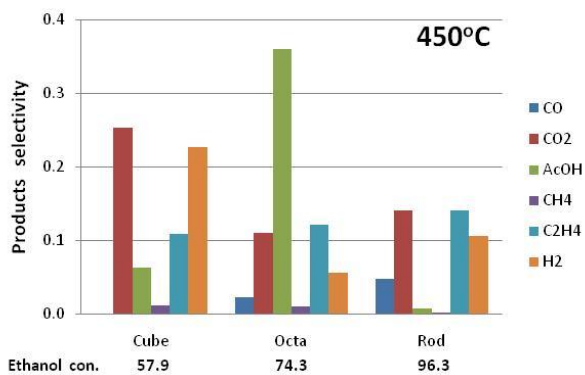


**Fig. 3** Product yield in ethanol oxidation vs particle shape.

rods, signaled by CO<sub>2</sub> onset. Ethylacetate occurs at lower T on rods suggesting (110) may be more active for coupling. Cubes have the highest selectivity for H<sub>2</sub>. H<sub>2</sub> onset is at higher T and H<sub>2</sub>/H<sub>2</sub>O ratio is smaller for octahedra because octahedra have the highest selectivity for acetaldehyde.

#### *Support effects in catalysis by Au and Au clusters*

Previously we have investigated the effects of oxide support upon stabilizing and altering catalytic pathways in Au catalysts. Continuing to probe support effects we have investigated the role of phosphates as supports, the role of hydroxide in Au catalytic pathways and in stabilizing Au clusters, the effect of alloying Au as a route to altering its selectivity and formation of heterostructured catalyst particles.

The interesting role of hydroxyls on the support surface prompted us to ask how the gold cluster interacts with the hydroxyl group. To address this question, we chose the basal plane of the Mg(OH)<sub>2</sub> support and explored its interaction with gold. Using a density functional theory-enabled local basin-hopping technique for global-minimum search, we found strong interaction of gold nanoclusters with the surface hydroxyls *via* a short bond between edge Au atoms and O atoms of the OH groups (Fig. 4). We expect that this strong interaction is ubiquitous on hydroxylated support surfaces and helps protect the gold nanoclusters against sintering, thereby contributing to their CO-oxidation activity at low temperatures.

Support effects in Au catalysis were further explored through direct comparison of Au on both reducible and non-reducible phosphate supports. The comparison reveals differences in the pathways for introduction of oxygen into the CO oxidation reaction. Au on reducible FePO<sub>4</sub> catalyzes CO oxidation through both a direct pathway (Au or Au interface activating O<sub>2</sub>) and by a redox pathway in which O from the FePO<sub>4</sub> lattice participates in CO oxidation. Au on non-reducible LaPO<sub>4</sub> also catalyzes CO oxidation through a direct pathway, but in addition, surface hydroxyls are found to be active for reacting with CO. This pathway may involve a

that the CO oxidation behavior is greatly influenced by the presence of defect sites and coordinatively unsaturated sites on ceria, whose nature and amount are intrinsically determined by the surface structure of the ceria nanoshapes.

Studies of partial ethanol oxidation also reveal pronounced structural differences between the different nanoshapes. Most striking is the much higher selectivity to acetaldehyde observed over the octahedra, compared to rods and cubes, both in temperature programmed surface reaction and in steady state reaction (Fig. 3). Total oxidation occurs at lower T on

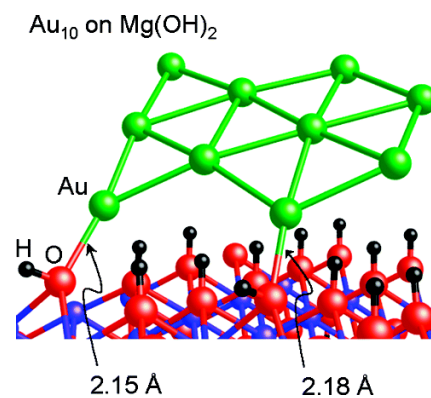


**Fig. 4** Computed structure of Au<sub>10</sub> cluster on hydroxylated MgO

hydroxycarbonyl intermediate that is proposed on other Au catalysts for the water– gas shift reaction. Depending upon treatment or reaction conditions, metallic, cationic and even anionic Au are observed with differences between the two supports. The most important pathway appears to be direct reaction catalyzed by metallic Au.

The effect of addition of alloying components on Au catalysis was explored. Using a new synthetic approach we showed that pre-formed Au nanoparticles supported on SiO<sub>2</sub> can be converted into supported intermetallic AuCu nanocrystals in a high temperature (300°C) organic solution of oleylamine, oleic acid and Cu acetate precursor. This synthetic method allows for the formation intermetallic AuCu nanoparticles with diameters averaging around 4.0 nm and tight size distribution. Although these silica supported intermetallic particles were relatively inactive, the copper oxidizes and segregates to form an intimate Au–CuO heterostructure when they are heated above 150°C in O<sub>2</sub>. These Au and amorphous CuO heterostructures are formed with a high degree of interfacial contact, increased thermal stability and high activity for CO oxidation. Interestingly, reduction in H<sub>2</sub> at 300 °C leads back to the intermetallic AuCu structure.

### **Future Plans**

Work will continue to explore how oxide supports and supported metal particles can be tailored to control selectivity. Our results show that rod-like CeO<sub>2</sub> provide high oxygen availability while octahedral (111) terminated particles provide lower activity but higher selectivity to partial oxidation. We will better characterize CeO<sub>2</sub> rods to define the reactive site structure. Results to date on ceria nanoshapes and on well-characterized CeO<sub>2</sub> oriented films are providing insight into steps of C-H bond cleavage, activation of methyl groups on adsorbed molecules, O<sub>2</sub> activation and utilization, and how an oxygen deficit on CeO<sub>2</sub> affects these pathways. Experiments with unsaturated or ringed oxygenates will further clarify the reaction pathways. Beyond the oxide surface itself, metals including Au, Cu or Rh will be deposited on oriented surfaces or on the pre-formed nanoshapes to create catalysts anticipated to have variable selectivity for dehydration/dehydrogenation in oxygenates. Synthetic routes to form ceria-metal heterostructures will be explored with the goal of achieving intimate contact between metal and oxide in nanosized bi-functional particles with high structural stability. Characterization techniques and *operando* methodology appropriate for high surface area samples will be utilized to explore the reactivity and surface chemistry of these systems. The effect of surface structure of the ceria nanoshapes upon the oxidation state of metals under reaction conditions; upon particle shape and orientation; and upon the synergism between the surface chemistry at metal, oxide and their interface will be studied. We will explore the role of the metal in managing hydrogen, OH or speeding up the reaction steps on reactions that already occur on the oxide.

### **Publications (2009-2011)**

Bauer, J. C., D. R. Mullins, M. Li, Z. Wu, A. Payzant, S. H. Overbury and S. Dai, *Synthesis of silica supported AuCu nanoparticle catalysts and the effects of pretreatment conditions for the CO oxidation reaction*, Physical Chemistry and Chemical Physics, **2011**, 13, 2571.

Brooks, J. D., T.-L. Chen, D. R. Mullins and D. F. Cox, *Reactions of ethylidene on a model chromia surface: 1,1-dichloroethane on stoichiometric  $\alpha$ -Cr<sub>2</sub>O<sub>3</sub> (10-12)*, Surface Science, **2011**, 605, 1170.

Calaza, F. C., T.-L. Chen, D. R. Mullins and S. H. Overbury, *Structure and Reactivity of Alkyl Ethers Adsorbed on CeO<sub>2</sub>(111) Model Catalysts*, Topics in Catalysis, **2011**, 54, 56-69.

Chen, T.-L. and D. R. Mullins, *Adsorption and Reaction of Acetaldehyde over CeO<sub>x</sub>(111) Thin Films*, Journal of Physical Chemistry C, **2011**, 115, 3385.

- Chen, T.-L. and D. R. Mullins, *Ethylene Glycol Adsorption and Reaction over CeO<sub>x</sub>(111) Thin Films*, Journal of Physical Chemistry C, **2011**, submitted.
- Jiang, D. E. and S. Dai, *The Role of Low-coordinate Oxygen on Co<sub>3</sub>O<sub>4</sub>(110) in Catalytic CO Oxidation*, Physical Chemistry Chemical Physics, **2011**, 13, 978.
- Jiang, D. E., S. H. Overbury and S. Dai, *Interaction of Gold Clusters with a Hydroxylated Surface*, Journal of Physical Chemistry Letter, **2011**, 2 1211-1215.
- Li, M., Z. Wu and S. H. Overbury, *CO oxidation on phosphate supported Au catalysts: Effect of support reducibility on surface reactions*, Journal of Catalysis, **2011**, 278, 133-142.
- Ma, Z. and S. Dai, *Development of Novel Supported Gold Catalysts: A Materials Perspective*, Nano Res., **2011**, 4, 3-32.
- Pei, Y., N. Shao, H. Li, D. E. Jiang and X. C. Zeng, *Hollow Polyhedral Structures in Small Gold-Sulfide Clusters*, ACS Nano, **2011**, 5, 1441.
- Tenney, S. A., W. He, J. S. Ratliff, D. R. Mullins and D. A. Chen, *Characterization of Pt-Au and Ni-Au Clusters on TiO<sub>2</sub>(110)*, Topics in Catalysis, **2011**, 54, 42.
- Yin, H. F., Z. Ma, M. F. Chi and S. Dai, *Heterostructured catalysts prepared by dispersing Au@Fe<sub>2</sub>O<sub>3</sub> core-shell structures on supports and their performance in CO oxidation*, Catalysis Today, **2011**, 160, 87-95.
- Allard, L. F., M. Flytzani-Stephanopoulos and S. H. Overbury, *Behavior of Au Species in Au/Fe<sub>2</sub>O<sub>3</sub> Catalysts Characterized by Novel In Situ Heating Techniques and Aberration-Corrected STEM Imaging*, Microscopy and Microanalysis **2010**, 16, 375-385.
- Chen, D. A., J. S. Ratliff, X. F. Hu, W. O. Gordon, S. D. Senanayake and D. R. Mullins, *Dimethyl methylphosphonate decomposition on fully oxidized and partially reduced ceria thin films*, Surface Science, **2010**, 604(5-6), 574-587.
- Dmowski, W., H. F. Yin, S. Dai, S. H. Overbury and T. Egami, *Atomic Structure of Au Nanoparticles on a Silica Support by an X-ray PDF Study*, Journal of Physical Chemistry C, **2010**, 114(15), 6983-6988.
- Durand, J. P., S. D. Senanayake, S. L. Suib and D. R. Mullins, *Reaction of Formic Acid over Amorphous Manganese Oxide Catalytic Systems: An In Situ Study*, Journal of Physical Chemistry C, **2010**, 114(47), 20000-20006.
- Hagaman, E. W., J. A. Jiao, B. H. Chen, Z. Ma, H. F. Yin and S. Dai, *Surface alumina species on modified titanium dioxide: A solid-state Al-27 MAS and <sup>3</sup>QMAS NMR investigation of catalyst supports*, Solid State Nuclear Magnetic Resonance, **2010**, 37(3-4), 82-90.
- Jiang, D. E., *Understanding and Predicting Thiolated Gold Nanoclusters from First Principles*, Acta Physico-Chimica Sinica, **2010**, 26(4), 999-1016.
- Jiang, D. E., M. Walter and J. Akola, *On the Structure of a Thiolated Gold Cluster: Au-44(SR)(28)(2-)*, Journal of Physical Chemistry C, **2010**, 114(38), 15883-15889.
- Jiang, D. E., M. Walter and S. Dai, *Gold Sulfide Nanoclusters: A Unique Core-In-Cage Structure*, Chemistry-a European Journal, **2010**, 16(17), 4999-5003.
- Ma, Z., H. F. Yin and S. Dai, *Performance of Au/MxOy/TiO<sub>2</sub> Catalysts in Water-Gas Shift Reaction*, Catalysis Letters, **2010**, 136(1-2), 83-91.
- Mullins, D. R., S. D. Senanayake and T.-L.Chen, *Adsorption and Reaction of C1 - C3 Alcohols over CeO<sub>x</sub>(111) Thin Films*, Journal of Physical Chemistry C, **2010**, 114, 17112.
- Rashkeev, S. N., S. Dai and S. H. Overbury, *Modification of Au/TiO<sub>2</sub> Nanosystems by SiO<sub>2</sub> Monolayers: Toward the Control of the Catalyst Activity and Stability*, Journal of Physical Chemistry C, **2010**, 114(7), 2996-3002.
- Senanayake, S. D., J. Evans, S. Agnoli, L. Barrio, T.-L. Chen, J. Hrbek and J. A. Rodriguez, *Water-gas Shift and CO Methanation Reactions over Ni-CeO<sub>2</sub>(111) catalysts*, Topics in Catalysis, **2010**, 54, 34 - 41.

Wang, C., H. Yin, S. Dai and S. Sun, *A General Approach to Noble Metal-Metal Oxide Dumbbell Nanoparticles and Their Catalytic Application for CO Oxidation*, Chem. Mater., **2010**, 22, 3277.

Wu, Z., M. Li, J. Howe, H. M. M. III and S. H. Overbury, *Probing Defect Sites on CeO<sub>2</sub> Nanocrystals with Well-Defined Surface Planes by Raman Spectroscopy and O<sub>2</sub> Adsorption*, Langmuir, **2010**, 26 (21), 16595-16606.

Wu, Z. K., D. E. Jiang, E. Lanni, M. E. Bier and R. C. Jin, *Sequential Observation of Ag<sub>n</sub>S<sup>d</sup> (1 ≤ n ≤ 7) Gas Phase Clusters in MS/MS and Prediction of Their Structures*, Journal of Physical Chemistry Letters, **2010**, 1(9), 1423-1427.

Yin, H. F., Z. Ma, H. G. Zhu, M. F. Chi and S. Dai, *Evidence for and mitigation of the encapsulation of gold nanoparticles within silica supports upon high-temperature treatment of Au/SiO<sub>2</sub> catalysts: Implication to catalyst deactivation*, Applied Catalysis a-General, **2010**, 386(1-2), 147-156.

Allard, L. F., A. Borisevich, W. Deng, R. Si, M. Flytzani-Stephanopoulos and S. H. Overbury, *Evolution of Gold Structure During Thermal Treatment of Au/FeO<sub>x</sub> Catalysts Revealed by Aberration-Corrected Electron Microscopy*, Journal of Electron Microscopy, **2009**, 58(3), 199-212.

Gordon, W. O., Y. Xu, D. R. Mullins and S. H. Overbury, *Temperature evolution of structure and bonding of formic acid and formate on fully oxidized and highly reduced CeO<sub>2</sub>(111)*, Physical Chemistry Chemical Physics, **2009**, 11(47), 11171-11183.

Jiang, D. E., *Au adatom-linked CH<sub>3</sub>S-Au-SCH<sub>3</sub> complexes on Au(111)*, Chemical Physics Letters, **2009**, 477(1-3), 90-94.

Jiang, D. E., W. Chen, R. L. Whetten and Z. F. Chen, *What Protects the Core When the Thiolated Au Cluster is Extremely Small?*, Journal of Physical Chemistry C, **2009**, 113(39), 16983-16987.

Jiang, D. E. and S. Dai, *Constructing Gold-Thiolate Oligomers and Polymers on Au(111) Based on the Linear S-Au-S Geometry*, J. Phys. Chem. C **2009**, 113, 7838-7842.

Jiang, D. E. and S. Dai, *From Superatomic Au-25(SR)(18)(-) to Superatomic M@Au-24(SR)(18)(q) Core-Shell Clusters*, Inorganic Chemistry, **2009**, 48(7), 2720-2722.

Jiang, D. E. and S. Dai, *Diffusion of the Linear CH<sub>3</sub>S-Au-SCH<sub>3</sub> Complex on Au(111) from First Principles*, Journal of Physical Chemistry C, **2009**, 113(9), 3763-3766.

Jiang, D. E. and S. Dai, *Cis-trans conversion of the CH<sub>3</sub>S-Au-SCH<sub>3</sub> complex on Au(111)*, Physical Chemistry Chemical Physics, **2009**, 11(38), 8601-8605.

Jiang, D. E., R. L. Whetten, W. D. Luo and S. Dai, *The Smallest Thiolated Gold Superatom Complexes.*, J. Phys. Chem. C, **2009**, 113, 17291.

Li, M. J., Z. L. Wu, Z. Ma, V. Schwartz, D. R. Mullins, S. Dai and S. H. Overbury, *CO oxidation on Au/FePO<sub>4</sub> catalyst: Reaction pathways and nature of Au sites*, Journal of Catalysis, **2009**, 266(1), 98-105.

Ma, Z., S. H. Overbury and S. Dai (2009). *Gold Nanoparticles as Chemical Catalysts* Nanomaterials: Inorganic and Bioinorganic Perspectives. C. M. Lukehart and R. A. Scott. Chichester, John Wiley & Sons.

Senanayake, S. D., W. O. Gordon, S. H. Overbury and D. R. Mullins, *Adsorption and Reaction of Acetone over CeO<sub>x</sub>(111) Thin Films*, Journal of Physical Chemistry C, **2009**, 113(15), 6208-6214.

Veith, G. M., A. R. Lupini, S. Rashkeev, S. J. Pennycook, D. R. Mullins, V. Schwartz, C. A. Bridges and N. J. Dudney, *Thermal stability and catalytic activity of gold nanoparticles supported on silica* Journal of Catalysis, **2009**, 262, 92-101.

Wang, C., H. Yin, R. Chan, S. Peng, S. Dai and S. Sun, *One-Pot Synthesis of Oleylamine Coated AuAg Alloy NPs and Their Catalysis for CO Oxidation*, Chem. Mater., **2009**, 21(3), 433-435.

Wu, Z. L., S. H. Zhou, H. G. Zhu, S. Dai and S. H. Overbury, *DRIFTS-QMS Study of Room Temperature CO Oxidation on Au/SiO<sub>2</sub> Catalyst: Nature and Role of Different Au Species*, Journal of Physical Chemistry C, **2009**, 113(9), 3726-3734.

**Investigation of the nature of active sites on heteroatom-containing carbon nano-structures for oxygen reduction reaction**

Post-doctoral Researchers: Xiaoguang Bao, Burcu Mirkelamoglu, Ann-Marie Alexander  
PhD Students: Elizabeth J. Biddinger, Dieter von Deak, Deepika Singh  
Undergraduate Students: Jesaiah King, Dan Valco  
Collaborators: Christopher Hadad, (Department of Chemistry, The Ohio State University), Jeffrey Miller (Argonne National Laboratory), Jean-Marc Millet (CNRS Catalysis Research Institute Lyon-France)  
Contacts: Ohio State University, Department of Chemical and Biomolecular Engineering, 140 W 19<sup>th</sup> Avenue, Columbus, OH 43210.  
Ozkan.1@osu.edu

**Goal**

The main objective of this project is to develop non-precious metal carbon-based fuel cell cathode electrocatalysts while investigating the fundamental catalytic phenomena underlying the oxygen reduction reaction. The project focuses on determining the nature of active sites and the ways to create these active sites for oxygen reduction reaction by molecular tailoring of the carbon nano-structures and surface moieties.

**DOE Interest**

The practical relevance of the work lies in the need for developing precious-metal-free ORR catalysts for proton exchange membrane (PEM) fuel cells and direct methanol fuel cells (DMFC). A fundamental understanding of the oxygen reduction reaction over heteroatom-containing nanostructured carbon catalysts is important for the development of precious-metal-free electrocatalysts for PEM and Direct Methanol Fuel Cells. Through an understanding of the nature of active sites and the ORR mechanism on these nanostructured materials, carbon-based catalysts can be tailored to improve ORR activity. Additionally, any insight gained into the role of heteroatoms incorporated into graphitic carbon and techniques to be developed for synthesis, characterization and electrochemical testing of these materials can be extended to tailor unique nanoscale catalysts and electrocatalysts for a variety of reactions. Another important objective for the project is to bridge the fields of heterogeneous catalysis and electrocatalysis as cross-fertilization of these areas will be very beneficial to both fields.

**Recent Progress:*****Doping by other heteroatoms***

The inclusion of heteroatoms (nitrogen, sulfur, phosphorus, etc.) into the hexagonal networks of graphitic carbons modifies the electronic and chemical properties due to variations in the electronic structure and nanostructure growth. Phosphorus and sulfur, like nitrogen, can impart an increase in electron donation ability in graphitic carbon catalysts. It is a natural extension that the inclusion of other heteroatoms into graphitic ORR electrocatalysts would alter the reaction properties.



In our recent studies, phosphorous, another n-type dopant, was added to the transition metal growth catalyst (Fe, Co) during  $CN_x$  synthesis to study the effect of phosphorus addition on oxygen reduction. The pyrolysis step again involved C and N-containing precursors. At low molar phosphorus loadings (P: Fe < 3), a significant increase in ORR activity of  $CN_x$  was observed, with higher onset potentials. Increasing amounts of phosphorus in the growth media was found to alter the growth of carbon nanostructures and make them more irregular with a “perforated” character. Through temperature programmed oxidation experiments, the inclusion of phosphorus in the growth media was found to increase the stability and graphitic nature of the catalyst materials.

***Probing the active sites by selective poisoning experiments.***

Since the role of the transition metal left behind from the pyrolysis process in the ORR activity of the  $CN_x$  catalysts is still debated, we designed a series of experiments to attempt to poison any exposed Fe sites. The rationale was that, if Fe centers are indeed the active sites, the use of known poisons for iron catalysts should lead to significant activity loss in ORR.

*Use of  $H_2S$  poisoning as a probe.* Activity loss in iron-based catalysts has been attributed to sulfur for many well-known reactions such as Fisher-Tropsch, water-gas shift, ammonia synthesis, ammonia decomposition and iron carburization. Hence, the conjecture of an iron-based catalytic site would only be proved if iron-containing  $CN_x$  exhibited a similar deactivation when exposed to hydrogen sulfide. To probe further into the nature of platinum-free ORR active site, and to establish the role of the transition metal in the activity of  $CN_x$ ,  $H_2S$ - a known metal poison, was introduced subsequent to catalyst synthesis. The incorporation of sulfur into the carbon matrix was verified by temperature-programmed oxidation and X-ray photoelectron spectroscopy. An identical treatment was used for platinum catalysts for comparison. Platinum showed a loss in ORR activity whereas deactivation was not observed by  $CN_x$ , which showed an increase in activity after  $H_2S$  treatment. The iron phase within the  $CN_x$  catalysts was investigated with X-ray absorption and was found to be similar for the treatments studied, suggesting that iron was not present as an exposed metal phase. XANES analysis of the  $CN_x$  Fe K-edge showed the iron phase in  $CN_x$  to be mostly metallic and to a smaller extent carbidic. Spectra showed no resemblance to the iron macrocycle standard, which is similar to the hypothesized nitrogen bonded transition metal ORR active site.

*Use of CO poisoning as a probe.* The effect of CO on ORR activity of Pt and  $CN_x$  catalysts was examined in half-cell experiments. During oxygen reduction carbon monoxide preferentially adsorbed to the platinum electrocatalysts causing all oxygen reduction to cease, however, the effect was reversible and the activity was recovered once carbon monoxide left the system. There was no loss of activity due to CO adsorption in  $CN_x$  catalysts. Carbon monoxide pulse chemisorption confirmed that CO is adsorbed to platinum on Vulcan carbon and not adsorbed on  $CN_x$ .

**Future Plans:**

To understand the change in the metal growth catalyst during pyrolysis, operando X-ray absorption studies were initiated where XAS spectra are obtained during pyrolysis. To perform in-situ XAS characterization during half-cell and full fuel cell operation, design and construction of operando cells are in progress.

## Publications (2010-2011)

1. Biddinger, E.J., Knapke, D.S., von Deak, D., Ozkan, U.S., “Effect of Sulfur as a Growth Promoter for CN<sub>x</sub> Nanostructures as PEM and DMFC ORR Catalysts” *Applied Catalysis B*, **96**, 72-82 (2010).
2. Woods, M.P., Biddinger, E.J., Matter, P.H., Mirkelamoglu, B. and Ozkan, U.S., “Correlation Between the ORR and ODH Activities of CN<sub>x</sub> Catalysts”, *Catalysis Letters*, **136** (1), 1-8 (2010)
3. Biddinger, E.J., von Deak, D., Marsh, H., Ozkan, U.S., “RRDE catalyst ink aging effects on selectivity to water formation in ORR,” *Electrochemistry and Solid State Letters*, **13** (8) B98-B100 (2010).
4. Von Deak, D., Biddinger, E.J., Luthman, K.A., Ozkan, U.S., “The effect of phosphorus in nitrogen-containing carbon nanostructures on oxygen reduction in PEM fuel cells,” *Carbon*, **48**, 3635-3638 (2010).
5. Biddinger, E.J., Ozkan, U.S., “Role of graphitic edge-plane exposure in carbon nanostructures for oxygen reduction reaction,” *J. Phys. Chem. C*, **114**, 15306–15314 (2010).
6. Bao, X., von Deak, D. Biddinger, E.J., Ozkan, U.S., Hadad, C.M., “A Computational Exploration of the Oxygen Reduction Reaction over a Carbon Catalyst Containing a Phosphinate Functional Group,” *Chemical Communications*. **46**, 8621-8623 (2010).
7. Biddinger, E.J., von Deak, D., Singh, D., Marsh, H., Knapke, D.S., Ozkan, U.S., “Examination of catalyst loading effects on the selectivity of CN<sub>x</sub> and Pt/VC ORR catalysts using RRDE” *Journal of Electrochemical Society*, **158** (4) B402-B409 (2011).
8. Von Deak, D., Biddinger, E.J., Ozkan, U.S., “Corrosion Characteristics of N-containing Carbon Nanostructures in a PEM Fuel Cell Environment” *Journal of Applied Electrochemistry*, **41**, 757-763 (2011).
9. Von Deak, D., Singh, D., Biddinger, E.J., King, J.C., Bayram, B., Miller, J.T., Ozkan, U.S., “Investigation of sulfur poisoning of CN<sub>x</sub> oxygen reduction catalysts for PEM fuel cells,” *Journal of Catalysis*. In review.

### Alcohol Dehydration on Oxide Catalysts: Activity and Selectivity

Authors: Ja Hun Kwak, Donghai Mei, Charles H.F. Peden, Roger Rousseau, Janos Szanyi, Yong Wang.

Contact information: C.H.F. Peden, Institute for Integrated Catalysis, Pacific Northwest National Laboratory, P.O. Box 999, MS K2-12, Richland, WA 99352  
 chuck.peden@pnl.gov

**Alcohol Dehydration on Alumina Surfaces:** Temperature programmed desorption (TPD) of ethanol, as well as ethanol and methanol dehydration reactions were studied on  $\gamma$ -Al<sub>2</sub>O<sub>3</sub> in order to identify the active catalytic sites for alcohol dehydration reactions. Two high temperature (> 473 K) desorption features were observed following ethanol adsorption (Figure 2). Samples calcined at  $T \leq 473$  K displayed a desorption feature in the 523-533 K temperature range, while those calcined at  $T \geq 673$  K showed a single desorption feature at 498 K. These two high temperature desorption features correspond to the exclusive formation of ethylene on the Lewis (498 K) and Brønsted acidic (~525 K) sites. The results demonstrate that in alcohol dehydration reactions on  $\gamma$ -Al<sub>2</sub>O<sub>3</sub>, the (100) facets are the active catalytic surfaces.

**The Origin of Regioselectivity in 2-butanol Dehydration on Solid Acid Catalysts:** The origin in the variations of trans-/cis-2-butene product selectivity ratios in 2-butanol dehydration over solid acid catalysts were investigated using a combined experimental-theory approach. Reactivity measurements over  $\gamma$ -Al<sub>2</sub>O<sub>3</sub>, AlO<sub>x</sub>/SBA-15, and H-form zeolites with widely varying Si/Al ratios and pore structures showed over two orders of magnitude change in the trans-/cis-2-butene product ratio. Activation energy barriers calculated for the concerted C-O and  $\beta$ -C-H bond breakings of adsorbed butoxy intermediates by dispersion-corrected DFT calculations correctly predicted the trans-/cis-2-butene product ratio observed on  $\gamma$ -Al<sub>2</sub>O<sub>3</sub> (Figure 3). The very low trans-2-butene selectivity on  $\gamma$ -Al<sub>2</sub>O<sub>3</sub> can now be understood by the formation of a late transition state with high energy barrier caused by the strong van der Waals interaction between the  $\gamma$ -H atoms and the flat catalyst surface. Trans-/cis-2-butene selectivity ratios much higher than that dictated by thermodynamic equilibrium can be achieved by introducing additional geometric constraints around the active catalytic site (e.g., varying the 3D environment around the active center in zeolites).

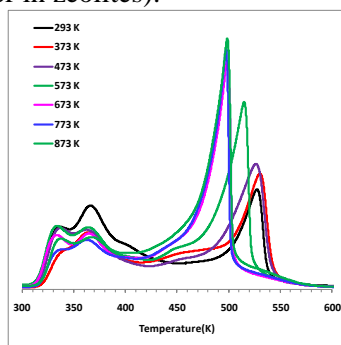


**Figure 2.** TPD profiles after room temperature ethanol adsorption on  $\gamma$ -Al<sub>2</sub>O<sub>3</sub> calcined at the indicated temperatures ( $T_{\text{ads}}=293$  K).

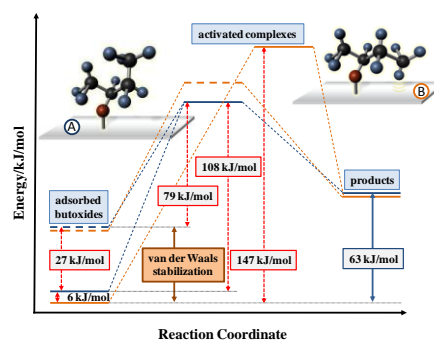


**Figure 3.** Calculated energetics for the rate determining step in the formation of cis-/trans-2-butene in accord with an E1 mechanism. Solid line is calculation based on dispersion-corrected DFT-D and dashed line is standard DFT without dispersion.

**Early Transition Metal Oxides as Catalysts:  
Crossing Scales from Clusters to Single Crystals to Functioning Materials**

Additional PIs: Prof. David. A. Dixon<sup>1</sup>, Dr. Zdenek Dohnalek<sup>2</sup>, Prof. Enrique Iglesia<sup>3</sup>, Dr. Bruce D. Kay<sup>2</sup>, Dr. Jun Liu<sup>2</sup>, Dr. Charles H. F. Peden<sup>2</sup>, Dr. Roger Rousseau<sup>2</sup>, Prof. Lai-Sheng Wang<sup>4</sup>, Prof. Yong Wang<sup>2,5</sup>.

Co-Investigators: Dr. F. Gao<sup>5</sup>, Dr. Jianzhi Hu<sup>2</sup>, Ja Hun Kwak<sup>2</sup>, Dr. Hua-Jin Zhai<sup>4</sup>.

Postdocs: Dr. H.-Y. Fan<sup>2</sup>, Dr. D. Acharya<sup>1</sup>, Dr. S. Li<sup>1</sup>, Dr. W.-Z. Li<sup>2</sup>, Dr. Z. Li<sup>2</sup>, Dr. J. Sun<sup>2</sup>, Dr. T. Stuchinskaya<sup>3</sup>, Dr. D. Wang<sup>2</sup>, Dr. X. Yin<sup>3</sup>, Dr. Y. Yoon<sup>2</sup>.

Graduate Students: R. Carr<sup>3</sup>, R. Craciun<sup>1</sup>.

Undergrad Students: N. Gist<sup>1</sup>, D Picone<sup>1</sup>, R.T. Long<sup>1</sup>.

<sup>1</sup>University of Alabama, <sup>2</sup>Pacific Northwest National Laboratory, <sup>3</sup>University of California, Berkeley, <sup>4</sup>Brown University, <sup>5</sup>Washington State University

Contact information: C.H.F. Peden, Institute for Integrated Catalysis, Pacific Northwest National Laboratory, P.O. Box 999, MS K2-12, Richland, WA 99352  
[chuck.peden@pnl.gov](mailto:chuck.peden@pnl.gov)

### Goal

We are employing an integrated experimental/theoretical approach to advance our current ability to understand, design, and control the catalytic and surface chemistry of transition metal oxides, specifically for redox and acid-base chemistries. The approach combines novel solid-state inorganic synthesis, surface science, experimental and theoretical/computational chemical physics, and mechanistic organic chemistry to address this complex and important challenge.

### DOE Interest

The proportion of chemical industry processes using catalysts exceeds 80%. Current commercial heterogeneous catalysts are structurally and chemically complex and data gathered from them can seldom be interpreted with atomic-level precision. We seek to reduce the complexity of TMO catalysts to levels addressable and controllable at the atomic level, while maintaining intimate linkages with practical catalysis and catalytic materials. The focus of the proposed work is to gain a fundamental understanding of chemical transformations in order to design and construct new catalysts with more precise control of specific chemical reactions. This will enable us to help DOE reach its goals of doing fundamental science to address the energy needs of the country by (1) improving energy conservation by new means of energy conversion and storage; (2) enable direct chemical conversions previously economically unfeasible and produce new routes to novel materials while at the same time minimizing by-products and environmental impact; and (3) protecting the environment

### Recent Progress

Selected highlights from the results obtained in the last year are presented in this section.

### ***Catalyst synthesis, characterization, and kinetics studies***

***Acid and Oxidation Catalysis on Polyoxometalate Clusters:*** Keggin polyoxometalate (POM) clusters exhibit uniform and well-defined size and atomic connectivity over a diverse chemical composition range, making them ideal catalytic materials to elucidate specific relations between composition and function. We have previously developed methods for dispersing W-based Keggin POM on amorphous SiO<sub>2</sub> as intact, nearly isolated species over a range of central atoms (P, Si, Al, Co) to prepare solid Brønsted acids with a broad range of acid strengths [1]. The relations between rate constants for butanol dehydration and n-hexene isomerization on Keggin POM and zeolites and their deprotonation energies (DPE), a rigorous measure of acid strength available from theory for Keggin POM because of their known structure, showed that acid strength affects the electrostatic stabilization of ion-pair transition states and that the charge distribution at transition states determines the sensitivity of each reaction to acid strength [2,3]. During this reporting period, we have extended these concepts to CH<sub>3</sub>OH dehydration [4] and 2-methylpentene (2MP) isomerization to discern the individual roles of acid strength and confinement on reactivity and have addressed mechanistic details for CH<sub>3</sub>OH dehydration and oxidative dehydrogenation (ODH) reactions on bifunctional Keggin clusters to develop concepts that render these reactions useful as rigorous probes of the independent effects of solvation, acid strength, and redox properties in oxidation and acid catalysis.

***CH<sub>3</sub>OH Dehydration and 2MP Isomerization on Solid Acids:*** We have combined kinetic and density functional theory (DFT) analyses to show that CH<sub>3</sub>OH dehydration proceeds via concerted reactions of gaseous and protonated CH<sub>3</sub>OH molecules mediated by transition states that form dimethyl ether (DME) and eliminate H<sub>2</sub>O simultaneously (Figure 1a) instead of sequential reactions involving methoxide intermediates, because methyl cations are better solvated by nearby molecules at transition states in concerted routes. Dehydration rates at low CH<sub>3</sub>OH pressures are more sensitive to DPE than at high pressures, as shown by the respective dependences of first-order ( $k_{\text{mono}}$ ) and zero-order ( $k_{\text{dimer}}$ ) rate constants on DPE (Figure 1a). Mechanism-based interpretations of  $k_{\text{mono}}$  and  $k_{\text{dimer}}$  indicate that they proceed via the same transition state, but have experimental barriers that reflect energy differences with respect to a different reactive intermediate. CH<sub>3</sub>OH monomers are the most abundant adsorbed species at low pressures, but acid sites become saturated with protonated dimers as CH<sub>3</sub>OH pressure increases. The similar charges at the ion-pairs for protonated dimers and transition states cause their stabilities to vary similarly with DPE and more strongly than uncharged monomers; as a result, activation barriers measured from dimers are attenuated to acid strength and lead to the weaker effects of DPE on  $k_{\text{dimer}}$  than on  $k_{\text{mono}}$  rate constants. Values of  $k_{\text{dimer}}$  measured on acid forms of zeolites coincide with the trend developed on Keggin POM, but their  $k_{\text{mono}}$  values differ among themselves and are much larger than the value predicted by POM clusters (Figure 1a). These results arise from greater stabilization of CH<sub>3</sub>OH at transition states and dimers via van der Waals forces relative to monomers, because both reactant molecules are confined within the pores of zeolites in the cases of dimers and transition states, but only one for monomers. The different stabilization of transition states and monomers by confinement decreases the barriers responsible for  $k_{\text{mono}}$  and causes reactivity differences among zeolites and between them and POM clusters as a result of van der Waals stabilization, and not just merely acid strength. These mechanistic conclusions render CH<sub>3</sub>OH dehydration reactions uniquely suited to discern the separate effects of solvation and acid strength on acid catalysis. In contrast, 2MP isomerizes to three products via different transition states that are preceded by a common alkoxide intermediate. The formation rates of these products differ by three orders of magnitude; yet the ratios of their respective isomerization rate constants do not depend on DPE or solvation (Figure 1b). Reactivity differences are commensurate with differences in the proton affinity of gaseous transition state analogs, while similar selectivities reflect the similar effects of confinement and acid strength on distinct transition states that have similar sizes and charge distributions. In such cases, product selectivities depend on acid strength only because the more facile reactions approach equilibrium and not because of different effects of DPE on the more facile or difficult reactions.

***Conversion of CH<sub>3</sub>OH on Bifunctional Keggin Polyoxometalates:*** Keggin clusters with Mo or V metal atoms exhibit significant reactivity in reduction-oxidation catalysis and also Brønsted acid catalysis

because of their charge-balancing protons. Mechanistic interpretations of turnover rates and isotopic effects for  $\text{CH}_3\text{OH}$  dehydration (to DME) and ODH (to formaldehyde) reactions were used to assess the effects of acid strength and redox properties for these materials. Transmission electron microscopy,  $^{31}\text{P}$ -MAS-NMR, and titrations of protons during catalysis indicate  $\text{H}_3\text{PMo}_{12}\text{O}_{40}$  clusters are present as intact, well-dispersed clusters supported on  $\text{SiO}_2$ . ODH rates and kinetic isotope effects on these supported clusters are consistent with Mars van Krevelen redox cycles, in which rates are limited by H-abstraction from methoxide intermediates in a reduction step that is coupled kinetically with the subsequent reoxidation of the reduced cluster by  $\text{O}_2$ . In-situ transient and steady-state UV-visible spectra confirmed these mechanistic conclusions and provide independent evidence for the number and reactivity of active centers during catalysis. Turnover rates from in-situ transient redox measurements and steady-state rates are being used to determine the actual number of active redox centers per Keggin cluster in  $\text{CH}_3\text{OH}$  ODH reactions. Dehydration rates and isotopic data on  $\text{H}_3\text{PMo}_{12}\text{O}_{40}$  and  $\text{H}_4\text{SiMo}_{12}\text{O}_{40}$  are consistent with the pathways reported in the previous section for W-POM clusters, but turnover rates are much lower than predicted from the data in Figure 1a and the DPE estimates for these clusters; these discrepancies reflect the extent of reduction during catalysis and its consequences for acid strength, which, taken together with the data in Figure 1a, can be used to estimate the extent to which each material reduces upon exposure to  $\text{CH}_3\text{OH-O}_2$  reactants. As part of this program, we have also developed synthetic protocols for dispersed Keggin clusters with V-metal atoms ( $\text{H}_{3+x}\text{PMo}_{12-x}\text{V}_x\text{O}_{40}$  ( $x = 0-3$ ),  $\text{H}_4\text{PW}_{11}\text{V}_1\text{O}_{40}$ ), which show much higher oxidation reactivity (but lower acid strength) than their V-free analogs. These materials allow us to probe the catalytic consequences of local and cluster-wide electronic properties and their relation to activation barriers for the reductive elementary steps in oxidation sequences. These latter studies combine kinetic and isotopic methods, V-NMR studies, in-situ UV-visible spectra as probes of reduction and HOMO-LUMO gaps, and DFT-derived energies for the addition of H-atoms as reductants at different O-atoms on POM cluster surfaces.

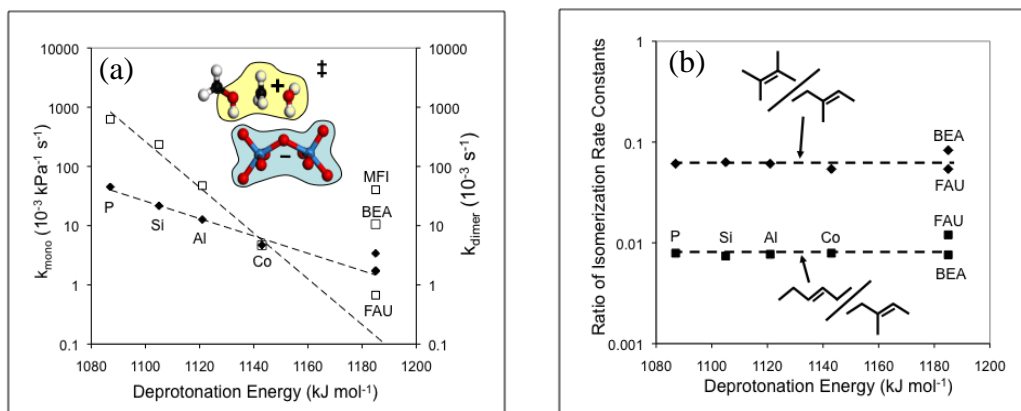


**Figure 1.** (a) First-order ( $k_{\text{mono}}$ ;  $\square$ ) and zero-order ( $k_{\text{dimer}}$ ;  $\blacklozenge$ ) rate constants for  $\text{CH}_3\text{OH}$  dehydration (433 K) on W-based Keggin POM (central atom indicated) and BEA, FAU, and MFI zeolites as a function of DPE. The structure of the DME formation transition state is shown in the inset. (b) Ratios of 2MP isomerization rate constants for different products as a function of DPE on Keggin POM (central atom indicated) and BEA and FAU zeolites.

**Alcohol Dehydration on Alumina Surfaces:** Temperature programmed desorption (TPD) of ethanol, as well as ethanol and methanol dehydration reactions were studied on  $\gamma\text{-Al}_2\text{O}_3$  in order to identify the active catalytic sites for alcohol dehydration reactions [5]. Two high temperature ( $> 473$  K) desorption features were observed following ethanol adsorption (Figure 2). Samples calcined at  $T \leq 473$  K displayed a desorption feature in the 523-533 K temperature range, while those calcined at  $T \geq 673$  K showed a single desorption feature at 498 K. These two high temperature desorption features correspond to the exclusive formation of ethylene on the Lewis (498 K) and Brønsted acidic ( $\sim 525$  K) sites. The amount of ethylene formed under conditions where the competition between water and ethanol for adsorption sites is minimized is identical over the two surfaces. Furthermore, a nearly 1-to-1

correlation between the number of under-coordinated  $\text{Al}^{3+}$  ions on the (100) facets of  $\gamma\text{-Al}_2\text{O}_3$  and the number of ethylene molecules formed in the ethanol TPD experiments on samples calcined at  $T \geq 673$  K was found. Titration of the penta-coordinate  $\text{Al}^{3+}$  sites on the (100) facets of  $\gamma\text{-Al}_2\text{O}_3$  by BaO completely eliminated the methanol dehydration reaction activity. These results demonstrate that in alcohol dehydration reactions on  $\gamma\text{-Al}_2\text{O}_3$ , the (100) facets are the active catalytic surfaces. The observed activities can be linked to the same  $\text{Al}^{3+}$  ions on both hydrated and dehydrated surfaces: penta-coordinate  $\text{Al}^{3+}$  ions (Lewis acid sites), and their corresponding -OH groups (Brønsted acid sites), depending on the calcination temperature.

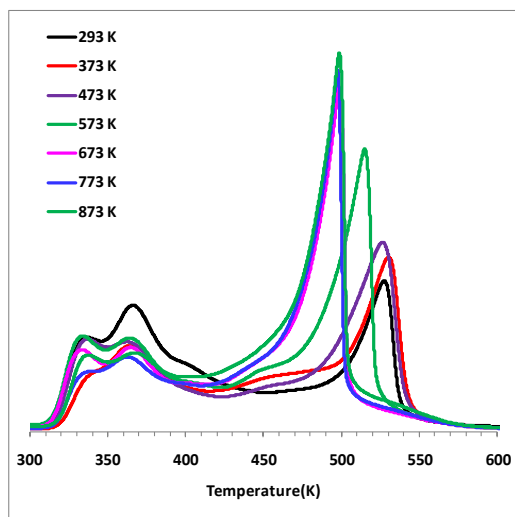


**Figure 2.** TPD profiles after room temperature ethanol adsorption on  $\gamma\text{-Al}_2\text{O}_3$  calcined at the indicated temperatures ( $T_{\text{ads}}=293$  K).

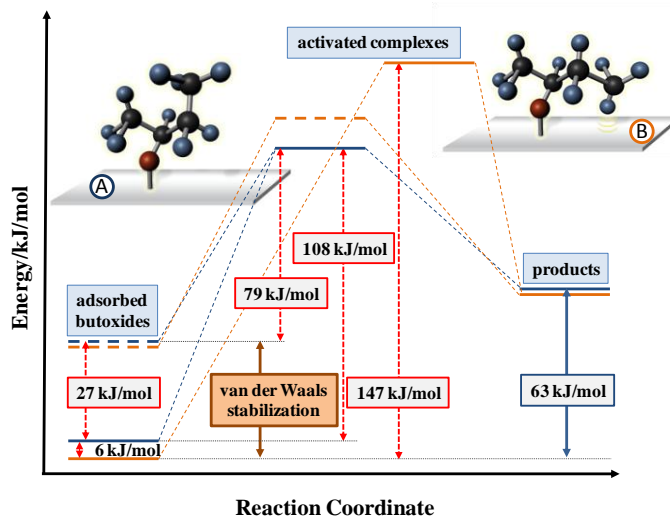


**Figure 3.** Calculated energetics for the rate determining step in the formation of cis-/trans-2-butene in accord with an E1 mechanism. Solid line is calculation based on dispersion-corrected DFT-D and dashed line is standard DFT without dispersion.

**The Origin of Regioselectivity in 2-butanol Dehydration on Solid Acid Catalysts:** The origin in the variations of trans-/cis-2-butene product selectivity ratios in 2-butanol dehydration over solid acid catalysts were investigated using a combined experimental-theory approach [6]. Reactivity measurements over  $\gamma\text{-Al}_2\text{O}_3$ ,  $\text{AlO}_x/\text{SBA-15}$ , and H-form zeolites with widely varying Si/Al ratios and pore structures showed over two orders of magnitude change in the trans-/cis-2-butene product ratio. Activation energy barriers calculated for the concerted C-O and  $\beta\text{-C-H}$  bond breakings of adsorbed butoxy intermediates by dispersion-corrected DFT calculations correctly predicted the trans-/cis-2-butene product ratio observed on  $\gamma\text{-Al}_2\text{O}_3$  (Figure 3). The very low trans-2-butene selectivity on  $\gamma\text{-Al}_2\text{O}_3$  can now be understood by the formation of a late transition state with high energy barrier caused by the strong van der Waals interaction between the  $\gamma\text{-H}$  atoms and the flat catalyst surface. Decreasing the dispersive attractive force between the adsorbed butoxide and the surface (e.g., by moving it further away from the support surface in  $\text{AlO}_x/\text{SBA-15}$ ) leads to almost equimolar formation of the trans- and cis-2-butene isomers. Trans-/cis-2-butene selectivity ratios much higher than that dictated by thermodynamic equilibrium can be achieved by introducing additional geometric constraints around the active catalytic site (e.g., varying the 3D environment around the active center in zeolites). We propose a model to explain the widely varying trans-/cis-2-butene selectivity in 2-butanol dehydration over solid acid catalysts that is consistent with the experimental results in this study. A key outcome of the study is the realization that van der Waals interactions between the reactant and the active catalyst surface must be included in the theoretic models in order to be able to accurately predict product selectivities. This information, in turn, significantly advances our ability to develop catalyst materials with designed active centers in order to achieve desired regioselectivities.

## Geometric and electronic structure of oxide clusters

### Stoichiometric and Oxygen-Rich $M_2O_n^-$ and $M_2O_n$ ( $M = Nb, Ta; n = 5-7$ ) Clusters: Molecular Models for Oxygen Radicals, Diradicals, and Superoxides:

Structural and electronic defects are common on the surfaces of transition-metal oxides. Among the wide catalytic applications of Nb and Ta oxides are their utilization as efficient catalytic promoters, whose mechanisms remain poorly understood at the molecular level. We have investigated the structures and bonding of two series of early transition-metal oxide clusters,  $M_2O_n^-$  and  $M_2O_n$  ( $M = Nb, Ta; n = 5-7$ ) using photoelectron spectroscopy (PES) and density-functional theory (DFT) [7]. The stoichiometric  $M_2O_5$  clusters are found to be closed-shell with large HOMO-LUMO gaps and their electron affinities (EAs) are measured to be 3.33 and 3.71 eV for  $M = Nb$  and  $Ta$ , respectively; whereas EAs for the oxygen-rich clusters are found to be much higher: 5.35, 5.25, 5.28, and 5.15 eV for  $Nb_2O_6$ ,  $Nb_2O_7$ ,  $Ta_2O_6$ , and  $Ta_2O_7$ , respectively, suggesting that these clusters are strong oxidizers and belong to the class of high EA species called “superhalogens”. Structural searches at the B3LYP level yield triplet and doublet ground states for the oxygen-rich neutral and anionic clusters, respectively. Spin density analyses reveal oxygen radical, diradical, and superoxide characters in the oxygen-rich clusters (Figure 4). The  $M_2O_7^-$  and  $M_2O_7$  clusters, which can be viewed to be formed by  $M_2O_5^{-/0} + O_2$ , are used as molecular models to understand dioxygen activation on  $M_2O_5^-$  and  $M_2O_5$  clusters. The  $O_2$  adsorption energies on the stoichiometric  $M_2O_5$  neutrals are shown to be surprisingly high (1.3-1.9 eV), suggesting strong capabilities to activate  $O_2$  by structural defects in Nb and Ta oxides. The PES data also provides valuable benchmarks for various density functionals (B3LYP, BP86, and PW91) for the Nb and Ta oxides.

### Probing the Electronic and Structural Properties of $M_3O_n^-$ ( $M = Nb, Ta; n = 1-8$ ) Clusters:

#### The Evolution of the Delocalized $\delta$ Orbital:

Delocalized multi-center  $\delta$ -bonding, that is,  $\delta$ -aromaticity, represents a new mode of chemical bonding, which was first discovered as part of this program during the previous funding period [8].  $\delta$ -Aromaticity is unique to transition metal systems. We have conducted systematic studies on the electronic and structural evolution, sequential oxidation, and chemical bonding in the  $M_3O_n^-$  ( $M = Nb, Ta; n = 1-8$ ) clusters [9,10]. In particular, the combined experimental and theoretical data allows us to follow the evolution of the  $\delta$  orbital as a function of O content. A  $\delta$ -type MO can be identified in the  $Ta_3O_n^-$  ( $n = 0-5$ ) clusters, along with the specific experimental PES band associated with it, as shown in Figure 5. Depending on the geometric shape and the O atom coordination environment in a  $Ta_3O_n^-$  cluster, the  $\delta$  orbital is found to be primarily localized on a single Ta center in  $Ta_3O_5^-$ , shared by two Ta centers in  $Ta_3O_4^-$ , partially delocalized over three Ta centers but distorted in  $Ta_3O_3^-$  and  $Ta_3O_2^-$ , and completely delocalized over three Ta centers in  $Ta_3O_1^-$  and  $Ta_3O_0^-$ . Although  $\delta$  bonding is substantially weaker than  $\sigma$  and  $\pi$  bonding, there is observable stabilization effect due to the delocalization of the  $\delta$  orbital. For example, the VDE of the  $\delta$  orbital in  $Ta_3O_3^-$  is the highest because this MO is highly delocalized in the  $D_{3h}$  cluster.

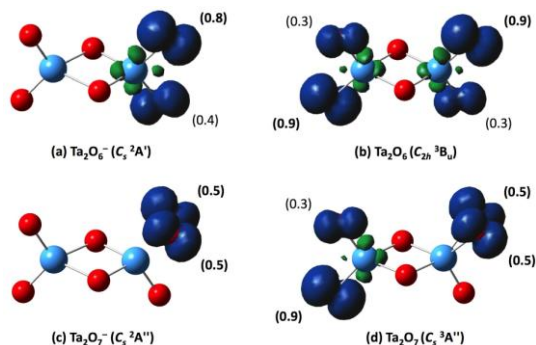


**Figure 4.** Numerical electron spin density (in  $|e|$ ) for the ground states of  $Ta_2O_n^-$  and  $Ta_2O_n$  ( $n = 6, 7$ ) clusters. All other O atoms have spin density of 0.0 (not labeled).

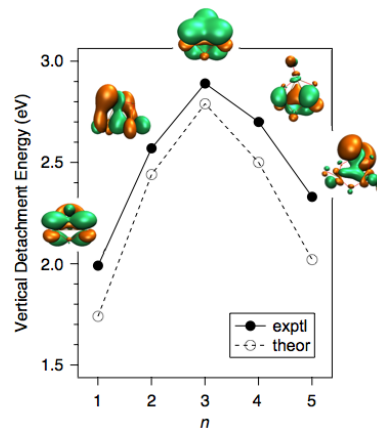


**Figure 5.** Experimental (solid line) and computational (dashed line) vertical detachment energies from the  $\delta$  orbital in  $Ta_3O_n^-$  ( $n = 1-5$ ) as a function of O content.



**Molecular Structures and Energetics of  $(\text{ZrO}_2)_n$  and  $(\text{HfO}_2)_n$  ( $n = 1-4$ ) Clusters and Their Anions:** Transition metal oxides form an important family of materials widely used as industrial catalysts or catalyst supports. Although considered less important than  $\text{TiO}_2$  for catalysis,  $\text{ZrO}_2$ ,  $\text{HfO}_2$ ,

and materials using these oxides are also known for their catalytic activities. The group IVB transition metal dioxide clusters and their anions,  $(\text{MO}_2)_n$  and  $(\text{MO}_2)_n^-$  ( $M = \text{Zr}, \text{Hf}; n = 1-4$ ), were studied with coupled cluster (CCSD(T)) theory and density functional theory (DFT). Similar to the results for  $M = \text{Ti}$ , these oxide clusters have a number of low-lying isomeric structures, which can make it difficult to predict the ground electronic state especially for the anion. Electron affinities for the low-lying structures are calculated and compared with those for  $M = \text{Ti}$ . Electron affinities of these clusters depend strongly on the cluster structures. Anion photoelectron spectra are calculated for the monomer and dimer, and demonstrate the possibility for structural identification at a spectral linewidth of  $\leq 0.05$  eV.

Electron excitation energies from the low-lying states to the singlet and triplet excited states were calculated self-consistently, as well as by the time-dependent DFT and equation-of-motion coupled cluster (EOM-CCSD) methods. The calculated excitation energies are compared to the band energies of bulk oxides indicating the excitation energy is not yet converged for  $n = 4$  for these clusters (Figure 6). The excitation energies of the low-lying isomeric clusters are less than the bulk metal oxide band gaps and suggest that these clusters could be useful photocatalysts with a visible light source.

**Structural and Electronic Near Degeneracy of  $\text{M}_3\text{O}_9^-$  ( $M = \text{Cr}, \text{Mo}, \text{W}$ ):** Density functional and coupled cluster theories were used to study several near degenerate structures/states of  $\text{M}_3\text{O}_9^-$  ( $M = \text{Cr}, \text{Mo}, \text{W}$ ). Electron addition to  $\text{M}_3\text{O}_9$  has a significant effect on the relative stability of the ring and the chain. For  $\text{M}_3\text{O}_9$ , the ring is much more stable than the chain, but for  $\text{M}_3\text{O}_9^-$ , the ring and the chain are nearly degenerate in energy. For  $\text{W}_3\text{O}_9^-$ , in addition to the structural near degeneracy, there is also an electronic near degeneracy for the ring. Accurate adiabatic and vertical electronic detachment energies of the anions are calculated for assessing the previous assignments of the experimental anion photoelectron spectra. Definitive assignments of these spectra for  $M = \text{Mo}$  and  $\text{W}$  are impossible due to their limited resolution and the closeness of the calculated electron detachment energies. Two transition states are found for the ring and the chain of  $\text{M}_3\text{O}_9$  ( $M = \text{Mo}, \text{W}$ ) and  $\text{M}_3\text{O}_9^-$  for the interconversion between the terminal  $\text{M}=\text{O}$  and bridge  $\text{M}-\text{O}$  bonds. The calculated reaction barriers for these transition states are sufficiently high that the interconversion between the ring and the chain is unlikely to occur at the low to moderate temperatures, at which the anion photoelectron spectra were taken. In addition, the fact that electron addition significantly lowers the above reaction barriers suggests that redox chemistries can have a significant impact on cluster/surface structures and may initiate cluster/surface re-structuring.

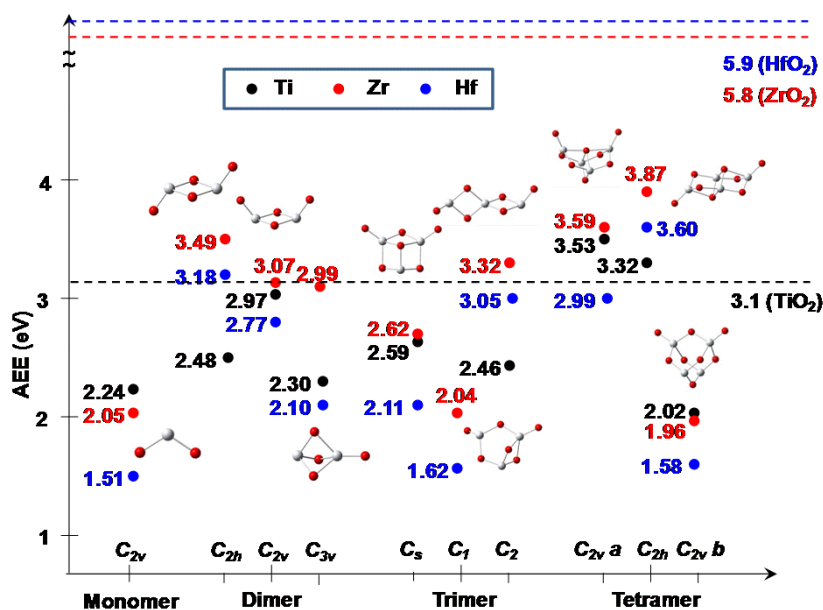


**Figure 6.** Adiabatic energy gaps in eV for the low-lying structures of the  $(\text{MO}_2)_n$  ( $n = 1-4$ ) clusters for  $M = \text{Ti}$  (black),  $\text{Zr}$  (red), and  $\text{Hf}$  (blue) calculated at the CCSD(T)/aD//B3LYP/aD level. The experimental values of the bulk metal oxide band gaps are shown.

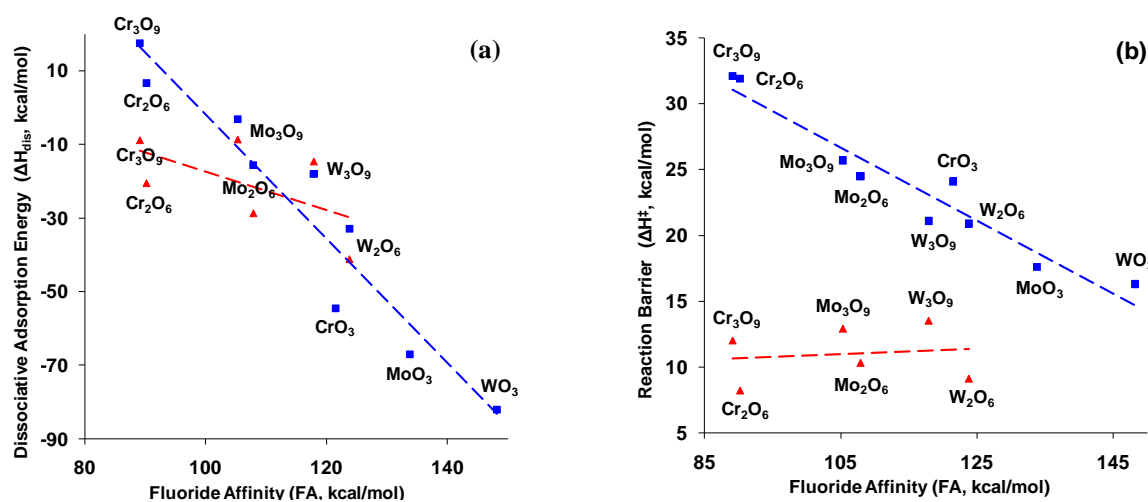


**Figure 7.** Plots of (a) the dissociative adsorption energies and (b) reaction barriers for hydrogen transfer in the dissociative chemisorption step vs. the Lewis acidities (fluoride affinities). In (b), the dissociative adsorption energies for hydrogen transfer to the terminal =O atoms are shown as the blue squares, and those to the bridge -O- atoms are shown as the red triangles.

**Molecular Structures, Acid-Base Properties, and Formation of Group 4 and 6 Transition Metal Hydroxides:**

Transition metal oxides (TMOs) and their associated compounds have received wide attention due to their rich acid/base and redox chemistries, and their ubiquitous applications in industry as catalysts and catalyst supports. DFT and coupled cluster theory (CCSD(T)) were used to study the group 6 metal ( $M = \text{Cr}, \text{Mo}, \text{W}$ ) hydroxides:  $\text{MO}_{3-m}(\text{OH})_{2m}$  ( $m = 1 - 3$ ),  $\text{M}_2\text{O}_{6-m}(\text{OH})_{2m}$  ( $m = 1 - 5$ ),  $\text{M}_3\text{O}_{9-m}(\text{OH})_{2m}$  ( $m = 1, 2$ ), and  $\text{M}_4\text{O}_{11}(\text{OH})_2$ . The calculations were done up to the complete basis set (CBS) limit with the CCSD(T) method. Brønsted acidities in the gas phase and  $\text{pK}_a$  values in aqueous solution were predicted for  $\text{MO}_{3-m}(\text{OH})_{2m}$  ( $m = 1 - 3$ ) and  $\text{M}_n\text{O}_{3n-1}(\text{OH})_2$  ( $n = 2 - 4$ ). In addition, Brønsted basicities and Lewis acidities (fluoride affinities) were predicted for  $\text{MO}_{3-m}(\text{OH})_{2m}$  ( $m = 1 - 3$ ) as well as the metal oxide clusters  $\text{M}_n\text{O}_{3n}$  ( $n = 1 - 3$ ). The metal hydroxides were predicted to be strong Brønsted acids, and weak to modest Brønsted bases and Lewis acids. The  $\text{pK}_a$  values can have values as negative as  $-31$ . Potential energy surfaces for the hydrolysis of the  $\text{M}_n\text{O}_{3n}$  ( $n = 1 - 4$ ) clusters were calculated (Figure 8). Heats of formation of the metal hydroxides were predicted from the calculated reaction energies and the agreement with the limited available experimental data is good. The hydrolysis reaction is initiated by the formation of a Lewis acid-base complex of different strengths, which can be as large as  $\sim 45$  kcal/mol and correlates with the calculated Lewis acidities. A hydrogen from the coordinated  $\text{H}_2\text{O}$  is then transferred to the

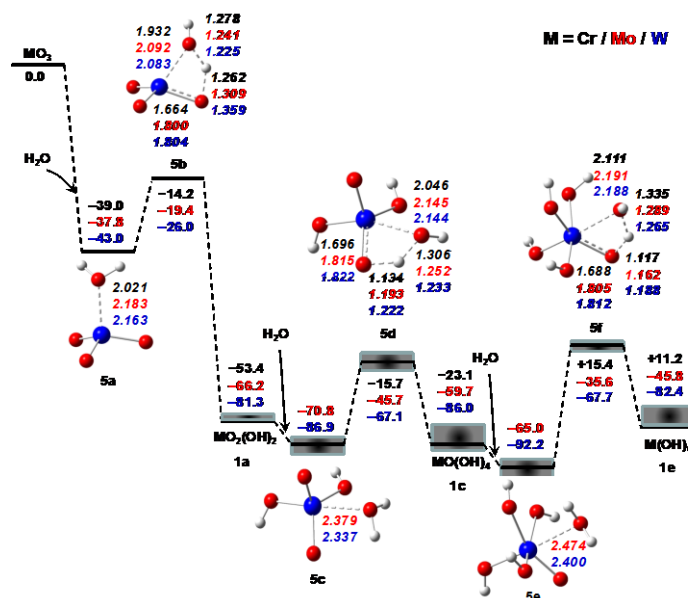


**Figure 8.** Potential energy surfaces for the reaction  $\text{MO}_3 + 3\text{H}_2\text{O} \rightarrow \text{M}(\text{OH})_6$  ( $M = \text{Cr}, \text{Mo}, \text{W}$ ) calculated at the CCSD(T)/CBS/B3LYP/aD level. Relative energies at 0 K from the reactants in kcal/mol and selected bond lengths in Å in italic.  $M = \text{Cr}$  (Black),  $\text{Mo}$  (Red),  $\text{W}$  (Blue).

terminal or bridge O for the dissociative chemisorptions step. The first hydrolysis step leading to the formation of  $M_nO_{3n-1}(OH)_2$  was predicted to be exothermic, with the exothermicity becoming less negative as  $n$  increases and essentially converged at  $n = 3$ . Further hydrolysis of  $M_nO_{3n-1}(OH)_2$  tends to be endothermic especially for  $M = Cr$ . 55 DFT exchange-correlation functionals were benchmarked for the calculations of the reaction energies, complexation energies, and reaction barriers by comparing to our CCSD(T) results. Linear correlations between the calculated reaction barrier and reaction energy for hydrogen transfer reactions to the terminal =O atom and to the bridge O atom were found to be quite different, indicating their different reaction properties. The calculated Lewis acidity (fluoride affinity) was found to best correlate with the calculated adsorption energy, the dissociative adsorption energy, and the reaction barrier for hydrogen transfer reactions to the terminal =O atom (Figure 2).

A similar set of studies has been done for  $(TiO_2)_n$  nanoclusters. The first  $H_2O$  adsorption (physisorption) energies for these  $TiO_2$  nanoclusters are predicted to be  $-10$  to  $-35$  kcal/mol for the singlet states and  $-10$  to  $-50$  kcal/mol for the triplet states. These physisorption energies depend on the cluster size and the site of adsorption, consistent with existing experimental studies. In general,  $H_2O$  prefers to physisorb on the Ti site with one Ti=O bond and two Ti-O bonds, and at the Ti site with no Ti=O bond and three Ti-O bonds. The first hydrolysis (dissociative chemisorption) reaction energies of the  $TiO_2$  nanoclusters are predicted to be  $-20$  to  $-70$  kcal/mol for the singlet states and  $-15$  to  $-80$  kcal/mol for the triplet states. Both singlet and triplet potential energy surfaces for the hydrolysis are calculated. Our calculations show that  $H_2O$  readily reacts with both the singlet and triplet states of the  $TiO_2$  nanoclusters to form the hydroxides with reaction barriers of 5 to 16 kcal/mol for the singlet states and 5 to 26 kcal/mol for the triplet states for the first hydrolysis steps, which are in general less than the  $H_2O$  complexation energies. Since  $H_2O$  splitting to form  $H_2$  and  $O_2$  is a strongly endothermic process by  $\sim 116$  kcal/mol, photocatalytic processes are necessary only in the subsequent steps.

### ***Surface structure and chemistry of Model, Planar Supported Oxides***

***Ultra-thin Tungsten Oxide Films on Pt(111): Preparation, Characterization and Catalytic Activity:*** In our previous studies we focused on the preparation and catalytic activity of supported  $(WO_3)_3$  clusters deposited via sublimation of  $WO_3$  in vacuum [11,12]. Here we show that unique tungsten oxide films, composed of molecularly bound  $(WO_3)_3$  trimers ordered in a  $(3 \times 3)$  superstructure, can be prepared on Pt(111) [13]. Our results show that well-ordered  $WO_3$  films can be prepared by depositing monodispersed cyclic  $(WO_3)_3$  clusters from the gas-phase onto Pt(111) at 700 K. In the first layer, a film with  $c(4 \times 2)$  periodicity composed of zig-zag chains is observed. Half of the tungsten atoms are reduced to the  $(5+)$  oxidation state. Theoretical calculations show that it is energetically favorable to open the  $(WO_3)_3$  cluster rings, and form linear tungsten oxide chains, which at higher coverage condense into a 2-dimensional wetting layer. In the second layer,  $(WO_3)_3$  clusters bind molecularly to the underlying  $c(4 \times 2)$  structure as demonstrated by high-resolution STM images (Figure 9a) and form an ordered  $(3 \times 3)$  overlayer as shown by LEED (Figure 9b). A few defects are found within the extended  $(3 \times 3)$  domains and are due to  $(WO_3)_3$  clusters rotated  $180^\circ$  with respect to the preferred orientation. The detailed structure of both the first  $c(4 \times 2)$  and second  $(3 \times 3)$  layers was obtained from DFT calculations.

The catalytic properties of such films are illustrated in polymerization reactions of formaldehyde,  $H_2CO$ , and acetaldehyde,  $CH_3CHO$  [14]. It was found that physisorbed  $H_2CO$  and  $CH_3CHO$  start to polymerize at  $\sim 70$  and 80 K, respectively. The formed paraformaldehyde is found to be more stable than the paraldehyde. Upon heating, both paraformaldehyde and paraldehyde simultaneously decompose and desorb in the form of monomers and oligomers around 250 and 190 K, respectively. The amount of polymerized species increases with increasing thickness of the  $H_2CO$  and  $CH_3CHO$  film and saturates at 5 and 8 ML, respectively, most likely due to crosslinking of the neighboring chains. The  $H_2CO$  and  $CH_3CHO$  heats of sublimation of 24 and 26 kJ/mol are determined from the TPD spectra of their multilayer films. Further, heats polymerization of 47 and 30 kJ/mol are estimated for  $H_2CO$  and  $CH_3CHO$  from the onset of the polymerization and the polymer decomposition temperatures. All values are found to be in a good agreement with the previously published values. A similar results were also obtained on a model  $(WO_3)_3/TiO_2(110)$  catalyst [15].

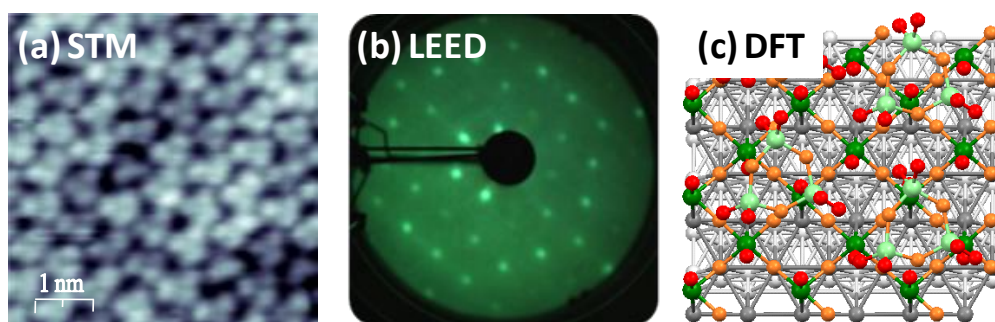


**Figure 9.** Structure of the two layer thick tungsten oxide film deposited on Pt(111) at 700 K. (a) High-resolution STM micrograph demonstrates that the films are composed of ordered array of  $(\text{WO}_3)_3$  clusters. (b) LEED image shows  $(3 \times 3)$  periodicity of the tungsten oxide film surface. (c) Film structure model based on DFT calculations. Pt atoms are shown as grey, W in first (second) layer as dark (light) green, O of  $\text{W}=\text{O}$  group as red, and O of  $\text{W}-\text{O}-\text{W}$  as orange.

**Imaging Hindered Rotations of Alkoxy Species on  $\text{TiO}_2(110)$ :** We carried out the first scanning tunneling microscopy (STM) study of the rotational dynamics of organic species on any oxide surface [16]. Specifically, variable-temperature STM and dispersion-corrected density functional theory (DFT-D) are used to study the alkyl chain conformational disorder and dynamics of 1-, 2-, 3- and 4-octoxy on rutile  $\text{TiO}_2(110)$  (Figure 10). The octoxy species together with the bridging hydroxyls ( $\text{HO}_b$ ) form as a result of octanol dissociation on the bridging oxygen ( $\text{O}_b$ ) vacancy ( $\text{V}_O$ ) defect sites. The STM images obtained at 150 and 300 K show that the alkyl chains of the octoxy species are positioned on the  $\text{Ti}^{4+}$  rows (neighboring the anchoring  $\text{O}_b$  row) where the attractive dispersion forces are maximized. The exact orientation of the alkyl chain depends on the position of the anchor ( $\text{C}-\text{O}_b$ ) as determined by the original position of OH in 1-, 2-, 3-, and 4-octanol. For isolated octoxy species, two rotational barriers are present, a small one for motion within the same  $\text{Ti}^{4+}$  row and a larger one for motion across the  $\text{O}_b$  row. In the presence of neighboring  $\text{HO}_b$ , the cross  $\text{O}_b$  row rotation of the octoxy leads to two structurally and energetically inequivalent configurations, a less favorable one with the  $\text{H}-\text{CO}$  hydrogen facing the  $\text{HO}_b$  and a more favorable one with the  $\text{H}-\text{CO}$  hydrogen facing away from the  $\text{HO}_b$ . The combination of atomistic simulation and our STM measurements have evolved a picture wherein, the observed alkyl chain orientations are found to be stabilized by  $\text{Ti} \cdots \text{C}$  vdW interactions which lead to a corrugated potential energy surfaces, with a resulting static and dynamic disorder amongst multiple binding configurations.

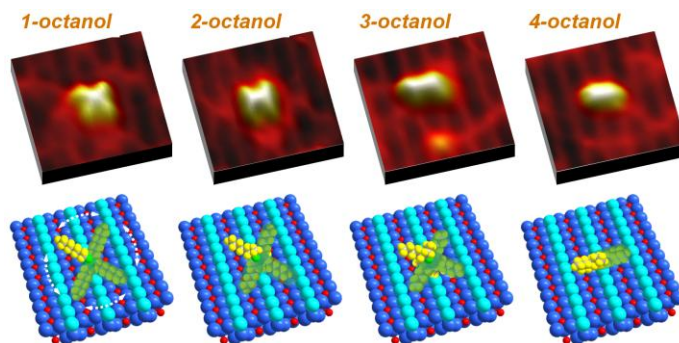


**Figure 10.** The STM images of partially reduced  $\text{TiO}_2(110)$  after adsorption of 1-, 2-, 3-, and 4-octanol at 300 K. The yellow lobes in the schematics show the octyl chains. Green lobes forming an “X” shape for 1-, 2-, and 3-octoxy and “I” shape for 4-octoxy indicate how fast rotation of the octoxy species leads to the formation of such features in the STM images. In all cases, the coverages were kept very low ( $< 2 \times 10^{13}$  molecules/ $\text{cm}^2$ ) to isolate the alkoxy species from each other. While not observable in the STM images the geminate  $\text{HO}_b$  species are present next to most of the octoxy species.

## Cited References

- [1] Macht, J; MJ Janik, M Neurock, and E Iglesia, *Angew. Chem. Int. Ed.*, **2007**, *46*, 7864.
- [2] Macht, J; MJ Janik, M Neurock, and E Iglesia, *J. Am. Chem. Soc.*, **2008**, *130*, 10369.
- [3] Macht, J; RT Carr, and E Iglesia. *J. Am. Chem. Soc.*, **2009**, *131*, 6554.
- [4] Carr, RT; M Neurock, and E Iglesia. *J. Catal.*, **2011**, *278*, 78.
- [5] Kwak, JH; D Mei, J Szanyi, Y Wang, CHF Peden, and RJ Rousseau. *Catal. Lett.* **2011**, *141* 649.
- [6] Kwak, JH; R Rousseau, D Mei, CHF Peden, and J Szanyi. *Chem. Cat. Chem.* **2011**, in press.
- [7] Zhai HJ, XH Zhang, WJ Chen, X Huang, and LS Wang, *J. Am. Chem. Soc.* **2011**, *133*, 3085.
- [8] Zhai HJ, BB Averkiev, DY Zubarev, LS Wang, and AI Boldyrev, *Angew. Chem. Int. Ed.* **2007**, *46*, 4277.
- [9] Chen WJ, HJ Zhai, YF Zhang, X Huang, and LS Wang, *J. Phys. Chem. A* **2010**, *114*, 5958.
- [10] Zhai HJ, B Wang, X Huang, and LS Wang, *J. Phys. Chem. A.* **2009**, *113*, 9804.
- [11] Bondarchuk, O.; Huang, X.; Kim, J.; Kay, B. D.; Wang, L. S.; White, J. M.; Dohnálek, Z. *Angew. Chem., Int. Ed. Engl.* **2006**, *45*, 4786.
- [12] Kim, Y. K.; Rousseau, R.; Kay, B. D.; White, J. M.; Dohnálek, Z. *J. Am. Chem. Soc.* **2008**, *130*, 5059.
- [13] Li, Z. J.; Zhang, Z. R.; Kim, Y. K.; Smith, R. S.; Netzer, F.; Kay, B. D.; Rousseau, R.; Dohnalek, Z. *J. Phys. Chem. C* **2011**, *115*, 5773.
- [14] Li, Z.; Zhang, Z.; Kay, B. D.; Dohnálek, Z. *J. Phys. Chem. C* **2011**, *115*, 9692.
- [15] Kim, J.; Kay, B. D.; Dohnalek, Z. *J. Phys. Chem. C* **2010**, *114*, 17017.
- [16] Zhang, Z.; Rousseau, R.; Gong, J.; Kay, B. D.; Dohnálek, Z. *J. Am. Chem. Soc.* **2009**, *131*, 17926.

## Publications 2009-2011

### 2009

- Kwak, JH; J Hu, DH Mei, C-W Yi, DH Kim, CHF Peden, LF Allard, J Szanyi. "Coordinatively Unsaturated Al<sup>III</sup> Centers as Binding Sites for Active Catalyst Phases: Strong Interactions Between Pt and  $\gamma$ -Al<sub>2</sub>O<sub>3</sub> Surfaces." *Science* **325** (2009) 1670-1673.
- Wan, H; S Li, TA Konovalova, Y Zhou, JS Thrasher, DA Dixon, and SC Street. "Experimental and Theoretical Studies of the Photoreduction of Metal Ion-Dendrimer Complexes: Observation of a Delocalized Organic Radical." *J. Phys. Chem. A* **113** (2009) 5358-5367.
- Zhu, K; J Hu, X She, J Liu, Z Nie, Y Wang, CHF Peden, JH Kwak. "Dispersion of Heteropoly Acid on Mesoporous Zeolite and Identification of the Surface Species by Solid State <sup>31</sup>P NMR Spin-Lattice Relaxation." *J. Am. Chem. Soc.* **131** (2009) 9715-9721.
- Tapu, D.; DA Dixon, and C Roe. "<sup>13</sup>C Spectroscopy of "Arduengo-type" Carbenes and Their Derivatives." *Chem. Rev.* **109** (2009) 3385-3407.
- Hu, JZ; JA Sears, JH Kwak, DW Hoyt, Y Wang, and CHF Peden. "An Isotropic Chemical Shift-Chemical Shift Anisotropic Correlation Experiment Using Discrete Magic Angle Turning." *J. Mag. Reson.* **198** (2009) 105-110.
- Konovalova, TA; S Li, NE Polyakov, L Focsan, DA Dixon, and LD Kispert. "Measuring Ti(III)-Carotenoid Radical Interspin Distances in TiMCM-41 by Pulsed EPR Relaxation Enhancement Method." *J. Phys. Chem. B* **113** (2009) 8704-8716.
- Janik, M; J Macht, E Iglesia, and M Neurock. "Correlating Acid Properties and Catalytic Function: A First-Principles Analysis of Alcohol Dehydration Pathways on Polyoxometalates." *J. Phys. Chem. C* **113** (2009) 1872-1885.
- Grant, DJ; DA Dixon, JS Francisco, D Feller, and KA Peterson. "Heats of Formation of the H<sub>1,2</sub>O<sub>m</sub>S<sub>n</sub> (m, n = 0 – 3) Systems from Electronic Structure Calculations." *J. Phys. Chem. A* **113** (2009) 11343-11353.
- Zhang, Z; Y Du, NG Petrik, GA Kimmel, I Lyubinsky, and Z Dohnálek. "Water as a Catalyst: Imaging Reactions of O<sub>2</sub> with Partially and Fully Hydroxylated TiO<sub>2</sub>(110) Surfaces." *J. Phys. Chem. C* **113** (2009) 1908-1916.
- Hu, JZ; JH Kwak, Y Wang, CHF Peden, H Zheng, D Ma, and X Bao. "Studies of the Active Sites for Methane Dehydroaromatization Using Ultra-High Field Solid State <sup>95</sup>Mo NMR Spectroscopy." *J. Phys. Chem. C* **113** (2009) 2936-2942.

- Stott, AC; PB Abel, GH Bozzolo, and DA Dixon. "Interfacial Phase Stability in TiV Multi-Laminate Thin Films." *J. Phys. Chem. C* **113** (2009) 21383-21388.
- Macht, J; RT Carr, E Iglesia. "Consequences of Acid Strength for Isomerization and Elimination Catalysis on Solid Acids." *J. Am. Chem. Soc.* **131** (2009) 6554-6565.
- Li, S; JM Hennigan, DA Dixon, and KA Peterson. "Accurate Thermochemistry for Transition Metal Oxide Clusters." *J. Phys. Chem. A* **113** (2009) 7681-7877.
- Du, Y; NA Deskins, Z Zhang, Z Dohnálek, M Dupuis, and I Lyubinetzky. "Imaging Consecutive Steps of O<sub>2</sub> Reaction with Hydroxylated TiO<sub>2</sub>(110): Identification of HO<sub>2</sub> and Terminal OH Intermediates." *J. Phys. Chem. C* **113** (2009) 666-671.
- Macht, J; RT Carr, E Iglesia. "Functional Assessment of the Strength of Solid Acid Catalysts." *J. Catal.* **264** (2009) 54-66.
- Zhu, K; J Hu, X She, J Liu, Z Nie, Y Wang, CHF Peden, and JH Kwak. "Dispersion of Heteropoly Acid on Mesoporous Zeolite and Identification of the Surface Species by Solid State <sup>31</sup>P NMR Spin-Lattice Relaxation." *J. Am. Chem. Soc.* **131** (2009) 9715-9721.
- Kim, YK; Z Dohnálek, BD Kay, and R Rousseau. "Competitive Oxidation and Reduction of Aliphatic Alcohols over (WO<sub>3</sub>)<sub>3</sub> Clusters." *J. Phys. Chem. C* **113** (2009) 9721-9730.
- Kim, YK; Z Zhang, GS Parkinson, S-C Li, BD Kay, and Z Dohnálek. "Reactivity of FeO(111)/Pt(111) with Alcohols." *J. Phys. Chem. C* **113** (2009) 20020-20028.
- Zhang, Z; R Rousseau, J Gong, BD Kay, and Z Dohnálek. "Imaging Hindered Rotations of Alkoxy Species on TiO<sub>2</sub>(110)." *J. Am. Chem. Soc.* **131** (2009) 17926-17932.
- Zhai, HJ; B Wang, X Huang, and LS Wang. "Probing the Electronic and Structural Properties of the Niobium Trimer Cluster and its Mono- and Di-oxides: Nb<sub>3</sub>O<sub>n</sub><sup>-</sup> and Nb<sub>3</sub>O<sub>n</sub> (n = 0–2)." *J. Phys. Chem. A* **113** (2009) 3866-3875.
- Zhai, HJ; B Wang, X Huang, and LS Wang. "Structural Evolution, Sequential Oxidation, and Chemical Bonding in Tri-Tantalum Oxide Clusters: Ta<sub>3</sub>O<sub>n</sub><sup>-</sup> and Ta<sub>3</sub>O<sub>n</sub> (n = 1–8)." *J. Phys. Chem. A* **113** (2009) 9804-9813.
- Sierka, M; J Döbler, J Sauer, HJ Zhai, and LS Wang. "The [(Al<sub>2</sub>O<sub>3</sub>)<sub>2</sub>]<sup>-</sup> Anion Cluster: Electron Localization-Delocalization Isomerism." *ChemPhysChem* **10** (2009) 2410-2413.
- Li, SG; HJ Zhai, LS Wang, and DA Dixon. "Structural and Electronic Properties of Reduced Transition Metal Oxide Clusters, M<sub>3</sub>O<sub>8</sub> and M<sub>3</sub>O<sub>8</sub><sup>-</sup> (M = Cr, W), from Photoelectron Spectroscopy and Quantum Chemical Calculations." *J. Phys. Chem. A* **113** (2009) 11273-11288.
- Dixon, DA. "Noble Gas Compounds: Reliable Computational Methods." In *Computational Inorganic and Bioinorganic Chemistry*, EI Solomon, RA Scott and RB King, Eds., John Wiley & Sons (Chichester, UK) 2009, pp 527-538.

## 2010

- Grant, DJ; T-H Wang, DA Dixon, and KO Christe. "Heats of Formation of XeF<sub>3</sub><sup>+</sup>, XeF<sub>3</sub><sup>-</sup>, XeF<sub>5</sub><sup>+</sup>, XeF<sub>7</sub><sup>+</sup>, XeF<sub>7</sub><sup>-</sup>, and XeF<sub>8</sub> from High Level Electronic Structure Calculations." *Inorg. Chem. A* **49** (2010) 261-270.
- Yang, Y; CA Mims, RS Disselkamp, CHF Peden, and CT Campbell. "(Non)Formation of Methanol by Hydrogenation of Formate on Copper Catalysts." *J. Phys. Chem. C* **40** (2010) 17205-17211. **Invited contribution in D. Wayne Goodman Festschrift Issue.**
- Henderson, MA; CHF Peden, JA Rodriguez, J Szanyi, JT Yates, Jr., and F Zaera. "Preface to the Festschrift in Honor of Professor D. Wayne Goodman." *J. Phys. Chem. C* **40** (2010) 16861-16862. **Invited contribution in D. Wayne Goodman Festschrift Issue.**
- Mei, D; JH Kwak, J Hu, SJ Cho, J Szanyi, LF Allard, and CHF Peden. "The Unique Role of Anchoring Penta-Coordinated Al<sup>3+</sup> Sites in the Sintering of  $\gamma$ -Al<sub>2</sub>O<sub>3</sub>-supported Pt Catalysts." *J. Phys. Chem. Lett.* **1** (2010) 2688-2691.
- Feller, D; KA Peterson, and DA Dixon. "Refined theoretical estimates of the atomization energies and molecular structures of selected small oxygen fluorides." *J. Phys. Chem. A* **114** (2010) 613-623.
- Dohnálek, Z; I Lyubinetzky, and R. Rousseau. "Thermally-Driven Processes on Rutile TiO<sub>2</sub>(110)-(1×1): A Direct View at the Atomic Scale." *Prog. Surf. Sci.* **85** (2010) 161. **Invited Review Article.**
- Craciun, R; D Picone, RT Long, S Li, DA Dixon, KA Peterson, and KO Christe. "Third Row Transition Metal Hexafluorides, Extraordinary Oxidizers and Lewis Acids: Electron Affinities, Fluoride Affinities, and Heats of Formation of WF<sub>6</sub>, ReF<sub>6</sub>, OsF<sub>6</sub>, IrF<sub>6</sub>, PtF<sub>6</sub>, and AuF<sub>6</sub>." *Inorg. Chem. A* **49** (2010) 1056-1070.

- Li, SG; and DA Dixon. "Structures and Energetics of the  $(\text{ZrO}_2)_n$  and  $(\text{HfO}_2)_n$  ( $n = 1-4$ ) Clusters and Their Anions." *J. Phys. Chem. A* **114** (2010) 2665-2683.
- Kim, J; BD Kay, and Z Dohnálek. "Formaldehyde Polymerization on  $(\text{WO}_3)_3/\text{TiO}_2(110)$  Model Catalyst." *J. Phys. Chem. C* **114** (2010) 17017. **Invited contribution in D. Wayne Goodman Festschrift Issue.**
- Grant, DJ; EB Garner III, MH Matus, MT Nguyen, KA Peterson, JS Francisco, and DA Dixon. "Thermodynamic Properties of the  $\text{XO}_2$ ,  $\text{X}_2\text{O}$ ,  $\text{XYO}$ ,  $\text{X}_2\text{O}_2$ , and  $\text{XYO}_2$  ( $\text{X}, \text{Y} = \text{Cl}, \text{Br}$  and  $\text{I}$ ) Isomers." *J. Phys. Chem. A* **114** (2010) 4254-4265.
- Chen, WJ; HJ Zhai, YF Zhang, X Huang, and LS Wang. "On the Electronic and Structural Properties of Tri-Niobium Oxide Clusters  $\text{Nb}_3\text{O}_n^-$  and  $\text{Nb}_3\text{O}_n$  ( $n = 3-8$ ): Photoelectron Spectroscopy and Density Functional Calculations." *J. Phys. Chem. A* **114** (2010) 5958-5966.
- Vasiliu, M; S Li, KA Peterson, D Feller, JL Gole, and DA Dixon. "Structures and Heats of Formation of Simple Alkali Metal Compounds: Hydrides, Chlorides, Fluorides, Hydroxides and Oxides for Li, Na and K." *J. Phys. Chem. A* **114** (2010) 4272-4281.
- Parkinson, GS; Z Dohnálek, RS Smith, and BD Kay. "Reactivity of  $\text{Fe}^0$  atoms with mixed  $\text{CCl}_4$  and  $\text{D}_2\text{O}$  films over  $\text{FeO}(111)$ ." *J. Phys. Chem. C* **14** (2010) 17136. **Invited contribution in D. Wayne Goodman Festschrift Issue.**
- Craciun, R; AJ Vincent, KH Shaughnessy, and DA Dixon. "Prediction of Reliable Metal- $\text{PH}_3$  Bond Energies for Ni, Pd and Pt in the 0 and +2 Oxidation States." *Inorg. Chem.* **49** (2010) 5546-5553.
- Zhai, HJ; and LS Wang. "Probing the electronic structure of early transition metal oxide clusters: Molecular models towards mechanistic insights into oxide surfaces and catalysis." *Chem. Phys. Lett.* **500** (2010) 185-195. **Invited Frontiers Article, and featured on the journal cover.**
- Christe, KO; DA Dixon, DJ Grant, R Haiges, FS Tham, A Vij, V Vij, T-H Wang, and WW Wilson. "Dinitrogen Difluoride Chemistry. Improved Syntheses of *cis*- and *trans*- $\text{N}_2\text{F}_2$ , Synthesis and Characterization of  $\text{N}_2\text{F}^+\text{Sn}_2\text{F}_9^-$ , Ordered Crystal Structure of  $\text{N}_2\text{F}^+\text{Sb}_2\text{F}_{11}^-$ , High-Level Electronic Structure Calculations of *cis*- $\text{N}_2\text{F}_2$ , *trans*- $\text{N}_2\text{F}_2$ ,  $\text{F}_2\text{N}=\text{N}$ , and  $\text{N}_2\text{F}^+$ , and Mechanism of the *trans*-*cis* Isomerization of  $\text{N}_2\text{F}_2$ ." *Inorg. Chem.* **49** (2010) 6823-6833. **Featured on the journal cover.**
- Du, Y; NA Deskins, Z Zhang, Z Dohnálek, M Dupuis, and I Lyubinetsky. "Water Interactions with Terminal Hydroxyls on  $\text{TiO}_2(110)$ ." *J. Phys. Chem. C* **14** (2010) 17080. **Invited contribution in D. Wayne Goodman Festschrift Issue.**
- Wang, TH; AM Navarrete-López, S Li, DA Dixon, and JL Gole. "Hydrolysis of  $\text{TiCl}_4$ : The Initial Steps in the Production of  $\text{TiO}_2$ ." *J. Phys. Chem. A* **114** (2010) 7561-7570.
- Craciun, R; RT Long, DA Dixon, and KO Christe. "Electron Affinities, Fluoride Affinities, and Heats of Formation of the Second Row Transition Metal Hexafluorides:  $\text{MF}_6$  ( $\text{M} = \text{Mo}, \text{Tc}, \text{Ru}, \text{Rh}, \text{Pd}, \text{Ag}$ )." *J. Phys. Chem. A* **114** (2010) 7571-7582.
- Li, K; N Li, S Li, DA Dixon, and TM Klein. "Tetrakis(dimethylamido) Hafnium Adsorption and Reaction on Hydrogen-Terminated  $\text{Si}(100)$  Surfaces." *J. Phys. Chem. C* **114** (2010) 14061-14075.
- Wang, T-H; DA Dixon, and MA Henderson. "C-C and C-Heteroatom Bond Dissociation Energies in  $\text{CH}_3\text{R}^+\text{C}(\text{OH})_2$ : Energetics for Photocatalytic Processes of Organic Diolates on  $\text{TiO}_2$  Surfaces." *J. Phys. Chem. C* **114** (2010) 14083-14092.
- Vasiliu, M; S Li, D Feller, JL Gole, and DA Dixon. "Structures and Heats of Formation of Simple Alkaline Earth Metal Compounds: Fluorides, Chlorides, Oxides, and Hydroxides for Be, Mg, and Ca." *J. Phys. Chem. A* **114** (2010) 9349-9358.
- Stott, AC; JI Brauer, A Garg, SV Pepper, PB Abel, C DellaCorte, RD Noebe, G Glennon, E Bylaska, and DA Dixon. "Bonding and microstructural stability in  $\text{Ni}_{55}\text{Ti}_{45}$  studied by experimental and theoretical methods." *J. Phys. Chem. C* **114** (2010) 19704-19713.

## 2011

- Grant, DJ; T-H Wang, M Vasiliu, DA Dixon, and KO Christe. "The  $\text{F}^+$  and  $\text{F}^-$  Affinities of Simple  $\text{N}_x\text{F}_y$  and  $\text{O}_x\text{F}_y$  Compounds." *Inorg. Chem.* **50** (2011) 1914-1925.
- Carr, RC; M Neurock, and E Iglesia. "Catalytic Consequences of Acid Strength in the Conversion of Methanol to Dimethyl Ether." *J. Catal.* **278** (2011) 78-93.
- Feller, D; KA Peterson, and DA Dixon. "Ab Initio Coupled Cluster Determination of the Heats of Formation of  $\text{C}_2\text{H}_2\text{F}_2$ ,  $\text{C}_2\text{F}_2$  and  $\text{C}_2\text{F}_4$ ." *J. Phys. Chem. A* **115** (2011) 1440-1451.

- Zhai, HJ; XH Zhang, WJ Chen, X Huang, and LS Wang. "Stoichiometric and Oxygen-Rich  $M_2O_n^-$  and  $M_2O_n$  ( $M = Nb, Ta; n = 5-7$ ) Clusters: Molecular Models for Oxygen Radicals, Diradicals, and Superoxides." *J. Am. Chem. Soc.* **133** (2011) 3085-3094.
- Wang, X; H-G Cho, L Andrews, M Chen, DA Dixon, H-S Hu, and J Li. "Matrix Infrared Spectroscopic and Computational Investigations of the Lanthanide Metal Atom-Methylene Fluoride Activation Products  $CH_2LnF_2$ ." *J. Phys. Chem. A* **115** (2011) 1913-1921.
- Stott, AC; PB Abel, C DellaCorte, SV Pepper, and DA Dixon. "Computational Studies of the NiTi Alloy System: Bulk, Supercell, and Surface Calculations." *MRS Proceedings* **1295** (2011) 15-20.
- Kwak, JH; D Mei, J Szanyi, Y Wang, CHF Peden, and RJ Rousseau. "The (100) Facets of  $\gamma$ - $Al_2O_3$ : the Active Surfaces for Alcohol Dehydration Reactions." *Catal. Lett.* **141** (2011) 649-655.
- Li, S; CL Guenther, MS Kelley, and DA Dixon. "Molecular Structures, Acid-Base Properties, and Formations of Group VIB Transition Metal Hydroxides." *J. Phys. Chem. C* **115** (2011) 8072-8103.
- Wang, TH; Z Fang, NW Gist, S Li, DA Dixon, and J L Gole. "Computational Study of the Hydrolysis Reactions of the Ground and First Excited Triplet States of Small  $TiO_2$  Nanoclusters." *J. Phys. Chem. C* **115** (2011) 9344-9360.
- Kwak, JH; CHF Peden, and J Szanyi. "Using a Surface Sensitive Chemical Probe and a Bulk Structure Technique to Monitor the  $\gamma$ - to  $\theta$ - $Al_2O_3$  Phase Transformation." *J. Phys. Chem. C* **115** (2011) in press.
- Li, K; L Zhang, DA Dixon, and TM Klein. "Undulating Topography for  $HfO_2$  Thin Films Deposited in a Meso-Scale Reactor using Hafnium (IV) tert butoxide." *AIChE Journal*, WEB Online Feb. 16, 2011, in press.
- Kwak, JH; R Rousseau, D Mei, CHF Peden, and J Szanyi. "The Origin of Regioselectivity in 2-Butanol Dehydration on Solid Acid Catalysts." *Chem. Cat. Chem.* (2011) in press.
- Vasiliu, M; S Li, AJ Arduengo, and DA Dixon. "Bond Energies in Models of the Schrock Metathesis Catalyst." *J. Phys. Chem. C* **115** (2011) in press
- Hu, JZ; JH Kwak, Y Wang, and CHF Peden. "Characterizing Surface Acid Sites of Dispersed Tungsten Oxide Catalysts on Mesoporous Silica Using Solid State  $^{15}N$  NMR." *J. Mag. Reson.*, submitted for publication.
- Li, Z; Z Zhang, YK Kim, RS Smith, F Netzer, BD Kay, R Rousseau, and Z Dohnálek. "Growth of Ordered Ultra-thin Tungsten Oxide Films on Pt(111)." *J. Phys. Chem. C* **115** (2011) in press.
- She, X; JH Kwak, J Sun, J Hu, MY Hu, CM Wang, CHF Peden, and Y Wang. "A Comparative Study of SBA-15 Mesoporous Silica Supported Tungsten Oxide and Rhenium Oxide Catalysts for 2-Butanol Dehydration." *J. Catal.*, submitted for publication.
- Sun, J; K Zhu, F Gao, CM Wang, J Liu, CHF Peden, and Y Wang. "High Yield Bio-Ethanol Conversion to Isobutene:  $ZnxZryOz$  Mixed Oxides for a Novel and Highly Selective Process to Value-Added Products from Biomass." *J. Am. Chem. Soc.*, submitted for publication.





solid-state (SS) NMR experiments and further refined by theoretical modeling (Fig. 1) [22]. These conformations include PFP groups in the upright position (PFP-u) and the in the prone position with the aromatic rings located above the siloxane bridges (PFP-p). The NMR measurements showed that in the presence of solvents (including water) all PFP rings are in prone arrangement on the surface.

In a subsequent study [44], bifunctionalized MSN catalyst containing a Brønsted acidic diarylammonium triflate (DAT) group and a PFP group was designed for the esterification reaction of different carboxylic acids with benzyl alcohol (Fig. 2). Rather than controlling the diffusional penetration of reactants to the catalytic sites inside the mesopores, we incorporated the PFP groups to the porous framework, so that the perfluorinated, water-resistant mesochannels could efficiently extrude water molecules produced during the esterification reaction. The bifunctional PFP/DAT MSN catalyst showed considerably higher reactivity than

the monofunctional DAT MSN, and surpassed other commercially available heterogeneous acid catalysts, such as Amberlyst-15 and Nafion NR-50<sup>®</sup> under the examined reaction conditions.

**(2) Interplay between anomalous transport and catalytic reaction kinetics in single-file nanoporous systems.** MSN generally have pore diameters in the range 2-10 nm. However, after functionalization, the effective diameter can be reduced below 2.0 nm. In this regime, the kinetics of catalytic reaction processes in these systems can be strongly impacted by the anomalous transport. The most extreme case corresponds to single-file diffusion for narrow pores in which species cannot pass each other. The associated sub-linear mean-square-displacement for tracer diffusion is well-recognized. However, there is still limited understanding of the behavior of chemical diffusion which controls reactivity in conversion reactions. We have shown that traditional mean-field-type reaction-diffusion equations fail to capture the initial evolution of concentration profiles, and they cannot describe the scaling behavior of steady-state reactivity. Hydrodynamic reaction-diffusion equations accounting for the single-file aspects of chemical diffusion can describe such initial evolution [36], but additional refinements are needed to incorporate fluctuation effects controlling, e.g., removal of reactant from the center of a pore for which only end regions catalytic (see Fig. 3a) [35].

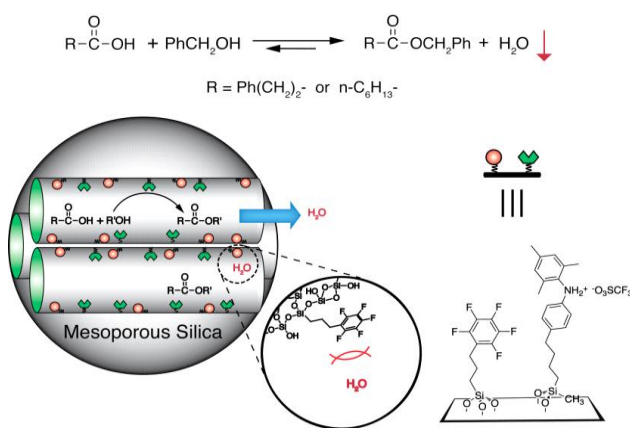


**Figure 2.** Schematic representation of a bifunctional PFP/DAT MSN catalyst for esterification reaction

For polymerization reactions in nanoporous materials with a single-file diffusion, no picture has been available for the spatiotemporal evolution of the oligomer distribution during growth. We found that initial behavior depends strongly on system details such as catalytic site loading and reaction rate. However, longer-time behavior often involves the formation of dominant large polymer near each end of the pore, initially within the pore but subsequently partly extruding (see Fig. 3b) [23,35]. In this partial extrusion regime, the growth kinetics are non-Markovian (i.e., conventional rate equations fail). They are controlled by unusual features of the random walk describing the motion of the end of the partly extruded polymer, noting that this extruded end must return within the pore for further growth [23].

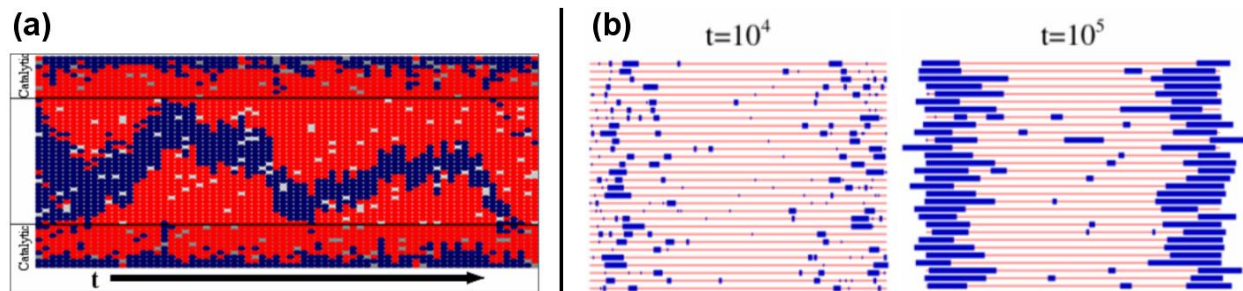


Fig. 3. (a) Conversion of A (blue) to B (red) inside a pore (aligned vertically) with catalytic end regions. Simulation snapshots for time increasing left to right. A in the central unreactive region is ultimately removed by anomalous diffusion to the reactive ends. (b) Simulated polymer distributions in an array of pores (aligned horizontally) modeling PPB formation within  $\text{Cu}^{2+}$ -functionalized MCM-41 silica.

**(3) Homogeneous reactions – development and mechanism toward new interfacial studies.** We have been developing new transition-metal complexes that maintain similar coordination geometries under homogeneous and surface-supported conditions for the preparation of well-defined catalytic sites. We have prepared bis(4,4-dimethyl-2-oxazolinyl)phenylborane [ $\text{PhB}(\text{Ox}^{\text{Me}_2})_2$ ] as an ancillary ligand that controls surface...transition-metal complex interactions and provides versatile spectroscopic handles for surface and solution characterization [18]. This bi-functional ligand provides a template for multisite catalysis under homogeneous and heterogeneous conditions. In one notable example, the oxazolinylborate metal compounds template C-N bond formation by coupling that step with a proton transfer [28,29,45]. In a second example, oxazolinylborate metal compounds facilitate C-H bond activation/functionalization for the derivatization of hydrocarbons [46].

We have also developed a rapid base-catalyzed reaction between rhodium hydrides and molecular oxygen that yields hydroperoxorhodium complexes capable of oxygen atom transfer to various substrates. The strongly pH-dependent kinetics, activation parameters, kinetic isotope effects, and an independent study of hydrogen exchange with the solvent all support a direct attack by hydroxide ion at the metal hydride as the key step in hydroperoxide formation [24].

**(4) Novel 3D catalyst synthesis.** We have synthesized a series of mesoporous mixed metal oxides combining earth alkaline metals with silica, which catalyzed the transesterification of animal fats for the production of biodiesel. These catalysts were not deactivated by the presence of free fatty acids, allowed the conversion to take place at low temperatures and saved purification steps, demonstrating a significant advantage over traditional homogeneous catalysts [21]. We have improved the control over particle morphology, pore structure and pore size of MSNs and applied these controls to prepare novel metal oxide and polymer nanoparticles. While the high surface area mesoporous oxides can act as catalysts, the mesoporous polymer particles

can serve as multivalent ligands for catalytic metal ions [15,17,38]. We developed multifunctionalized MSNs capable of performing sequential reactions in a single pot, and of controlling the stereochemistry of products through cooperative interactions [15,20,40,41].

An important step towards our goal of combining biological and photochemical catalysis involves incorporating photo deposition of metal particles on semiconductor nanorods. This was achieved with a high degree of site-selectivity (95:5 surface-bound vs. free-standing), as well as on axially anisotropic semiconductor nanorods with unprecedented control over site-specificity. In addition, we have made good progress on the immobilization and protection of semiconductor nanorods in MSNs via co-condensation, as well as on the photochemical dehydrogenation of alcohols to molecular hydrogen using bare semiconductor-metal heterostructures.

### Future Plans

- *Develop single-site catalysts for oxidative conversion of biomass and understand the fundamental mechanisms of such reactions.* Our current work has set the stage for this in that we have found reactions for deoxygenation of alcohols. We are also developing heterogeneous single-site catalysts based on our oxazolinylborate platform.
- *Influence of the mesopore environment on oxygen binding and activation.* Now that we have developed an understanding of oxygen activation with rhodium complexes in homogeneous solution, we will immobilize such complexes on MSNs and attempt to generate and characterize various intermediates (superoxo, hydroperoxo, peroxy) on the surface. Kinetic and mechanistic studies combined with solid-state NMR are expected to provide an understanding of O<sub>2</sub> activation by MSN-supported species and to lead to efficient heterogeneous catalysts for oxidations with molecular oxygen.
- *Develop multifunctional mesoporous catalysts for sequential redox and carbon-carbon bond forming reactions in a single pot.* We have optimized catalysts for two types of reactions, based on our ability to prepare multifunctionalized catalysts, we plan to combine both catalysts into a single one to achieve an efficient catalyst for sequential reactions.
- *Study catalytic processes in nanodomains by selectively exciting energy absorbing nanoparticles embedded in mesoporous supports.* We have prepared a series of mesoporous materials containing nanoparticles capable of absorbing different types of energy (microwave, UV-visible, alternating magnetic fields), and we will use the energy collected by these species to activate catalysts immobilized in the mesoporous supports.
- *Investigate effects of pore parameters on the activity of mesoporous catalysts.* We have achieved the ability to control the morphology, width and length of pores in mesoporous materials. With the assistance of SSNMR characterization and statistical mechanical modeling, we plan to establish the ideal combination of these variables to obtain optimized catalysts.
- *Photoactive heterostructures for solar-to-chemical conversion.* Our immediate future plans include the selective photo-deposition of metal particles on heterostructured and immobilized semiconductors, investigating electron transfer rates as a function of dielectric constant and pore functionalization inside mesoporous materials, and testing the resulting nanocomposites as photo catalysts for solar-to-chemical energy conversion of biomass feedstocks.
- *Catalyst characterization by solid-state NMR spectroscopy.* The development of SSNMR techniques will focus on new multidimensional protocols for studying the internuclear correlations on solid-liquid interfaces and transport phenomena within the pores.
- *Modeling of transport and reaction in mesoporous systems.* We will develop models for conversion reactions with inhibited passing of reactants and products which can account for

observed pore-diameter-dependence of yield. We will also pursue detailed modeling for cross-coupling polymerization reactions.

### Publications (2009-present)

1. J. L. Rapp, Y. Huang, M. Natella, Y. Cai, V. S. -Y. Lin, M. Pruski, *A Solid-State NMR Investigation of the Structure of Mesoporous Silica Nanoparticle Supported Rhodium Catalysts*, *Solid State NMR* 35, 82-86 (2009).
2. K. Mao, J. W. Wiench, V. S. -Y. Lin, M. Pruski, *Indirectly Detected Through-Bond Chemical Shift Correlation NMR Spectroscopy under Fast MAS: Studies of Organic-Inorganic Hybrid Materials*, *J. Magn. Reson.* 196, 92-95 (2009).
3. E. Szajna-Fuller, Y. Huang, J.R. Rapp, G. Chaka, V. S.-Y. Lin, M. Pruski, A. Bakac, *Kinetics of Oxidation of an Organic Amine With a Cr(V) Salen Complex in Homogeneous Aqueous Solution and on the Surface of Mesoporous Silica*, *Dalton Trans.* 17, 3237-3246 (2009).
4. D. -J. Liu, H. -T. Chen, V. S. -Y. Lin, J. W. Evans, *Statistical Mechanical Modeling of Catalytic Polymerization within Surface Functionalized Mesoporous Materials*, *Phys. Rev. E* 80, 011801 (2009).
5. J. W. Wiench, C. Michon, A. Ellern, P. Hazendonk, A. Iuga, R.J. Angelici, M. Pruski, *Solid-State NMR Investigations of the Immobilization of a  $BF_4^-$  Salt of a Palladium(II) Complex on Silica*, *J. Am. Chem. Soc.* 131, 11801-11810 (2009).
6. G. Chaka, A. Bakac, *Two-Electron Oxidation of N,N,N',N'-Tetramethylphenylenediamine with a Chromium(V) Salen Complex*, *Dalton Trans.* 318-321, (2009).
7. A. Bakac, O. Pestovsky, *Iron Catalysis in Oxidation by Ozone*, US patent 7618546 (2009).
8. K. Mao, J. R. Rapp, J. W. Wiench, M. Pruski, *Characterization of Mesoporous Organic-Inorganic Hybrid Materials using Advanced Solid-State NMR Spectroscopy*, *Mat. Res. Soc. Symp. Proc. Ser.*, 1184, 175-183 (2009).
9. K. Yan, A. V. Pawlikowski, C. Ebert, A. D. Sadow, *A tris(alkyl)yttrium Compound Containing Six  $\beta$ -agostic Si-H Interactions*, *Chem. Commun.* 6, 656-658 (2009).
10. A. V. Pawlikowski, T. S. Gray, G. Schoendorff, B. Baird, A. Ellern, T. L. Windus, A. D. Sadow, *Structure, Bonding, and Ligand-based Reactions of Zwitterionic Boratoiridium(I) Complexes with Oxazoline-based Scorpionate Ligands*, *Inorg. Chim. Acta.* 362, 4517-4525 (2009).
11. K. Yan, B. Upton, A. Ellern, A. D. Sadow, *Lewis Acid Mediated  $\beta$ -Hydride Abstraction Reactions of Divalent  $M(C(SiHMe_2)_3)_2THF_2$  ( $M=Ca, Yb$ )*, *J. Am. Chem. Soc.* 131, 15110-15111 (2009).
12. K. Mao, M. Pruski, *Directly and Indirectly Detected Through-Bond Heteronuclear Correlation Solid-State NMR Spectroscopy under Fast MAS*, *J. Magn. Reson.* 201, 165-174 (2009).
13. I. I. Slowing, C. -W. Wu, J. L. Vivero, V. S. -Y. Lin, *Mesoporous Silica Nanoparticles for Reducing Hemolytic Activity Towards Mammalian Red Blood Cells*, *Small* 5, 57-62 (2009).
14. R. Mortera, J. L. Vivero, I. I. Slowing, E. Garrone, B. Onida, V. S. -Y. Lin, *Cell-induced Intracellular Controlled Release of Membrane Impermeable Cysteine from a Mesoporous Silica Nanoparticle-based Drug Delivery System*, *Chem. Commun.* 3219-3221 (2009).
15. S. G. Wang, C.-W. Wu, K. M. Chen, V. S. -Y. Lin, *Fine-Tuning Mesochannel Orientation of Organically Functionalized Mesoporous Silica Nanoparticles*, *Chem.-Asian J.* 4, 658-661 (2009).
16. I. I. Slowing, J. L. Vivero, B. G. Trewyn, V. S. -Y. Lin, *Mesoporous Silica Nanoparticles: Structural Design and Applications*, *J. Mater. Chem.* 20, 7924-7937 (2010).
17. T. -W. Kim, P. -W. Chung, V. S. -Y. Lin, *Facile Synthesis of Monodisperse Spherical MCM-48 Mesoporous Silica Nanoparticles with Controlled Particle Size*, *Chem. Mater.* 22, 5093-5104 (2010).
18. J. F. Dunne, K. Manna, J. W. Wiench, A. Ellern, M. Pruski, A. D. Sadow, *Bis(oxazolanyl)borane: A Lewis Acid-containing Ligand for Aluminum(III), Methide Abstraction-based Coordination, and Comparisons with Tris(oxazolanyl)boratoaluminum Catalyzed Lactide Ring Opening Polymerization*, *Dalton Trans.* 39, 641-653 (2010).
19. K. Mao, M. Pruski, *Homonuclear Dipolar Decoupling under Fast MAS: Resolution Patterns and Simple Optimization Strategy*, *J. Magn. Reson.* 203, 144-149 (2010).

20. H. -T. Chen, B. G. Trewyn, J. W. Wiench, M. Pruski, V.S.-Y. Lin, *Urea and Thiourea-Functionalized Mesoporous Silica Nanoparticle Catalysts with Enhanced Catalytic Activity for Diels-Alder Reaction*, *Top. Catal.* 53, 187-191 (2010).
21. T. -M. Hsin, S. Chen, E. Guo, C. -H. Tsai, M. Pruski, V. S.-Y. Lin, *Calcium Containing Silicate Mixed Oxide-based Heterogeneous Catalysts for Biodiesel Production*, *Top. Catal.* 53, 746-754 (2010).
22. K. Mao, T. Kobayashi, J. W. Wiench, H. -T. Chen, C. -H. Tsai, V. S. -Y. Lin, M. Pruski, *Conformations of Silica-Bound (Pentafluorophenyl)Propyl Groups Determined by Solid-State NMR Spectroscopy and Theoretical Calculations*, *J. Am. Chem. Soc.* 132, 12452-12457 (2010).
23. D. -J. Liu, H. -T. Chen, V. S.-Y. Lin, J. W. Evans, *Polymer Length Distributions for Catalytic Polymerization in Mesoporous Materials: Non-Markovian Behavior Associated with Partial Extrusion*, *J. Chem. Phys.*, 132, 154102 (2010).
24. E. Szajna-Fuller, A. Bakac, *Base-Catalyzed Insertion of Dioxygen into Rhodium-Hydrogen Bonds. Kinetics and Mechanism*, *Inorg. Chem.* 49, 781-785 (2010).
25. A. Bakac, *Oxygen Activation With Transition Metal Complexes in Aqueous Solution*, *Inorg. Chem.* 49, 3584-3593 (2010).
26. D. Mukherjee, A. Ellern, A. D. Sadow, *Conversion of a Zinc Disilazide to a Zinc Hydride Mediated by LiCl*, *J. Am. Chem. Soc.* 132, 7582-7583 (2010).
27. H.-A. Ho, J.F. Dunne, A. Ellern, A. D. Sadow, *Reactions of Tris(oxazolinyl)phenylborato Rhodium(I) with C-X (X = Cl, Br, OTf) Bonds: Stereoselective Intermolecular Oxidative Addition*, *Organometallics* 29, 4105-4114 (2010).
28. K. Manna, A. Ellern, A. D. Sadow, *A Zwitterionic Zirconium Complex that Catalyzes Hydroamination at Room Temperature*, *Chem. Commun.* 46, 339-441 (2010).
29. J. F. Dunne, D. B. Fulton, A. Ellern, A. D. Sadow, *Concerted C–N and C–H Bond Formation in a Magnesium-Catalyzed Hydroamination*, *J. Am. Chem. Soc.* 132, 17680-17683 (2010).
30. E. Szajna-Fuller, A. Bakac, *Catalytic Generation of Hydrogen with Titanium Citrate and a Macrocyclic Cobalt Complex*, *Eur. J. Inorg. Chem.* 2488-2494 (2010).
31. J. -E. Jee, O. Pestovsky, I. Hidayat, E. Szajna-Fuller, A. Bakac, *Mechanism of Oxidation of Alkyl And Superoxo Complexes of Chromium by Aquamanganese(III) Ions*, *J. Coord. Chem.* 63, 2578-2585 (2010).
32. J. -E. Jee, O. Pestovsky, A. Bakac, *Preparation and Characterization of Manganese(IV) in Aqueous Acetic Acid*, *Dalton Trans.* 39, 11636-11642 (2010).
33. A. *Chemical Kinetics as a Mechanistic Tool* in *Physical Inorganic Chemistry. Principles, Methods and Models*" A. Bakac, Ed., Wiley, Hoboken, (2010).
34. B. Jana, A. Ellern, O. Pestovsky, A. D. Sadow, A. Bakac, *Synthesis of Fe(II) and Ru(II) Complexes of Tetradentate Phosphines*, *Inorg. Chem.* 50, 3010 – 3016 (2011).
35. D. -J. Liu, J. Wang, D. Ackerman, I. I. Slowing, M. Pruski, H. -T. Chen, V. S. -Y. Lin, J. W. Evans, *Interplay between Anomalous Transport and Catalytic Reaction Kinetics in Single-file Mesoporous Systems*, *ACS Catalysis* 1, 751-763 (2011).
36. D. M. Ackerman, J. Wang, J. H. Wendel, D. -J. Liu, M. Pruski, J. W. Evans, *Catalytic Conversion Reactions Mediated by Single-File Diffusion in Linear Nanopores: Hydrodynamic vs stochastic Behavior*, *J. Chem. Phys.*, 134, 114107 (2011).
37. O. Pestovsky, S. Veysey, A. Bakac, *Kinetics and Mechanism of Hydrogen Atom Abstraction from Rhodium Hydrides by Alkyl Radicals in Aqueous Solutions*, *Chem. Eur. J.* 17, 4518-4522 (2011).
38. T. -W. Kim, I. I. Slowing, P. -W. Chung, V. S. -Y. Lin, *Ordered Mesoporous Polymer-Silica Hybrid Nanoparticles as Vehicles for the Intracellular Controlled Release of Macromolecules*, *ACS Nano* 5, 360-366 (2011).
39. Y. Huang, X. Shu, V. S. -Y. Lin, *Bifunctionalized Mesoporous Materials with Site-Separated Brønsted Acids and Bases: Catalyst for a Two-Step Reaction Sequence*, *Angew. Chem. Int. Ed.* 50, 661–664 (2011).
40. Y. Huang, X. Shu, V. S. -Y. Lin, *New Strategy for Enantioselective Heterogeneous Catalysis: Immobilization of both Metal Nanoparticles and Chiral Modifiers in Mesoporous Silica Nanoparticles*, *ChemCatChem.* 3, 690-694 (2011).

41. Y. Huang, X. Shu, V. S. -Y. Lin, *Changing from Symmetric to Asymmetric Simply by Immobilizing the Catalyst on Mesoporous Silica Nanoparticle*, ChemCatChem 3, 131-134 (2011).
42. S. R. Neal, A. Ellern, A. D. Sadow, *Optically Active, Bulky Tris(oxazolanyl)borato Magnesium and Calcium Compounds for Asymmetric Hydroamination/cyclization*, J. Organomet. Chem. 696, 228-234 (2011).
43. D. Mukherjee, R. Thompson, A. Ellern, A. D. Sadow, *A Coordinatively Saturated Tris(oxazolanyl)borato Zinc Hydride-Catalyzed Cross Dehydrocoupling of Silanes and Alcohols*, ACS Catal. 1, 698-702 (2011).
44. C. -H. Tsai, H. -T. Chen, S. M. Althaus, K. Mao, T. Kobayashi, M. Pruski, V. S. -Y. Lin, *Rational Catalyst Design: A Multifunctional Mesoporous Silica Catalyst for Shifting the Equilibrium Reaction by Removal of Byproduct*, ACS Catal. 1, 729-732 (2011).
45. K. Manna, S. Xu, A. D. Sadow, *A Highly Enantioselective Zirconium Catalyst for Intramolecular Alkene Hydroamination: Activity Below Room Temperature and a New Mechanism*, Angew. Chem. Int. Ed. 50, 1865-1868 (2011).
46. H. -A. Ho, T. S. Gray, B. Baird, A. Ellern, A. D. Sadow, *Allylic C-H Bond Activation and Functionalization Mediated by Tris(oxazolanyl)borato Rhodium(I) and Iridium(I) Compounds*, Dalton Trans., 40, 6500-6514 (2011).

## Controlling Structural, Electronic, and Energy Flow Dynamics of Catalytic Processes through Tailored Nanostructures

**Additional PIs:** Tony F. Heinz (Columbia U.), Ludwig Bartels (UC Riverside), Donna Chen (U. South Carolina)

**Post-docs:** Salai Ammal (USC), Zhihai Cheng (UCR), Vasse Chis (UCF), Daejin Eom (Columbia), Wei He (USC), Sampyo Hong (UCF), Limin Huang (Columbia), Christophe Huchon (UCR), Kedar Manandhar (USC), Marisol Alcantara Ortigoza (UCF), Volodymyr Turkowski (UCF).

**Graduate Students:** Brett Cagg (USC), Zhang Jia (Columbia), D. H. Kim (UCR), Duy Tran Le (UCF), Mara Levine (USC), Miaomiao Luo (UCR), Kin Fai Mak (Columbia), John Mann (UCR), Jay S. Ratliff (USC), Abraham A. Rodriguez (USC), Christopher C. Roberts (USC), Ghazal Shafai (UCF), S. Islamuddin Shah (UCF), Dezheng Sun (UCR), Samuel Tenney (USC), Jon Wyrick (UCR), Hui Zhou (Columbia)

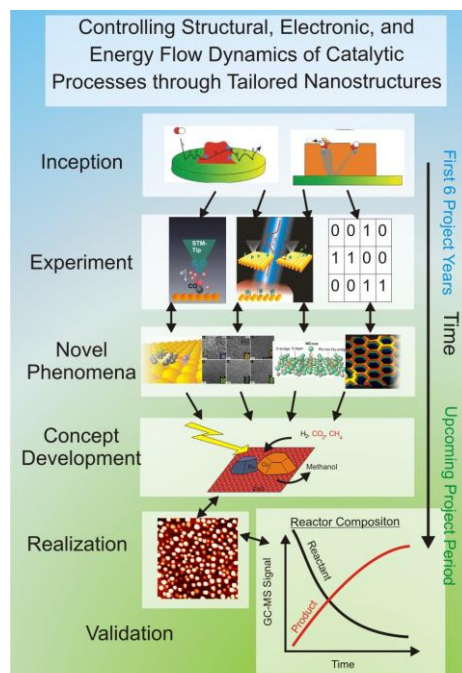
**Undergraduate Students:** Amanda Chee (UCR), Kamelia Cohen (UCR), KatieMarie Magnone (UCR), Connor Holzke (UCR), Daniel Salib (UCR)

**Collaborators:** Radoslav R. Adzic (Brookhaven), Louis E. Brus (Columbia University), Gerhard Ertl (Fritz-Haber Inst., Berlin), George W. Flynn (Columbia University), Irving Herman (Columbia University), Andreas Heyden (USC), Jim Hone (Columbia University), Mark Hybertsen (Brookhaven), Karl Jakobi (Fritz-Haber Inst., Berlin), Maki Kawai (Riken), Yousoo Kim (Riken), John R. Monnier (USC), David R. Mullins (Oak Ridge National Laboratory), Christopher Murray (U. Penn), Gertrude Neumark (Columbia University), Colin Nuckolls (Columbia University), Matthew Sfeir (Brookhaven), Nicholas Turro (Columbia University), Feng Wang (UC Berkeley), Yumei Zhu (Brookhaven)

**Contact:** Talat S. Rahman, Dept. of Physics, University of Central Florida, Orlando, FL 32816; tel: 407-823 1480; email: [trahman@mail.ucf.edu](mailto:trahman@mail.ucf.edu)  
 Tony F. Heinz, Dept. of Physics, Columbia University, New York, NY, 10027; tel: 212-854-6564 email: [tony.heinz@columbia.edu](mailto:tony.heinz@columbia.edu)  
 Ludwig Bartels, Dept. of Chemistry, U. of California, Riverside, CA 92506; tel: 951-827-2041; email: [ludwig.bartels@ucr.edu](mailto:ludwig.bartels@ucr.edu)  
 Donna Chen, Dept. of Chemistry, U. of South Carolina, Columbia, SC 29208, tel: 803-777-1050; email: [chen@chem.sc.edu](mailto:chen@chem.sc.edu)

### Goal

*Throughout this project we focus on the idea that controlling the dynamics of a catalytic system in a pre-determined fashion may hold the key to fundamental improvements in the efficiency of catalytic reactions.* In this context, we consider both the dynamics of reactants, as they undergo chemical transformation at the active sites of a heterogeneous catalyst and highlight the importance of the dynamics of the catalyst, i.e. its constant structural (e.g., morphology, density and nature of surface defect sites) and chemical (e.g., oxidation state of surface atoms, variation in the composition of the surface layer) reorganization during the course of catalyzing a chemical process in a reactive environment. In addition, we pursue the idea that control of the flow of energy, typically in the form of electronic excitations, will emerge as an important concept, in particular with regards to photo-activation of catalytic reactions, as set forth in the DOE *Catalysis for Energy* report. In this regard we develop methods for the catalytic growth of MoS<sub>2</sub> monolayers as photon-harvesting components. Over the course of the past two years, our project has made significant progress in *understanding reactant transport at surfaces* through application of novel theoretical methods and through experiments that offer precise





imaging or spectroscopic resolution of reactant dynamics. We have obtained both experimental and theoretical data on the *rearrangement of the catalyst during reaction* and how such processes are affected by the presence of reactants. Originally working predominantly on metal substrates, we have devised methods for *simulating complex catalyst while maintaining the atomic scale focus* that is fundamental to our approach. We have *developed theoretical methods to investigate reaction prefactors, reaction rates and dispersive, non-local interaction*. In the choice of the catalytic reactions we *continue juxtaposing conventional heterogeneous catalytic processes with emerging ones*, for instance addressing on the one hand side CO and methanol oxidation at bimetallic particles on chalcogenide (including oxide) support, and on the other hand the synthesis of MoS<sub>2</sub> and graphene on copper.

## DOE Interest

The DOE “New Science for a Secure and Sustainable Energy Future” outlines in its synopsis that “the U.S. will have to create fundamentally new technologies with performance levels far beyond what is now possible” and that “development of these advances will require scientific breakthroughs that come only with fundamental understanding of new materials and chemical processes”. This is exactly the focus of this research project, in which we develop new approaches to the optimization of catalytic reactions by means of gaining understanding of the underlying processes. Led by a theorist and combining the expertise of scientists with backgrounds a) in the microelectronics fabrication/control of charge and excitation energy in engineered process b) in imaging at the atomic scale and control of processes at the single molecule level and c) in the synthesis of chemically structured nanoparticles and layers and analysis of their catalytic activity, this project combines the outside stimulus and internal focus necessary for the invention of the “fundamentally new technologies” based on “fundamental understanding” of the dynamics processes at surfaces whose combination leads to heterogeneous catalysis of energy carriers and optical capture of energy.

## Recent Progress

### \* Preparation and Properties of Atomically Thin Films for Energy and Catalytic Applications

The activity of heterogeneous catalysts is largely a property of their surface, i.e. the portion of the catalyst in direct contact with the reactant. This renders atomically thin materials particularly appealing, as all their atoms are part of the surface preventing material from being ‘dormant’ in the bulk. Such high-surface-area materials are generally far from the thermodynamically most stable form of their constituents and require careful and *catalytic* control during their fabrication, highlighting the dual role catalysis plays in our research project: once as the ultimate goal of application of the materials employed and once as a means to their fabrication. The particular focus of this project on atomic scale visualization of structural and energy flow dynamics is particularly well suited for elucidation of the latter. In the current project period, we focused on the catalytic formation and energy flow properties of MoS<sub>2</sub> and graphene monolayers.

#### a) Molybdenum Disulfide (MoS<sub>2</sub>)

Although sulfur poisoning is a common phenomenon in heterogeneous catalysis, there are also a variety of sulfur based catalytic systems, in which sulfur is an essential part of the system. In this project we work towards understanding the dynamics of the sulfur atoms under elevated temperatures and to which extent sulfur atoms migrate between metallic islands and an underlying sulfide substrate. To this end we have established parameters for the formation of a sulfur terminated copper substrate by means of exposure to an organic thiol like benzene thiol followed by removal of the carbon-based portion of the reactant through annealing. Depending on the experimental conditions, experiments at UCR find a variety of CuS<sub>x</sub> adlayers, whose structure we are currently exploring theoretically at UCF.

These CuS<sub>x</sub> coverages have in turn been used for the controlled and epitaxial growth of MoS<sub>2</sub> films through deposition of molybdenum. In this approach the copper substrate is used as a sulfur source whose loading can be adjusted at will. Atomically perfect MoS<sub>2</sub> islands/flakes

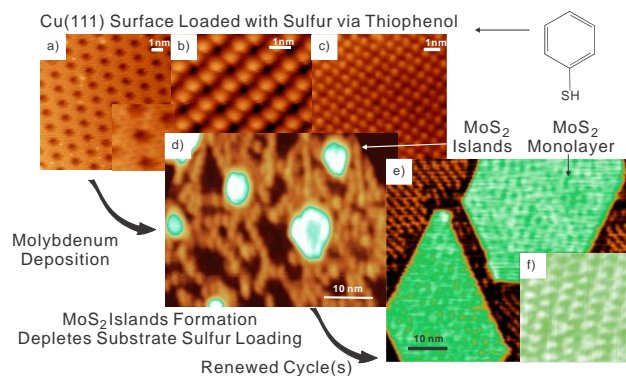


**Figure 1.** Preparation of MoS<sub>2</sub> monolayer islands (panel d) and larger flakes (panel e) on a Cu(111) surface through initial loading of the substrate with sulfur (panels a-c) via thiophenol (top right) exposure. The resultant MoS<sub>2</sub> monolayer is highly ordered and oriented in the same crystallographic direction across all islands on the surface.

have been produced from the range of a few nanometers to several tenths of nanometers in size.

Molybdenum disulfide occurs naturally as molybdenite and is a stable layered metal dichalcogenides. It is built up from layers consisting of an atomic planes of Mo sandwiched between two atomic planes of S in a trigonal prismatic arrangement. The material has attracted interest for diverse applications. In addition to its role as a catalyst in dehydrosulfurization, the layered structure of MoS<sub>2</sub> allows its use as a dry lubricant. The material has also been investigated for photovoltaic power generation and photo-electrochemical hydrogen production. A recent study demonstrated that nanoclusters of MoS<sub>2</sub> can significantly enhance photocatalytic hydrogen production when it is mixed with CdSe. Also, because of its capability to form intercalation compounds, MoS<sub>2</sub> is an ingredient of some Li ion batteries.

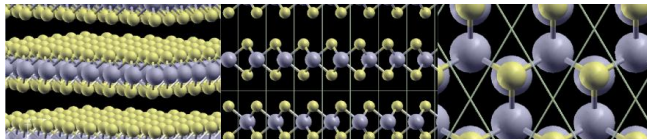
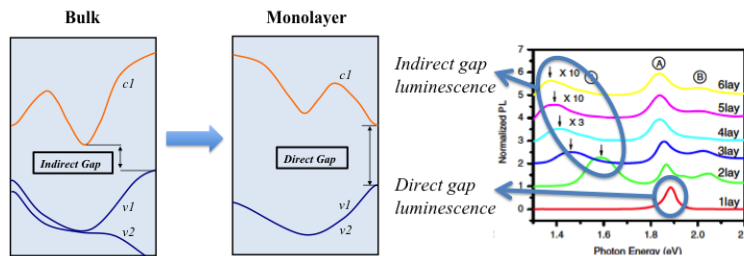


Figure 2. The structure of MoS<sub>2</sub>.

We investigated the properties of mechanical exfoliation MoS<sub>2</sub> films of with thicknesses of  $N = 1, 2, 3, \dots, 6$  layers of the basic MoS<sub>2</sub> building block. These films were found to have significantly different properties from the bulk material. In particular, in the bulk, MoS<sub>2</sub> is an indirect gap semiconductor with a gap of 1.2 eV. We have shown that as the thickness decreases towards a single monolayer, the indirect-gap energy increases sharply. At the monolayer limit, the indirect gap energy exceeds that of the direct gap energy and a new direct-gap material is produced. This is an important result for many applications, including, notably for photocatalysis where the higher band gap is expect to significantly increase the efficiency of photo-driven surface reactions. Strikingly, an enhancement of the luminescence quantum yield by more than a factor of 1000 is observed in the monolayer limit compared with the bulk material.



**Figure 3.** Summary of the indirect-to-direct band gap crossover in atomically thin MoS<sub>2</sub>. The crossover is accompanied by significant enhancement in photoluminescence quantum yield, up-shift of the indirect gaps and differences in absorption rate.

We studied the vibrational spectrum of bulk MoS<sub>2</sub> by means of DFT calculations. Our results show that semilocal DFT pseudopotentials can describe very well the intralayer interactions between molybdenum and sulfur since the DFT-GGA lattice parameter (3.192 Å) is in very good agreement with the experimental value. MoS<sub>2</sub> has 6 pairs of *almost* degenerate modes and 3 quasi-acoustical modes corresponding to the vibrations of the layers as rigid objects, plus the three acoustical modes that account for the translational invariance of the system. In our calculations, for which MoS<sub>2</sub> layers are under-bound, the degeneracy is broken by no more than 1 cm<sup>-1</sup> and each mode is consistently associated with whether the 4.6Å nearest interlayer S-S bond is stretched or not. The mode predicted by Raman scattering at 519 cm<sup>-1</sup> does not exist in our calculation. However, we find two almost degenerate modes at 283 cm<sup>-1</sup> that have the expected symmetry and polarization. In these mode, every other molecular unit stays static and every other performs an out-of-phase expansion/contraction of each Mo-S bond. Our calculated frequency, incidentally, matches that obtained by NIS measurements.

## b) Graphene

Complementary investigations were carried out to examine the nature of graphene growth on copper surfaces. The present studies, carried out in collaboration with the Pasupathy group and other colleagues at Columbia, investigated the role of the crystallographic face of the copper surface and of atomic registry for the synthesis of high-quality graphene monolayer films. The growth is not epitaxial in character on Cu(111). Although the graphene films were able to grow over steps, such structural features in the Cu substrate often coincided with extended defects in the graphene monolayers. Growth on the Cu(100) facet (not shown) was of substantially lower quality, with smaller grain size and higher defect densities. We also examined the nature of incorporation of impurity atoms in the graphene lattice for chemical doping. Nitrogen doping was achieved by adding as a precursor a small concentration of ammonia during the catalytic growth of the film. In particular, films were grown using a mixture of

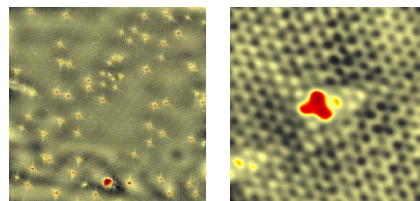


**Figure 5.** Structure of graphene monolayers with substitutional N impurities. The left panel shows a large area STM image with many individual impurities. The right panel zooms-in on a single impurity.

CH<sub>4</sub>, H<sub>2</sub> and NH<sub>3</sub> at a total pressure of 1.9 torr and a temperature of 1000 °C with a polycrystalline Cu film as the catalytic surface. The resulting graphene layers were analyzed using STM, but complemented by XPS measurements and Raman spectroscopy. From the combination of the various experimental techniques and theoretical support, we conclude that individual N atoms are incorporated substitutionally into the graphene lattice. The amount of delocalized charge injected into the graphene film and the degree of localization of the remaining charge could be determined quantitatively by analysis of the STM tunneling spectra in different spatial regimes.

### \* *The Impact of the Reactant on the Catalyst*

Metal nanoparticles are the crucial active component of heterogeneous catalysts for a wide spectrum of applications. Although their surface to volume ratio is not quite as extreme as in monolayer materials, mandated by the metallic nature of the interatomic interaction, we find that they are still very much affected by catalytic processes occurring at their surface. In this project we focus on the structural dynamic of metal nanoparticles during support of catalytic model reactions, in particular on Ni/Au, Pt/Au and Co/Au bimetallic clusters on TiO<sub>2</sub>, and investigated encapsulation by the substrate and alloying/dealloying processes.

Pt nanoparticles are known to be encapsulated by a Ti<sup>+3</sup> containing reduced titania film when heated on TiO<sub>2</sub>(110), whereas Au nanoparticles remain bare. On a support with 2 ML Pt + 2 ML Au we find the contribution of Ti<sup>+3</sup> is 3% at room temperature, but after heating to 800 K, there is little change in the spectrum, with the Ti<sup>+3</sup> accounting for 6% of the total Ti signal. Since it has been well established that the reduction of titania occurs on top of the Pt clusters rather than at the interface at the base of the clusters, this result suggests that Pt is completely covered by Au and consequently there is no surface Pt to be encapsulated by reduced titania. If the Au coverage is chosen smaller, at 0.4 ML a regime is accessed, in which the Pt is not completely covered by Au. In this case the titania spectrum at room temperature is identical to that of TiO<sub>2</sub> itself, but the low binding energy shoulder first appears at 500 K and continues to grow upon further heating, as in the case of pure Pt.

STM studies demonstrate that bimetallic clusters can be grown by sequential deposition when the less mobile Pt or Ni atoms are deposited first, followed by the more mobile Au atoms. In the second deposition step almost no new clusters are nucleated on the surface and the existing clusters increase in size with increasing Au deposition; this implies that the incoming Au atoms are incorporated into the existing Ni/Pt clusters to make bimetallic clusters.

The surface compositions of such clusters have been studied by low energy ion scattering (LEIS) experiments, which probe only the first monolayer of surface. Bulk thermodynamics predicts that the surface of the clusters should be pure Au because the surface free energy of Au is lower than that of Ni or Pt, and neither Ni nor Pt are miscible with Au in the bulk. This is confirmed experimentally. However, when the surface activity of the clusters is probed by the adsorption and desorption of CO we find evidence that the presence of the CO molecules induce diffusion of Ni or Pt to the cluster surface. This process is thermodynamically driven by the formation of strong Ni-CO or Pt-CO bonds. Moreover, the desorption profiles for the CO are characteristic of binding at Ni/Pt sites. DFT calculations on supported Ni<sub>1</sub>Au<sub>121</sub> clusters indicate that the Ni atoms prefer to reside in the second layer from the surface initially, but exposure to CO results in the formation of the strong Ni-CO bond with Ni at the surface. *Ab initio* molecular dynamics simulations indicate that for small unsupported Ni<sub>1</sub>Au<sub>12</sub> clusters, Ni will not diffuse to the surface of the clusters even at temperatures as high as 1500 K, but in the presence of CO, diffusion of Ni to the cluster surface occurs readily at room temperature. Similar behavior was observed for CO-induced diffusion of Pt to the surface in Au-Pt clusters. Furthermore, investigations for methanol chemistry on the Au-Ni and Au-Pt clusters demonstrate that methanol exposure at low temperature (100 K) also induces

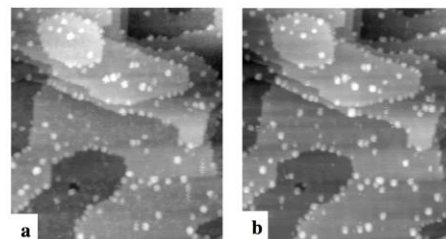


Figure 6. a) 0.02 ML of Ni; followed by b) 0.10 ML Au. All depositions were carried out at room temperature.

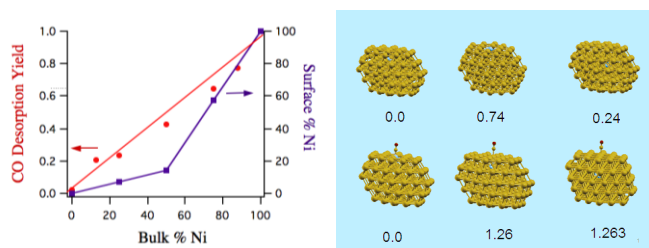


Figure 7 Left: CO desorption yields from TPD experiments on Ni-Au clusters (red) and surface Ni composition as determined from LEIS experiments (purple) as a function of bulk Ni composition. Right: Optimized structures for the unsupported Ni<sub>1</sub>Au<sub>121</sub> clusters with the Ni atom in different layers with and without adsorbed CO molecule. Relative energies (in eV) are given below each cluster.

diffusion of Ni and Pt to the surface of the clusters, resulting in methanol chemistry that is characteristic of reaction on Ni and Pt. These experiments illustrate the dynamic nature of bimetallic surfaces in the presence of adsorbates even at room temperature and very low adsorbate exposures (<1 Langmuir).

### \* Adsorbate Dynamics and Reaction Rates at Surfaces and under Confinement

We explore experimentally and theoretically effects that influence the rate of surface reactions and are a direct consequence of interaction of adsorbates with the substrate, their interaction with one another and their confinement on surface structures (as opposed to idealized extended terraces).

For nanoscale confinement we use a molecular honeycomb network providing pores of 4 nm in diameter, in which we study the dynamics of CO molecules as a function of the pore filling. We find that confinement increases the diffusivity of CO and stabilizes the dispersion of individual vacancies in the film. Through incommensurability between the pore size and CO ( $\sqrt{3}\times\sqrt{3}$ )R30° structure, dislocation lines are forced into the overlayer at complete coverage, much in contrast to the homogeneous coverage of extended terraces. All effects observed lead to higher accessibility of the CO adsorbates and likely to higher potential activity of the film, highlighting that confinement on the nanoscale by itself (as it necessarily occurs on nanoscale catalytic clusters) increases adsorbate reactivity even absent any substrate-induced effects.

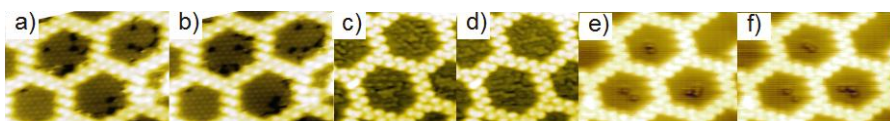
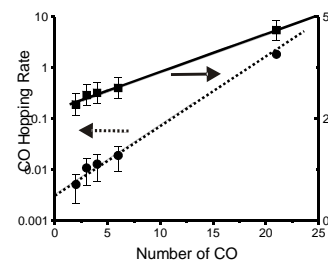


Figure 8. 2 images from STM movies showing the diffusion of a,b) vacancies in a ( $\sqrt{3}\times\sqrt{3}$ )R30° CO coverage in confinement (23 K); c,d) 1/3 filled pores (22 K); e,f) and 2-3 CO molecules per pore (27 K), as well as the coverage dependence of the diffusivity (right).



Quite generally, anharmonic effects (such as electron-hole pair creation and phonon-phonon coupling) can either dissipate or provide the energy to excite the CO modes that are precursors of diffusion. Previous calculations, however, found that electron-hole pair creation and phonon-phonon coupling (only among CO-localized modes) cannot explain the observed differences in the diffusion rate of CO on Ag(110) and Cu(110). In order to determine phonon-phonon coupling, however, the full dispersion of all phonons in the system is required as input information. Our earlier calculations, for example, have shown that, in addition to the hybridization of the frustrated translation mode of CO with the bulk and surface modes, there is a strong hybridization of the frustrated rotation mode of CO with surface modes of Ag(001). This latter mixing is not found in the case of CO on Cu(001). None of these effects have been taken into account in theoretical calculations so far. Using first principles methods, we have calculated the diffusion path and energy barriers of CO on Ag(001) and more importantly extracted the diffusion prefactors  $v_0$ , and diffusion rate.

The free energy (static and vibrational parts) at each CO site (including intermediates) is calculated according to the statistical-mechanical treatment of transition state theory. The *pre-exponential factor* ( $hv_0$ ) that enters in the calculation of the diffusion rate indicates that the diffusion from bridge to top follows from the frustrated-rotation mode. To our knowledge this is the first calculation to show large variations in the prefactor with temperature.

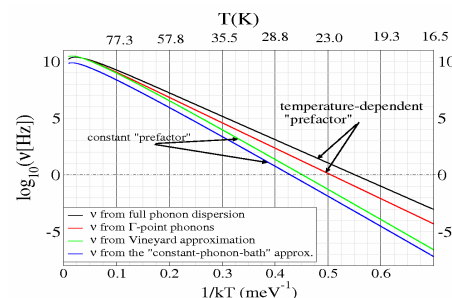


Figure 9. Comparison of diffusion rate of CO on Ag(110) as predicted by different methods.

### Publications (2009-2011)

1. S. Berciaud, S. Ryu, L. Brus, and T. F. Heinz, "Probing the Intrinsic Properties of Exfoliated Graphene: Raman Spectroscopy of Free-Standing Monolayers", **Nano Lett.** **9**, 346 (2009).
2. D. Song, F. Wang, G. Dukovic, M. Zheng, E. D. Semke, L. E. Brus, and T. F. Heinz, "Measurement of the Optical Stark Effect in Semiconducting Carbon Nanotubes", **Appl. Phys. A** **96**, 283 (2009).
3. D. Eom, D. Prezzi, K. T. Rim, H. Zhou, M. Lefenfeld, S. Xiao, C. Nuckolls, M. S. Hybertsen, T. F. Heinz, and G. W. Flynn, "Structure and Electronic Properties of Graphene Nanoislands on Co(0001)", **Nano Lett.** **9**, 2844 (2009).
4. M. Alcántara-Ortigoza, T. S. Rahman, R. Heid, and K. P. Bohnen, "Effect of c(2x2)-CO overlayer on the phonons of

- Cu(001): A first-principles study”, **Phys. Rev. B** **79**, 125432 (2009).
5. D. T. Le, S. Stolbov, and T. S. Rahman, “Reactivity of the Cu<sub>2</sub>O(100) surface: Insight from first principles calculations”, **Surf. Sci.** **603**, 1637 (2009)
  6. Faisal Mehmood, Abdelkader Kara, Talat S. Rahman, Claude R. Henry”, Comparative study of CO adsorption on flat, stepped and kinked Au surfaces using density functional theory”, **Phys. Rev. B** **79**, 075422 (2009)
  7. S. Stolbov, M. Alcántara Ortigoza and T. S. Rahman, “Application of the density functional theory to CO tolerance in fuel cells: a brief review”, **J. Phys. Condens. Matter.** **21**, 474226 (2009).
  8. E.Z. Ciftlikli, L.V. Goncharova, B.J. Hinch, M. Alcántara Ortigoza, S. Hong, and T.S. Rahman, “Vibrational Dynamics of a c(2x2) phase Induced by nitrogen adsorption on Cu(001)”, **Phys. Rev. B** **81**, 115465 (2010).
  9. L. Bartels, “Tailoring Molecular Layers at Metal Surfaces”, **Nature Chem.** **2**, 87 (2010)
  10. Cheng Z., Wyrick J., Luo M., Sun, D., Kim D., Zhu Y., Lu W., Kim K., Einstein T.L., Bartels L., “Adsorbates in a Box: Titration of Substrate Electronic States”, **Phys. Rev. Lett.** **105**, 066104 (2010)
  11. Cheng Z., Luo M., Wyrick J., Sun, D., Kim D., Zhu Y., Lu W., Kim K., Einstein T.L., Bartels L., “Power of Confinement: Adsorbate Dynamics on Nanometer-Scale Exposed Facets”, **Nano Lett.** **10**, 1022018 (2010)
  12. Cheng Z., Chu E., Sun, D., Kim D., Zhu Y., Luo M., Pawin G., Lu W., Wong K.L., Kwon K.Y., Carp R., Marsella M., Bartels L., “Tunability in Polyatomic Molecule Diffusion through Tunneling versus Pacing”, **J. Am. Chem. Soc.** **132**, 13578 (2010)
  13. Sun D., Kim D., Le D., Borck Ø., Berland K., Kim K., Lu W., Zhu Y., Luo M., Wyrick J., Cheng Z., Einstein T.L., Rahman T.S., Hyldgaard P., Bartels L., “Effective elastic properties of a van der Waals molecular monolayer at a metal surface”, **Phys. Rev. B** **82**, 201410(R) (2010)
  14. Tenney S. A., Ratliff J. S., Heyden A., Ammal S. C., Mullins D. R., Roberts C. R., Chen D. A., “Adsorbate-Induced Changes in the Surface Composition of Bimetallic Clusters: Au-Pt on TiO<sub>2</sub>(110)”, **J. Phys. Chem. C** **114**, 21652-21663, (2010).
  15. Lee C., Yan H., Bus L. E., Heinz T. F., Hone J., and Ryu S., “Anomalous Lattice Vibrations of Single- and Few-Layer MoS<sub>2</sub>”, **ACS Nano** **4**, 2695 (2010).
  16. Sfeir M. Y., Misewich J. A., Rosenblatt S., Wu Y., Vosin C., Yan H. G., Berciaud S., Heinz T. F., B. Chandra, R. Caldwell, Y. Y. Shan, J. Hone, G. Flynn, “Infrared Spectra of Individual Semiconducting Single-Walled Carbon Nanotubes: Testing the Scaling of Transition Energies for Large Diameter Nanotubes”, **Phys. Rev. B** **82**, 195424 (2010).
  17. Mak K. F., Lee C., Hone J., Shan J., Heinz T. F., “Atomically Thin MoS<sub>2</sub>: A New Direct-Gap Semiconductor”, **Phys. Rev. Lett.** **105**, 136805 (2010)
  18. Lui C. H., Li Z., Chen Z., Klimov P. V., Brus L. E., Heinz T. F., “Imaging Stacking Order in Few-Layer Graphene”, **Nano Lett.** **11**, 164-169 (2010)
  19. Alcántara Ortigoza M., Rahman T. S., Heid R., Bohnen K. P., “Ab initio Calculations of the Dispersion of Surface Phonons of a c(2x2) CO overlayer on Ag(001)”, **J. Phys.: Condens. Matter** **22** 395001 (2010)
  20. Tenney S. A., Ratliff J. S., He W., Mullins D. R., and Chen D. A., “Characterization of Au-Pt and Au-Ni Clusters on TiO<sub>2</sub>(110)”, **Topics in Catalysis** **54**, 42-55 (2011)
  21. Zhao L., Rim K. T., Zhou H., He R., Heinz T. F., Pinczuk A., Flynn G. W., Pasupathy A. N., “Influence of Copper Crystal Surface on the CVD Growth of Large Area Monolayer Graphene”, **Solid State Commun.** **151**, 509-513 (2011).
  22. Tenney S. A., He W., Roberts C. C., Ratliff J. S., Shah S. I., Shafai G. S., Turkowski V., Rahman T. S., Chen D. A., “CO-induced Diffusion of Ni Atoms to the Surface of Ni-Au Clusters on TiO<sub>2</sub>(110)”, **J. Phys. Chem. C**, **115**, 11112-11123 (2011).
  23. Hong S., Alcántara Ortigoza M., Rahman T. S., Ciftlikli E. Z., Hinch B. J., “Stress balance in nanopatterned N/Cu(001) surfaces”, **Phys. Rev. B**, in press
  24. Wyrick J., Kim D., Sun D., Cheng Z., Lu W., Zhu Y., Berland K., Kim Y.S., Rotenberg E., Luo M., Hyldgaard P., Einstein T. L., Bartels L., “Do 2D ‘Noble Gas Atoms’ Produce Molecular Honeycombs at a Metal Surface?”, **Nano Lett.**, in press
  25. Wong K. L., Cheng Z., Pawin G., Sun D., Kwon K., Kim D., Carp R., Marsella M., Bartels L., “Steric-Blocking as a Tool to Control Molecular Film Geometry at a Metal Surface”, **Langmuir**, in press
  26. Zhao L., He R., Rim K. T., Kim K. S., Zhou H., Gutierrez C., Chockalingam S., Arguello C., Paolova L., Schiros T., Norlund D., Hybertsen M. S., Reichman D. R., Heinz T. F., Kim P., Pinczuk A., Flynn G. W., Pasupathy A. N., “Visualizing Individual Nitrogen Dopants in Monolayer Graphene”, **Science**, in press
  27. Alcántara Ortigoza M., Heid R., Bohnen K. P., Rahman T. S.; “Nature of the Binding of a c(2x2)-CO Overlayer on Ag(001) and Surface Mediated Intermolecular Coupling”, **J. Phys. Chem. A** **115**, 7291-7299 (2011).
  28. S. Hong, G. Shafai, M. Bertino, and T. S. Rahman, “Ligand Spacer Controlled Size Selectivity of Gold Clusters”, **J. Phys. Chem. C** **115**, 14478 (2011).

**Polarization-dependence of palladium deposition on ferroelectric lithium niobate (0001) surfaces**

Additional PIs: N/A

Postdoc: Seungchul Kim

Undergrad student: Michael Rutenberg Schoenberg

Collaborators: John M. Vohs (UPenn)

Contacts: Department of Chemistry, University of Pennsylvania  
231 South 34<sup>th</sup> Street, Philadelphia, PA 19104-6323  
[rappe@sas.upenn.edu](mailto:rappe@sas.upenn.edu)**Goal**

The main objectives of the research program goals of this project are: the study of catalysis on known nonstoichiometric surfaces, the discovery of new nonstoichiometric surfaces guided by understanding how changes in surface composition affect surface reactivity, exploration of the catalytic properties of the newly-discovered surfaces, and the development of new nonstoichiometric oxide surfaces incorporating catalytic and base metal atoms to enhance catalysis. Currently, catalysis on oxide surfaces is not as well understood as catalysis on metal surfaces. This is especially true for the multi-component complex oxides for which the surface often has a different stoichiometry than the bulk. It is therefore of great practical and fundamental interest to determine how unusual surface stoichiometries can be stabilized and used to promote heterogeneous catalysis impossible for the standard stoichiometric surfaces.

**DOE Interest**

The development of a new class of heterogeneous catalyst is of great practical and fundamental interest. The unusual stoichiometry of the surface nanoshells stabilized by the attachment to the bulk of the  $ABO_3$  perovskite oxide has the potential to achieve reactivity unavailable in standard materials. This will allow the creation of inexpensive catalysts without precious metals that will exhibit the same reactivity as the best current precious metal based catalysts. Furthermore, the surface stoichiometry and reactivity are responsive to the changes in reaction conditions and the change of the bulk polarization through an applied mechanical stress or an electric field. This offers a further avenue for increasing catalytic performance for a variety of reaction conditions. Thus, catalytic nonstoichiometric surfaces would bring significant advantages, enhancing reactivity in harsh environments where control of conditions is difficult, making new chemical transformations feasible, and reducing the process requirements for others. Due to the great importance of heterogeneous catalysis in modern industry, their development would be highly beneficial for a wide range of chemical technologies.

**Recent Progress**

We investigate the effect of ferroelectric polarization direction on the geometric properties of Pd deposited on the positive and negative surfaces of  $LiNbO_3$  (0001). We predict preferred geometries and diffusion properties of small Pd clusters using density functional theory, and use these calculations as the basis for kinetic Monte Carlo simulations of Pd deposition on a larger scale. Our results show (see Figure 1) that on the positive surface, Pd atoms favor a clustered configuration, while on the negative surface, Pd atoms are adsorbed in a more dispersed pattern due to suppression of diffusion and

agglomeration. This suggests that the effect of  $\text{LiNbO}_3$  polarization direction on the catalytic activity of Pd [*J. Phys. Chem.* **88**, 1148 (1984)] is due, at least in part, to differences in adsorption geometry. Further investigations using these methods can aid the search for catalysts whose activities switch reversibly with the polarization of their ferroelectric substrates.

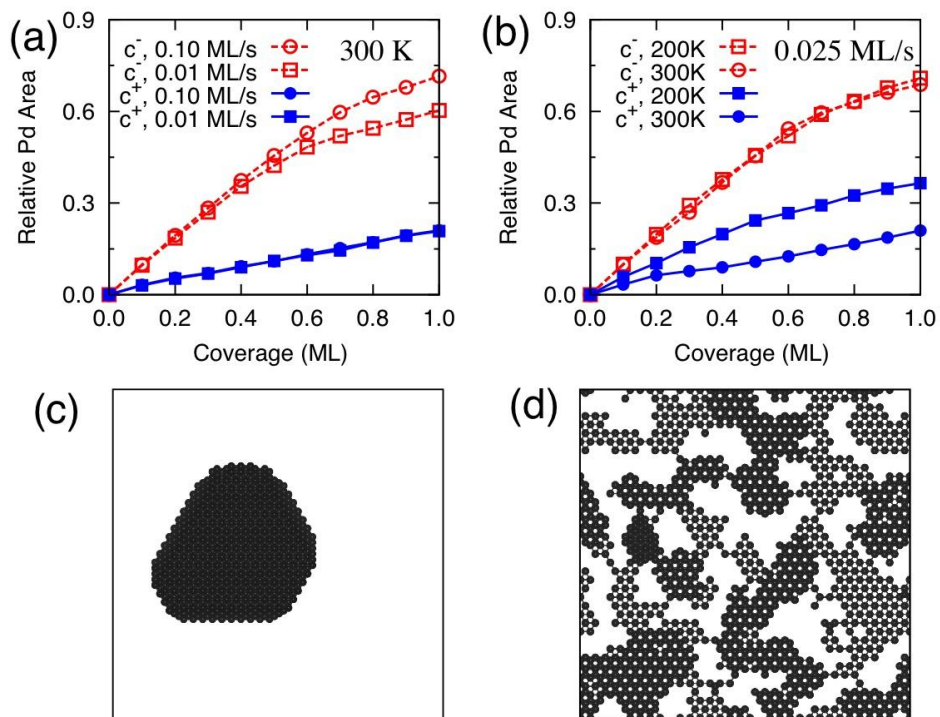


Figure 1: : Proportion of surface area covered by Pd for simulations at a range of (a) deposition rates at 300 K and (b) temperatures with a deposition rate of 0.025 ML/s. KMC snapshots of 1.0 ML on (c) c+ and (d) c- at 300 K with a 0.025 ML/s deposition rate.

### Future plans

Firstly, we plan to investigate the diffusion of oxygen through perovskite oxides, in order to understand oxygen availability for catalyzed redox reactions with different substrate compositions. Secondly, we plan to investigate the surface properties of additional perovskites, including additional *B*-site cations, to broaden the palette of potential nonstoichiometric catalysts. Thirdly, we plan to investigate directly the surface catalytic properties of nonstoichiometric surfaces for redox transformations.

### Publications (2009-2010)

1. R. V. Wang, D. D. Fong, F. Jiang, M. J. Highland, P. H. Fuoss, C. Thompson, A. M. Kolpak, J. A. Eastman, S. K. Streiffer, A. M. Rappe, and G. B. Stephenson, "Reversible chemical switching of a ferroelectric film", *Phys. Rev. Lett.* **102**, 047601 (1-4) (2009).
2. S. E. Mason, E. A. Sokol, V. R. Cooper, and A. M. Rappe, "Spontaneous Formation of Dipolar Metal Nanoclusters", *J. Phys. Chem. A* **113**, 4134-7 (2009).
3. S. Srinivasan, M. W. Lee, M. C. Grady, M. Soroush, and A. M. Rappe, "Computational Study of the Self-Initiation Mechanism in Thermal Polymerization of Methyl Acrylate", *J. Phys. Chem. A* **113**, 10787-94 (2009).

4. T. Qi, S. V. Levchenko, J. W. Bennett, I. Grinberg, and A. M. Rappe, “New Prospects for High Performance SONAR, Chemical Sensor, and Communication Device Materials”, *2009 DoD HPCMP Users Group Conference*, 197-204 (2009).
5. V. R. Aravind, A. N. Morozovska, S. Bhattacharyya, D. Lee, S. Jesse, I. Grinberg, Y. L. Li, S. Choudhury, P. Wu, K. Seal, A. M. Rappe, S. V. Svechnikov, E. A. Eliseev, S. R. Phillpot, L. Q. Chen, V. Gopalan, and S. V. Kalinin, “Correlated polarization switching in the proximity of a 180° domain wall”, *Phys. Rev. B* **82**, 024111 (1-11) (2010).
6. W. A. Al-Saidi and A. M. Rappe, “Density functional study of PbTiO<sub>3</sub> nanocapacitors with Pt and Au electrodes”, *Phys. Rev. B* **82**, 155304 (1-7) (2010).



**Fundamental Studies on the Kinetics of Oxidation Reactions**

Students: Wen-Sheng Lee

Collaborators: W. Nicholas Delgass (Purdue), W. F. Schneider (Notre Dame U.), Jeffrey T. Miller (ANL-APS), Eric Stach (BNL), D. Zemlyanov (Purdue University), A. Jeremy Kropf (ANL)

Contact: Fabio H. Ribeiro, Purdue University, 480 Stadium Mall Drive, West Lafayette, IN 47907-2100, phone: (765) 494-7799, E-mail: fabio@purdue.edu

**Goal**

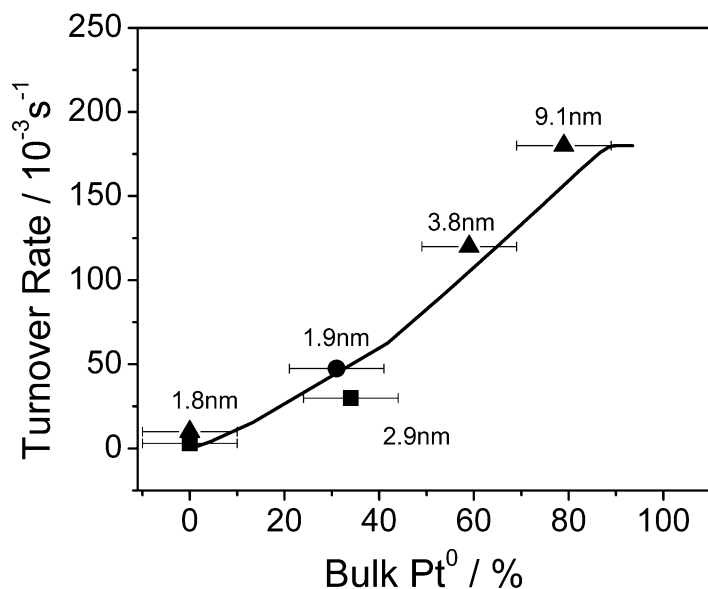
The goal is to develop model catalysts and time-resolved kinetic tools at steady state to study the mechanism of heterogeneous catalytic reactions. We will study oxidation reactions on PdAu alloys and try to control their selectivity. A key descriptor for these reactions is oxygen lability, which is controlled by the oxygen bond energy. Since this energy is a strong function of surface composition, alloying offers an opportunity for fundamental understanding of control of catalytic oxidation on metals. We propose to use PdAu alloys to study the oxidation of methane, NO and propylene.

**DOE Interest**

Development of techniques based on model catalysts and time-resolved kinetic tools at steady state will help to understand the mechanism of heterogeneous catalytic reactions. Model catalysts, due to the control afforded by the precise variation of surface morphology, allow the testing of mechanisms with an unprecedented level of detail. In addition, the collaboration with our colleagues who work on theory is facilitated.

**Recent Progress**

*The rate of Pt-catalyzed NO oxidation is proportional to the amount of surface Pt that is not oxidized:* Kinetic measurements and in situ x-ray adsorption spectroscopy show that the rate of formation of NO<sub>2</sub> from NO and O<sub>2</sub> on a Pt catalyst is the same on Pt(111) and Pt(321) large single crystals and Pt clusters with average diameters 2-9 nm supported on silica, alumina, and carbon, when normalized by the amount of metallic surface Pt. In addition, the apparent reaction orders and activation energies are constant with Pt cluster size, indicating that the active sites are similar. DFT calculations indicate that metallic Pt is active in O coverage windows dictated by the NO<sub>2</sub> to NO ratio but at these same conditions is thermodynamically metastable to surface and bulk oxides. Formation of the oxide is uniformly observed to decrease activity and to be a strong function of particle size and support. The apparent dependence of rates on particle size and support is thus a result of different extents of Pt oxidation rather than intrinsic sensitivity of rate to structure. The activity of Pt catalysts for NO oxidation is a function of their ability to resist transformation into the thermodynamically stable oxide.



Comparison of the “best-fit” particle oxidation model to the turnover rate as a function of total Pt fraction remaining metallic after 20 min exposure to the standard NO oxidation conditions (at 250 °C, with 300 ppm NO, 170 ppm NO<sub>2</sub>, 10% O<sub>2</sub>, He) for Pt/SBA-15 (▲), Pt/C (●), and Pt/Al<sub>2</sub>O<sub>3</sub> (■) catalysts.

*Probing the Gold Active Sites in Au/TS-1 for Gas Phase Epoxidation of Propylene in the Presence of Hydrogen:* While gold particles with sizes in the range 2-5 nm in Au/TiO<sub>2</sub> are assigned as the active sites in propylene oxidation (PO) reaction, previous work suggests that gold clusters smaller than 2 nm are much more active in propylene epoxidation. However, the issue of whether gold clusters inside the TS-1 micropores are active in the PO reaction has not been settled. We addressed this question and attempted to further understand the gold active sites in Au/TS-1.

A TS-1 support coated with an inert layer of S-1 (silicalite-1) was designed and prepared for probing the activity of the gold clusters inside the TS-1 micropores for the PO reaction. This coated material (S-1/TS-1) was characterized via TEM, XRD, XPS, DRUV-vis and nitrogen adsorption analysis at LN<sub>2</sub> temperature to understand the result of the silicalite-1 coating and the corresponding influence on the spatial distribution of the titanium. Au/S-1/TS-1 was then prepared by using optimized deposition-precipitation (DP) conditions. Since neither Au nor Ti alone would give any significant PO activity, any significant PO activity observed from Au/S-1/TS-1 must come from the intimate Au-Ti contact inside the TS-1 core. The experimental results showed that this Au/S-1/TS-1 sample had at least 25 times higher PO production rate (gPO/h/kgCat), compared to that of an Au/S-1 sample. **This is an indication, as well as the first direct experimental evidence, showing that the gold clusters inside the TS-1 are the active ones for the PO reaction.**

### Future Plans

*Catalytic combustion of methane on PdAu:* Studies on PdAu large single crystals and on nanometer sized PdAu clusters supported on TiO<sub>2</sub> and Al<sub>2</sub>O<sub>3</sub>.

*NO oxidation on PdAu:* Test if the addition of Au to Pd make Pd nobler and thus accelerate the rate of NO oxidation.

*Oxidation of propylene to propylene oxide on PdAu*: Confirm the prediction that PdAu clusters supported on titania should be a good catalyst for PO formation.

### **Publications**

1. R. B. Getman, W. F. Schneider, A. D. Smeltz, W. N. Delgass, and F. H. Ribeiro, "Oxygen Coverage Effects on Molecular Dissociations at a Pt Metal Surface" *Physical Review Letters*, **102** (2009) 076101.
2. B. R. Fingland, F. H. Ribeiro, J. T. Miller, "Simultaneous measurement of x-ray absorption spectra and kinetics: a fixed-bed, plug-flow *operando* reactor" *Catalysis Letters*, **131** (2009) 1-6.
3. Worajit Setthapun, W. Damion Williams, Seung Min Kim, Hao Feng, Jeffrey W. Elam, Federico A. Rabuffetti, Kenneth R. Poepelmeier, Peter C. Stair, Eric A. Stach, Fabio H. Ribeiro, Jeffrey T. Miller, and Christopher L. Marshall, "Genesis and evolution of surface species during Pt atomic layer deposition on oxide supports characterized by in-situ XAFS analysis and water-gas shift reaction" *Journal of Physical Chemistry C*, **114** (21), (2010) 9758–9771.
4. Neng Guo, Bradley R. Fingland, W. Damion Williams, Vincent F. Kispersky, Jelena Jelic, W. Nicholas Delgass, Fabio H. Ribeiro, Randall J. Meyer, and Jeffrey T. Miller, "Determination of CO, H<sub>2</sub>O and H<sub>2</sub> Coverage by XANES and EXAFS on Pt and Au During Water Gas Shift Reaction" *Physical Chemistry Chemical Physics*, **12** (2010) 5678 - 5693.
5. Andrew D. Smeltz, W. Nicholas Delgass, and Fabio H. Ribeiro, "Oxidation of NO with O<sub>2</sub> on Pt(111) and Pt(321) large single crystals", *Langmuir*, **26**(21) (2010)16578–16588.
6. Wen-Sheng Lee, Rong Zhang, M. Cem Akatay, Chelsey Baertsch, Eric Stach, Fabio H. Ribeiro and W. Nicholas Delgass, "The Catalytic Sites for CO oxidation and Propylene Epoxidation on Au Nanoparticles are Different" Submitted to *Chemical Communications*, June 2011.

## Water-tolerant Lewis acids for the activation of biomass-derived molecules

Principal Investigator: Yuriy Román

Contact: Massachusetts Institute of Technology, 77 Massachusetts Ave – 66-456, Cambridge, MA 02139, yroman@mit.edu

### Goal

The objective of this project is to understand the activation of carbonyl functional groups using Lewis acids in aqueous media and to devise rational pathways for the synthesis of highly active catalysts featuring isolated Lewis acid sites embedded within crystalline (i.e., zeolites) and amorphous silica matrices.

### DOE Interest

The depolymerization of the constituents of biomass by way of thermochemical or biological routes results in the production of a wide variety of oxygenated intermediates. Although the composition of these intermediates is quite diverse, carbonyl functionalities are prevalent (e.g. aldehydes, ketones, carboxylic acids, etc). In order to transform these functional intermediates into useful chemicals and fuels, robust and active catalysts need to be developed to selectively

activate these molecules. Lewis acids are known to form strong complexes with carbonyl groups. A particular instance involves the complexation of the lone pair of electrons from the oxygen to the Lewis acid, effectively polarizing the carbonyl carbon atom, thereby making it prone to nucleophilic attack. Unfortunately, biomass-derived molecules are commonly found in aqueous solutions and, in most cases, Lewis acidity is suppressed in the presence of water, since the hydroxyl group of water also forms strong complexes with Lewis acid sites. The incorporation of metal centers (e.g. tin, titanium, and zirconium) into the framework of pure silica zeolites results in materials that maintain Lewis acidity in purely aqueous environments. Controlling pore topology, hydrophobicity, and the type and arrangement of Lewis acidic metal centers in the framework will open a host of new transformations of biomass-derived oxygenates, particularly, in the critical areas of selective oxidation, hydrogen-transfer, and C-C bond forming reactions.

### Recent Progress

The isomerization of glucose into fructose using Sn-Beta zeolites has been recently demonstrated to follow a Lewis-acid-mediated intramolecular hydride shift mechanism. Experimental evidence suggests that the carbonyl and hydroxyl moieties in glucose attach to the tin metal center in Sn-Beta forming a six-membered transition state intermediate. We are currently exploring novel methods to exploit the

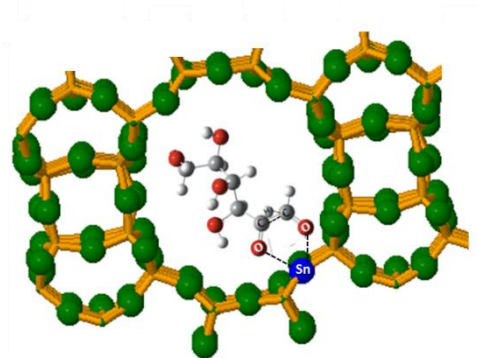


Figure 1. Solid Lewis acid activating a carbohydrate molecule

remarkable activity of these materials in water, while aiming to enhance the reactivity of Sn-, Zr-, Ta-, and Nb-based zeolites. A strong emphasis is placed on investigating C-C bond forming reactions including condensations and 4+2 cycloadditions.

### **Future Work**

Some of the most extraordinary rate enhancements in Lewis acid chemistry arise from the synergistic effect of multiple sites working cooperatively, including Lewis acid-Lewis acid, Lewis acid-Brønsted acid, and Lewis acid-Lewis base interactions. Future work is geared at understanding the effect of reactivity enhancement by dual-site Lewis acid activation. Briefly, polysilsesquioxane moieties will be investigated as sources of isolated Lewis acid centers with pre-determined distances between metal centers that are easy to manipulate and that can be incorporated into silica matrices.

### **Recent relevant publications**

- (1) Román-Leshkov, Y.; Moliner, M.; Labinger, J. A.; Davis, M. E. *Angew. Chem. Int. Ed.* 2010, 49, 8954.
- (2) Moliner, M.; Román-Leshkov, Y.; Davis, M. E. *Proc. Nat. Acad. Sci.* 2010, 107, 6164.

## Atomic Resolution Imaging and Quantification of Chemical Functionality of Surfaces

Additional PIs: Eric I. Altman  
Postdocs: Harry Mönig (50 %), Ozhan Unverdi (35 %)  
Students: Mehmet Baykara (80 %)  
Collaborators: Todd Schwendemann, Yale University; Ruben Perez, Universidad Autonoma de Madrid, Spain (unfunded collaborators)  
Contact: Department of Mechanical Engineering & Materials Science, Yale University, PO Box 208284, New Haven, CT 06520-8284; Phone (203) 432-7525; E-mail: udo.schwarz@yale.edu

### Goal

The work carried out in this project comprises an atomic-scale study of the local chemical interactions that govern the catalytic properties of model catalysts that are of interest to DoE. This goal will be achieved through three-dimensional atomic force microscopy (3D-AFM), a new measurement mode that allows the mapping of the complete surface force and energy fields with picometer resolution in space ( $x$ ,  $y$ , and  $z$ ) and piconewton/millielectronvolts in force/energy. In combination with chemically well-defined tips, chemical interactions can be precisely quantified and assigned to exact positions within the lattice. To further improve on imaging robustness, we are also pursuing several routes for instrumental and methodological upgrades.

### DOE Interest

Widely used in industrial processes such as catalytic cracking, silica and silicates are among the most important catalytic model systems.  $\text{TiO}_2$ , on the other hand, represents the most widely studied photocatalyst with a potential for fuel production. Full understanding of chemical reactions at these and other surfaces requires the availability of a tool that allows not only the *identification* of the chemical nature of specific atoms at surfaces, but also the precise *quantification* of the interaction strengths of these surface atoms with adsorbed atoms and molecules. With our approach, which ultimately delivers complete 3D force maps of a surface with atomic resolution, we aim to achieve substantial progress in this direction.

### Recent Progress

Surface catalytic reactions are inherently determined by the site-specific interactions between the reactive molecules and the catalytically active surface triggering the desired process. Full knowledge of the reaction specifics requires, therefore, not only atomic-scale structural information, but also a quantitative, site-specific elaboration of the surface force and energy fields. Until now, such information has only been theoretically accessible, and is thus subject to computational limitations. It is, however, possible to obtain such information by using a new experimental approach called three-dimensional atomic force microscopy (3D-AFM; see Ref. 1). Within the framework of a previous DoE-supported study, we were able to successfully quantify the interactions between a sample surface and a probe tip with piconewton (force) and

millielectronvolt (energy) resolution while maintaining picometer accuracy in the  $x$ ,  $y$ , and  $z$  position of the tip (see Ref. 4).

The objective of our recent work reported here has been to capitalize on this previous success by focusing first on the oxygen on the copper (100)  $\text{Cu}_3\text{O}_2$  surface phase [a  $(2\sqrt{2}\times\sqrt{2})R45^\circ$  missing row reconstruction] and rutile  $\text{TiO}_2$  as model surface oxide systems to perform 3D-AFM/STM on. The  $\text{Cu}_3\text{O}_2$  surface phase was chosen as model system because it consists of multiple chemical species and includes several defects and domain boundaries so that 3D-AFM/STM can be employed to quantify the chemical reactivity of individual surface atoms as well as to perform local chemical identification through comparison of multiple data channels.

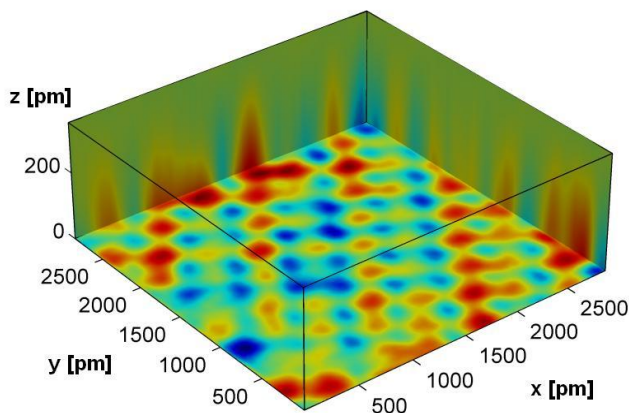


**Fig. 1.** Three-dimensional, atomically resolved interaction force field on the surface oxide layer of Cu(100). Interaction differences on individual oxygen atoms (force maxima) are detected that are caused by stress fields caused by filled-row copper defects (see Fig. 2b).

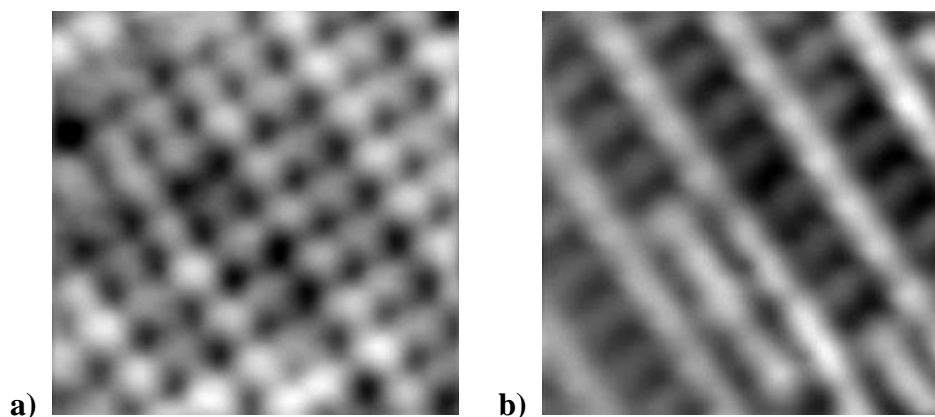


**Fig. 2.** Maps of the tip-sample interaction force (a) and tunneling current (b). Due to the different physical nature of the interactions that give rise to the contrast modes exploited, the two data channels provide complementary information: Oxide atoms are imaged in force, while the current is sensitive to the position of the four-fold coordinated copper atoms. This ultimately enables chemically sensitive imaging. Note that in particular, the current image reveals filled-row copper defects invisible in the force channel.

We imaged the  $\text{Cu}_3\text{O}_2$  surface applying 3D-AFM with simultaneous recording of the tunneling current. Figure 1 shows three a full three-dimensional map of interaction forces on the surface oxide layer of Cu(100) with pm and pN resolution. It can be observed that significant differences

in interaction force exist on top of force maxima, which are assigned to oxygen atoms of the reconstructed surface due to the alternating rectangular symmetry exhibited. The reason for this significant variation in interaction forces on individual oxygen atoms becomes apparent when the contrast in the force channel is compared with the simultaneously recorded tunneling current data for constant heights above the surface as shown in Fig. 2. The contrast in the current channel, which essentially consists of a missing-row type of structure with bright rows and faint stripes in-between, is very different from the oxygen atom based contrast observed in the force channel. Moreover, several defects in the form of *nonmissing rows* are detected in the current channel, which are not recognizable from the force images alone. Carrying over the assignment of oxygen atoms to the current channel, one can determine that the bright spots in the current channel correspond to Cu atoms in the filled rows of the oxygen reconstructed surface and that the *nonmissing rows* are indeed rows of Cu atoms that have not been removed from the surface during reconstruction. The differences in interaction force on individual O atoms can be attributed to the existence of these *nonmissing row* defects and the stress fields associated with them, thus proving that atom-specific interaction quantification at defects is possible.

### Future Plans

An immediate objective of our future work would be to finalize the analysis and interpretation of our 3D-AFM/STM data sets in collaboration with our Spanish theory partner (Prof. Ruben Perez from the Universidad Autonoma de Madrid). Furthermore, we have recently started applying our improved 3D-AFM/STM technique to the study of the rutile (110) surface, a model oxide system of major catalytic relevance, for which we will also present preliminary results that include interaction quantification at defects. Future research efforts will include 3D force and tunneling current spectroscopy of organic molecules adsorbed on rutile (110) as well as efforts to chemically sensitize tips for chemically selective imaging.

### Recent Publications (2009-2011)

1. M. Z. Baykara, T. C. Schwendemann, E. I. Altman, and U. D. Schwarz. *Three-dimensional atomic force microscopy – Taking surface imaging to the next level*. *Advanced Materials* **22**, 2838 (2010).
2. E. I. Altman and U. D. Schwarz. *Mechanisms, kinetics, and dynamics of oxidation and reactions on oxide surfaces investigated by scanning probe microscopy*. *Advanced Materials* **22**, 2854 (2010).
3. A. Schirmeisen, H. Hölscher, and U. D. Schwarz. *Force field spectroscopy in three dimensions*. In: *Non-contact Atomic Force Microscopy*, 2<sup>nd</sup> edition, Eds. S. Morita, R. Wiesendanger, F. Giessibl, Springer-Verlag, Heidelberg, Germany (2009)
4. B. J. Albers, T. C. Schwendemann, M. Z. Baykara, N. Pilet, M. Liebmann, E. I. Altman, and U. D. Schwarz. *Three-dimensional probing of short-ranged chemical forces with picometer resolution*. *Nature Nanotechnology* **4**, 307 (2009).
5. B. J. Albers, T. C. Schwendemann, M. Z. Baykara, N. Pilet, M. Liebmann, E. I. Altman, and U. D. Schwarz. *Data acquisition and analysis procedures for high-resolution atomic force microscopy in three dimensions*. *Nanotechnology* **20**, 264002 (2009).
6. C. A. F. Vaz, H.-Q. Wang, C. H. Ahn, V. E. Henrich, M. Z. Baykara, T. C. Schwendemann, N. Pilet, B. J. Albers, U. D. Schwarz, L. H. Zhang, Y. Zhu, J. Wang, and E. I. Altman. *Interface and electronic characterization of thin epitaxial  $Co_3O_4$  films*. *Surface Science* **603**, 291-297 (2009).



**CATALYSIS SCIENCE INITIATIVE:**  
**Hierarchical Design of Heterogeneous Catalysts for Hydrocarbon Transformations**

Additional PIs: Bradley F. Chmelka, Baron Peters  
Postdoctoral fellows: Ryan Nelson, Ming-Yung Lee, Brian Vicente, Haiyan Xia\*  
Graduate students: Ramzy Shayib, S. Michael Stewart,\*\* Trenton Tovar,\*\*\* Ming-Feng Hsieh, Anthony Fong, Bryan Goldsmith, Taeho Hwang, Xiaoying Ouyang, Robert Savinelli, Jing Huang\*\*\*\*  
\* Stipend from NNSF-China. \*\* NSF Graduate Fellowship recipient. \*\*\* IGERT Fellowship recipient. \*\*\*\* China Scholarship Council recipient.

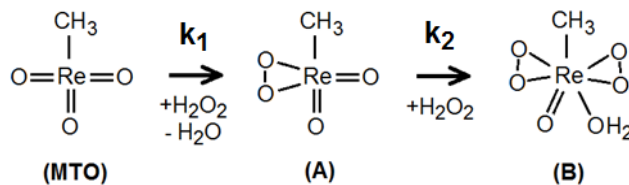
Contact: Department of Chemical Engineering, University of California, Santa Barbara CA 93106-5080; [sscott@engineering.ucsb.edu](mailto:sscott@engineering.ucsb.edu); [bradc@engineering.ucsb.edu](mailto:bradc@engineering.ucsb.edu); [baronp@engineering.ucsb.edu](mailto:baronp@engineering.ucsb.edu)

**Goal:** This project aims to improve heterogeneous catalysts for hydrocarbon transformations such as olefin metathesis and cyclopropanation, giving them higher activities and stabilities and improved functional-group tolerance through rational design. The major challenges are (1) to understand the origins of support-induced activity in dispersed metal oxides; (2) to understand catalyst deactivation at the molecular level; and (3) to modify active site structures to promote activation, improve functional-group tolerance and slow deactivation. The overall goals of this project are to develop a fundamental understanding of active site formation, structure and reactivity, and to use this information to design materials better suited to a wide range of applications. A second overall goal of this project is to enable the design of more robust, low-PGM oxidation catalysts, combining the materials chemistry of crystalline mixed metal oxides with detailed reactivity studies linking structure and function.

**DOE Interest:** The nature of the interaction between the active site and the catalyst support leading to activation of dispersed metal oxides is a perplexing problem in heterogeneous catalysis, because of the difficulty in probing amorphous materials. Support acidity, which varies widely even among similar oxides such as silica, alumina, silica-alumina and aluminosilicates, is likely key to the activation process. A better understanding of the origin and role(s) of Lewis and Brønsted acidity can lead to more effective catalyst supports, and more efficient activation processes.

### Recent Progress

*Modeling the reaction of methyltrioxorhenium (MTO) with H<sub>2</sub>O<sub>2</sub>.* The reactions between MTO and H<sub>2</sub>O<sub>2</sub> provide a good benchmark for computational models involving MTO, because they have been investigated in detail by several groups. H<sub>2</sub>O<sub>2</sub> reacts with MTO in two steps, giving first the monoperoxo intermediate **A**, then the diperoxo product **B**, as shown in Scheme 1. Espenson and coworkers measured forward rates and equilibrium constants for the conversion from MTO to **A** ( $k_1$ ) and for conversion from **A** to **B** ( $k_2$ ) in water and water-CH<sub>3</sub>CN mixtures. They reported only weak solvent and pH effects, although some experiments suggested a significant role for water in the equilibrium constants and in the rate constants  $k_1$  and  $k_2$ .



**Scheme 1:** Products of successive reactions of MTO with  $\text{H}_2\text{O}_2$

Computational chemistry has been used to try to understand the reactions between MTO and hydrogen peroxide. However, published results using a B3LYP density functional and LANL2 basis set deviated markedly from experiment: the calculated activation enthalpies were in excess of 25 kcal/mol for both steps, in contrast to much smaller experimental values (between 5 and 7 kcal/mol for the first step). Furthermore, the overall reaction enthalpy was predicted to be uphill, yet the net enthalpy must be significantly downhill to overcome the loss of translational entropy involved in forming **B** by the reaction  $\text{MTO} + 2 \text{H}_2\text{O}_2 \rightarrow \text{B} + \text{H}_2\text{O}$ .

We used density functional theory to investigate the mechanisms of the reactions shown in Scheme 1. All electronic structure calculations were performed using Gaussian 03. An extensive validation of basis sets and functionals revealed that basis sets should be augmented with two reoptimized  $f$ -functions, as first suggested by Pietsch et al., and that the functional mPW1PW91 performs better than B3LYP. We used a def2-TZVP basis augmented with two  $f$  functions and a Stuttgart effective core potential. Transition states were optimized using the eigenvector-following algorithm. Free energies include rotational, translational, vibrational, and zero-point contributions. Single-point conductor-type polarizable continuous medium (CPCM) solvent corrections were used to model the high dielectric aqueous and acetonitrile solvents. Rates were computed using transition state theory and a tunneling correction [ $\Gamma = (\beta\hbar|\omega_{\ddagger}|/2)/\sin[\beta\hbar|\omega_{\ddagger}|/2]$  with  $\beta = 1/k_{\text{B}}T$ ], because all steps involve hydrogen transfer.

We computed free energies for all intermediates and transition states at 300 K and for a standard reference concentration of 1 M. The key finding is the  $\text{H}_2\text{O}$  is directly involved in the transition states. The standard free energies at each stage of the reaction *with water-assisted hydrogen transfer steps* are plotted in Figure 1. All activation barriers are much lower with water assistance than without (not shown). Furthermore, the predicted kinetics, like the experiments, show acceleration with increasing water concentration in the solvent. Consequently, we remeasured the biexponential kinetics of the MTO- $\text{H}_2\text{O}_2$  reaction experimentally. We found a strong water dependence of both apparent second-order rate constants on the concentration of water, as predicted computationally. Apparent activation enthalpy and entropy parameters were extracted from the computed rate constants using an Eyring plot [ $\ln(hk/k_{\text{B}}T)$  vs  $1/k_{\text{B}}T$ ]. The effective experimental activation parameters for the first step are  $\Delta H^{\ddagger} = 5.9$  kcal/mol and  $\Delta S^{\ddagger}/k_{\text{B}} = -25.5$ ; for the second step, they are  $\Delta H^{\ddagger} = 6.9$  kcal/mol and  $\Delta S^{\ddagger}/k_{\text{B}} = -25.7$ . For our water-assisted mechanism, the calculated activation

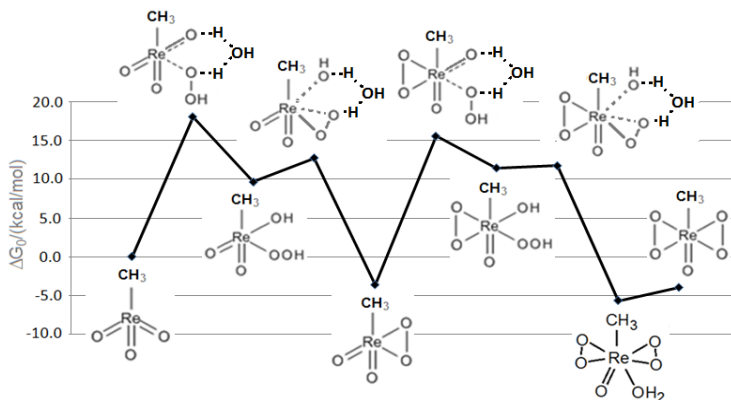


**Figure 1.** Standard free energies (at 300 K and with all species at 1 M concentration) for reaction mechanisms with water assistance.

parameters are in reasonable agreement with experiments:  $\Delta H^\ddagger = 8.3$  kcal/mol and  $\Delta S^\ddagger/k_B = -30.4$  for the first step, and  $\Delta H^\ddagger = 9.0$  kcal/mol,  $\Delta S^\ddagger/k_B = -31.0$  for the second step.

Although our work on the MTO/H<sub>2</sub>O<sub>2</sub> system began as a benchmarking exercise, we anticipate publishing an article about these new mechanistic insights, as an exemplar of the complementarity of theory and experiment in deducing reaction mechanisms.

*Modeling site distributions on amorphous supports.* Our early attempts to model the activation of MTO by solid Lewis acids such as silica-alumina, and its subsequent reactivity, revealed a problem that *always* arises for catalysis on amorphous supports, namely, that different structural models yield different reactivity. We do not know a priori which sites are present or how to build models of sites with desirable catalytic properties.

The solution we have found involves reversing the conventional modeling strategy. Typically, calculations start from crystalline structures (e.g., zeolites, metals, metal oxides) and predict chemical properties from a limited set of structural possibilities. Because amorphous materials present a true distribution of sites, and therefore a distribution of chemical properties, we developed a novel, constrained optimization strategy to identify the lowest energy site with a given Lewis acidity towards a probe base, or with a given activation barrier for a reaction of interest. This will allow us to design simple models of active sites in amorphous materials that have a spectrum of turnover rates, and to thereby understand how different active site characteristics affect different catalytic properties. We expect this approach will impact not only this project, involving amorphous silica-alumina, but also many other applications of amorphous supports in catalysis.

*Coupled Brønsted and Lewis acidities in silica-alumina.* We established that the strengths of Brønsted acid sites in amorphous silica-aluminas depend on the presence of nearby electron-withdrawing Lewis acid sites. A consequence of this coupling of Brønsted and Lewis acidity is that adsorption on one acid site influences the apparent acidity of adjacent sites. To show this, we compared acidity in the presence of different site-selective adsorbed molecules on silica-alumina. For example, selective adsorption of pyridine and 2,6-dimethylpyridine (lutidine) on Lewis and Brønsted acid sites, respectively, establishes coupling of the Brønsted and Lewis acidities, as manifested by 1D- and 2D-NMR and IR spectra, as well as TPD measurements. In particular, 2,6-dimethylpyridine adsorbs strongly and selectively on Brønsted acid sites, but not on Lewis acid sites, for steric reasons. By comparison, pyridine adsorbs on both types of acid sites. Consequently, when Brønsted acid sites are saturated first with adsorbed 2,6-dimethylpyridine, followed by adsorption of pyridine on the remaining Lewis acid sites, the different types of acidity can be distinguished and analyzed quantitatively.

Based on these results, we established that adsorption of pyridine onto the Lewis acidic *cus* Al sites in silica-alumina weakens the Brønsted acidity of nearby silanol protons. This is manifested by diminished intensity of characteristic IR bands at 1630-1645 cm<sup>-1</sup> associated with 2,6-dimethylpyridine in the presence of co-adsorbed pyridine, reflecting reduced lutidine adsorption (**Figure 2a**). The corresponding 2D <sup>29</sup>Si{<sup>1</sup>H} heteronuclear correlation (HETCOR) NMR spectrum shown in **Figure 2b** resolves correlated signals at -103 ppm in the <sup>29</sup>Si dimension and at 2.9 ppm in the <sup>1</sup>H dimension that establish adsorption of 2,6-dimethylpyridine at the Q<sup>3</sup>(0 Al) sites. Comparison of the relative intensities of this correlated 2D signal after heating at 100 or 200 °C (**Figure 2c**) corroborates the weaker adsorption of 2,6-dimethylpyridine on these sites. Such analyses provide comprehensive understanding of the molecular-level origins of surface acidities in porous silica-aluminas, in particular, the mutual proximities of

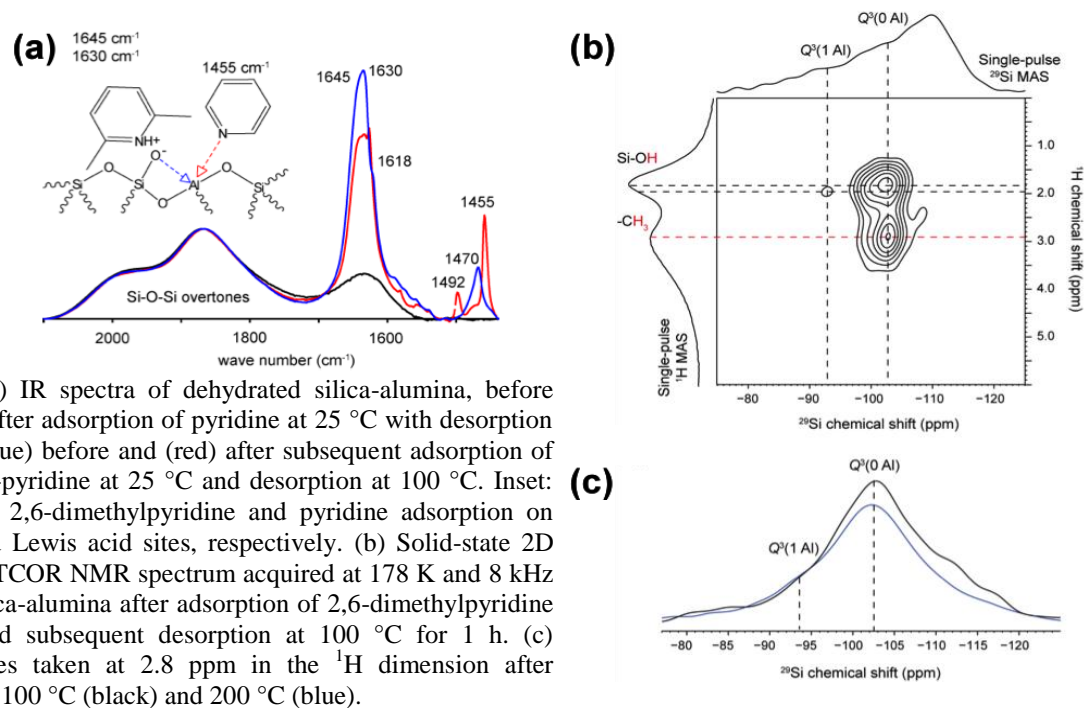
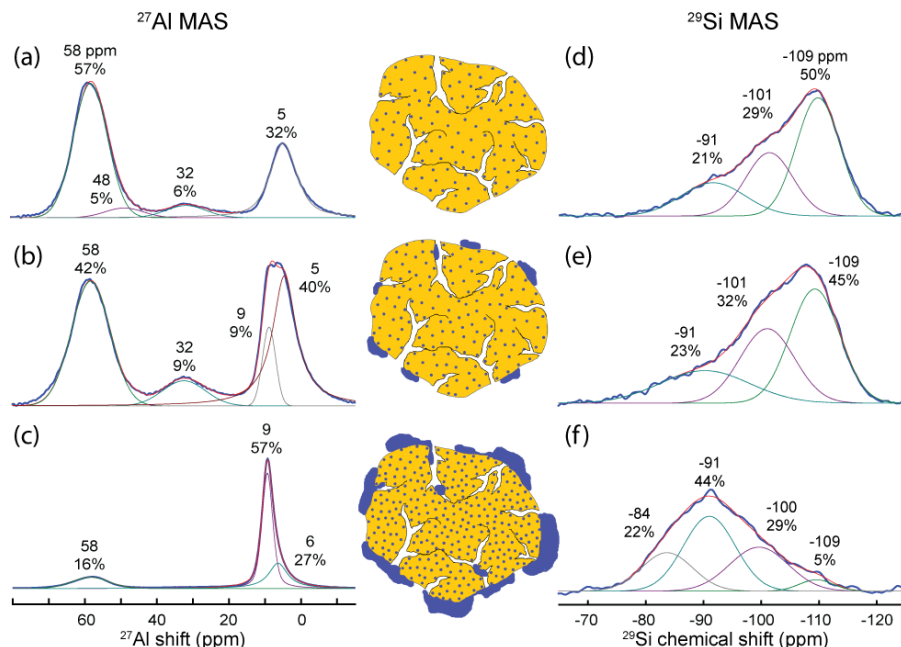


**Figure 2.** (a) IR spectra of dehydrated silica-alumina, before (black) and after adsorption of pyridine at 25 °C with desorption at 100 °C (blue) before and (red) after subsequent adsorption of 2,6-dimethyl-pyridine at 25 °C and desorption at 100 °C. Inset: schematic of 2,6-dimethylpyridine and pyridine adsorption on Brønsted and Lewis acid sites, respectively. (b) Solid-state 2D  $^{29}\text{Si}\{^1\text{H}\}$  HETCOR NMR spectrum acquired at 178 K and 8 kHz MAS for silica-alumina after adsorption of 2,6-dimethylpyridine at 25 °C and subsequent desorption at 100 °C for 1 h. (c) Contour slices taken at 2.8 ppm in the  $^1\text{H}$  dimension after desorption at 100 °C (black) and 200 °C (blue).

Brønsted and Lewis acid sites and their adsorption-dependent influences on one another. These include the relative surface concentrations, strengths, and distributions of Brønsted and Lewis acid sites, as well as their mutual interactions.

The distribution of acidity types and strengths in amorphous silica-alumina depends on the aluminum content, which has been investigated using NMR. In particular, the combination of solid-state  $^{27}\text{Al}$  and  $^{29}\text{Si}$  MAS NMR (**Figure 3**) provides detailed insight regarding the distribution of local aluminum atom environments in amorphous silica-alumina. We have shown these are correlated with bulk aluminum content, steaming treatment, and catalytic activity. For example, single-pulse  $^{27}\text{Al}$  MAS measurements conducted on different silica-aluminas at very high magnetic field (19.6 Tesla, 830 MHz for  $^1\text{H}$  at the National High Magnetic Field Laboratory, Tallahassee, Florida) resolve signals from  $^{27}\text{Al}$  atoms in four-, five-, and six-coordinate environments (58, 32, and 5 ppm, respectively), the relative populations of which are determined quantitatively based on their integrated signal intensities. The  $^{27}\text{Al}$  MAS spectra in **Figure 3a** establish that aluminum atoms are distributed predominantly in the siliceous domains of as-synthesized Davicat 3113 silica-alumina with relatively low aluminum content ( $\text{Si}/\text{Al} = 9$ ). Silica-aluminas with moderate ( $\text{Si}/\text{Al} = 4$ , **Figure 3b**) or high ( $\text{Si}/\text{Al} = 0.5$ , **Figure 3c**) bulk aluminum contents exhibit resolved  $^{27}\text{Al}$  signals associated with both silica-alumina and alumina domains, the latter manifested by a signal associated with  $^{27}\text{Al}_2\text{O}_3$  species at 9 ppm. The fractions of aluminum species in alumina domains correlate directly with bulk aluminum contents of the materials. Such insights are corroborated by complementary single-pulse  $^{29}\text{Si}$  MAS NMR spectra (**Figure 3d,e**) that exhibit quantitatively similar  $^{29}\text{Si}$  signals and population distributions for as-synthesized silica-aluminas with relatively low ( $\text{Si}/\text{Al}=9$ ) and moderate ( $\text{Si}/\text{Al}=4$ ) aluminum contents, despite their different heteroatom loadings. In contrast, silica-alumina with the highest bulk aluminum content ( $\text{Si}/\text{Al}=0.5$ ) yields a single-pulse  $^{29}\text{Si}$  MAS spectrum (**Figure 3f**) that is significantly different from the others, reflecting much higher

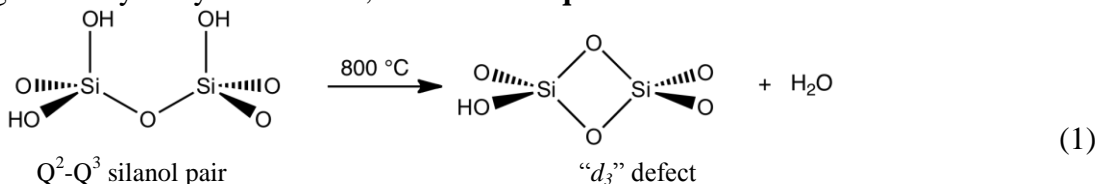
**Figure 3.** Quantitative solid-state (a-c)  $^{27}\text{Al}$  and (d-f)  $^{29}\text{Si}$  MAS NMR spectra acquired at room temperature of *as-synthesized* silica-aluminas with bulk Si/Al ratios of (a,d) 9, (b,e) 4, and (c,f) 0.5. The  $^{27}\text{Al}$  MAS spectra were acquired at 19.6 T and 32 kHz MAS; the  $^{29}\text{Si}$  MAS spectra were acquired at 11.7 T and 10 kHz MAS. Deconvoluted signals, their corresponding shifts, and relative integrated areas are shown for each  $^{27}\text{Al}$  and  $^{29}\text{Si}$  signal. The schematic diagrams depict the different aluminum contents of the respective materials, including distinct alumina-rich domains that appear to be present.



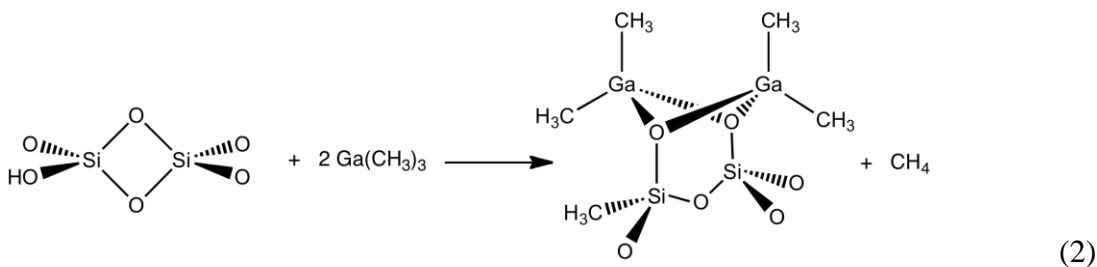
contributions from  $^{29}\text{Si}$  signals at -84 and -91 ppm associated with  $Q^4(4\text{ Al})$  and  $Q^4(3\text{ Al})$  sites that are bonded covalently to multiple Al atoms via bridging oxygen atoms.

*Probing the spatial distribution of grafting sites on oxide surfaces.* Molecules encountering silica interfaces interact primarily with the hydroxyl groups that terminate the bulk structure. When the nominal surface density is very low, these “silanols” are presumed to be isolated. Nevertheless, silicas that are highly dehydroxylated by pretreatment at 800 °C react with  $\text{Ga}(\text{CH}_3)_3$  at room temperature to give primarily disilanolate-bridged digallium sites,  $[(\text{CH}_3)_2\text{Ga}(\mu\text{-OSi}\equiv)]_2$ . The EXAFS at the Ga *K*-edge shows a prominent Ga-Ga scattering path, regardless of whether an excess or a limiting amount of  $\text{Ga}(\text{CH}_3)_3$  is used.

Some dimers are formed by the concerted reaction of  $\text{Ga}(\text{CH}_3)_3$  with an “isolated” silanol and an adjacent siloxane bond. These grafting sites are proposed to be hydroxyl-substituted 2-rings, formed by condensation within a vicinal  $Q^2$ - $Q^3$  pair. The high uniformity of the  $\text{Ga}_2\text{O}_2$  rings suggests a precise relationship between the silanol and the reactive siloxane bond. During silica pretreatment at 800 °C, condensation of a vicinal pair of silanols (i.e., those separated by a single bridging oxygen) leads to the formation of a highly strained 2-ring ( $\text{Si}_2\text{O}_2$ ). When one of the silanols is also a member of a geminal silanol pair (i.e., a vicinal  $Q^2$ - $Q^3$  site pair), the result is a 2-ring with a hydroxyl substituent, as shown in eq 1.



As silica is heated, 2-rings first arise via the condensation reaction shown in eq 1, since they impose less strain on the silica framework than do 2-rings lacking a hydroxyl substituent (i.e., which are anchored via an additional siloxane linkage to the lattice). The proposed reaction of  $\text{Ga}(\text{CH}_3)_3$  with a hydroxyl-substituted 2-ring is depicted in eq 2.



It is possible that siloxane bond cleavage occurs prior to protonolysis of  $\text{Ga}(\text{CH}_3)_3$  by the remaining silanol, due to the very high reactivity of the strained 2-rings. Other dimers are formed by reaction of  $\text{Ga}(\text{CH}_3)_3$  with vicinal  $\text{Q}^3$ - $\text{Q}^3$  pairs which have not condensed, even at  $800^\circ\text{C}$ . In a computational model for the dimer sites, the O-O distance is  $<2.6 \text{ \AA}$ , which is far shorter than the calculated mean interhydroxyl separation for the thermally treated silicas ( $12.2 \text{ \AA}$ ). This highly non-random distribution of surface silanols, in combination with the coupled reaction of “isolated” silanols and strained siloxane bonds, accounts for the preferential formation of grafted site pairs rather than isolated grafted sites when silica surfaces are chemically modified. This finding has profound implications for site isolation strategies in supported organometallic catalysts.

**Future Plans:** We will continue to implement a combined experimental-computational approach to the structure and strength of Lewis and Brønsted sites on a variety of silica/aluminas and related materials used widely as supports for dispersed metal oxides. We are also studying initiation mechanisms for the active sites, involving reaction with the olefinic substrate.

#### Publications acknowledging this grant (2009-2011)

1. M. Hisamoto, R.C. Nelson, M.-Y. Lee, J. Eckert, S.L. Scott, “Mode of Adsorption of  $(\text{CH}_3)_2\text{Au}(\text{acac})$  onto Partially Dehydroxylated Silica”, *J. Phys. Chem. C*, **2009**, *113*, 8794–8805.
2. M. Hisamoto, S. Chattopadhyay, J. Eckert, G. Wu, S.L. Scott, “Solid-state Spectroscopic and Structural Investigation of *cis*- $(\text{CH}_3)_2\text{Au}(\text{O},\text{O}'\text{-acac})$ ” *J. Chem. Crystallogr.* **2009**, *39*, 173-177.
3. D. Serrano, J. Aguado, G. Morales, J. M. Rodríguez, A. Peral, M. Thommes, J.D. Epping, B.F. Chmelka, “Molecular, meso- and macroscopic properties of hierarchical nanocrystalline ZSM-5 zeolite prepared by seed silanization,” *Chem. Mater.*, **2009**, *21*, 641-654.
4. S. Cadars, D.H. Brouwer, B.F. Chmelka, “Probing the Local Structures of Siliceous Zeolite Frameworks Using Solid-State NMR and DFT Calculations of  $^{29}\text{Si}$ -O- $^{29}\text{Si}$  Scalar Couplings,” *Phys. Chem. Chem. Phys.*, **2009**, *11*, 1825-1837.
5. G.L. Athens, R. Shayib, B.F. Chmelka, “Functionalization of Mesostructured Inorganic-Organic and Porous Inorganic Materials,” *Curr. Opin. Coll. Interf. Sci.*, *14*, 281-292 (2009)
6. J.A. Kurzman, X. Ouyang, W.B. Im, J. Li, J. Hu, S.L. Scott, R. Seshadri, “ $\text{La}_4\text{LiAuO}_8$  and  $\text{La}_2\text{BaPdO}_5$ : Comparing Two Highly Stable  $d^8$  Square-Planar Oxides,” *Inorg. Chem.* **2010**, *49*, 4670–4680.
7. X. Ouyang, S.L. Scott, “Mechanism for CO oxidation catalyzed by Pd-substituted  $\text{BaCeO}_3$ , and the local structure of the active sites”, *J. Catal.*, **2010**, *273*, 83-89.
8. R.O. Savinelli, S.L. Scott, “Wavelet Transform EXAFS Analysis of Mono- and Dimolybdate Model Compounds and a Mo/HZSM-5 Dehydroaromatization Catalyst,” *Phys. Chem. Chem. Phys.* **2010**, *12*, 5660 - 5667.
9. W.B. Im, N. George, J. Kurzman, S. Brinkley, A. Mikhailovsky, J. Hu, B.F. Chmelka, S.P. DenBaars, Ram Seshadri, “Efficient and Color-Tunable Oxyfluoride Solid Solution Phosphors for Solid-State White Lighting”, *Adv. Mater.* **2011**, *23*, 2300–2305.
10. B.C. Vicente, R.C. Nelson, A.W. Moses, S. Chattopadhyay, S.L. Scott, “Interactions Involving Lewis Acidic Aluminum Sites in Oxide-Supported Perhenate Catalysts”, *J. Phys. Chem. C* **2011**, *115*, 9012-9024
11. S.D. Fleischman, S.L. Scott, “Evidence for the Pairwise Disposition of Grafting Sites on Highly Dehydroxylated Silicas via Their Reactions with  $\text{Ga}(\text{CH}_3)_3$ ”, *J. Am. Chem. Soc.* **2011**, *133*, 4847-4855 (Cover Article).

## Towards a Molecular Scale Understanding of Surface Chemistry and Photocatalysis on Metal Oxides: Surface Science Experiments and First Principles Theory

Students and Postdocs: Ulrich Aschauer, Shao-Chun Li

Collaborators: C. Di Valentin (University of Milano-Bicocca), G. Pacchioni (University of Milano-Bicocca), Antonio Tilocca (University College London)

Contacts: U. Diebold, Tulane U.; phone: (504) 862-8279; Email: [diebold@tulane.edu](mailto:diebold@tulane.edu)

A. Selloni, Princeton University; phone (609) 258-3837; Email: [aselloni@princeton.edu](mailto:aselloni@princeton.edu)

### Goal

The overall objective is to provide a complete picture of the relationship between atomic structure, electronic properties and (photo-)reactivity of TiO<sub>2</sub> surfaces. Macroscopic single crystalline surfaces are being studied, where these interrelated aspects can be identified.

### DOE Interest

The project provides an increased understanding of molecular processes and structure-activity relationships in photocatalytic systems. This can lead to guidelines on how to make TiO<sub>2</sub>-based photocatalytic systems more efficient. This directly relates to the Program's mission to develop a mechanistic understanding of chemical reactions that pertain to environmental remediation and pollution control; energy production (photoelectrochemical and production of hydrogen); and novel materials synthesis.

### Recent Progress (2009- 2011)

Importance of subsurface defects at the anatase TiO<sub>2</sub>(101) surface. We showed that on the anatase (101) surface oxygen vacancies are preferentially located at subsurface rather than at surface sites, as found on rutile TiO<sub>2</sub>(110). Using STM measurements and DFT calculations, we studied the influence of subsurface defects on the reactivity of anatase (101). We observed that subsurface defects lead to a higher desorption temperature of adsorbed water. DFT calculations found a strong selectivity for water binding to sites in the vicinity of the subsurface defects. The water adsorption energy at these sites is considerably higher than that on the stoichiometric surface, consistent with the experiment. Similar to water, also the adsorption of O<sub>2</sub>, is strongly enhanced close to subsurface defect.

Water /anatase TiO<sub>2</sub>(101) interaction. By combined STM and DFT studies, we obtained a detailed atomic-scale picture of the structural, dynamical, and electronic properties of submonolayer water on anatase (101). Using First Principles Molecular Dynamics (FPMD) simulations we also investigated the structure and electronic properties of an adsorbed OH<sup>-</sup> at the interface between liquid water and stoichiometric anatase TiO<sub>2</sub>(101). Analysis of the interface electronic structure along the FPMD trajectories shows that thermal fluctuations have an important effect on the electronic energy levels. While the topmost occupied levels of OH<sup>-</sup> (water) typically lie below (well below) the TiO<sub>2</sub> valence band edge (VBE), thermal fluctuations can lead to special, poorly solvated configurations where the topmost OH<sup>-</sup> energy levels are *above* the TiO<sub>2</sub> VBE. In these configurations, holes generated by UV light absorption can be transferred from anatase to OH<sup>-</sup>, though such transfer is usually forbidden.

*Organic molecules on TiO<sub>2</sub> surfaces* We have investigated the bonding geometry of different organic and metallo-organic molecules, and how the bonding to the substrate relates to the electronic structure. This information is key to understanding charge-transfer mechanisms across the organic/TiO<sub>2</sub> interface. In particular, we have studied the adsorption of azobenzene and aniline. Our STM studies revealed the prominent role of the TiO<sub>2</sub> surface in cleaving the N=N double bond. Catechol is a model organic sensitizer for dye-sensitized solar cells. By STM and DFT calculations we studied the growth and organization of a catechol monolayer on the anatase (101) surface (Figure 1). On anatase terraces, monodentate (D1) and bidentate (D2) conformations are both present in the dilute limit, and frequent interconversions can take place between these two species. A D1 catechol is mobile at room temperature and can explore the most favorable surface adsorption sites, whereas D2 is essentially immobile. When a D1 molecule arrives in proximity of another adsorbed catechol in an adjacent row, it is energetically convenient for them to pair up in nearest-neighbor positions taking a D2-D2 or D2-D1 configuration. This intermolecular interaction, largely substrate-mediated, causes the formation of one-dimensional catechol islands that can change in shape but are stable to break-up.

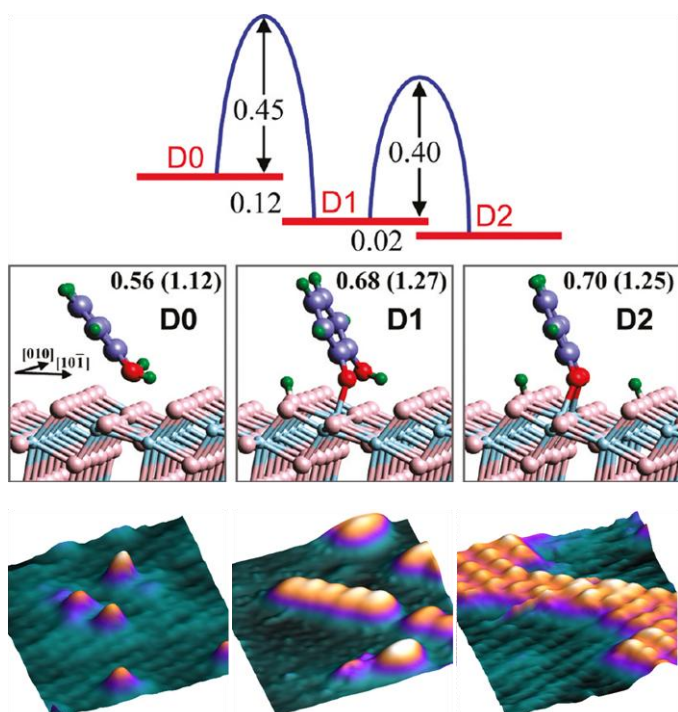


**Figure 1.** Upper panel: Computed adsorption configurations of isolated catechol molecules on anatase TiO<sub>2</sub>(101). (a) Molecularly adsorbed ‘D0’, (b) singly dissociated ‘D1’, and (c) doubly dissociated ‘D2’. Listed for each configuration are adsorption energies (in eV), without (with) taking into account vdW interactions. The scheme in the top part of the figure shows the energy barriers and energy differences (in eV) of the D0→D1 and D1→D2 transformations, from PBE calculations without vdW corrections. Lower panel: Submonolayer of catechol on anatase TiO<sub>2</sub>(101). STM images ( $U_{\text{sample}} = +1.40$  V,  $I_{\text{tunnel}} = 0.20$  nA) of  $\sim 0.2$  ML (left),  $\sim 0.3$  ML (middle), and  $\sim 0.5$  ML (right) catechol, adsorbed and imaged at room temperature.

### Future Plans:

Building on our previous results, we intend to carry out theoretical/computational studies of the atomic structure, electronic properties and reactivity of *anatase surfaces covered by a few up to several layers of water*, which represent more realistic models of the surfaces that occur in real photocatalysis. In particular, we intend to focus on the characterization of the structure of anatase TiO<sub>2</sub> surfaces in aqueous environment, the study of molecular adsorption at the anatase/water interface, the properties of excess electron and hole states at the anatase-water interface.



**Publications 2009 – 2011** (in reverse chronological order)

1. L.-M. Liu, S.-C. Li, H. Cheng, U. Diebold, A. Selloni, Growth and Organization of an Organic Molecular Monolayer on TiO<sub>2</sub>: Catechol on Anatase (101), *J. Am. Chem. Soc.* **2011**, *133*, 7816-7823
2. S.-C. Li, U. Diebold, Adsorption-site dependent electronic structure of catechol on TiO<sub>2</sub> anatase (101) surface, *Langmuir Letters* **2011**, in press
3. S.-C. Li, Y. Losovyi, V. K. Paliwal, and U. Diebold, Photoemission study of azobenzene and aniline adsorbed on TiO<sub>2</sub> anatase (101) and rutile (110) surfaces, *J. Phys Chem C* **2011**, *115* 10173-1017
4. U. Aschauer, A. Selloni, Structure of the Rutile TiO<sub>2</sub>(011) Surface in an Aqueous Environment, *Phys. Rev. Lett.* **2011**, *106*, 166102
5. U. Aschauer, A. Selloni, Influence of subsurface Ti interstitials on the reactivity of anatase TiO<sub>2</sub> (101), Proc. of SPIE Vol. 7758, 77580B ·**2010**
6. U. Aschauer, J. Chen, A. Selloni, Peroxide and superoxide states of adsorbed O<sub>2</sub> on anatase TiO<sub>2</sub> (101) with subsurface defects, *Phys. Chem. Chem. Phys.*, **2010**, *12*, 12956 – 12960
7. S.-C. Li, U. Diebold, L.-N. Chu, X.-Q. Gong “Hydrogen controls the dynamics of catechol adsorbed on a TiO<sub>2</sub>(110) surface” *Science* **2010**, *328*, 882 – 884 (Paper highlighted in C&EN News)
8. O. Dulub, U. Diebold “Preparation of a Pristine TiO<sub>2</sub> Anatase (101) Surface by Cleaving” *J. Phys: Condensed Matter* **2010**, *22* 084014 (Special Issue Honoring the Memory of Prof. T.E. Madey)
9. U. Diebold, S.-C. Li, M. Schmid “Oxide Surface Science” *Ann. Rev. Phys. Chem.* 2010 61 (Invited Review)
10. S.-C. Li, U. Diebold, Reactivity of TiO<sub>2</sub> Rutile and Anatase Surfaces towards Nitroaromatics, *J. Am Chem. Soc. (Communication)* **2010**, *132*, 64 – 66
11. A. Vittadini, M. Casarin, A. Selloni, Hydroxylation of TiO<sub>2</sub>-B: insights from Density Functional calculations, *J. Mater. Chem.* **2010**, *20*, 5871.
12. H. Cheng and A. Selloni, Hydroxide ions at the water/anatase(101) interface: structure and electronic states from first principles molecular dynamics, *Langmuir* **2010**, *26*, 11518
13. F. De Angelis, S. Fantacci, A. Selloni, M.K. Nazeeruddin and M. Graetzel, First-Principles Modeling of the Adsorption Geometry and Electronic Structure of Ru(II) Dyes on Extended TiO<sub>2</sub> Substrates for Dye-Sensitized Solar Cell Applications, *J. Phys. Chem. C* **2010**, *114*, 6054-6061
14. U. Aschauer, Y. He, H. Cheng, S.C. Li, U. Diebold, A. Selloni, Influence of subsurface defects on the surface reactivity of TiO<sub>2</sub>: water on anatase (101), *J. Phys. Chem. C* **2010**, *114*, 1278-1284
15. C. Di Valentin, G. Pacchioni, A. Selloni, Reduced and n-type doped TiO<sub>2</sub>: Nature of Ti<sup>3+</sup> species, *J. Phys. Chem. C* **2009**, *113*, 20543 (Feature Article)
16. H. Cheng and A. Selloni, Energetics and diffusion of intrinsic surface and subsurface defects on anatase TiO<sub>2</sub>(101), *J. Chem. Phys.* **2009**, *131*, 054703
17. Y. He, A. Tilocca, O. Dulub, A. Selloni, U. Diebold, Submonolayer water on TiO<sub>2</sub> anatase (101): structural, dynamical, and electronic signatures, *Nature Materials* **2009**, *8*, 585-589.
18. Y. He, W.-K. Li, X.-Q. Gong, O. Dulub, A. Selloni, U. Diebold, Nucleation and Growth of 1D Water Clusters on Rutile TiO<sub>2</sub> (011)-2×1, *J. Phys. Chem. C* **2009**, *113*, 10329-10332.
19. S.-C. Li and U. Diebold “Direction-dependent intermolecular interactions: catechol on TiO<sub>2</sub>(110)-1×1” Proc. SPIE, Vol. 7396, 73960P, **2009**
20. S.-C. Li, J.-g. Wang, P. Jacobson, X.-Q. Gong, A. Selloni, and U. Diebold “Correlation between bonding geometry and band gap states at organic-inorganic interfaces: catechol on rutile TiO<sub>2</sub>(110)” *J. Am Chem Soc.* **2009**, *131*, 980 – 984
21. X.-Q. Gong, N. Khorshidi, A. Stierle, V. Vonk, C. Ellinger, H. Dosch, H. Cheng, A. Selloni, Y. He, O. Dulub, U. Diebold “The 2x1 Reconstruction of the Rutile TiO<sub>2</sub>(011) Surface: a Combined Density Functional Theory, X-ray Diffraction, and Scanning Tunneling Microscopy Study” *Surf Sci* **2009**, *603*, 138 – 144

# Increasing the Hydrothermal Stability of Heterogeneous Catalysts for Biomass Conversion

Carsten Sievers – Georgia Institute of Technology

Email: carsten.sievers@chbe.gatech.edu - Phone: 404-385-7685

## Introduction

Aqueous phase processes are expected to play a key role in the production of renewable chemicals and fuels from biomass. Facile separation makes heterogeneous catalysts an attractive option for achieving high efficiency in these processes. Therefore, it is not surprising that a number of recent publications described heterogeneously catalyzed reactions in water including aqueous phase reforming<sup>1</sup> and dehydration of sugars.<sup>2</sup> However, little is known about the stability of the catalysts under reaction conditions (liquid water at 150-265 °C).<sup>3-5</sup> We recently demonstrated that faujasite type zeolites with high Si/Al ratios are degraded by hydrolysis of siloxane bonds, whereas ZSM-5 showed remarkable stability.<sup>4</sup> In this paper, we extend these studies to  $\gamma$ -Al<sub>2</sub>O<sub>3</sub>, Pt/ $\gamma$ -Al<sub>2</sub>O<sub>3</sub>, and Ni/ $\gamma$ -Al<sub>2</sub>O<sub>3</sub>,<sup>5</sup> and demonstrate that these materials can be stabilized significantly by silylation.

## Experimental

Pt/ $\gamma$ -Al<sub>2</sub>O<sub>3</sub> and Ni/ $\gamma$ -Al<sub>2</sub>O<sub>3</sub> were prepared by wet impregnation of  $\gamma$ -Al<sub>2</sub>O<sub>3</sub> with H<sub>2</sub>PtCl<sub>6</sub> and Ni(NO<sub>3</sub>)<sub>2</sub>, respectively. The metal loading was 1 wt% in both cases. Silylated samples were prepared from Pt/ $\gamma$ -Al<sub>2</sub>O<sub>3</sub> using tetraorthosilicate (TEOS) or polydimethylsiloxane (PDMS) as reagents. The stability tests were performed by exposing the samples to liquid water at 200 °C and autogenous pressure using an autoclave reactor. Transformations were analyzed by XRD, <sup>27</sup>Al and <sup>1</sup>H MAS NMR, nitrogen physisorption, adsorption of pyridine, and TEM. Aqueous phase reforming was studied in a batch reactor at 225 °C and 5 bar N<sub>2</sub> initial pressure using 100 mg of catalyst in 100 mL of a 5 wt% glycerol solution. Reaction products after 4 h were analyzed by HPLC and GC.

## Results and Discussion

XRD analysis of  $\gamma$ -Al<sub>2</sub>O<sub>3</sub> supported catalysts indicated the formation of crystalline phase upon treatment in liquid water at 200 °C. The new phase was identified as boehmite (AlOOH) based on comparison with reference spectra. <sup>27</sup>Al MAS NMR spectra were used to quantify the concentration of boehmite after different treatment times (Figure 1).<sup>5</sup> This was possible because Al nuclei are found in tetrahedral and octahedral coordination in  $\gamma$ -Al<sub>2</sub>O<sub>3</sub>, whereas in boehmite, all Al nuclei are octahedrally coordinated. The conversion of metal free  $\gamma$ -Al<sub>2</sub>O<sub>3</sub> was completed within 10 h. The incorporation of metal (1 wt% Ni and 1 wt% Pt) caused a significant delay in the phase transition compared to metal-free  $\gamma$ -Al<sub>2</sub>O<sub>3</sub>.<sup>5</sup> It appears that approximately 15% of the  $\gamma$ -alumina support is readily converted into boehmite, whereas the remaining support is reasonably stable for 6 h. A longer treatment results in the formation of substantial amounts of boehmite from Pt/ $\gamma$ -Al<sub>2</sub>O<sub>3</sub> and Ni/ $\gamma$ -Al<sub>2</sub>O<sub>3</sub>. The formation of boehmite resulted in a loss of surface area and a significant decrease of the concentration of acid sites. Only Lewis acid sites were detected for the treated and untreated samples. The size of the supported metal particles barely changed during the first 4 h of the treatment but notable sintering was observed as the formation of boehmite accelerated.

The stabilizing effect of the metal particles was investigated by <sup>1</sup>H MAS NMR (Figure 2). The spectrum of untreated  $\gamma$ -Al<sub>2</sub>O<sub>3</sub> showed peaks corresponding to hydroxyl group that interact with

one (-0.3 and 0.7 ppm), two (1.5 and 2.5 ppm) and three (4.1 ppm) aluminium atoms as well as traces of adsorbed water (6.1 ppm). In particular, the peaks corresponding to hydroxyl groups interacting with a single aluminium atoms decreased upon incorporation of metal particles. Therefore, it is proposed that these sites serve as nucleation sites for the formation of boehmite.

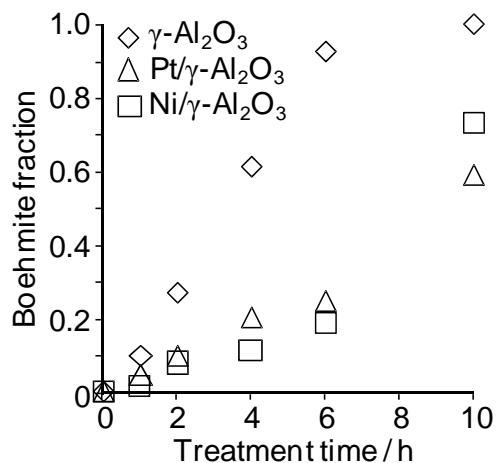


**Figure 1:** Kinetics of boehmite formation from  $\gamma\text{-Al}_2\text{O}_3$  supported catalysts.

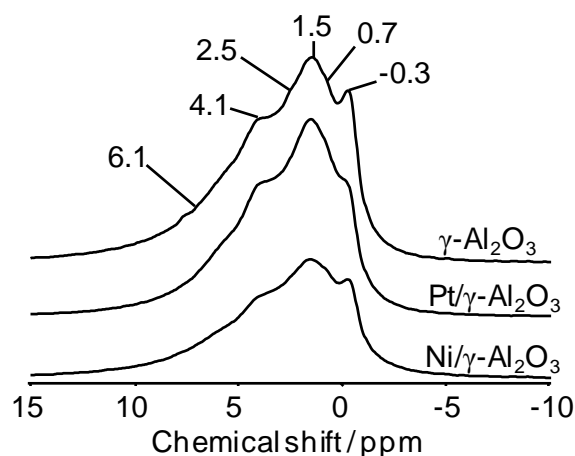


**Figure 2:**  $^1\text{H}$  MAS NMR spectra of  $\gamma\text{-Al}_2\text{O}_3$ ,  $\text{Pt}/\gamma\text{-Al}_2\text{O}_3$  and  $\gamma\text{-Al}_2\text{O}_3$ .

Further stabilization was achieved by capping the remaining surface hydroxyl groups on  $\text{Pt}/\gamma\text{-Al}_2\text{O}_3$  with tetraorthosilicate (TEOS) or polydimethylsiloxane (PDMS). Only minimal changes between the  $^{27}\text{Al}$  MAS NMR spectra of these samples before and after treatment in water at 200 °C for 10 h (Figure 3), and there were no peak corresponding to boehmite in the x-ray diffractograms of treated samples. Moreover, a notable increase of the hydrogen yield was observed when the silylated catalysts were used for aqueous phase reforming of glycerol.

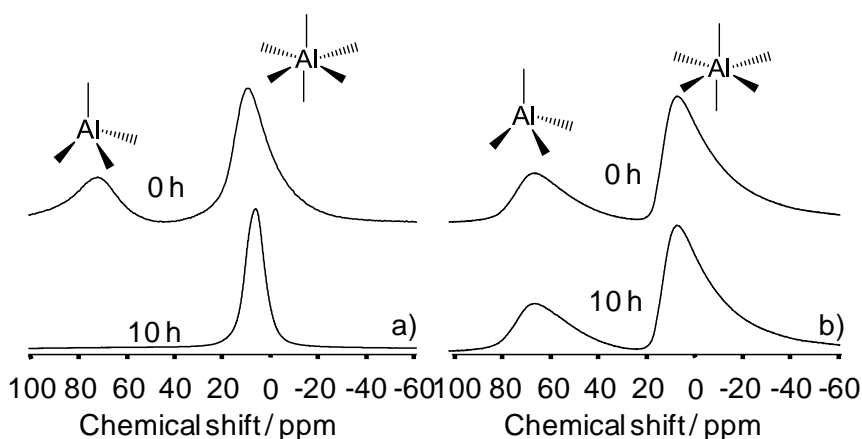


**Figure 3:**  $^{27}\text{Al}$  MAS NMR spectra of  $\text{Pt}/\gamma\text{-Al}_2\text{O}_3$  before and after treatment in water at 200 °C for 10 h: a) unstabilized  $\text{Pt}/\gamma\text{-Al}_2\text{O}_3$ , b)  $\text{Pt}/\gamma\text{-Al}_2\text{O}_3$  after silylation with TEOS.

## References

(1) Cortright, R. D.; Davda, R. R.; Dumesic, J. A. *Nature* **2002**, *418*, 964-967.

- (2) Watanabe, M.; Aizawa, Y.; Iida, T.; Aida, T.M.; Levy, C.; Sue, K.; Inomata, H. *Carbohydr. Res.* **2005**, *340*, 1925-1930.
- (3) Ketchie, W. C.; Maris, E. P.; Davis, R. J. *Chem. Mat.* **2007**, *19*, 3406-3411.
- (4) Ravenelle, R. M.; Schüßler, F.; D'Amico, A.; Danilina, N.; van Bokhoven, J. A.; Lercher, J. A.; Jones, C. W.; Sievers, C. *J. Phys. Chem. C* **2010**, *114*, 19582-19595.
- (5) Ravenelle, R. M.; Copeland, J. R.; Kim, W. G.; Crittenden, J. C.; Sievers, C. *ACS Catal.* **2011**, *1*, 552-561.

### Catalysis and the nature of mixed-metal oxides at the nanometer level

Lead PI: José A. Rodriguez  
Additional PIs: Jan Hrbek, Ping Liu  
Postdocs: Joon B. Park, Fan Yang  
Contact: Department of Chemistry, Brookhaven National Laboratory, Upton, NY11973;  
[djs@bnl.gov](mailto:djs@bnl.gov)

Metal oxide catalysts are more complex than conventional metal catalysts because they can terminate with different functionalities and expose cations in multiple oxidation states. The combination of two metals in an oxide matrix can produce materials with novel structural or electronic properties that can lead to distinct catalytic activity or selectivity. To rationalize structure-reactivity relationships for mixed-metal oxide catalysts at the atomic level, well-defined systems are required [1]. Our recent studies involving the deposition of nanoparticles and clusters of  $\text{RuO}_x$  or  $\text{CeO}_x$  on  $\text{TiO}_2(110)$  have shown novel structures that have special chemical properties. After deposition on  $\text{TiO}_2(110)$ , we have found the formation of ceria dimers and 1D structures of  $\text{RuO}_x$ . The non-typical coordination modes imposed by  $\text{TiO}_2(110)$  on ceria nanoparticles make possible the direct participation of this oxide in catalytic reactions and enhance the dispersion of metals on the titania substrate.  $\text{M/CeO}_x/\text{TiO}_2(110)$  ( $\text{M} = \text{Au}, \text{Cu}, \text{Pt}$ ) surfaces display an extremely high catalytic activity for CO oxidation and the water-gas shift reaction [2, 3]. The 1D structures for  $\text{RuO}_2$  deposited on  $\text{TiO}_2(110)$  can be easily reduced and re-oxidized, displaying a very high catalytic activity for CO oxidation [4]. In general, the chemical behavior of the  $\text{MO}_x/\text{TiO}_2(110)$  ( $\text{M} = \text{V}, \text{W}, \text{Ce}$  or  $\text{Ru}$ ) surfaces reflects their unique structure at the nanometer level [1,4]. These simple models can provide a conceptual framework for modifying or controlling the chemical properties of mixed-metal oxides and for guiding the engineering of novel industrial catalysts.

#### References

1. Rodriguez, J.A. and D. Stacchiola, *Catalysis and the nature of mixed-metal oxides at the nanometer level: special properties of  $\text{MO}_x/\text{TiO}_2(110)$  ( $\text{M} = \text{V}, \text{W}, \text{Ce}$ ) surfaces*. Physical Chemistry Chemical Physics, 2010. **12**(33): p. 9557-9565.
2. Park, J.B., et al., *Gold, Copper, and Platinum Nanoparticles Dispersed on  $\text{CeO}_x/\text{TiO}_2(110)$  Surfaces: High Water-Gas Shift Activity and the Nature of the Mixed-Metal Oxide at the Nanometer Level*. Journal of the American Chemical Society, 2010. **132**(1): p. 356-363.
3. Park, J.B., et al., *High catalytic activity of  $\text{Au/CeO}_x/\text{TiO}_2(110)$  controlled by the nature of the mixed-metal oxide at the nanometer level*. Proceedings of the National Academy of Sciences of the United States of America, 2009. **106**(13): p. 4975-4980.
4. Yang, F., et al., *Unravelling the behaviour of  $\text{RuO}_x$  nanoparticles in Mixed-Metal Oxides: Special Structural and Catalytic Properties of  $\text{RuO}_2/\text{TiO}_2(110)$  Surfaces*. Submitted.

**Institute for Catalysis in Energy Processes (ICEP)**

Additonal PIs: Argonne: Larry Curtiss, Jeff Elam, Nada Dimitrijevic, Jeff Miller, Peter Zapol  
Northwestern University: Mike Bedzyk, Linda Broadbelt, Don Ellis, Franz Geiger, Kim Gray, Mark Hersam, Joe Hupp, Harold Kung, Mayfair Kung, Laurence Marks, Tobin Marks, SonBinh Nguyen, Ken Poeppelmeier, Randy Snurr, Rick Van Duyne, Eric Weitz

Research Staff: Hack-Sung Kim (NU/ANL)

Postdocs: Kaustava Bhattacharyya, Haiying He (ANL), Linhua Hu, Dragos Seghete, Sven Stoltz, Baiju Vijayan

Graduate Students: Avram Buchbinder, Alon Danon, Paul Desario, Christopher Downing, Tasha Drake, James Enterkin, Zhenxing Feng, Ivan Konstantinov, Stephanie Kwon, Jonathan Lelah, Tony Liang, Yu Yuan Lin, Renhu Ma, Sicelo Masango, Neema Mashayekhi, Martin McBriarty, Huong Giang Nguyen, Alex Peroff, Patrick Ryan, Audrey Salazar, Abraham Shultz, Miles Tan, Chuandao Wang, Staci Wegener.

Collaborators: Chris Marshall (ANL), Tijana Rajh (ANL), Stan Zygmunt (Valpariso U.)

Contacts:

P. Stair, <a href="mailto:pstair@northwestern.edu">pstair@northwestern.edu</a>	M. Hersam, <a href="mailto:m-hersam@northwestern.edu">m-hersam@northwestern.edu</a>
L. Curtiss, <a href="mailto:curtiss@anl.gov">curtiss@anl.gov</a>	J. Hupp, <a href="mailto:j-hupp@northwestern.edu">j-hupp@northwestern.edu</a>
N. Dimitrijevic, <a href="mailto:dimitrijevic@anl.gov">dimitrijevic@anl.gov</a>	H. Kung, <a href="mailto:hkung@northwestern.edu">hkung@northwestern.edu</a>
J. Elam, <a href="mailto:jelam@anl.gov">jelam@anl.gov</a>	M. Kung, <a href="mailto:m-kung@northwestern.edu">m-kung@northwestern.edu</a>
J. Miller, <a href="mailto:millerjt@anl.gov">millerjt@anl.gov</a>	L. Marks, <a href="mailto:l-marks@northwestern.edu">l-marks@northwestern.edu</a>
P. Zapol, <a href="mailto:zapol@anl.gov">zapol@anl.gov</a>	T. Marks, <a href="mailto:t-marks@northwestern.edu">t-marks@northwestern.edu</a>
M. Bedzyk, <a href="mailto:bedzyk@northwestern.edu">bedzyk@northwestern.edu</a>	S. Nguyen, <a href="mailto:stn@northwestern.edu">stn@northwestern.edu</a>
L. Broadbelt, <a href="mailto:broadbelt@northwestern.edu">broadbelt@northwestern.edu</a>	K. Poeppelmeier, <a href="mailto:krp@northwestern.edu">krp@northwestern.edu</a>
D. Ellis, <a href="mailto:don-ellis@northwestern.edu">don-ellis@northwestern.edu</a>	R. Snurr, <a href="mailto:snurr@northwestern.edu">snurr@northwestern.edu</a>
F. Geiger, <a href="mailto:f-geiger@northwestern.edu">f-geiger@northwestern.edu</a>	R. VanDuyne, <a href="mailto:vanduyne@northwestern.edu">vanduyne@northwestern.edu</a>
K. Gray, <a href="mailto:k-gray@northwestern.edu">k-gray@northwestern.edu</a>	E. Weitz, <a href="mailto:weitz@northwestern.edu">weitz@northwestern.edu</a>

**Goal**

The Institute for Catalysis in Energy Processes (ICEP) is a joint venture of the Northwestern University Center for Catalysis and Surface Science (NU) and Argonne National Laboratory (ANL). It is organized into three (3) highly integrated efforts. Two of these comprise the **Scientific Themes**: *Chemical Catalysis: Selective Oxidation of Light Alkanes to Fuels* and *Photocatalysis: Reduction of Carbon Oxides*. Research activities of ICEP are in synthesis of catalytic materials, in measurements that reveal catalyst properties and chemistry, and in theory and modeling to understand properties, measurements, and chemistry. In many cases ICEP researchers are the inventors or developers of the methods that can be brought to bear on catalytic systems. The third effort is a natural outgrowth of these strengths. It provides the **Research Expertise** for advancing the scientific themes through the application and development of both experimental methods and theory.

Understanding the elementary catalytic steps in selective oxidation of light alkanes to oxygenates, with an ultimate goal to achieve the ability to design and manipulate selective catalytic sites is the major objective of the *Chemical Catalysis* theme. Understanding the elementary steps in the photocatalytic reduction of CO<sub>2</sub> on oxide surfaces is the major objective of the *Photocatalysis* theme. An important aspect of the ongoing ICEP research is the continued advancement and development of both synthesis and characterization methods. Significant progress has been achieved in each of these areas as described in ICEP publications.

### **DOE Interest**

As emphasized in both the DOE-BES reports “Catalysis for Energy” and “Directing Matter and Energy: Five Challenges for Science and the Imagination,”, catalytic technology is essential for economic prosperity, energy security and environmental preservation in the 21st Century. Due to the abundance of light alkanes in natural gas there is a strong incentive to convert them into higher boiling liquids usable for transportation. Likewise, the development of solar fuels technology from the photocatalytic reduction of carbon dioxide would have a major effect on the nation’s reliance on foreign sources of energy and the reduction of green house gases. These are difficult chemistries. Therefore, an improved understanding of the relevant catalytic materials and chemistry combined with the development of advanced catalyst synthesis techniques required to achieve practical technologies are relevant to the interests of DOE.

### **Recent Progress**

#### *Chemical Catalysis Highlights*

The goal of this subtask is new fundamental understanding of selective oxidation of hydrocarbons to alcohols and oxygenates. The emphasis is to develop novel catalytic sites with atomic level control that enables unprecedented, detailed understanding of catalytic chemistry. The experimental work is supported by quantum chemical computational investigation of the reaction energetics and spectroscopic characterization of relevant adsorbed molecules.

- A strategy was developed that is capable of generating a plethora of metal-organic frameworks (MOFs) from a single highly porous, robust MOF incorporating a wide variety of catalytically active metal centers in essentially a crystal-to-crystal transformation.
- DFT calculations suggested that exposed metal sites on the exterior surfaces of MOF crystals may be the active catalytic sites for the decomposition of hydroperoxides during tetralin autooxidation using O<sub>2</sub>.
- A structure consisting of Ti-oxo species placed around Au nanoparticles was synthesized and shown to yield a higher selectivity for acetone in partial oxidation of propane than a sample in which the Ti-oxo species was placed randomly, suggesting that Au-oxoTi-interface is important for partial oxidation of propane.
- The local structures and reactivity of supported vanadia hydrocarbon oxidation catalysts were found to be sensitive to the nuclearity (monomeric, dimeric, tetrameric) of grafted organometallic precursor molecules.
- Molecular orientation and ordering of adsorbates at the liquid/solid interface of model selective oxidation catalysts were determined successfully.

#### *Photocatalysis Highlights*

An overarching goal of our work on the photoreduction of CO<sub>2</sub> is to develop a detailed molecular level understanding of the factors that control the chemical efficiency of this process with the

expectation that an increased level of understanding will ultimately lead to the ability to design and synthesize a multifunctional catalyst capable of a feasible CO<sub>2</sub> photoreduction process. Work has centered on the synthesis, characterization, and evaluation of new materials for CO<sub>2</sub> PCR along with effort directed toward the elucidation of the details of the mechanism for CO<sub>2</sub> PCR. The population of photocatalytically active, under-coordinated Ti in titania nanotubes is controlled by calcination temperature

- Pt-doped titania nanotubes show enhanced photocatalytic oxidation but not reduction.
- Amine and hydroxyl functionality show cooperative effects on CO<sub>2</sub> binding to surfaces
- Complexes of solvent-exfoliated-graphene and TiO<sub>2</sub> show exceptional CO<sub>2</sub> photocatalytic reduction due to enhanced electron transport

#### *Research Expertise Highlights*

An important aspect of the ongoing ICEP research is the continued advancement and development of both synthesis and characterization methods. ICEP researchers are world-class experts in and in some cases the inventors of new materials and methods of synthesis. ICEP has similar strength in the methods for characterization of molecules, materials, and reactions, both experimentally and computationally.

- A method has been developed for synthesizing face-selective catalysts by epitaxial growth
- Resonance Raman spectroscopy has shown that bidentate surface vanadia are the most redox active monomer species and that the conventional tridentate species is likely to be a spectator under catalytic reaction conditions.
- XSW and XPS measurements show that an epitaxial rutile VO<sub>2</sub> film was formed by hydrogen reduction with V<sup>4+</sup> cations in lateral alignment with Ti lattice positions. Oxidation was found to produce V<sup>5+</sup> cations uncorrelated to the substrate lattice.
- DFT provides a plausible theoretical explanation of reaction-induced cation rearrangements observed by XSW.

#### **Publications (2009-2011)**

1. "Hydration and Reduction of Molecular Beam Epitaxy Grown VO<sub>x</sub>/α-Fe<sub>2</sub>O<sub>3</sub> (0001): Ambient Pressure Study", C.-Y. Kim, J. A. Klug, P. C. Stair, and M. J. Bedzyk, *J. Phys. Chem. C* 113, 1406-1410 (2009).
2. "Nanoscale Structure and Morphology of Atomic Layer Deposition Platinum on SrTiO<sub>3</sub> (001)", S. T. Christensen, J. W. Elam, B. Lee, Z. Feng, M. J. Bedzyk and M. C. Hersam, *Chem. Mater.* 21 516-521 (2009).
3. (Cover)"Controlled Growth of Platinum Nanoparticles on Strontium Titanate Nanocubes By Atomic Layer Deposition", S.T. Christensen, J.W. Elam, F.A. Rabuffetti, Q. Ma, S.J. Weigand, B. Lee, S. Seifert, P.C. Stair, K.R. Poeppelmeier, M.C. Hersam, M.J. Bedzyk, *Small* 5, 750-757 (2009).
4. "Hierarchical nanoparticle morphology for platinum supported on SrTiO<sub>3</sub> (0 0 1): A combined microscopy and X-ray scattering study", S.T. Christensen, B. Lee, Z. Feng, M. C. Hersam, M. J. Bedzyk, *Appl. Surf. Sci.* 256, 423-427 (2009).
5. "Direct Atomic-Scale Observation of Redox-Induced Cation Dynamics in an Oxide-Supported Monolayer Catalyst: WOX/α-Fe<sub>2</sub>O<sub>3</sub>(0001)", Z. Feng, C.-Y. Kim, J. W. Elam, Q. Ma, Z. Zhang, M. J. Bedzyk, *J. Am. Chem. Soc.* 131, 18200-18201 (2009).
6. Yin, S. and D. E. Ellis (2009). "DFT studies of Cr(VI) complex adsorption on



- hydroxylated hematite (1102) surfaces." *Surf. Sci.* **603**(4): 736-746.
7. Yin, S. and D.E. Ellis (2010) "First-principles Investigations of Ti-substituted Hydroxyapatite Electronic Structure", *Phys. Chem. Chem. Phys.* **12**, 156-163.
  8. Christensen, S. T., J. W. Elam, et al. (2009). "Nanoscale Structure and Morphology of Atomic Layer Deposition Platinum on SrTiO<sub>3</sub> (001)." *Chem. Mater.* **21**(3): 516-521.
  9. Ostojic, G. N., Y. T. Liang, et al. (2009). "Catalytically active nanocomposites of electronically coupled carbon nanotubes and platinum nanoparticles formed via vacuum filtration." *Nanotechnology* **20**(43): 434019/434011-434019/434016.
  10. Sung, C.-Y., L. J. Broadbelt, et al. (2009). "QM/MM Study of the Effect of Local Environment on Dissociative Adsorption in BaY Zeolites." *J. Phys. Chem. C* **113**(35): 15643-15651.
  11. Sung, C.-Y., R. Q. Snurr, et al. (2009). "DFT Study of deNO<sub>x</sub> Reactions in the Gas Phase: Mimicking the Reaction Mechanism over BaNaY Zeolites." *J. Phys. Chem. A* **113**(24): 6730-6739.
  12. Buchbinder, A. M., E. Weitz, et al. (2010). "Pentane, hexane, cyclopentane, cyclohexane, 1-hexene, 1-pentene, cis-2-pentene, cyclohexene, and cyclopentene at vapor/alpha -alumina and liquid/alpha -alumina interfaces studied by broadband sum frequency generation." *J. Phys. Chem. C* **114**(1): 554-566.
  13. Geiger, F. M. (2009). "Second harmonic generation, sum frequency generation, and c(3): dissecting environmental interfaces with a nonlinear optical Swiss army knife." *Annu. Rev. Phys. Chem.* **60**: 61-83.
  14. Savara, A., C. M. Schmidt, et al. (2009). "Adsorption Entropies and Enthalpies and Their Implications for Adsorbate Dynamics." *J. Phys. Chem. C* **113**(7): 2806-2815.
  15. Stokes, G. Y., A. M. Buchbinder, et al. (2009). "Chemically diverse environmental interfaces and their reactions with ozone studied by sum frequency generation." *Vib. Spectrosc.* **50**(1): 86-98.
  16. Stokes, G. Y., E. H. Chen, et al. (2009). "Atmospheric Heterogeneous Stereochemistry." *J. Am. Chem. Soc.* **131**(38): 13733-13737.
  17. Elam, J. W., J. A. Libera, et al. (2009). Spatially controlled atomic layer deposition in porous materials. Application: US, (UChicago Argonne, LLC, USA). 18pp.
  18. Feng, H., J. W. Elam, et al. (2009). "Catalytic nanoliths." *Chem. Eng. Sci.* **64**(3): 560-567.
  19. Kim, H.-S. and P. C. Stair (2009). "Resonance Raman Spectroscopic Study of Alumina-Supported Vanadium Oxide Catalysts with 220 and 287 nm Excitation." *J. Phys. Chem. A* **113**(16): 4346-4355.
  20. Kim, H.-S., S. A. Zygmunt, et al. (2009). "Monomeric Vanadium Oxide on a q-Al<sub>2</sub>O<sub>3</sub> Support: A Combined Experimental/Theoretical Study." *J. Phys. Chem. C* **113**(20): 8836-8843.
  21. Lu, J., K. M. Kosuda, et al. (2009). "Surface Acidity and Properties of TiO<sub>2</sub>/SiO<sub>2</sub> Catalysts Prepared by Atomic Layer Deposition: UV-visible Diffuse Reflectance, DRIFTS, and Visible Raman Spectroscopy Studies." *J. Phys. Chem. C* **113**(28): 12412-12418.
  22. Stair, P. C., J. W. Elam, et al. (2009). "Performance and characterization of ALD vanadium oxide catalytic nanoliths." *ECS Trans.* **25**(4, Atomic Layer Deposition Applications 5): 49-55.
  23. Savara, A., A. Danon, et al. (2009). "TPD of nitric acid from BaNa-Y: evidence that a nanoscale environment can alter a reaction mechanism." *Phys. Chem. Chem. Phys.* **11**(8): 1180-1188.

24. Savara, A., W. M. H. Sachtler, et al. (2009). "TPD of NO<sub>2</sub> - and NO<sub>3</sub> - from Na-Y: The relative stabilities of nitrates and nitrites in low temperature DeNO<sub>x</sub> catalysis." *Appl. Catal., B* **90**(1-2): 120-125.
25. L. Chen, M.E. Graham, K.A. Gray (2009) "Nitrogen stabilized reactive sputtering of optimized TiO<sub>2-x</sub> photocatalysts with visible light reactivity," *Journal Vacuum Science & Technology*, 27(4):712-715.
26. L. Chen, M.E. Graham, G. Li, D. Gentner, K.A. Gray (2009) "Photoreduction of CO<sub>2</sub> by TiO<sub>2</sub> Nanocomposites Synthesized through Reactive DC Magnetron Sputter Deposition," *Thin Solid Films*, 517:5641–5645.
27. C. H. Lanier, A. N. Chiaramonti, L. D. Marks, and K. P. Poepelmeier, (2009) "The Fe<sub>3</sub>O<sub>4</sub> Origin of the "Biphase" Reconstruction on  $\alpha$ -Fe<sub>2</sub>O<sub>3</sub> (0001)", *Surface Science*, 603, 2574-2579.
28. C.-Y. Kim, J. W. E., P. C. Stair and M. J. Bedzyk (2010), "Redox driven crystalline coherent-incoherent transformation for a 2 ML VO<sub>x</sub> film grown on  $\alpha$ -TiO<sub>2</sub>(110)." *J. Phys. Chem C* **114**: 19723-19726.
29. Kim, H., Kosuda, K. M., Van Duyne, R. P., and Stair, P. C. (2010). "Resonance Raman and surface- and tip-enhanced Raman spectroscopy methods to study solid catalysts and heterogeneous catalytic reactions". *Chemical Society Reviews* **39**(12), 4820-4844.
30. Ellis, S. Y. a. D. E. (2010), "First-principles Investigations of Ti-substituted Hydroxyapatite Electronic Structure", *Phys. Chem. Chem. Phys.* **12**.
31. Enterkin, J. A., Subramanian, A. K., Russell, B. C., Castell, M. R., Poepelmeier, K. R., and Marks, L. D. (2010). "A homologous series of structures on the surface of SrTiO<sub>3</sub>(110)". *Nat. Mater.* **9**(3), 245-248.
32. J. Terra, A. M. R., G.A. Gonzalez, and D.E. Ellis (2010), " Theoretical and Experimental Studies of Substitution of Cadmium into Hydroxyapatite", *J.Phys.Chem* **12**.
33. Konstantinov, I. A. and L. J. Broadbelt "Reaction free energies in organic solvents: comparing different quantum mechanical methods" *Molecular Simulation* **36**(15): 1197-1207.
34. Konstantinov, I. A. and L. J. Broadbelt "The Role of Oxazolidinones in l-Proline-Assisted Aldol-Type Reactions." *Topics in Catalysis* **53**(15-18): 1031-1038.
35. Liang, Y. T. and M. C. Hersam (2010), "Highly concentrated graphene solutions via polymer enhanced solvent exfoliation and iterative solvent exchange" *Journal of the American Chemical Society* **132**: 17661-17663.
36. Libera, J. A., Elam, J. W, Sather, N. F, Rajh, T., Dimitrijevic, N. M. (2010), "Iron(III)-oxo Centers on TiO<sub>2</sub> for Visible-Light Photocatalysis." *Chem. Mater.* **22**: 409-413.
37. Lin, X. F., K.R. Poepelmeier, and E. Weitz (2010), "Oxidative dehydrogenation of ethane with oxygen catalyzed by K-Y zeolite supported first-row transition metals" *Applied Catalysis A-General* **381**(1-2): 114-120.
38. M. Matos, J. T., and D.E. Ellis (2010), "A Combined Quantum Theoretical Methodology to Study Zn Substitution in (001) Hydrated Hydroxyapatite Surfaces." *J.Phys: Cond. Matt.* **22**.
39. Missaghi, M. N., J. M. Galloway, et al. (2010), "Bis(pyridyl)siloxane Oligomeric Ligands for Palladium(II) Acetate: Synthesis and Binding Properties." *Organometallics* **29**(17): 3769-3779.
40. Rabuffetti, F. A., P.C. Stair, and K.R. Poepelmeier (2010), "Synthesis-Dependent Surface Acidity and Structure of SrTiO<sub>3</sub> Nanoparticles." *Journal of Physical Chemistry C* **114**(25): 11056-11067.

41. Savara, A. and E. Weitz (2010), "Kinetics of  $\text{NO} + \text{H}^+ + \text{NO}_3^- \rightarrow \text{NO}_2 + \text{HNO}_2$  on BaNa-Y: Evidence for a Diffusion-Limited  $\text{A} + \text{B} \rightarrow 0$  Reaction on a Surface", Journal of Physical Chemistry C **114**: 20621-20628.
42. Vijayan, B., Dimitrijevic, N. M., Rajh, T., Gray, K.A. (2010), "Effect of Calcination Temperature on the Photocatalytic Reduction and Oxidation Processes of Hydrothermally Synthesized Titania Nanotubes", J. Phys. Chem. C **114**: 12994-13002
43. Vijayan, B., Dimitrijevic, N. M., Wu, J., Gray, K.A. (2010), "The Effects of Pt Doping on the Structure and Visible Light Photoactivity of Titania Nanotubes", J. Phys. Chem C **114**: 21262-21269.
44. He, H. Y., Zapol, P., and Curtiss, L. A. (2010). "A Theoretical Study of  $\text{CO}_2$  Anions on Anatase (101) Surface". Journal of Physical Chemistry C **114**(49), 21474-21481
45. Missaghi, M. N., J. M. Galloway, et al. (2011), "Bis(pyridyl)siloxane-Pd(II) complex catalyzed oxidation of alcohol to aldehyde: Effect of ligand tethering on catalytic activity and deactivation behavior." Appl. Catal., A **391**(1-2): 297-304.
46. Wegener, S.L.; Kim, H.-S., Marks, T.J.; Stair, P.C. (2011) "Supported Vanadium Oxides Prepared by Organometallic Grafting", J. Phys. Chem. Lett., **2**, 170-175.
47. Williams, L.A.; Marks, T.J. (2011), "Synthesis, Characterization, and Heterogeneous Catalytic Implementation of Sulfated Alumina Nanoparticles. Arene Hydrogenation and Olefin Polymerization Properties of Supported Organo-Group 4 Complexes", ACS Catalysis, **1**, 238-245.
48. Danon, A., P.C. Stair, and E. Weitz, (2011) "FTIR Study of  $\text{CO}_2$  Adsorption on Amine-Grafted SBA-15: Elucidation of Adsorbed Species." J. Phys. Chem. C. **115**, 11540-11549.
49. Frontiera, R.R., A.I. Henry, N.L. Gruenke, and R.P. Van Duyne, (2011) "Surface-Enhanced Femtosecond Stimulated Raman Spectroscopy." J. Phys. Chem. Lett. **2**, 1199-1203.
50. Dimitrijevic, N. M.; Vijayan, B. K.; Poluektov, O. G.; Rajh, T.; Gray, K. A.; He, H.; Zapol, P. (2011) "Role of Water and Carbonates in Photocatalytic Transformation of  $\text{CO}_2$  to  $\text{CH}_4$  on Titania", J. Am. Chem. Soc. **133**, 3964-3971.
51. Enterkin, J. A., Poeppelmeier, K. R., and Marks, L. D. (2011). "Oriented Catalytic Platinum Nanoparticles on High Surface Area Strontium Titanate Nanocuboids". Nano Lett. **11**(3), 993-997.
52. Enterkin, J. A., Setthapun, W., Elam, J. W., Christensen, S. T., Rabuffetti, F. A., Marks, L. D., Stair, P. C., Poeppelmeier, K. R., and Marshall, C. L. (2011). "Propane Oxidation over Pt/SrTiO<sub>3</sub> Nanocuboids". ACS Catal. **1**(6), 629-635.
53. Setthapun, W., Williams, W. D., Kim, S. M., Feng, H., Elam, J. W., Rabuffetti, F. A., Poeppelmeier, K. R., Stair, P. C., Stach, E. A., Ribeiro, F. H., Miller, J. T., and Marshall, C. L. (2010). "Genesis and Evolution of Surface Species during Pt Atomic Layer Deposition on Oxide Supports Characterized by in Situ XAFS Analysis and Water-Gas Shift Reaction". J. Phys. Chem. C **114**(21), 9758-9771

## Microporous and Mesoporous Nano-Size Transition Metal Oxides: Preparation, Characterization, and Applications

**Postdocs:** W. S. Willis.

**Students:** C. H. Chen, T. Coons, A. Espinal, S. Frueh, B. Hu, H. Huang, A. Iyer, L. Jin, J. Kona, A. Morey, N. Opembe, S. Sithambaram, L. Xu., Y. Zhang.

**Collaborators:** M. Aindow; A. Doble; A. Frenkel; J. Hanson; D. Mullins.

**Contacts:** Department of Chemistry, Unit 3060, University of Connecticut, Storrs, CT 06269-3060.

[Steven.Suib@Uconn.edu](mailto:Steven.Suib@Uconn.edu)

### Goal

The goals of this project are to prepare and characterize porous nano-size metal oxide systems for activation of CO<sub>2</sub>, H<sub>2</sub>O, and selective oxidations.

### DOE Interest

Fundamental understanding of the mechanisms of selective catalytic oxidations is important in the areas of energy and catalysis. Selective catalytic oxidations, activation of CO<sub>2</sub>, solar photocatalysis, novel batteries and electrocatalysis are areas being pursued. Porous nano-size metal oxides<sup>1-40</sup> are useful in these green applications. Redox catalysis, electron and energy transfer, mixed valency, mechanistic studies, characterization of molecular transformations, and detailed knowledge of structure are controlled to improve energy efficiency in these reactions.

### Recent Progress

#### *Synthesis of Nanomaterials.*

The focus of our synthetic work<sup>3,7,8,10,25,27,28,30,33</sup> involves novel syntheses and phases, new morphologies, and framework substitutions.<sup>1-40</sup> Metal and mixed metal oxides of manganese, titanium, copper, zinc, iron, and mixed metal systems have been the focus of this work. Unique ultrathin materials,<sup>12</sup> controlled morphologies<sup>36</sup> of various nano-size metal oxides, and control of particle sizes<sup>1-3,6,9-10,15,17</sup> have been realized. Pore size<sup>23</sup> and hydrophobicity<sup>18</sup> control have been used.

#### *Characterization Studies.*

*In situ* X-ray powder diffraction (XRD), *In situ* synchrotron XRD,<sup>24</sup> adsorption, electron microscopy, soft XPS,<sup>31</sup> X-ray absorption, infrared, Raman, thermal, chemical analysis, and other methods have been used to study the above systems after synthesis, after reaction and *in situ* during catalytic reactions. Synchrotron work is being done at Brookhaven National Labs.

#### *Catalysis.*

All materials described above have been studied in various catalytic reactions. Selective oxidations<sup>1,2,5,6,15,20,22,26,29,37,38</sup> of various substrates with O<sub>2</sub> or with peroxides; photocatalytic degradations of toxic species,<sup>4,9,14,17,32,34</sup> activation of CO<sub>2</sub>,<sup>11,19</sup> improved

battery<sup>26</sup> and fuel cell catalysts,<sup>13,16,21,35,40</sup> fuel reforming<sup>39</sup> and other reactions have been studied. Evidence of catalytic redox cycling, multifunctional catalysis, morphological effects in catalysis, hydrophobic effects on catalytic reactions, catalytic intermediates, and other phenomena have been observed with these systems.

### Future Plans

Future plans include studies of efficient activation of CO<sub>2</sub>, degradation of toxic species, control of pore sizes, and understanding the role of morphology in selective catalytic reactions.

### Publications (2009-2011)

1. Sithambaram, S.; Xu; Chen; Ding, Kumar; Calvert; Suib, S. L., Manganese Octahedral Molecular Sieve Catalysts for Selective Oxide Ring Opening, *Catal. Today*, 2009, **140**, 162-168.
2. Jin, L.; Chen, C.; Crisostomo, V. M. B.; Xu, L.; Son, Y. C.; Suib, S. L., gamma-MnO<sub>2</sub> Octahedral Molecular Sieve: Preparation, Characterization, and Catalytic activity in the Atmospheric Oxidation of Toluene, *J. Appl. Catal.*, 2009, **355**, 169-175.
3. Nosheen, S.; Galasso, F.; Suib, S. L., Synthesis of mordenite aggregates of nano-sized crystallites, *Sci. Adv. Mat.*, 2009, **1**, 31-37.
4. Sriskandakumar, T.; Opembe, N.; Chen, C.; Morey, A.; King'onde, C., Suib, S. L., Green Decomposition of Organic Dyes using Octahedral Molecular Sieves Manganese Oxide Catalysts, *J. Phys. Chem. A*, 2009, **113**, 1523-1530.
5. Kumar, R.; Sithambaram, R.; Suib, S. L., Cyclohexane Oxidation Catalyzed by Manganese Oxide Octahedral Molecular Sieves - Effect of Acidity of the Catalyst, *J. Catal.*, 2009, **262**, 304-313.
6. Xu, L.; Sithambaram, S.; Zhang, Y.; Chen, C.; Jin, L.; Joesten, R., Suib, S. L., Novel Urchin-like CuO Synthesized by a Facile Reflux Method with Efficient Olefin Epoxidation Catalytic Performance, *Chem. Mat.*, 2009, **21**, 1253-1259.
7. Acquah, C.; Karunanithi, A. T.; Cagnetta, M.; Achenie, L. E. K.; Suib, S. L., Linear Models for Prediction of Ibuprofen Crystal Morphology based on Hydrogen Bonding Propensities, *Fluid Phase Equilibria*, 2009, **277**, 73-80.
8. Nosheen, S.; Galasso, F. S.; Suib, S. L., Role of Ti-O Bonds in Phase Transitions of TiO<sub>2</sub>, *Langmuir*, 2009, **25**, 7623-7630.
9. Xu, L.; Hu, Y.L.; Pelligra, C.; Chen, C. H. ; Jin, L.; Huang, H.; Sithambaram, S.; Aindow, M.; Joesten, R.; Suib, S. L., ZnO with Different Morphologies Synthesized by Solvothermal Methods for Enhanced Photocatalytic Activity, *Chem. Mat.*, 2009, **21**, 2875-2885.
10. Karunanithi, A. T.; Acquah, C.; Achenie, Luke E. K.; Sithambaram, S.; Suib, S. L., Solvent design for crystallization of carboxylic acids, *Computers Chem. Eng.*, 2009, **33**, 1014-1021.
- Garces, F.; Galindo, H. M.; Garces, J.; Hunt, J.; Morey, A.; Suib, S. L., Low Temperature H<sub>2</sub>S Dry-Desulfurization with Zinc Oxide, *Micr. Mesopor. Mat.*, 2010, **127**, 190-197.
11. Jin, L.; Reutenauer, J.; Opembe, N.; Lai, M.; Martenak, D. J.; Han, S.; Suib, S. L., Studies on Dehydrogenation of Ethane in the Presence of CO<sub>2</sub> over Octahedral Molecular Sieve (OMS-2) Catalysts, *ChemCatChem.*, 2009, **1**, 441-444.

12. Espinal, A.; Zhang, L.; Chen, C. H.; Morey, A.; Nie, Y.; Espinal, L.; Wells, N. O.; Joesten, R.; Aindow, M.; Wells, B.; Suib, S. L. Nanostructured arrays of semiconducting octahedral molecular sieves by pulsed laser deposition, *Nature Materials*, 2009, **9**, 54-59.
13. Li, X.; Hu, B.; Suib, S. L.; Lei, Y.; Li, B., Manganese Dioxide as a New Cathode Catalyst in Microbial Fuel Cells (MFC), *J. Power Sources*, 2010, **195**, 2586-2591.
14. Iyer, A.; Galindo, H.; Sithambaram, S.; King'onde, C.; Chen, C. H.; Suib, S. L., Nanoscale Manganese Oxide Octahedral Molecular Sieves (OMS-2) as Efficient Photocatalysts in 2-propanol Oxidation, *Appl. Catal. A: General*, 2010, **375**, 295-302.
15. Chen, C. H.; Njagi, E.; Sun, S. P.; Genuino, H.; Hu, B.; Suib, S., Hydrophobic Polymer Coated Metal Oxide Catalysts for Effective Low Temperature Oxidation of CO under Moisture-Rich Conditions, *Chem. Mat.*, 2010, **22**, 3313-3315.
16. Zhang, X.; Galindo, H. M.; Garces, H. F.; Baker, P.; Wang, X.; Pasaogullari, U.; Suib, S. L.; Molter, T., Influence of Formic Acid Impurity on Proton Exchange Membrane Fuel Cell Performance, *J. Electrochem. Soc.*, 2010, **157**, B409-B414.
17. Chen, C. H.; Jin, L.; Espinal, A. E.; Firliet, B. T.; Xu, L.; Aindow, M.; Joesten, R.; Suib, S. L., Heteroepitaxial Growth of Nanoscale Oxide Shell/Fiber Superstructures by Mild Hydrothermal Processes, *Small*, 2010, **6**, 988-992.
18. Hu, B.; Chen, C. H.; Frueh, S.; Jin, L.; Joesten, R.; Suib, S. L., Removal of Aqueous Phenol by Adsorption and Oxidation with Doped Hydrophobic Cryptomelane-Type Manganese Oxide (K-OMS-2) Nanofibers, *J. Phys. Chem. C*, 2010, **114**, 9835-9844.
19. Hu, B.; Stancovski, V.; Morton, M.; Suib, S. L., Enhanced Electrocatalytic Reduction of CO<sub>2</sub>/H<sub>2</sub>O to Paraformaldehyde at Pt/Metal Oxide Interfaces, *Appl. Catal., A: General*, 2010, **382**, 277 - 283.
20. Huang, H.; Sithambaram, S.; Chen, C. H.; King'onde Kithongo, C.; Xu, L.; Iyer, A.; Garces, H.; Suib, S. L., Microwave-assisted Hydrothermal Synthesis of Cryptomelane-type Octahedral Molecular Sieves (OMS-2) and Their Catalytic Studies, *Chem. Mater.*, 2010, **22**, 3664-3669.
21. Zhang, X.; Galindo, H. M.; Garces, H. F.; Baker, P.; Wang, X.; Pasaogullari, U.; Suib, S. L.; Molter, T., Influence of formic acid impurity on proton exchange membrane fuel cell performance, *ECS Trans.*, 2009, **25**, 1633-1644.
22. Njagi, E.; Chen, C. H.; Genuino, H.; Galindo, H.; Huang, H.; Suib, S. L., Total oxidation of CO at ambient temperature using copper manganese oxide catalysts prepared by a redox method, *Appl. Catal. B*, 2010, **99**, 103-110.
23. Huang, H.; Chen, C. H.; Xu, L.; Genuino, H.; Garcia-Martinez, J.; Garces, H. F.; Jin, L.; King'onde Kithongo, C.; Suib, S. L., Single-Step Synthesis of Manganese Oxide Octahedral Molecular Sieves with Large Pore Sizes, *J. Chem. Soc. Chem. Comm.*, 2010, **46**, 5945-5947.
24. Sithambaram, S.; Suib, S. L., H<sub>2</sub> Production Through the Water-gas-shift Reaction: an in situ Time-resolved X-ray Diffraction Investigation of Manganese OMS-2 Catalyst Catalysis Today, *Catal. Today*, 2010, **156**, 2-7.
25. Galindo, H.; Suib, S. L., Sulfonation of the surface of cordierite monoliths through a novel multi-step wet chemical process, *Micropor. Mesopor. Mat.*, 2010, **135**, 37-44.

26. Jin, Lei; Xu, L.; Morein, C.; Chen, C. H.; Lai, M.; Dharmarathna, S.; Doble, A.; Suib, S. L., Titanium Containing  $\gamma$ -MnO<sub>2</sub> (TM) Hollow Spheres: One-step Synthesis and Catalytic Activities in Li/Air Batteries and Oxidative Chemical Reactions, *Adv. Funct. Mat.*, 2010, **20**, 3373-3382.
27. Galindo, H.; Carvajal, Y.; Njagi, E.; Ristau, R.; Suib, S. L., A facile one-step template-free synthesis of uniform hollow microstructures of cryptomelane-type manganese oxide K-OMS-2, *Langmuir*, 2010, **26**, 13677-13683.
28. Opembe, N. King'onde, C.; Nyutu, E.; Espinal, A.; Chen, C. H.; Crisostomo, V. M., Suib, S. L., Microwave-Assisted Synthesis of Manganese Oxide Octahedral Molecular Sieves (OMS-2) Nanomaterials under Continuous Flow Conditions, *J. Phys. Chem. C*, 2010, **114**, 14417-14426.
29. Ruettinger, W.; Benderly, A.; Han, S.; Shen, X.; Ding, Y.; Suib, S. L., Influence of support surface area and niobium addition on the reactivity of vanadium catalysts for propane oxidative dehydrogenation, *Catal. Lett.*, 2011, **141**, 15-21.
30. Gulbinska, M.; Suib, S. L. Vanadium-Substituted Porous Manganese Oxides with Li-ion Intercalation Properties, *J. Power Sources*, 2011, **196**, 2149-2154.
31. Durand, Jason; Senanayake, Sanjaya; Suib, Steven; Mullins, David, The Reaction of Formic Acid over Amorphous Manganese Oxide Catalytic Systems: An *In-Situ* Study, *J. Phys. Chem. C*, 2010, **114**, 20000-20006.
32. Genuino, H.; Njagi, E. C.; Benbow, E. V.; Horvath, D. T.; Hoag, G. E.; Collins, J. B.; Suib, S. L.; Enhancement of the Photodegradation of N-nitrosodimethylamine in Water Using Amorphous and Platinum Manganese Oxide Catalysts, *J. Photochem. Photobiol. A: Chem.*, 2011, **217**, 284-92.
33. Frueh, S.; Kellett, R.; Mallery, C.; Molter, T.; Willis, W.; King'onde, C.; Suib, S., Pyrolytic Decomposition of Ammonia Borane to Boron Nitride, *Inorg. Chem.*, 2011, **50**, 783-792.
34. King'onde, C.; Iyer, A.; Njagi, E.; Opembe, N.; Genuino, H.; Huang, H.; Ristau, R.; Suib, S., Light-Assisted Synthesis of Metal Oxide Hierarchical Structures and Their Catalytic Applications, *J. Am. Chem. Soc.*, 2011, **133**, 4186-4189.
35. Jiang, D.; Curtis, M.; Troop, E.; Scheible, K.; McGrath, J.; Hu, B.; Suib, S.; Raymond, D.; Li, B., A pilot scale study on utilizing multi-anode/cathode microbial fuel cells (9MAC MFCs) to enhance The power production in waste water treatment, *Int. J. of Hydrogen Energy*, 2011, **36**, 876-884.
36. King'onde, C. K.; Opembe, N.; Chen, C. – H.; Ngala, K.; Huang, H.; Iyer, A.; Garces, H. F.; Suib, S. L., Manganese Oxide Octahedral Molecular Sieves (OMS-2) Multiple Framework Substitutions: A New Route to OMS-2 Particle Size and Morphology Control, *Adv. Funct. Mat.*, 2011, **21**, 312-323.

37. Njagi, E.; Suib, S. L., Preferential oxidation of CO in H<sub>2</sub>-rich feeds over mesoporous copper manganese oxides synthesized by a redox method, *Int. J. Hydrogen Energy*, 2011, in press.
38. Arshadia, M.; Ghiacia, M.; Ensafia, A. A.; Karimi-Maleha, H.; Suib, S. L. Oxidation of ethylbenzene using some recyclable cobalt nanocatalysts: The role of linker and electrochemical study, *J. Mol. Catal.*, 2011, 338, 71-83.
39. Xing, Y.; Khare, G. P.; Suib, S. L., Deactivation of Pt/F-KL Zeolite-type Naphtha Reforming Catalysts: in-situ IR and on-line Mass Spectrometry Studies of Fluorine Loss, *J. Appl. Catal., A*, 2011, in press.
40. Li, X.; Hu, B.; Suib, S.; Lei, Y.; Li, B., Electricity generation in continuous flow Microbial fuel cells (MFCs) with manganese dioxide (MnO<sub>2</sub>) cathodes, *Biochem. Eng. J.*, 2011, **54**, 10-15.



### Ultrafast and Chemically Specific Microscopy for Atomic Scale Imaging of Nano-Photocatalysis

**Contacts:** P. Sutter, Nanoscience Department and Center for Functional Nanomaterials  
Brookhaven National Laboratory, Upton, NY 11973  
Phone: (631) 344-4412; Email: [psutter@bnl.gov](mailto:psutter@bnl.gov)  
N. Camillone, Chemistry Department  
Brookhaven National Laboratory, Upton, NY 11973  
Phone: (631) 344-4412; Email: [nicholas@bnl.gov](mailto:nicholas@bnl.gov)

#### Goal

This program's objective is to develop and apply novel techniques to understand photocatalytic reactions at the single-electron and individual-molecule level. Our work focuses on combining subnanometer spatial resolution, subpicosecond temporal resolution and chemical specificity, to study in unprecedented detail the links between optical and electronic excitation, charge and energy transfer, and the resulting reactions that underlie heterogeneous photocatalysis.

#### DOE Interest

This effort addresses the long-standing challenge of characterizing chemical transformations with simultaneous temporal, spatial and chemical resolution at the molecular level. We are working to understand photoinduced processes on nanostructures and model catalyst surfaces by (1) mapping the dynamics of nonequilibrium charge populations ("hot carriers") and the chemical reactions they drive, and (2) identifying chemical species on photocatalysts and investigating the mechanisms of their non-thermal, electron-mediated chemistry. Because photoinduced heterogeneous catalysis depends on the transfer of charge or energy from the photoexcited catalyst to an adsorbate molecule, its efficiency depends on the hot-carrier relaxation rate near the binding site, the cross section for electron (or hole) capture into adsorbate affinity levels, and the lifetime of the electronic excitation of the adsorbate. Our effort is aimed at breaking new ground in probing these fundamental mechanistic steps to contribute to the rational design of next-generation materials for solar photocatalysis.

#### Recent Progress

##### 1. Ultrafast Scanning Tunneling Microscopy

To probe hot-carrier dynamics with near-atomic resolution, we have been developing a new laser-based approach to time-resolved scanning tunneling microscopy (STM). The idea of observing laser-stimulated phenomena with atomic resolution has been pursued since the invention of STM; recent work has suggested that femtosecond laser excitation of the tip-sample junction may enable probing ultrafast dynamic phenomena. However, truly simultaneous subpicosecond- and subnanometer-resolved measurements have proven elusive to date.

We have recently demonstrated a new method for simultaneous sub-ps and sub-nm surface electron

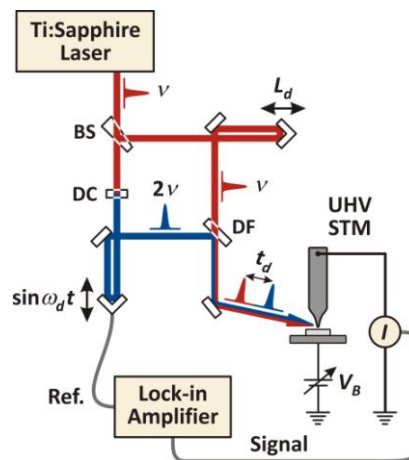


**FIG. 1.** Schematic of our two-color cross-correlation setup. The Ti:Sapphire oscillator output is split, frequency doubled, recombined, and focused onto the tip-sample junction. Modulation of the optical delay and lock-in amplification enables extraction of the photoexcited current signal from the conventional tunneling current.

dynamics measurements by ultrafast-laser-excited STM. Our approach involves ultrafast-laser two-color two-photon excitation of a metal surface detected using the STM tip as a proximate anode (Fig. 1). We have shown that a delay modulation technique effectively isolates the two-photon photoexcited current from the conventional tunneling current enabling sub-ps time-resolved detection of photoexcited surface electrons. When applied with the tip in tunneling range, the two-color approach has the unique advantage of completely eliminating parasitic effects due to optical interference and thermal expansion that have historically hindered photoexcited time-resolved STM on timescales of the order of the incident laser pulses. The successful demonstration of this approach represents an important step toward simultaneous spatially and ultrafast time-resolved measurements.

Application of the two-color method to time-resolved photoassisted imaging of a silver nanoparticle (Fig. 2) demonstrates that simultaneous sub-ps temporal and sub-nm spatial resolution can be achieved—local detection of ultrafast surface electron dynamics by STM is feasible. Our observations are consistent with highly-localized field enhancements, but further study is required to understand the mechanism(s) at play and generalize the approach. Extension of this work to measuring electron dynamics in individual nanoparticles is well within reach, as is the spatial mapping of the surface electron dynamics of other nanostructures

## 2. Site-Specific Electron-Mediated Surface Chemistry

The STM can be used to inject charge carriers with well-defined energy into individual surface sites and adsorbates. We are using local charge injection at cryogenic temperatures combined with temperature-dependent imaging to investigate electron-mediated reactions in model systems relevant to heterogeneous photocatalytic water splitting and CO<sub>2</sub> reforming. Specifically, we have characterized the adsorption, thermal and electron-mediated diffusion, dissociation and desorption of various species (H, OH, H<sub>2</sub>O, and CO<sub>2</sub>) on rutile TiO<sub>2</sub>(110).

For example, our studies of H-atom desorption from bridging hydroxyls on TiO<sub>2</sub>(110) at 77 K have addressed long-standing mechanistic questions regarding this model system. Based on

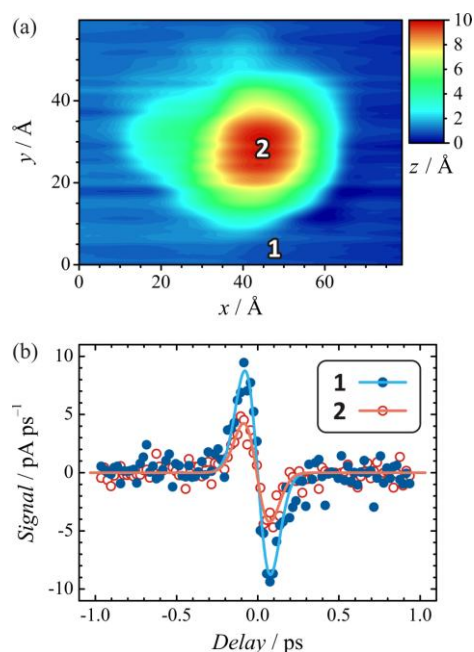


**FIG. 2.** (a) STM topograph of a silver particle atop a Ag(111) surface. (b) Two-color cross-correlation measurements made with subpicosecond pulses near (point 1) and atop (point 2) the particle. The marked dependence of the signal level on both tip location and optical delay shows that simultaneous subpicosecond temporal and subnanometer spatial resolution is achieved.

study is required to understand the mechanism(s) at play and generalize the approach. Extension of this work to measuring electron dynamics in individual nanoparticles is well within reach, as is the spatial mapping of the surface electron dynamics of other nanostructures

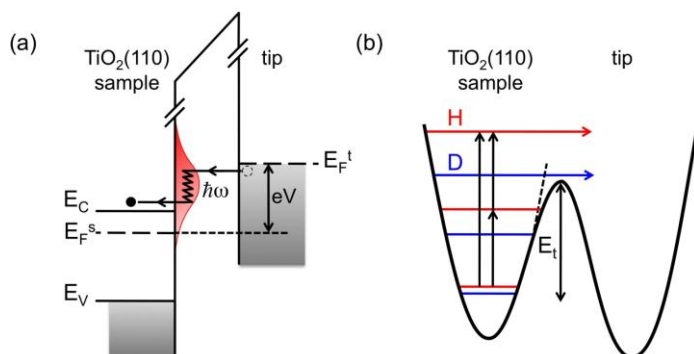


**FIG. 3.** Schematics of (a) vibrational excitation by inelastic tunneling on a wide-bandgap oxide, and (b) the vibrational “ladder-climbing” responsible for H/D desorption. Electron injection from the STM tip into empty states of the sample at energy  $eV$  promotes the H (or D) to vibrationally-excited states above the activation barrier ( $E_t$ ) for surface–tip atom transfer.

extensive measurements of the desorption-yield dependence on current, voltage and isotope, we have identified the electron-mediated desorption as due to atom transfer from the surface to the STM tip triggered by excitation of the O–H stretch by inelastic one- and two-electron tunneling (Fig. 3). The highly efficient removal of H atoms under moderate conditions can be used as a tool to distinguish the H atoms from other adsorbates and defects, and opens new avenues for atomic-scale control of the H-atom population by selective H-atom removal and redeposition.

We have also studied the adsorption, diffusion, thermal desorption and electron-mediated reactions of CO<sub>2</sub> on TiO<sub>2</sub>(110). Our measurements show that at cryogenic temperatures CO<sub>2</sub> adsorbs molecularly with three distinct geometries: one atop five-fold coordinated Ti sites (Ti<sub>5f</sub>) and two—one symmetric and one asymmetric—at the bridging oxygen vacancy sites (V<sub>O,br</sub>). Analysis of detailed time-resolved images of the thermal diffusion has led us to infer that there is an activation barrier that effectively isolates the Ti<sub>5f</sub>- and V<sub>O,br</sub>-adsorbed CO<sub>2</sub> populations. Our STM images provide direct real-space evidence supporting understanding of the thermal desorption derived from less direct methods, and site population analysis has provided new insight into the adsorption dynamics. Significantly, injection of tunneling electrons at elevated electron energies was found to lead to healing of oxygen vacancies (Fig. 4) as a by-product of electron-mediated CO<sub>2</sub> reduction, a process that is not thermally activated up to the desorption temperature.

### Future Plans

We are working toward sub-ps local-probe investigations of size-dependent hot-carrier dynamics in and spatially-resolved photocatalysis on oxide-supported metal nanoparticles. We will investigate water splitting and related chemistries on metal oxides and oxide-supported metal nanoparticles. Combining ultrafast laser excitation, local electronic excitation probing, local charge injection and STM imaging, we will be uniquely positioned to study reaction dynamics relevant to a fundamental understanding of electron/hole and molecular dynamics at regular lattice sites, defect sites, and on supported nanoparticles. Ultimately we aim to understand the fundamental connections relating photocatalyst structure, thermal and non-thermal excitation, carrier dynamics and reaction efficiency and selectivity.

### Publications

1. D. P. Acharya, N. Camillone III, and P. Sutter, “CO<sub>2</sub> Adsorption, Diffusion, and Electron-Induced Chemistry on Rutile TiO<sub>2</sub>(110): A Low-Temperature Scanning Tunneling Microscopy Study,” *J. Phys. Chem. C*, **in press** (2011).
2. A. Dolocan, D. P. Acharya, P. Zahl, P. Sutter, and N. Camillone III, “Two-Color Ultrafast Photoexcited Scanning Tunneling Microscopy,” *J. Phys. Chem. C*, **115**, 10033 (2011).
3. D. P. Acharya, C. V. Ciobanu, N. Camillone III, and P. Sutter, “Mechanism of Electron-Induced Hydrogen Desorption from Hydroxylated Rutile TiO<sub>2</sub>(110),” *J. Phys. Chem. C*, **114**, 21510 (2010).

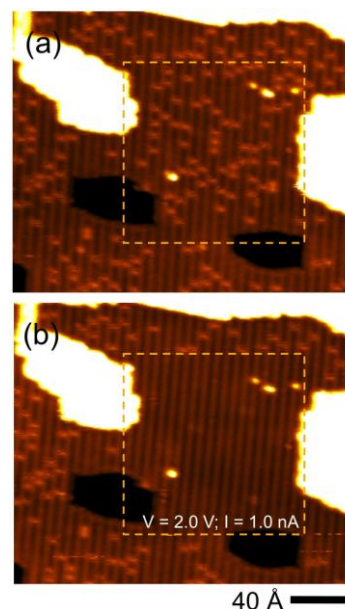


**FIG. 4.** Electron-stimulated healing of oxygen vacancies by reaction with adsorbed CO<sub>2</sub>. (a) STM image of CO<sub>2</sub> bound to oxygen vacancies on TiO<sub>2</sub>(110). (b) Same sample area, imaged after scanning the outlined region at V = 2.0 V, I = 1.0 nA. (Imaging conditions: V = 1.2 V, I = 0.25 nA, T = 140 K.)

## Chemistry on Base-Metal Oxide Nanostructures on Oxide Substrates: A Model System Approach

Postdoc: Kumudu Mudiyansele

Collaborators: Ja Hun Kwak (PNNL), Donghai Mei (PNNL), Chuck H.F. Peden (PNNL), Jason F. Weaver (U. Florida), Larry F. Allard (ORNL), Cheol Woo Yi (Sungshin Women's University, S.Korea)

Contacts: Pacific Northwest National Laboratory, 902 Battelle Blvd, MSIN: K8-83, Richland, WA 99352, [janos.szanyi@pnnl.gov](mailto:janos.szanyi@pnnl.gov)

### Goal

To develop fundamental understanding of the chemistry (specifically  $\text{CO}_x$  and  $\text{NO}_x$ ) on base metal oxide nanostructures supported on metal and metal oxide substrates. Use high resolution spectroscopy/microscopy techniques in combination with theory to elucidate the nature of defect sites on alumina support materials, and their roles in the phase stability, active catalyst component anchoring and stabilization, as well as in catalytic chemistry.

### DOE Interest

Beside the fundamental scientific importance of understanding the interactions of molecules with base-metal oxides, there are a number of practical reasons these studies support the mission of DOE. The results of these investigations help understanding how environmental pollutants (e.g.  $\text{CO}_x$ ,  $\text{NO}_x$ ) interact with oxide nanostructures. In order to design tailor made catalysts for specific reactions it is critical to learn how active catalyst components anchor and get stabilized on the surfaces of support materials. On the practical side, the recent advances in lean  $\text{NO}_x$  technologies (in particular  $\text{NO}_x$  storage/reduction) may promote the widespread use of highly fuel efficient diesel and lean-burn gasoline engines. Understanding of the chemistry on and the structure of base-metal oxide-based catalyst systems is critical in the development of highly efficient catalysts.

### Recent Progress

**BaO-based Model Systems:** *Oxygen on BaO/Pt(111):* The formation of adsorbed O ( $\text{O}_{\text{ad}}$ ) species and their reactivities in CO oxidation on BaO/Pt(111) (at two BaO coverages) were studied. In neither of these two systems was the Pt(111) surface completely covered with BaO. At lower BaO coverage (~45 % of the Pt(111) surface is covered by BaO), two different  $\text{O}_{\text{ad}}$  species form following the adsorption of  $\text{O}_2$  at 300 K: O adsorbed on BaO-free Pt(111) sites ( $\text{O}_{\text{Pt}}$ ) and at the Pt-BaO interface ( $\text{O}_{\text{int}}$ ). At higher BaO coverage (~60 % of the Pt(111) surface is covered by BaO), two types of  $\text{O}_{\text{int}}$  are seen at the Pt-BaO interface. The desorption of  $\text{O}_{\text{Pt}}$  from the BaO-free portion of the Pt(111) surface gives an  $\text{O}_2$  desorption peak with a maximum desorption rate at ~690 K. Migration of  $\text{O}_{\text{int}}$  to the Pt(111) sites and their recombinative desorption give two explosive desorption features at ~760 and ~790 K in the TPD spectrum. The reactivities of these  $\text{O}_{\text{ad}}$  species with CO to form  $\text{CO}_2$  follow their sequence of desorption; i.e., the  $\text{O}_{\text{Pt}}$  associated with the BaO-free Pt(111) surface, which desorbs at 690 K, reacts first with

CO, followed by the  $O_{\text{int}}$  species at the Pt-BaO interface (first the one that desorbs at  $\sim 760$  K and finally the one that is bound the most strongly to the interface, and desorbs at  $\sim 790$  K).

*$NO_2$  on  $Ba(OH)_2/Pt(111)$ :* The interaction of  $NO_2$  with amorphous and crystalline  $Ba(OH)_2$  supported on Pt(111) was studied in the wide pressure range of  $1.0 \times 10^{-9} - 1.0 \times 10^{-4}$  Torr and compared to that with a thick ( $> 20$  monolayer equivalent (MLE)) BaO film. The amorphous and crystalline  $Ba(OH)_2$  layers were prepared by exposing a thick BaO ( $> 20$  MLE) layer on Pt(111) to  $H_2O$  at 300 and 425 K, respectively. The amorphous and crystalline  $Ba(OH)_2$  layers partially convert to  $Ba(NO_x)_2$  (nitrites and nitrates) following their exposure to elevated  $NO_2$  pressure ( $\sim 1.0 \times 10^{-4}$  Torr) at 300 K. The exposure of the crystalline- $Ba(OH)_2/Pt(111)$  system to  $NO_2$  at 425 K, however, leads to the desorption of  $H_2O$  and the complete conversion of the crystalline  $Ba(OH)_2$  layer to  $Ba(NO_x)_2$ , which consists of mainly crystalline nitrates and a small amount of nitrites. The amounts of  $NO_x$  stored by BaO ( $> 20$  MLE)/Pt(111) and crystalline  $Ba(OH)_2/Pt(111)$  systems upon their exposure to  $NO_2$  at 425 K are comparable. The thus-formed bulk crystalline  $Ba(NO_3)_2$  phase decomposes in two steps, both releasing NO and  $O_2$ , in accord with the melting/decomposition scheme for bulk  $Ba(NO_3)_2$ .

*Reduction of  $Ba(NO_3)_2/Pt(111)$  with CO:* The decomposition of  $Ba(NO_3)_2$  formed on BaO/Pt(111) (Pt(111) surface is partially covered by BaO) in the presence of CO was studied. The exposure of BaO/Pt(111) to elevated  $NO_2$  pressure ( $1.0 \times 10^{-4}$  Torr) at 450 K leads to the formation of  $Ba(NO_3)_2$ , chemisorbed O ( $O_{\text{Pt}}$ ) and Pt-oxide-like domains. During TPD, the  $Ba(NO_3)_2$  begins to thermally decompose near 490 K, releasing NO and  $NO_2$  with the maximum  $NO_x$  desorption rate seen at 605 K. The  $O_{\text{Pt}}$  species formed following the exposure of BaO/Pt(111) to  $NO_2$  react with CO to release  $CO_2$  at 450 K. The consumption of  $O_{\text{Pt}}$  during CO oxidation initiates the migration of O from the Pt-oxide-like domains to the chemisorbed phase, where the CO oxidation reaction occurs. Therefore, the removal of  $O_{\text{Pt}}$  by CO leads to the reduction of oxidized Pt, and to the formation of metallic Pt(111) domains, where, subsequently, catalytic decomposition of  $Ba(NO_3)_2$  can take place. The Pt-catalyzed decomposition of  $Ba(NO_3)_2$  occurs readily at 450 K, a temperature much lower than the onset of  $Ba(NO_3)_2$  decomposition in the presence of oxidized Pt.

**High Surface Area Pt/ $\gamma$ - $Al_2O_3$  Catalysts:** *Anchoring and Stability of Pt on  $\gamma$ - $Al_2O_3$ :* We used a combination of ultrahigh magnetic field, solid-state magic-angle spinning nuclear magnetic resonance spectroscopy, and high-angle annular dark-field scanning transmission electron microscopy coupled with density functional theory calculations to reveal the nature of anchoring sites of a catalytically active phase of platinum on the surface of a  $\gamma$ - $Al_2O_3$  catalyst support material. The results obtained show that coordinatively unsaturated pentacoordinate  $Al^{3+}$  ( $Al^{3+}_{\text{penta}}$ ) centers present on the (100) facets of the  $\gamma$ - $Al_2O_3$  surface are anchoring Pt. At low loadings, the active catalytic phase is atomically dispersed on the support surface ( $Pt/Al^{3+}_{\text{penta}} = 1$ ), whereas two-dimensional Pt rafts form at higher coverages. HRTEM and EXAFS measurements combined with theoretical DFT calculations show that  $Al^{3+}_{\text{penta}}$  sites on the  $\gamma$ - $Al_2O_3(100)$  surface can inhibit Pt sintering both thermodynamically and kinetically due to its strong interactions with atomic Pt or Pt oxide species.

## Future Plans

*Preparation and  $CO_2$  chemistry on model  $CeO_x$ /metal catalysts:*  $CeO_x$  thin films with different extent of reduction will be prepared on metal single crystals (Pt(111), Ru(0001), and Au(111))

and investigated in their interactions with CO<sub>2</sub>. The new focus of the program is to understand the fundamentals of the interaction between CO<sub>2</sub> and reducible oxides critical in CO<sub>2</sub> activation.

*Metals on  $\gamma$ -Al<sub>2</sub>O<sub>3</sub>*: The anchoring and chemical reactivities of transition metals, other than Pt, will be studied on  $\gamma$ -Al<sub>2</sub>O<sub>3</sub> in order to learn about the catalytic chemistry of oxide supported metal catalysts when the metal distribution approaches the atomic level. The focus of this work will be on CO<sub>2</sub> activation.

### Publications (2009-2011)

1. Reactivity of a Thick BaO Film Supported on Pt(111): Adsorption and Reaction of NO<sub>2</sub>, H<sub>2</sub>O, and CO<sub>2</sub>, Mudiyanselage K, Yi CW, Szanyi J, **Langmuir**, **25**, 10820-10828, (2009)
2. Coordinatively Unsaturated Al<sup>3+</sup> Centers as Binding Sites for Active Catalyst Phases of Platinum on gamma-Al<sub>2</sub>O<sub>3</sub>, Kwak JH, Hu JZ, Mei D, Yi CW, Kim DH, Peden CHF, Szanyi J, **Science**, 1670-1673, (2009)
3. Catalyst size and morphological effects on the interaction of NO<sub>2</sub> with BaO/gamma-Al<sub>2</sub>O<sub>3</sub> materials, Mei DH, Kwak JH, Szanyi J, Peden CHF, **Catalysis Today**, **151**, 304-313, (2010)
4. Unique Role of Anchoring Penta-Coordinated Al<sup>3+</sup> Sites in the Sintering of gamma-Al<sub>2</sub>O<sub>3</sub>-Supported Pt Catalysts, Mei DH, Kwak JH, Hu JZ, Szanyi J, Peden CHF, **Journal of Physical Chemistry Letters**, **1**, 2688-2691, (2010)
5. Reactions of NO<sub>2</sub> with Ba(OH)<sub>2</sub> on Pt(111), Mudiyanselage K, Yi CW, Szanyi J, **Journal of Physical Chemistry C**, **114**, 16955-16963, (2010)
6. Formation, Characterization, and Reactivity of Adsorbed Oxygen on BaO/Pt(111), Mudiyanselage K, Mei DH, Yi CW, Weaver JF, Szanyi J, **Journal of Physical Chemistry C**, **114**, 20195-20206 (2010)
7. Catalytic Decomposition of Ba(NO<sub>3</sub>)<sub>2</sub> on Pt(111), Mudiyanselage K, Weaver JF, Szanyi J, **Journal of Physical Chemistry C**, **115**, 5903-5909, (2011)
8. Reactions of NO<sub>2</sub> with BaO/Pt(111) Model Catalysts: The Effects of BaO Film Thickness and NO<sub>2</sub> Pressure on the Formation of Ba(NO<sub>x</sub>)<sub>2</sub> Species, Mudiyanselage K, Yi C, Szanyi J, **Phys. Chem. Chem. Phys.**, **13**, 11016 – 11026, (2011)
9. (100) facets of  $\gamma$ -Al<sub>2</sub>O<sub>3</sub>: The Active Surfaces for Alcohol Dehydration Reactions, Kwak JH, Mei DH, Peden CHF, Rosseau R, Szanyi J, **Catalysis Letters**, **141**, 649-655 (2011)
10. Using a Surface-Sensitive Chemical Probe and a Bulk Structure Technique to Monitor the  $\gamma$ - to  $\theta$ -Al<sub>2</sub>O<sub>3</sub> Phase transformation, Kwak JH, Peden CHF, Szanyi J, **Journal of Physical Chemistry C**, DOI 10.1021/jp203541a

## **Metal—Organic Surface Catalyst for Low-temperature Methane Oxidation: Bi-functional Union of Metal—Organic Complex and Chemically Complementary Surface**

Steven L. Tait

Indiana University, Department of Chemistry, Bloomington, Indiana 47405

e-mail: [tait@indiana.edu](mailto:tait@indiana.edu)

Metal-organic complexes at surfaces provide an efficient route to homogeneous, undercoordinated metal sites at a solid surface. The self-assembly and structure of these systems have been studied with growing interest in recent years, but most of these studies have focused on structural characterization.<sup>1-5</sup> We are working to develop catalytic function from these systems. This project explores new possibilities in catalysis by combining features of homogeneous catalysts with those of heterogeneous catalysts to develop new, bi-functional systems. The surface supported metal-organic complexes are structurally and chemically similar to complexes used in homogeneous catalysts. The addition of a solid support serves two purposes. First, the support can play a catalytic role in preliminary steps of the target reaction. Second, stabilizing the catalyst complex at the solid support allows us to combine the selectivity (tuning) of a ligand coordinated metal complex with the facile recovery inherent in a homogeneous catalyst. We study the interactions of metal—organic catalysts with surface supports and their interactions with reactants to enable the catalysis of critical reactions at lower temperatures. The initial focus of this research program is the methane oxidation reaction. This project addresses several fundamental chemistry problems in these systems. How do the metal—organic complexes interact with the surface? Can those metal center sites be tuned for selectivity and activity, as they are in the homogeneous system, by ligand design? What steps are necessary to enable a cooperative chemistry to occur and open opportunities for bi-functional catalyst systems? Study of these systems will develop the concept of bringing together the advantages of heterogeneous catalysis with those of homogeneous catalysis, and take this a step further by pursuing the objective of a bi-functional system.

1. Langner, A.; Tait, S. L.; Lin, N.; Rajadurai, C.; Ruben, M.; Kern, K., *Proceedings Of The National Academy Of Sciences Of The United States Of America* **2007**, *104* (46), 17927-17930.
2. Lin, N.; Langner, A.; Tait, S. L.; Rajadurai, C.; Ruben, M.; Kern, K., *Chemical Communications* **2007**, 4860-4862.
3. Tait, S. L.; Wang, Y.; Costantini, G.; Lin, N.; Baraldi, A.; Esch, F.; Petaccia, L.; Lizzit, S.; Kern, K., *Journal Of The American Chemical Society* **2008**, *130* (6), 2108-2113.
4. Tseng, T.-C.; Lin, C.; Shi, X. Q.; Tait, S. L.; Liu, X.; Starke, U.; Lin, N.; Zhang, R. Q.; Minot, C.; Vanhove, M. A.; Cerda, J. I.; Kern, K., *Physical Review B* **2009**, *80*, 155458.
5. Lingenfelder, M. A.; Spillmann, H.; Dmitriev, A.; Stepanow, S.; Lin, N.; Barth, J. V.; Kern, K., *Chemistry-A European Journal* **2004**, *10* (8), 1913-1919.

## Integration of Operando Studies into Nanocatalysis for Efficient Energy Conversion

Franklin (Feng) Tao

Department of Chemistry and Biochemistry, University of Notre Dame, Notre Dame, IN 46556

Email: [ftao@nd.edu](mailto:ftao@nd.edu)

Catalysis plays a crucial role in energy conversion. Heterogeneous catalysis occurs on surfaces of catalysts at an ambient or high temperature in reactant gases at ambient or high pressure, or at solid-liquid interfaces. The relationship between chemistry and structure of catalyst surfaces during operation and their catalytic performance needs to be established in order to understand the mechanisms at work and to enable the design of new and better catalysts. Although studies of the structure, composition, chemical state, and phase transformation during pretreatment and under working conditions are challenging, progress in the development of new techniques that operate under a variety of reactive environments has been made in recent years. In the development of techniques capable of operando studies, we designed in-house ambient pressure XPS and ambient pressure STM for exploring chemistry and structure of catalyst surfaces under reaction conditions. These operando techniques available in our group are integrated into our studies of catalysis including production of clean energy and conversion of sustainable energy sources to liquid fuels. Examples of the operando studies of catalysis using AP-XPS and AP-STM will be presented. Different surface chemistry and structure of catalysts in contrast to those attained at an ex-situ condition will be discussed. With the information obtained from operando studies, the active phases and catalytic sites responsible for catalysis can be identified. Such information on the active phases and reactive sites will provide a “goal” for tuning synthesis and designing efficient catalysts.

### References

1. F. Tao, M. Salmeron, *Science* 331 (2011) 171-174.
2. B. Sun, et al. *ChemCatChem* 3 (2011) 542-545.



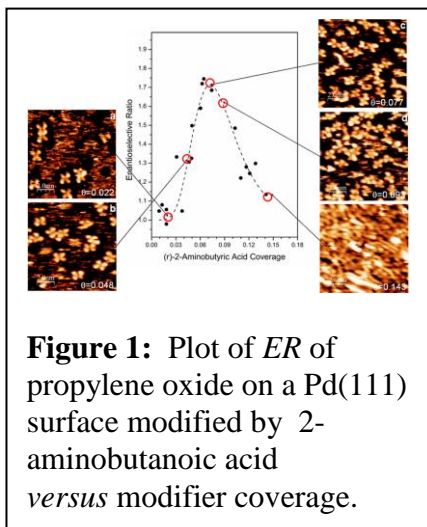
## Molecular-level Design of Heterogeneous Chiral Catalysts

Lead PI: Andrew Gellman

Postdoc: Luke Burkholder, Yun Bai

Student : Zhenjun Li, Michael Garvey, Mausumi Mahapatra

Contact: Department of Chemistry and Biochemistry, University of Wisconsin-Milwaukee, 3210 N Cramer Street, Milwaukee, WI 53211; wtt@uwm.edu



We have explored the surface chemistry of various chiral modifiers, chiral probes and prochiral reactants on single crystal surfaces in ultrahigh vacuum to identify the mode of chiral modification. This has been proposed to occur either via a templating mechanism, in which several chiral modifying molecules act in concert to provide a chiral reaction site, or via a one-to-one interaction to form a docking complex between the modifier and prochiral reactant. It has been found, by correlating the chemisorptive enantioselectivity of propylene oxide on various aminoacid-modified surfaces with the structures formed on the surface using scanning-tunneling microscopy that tetrameric units of aminocids formed on the surface provide ensembles that act as chiral

templates. Confirming this conclusion, the data in Fig. 1 reveals that the number of such tetrameric units increases as the enantioselectivity increases, but then starts to decrease as the aminoacid coverage increases further to cause the tetramers to coalesce as the surface forms a saturated overlayer. Similar experimntnal stratgies are used to explore one-to-one interactions with  $\alpha$ -1-(1-Naphthylethylamine) on Pd(111).

## References

1. Luke Burkholder, Darío Stacchiola, Jorge. A. Boscoboinik and Wilfred. T. Tysoe, Enantioselective Chemisorption on Model Chirally Modified Surfaces: 2-Butanol on  $\alpha$ -1-(1-Naphthylethylamine)/Pd(111), *J. Phys. Chem C.*, **113**, 13877-13885 (2009)
2. L. Burkholder and W. T. Tysoe. Structure and Reaction Pathways of Methyl Pyruvate on Pd(111), *J. Phys. Chem. C.*, **113**, 15298-15306 (2009)
3. Luke Burkholder and Wilfred. T. Tysoe, Structure and Reaction Pathways of Methyl Lactate on Pd(111), *Surf. Sci.*, **603**, 2714-2720 (2009)
4. Luke Burkholder, Michael Weinert, Michael Garvey, Wilfred. T. Tysoe, Structure of Methyl Pyruvate and  $\alpha$ -(1-Naphthyl)ethylamine on Pd(111), *J. Phys. Chem. C.*, **115**, 8790-8797 (2011)
5. Jorge A. Boscoboinik, Yun Bai, Luke Burkholder and Wilfred T. Tysoe, Structure and Distribution of S- $\alpha$ -(1-Naphthyl)-Ethylamine on Pd(111), *J. Phys. Chem C.*, **33**, 16488-16494 (2011)

### Fundamental Studies of the Steam Reforming of Alcohols on Pd/ZnO and Co/ZnO Catalysts

Students: Eddie Martono  
Collaborators: Abhaya Datye (University of New Mexico), Yong Wang (Pacific Northwest National Laboratory).  
Contacts: University of Pennsylvania, Department of Chemical and Biomolecular Engineering, 220 S. 33<sup>rd</sup> Street, Philadelphia, PA 19104-6393  
215-898-6318 [vohs@seas.upenn.edu](mailto:vohs@seas.upenn.edu)

#### Goal

The goal of this project is to elucidate the relationships between the structure and reactivity of Pd/ZnO methanol, and Co/ZnO ethanol steam reforming catalysts and to determine the origins of the unique reactivity of these catalytic systems. The effect of alloying Pd and Co with small amounts of Zn and the role of the support in influencing the selectivity for alcohol steam reforming will be determined. Insights obtained in this study will be useful in the development of more highly active and selective alcohol reforming catalysts.

#### DOE Interest

H<sub>2</sub> is recognized as a clean energy carrier, but renewable methods for its production are needed in order for H<sub>2</sub> to be widely used as a fuel for highly efficient energy conversion devices such as fuel cells. While alcohols are potentially a bio-renewable feedstock for H<sub>2</sub> production, highly active and selective catalysts for the steam reforming of alcohols to produce H<sub>2</sub> and CO<sub>2</sub> are needed. This project focuses on providing fundamental insights that will aid in the development of such catalysts.

#### Recent Progress

Our recent studies have focused on Co-based catalysts for steam reforming of ethanol (SRE). Base case studies of the reactivity of a Co foil have provided insights into the possible roles of the various Co oxidation states in the SRE reaction. Metallic Co has been shown to be highly active for decarbonylation of CO which likely proceeds via an oxametallacycle intermediate. Since previous studies have implicated acetaldehyde as an important intermediate in SRE it is unlikely that Co<sup>0</sup> are the active sites for this reaction, although they may play a role in catalyst deactivation, since decarbonylation also results in carbon deposition. In contrast, Co<sup>2+</sup> sites were found to be highly active for the dehydrogenation of ethoxide species to produce acetaldehyde. This reaction was facile and occurred near 355 K. Based on these observations we initially proposed that acetaldehyde production during SRE proceeds via  $\alpha$ -H abstraction from ethoxide groups adsorbed on Co<sup>2+</sup> sites.

Studies of the structure and reactivity of model Co/ZnO catalysts have shown that vapor deposited Co films grow in a nearly layer-by-layer fashion at 300 K but agglomerate upon heating to 700 K. At higher temperatures the Co reacts with the ZnO support to form CoO particles which then redisperse over the ZnO(0001) surface. The structural evolution of Co films

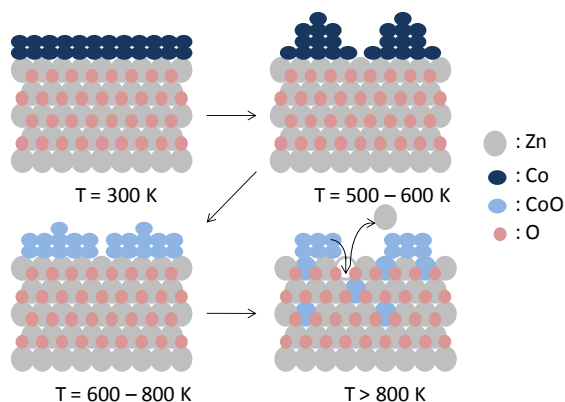


Fig. 1. Schematic of the structural evolution of Co films on ZnO(0001)

on ZnO(0001) as a function of temperature are shown in Figure 1. Ethanol TPD studies obtained for as-deposited Co films on ZnO(0001) which were partially oxidized exhibited reactivity trends similar to those observed for the Co foil with dehydrogenation and decarbonylation reactions occurring on  $\text{Co}^{2+}$  and  $\text{Co}^0$  sites, respectively. The results obtained for annealed Co/ZnO(0001) samples in which the Co was primarily in the +2 oxidation state were somewhat at odds with this conclusion, however, with the CoO particles in these samples being unreactive towards ethanol.

Together our studies of the reactivity of CO foils and Co/ZnO(0001) model catalysts indicate that the most active and selective surfaces for the dehydrogenation of adsorbed ethoxide species to produce acetaldehyde contain a mixture of  $\text{Co}^0$  to  $\text{Co}^{2+}$  sites. Studies of high surface area Co/ZnO catalysts by Llorca et al. have led to a similar conclusion. These observations coupled with the fact that bulk CoO particles supported on ZnO exhibit low reactivity towards ethanol have led us to hypothesize that a surface CoO layer on metallic Co may provide the active sites for the dehydrogenation reaction. We are currently studying this possibility in more detail.

### Future Plans

Over the next year we will pursue two avenues of investigation. First we will resolve how the oxidation state of the Co affects its reactivity toward ethanol and whether a surface “CoO” phase is active for the dehydrogenation of adsorbed ethoxide groups to produce acetaldehyde. We will investigate this possibility further using a Co(0001) single crystal for which we will be able to more precisely control the oxidation state of the surface Co atoms. The second avenue of research will be to expand the number of supports that we use in our studies of the reactivity of supported Co films and particles. Specific supports that we will investigate will be  $\text{ZrO}_2$  and  $\text{CeO}_2$ .  $\text{ZrO}_2$  was chosen because Ozkin’s group has shown that like Co/ZnO, Co/ $\text{ZrO}_2$  exhibits high selectivity for the steam reforming of ethanol to produce  $\text{H}_2$  and  $\text{CO}_2$ . Results for the unreducible  $\text{ZrO}_2$  support along with our results for the reducible ZnO support will allow us to study how the redox properties of the support affect catalyst activity and stability. Ceria has been used as a promoter that improves catalyst activity possibly by donating oxygen to the Co which can then be used to oxidize carbon deposits. Supports consisting of epitaxial films of  $\text{CeO}_2$  on  $\text{ZrO}_2$  single crystal supports will be used to study this effect in detail.

### Publications (2010-2011)

1. Studies of the Structure and Interfacial Chemistry of Co Layers on ZnO(0001), M. Hyman, E. Martono, and J.M. Vohs, *J. Phys. Chem. C*, **114** (2010) 16892-16899.
2. Reaction of Ethanol on Oxidized and Reduced Cobalt Surfaces, M.P. Hyman and J.M. Vohs, *Surface Science*, **605** (2011) 383-389.
3. Aerosol-Derived Bimetallic Alloy Powders: Bridging the Gap. B. Halevi, E.J. Peterson, A. Delariva, E. Jerero, V.M. Lebarbier, Y. Wang, J.M. Vohs, E. Kunkes, M. Havecker, M. Behrens, R. Schlogl, A.K. Datye, *J. Phys. Chem. C*, **114** (2010) 17181-17190.

4. Reaction Pathways for Ethanol on Model Co/ZnO(0001) Catalysts, E. Martono and J.M. Vohs, *Phys. Chem. Chem. Phys.*, **13** (2011) 9880-9886.

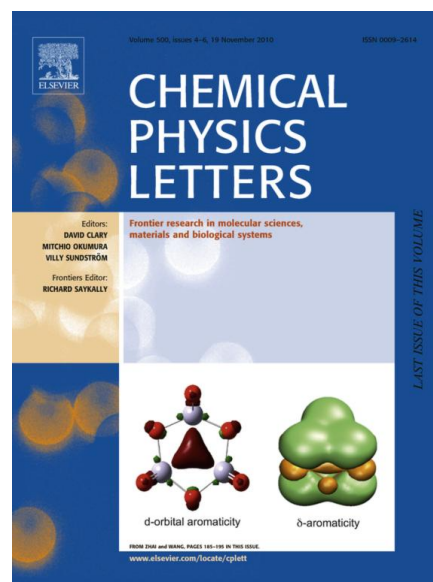
## Oxide Cluster Model Studies: Toward a Molecular Level Understanding of Oxide Surfaces and Defect Structures

Lead PI: Lai-Sheng Wang  
 Co-Investigator: Hua-Jin Zhai  
 Contact: Department of Chemistry, Brown University, 324 Brook Street,  
 Providence, RI 02912; Email: Lai-Sheng\_Wang@brown.edu

Gas-phase transition-metal oxide clusters provide well-defined and controllable molecular models towards mechanistic insights into the complex surface chemistry and catalytic processes. We will present combined photoelectron spectroscopy and theoretical studies on selected oxide cluster systems. (1) A comparative study on two group VIB oxide clusters,  $M_3O_8^-$  and  $M_3O_8$  ( $M = Cr, W$ ). The concerted experimental and theoretical investigation allows critical benchmarking of DFT methods for the Cr and W oxide clusters. (2) Stoichiometric and oxygen-rich group VB oxide clusters,  $M_2O_n^-$  and  $M_2O_n$  ( $M = Nb, Ta; n = 5-7$ ), as molecular models for oxygen radicals, diradicals, and superoxides. (3)  $\delta$ -aromaticity and delocalized multi-center  $d-d$  bonding in transition metal oxide clusters (see figure). Systematic studies for the  $M_3O_n^-$  ( $M = Nb, Ta; n = 1-8$ ) clusters reveal the electronic and structural evolution, sequential oxidation, and chemical bonding as a function of oxygen content. In particular, a  $\delta$ -type orbital can be identified in the  $Ta_3O_n^-$  ( $n = 0-5$ ) clusters, along with the specific spectral band associated with it. Although  $\delta$  bonding is substantially weaker than  $\sigma$  and  $\pi$  bonding, there is observable stabilization effect due to the delocalization of the  $\delta$  orbital.

### References:

- (1) S. G. Li, H. J. Zhai, L. S. Wang, and D. A. Dixon, "Structural and Electronic Properties of Reduced Transition Metal Oxide Clusters,  $M_3O_8$  and  $M_3O_8^-$  ( $M = Cr, W$ ), from Photoelectron Spectroscopy and Quantum Chemical Calculations" *J. Phys. Chem. A* **113**, 11273 (2009).
- (2) H. J. Zhai, B. Wang, X. Huang, and L. S. Wang, "Structural Evolution, Sequential Oxidation, and Chemical Bonding in Tri-Tantalum Oxide Clusters:  $Ta_3O_n^-$  and  $Ta_3O_n$  ( $n = 1-8$ )" *J. Phys. Chem. A* **113**, 9804 (2009).
- (3) W. J. Chen, H. J. Zhai, Y. F. Zhang, X. Huang, and L. S. Wang, "On the Electronic and Structural Properties of Tri-Niobium Oxide Clusters  $Nb_3O_n^-$  ( $n = 3-8$ ): Photoelectron Spectroscopy and Density Functional Calculations" *J. Phys. Chem. A* **114**, 5958 (2010).
- (4) H. J. Zhai and L. S. Wang, "Probing the Electronic Structure of Early Transition Metal Oxide Clusters: Molecular Models Towards Mechanistic Insights into Oxide Surfaces and Catalysis," *Chem. Phys. Lett.* **500**, 185-195 (2010).
- (5) H. J. Zhai, X. H. Zhang, W. J. Chen, X. Huang, and L. S. Wang, "Stoichiometric and Oxygen-Rich  $M_2O_n^-$  and  $M_2O_n$  ( $M = Nb, Ta; n = 5-7$ ) Clusters: Molecular Models for Oxygen Radicals, Diradicals, and Superoxides," *J. Am. Chem. Soc.* **133**, 3085 (2011).



**Acid/base and Redox Properties of Metal Oxides Catalysts**

Co-PI: Jun Liu

Lead PI: Charles H.F. Peden

Postdoc: Junming Sun, Wenzhen Li, Feng Gao

Student: Yan Li

Contact: MSIN: Pacific Northwest National Laboratory, MSIN: K2-12, 902 Battelle Blvd, Richland, WA 99354; [yongwang@pnl.gov](mailto:yongwang@pnl.gov).

Two types of metal oxide catalysts were studied. First, ZnO was added to mesoporous ZrO<sub>2</sub> in order to selectively passivate zirconia's strong Lewis acidic sites and weaken Brønsted acidic sites, while simultaneously introducing basicity. As a result, a surface basic site-catalyzed ethanol dehydrogenation and aldol-condensation, followed by Brønsted acidic site-catalyzed acetone-to-isobutene reaction pathway dominates on the Zn<sub>x</sub>Zr<sub>y</sub>O<sub>z</sub> mixed oxide catalyst, leading to a highly selective and stable catalyst for direct conversion of bio-ethanol to isobutene while the undesired reactions of bio-ethanol dehydration and acetone polymerization/coking are suppressed. The design and synthesis of Zn<sub>x</sub>Zr<sub>y</sub>O<sub>z</sub> mixed oxides allows for direct and high (~83%) yield conversion of bio-ethanol to isobutene, which is an important intermediate for butyl rubber production and upgrading ethanol to gasoline or jet fuels. Second, vanadia on TiO<sub>2</sub> with control facets were synthesized and studied for methanol oxidation. FTIR, Raman, high-field NMR and XPS revealed that the Lewis acidity of Ti sites plays a key role of support effect, and the weaker Lewis acidity of Ti sites on TiO<sub>2</sub> results in a higher reactivity of the supported vanadia.

**References**

Sun, J; K Zhu, F Gao, CM Wang, J Liu, CHF Peden, and Y Wang. "High Yield Bio-Ethanol Conversion to Isobutene: Zn<sub>x</sub>Zr<sub>y</sub>O<sub>z</sub> Mixed Oxides for a Novel and Highly Selective Process to Value-Added Products from Biomass." *J. Am. Chem. Soc* (in press).

**Growth and Reactivity of Oxide Phases on Crystalline Pd and Pt Surfaces**

Additional PIs: Aravind Asthagiri (The Ohio State University)

Students: Heywood H. Kan, Can Hakanoglu, Jose A. Hinojosa Jr., Jeffery Hawkins, Abbin Antony

Contact: Department of Chemical Engineering, University of Florida, Gainesville, FL 32611, Tel. 352-392-0869, [weaver@che.ufl.edu](mailto:weaver@che.ufl.edu)

**Goal**

The main goals of our project are to elucidate the mechanisms governing the oxidation of crystalline Pd and Pt surfaces, and to advance the fundamental understanding of the reactivity of the resulting oxide phases. We are focusing particularly on characterizing mechanistic aspects of alkane adsorption and chemical transformations on a PdO(101) thin film. This effort is motivated largely by the need to develop more efficient methods for utilizing alkanes as fuel sources and also as feedstocks for chemical production.

**DOE Interest**

Understanding the growth and reactivity of oxide phases on late transition metal surfaces is critically important for rationally designing catalytic oxidation processes for oxygen-rich applications, including the catalytic combustion of natural gas, exhaust gas remediation in lean-burn diesel engines and the selective oxidation of organic compounds. Improving the efficiency of these catalytic processes would positively impact important technologies for energy conversion and utilization.

**Recent Progress**

*Growth and decomposition of PdO(101) thin films on Pd(111).* By using oxygen atom beams to prepare surface oxygen phases, we have been successful in broadly extending the range of oxygen concentrations that can be cleanly generated on Pt and Pd surfaces in ultrahigh vacuum (UHV). During 2009 to 2011, we conducted investigations of the growth and thermal reduction of PdO(101) thin films on Pd(111), with particular emphasis on characterizing structural properties of the PdO(101) surface using scanning tunneling microscopy (STM). This work shows that PdO(101) films grown on Pd(111) at moderate temperature have high-quality surface structures that are characterized by large crystalline terraces with minimal quantities of defects. Our work also reveals that the PdO(101) films decompose by an autocatalytic mechanism wherein the isothermal rate of oxygen desorption increases as the oxide decomposes.

Our STM results demonstrate that reduced sites act to catalyze PdO decomposition, and reveal strong spatial anisotropies in the decomposition kinetics. These anisotropies cause one-dimensional reaction fronts to propagate preferentially along the atomic rows of the oxide, generating long chains of reduced sites. Reduced sites also promote oxygen recombination in neighboring rows of the PdO(101) structure as evidenced by the formation of loops and larger aggregates of reduced sites. Finally, the

STM images provide evidence that underlying PdO(101) layers transfer oxygen to reduced surface domains, thus producing large domains of PdO(101) islands at the surface. Re-oxidation of the surface acts to sustain the autocatalytic decomposition kinetics, and provides a mechanism for oxygen atoms to ultimately evolve from the subsurface of the PdO(101) film. These results demonstrate that diverse structural transformations occur during PdO reduction, and provide insights into the couplings among these structural changes and the kinetic processes that control oxide decomposition.

*Reactivity of a PdO(101) thin film.*

We find that the PdO(101) surface has a high affinity for binding various types of molecules as well as strong oxidizing capabilities. Of particular interest are our findings that *n*-alkanes larger than ethane undergo facile C-H bond activation and oxidation on the PdO(101) surface. Our results reveal that alkane activation on PdO(101) occurs by a precursor-mediated mechanism wherein a molecularly adsorbed state acts as

a precursor for initial C-H bond cleavage and a kinetic competition between desorption and dissociation of the precursor determines the net dissociation probability. We have presented evidence based on experimental measurements as well as density functional theory (DFT) calculations that alkanes form  $\sigma$ -complexes on PdO(101) by bonding with coordinatively unsaturated (cus) Pd atoms at the surface, and that these complexes act as precursors for initial C-H bond activation. The formation of  $\sigma$ -complexes causes the binding energies of *n*-alkanes on PdO(101) to exceed those on Pd(111) by a nearly constant amount (~20-25 kJ/mol). DFT calculations show clearly that dative bonding with the cus-Pd atoms significantly weakens the C-H bonds of alkanes, thus making them easier to cleave. We have also been examining regioselectivity in the activation of alkanes on PdO(101). Both experimental and computational results reveal a strong preference for primary C-H bond cleavage of propane  $\sigma$ -complexes on PdO(101). DFT calculations predict that the relative stabilities of the carbanion transition structures play a key role in determining the initial C-H bond selectivity for alkane activation on PdO(101).

**Future Plans**

*Structural characterization of clean and adsorbed-covered oxides.* Characterize the structural properties of bulk Pd and Pt oxides using STM. We plan to focus particularly on characterizing the structural changes that occur as oxides are reduced by reaction with alkanes and other molecules.

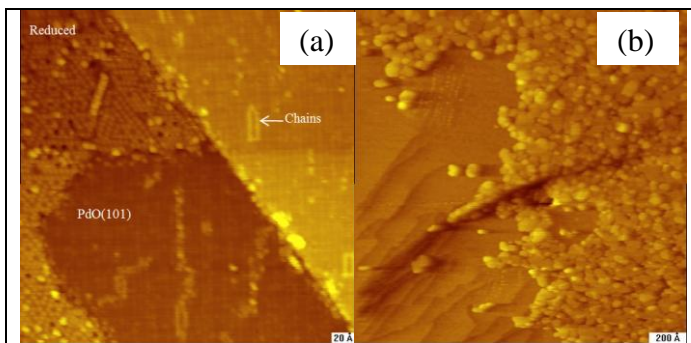


**Figure 1:** STM images obtained from a PdO(101) film after desorbing ~1 ML of oxygen atoms at 720 K. (a) Initial PdO(101) terraces coexisting with reduced structures; (b) PdO(101) islands formed by re-oxidation of reduced surface domains.



*Reaction selectivity of alkanes on PdO(101)*. Clarify factors that determine selectivity in the initial C-H bond cleavage of alkanes on PdO(101) and investigate the effects of co-adsorbed species in altering the oxidation selectivity of the resulting alkyl groups.

*Alkane activation on transition-metal doped PdO(101)*. Determine how transition-metal dopants alter the growth of PdO(101) films and influence the surface activity toward C-H bond cleavage.

### **Publications (2009-11)**

1. “High selectivity for 1° C-H bond cleavage of propane  $\sigma$ -complexes on the PdO(101) surface”, J.F. Weaver, C. Hakanoglu, A. Antony and A. Asthagiri, submitted.
2. “Surface structural evolution during the thermal decomposition of a PdO(101) thin film”, J.A. Hinojosa, Jr. and J.F. Weaver, *Surf. Sci.* (2011) in press.
3. “Oxidation of methanol on a PdO(101) thin film”, C. Hakanoglu, J.A. Hinojosa, Jr. and J.F. Weaver, *J. Phys. Chem. C* 115 (2011) 11575–11585.
4. “Catalytic decomposition of Ba(NO<sub>3</sub>)<sub>2</sub> on Pt(111)”, K. Mudiyansele, J.F. Weaver and J. Szanyi, *J. Phys. Chem. C* 115 (2011) 5903-5909.
5. “Precursor-mediated dissociation of *n*-butane on a PdO(101) thin film”, J.F. Weaver, C. Hakanoglu, J.A. Hinojosa, Jr., A. Antony, J.M. Hawkins and A. Asthagiri, *Catalysis Today* 160 (2011) 213-227.
6. “Formation, characterization and reactivity of adsorbed oxygen on BaO/Pt(111)”, K. Mudiyansele, D.H. Mei, C.W. Yi, J.F. Weaver and J. Szanyi, *J. Phys. Chem. C* 114 (2010) 20195-20206.
7. “Strong kinetic isotope effect in the dissociative chemisorption of H<sub>2</sub> on a PdO(101) thin film”, C. Hakanoglu, J.M. Hawkins, A. Asthagiri, and J.F. Weaver, *J. Phys. Chem. C* 114 (2010) 11485-11497.
8. “Molecular adsorption of small alkanes on a PdO(101) thin film: Evidence of  $\sigma$ -complex formation”, J.F. Weaver, C. Hakanoglu, J.M. Hawkins and A. Asthagiri, *J. Chem. Phys.* 132 (2010) 024709:1-10.
9. “Mechanism of PdO thin film formation during the oxidation of Pd(111)”, H.H. Kan and J.F. Weaver, *Surf. Sci.* 603 (2009) 2671-2682.
10. “Facile C-H bond cleavage and deep oxidation of propane on a PdO(101) thin film”, J.F. Weaver, S.P. Devarajan and C. Hakanoglu, *J. Phys. Chem. C* 113 (2009) 9773-9782.
11. “Adsorption of water on a PdO(101) thin film: Evidence of an adsorbed HO-H<sub>2</sub>O complex”, H.H. Kan, R.J. Colmyer, A. Asthagiri and J.F. Weaver”, *J. Phys. Chem. C* 113 (2009) 1495-1506.

KC0302010 (CO-019)

Ping Liu (BNL)  
Jose A. Rodriguez (BNL)  
Dario J. Stacchiola (BNL)  
Michael G. White (BNL/SUNYSB)

### Catalysis on the Nanoscale: Preparation, Characterization and Reactivity of Metal-Based Nanostructures

post docs (100%): Y.-M. Choi, A. Baber  
graduate students: J. Zhou, Y. Yang (Stony Brook University)

Chemistry Department  
Brookhaven National Laboratory  
Upton, NY 11973  
[pingliu3@bnl.gov](mailto:pingliu3@bnl.gov); [rodriguez@bnl.gov](mailto:rodriguez@bnl.gov); [djs@bnl.gov](mailto:djs@bnl.gov); [mgwhite@bnl.gov](mailto:mgwhite@bnl.gov)

Department of Chemistry  
SUNY Stony Brook  
Stony Brook, NY 11794;

### Program Goals

The general goals of this program are to identify and characterize the catalytically active sites of supported nanocatalysts and investigate how these are influenced by variations in particle size, morphology and support. Nanocluster preparation techniques include soft-landing of *size-selected* clusters and reactive layer deposition and these have been used to investigate the activity of novel transition metal carbide, oxide and sulfide nanocatalysts for desulfurization, hydrogen production and oxygenate synthesis. The model systems include “inverse” nanocatalysts of metal oxide clusters deposited on metal supports which exhibit unique electronic, morphological and reactivity properties. Theoretical modeling using DFT is an integral part of this program and is used to explore the role of light atoms (C, S, P) in modifying the activity of metal compounds, the influence of cluster-support interactions on reactivity, and the identification of key intermediates and reaction steps in complex surface reactions. Proposed work will focus on C<sub>1</sub>-C<sub>4</sub> oxygenate synthesis via CO/CO<sub>2</sub> hydrogenation using oxide-supported metal, metal oxide and metal sulfide nanoclusters. This effort will make use of a new instrument with capabilities for UHV surface science, cluster deposition, and characterization of model nanocatalysts under electrochemical conditions.

### DOE Interest

This research program uses both experiments and theory to investigate the properties of small supported nanoparticles in an effort to understand how size, morphology, composition and substrate interactions influence their catalytic activity and selectivity. It is expected that this effort will help develop basic principles for the design and optimization of better catalysts for the synthesis and utilization of chemical energy.

### Recent Progress

**Reactivity and Electronic Structure of size-selected Mo<sub>x</sub>S<sub>y</sub> nanoclusters:** Commercial desulfurization catalysts are based on nanometer-scale molybdenum sulfide (MoS<sub>2</sub>) nanoparticles supported on a  $\delta$ -Al<sub>2</sub>O<sub>3</sub> support. The active sites are edge or corner vacancy sites with exposed under-coordinated Mo atoms, but the influence of the alumina support on the electronic properties of the active sites is not well established. Our recent work explored the size-dependent interaction of small molybdenum nanoclusters (Mo<sub>x</sub>S<sub>y</sub>) deposited on an alumina support using two-photon photoemission to measure changes in work function with

cluster coverage. A thin alumina film was prepared by oxidation of NiAl(110) crystal and  $\text{Mo}_x\text{S}_y$  clusters ( $x/y = 2/6, 4/6, 5/7, 6/8$ ) were prepared by size-selected cluster deposition using reactive sputtering and soft-landing ( $<0.2$  eV/atom) of cluster cations with precisely controlled mass and coverage. The density of the clusters are well-described by a Gaussian distribution from the center of the crystal and the small laser spot (200  $\mu\text{m}$  dia) could probe the photoemission spectrum as function cluster coverage by scanning across the surface. The 2PPE results show that the surface work function is a local property that is larger than the bare surface in the presence of  $\text{Mo}_x\text{S}_y$  clusters and is proportional to the local cluster coverage. The increase of the work function indicates significant electron transfer from the surface to the  $\text{Mo}_x\text{S}_y$  clusters and the magnitude of the work function change is cluster size dependent. Dipole moments for each  $\text{Mo}_x\text{S}_y$  cluster could be derived from the coverage-dependent work function change. The highly symmetric clusters,  $\text{Mo}_6\text{S}_8$  and  $\text{Mo}_4\text{S}_6$ , have the highest interfacial dipole moments (see Figure 1) despite having no permanent dipole moments in the isolated clusters. These results demonstrate that the  $\text{Mo}_x\text{S}_y$  clusters have strong interaction with the alumina film and the distinct electronic properties of different  $\text{Mo}_x\text{S}_y$  clusters might induce unique catalytic activities on  $\text{Al}_2\text{O}_3$  support.

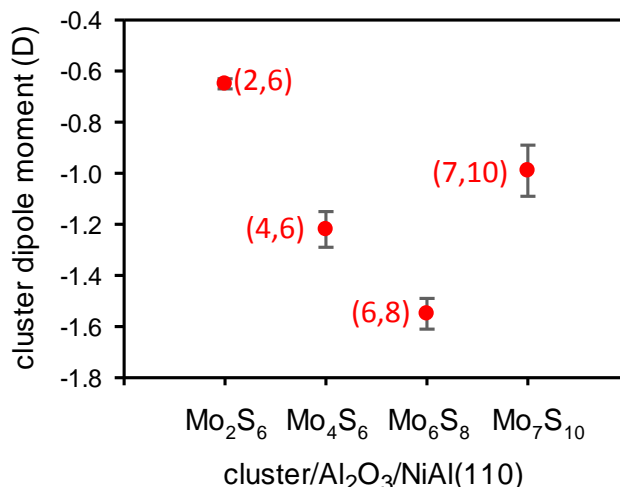


**Figure 1:** Dipole moments of  $\text{Mo}_x\text{S}_y$  clusters deposited on a  $\text{Al}_2\text{O}_3/\text{NiAl}(110)$  surface as determined by coverage dependent changes in work function.

**Controlled Assembly of  $\text{CeO}_2(111)$  and  $\text{CeO}_2(100)$  Nanoparticles on an Oxidized  $\text{Cu}(111)$  Substrate:** The catalytic performance of ceria-based heterogeneous catalysts in many chemical transformations (water-gas shift reaction, CO oxidation, alcohol synthesis from  $\text{CO}/\text{CO}_2$  hydrogenation, etc) is affected by the surface structure of the ceria. To control the performance of ceria-containing inverse catalysts, we devised a method to grow ceria nanoparticles (NPs) exposing exclusively either (111) or (100) surfaces and characterized their surface structures by scanning tunneling microscopy (STM). When vapor-depositing cerium on  $\text{Cu}(111)$  in a background of molecular  $\text{O}_2$  only  $\text{CeO}_2(111)$  NPs grow. However, if the surface of  $\text{Cu}(111)$  is pre-oxidized with  $\text{O}_2$  or  $\text{NO}_2$  to form a rectangular copper oxide phase, probably  $\text{Cu}_4\text{O}_3(001)$ ,  $\text{CeO}_2(100)$  NPs grow on the oxide template instead. These experimental findings are interpreted using results of density functional calculations. The (100)

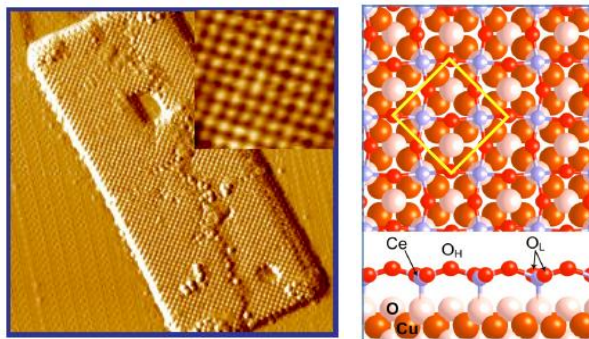


**Figure 2:** Left: STM image of  $\text{CeO}_2(100)$  NP prepared by Ce deposition in  $\text{O}_2$  at 650 K on a copper oxide surface ( $40 \times 40$   $\text{nm}^2$ ). Right: Top and side views of DFT-optimized  $\text{CeO}_2$  structures on  $\text{Cu}_4\text{O}_3(001)$ .

surface of bulk ceria reconstructs in order to preserve charge neutrality. This is not necessary for CeO<sub>2</sub>(100) NPs grown on Cu<sub>4</sub>O<sub>3</sub>(001), where the top most oxygen layer of Cu<sub>4</sub>O<sub>3</sub> is shared with the interfacial layer of cerium. After exposing the CeO<sub>2</sub>(100)/CuO<sub>x</sub>/Cu(111) surfaces to CO, the copper oxide was reduced but the shape of the CeO<sub>2</sub>(100) NPs remained intact. This opens the door for diverse applications in catalysis.

**CO<sub>2</sub> hydrogenation and alcohol synthesis over Cu nanoparticles dispersed on ZnO(000 $\bar{1}$ ), TiO<sub>2</sub>(110) and CeO<sub>x</sub>/TiO<sub>2</sub>(110):**

The synthesis of methanol from CO<sub>2</sub> and H<sub>2</sub> has attracted considerable attention due to its potential application in reducing CO<sub>2</sub> emissions, but also because the methanol product can serve as a liquid fuel as well as a raw material for the synthesis of other organic compounds. It has been shown that CO<sub>2</sub> is the predominant carbon source for methanol using the industrial Cu-Zn O/Al<sub>2</sub>O<sub>3</sub> catalyst under reaction conditions. Despite extensive experimental and theoretical efforts devoted to understanding the underlying reaction mechanism of methanol synthesis on Cu-based catalysts controversies over the mechanism still remain. Recent work in this project have combined experimental and theoretical studies to investigate the methanol synthesis via CO<sub>2</sub> hydrogenation on Cu(111) and Cu<sub>n</sub> nanoparticles (unsupported and deposited on ZnO(000 $\bar{1}$ )). Both experiment and theory show that Cu nanoparticles with or without ZnO support exhibit a higher catalytic activity than Cu(111). According to our calculated results, methanol synthesis on both surfaces follows the formate pathway via intermediates HCOO, H<sub>2</sub>COO, H<sub>2</sub>CO and H<sub>3</sub>CO, and the rate-limiting step is H<sub>2</sub>COO hydrogenation (see Figure 3). Compared with that on Cu(111), the barrier for the rate-limiting step of methanol synthesis reaction on Cu<sub>29</sub> is 0.19 eV lower which corresponds to a reaction rate ~50 times faster (T = 573 K), which is in qualitative agreement with our experimental measurements. The activity enhancement can be attributed to the flexibility and the presence of the active low-coordinated Cu sites in the nanoparticle, which significantly stabilize the key intermediates, the corresponding transition states, and therefore lower the barrier for the rate-limiting hydrogenation process. These results clearly illustrate the need to consider catalyst particle-size effects in methanol synthesis reaction. The competing RWGS reaction was also considered. Compared to the methanol synthesis, the barrier of the slowest step of the RWGS is calculated to be 0.27 eV lower, with a corresponding reaction rate that is faster by a factor of ~10<sup>2</sup> at T = 573 K. This is consistent with our experimental observations, showing that the RWGS reaction is 2–3 orders of magnitude faster and that the dominant product on Cu catalyst is CO rather than methanol. Our calculations indicate that methanol production from CO hydrogenation via the RWGS pathway is hindered by the first hydrogenation of CO to HCO. The latter is not stable

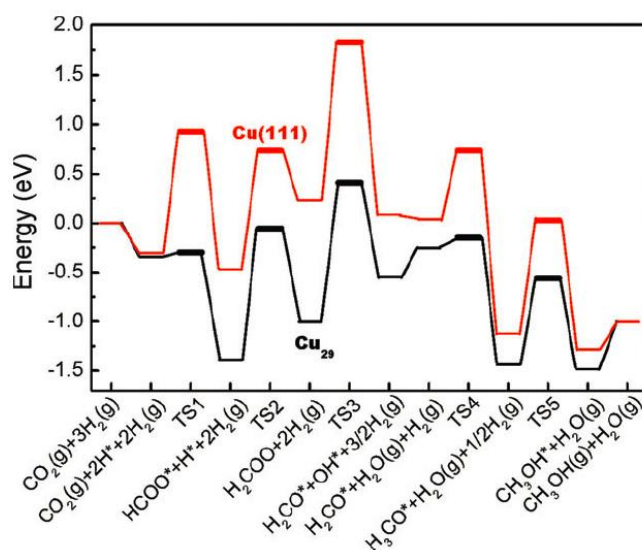


**Figure 3:** Potential energy diagram for the methanol synthesis reaction on the Cu(111) surface (upper diagram) and Cu<sub>29</sub> nanoparticle (lower diagram), where the thin bar represents the intermediates and the thick bar represents the transition states.

These results clearly illustrate the need to consider catalyst particle-size effects in methanol synthesis reaction. The competing RWGS reaction was also considered. Compared to the methanol synthesis, the barrier of the slowest step of the RWGS is calculated to be 0.27 eV lower, with a corresponding reaction rate that is faster by a factor of ~10<sup>2</sup> at T = 573 K. This is consistent with our experimental observations, showing that the RWGS reaction is 2–3 orders of magnitude faster and that the dominant product on Cu catalyst is CO rather than methanol. Our calculations indicate that methanol production from CO hydrogenation via the RWGS pathway is hindered by the first hydrogenation of CO to HCO. The latter is not stable

on Cu and prefers to dissociate into CO and H. Therefore, the faster RWGS only leads to the accumulation of CO, rather the methanol formation.

## Future

Future work in this program will continue to focus on the manipulation of nanostructured materials as catalysts for (1) the more efficient utilization of fossil-derived fuels (desulfurization), and (2) the synthesis and utilization of new energy sources such as H<sub>2</sub> (water-gas-shift) and methanol/ethanol (CO<sub>2</sub>/CO hydrogenation; ethanol reforming). Our current studies of the electronic structure of size-selected clusters of molybdenum sulfide on Al<sub>2</sub>O<sub>3</sub>/NiAl(110) will be expanded to include the TiO<sub>2</sub>(110) surface as well as to include correlations with reactivity with S-containing compounds. Similar studies will be performed with supported RuS<sub>x</sub> nanoparticles, as bulk RuS<sub>2</sub> is one of the most active materials known for desulfurization reactions. We also propose to synthesize model graphene supported MoA<sub>x</sub> (A = C, O, S) catalysts, for fundamental studies of new hydroprocessing catalysts. It has been suggested that carbon supports can act as a source of hydrogen for the hydrogenation steps during HDS and/or can provide carbon for the formation of active metal carbide or oxycarbide particles.

New efforts will also study nanocatalysts for alcohol reforming and synthesis as processes that can yield renewable sources of energy as hydrogen or as a liquid fuel, respectively. Potential catalyst materials include those that promote C-C bond formation (Rh), hydrogenation (Pt, Pd, Fe, Ni, metal sulfides) and CO oxidation (Au, Cu), many of which we have gained experience with in previous studies of hydrodesulfurization and the water gas shift reaction. Current DFT and kinetic Monte Carlo studies suggest that transition metal doping may be an effective way to improve the alcohol synthesis capabilities of Cu-based catalysts by promoting the hydrogenation steps of adsorbed CO formed by the reverse-water-gas-shift reaction. These predictions will be experimentally explored by a combination of surface science characterization studies and infrared reflectance measurements to identify surface intermediates. Other work will explore the alcohol synthesis properties of novel inverse nanocatalysts such as CeO<sub>x</sub>/CuO<sub>x</sub>/Cu(111) and Cu/CeO<sub>x</sub>/TiO<sub>2</sub> developed at BNL. A very new component of this program is to explore nanostructured metal/oxide catalysts for the efficient electrooxidation of ethanol (EOR) for fuel cell applications. This effort involves the use of a new instrument which can be used to prepare and characterize nanocatalysts under UHV conditions (XPS, ISS, LEED, TPD) before and after electrochemical activity measurements. The latter are made possible by *in vacuo* sample transfer to a liquid electrochemical cell. Of particular interest are nanostructured Pt/SnO<sub>x</sub>/Pt(111) surfaces as model electrocatalysts for understanding the high EOR activity of recently discovered Pt/Rh/SnO<sub>x</sub> powdered catalysts at BNL.

## Publications 2009-2011

1. J.B. Park, J. Graciani, J. Evans, D. Stacchiola, S. Ma, P. Liu, A. Nambu, J. Fernandez-Sanz, J. Hrbek, and J.A. Rodriguez, High Catalytic Activity of Au/CeO<sub>x</sub>/TiO<sub>2</sub>(110) Controlled by the Nature of the Mixed-Metal Oxide at the Nanometer Level, *Proc. Nat. Acad. Sci. (PNAS)*, **106**, 4975-4980 (2009).
2. E. Florez, F. Viñes, J.A. Rodriguez, and F. Illas, Adsorption and Diffusion of Au Particles on the (001) Surface of Ti, Zr, Hf, V, Nb, Ta, and Mo Carbides, *J. Chem. Phys.* **130**, 2444706-1,7, (2009).

3. J.A. Rodriguez, P. Liu, Y. Takahashi, K. Nakamura, F. Viñes, and F. Illas, Desulfurization of Thiophene on Au/TiC(001): Au-C Interactions and Charge Polarization, *J. Am. Chem. Soc.* **131**, 8592-8602 (2009).
4. E. Florez, L. Feria, F. Viñes, J.A. Rodriguez, and F. Illas, Effect of the Support on the Electronic Structure of Au Nanoparticles Supported on Transition Metal Carbides: Choice of the best substrate for Au activation, *J. Phys. Chem. C*, **113**, 19994-20001 (2009).
5. J.A. Rodriguez, J. Graciani, J. Evans, J.B. Park, F. Yang, D. Stacchiola, S.D. Senanayake, S. Ma, M. Perez, P. Liu, J.F. Sanz, and J. Hrbek, Water-Gas Shift Reaction on a Highly Active Inverse CeO<sub>x</sub>/Cu(111) Catalyst: Unique Role of Ceria Nanoparticles., *Angew. Chem. Int. Ed.*, **48**, 8047 (2009).
6. Y. Choi and P. Liu, Mechanism of ethanol synthesis from syngas on Rh(111), *J. Am. Chem. Soc.* **131**, 13054 (2009).
7. P. Liu, J.A. Rodriguez, Y. Takahashi and K. Nakamura, Water-gas-shift reaction on a Ni<sub>2</sub>P(001) catalyst: Formation of oxy-phosphides and highly active reaction sites, *J. Catal.* **262**, 294 (2009).
8. M. Kowal, M. Li, M. Shao, K. Sasaki, M. B. Vukmirovic, J. Zhang, N. S. Marinkovic, P. Liu, A. Frenkel, and R. R. Adzic, Ternary Pt/Rh/SnO<sub>2</sub> Electrocatalysts for Oxidizing Ethanol to CO<sub>2</sub>, *Nature Mater.* **8**, 325 (2009).
9. J.A. Rodriguez and J. Hrbek, Inverse Oxide/Metal Catalysts: A Versatile Approach for Activity Tests and Mechanistic Studies, *Surf. Sci.* **604**, 241-244 (2010) (**invited**).
10. T. Gómez, E. Florez, J.A. Rodriguez and F. Illas, Theoretical Analysis of the Adsorption of Late Transition Metal Atoms on the (001) Surface of Early Transition Metal Carbides, *J. Phys. Chem. C*, **114**, 1622-1626 (2010).
11. J.B. Park, J. Graciani, J. Evans, D. Stacchiola, S.D. Senanayake, L. Barrio, P. Liu, J.F. Sanz, J. Hrbek, and J.A. Rodriguez, Gold, Copper and Platinum Nanoparticles dispersed on CeO<sub>x</sub>/TiO<sub>2</sub>(110) Surfaces: High Water-Gas Shift Activity and the Nature of the Mixed-Metal Oxide at the Nanometer Level, *J. Am. Chem. Soc.*, **132**, 356-363 (2010).
12. Y. Yang, J. Evans, J.A. Rodriguez, M.G. White, P. Liu, Fundamental Studies of Methanol Synthesis from CO<sub>2</sub> Hydrogenation on Cu(111), Cu Clusters and Cu/ZnO(0001), *Phys. Chem. Chem. Phys.*, **12**, 9909-9917 (2010).
13. P. Liu, Y.-M. Choi, Y. Yang and M. G. White, Methanol Synthesis from H<sub>2</sub> and CO<sub>2</sub> on a Mo<sub>6</sub>S<sub>8</sub> Cluster: A Density Functional Study, *J. Phys. Chem. A* **114**, 3888-3895 (2010).
14. F. M. Hoffmann, Y. Yang, J. Paul, M. G. White, J. Hrbek, Hydrogenation of Carbon Dioxide by Water: Alkali-Promoted Synthesis of Formate, *J. Phys. Chem. Lett.*, **1**, 2130-2134 (2010).
15. F. Yang, Y.-M. Choi, P. Liu, J. Hrbek, and J. A. Rodriguez, Autocatalytic Reduction of a Cu<sub>2</sub>O/Cu(111) Surface by CO: STM, XPS, and DFT Studies, *J. Phys. Chem. C*, **114**, 17042-17050 (2010).
16. J.A. Rodriguez, D. Stacchiola, Catalysis and the nature of mixed-metal oxides at the nanometer level: Special properties of MO<sub>x</sub>/TiO<sub>2</sub>(110) {M= V, W, Ce} surfaces, *PCCP, Perspectives*, **12** 9557-9565 (2010) (**invited**).
17. Y.-M. Choi, P. Liu, Understanding of Ethanol Decomposition on Rh(111) from Density Functional Theory and Kinetic Monte Carlo Simulations, *Catal. Today*, **165**, 64-70 (2011).
18. F. Yang, Y.-M. Choi, P. Liu, D. Stacchiola, J. Hrbek, and J. A. Rodriguez, Identification of 5\_7 Defects in a Copper Oxide Surface, *J. Am. Chem. Soc.*, **133**, 11474-11477 (2011).
19. W.-P. Zhou, S. Axnanda, M. G. White, R. R. Adzic, Jan Hrbek, Enhancement in Ethanol Electro-oxidation by SnO<sub>x</sub> Nanoislands Grown on Pt(111): Effect of Metal Oxide-metal Interface Sites, *J. Chem. Phys.*, 2011 (in press).

**Structure dependence of CO oxidation over ceria nanoshapes**

Lead PI: **Steven H. Overbury**

Postdoc: Meijun Li

Contact: Chemical Science Division, Oak Ridge National Laboratory, 1 Bethel Valley Rd, Oak Ridge, TN 37831. Email: [wuzl@ornl.gov](mailto:wuzl@ornl.gov)

CO oxidation is a model reaction for probing the redox property of ceria-based catalysts. Although it was found experimentally and predicted theoretically that CO oxidation is sensitive to the surface structure of ceria catalysts, there is still a lack of detailed understanding of how CO interacts with different ceria surfaces and how the reactivity and mobility of surface oxygen of ceria are affected by the surface structure. In this research, we made use of ceria nanocrystals with define surface structures (rods ( $\{110\} + \{100\}$ ), cubes ( $\{100\}$ ), octahedra ( $\{111\}$ )) and targeted for a molecular level insights into the structure dependent CO oxidation phenomenon over ceria catalysts utilizing *in situ* techniques including infrared and Raman spectroscopy coupled with isotopic labeling. It is shown that CO interacts more strongly with the open surfaces on rods and cubes ( $\{110\}$  and  $\{100\}$ ) than on the rather inert octahedra surface ( $\{111\}$ ), all leading to surface carbonate species. The lattice oxygen reactivity (accessed by CO-TPR) and mobility (accessed by oxygen isotopic exchange) are also found strongly surface dependent. We suggest that the difference in nature and amount of defect sites and coordinatively unsaturated sites, ultimately determined by the surface planes of ceria nanoshapes [1], is the driving force for the surface dependent behaviors of CO interaction with ceria, lattice oxygen reactivity and mobility, and thus the CO oxidation performance. The majority of the carbonate species observed under steady state CO oxidation condition is reaction spectator while the carbonate species associated with reduced ceria surface are possibly among the reaction intermediates in CO oxidation over ceria catalysts [2].

**References:**

1. Wu, Z. L.; Li, M. J.; Howe, J.; Meyer, H. M.; Overbury, S. H., "Probing Defect Sites on CeO<sub>2</sub> Nanocrystals with Well-Defined Surface Planes by Raman Spectroscopy and O<sub>2</sub> Adsorption," *Langmuir* **2010**, *26*, 16595.
2. Wu, Z. L.; Li, M. J.; Overbury, S. H., "On the Structure Dependence of CO Oxidation over Ceria Nanocrystals with Defined Surface Planes," *Journal of Catalysis* **2011**, submitted.

**Acknowledgements:** This Research is sponsored by the Division of Chemical Sciences, Geosciences, and Biosciences, Office of Basic Energy Sciences, U.S. Department of Energy. Part of the work was conducted at the Center for Nanophase Materials Sciences, which is sponsored at Oak Ridge National Laboratory, by the Office of Basic Energy Science, U. S. Department of Energy. The research was supported in part by the appointment for M.J. Li to the ORNL Postdoctoral Research Associates Program, administered jointly by ORNL and the Oak Ridge Associated Universities.

## **Electrocatalysis at Single Metal Nanoparticles and Single Molecules**

Jonathan Cox, Yongxin Li, and Bo Zhang

Department of Chemistry, University of Washington, Seattle, WA 98195

Electrode-supported metal nanoparticles form the basis for many catalysts of importance in energy technologies. The electrocatalytic activity of such nanoparticle-arrays can vary with size, shape, composition, and particle spacing. In general, these effects are poorly understood due to difficulty to structurally characterize the large-area electrocatalysts in sufficient detail, resulting in an inability to analyze thoroughly any structure-reactivity relationships that control the effects.

Our group uses single nanoparticles to characterize the structure-activity relationships in nanoparticle electrocatalysts. This strategy removes the averaging effects from particle-arrays and enables precise correlation of structure and activity of nanoparticle electrocatalysts. Our approach is based upon the use of single molecular-scale nanoelectrodes. We have developed and used platinum and gold nanoelectrodes as small as 1nm to directly measure and correlate the electrocatalytic response of single Au nanoparticles and their structures. In addition, we have developed a new method to monitor individual electron-transfer events at single nanoparticles and single enzyme molecules supported on nanoelectrode. Our research will reveal information of key importance in technological applications in the areas of energy conversion and storage.



# **Additional Abstracts of Funded Projects**

This page is intentionally blank.

### Characterization of fundamental catalytic properties of MoS<sub>2</sub>/WS<sub>2</sub> nanotubes and nanoclusters for desulfurization catalysis – a surface chemistry study

**Additional PIs:** none

**Postdocs:** Evgueni Kadossov (up to Dec. 2010), Junjun Shan (since Jan 2011)

**Students:** Mallikharjuna Komarneni (current), J. Goering (graduated)

**Undergraduate students:** Andrew Sand (chemistry, graduated in 2010 and joined the graduate school of the University of Chicago), Philip Nevin (biotechnology, 2009 summer exchange student from Sweden, joined the graduate school of Northeastern University in 2010), Razdan Mahalakshmi (biotechnology, joined grad. school in New York in 2009), John Justin (chemistry, 2009/10), Jordan Schmidt (physics, 2010)

**Collaborators:** M. Lu (Brookhaven National Laboratory – SEM sample characterization); B.W. Arey (Pacific Northwest National Laboratory – SEM sample characterization); R. Tenne, A. Zak, O. Eidelman (Weizmann Institute of Science, Israel – nanomaterials fabrication); L. Monica Veca (grad. student), Ya-Ping Sun (Clemson University)

#### Goal

Developing and characterizing novel hydrodesulfurization (HDS) catalysts using nanofabrication and surface science techniques.

#### DOE Interest

Despite tremendous and pertinent efforts to develop a variety of novel processes to replace petroleum as a transportation fuel as well as to utilize CO<sub>2</sub>, petroleum will remain paramount for the US for the foreseeable future since the synthesis of plastics, paints, and even pharmaceuticals are based on petroleum-derived products as a feedstock. HDS catalysts are required to clean up raw oil. Improved catalysts may become even more pertinent when depleting resources demand utilization of lower quality (higher sulfur content) raw oil. In addition to HDS, applications of Mo catalysts include further the isomerization and hydrogenation of olefins, synthesis of alcohols from CO (as alternative fuels) and CO<sub>2</sub>, hydrodenitrogenation, hydrodeoxygenation, metathesis of alkenes/olefines, methanation, and the H<sub>2</sub> evolution reaction. Most of these applications are energy related.

#### Recent Progress

The project consisted of two main components. *First*, characterization of novel nanomaterials for HDS. *Second*, studying more traditional model systems for HDS such as vapor-deposited (PVD) silica-supported Mo and MoS<sub>x</sub> clusters.

Studying new materials and systems has the potential to impact science and technology. The systems investigated are closely related to energy and environmental-related surface science/catalysis.

In the first subproject, we studied WS<sub>2</sub> and MoS<sub>2</sub> fullerene-like nanoparticles as well as WS<sub>2</sub> nanotubes. Thiophene (C<sub>4</sub>H<sub>4</sub>S) was used as the probe molecule. Interestingly, metallic and sulfur-like adsorption sites could be identified on the silica-supported inorganic fullerenes. Similar structures are seen for PVD system. Thus, this may be a kinetics fingerprint feature of modern HDS model systems. In addition, kinetics data allowed characterization of the different adsorption sites for thiophene on the surfaces and *inside* WS<sub>2</sub> nanotube bundles. The latter is a unique feature of nanotubes that has not been reported before for any inorganic nanotube system;

however, examples are known for carbon nanotubes, including work of the PI. Although HDS has been studied for decades, utilizing nanotubes as nanosized HDS reactors has never been tried before, as far as we know. This is of interest from a fundamental perspective.

In the *second* subproject, we studied HDS-related chemistry on more traditional supported cluster catalysts. PVD Mo clusters supported on silica have been characterized. Two reaction pathways are evident when adsorbing thiophene on Mo and MoS<sub>x</sub> clusters: molecular adsorption and dissociation. PVD Mo clusters are very reactive toward thiophene bond activation. In addition to S and C deposits, H<sub>2</sub>, H<sub>2</sub>S, and small organic molecules were detected in the gas phase. Cluster size effects have been seen: thiophene adsorbs molecularly with larger binding energies on smaller clusters. However, larger clusters have smaller activation energy for C<sub>4</sub>H<sub>4</sub>S bond activation than smaller clusters. The latter is consistent with early catalysis studies. Kinetics and dynamics parameters have been determined quantitatively.

We spent a significant amount of time on upgrades of our equipment. A 2<sup>nd</sup>-hand refurbished X-ray photoelectron spectrometer (XPS) has been integrated into the existing molecular beam scattering system and is already operational (supported by the DoE supplemental grant available in October 2009). We also added a time of flight system to the beam scattering apparatus and improved on the accessible impact energy range for the beam scattering experiments. This will be important for our future projects on HDS. In addition, a GC-based powder atmospheric flow reactor for studies on powder samples is now operational. Furthermore, a 2<sup>nd</sup> UHV kinetics system has been upgraded as well.

Very recently Co doped WS<sub>2</sub> nanotubes (from R. Tenne) were characterized towards HDS activity at ambient pressure. Thiophene conversion rates above 50% were obtained which is close to the industrial Haldor Topsoe standard (see Fig.). A further optimization of the materials is on the way as well as a UHV characterization using spectroscopy and kinetics techniques.

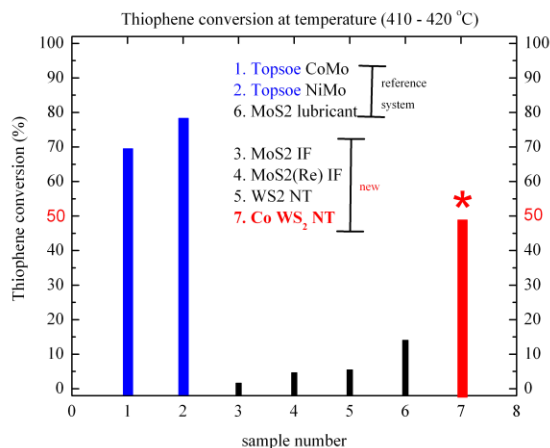
### Future Plans

Utilizing electron beam lithography, in summer 2010 Mo cluster samples of various shapes and sizes (dots, cigars) were made at Molecular Foundry (S. Cabrini) (involving a student from NDSU). These samples consist of very different rim length-to-surface area ratios. The plan is to characterize these samples for HDS processes at UHV to better understand the importance of rim side effects. Furthermore, PVD will be used to study Mo cluster samples. We would focus on molecular beam scattering of hydrogen.

In addition, in collaboration with R. Tenne, Co/Ni doped inorganic nanotubes and nanoparticles including alloys will be tested for HDS at UHV and ambient pressure.

### Publications (2009-2011)

- 1) *Adsorption of thiophene on inorganic MoS<sub>2</sub> fullerene-like nanoparticles*, Catalysis Letters 129 (2009) 66-70, by M. Komarneni, A. Sand, U. Burghaus



- 2) *Adsorption and reaction kinetics of small organic molecules on WS<sub>2</sub> nanotubes: an ultra-high vacuum study*, Chemical Physics Letters 479 (2009) 109-112, by M. Komarneni, A. Sand, P. Nevin, A. Zak, U. Burghaus
- 3) *Adsorption of thiophene on silica supported Mo clusters*, Surface Science 604 (2010) 1221-1229 by M. Komarneni, E. Kadossov, J. Justin, M. Ming, U. Burghaus
- 4) *Bond activation in thiophene and catalyst poisoning – nanosize Mo clusters supported on silica for desulfurization catalysis*, Am. Chem. Soc., Div. Fuel Chem. 55 (2010) 594, by E. Kadossov, M. Komarneni, J. Justin, U. Burghaus
- 5) *Reactive and non-reactive interactions of thiophene with WS<sub>2</sub> fullerene-like nanoparticles: an ultra-high vacuum surface science study*, Catalysis Letters 125 (2008) 236–242, by J. Goering, U. Burghaus, B.W. Arey, O. Eidelman, A. Zak, R. Tenne
- 6) *Multi-site kinetic Monte Carlo simulations of thermal desorption spectroscopy data*, Surface Science 603 (2009) 2494-2501, by E. Kadossov and U. Burghaus
- 7) *Surface science perspective of carbon dioxide chemistry - adsorption kinetics and dynamics of CO<sub>2</sub> on selected model surfaces*, Catalysis Today 148 (2009) 212-220, by U. Burghaus (invited and peer-reviewed)
- 8) *Adsorption kinetics of small organic molecules on thick and thinner layers of carbon nanotubes*, Chemical Physics Letters 470 (2009) 300-303, by M. Komarneni, A. Sand, M. Lu, U. Burghaus
- 9) *Possible effect of carbon nanotube diameter on gas-surface interactions – the case of benzene, water, and n-pentane adsorption on SWCNTs at ultra-high vacuum conditions*, Chemical Physics Letters 476 (2009) 227-231, by M Komarneni, A. Sand, J. Goering, U. Burghaus, M. Lu, L. Monica Veca, Ya-Ping Sun
- 10) *Adsorption kinetics of methanol on carbon nanotubes revisited – solvent effects and pitfalls in ultra-high vacuum surface science experiments*, Chemical Physics Letters 473 (2009) 131-134, by J. Goering, M. Komarneni, A. Sand, U. Burghaus
- 11) *Gas-carbon nanotubes interactions: a review of ultra-high vacuum surface science studies on CNTs*, book chapter, chapter 1 (pages 1- 56) in: Carbon Nanotubes: New Research, Avery P. Ottenhouse (Ed.), Nova Science, Inc. (NY), 2009, ISBN 978-1-60692-236-1, by U. Burghaus
- 12) *Effect of carbon nanotubes crystal structure on adsorption kinetics of small molecules – an experimental study utilizing ultra-high vacuum thermal analysis techniques*, conference proceedings (9 pages), invited (40 min) talk at the 38<sup>th</sup> NATAS conference, North American Thermal Analysis Society, Philadelphia, 2010, by Uwe Burghaus will additionally be printed by Elsevier in Journal of Thermal Analysis xx (2011) xx
- 13) *Nanotechnology for Sustainable Energy and Fuels*, conference report about this session of the ACS meeting in Boston, 2010, published as a Focus article in ACS Nano, invited (and edited), ACS Nano 4 (2010) 5517-5526, by Chang-jun Liu, Uwe Burghaus, Flemming Besenbacher, and Zhong Lin Wang
- 14) *Short review: site-specific surface chemistry on nanotubes*, Israel Journal of Chemistry, 50 (2010) 449–452, by U. Burghaus, A. Zak, and R. Rosentsveig (invited and peer-reviewed)
- 15) *New and future developments in catalysis: activation of carbon dioxide*, S.L. Suib (Editor), A. Koch (Senior Editorial Project Manager at Elsevier), book chapter, *Surface Science Studies of Carbon Dioxide Chemistry*, by U. Burghaus, Dec. 2011

**Platinum-group metal (PGM) substituted complex oxide catalysts**

Graduate Students: Joshua A. Kurzman, Lauren M. Misch  
Undergraduate Student: Stephanie L. Moffitt  
Collaborators: Professors Susannah L. Scott, Galen D. Stucky, Eric W. McFarland, and Dr. Maosheng Miao (UC Santa Barbara), Dr. Jeffrey Miller (Argonne National Laboratory), Professor Alexandra Navrotsky (UC Davis)  
Contact: Materials Research Laboratory, University of California Santa Barbara, Santa Barbara, CA 93106-5121  
[seshadri@mrl.ucsb.edu](mailto:seshadri@mrl.ucsb.edu)

**Goal**

The key research goals explored in this proposal are: (i) to expand evidence for the role of PGM ions substituted at low levels into oxide hosts in catalytic redox transformations of energy carrier substrates and pollutants arising from energy conversion, and extending the exploration to ions other than Pd<sup>2+</sup>, including isoelectronic Au<sup>3+</sup>, and (ii) to develop model Pd<sup>2+</sup>, Au<sup>3+</sup>, Rh<sup>3+</sup> and Pt<sup>4+</sup>-containing bulk oxides (*e.g.*, Y<sub>2</sub>BaPdO<sub>5</sub>, La<sub>4</sub>LiAuO<sub>8</sub>, LaRhO<sub>3</sub>, and Ba<sub>2</sub>CePtO<sub>6</sub>) and to use them to shed light on the critical question regarding the active sites: metal ion or nanoparticle?

**DOE Interest**

Developing strategies for increasing the efficiency of use of platinum-group metals in catalysis for energy-related conversions.

**Recent Progress**

*Complex oxide redox hosts for Pd<sup>2+</sup>*: Complex oxides, containing multiple cations on crystallographically distinct sites, have recently been shown to display redox cycling of PGMs such as Pd; for example, Pd-substituted complex oxides can reversibly extrude metallic Pd under reducing conditions and then reincorporate Pd<sup>2+</sup> ions into the lattice under oxidizing conditions. Regenerative materials of this type are appealing alternatives to conventional oxide-supported PGM catalysts, potentially offering improved resistance to sintering and poisoning of the active element(s). In contrast to previously studied host compounds, hexagonal YMnO<sub>3</sub>-type YMn<sub>0.5</sub>Fe<sub>0.5-x</sub>Pd<sub>x</sub>O<sub>3-δ</sub> is only modestly tolerant to cycling: repeated redox cycling leads to the formation of PdO. Although Pd<sup>2+</sup> is fully dispersed throughout the lattice in the as-prepared materials, their activity for CO oxidation is not enhanced beyond that of PdO on an inert support, suggesting that the corner-connected trigonal bipyramids which characterize this structure type, are not a structural motif that promotes oxygen mobility.

*Model Pd<sup>2+</sup> and Au<sup>3+</sup> compounds:* To inform an understanding of catalysis by substituted complex oxides, we have probed the activity of well-defined compounds containing PGM and noble metal ions. The exceptionally stable oxides of Pd<sup>2+</sup> and Au<sup>3+</sup>, La<sub>2</sub>BaPdO<sub>5</sub> and La<sub>4</sub>LiAuO<sub>8</sub>, both contain the isoelectronic d<sup>8</sup> species as isolated square planes. Despite similarities between the compounds, La<sub>2</sub>BaPdO<sub>5</sub> is very effective at catalyzing the oxidation of CO under CO-lean conditions, while La<sub>4</sub>LiAuO<sub>8</sub> is not. The pronounced difference in activity can be understood on the basis of the relative positions of the Pd 4d and Au 5d bands: density functional calculations reveal that the center of the Pd d-states are much nearer to the Fermi level (*ca.* -2.5 eV) – i.e. more accessible to adsorbates – than the Au d-states (*ca.* -5.0 eV).

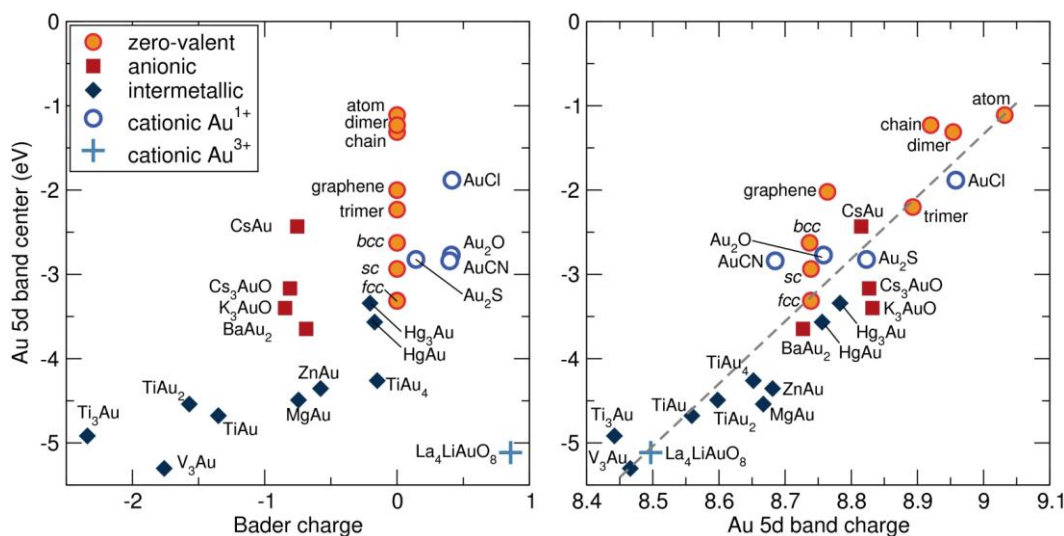


**Figure 1.** **Left panel:** Correlation of the Au 5d band center with the charge on Au (as obtained from Bader charge analysis) for a number of Au-based species including gold atoms, dimers, trimers, extended systems, and compounds. Note the absence of simple correlations, for example, the large variation in the 5d band center for a given charge state. **Right panel:** Correlation of the Au 5d band center with the Au 5d band charge. This is clearly a better correlation and suggests the difficulty of attempting to recreate key aspects of the electronic structure of gold clusters and nanoparticles in extended compounds such as oxides and intermetallics.

*Electronic signatures in extended solids of gold:* Strong association between the d-band center and the catalytic activity of transition metals has been well established by both first principles calculations and experimental observations. Despite the enormous amount of research on catalysis by gold nanoparticles, there is still some lack of consensus on the catalytic mechanisms at play and the nature of the active species. Prompted by the finding that Au<sup>3+</sup> in La<sub>4</sub>LiAuO<sub>8</sub> is ineffective at catalyzing the CO oxidation reaction, which we attribute to the Au 5d-states being inaccessible to adsorbates, we have calculated the electronic structure of a large number of well defined Au compounds with the aim of establishing the relation between Au charge states and its catalytic activity. As shown in **Figure 1**, our calculations reveal a remarkable correlation between the position of the d-band center and the d-band charge, *i.e.* the d-band center shifts toward the Fermi

level with increasing d-band charge. On the other hand, neither the d-band center nor the d-band charge shows any correlation with the total charge on Au.

## Future Plans

*Rh-substituted perovskites:* We have prepared a series of Rh<sup>3+</sup>-substituted perovskite La<sub>0.7</sub>Sr<sub>0.3</sub>Mn<sub>1-x</sub>Rh<sub>x</sub>O<sub>3</sub> samples and characterized them using time-of-flight neutron diffraction (SNS, Oak Ridge) and these samples are currently being subject to catalytic testing for NO<sub>x</sub> abatement.

*Electronic signatures in Pd oxides:* The relation between the d-band center and catalytic activity is well established in transition metal alloys but has not been widely employed in understanding catalysis by complex metal oxides. In light of our recent work on catalysis by Pd<sup>2+</sup>-substituted oxides, and the electronic structural correlations seen in the gold species in **Figure 1**, we intend to carry out a similar comprehensive study of the electronic structure of Pd-containing oxides, and look for signatures that could correlate with catalytic activity.

## Publications (2009-2011)

1. J. A. Kurzman, X. Ouyang, W. B. Im, J. Li, J. Hu, S. L. Scott, and R. Seshadri, La<sub>4</sub>LiAuO<sub>8</sub> and La<sub>2</sub>BaPdO<sub>5</sub>: Comparing two highly stable d<sup>8</sup> square-planar oxides, *Inorg. Chem.* **49** (2010) 4670–4680.
2. J. A. Kurzman, S. L. Moffitt, A. Llobet, and R. Seshadri, Neutron diffraction study of La<sub>4</sub>LiAuO<sub>8</sub>: Understanding Au<sup>3+</sup> in an oxide environment, *J. Solid State Chem.* **184** (2011) 1439–1444.
3. T. Z. Forbes, J. A. Kurzman, R. Seshadri, and A. Navrotsky, The energetics of La<sub>4</sub>LiAuO<sub>8</sub>, *J. Mater. Res.* **26** (2011) 1188–1192.
4. J. A. Kurzman, J. Li, T. D. Schladt, C. R. Parra, X. Ouyang, R. Davis, J. T. Miller, S. L. Scott, and R. Seshadri, Pd<sup>2+</sup>/Pd<sup>0</sup> redox cycling in hexagonal YMn<sub>0.5</sub>Fe<sub>0.5</sub>O<sub>3</sub>: Implications for catalysis by PGM-substituted complex oxides (*under review*).



## Fundamental Surface Structure-Photoactivity Relationships of Semiconductor Mixed Oxides for Splitting of H<sub>2</sub>O to H<sub>2</sub>/O<sub>2</sub>

Students: S. Phivalay, C.A. Roberts

Collaborators: A. Puretsky, Oak Ridge National Labs, Oak Ridge, TN  
K. Domen, University of Tokyo, Tokyo, Japan

Contact: I.E. Wachs, Chemical Engineering Department, Lehigh University,  
Bethlehem, PA 18105

Phone: (610)758-4274; E-mail: [iew0@lehigh.edu](mailto:iew0@lehigh.edu)

Web page : [www.lehigh.edu/operando](http://www.lehigh.edu/operando)

### Goal:

Determination of (1) molecular/electronic structure-photocatalytic relationship for water splitting on well-defined supported TiO<sub>2</sub>/SiO<sub>2</sub> catalysts and (2) nature of the catalytic active sites present on the surface of advanced bulk tantalum mixed oxide photocatalysts.

### Recent Progress

**Molecular/Electronic Structure-Photocatalytic Relationship for Water Splitting on Well-Defined Supported TiO<sub>2</sub>/SiO<sub>2</sub> Catalysts:** Model supported TiO<sub>2</sub>/SiO<sub>2</sub> catalysts were synthesized by incipient-wetness impregnation of Ti-isopropoxide/isopropanol precursor solutions onto a SiO<sub>2</sub> support (Cab-O-Sil, 330 m<sup>2</sup>/g), followed by drying and calcination in air. The supported titania phases were extensively characterized with *in situ* (dehydrated) Raman, IR, UV-vis, photoluminescence (PL) spectroscopy, XANES and electron microscopy (*aberration corrected* HR-TEM) to determine their molecular and electronic structures as well as the titania domain size. The catalysts were dehydrated under flowing 10% O<sub>2</sub> at 400 °C and the lifetimes of the excited states of the samples were determined *in situ* at room temperature using a pulsed laser for excitation and a gated detector with picosecond time resolution. The production of H<sub>2</sub> was monitored by gas chromatography for the water splitting reaction in a UV-irradiated reactor. The excitation lifetime measurements revealed that electron-hole decay is characterized by both fast and slow components. The slow component of decay is dominant in the higher wt% loading samples, larger titania domain size, and correlates with increased activity for photocatalytic water splitting (Fig. 1).

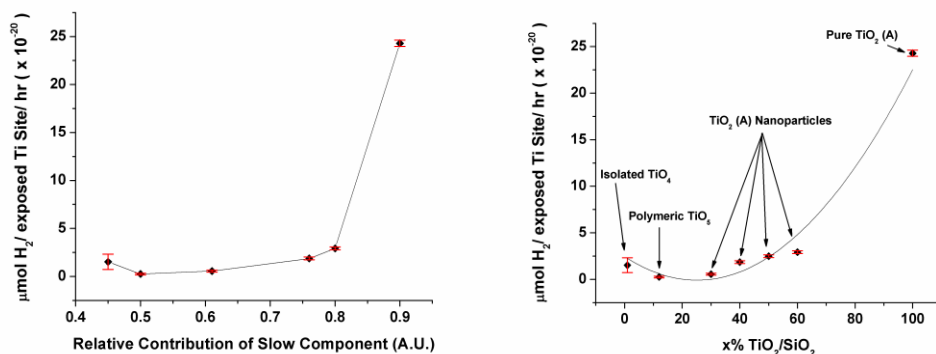


**Figure 1:** (a) Production of H<sub>2</sub> normalized by exposed Ti site as a function of the relative contribution of the slow component of decay. (b) Production of H<sub>2</sub> normalized by exposed Ti site as a function of wt% loading. Domain type is indicated.

The trend of increasing photoactivity with increasing domain size is not unique to water splitting and has also been shown to be true for the photo-oxidation of cyclohexane to cyclohexanone. The consistent trend in two separate photocatalytic reactions indicates that this finding is a general structure-activity relationship for photocatalysis, especially with TiO<sub>2</sub> based materials.

**Determination of the Nature of the Catalytic Active Sites Present on the Surface of Advanced Bulk Tantalum Mixed Oxide Photocatalysts:** Tantalum-based photocatalysts such as Ta<sub>2</sub>O<sub>5</sub>, NaTaO<sub>3</sub>, and NaTaO<sub>3</sub>:La have been found to be among the most active photocatalysts for the photocatalytic conversion of H<sub>2</sub>O into H<sub>2</sub>/O<sub>2</sub>, with NaTaO<sub>3</sub>:La loaded with a NiO co-catalyst being the most active with a quantum efficiency of 56% under UV-irradiation. *In situ* and *operando* optical spectroscopic characterization methods (Raman, IR, UV-vis, photoluminescence (PL) and time-resolved picosecond PL-Raman) were utilized to give further insight into the molecular and electronic structure of these mixed oxide photocatalysts. The unique surface science characterization techniques (high-resolution x-ray photoelectron spectroscopy (HR-XPS) and high-sensitivity low energy ion scattering (HS-LEIS)) available at Lehigh University were employed to determine the nature of the outermost atomic layer of the 0.2NiO/2% La<sub>2</sub>O<sub>3</sub>/NaTaO<sub>3</sub> bulk mixed oxide photocatalysts as shown in Figure 2.

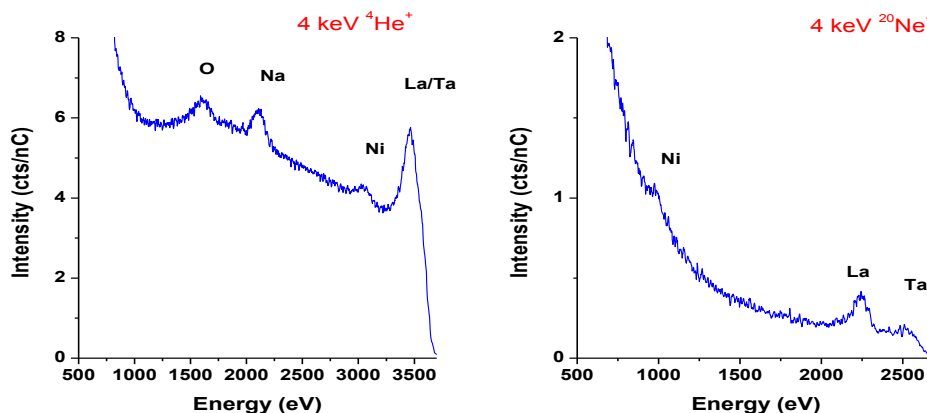


**Figure 2.** HS-LEIS Spectra of NaTaO<sub>3</sub> doped with 2% La<sub>2</sub>O<sub>5</sub> and 0.2% NiO using 4 keV (left) He<sup>+</sup> and (right) Ne<sup>+</sup> ion beams. Heavier Ne<sup>+</sup> ions allow discrimination of La and Ta.

The ION-TOF Qtac<sup>100</sup> HS-LEIS spectrometer is the first such cutting edge instrument in North America. The HS-LEIS measurements reveal that Na, Ni, La and Ta, as well as O, are present on the topmost layer of this mixed oxide. Corresponding sputtering studies revealed that Na, La and Ni are surface segregated with Ni and La being concentrated on the outermost surface layer. Comparison of this surface compositional information with corresponding photocatalytic activity for H<sub>2</sub>O splitting reveals that (1) the function of LaO<sub>x</sub> is to stabilize smaller NaTaO<sub>3</sub> nanoparticles with greater surface area and (2) the function of NiO is to enhance trapping of e<sup>-</sup> for evolution of H<sub>2</sub>. These unprecedented surface insights into the fundamental structure-photoactivity relationship of very active tantalum-based photocatalysts have *for the first time* revealed the important function of the surface characteristics of mixed oxide photocatalysts for H<sub>2</sub>O splitting.

## DOE Interest

The conversion of abundant and inexpensive H<sub>2</sub>O to H<sub>2</sub> fuel via photocatalysts activated by sunlight is one of the ultimate objectives of sustainable energy research.

## Future Studies

These new insights will be used to guide the design of improved photocatalysts for H<sub>2</sub> generation from H<sub>2</sub>O in future studies (e.g., different titania structures and surface modification of bulk tantalum mixed oxides). The photoactivity of supported Ta<sub>2</sub>O<sub>5</sub> catalysts for water splitting will also be investigated to establish their molecular/electronic structure-photoactivity relationship. Additional photocatalytic reactions will also be investigated to further establish that the observed structure-photoactivity relationship is a universal relationship that is not dependent on the specific photoactivity reaction (e.g., splitting of H<sub>2</sub>O and cyclohexane oxidation).

## Publications 2010-2011:

"Characterization of Hydrothermally Prepared Titanate Nanotube Powders by Ambient and *In Situ* Raman Spectroscopy," S.-J. Kim, Y.-U. Yun, H.-J. Oh, S. H. Hong, C. A. Roberts, K. Routray and I.E. Wachs, *J. Phys. Chem. Lett.* 1 (2010) 130-135.

"Molecular Structural determination of Molybdena in Different Environments: Aqueous Solutions, Bulk Mixed Oxides and Supported MoO<sub>3</sub> Catalysts," H. Tian, C.A. Roberts and I.E. Wachs, *J. Phys. Chem. C*, 114 (2010) 14110-14120.

"Anomalous Surface Compositions of Stoichiometric Mixed Oxide Compounds," Sergiy V. Merzlikin, Nikolay N. Tolkachev, Laura E. Briand, Thomas Strunskus, Christof Wöll, Israel E. Wachs and Wolfgang Grünert *Angewandte Chemie*, 47 (2010) 8037-8041.

"Origin of the synergistic interaction between MoO<sub>3</sub> and iron molybdate for the selective oxidation of methanol to formaldehyde," K. Routray, W. Gruenert, W. Zhou, C.J. Kiely and I.E. Wachs, *J. Catal.* 275 (2010) 84-98.

"Monitoring Surface Metal Oxide Catalytic Active Sites with Raman Spectroscopy, I.E. Wachs in *Understanding the Nature of Active Sites in Heterogeneous Catalysis: Lessons from In Situ Spectroscopy Studies*," Special Issue, *Chemical Soc. Reviews* 39 (2010) 5002-5017, invited article.

"The Generality of Surface Vanadium Oxide Phases in Mixed Oxide Catalysts," I.E. Wachs, *Appl. Catal. A: General* 391 (2011) 36-42 (DOI:10.1016/j.apcata.2010.08.048) invited article.

"Catalysis Science of Methanol Oxidation over Iron Vanadate Catalysts," K. Routray and I.E. Wachs, *ACS Catalysis* 1 (2011) 54-66 (DOI.org/10.1021/cs1000569).

"Determination of a Structure-Photocatalytic Relationship for Water Splitting on Well-Defined TiO<sub>2</sub> Nanodomains," C.A. Roberts, A.A. Puzovskiy, S.P. Phivilay and I.E. Wachs (to be submitted to *JACS*).

## Spectroscopic Observation of Dual Catalytic Sites During Oxidation of CO on a Au/TiO<sub>2</sub> Catalyst

Lead PI: John T. Yates, Jr.

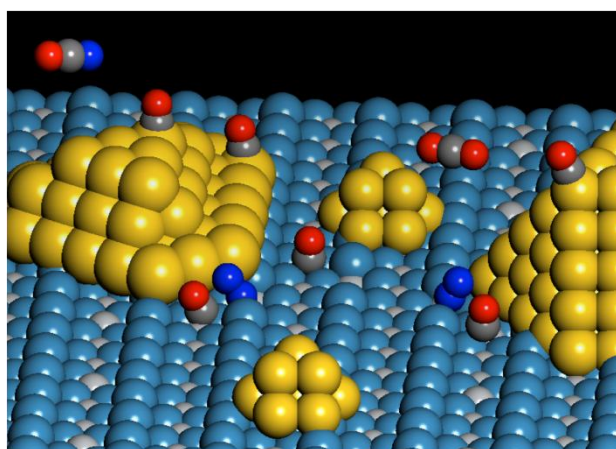
Co-PI: Matthew Neurock

Postdoc: Zhen Zhang and Wenjie Tang

Student: Isabel X. Green

Contact: Department of Chemistry, University of Virginia, Charlottesville VA 22904;  
johnt@virginia.edu

The prevailing view of CO oxidation on gold-titanium oxide (Au/TiO<sub>2</sub>) catalysts is that the reaction occurs on metal sites at the Au/TiO<sub>2</sub> interface. We observed dual catalytic sites at the perimeter of 3-nanometer Au particles supported on TiO<sub>2</sub> during CO oxidation. Infrared-kinetic measurements indicate that O-O bond scission is activated by the formation of a CO-O<sub>2</sub> complex at dual Ti-Au sites at the Au/TiO<sub>2</sub> interface. Density functional theory calculations, which provide the activation barriers



for the formation and bond scission of the CO-O<sub>2</sub> complex, confirm this model as well as the measured apparent activation energy of 0.16 electron volts. The observation of sequential delivery and reaction of CO first from TiO<sub>2</sub> sites and then from Au sites indicates that catalytic activity occurs at the perimeter of Au nanoparticles.

### Publications Since Beginning of Grant (09-15-09):

1. I. X. Green and J. T. Yates, Jr., "Vibrational Spectroscopic Observation of Weakly-Bound Adsorbed Molecular Oxygen on Powdered Titanium Dioxide," *The Journal of Physical Chemistry C*, 2010, **114**, 11924-11930.
2. Z. Zhang and J. T. Yates, Jr., "Effects of Adsorbed Donor and Acceptor Molecules on Electron Stimulated Desorption: O<sub>2</sub>/TiO<sub>2</sub>," *The Journal of Physical Chemistry Letters*, **1**, 2185-2188 (2010)
3. J. T. Yates, Jr. and C. T. Campbell, "Surface Chemistry: Key to Control and Advance Myriad Technologies," *PNAS*, **108**, 911-916 (2011).
4. J. Lee, Z. Zhang, X. Deng, D. Sorescu, C. Matranga, and J. T. Yates, Jr., "Interaction of CO and Oxygen Adatoms on TiO<sub>2</sub>(110)," *The Journal of Physical Chemistry C*, **115**, 4163 (2011).

5. I. X. Green, W. Tang, M. Neurock, and J. T. Yates, Jr., "Low Temperature H<sub>2</sub> Catalytic Oxidation over Nanoparticle Au/TiO<sub>2</sub>-Dual Perimeter Sites at Work," *Angewandte Chemie International Edition*, **50**, 1 (2011).
6. I. X. Green, W. Tang, M. Neurock and J. T. Yates, Jr., "Spectroscopic Observation of Dual Catalytic Sites During Oxidation of CO on a Au/TiO<sub>2</sub> Catalyst," *Science*, **Accepted**, to appear 05 Aug. 2011.
7. J. T. Yates, Jr., "The Search for the Active Site on Catalysts," *The Jefferson Journal of Science and Culture*, **Submitted**, 06 Jul. 2011

This page is intentionally blank.

# Participant List

This page is intentionally blank.



# Participant List

Name	Organization	E-mail
Adzic, Radoslav	Brookhaven National Laboratory	adzic@bnl.gov
Altman, Eric	Yale University	eric.altman@yale.edu
Asthagiri, Aravind	The Ohio State University	asthagiri@chbmeng.ohio-state.edu
Balbuena, Perla	Texas A&M University	balbuena@tamu.edu
Bao, Xinhe	Dalian Institute of Chemical Physics, CAS	xhbao@dicp.ac.cn
Bartels, Ludwig	University of California	bartels@ucr.edu
Bartynski, Robert	Rutgers University	bart@physics.rutgers.edu
Batzill, Matthias	University of South Florida	mbatzill@usf.edu
Bell, Alexis	Dept. of Chemical & Biomolecular Eng.	bell@cchem.berkeley.edu
Bernhardt, Thorsten	University of Ulm, Germany	thorsten.bernhardt@uni-ulm.de
Bessel, Carol	U. S. Department of Energy	carol.bessel@science.doe.gov
Bhan, Aditya	University of Minnesota, Twin Cities	abhan@umn.edu
Bouchard, Louis	University of California, Los Angeles	bouchard@chem.ucla.edu
Brinker, Jeff	University of New Mexico	cjbrink@sandia.gov
Britt, Phillip	Oak Ridge National Laboratory	brittpf@ornl.gov
Bullock, Morris	Pacific Northwest National Laboratory	morris.bullock@pnnl.gov
Bunel, Emilio	Argonne National Laboratory	ebunel@anl.gov
Burghaus, Uwe	North Dakota State University	uwe.burghaus@ndsu.edu
Camaioni, Donald	Pacific Northwest National Laboratory	donald.camaioni@pnnl.gov
Camillone, Nicholas	Brookhaven National Laboratory	nicholas@bnl.gov
Campbell, Charles	University of Washington	campbell@chem.washington.edu
Chen, Jingguang	University of Delaware	ygchen@udel.edu
Chen, Peng	Cornell University	pc252@cornell.edu
Chen, Donna	University of South Carolina	chen@chem.sc.edu
Cox, David	Virginia Tech	dfcox@vt.edu
Crooks, Richard	University of Texas	crooks@cm.utexas.edu
CUK, TANJA	University of California at Berkeley	tanjacuk@berkeley.edu
Curtiss, Larry	Argonne National Lab	curtiss@anl.gov
Dai, Sheng	Oak Ridge National Laboratory	dais@ornl.gov
Datye, Abhaya	University of New Mexico	datye@unm.edu
Dauenhauer, Paul	University of Massachusetts	dauenhauer@ecs.umass.edu
Davis, Robert	University of Virginia	rjd4f@virginia.edu
Delgass, William	Purdue University	delgass@purdue.edu
Dimitrijevic, Nada	Argonne National Laboratory	dimitrijevic@anl.gov
Dixon, David	University of Alabama	dadixon@bama.ua.edu
Dohnálek, Zdenek	Pacific Northwest National Laboratory	Zdenek.Dohnalek@pnnl.gov
Erlebacher, Jonah	Johns Hopkins University	Jonah.Erlebacher@jhu.edu
Evans, James	Ames Laboratory	evans@ameslab.gov
Flytzani-Stephanopoulos, Maria	Tufts University	maria.flytzani-stephanopoulos@tufts.edu

<b>Name</b>	<b>Organization</b>	<b>E-mail</b>
Frei, Heinz	Lawrence Berkeley National Laboratory	HMFrei@lbl.gov
Frenkel, Anatoly	Yeshiva University	anatoly.frenkel@yu.edu
Friend, Cynthia	Harvard University	cfriend@seas.harvard.edu
Gao, Pu-Xian	University of Connecticut	puxian.gao@ims.uconn.edu
Garrett, Bruce	Pacific Northwest National Laboratory	bruce.garrett@pnnl.gov
Gates, Bruce	University of California	bcgates@ucdavis.edu
Gellman, Andrew	Carnegie Mellon University	gellman@cmu.edu
Gorte, Raymond	University of Pennsylvania	gorte@seas.upenn.edu
Haller, Gary	Yale University	gary.haller@yale.edu
Harris, Alex	Brookhaven National Laboratory	alexh@bnl.gov
Heinz, Tony	Columbia University	tony.heinz@columbia.edu
Henderson, Michael	Pacific Northwest National Laboratory	ma.henderson@pnnl.gov
Henkelman, Graeme	University of Texas at Austin	henkelman@mail.utexas.edu
Heyden, Andreas	University of South Carolina	heyden@cec.sc.edu
Hrbek, Jan	U. S. Department of Energy	jan.hrbek@sceince.doe.gov
Jackson, James	Michigan State University	jackson@chemistry.msu.edu
Jaramillo, Thomas	Stanford University	jaramillo@stanford.edu
Jenks, Cynthia	Ames Laboratory	cjenks@ameslab.gov
Jentoft, Friederike	University of Oklahoma	fcjentoft@ou.edu
Jiang, De-en	Oak Ridge National Laboratory	jiangd@ornl.gov
Johnson, Duane	Ames Laboratory	ddj@ameslab.gov
Jones, Christopher	Georgia Institute of Technology	cjones@chbe.gatech.edu
Katz, Alexander	University of California	askatz@berkeley.edu
Kitchin, John	Carnegie Mellon University	jkitchin@andrew.cmu.edu
Kung, Harold	Northwestern University	hkung@northwestern.edu
Lercher, Johannes A.	Technische Universität München	johannes.lercher@ch.tum.de
Linic, Suljo	University of Michigan	linic.su@gmail.com
Liu, Ping	Brookhaven National Laboratory	pingliu3@bnl.gov
Lobo, Raul	University of Delaware	lobo@udel.edu
Marceau, Diane	U. S. Department of Energy	diane.marceau@science.doe.gov
Marks, Tobin	Northwestern University	t-marks@northwestern.edu
Marshall, Christopher	Argonne National Laboratory	marshall@anl.gov
Maupin, Paul	U. S. Department of Energy	Paul.maupin@science.doe.gov
Mavrikakis, Manos	University of Wisconsin	manos@engr.wisc.edu
McFarland, Eric	University of California	mcfar@engineering.ucsb.edu
McIntosh, Steve	Lehigh University	stm310@lehigh.edu
Medlin, James	University of Colorado	will.medlin@colorado.edu
Miller, John	U. S. Department of Energy	john.miller@science.doe.gov
Miller, Jeff	Argonne National Lab	millerjt@anl.gov
Miranda, Raul	U.S. Department of Energy	raul.miranda@science.doe.gov
Mullins, David	Oak Ridge National Laboratory	mullinsdr@ornl.gov
Mullins, Charles	University of Texas	mullins@che.utexas.edu

<b>Name</b>	<b>Organization</b>	<b>E-mail</b>
Mustain, William	University of Connecticut	mustain@engr.uconn.edu
Nilsson, Anders	SLAC National Accelerator Laboratory	nilsson@slac.stanford.edu
Nørskov, Jens	SLAC National Accelerator Laboratory	norskov@stanford.edu
Notestein, Justin	Northwestern University	j-notestein@northwestern.edu
Nuzzo, Ralph	University of Illinois	r-nuzzo@illinois.edu
Overbury, Steve	Oak Ridge National Laboratory	overburysh@ornl.gov
Ozkan, Umit	Ohio State University	ozkan.1@osu.edu
Peden, Charles	Institute for Integrated Catalysis	chuck.peden@pnl.gov
Pophale, Ramdas	Rice University	ramdas@rice.edu
Pruski, Marek	Ames Laboratory	mpruski@iastate.edu
Rahman, Talat	University of Central Florida	Talat.Rahman@ucf.edu
Rappe, Andrew	University of Pennsylvania	rappe@sas.upenn.edu
Ribeiro, Fabio	Purdue University	fabio@purdue.edu
Rodriguez, Jose	Brookhaven National Laboratory	rodrigez@bnl.gov
Roldán Cuenya, Beatriz	University of Central Florida	roldan@ucf.edu
Román, Yuriy	Massachusetts Institute of Technology	yroman@mit.edu
Rousseau, Roger	Pacific Northwest National Laboratory	roger.rousseau@pnnl.gov
Schneider, William	University of Notre Dame	wschneider@nd.edu
Schwarz, Udo	Yale University	udo.schwarz@yale.edu
Scott, Susannah	University of California	sscott@engineering.ucsb.edu
Selloni, Annabella	Princeton University	aselloni@princeton.edu
Sievers, Carsten	Georgia Institute of Technology	carsten.sievers@chbe.gatech.edu
Spitler, Mark	U.S. Department of Energy	Mark.Spitler@science.doe.gov
Stacchiola, Dario	Brookhaven National Laboratory	djs@bnl.gov
Stack, Robert	U.S. Department of Energy	Robert.Stack@science.doe.gov
Stair, Peter	Northwestern University	pstair@northwestern.edu
Steinrück, Hans-Peter	Universität Erlangen-Nürnberg	steinrueck@chemie.uni-erlangen.de
Suib, Steve	University of Connecticut	Steven.Suib@uconn.edu
Szanyi, Janos	Pacific Northwest National Laboratory	janos.szanyi@pnnl.gov
Tait, Steven	Indiana University	tait@indiana.edu
Tao, Franklin (Feng)	University of Notre Dame	ftao@nd.edu
Tong, YuYe J.	Georgetown University	yyt@georgetown.edu
Tysoe, Wilfred	University of Wisconsin	wtt@uwm.edu
Vlachos, Dion	University of Delaware	vlachos@udel.edu
Vohs, John	University of Pennsylvania	vohs@seas.upenn.edu
Wang, Guofeng	Univeristy of Pittsburgh	guw8@pitt.edu
Wang, Jia	Brookhaven National laboratory	jia@bnl.gov
Wang, Lai-Sheng	Brown University	Lai-Sheng_Wang@brown.edu
Wang, Linlin	Ames Laboratory	llw@ameslab.gov
Wang, Yong	Pacific Northwest National Laboratory	yongwang@pnl.gov
Weaver, Jason	University of Florida	weaver@che.ufl.edu
Weckhuysen, Bert	Utrecht University	b.m.weckhuysen@uu.nl

<b>Name</b>	<b>Organization</b>	<b>E-mail</b>
White, Michael	Brookhaven National Laboratory	mgwhite@bnl.gov
Wu, Zili	Oak Ridge National Laboratory	wuz1@ornl.gov
Yang, Judith	University of Pittsburgh	judyyang@pitt.edu
Yang, Peidong	University of California	p_yang@berkeley.edu
Zaera, Francisco	University of California	zaera@ucr.edu
Zapol, Peter	Argonne National Laboratory	zapol@anl.gov
Zhang, Bo	University of Washington	zhang@chem.washington.edu

# Author Index

This page is intentionally blank.

## Author Index

Abild-Pedersen, Frank .....	83	Davis, Mark .....	101
Abu-Omar, M.....	161	Davis, Robert J.....	14, 155
Adzic, Radoslav R.....	71, 113, 141, 236	Deem, Michael W.....	158
Alexandrova, Anastassia N. ....	119	Delgass, W. Nicholas .....	161
Altman, Eric I. ....	120, 302	Diebold, Ulrike .....	311
Asthagiri, Aravind .....	124, 343	Dimitrijevic, Nada M. ....	167, 318
Auerbach, Scott .....	101	Dixon, David A.....	168, 184, 268
Bakac, Andreja.....	281	Dohnálek, Zdenek .....	169, 199, 268
Balbuena, Perla B. ....	72, 125	Doren, Douglas.....	101, 218
Bao, Xinhe.....	53	Dumesic, James A.....	221, 236
Bardeen, Christopher J.....	32	Eichhorn, B. ....	236
Bare, Simon R. ....	141	Elam, Jeff.....	20, 318
Barteau, Mark.....	101, 221	Ellis, Don.....	318
Bartels, Ludwig .....	56, 288	Erlebacher, Jonah.....	170
Bartynski, Robert A.....	107	Evans, James .....	281
Batzill, Matthias.....	128	Fan, Wei .....	101
Bedzyk, Mike .....	318	Flynn, George .....	65
Bell, Alexis T.....	131	Flytzani-Stephanopoulos, Maria .....	65
Bernhardt, Thorsten M.....	63	Frei, Heinz .....	173
Bhan, Aditya .....	101, 134	Frenkel, Anatoly .....	101, 141, 252
Bligaard, Thomas.....	83	Friend, Cynthia M.....	174
Bouchard, L.-S.....	136	Fulton, John.....	137
Brinker, C. Jeffrey .....	4	Gao, P.X.....	177
Broadbelt, Linda .....	318	Gates, Bruce .....	178, 184
Bullock, R. Morris .....	41	Geiger, Franz .....	318
Burghaus, Uwe .....	355	Gellman, Andrew J.....	190, 337
Buttrey, Doug .....	101	Gorte, Raymond J.....	48, 101
Camaioni, Donald .....	137	Gray, Kimberly A. ....	167, 318
Camillone, Nicholas.....	329	Haller, Gary L.....	196
Campbell, Charles T.....	138	Hanson, Jonathan C. ....	26, 141
Caruthers, J. M. ....	161	Haw, James F.....	184
Chan, Siu-Wai .....	65	Heinz, Tony F.....	56, 288
Chen, Donna .....	56, 288	Henderson, Michael A.....	199
Chen, Jingguang G. ....	78, 101, 141	Henkelman, Graeme .....	147
Chen, Peng.....	64	Herman, Irving .....	65
Chmelka, Bradley F.....	305	Hersam, Mark.....	318
Cox, David F. ....	144	Heyden, Andreas.....	204
Cox, Jonathan .....	352	Hrbek, Jan.....	317
Crooks, Richard M. ....	147, 221	Hu, Jianzhi .....	137
Cuk, Tanja.....	150	Huber, George.....	101
Curtiss, Larry.....	20, 318	Hulbert, Steve L.....	141
Dai, Sheng.....	258	Hupp, Joe .....	318
Datye, Abhaya .....	151	Iglesia, Enrique .....	268
Dauenhauer, Paul J.....	101, 154	Jackson, James E. "Ned" .....	207

Jaramillo, Thomas F.....	208	Poeppelmeier, Ken.....	318
Jentoft, Friederike C. ....	209	Pruski, Marek .....	281
Jiang, De-en .....	258	Rahman, Talat S. ....	56, 288
Jiao, Feng.....	101	Rappe, Andrew M. ....	294
Johnson, Duane .....	252	Ribeiro, Fabio H.....	161, 297
Jones, Christopher.....	14	Rodriguez, Jose A. ....	26, 71, 141, 317, 346
Katz, Alexander.....	7	Roldán Cuenya, Beatriz .....	57
Kay, Bruce D. ....	268	Román, Yuriy .....	300
Kimmel, Greg.....	199	Rousseau, Roger.....	267, 268
Kitchin, John .....	210	Sadow, Aaron .....	281
Klein, Mike.....	101	Saltsburg, Howard.....	65
Koel, Bruce .....	101	Sandler, Stan .....	101
Kung, Harold H.....	213, 318	Sasaki, Kotaro.....	113
Kung, Mayfair .....	318	Schneider, William F. ....	87, 161
Kwak, Ja Hun .....	267	Schwartz, Daniel K.....	242
Lauterbach, Jochen A. ....	221	Schwarz, Udo D. ....	302
Lee, Kelvin .....	101	Scott, Susannah.....	305
Lercher, Johannes A. ....	97, 137	Selloni, Annabella.....	311
Li, Yongxin.....	352	Seminario, Jorge M. ....	125
Linic, Suljo.....	215	Seshadri, Ram.....	358
Liu, Jun.....	268, 342	Sharma, R. ....	136
Liu, Ping .....	26, 71, 113, 317, 346	Sherrill, C. David.....	14
Lobo, Raul F. ....	101, 218, 221	Sholl, Davis S. ....	190
Ludovice, Peter.....	14	Sievers, Carsten.....	314
Lyubinetsky, Igor .....	199	Slowing, Igor.....	281
Marks, Laurence .....	318	Snurr, Randy.....	318
Marks, Tobin J. ....	227, 318	Snyder, Mark.....	101
Marshall, Christopher L. ....	20, 230	Stacchiola, Dario J. ....	26, 317, 346
Mavrikakis, Manos .....	221, 236	Stair, Peter C. ....	20, 245, 318
McFarland, Eric.....	90	Steinrück, Hans-Peter .....	13
Medlin, J. Will .....	242	Studt, Felix .....	83
Mei, Donghai .....	137, 267	Suib, Steven L. ....	324
Metiu, Horia .....	90	Sutter, Peter .....	329
Miller, Jeffrey T.....	20, 245, 318	Szanyi, János .....	267, 332
Mullins, Charles Buddie.....	246	Tait, Steven T.....	335
Mullins, David R.....	141, 249, 258	Tao, Franklin (Feng).....	336
Mustain, William E. ....	45	Thomson, K. T.....	161
Neurock, Matthew .....	364	Tong, YuYe J. ....	98
Nguyen, SonBinh .....	318	Tsapatsis, Michael.....	101
Nilsson, Anders.....	83, 250	Tysoe, Wilfred T. ....	190, 337
Nørskov, Jens K.....	83	Van Duynne, Rick .....	318
Notestein, Justin M. ....	251	Vela, Javier .....	281
Nuzzo, Ralph.....	252	Vlachos, Dionisios G. ....	101, 221
Overbury, Steven H. ....	141, 249, 258, 351	Vohs, John M.....	101, 338
Ozkan, Umit S. ....	264	Vukmirovic, Miomir .....	113
Peden, Charles H. F.....	168, 169, 267, 268, 342	Wachs, Israel E. ....	361
Peters, Baron.....	305	Wang, Guofeng .....	42
Petrik, Nick .....	199	Wang, Jia.....	113



Wang, Lai-Sheng.....	268, 341
Wang, Yong .....	137, 151, 267, 268, 342
Weaver, Jason F.....	124, 343
Weck, Marcus.....	14
Weckhuysen, Bert M.....	77
Weitz, Eric.....	318
Westmoreland, Phil.....	101
White, Michael G.....	71, 346
Wu, Zili.....	258, 351
Xia, Younan.....	221
Xu, Ye.....	249, 258
Yan, Yushan .....	101
Yang, Judith .....	252
Yang, Peidong.....	3
Yates, John T., Jr. ....	364
Yin, Yadong.....	32
Zaera, Francisco.....	32, 190
Zapol, Peter .....	318
Zhang, Bo.....	352
Zhang, Miao.....	173